# PROTEIN EXPORT AND SECRETION AMONG BACTERIAL PATHOGENS

EDITED BY: Sophie Bleves, Romé Voulhoux, Bérengère Ize, Thibault Géry Sana and Denise Monack

PUBLISHED IN: Frontiers in Cellular and Infection Microbiology

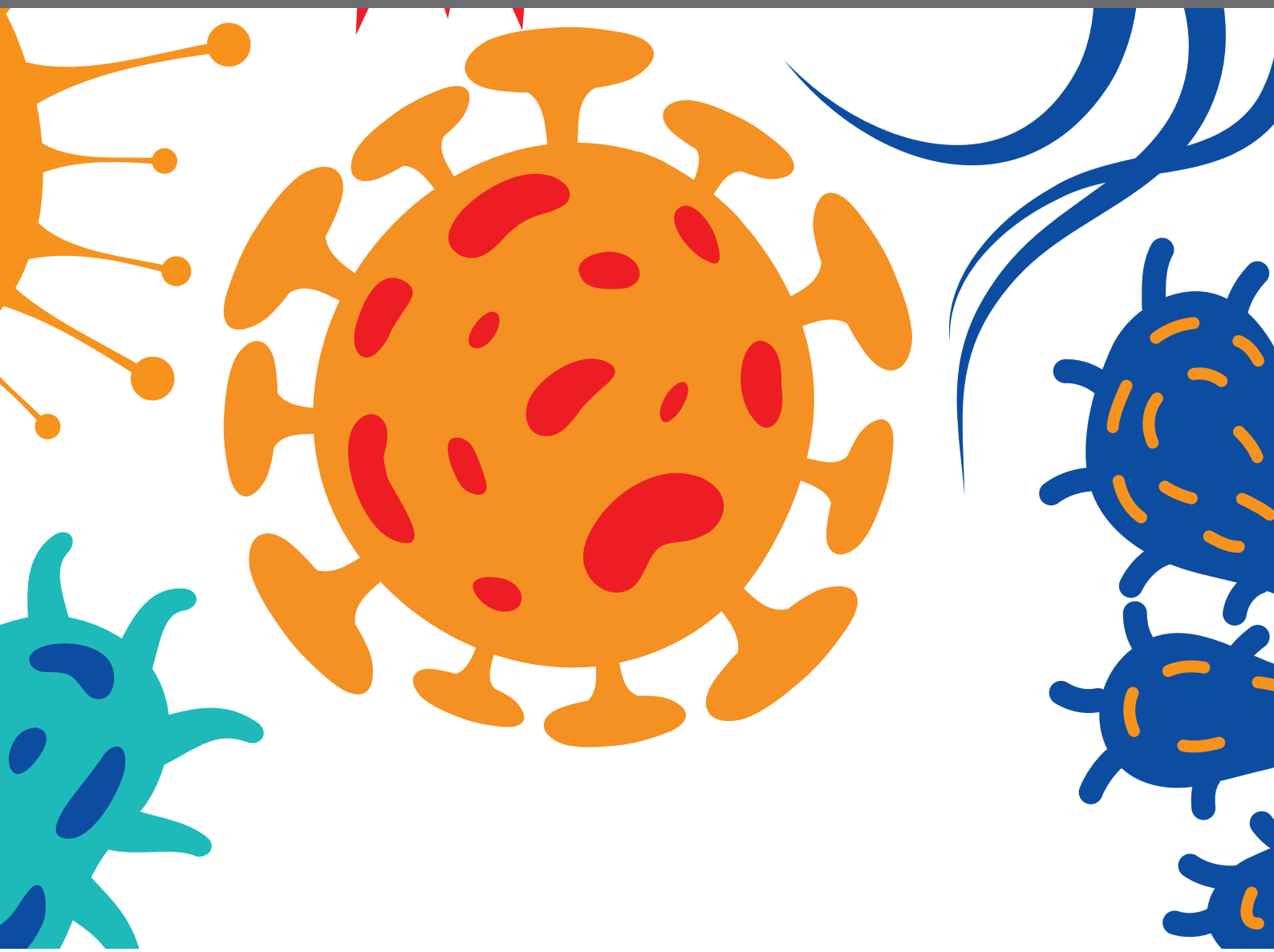

frontiers Research Topics

# frontiers



ISSN 1664-8714
ISBN 978-2-88963-516-0
DOI 10.3389/978-2-88963-516-0

## About Frontiers

Frontiers is more than just an open-access publisher of scholarly articles: it is a pioneering approach to the world of academia, radically improving the way scholarly research is managed. The grand vision of Frontiers is a world where all people have an equal opportunity to seek, share and generate knowledge. Frontiers provides immediate and permanent online open access to all its publications, but this alone is not enough to realize our grand goals.

## Frontiers Journal Series

The Frontiers Journal Series is a multi-tier and interdisciplinary set of open-access, online journals, promising a paradigm shift from the current review, selection and dissemination processes in academic publishing. All Frontiers journals are driven by researchers for researchers; therefore, they constitute a service to the scholarly community. At the same time, the Frontiers Journal Series operates on a revolutionary invention, the tiered publishing system, initially addressing specific communities of scholars, and gradually climbing up to broader public understanding, thus serving the interests of the lay society, too.

## Dedication to Quality

Each Frontiers article is a landmark of the highest quality, thanks to genuinely collaborative interactions between authors and review editors, who include some of the world's best academicians. Research must be certified by peers before entering a stream of knowledge that may eventually reach the public - and shape society; therefore, Frontiers only applies the most rigorous and unbiased reviews.
Frontiers revolutionizes research publishing by freely delivering the most outstanding research, evaluated with no bias from both the academic and social point of view. By applying the most advanced information technologies, Frontiers is catapulting scholarly publishing into a new generation.

## What are Frontiers Research Topics?

Frontiers Research Topics are very popular trademarks of the Frontiers Journals Series: they are collections of at least ten articles, all centered on a particular subject. With their unique mix of varied contributions from Original Research to Review Articles, Frontiers Research Topics unify the most influential researchers, the latest key findings and historical advances in a hot research area! Find out more on how to host your own Frontiers Research Topic or contribute to one as an author by contacting the Frontiers Editorial Office: researchtopics@frontiersin.org

# PROTEIN EXPORT AND SECRETION AMONG BACTERIAL PATHOGENS

Topic Editors:
**Sophie Bleves,** Aix-Marseille Université, France
**Romé Voulhoux,** UMR7255 Laboratoire d'ingénierie des systèmes macromoléculaires (LISM), France
**Bérengère Ize,** Centre National de la Recherche Scientifique (CNRS), France
**Thibault Géry Sana,** Federal Institute of Technology in Lausanne, Switzerland
**Denise Monack,** Stanford University, United States

**Citation:** Bleves, S., Voulhoux, R., Ize, B., Sana, T. G., Monack, D., eds. (2020). Protein Export and Secretion Among Bacterial Pathogens. Lausanne: Frontiers Media SA. doi: 10.3389/978-2-88963-516-0

# Table of Contents

frontiers in Cellular and Infection Microbiology

EDITORIAL
published: 22 January 2020
doi: 10.3389/fcimb.2019.00473

# Editorial: Protein Export and Secretion Among Bacterial Pathogens

*Thibault G. Sana[1*†], Romé Voulhoux[2†], Denise M. Monack[1], Bérengère Ize[2] and Sophie Bleves[2*]*

[1] Department of Microbiology and Immunology, Stanford School of Medicine, Stanford University, Stanford, CA, United States, [2] Laboratoire d'Ingénierie des Systèmes Macromoléculaires, Institut de Microbiologie de la Méditerranée, CNRS, Aix-Marseille University, Marseille, France

**Keywords: T2SS, T3SS, T6SS, T8SS, secretion systems, outer membrane proteins**

OPEN ACCESS

***Edited and reviewed by:***
*Thomas Rudel, Julius Maximilian University of Würzburg, Germany*

***Correspondence:**
*Thibault G. Sana*
*thibault.sana@epfl.ch*
*Sophie Bleves*
*bleves@imm.cnrs.fr*

***†Present address:***
*Thibault G. Sana, Laboratory of Molecular Microbiology, School of Life Sciences, Global Health Institute, Ecole Polytechnique Fédérale de Lausanne, Lausanne, Switzerland*
*Romé Voulhoux, Laboratoire de Chimie Bactérienne, Institut de Microbiologie de la Méditerranée, CNRS, Aix-Marseille University, Marseille, France*

***Specialty section:***
*This article was submitted to Bacteria and Host, a section of the journal Frontiers in Cellular and Infection Microbiology*

***Received:*** *22 October 2019*
***Accepted:*** *24 December 2019*
***Published:*** *22 January 2020*

***Citation:***
*Sana TG, Voulhoux R, Monack DM, Ize B and Bleves S (2020) Editorial: Protein Export and Secretion Among Bacterial Pathogens. Front. Cell. Infect. Microbiol. 9:473. doi: 10.3389/fcimb.2019.00473*

## Editorial on the Research Topic

## Protein Export and Secretion Among Bacterial Pathogens

Micro-organisms have colonized virtually every possible niche on Earth, including the bottom of the oceans and the upper atmosphere. Indeed, bacteria successfully evolved a myriad of complex systems to acclimate to, or to control, such different environments. In addition, bacterial pathogens face various environments within a host, including the microbiome and the immune system. In order to adapt to these harsh environments, pathogens often time utilize secretion systems. Secretion systems are machineries used to secrete proteins in the extracellular medium, or directly into the targeted cell.

Several secretion systems have been described in the scientific literature. Gram-negative bacteria have evolved eight secretion systems: T1SS (Type I Secretion System) to T6SS and the T9SS restricted so far to the phylum *Bacteroidetes*. The transport across the envelope can be a two-step process, in which exoproteins are first exported into the periplasm through the Sec or Tat export machineries, then attached on the surface or released into the extracellular medium which corresponds to the secretion step (T2-, T5-, and T9SS). The T1-, T3-, T4-, and T6SSs facilitate a one-step secretion process across the cell envelope leading to delivery of the effector in the medium (T1SS) or into host cells (T3-, T4-, and T6SS). All these secretion machinery components are made of proteins. However, an additional mechanism of secretion has been described and involves membrane shuffling which leads to the release of outer membrane vesicles (OMVs) loaded with proteins. Pathogens also use outer membrane proteins (OMPs), that are translocated through the inner membrane and then inserted in the outer membrane, for full virulence. In this special issue focused on the role of bacterial secretion systems during infections of mammalian hosts, several original research papers and reviews explore different facets of secretion systems amongst bacterial pathogens, as well as the different tools available in the scientific community to study them.

Several excellent reviews highlight and discuss important advances in the field.

A first review discuss about *Burkholderia pseudomallei*, the causative agent of melioidosis, a disease that can result in rapid, fatal infections in humans and animals. The mortality rate of melioidosis can reach 40% despite appropriate antibiotic therapies. Furthermore, diagnosis of *B. pseudomallei* infection is difficult because it can lead to a vast array of non-specific clinical manifestations, it is therefore predicted to be vastly under-reported. The genome of *B. pseudomallei* encodes three independent T3SS, named T3SS-1 to -3. While T3SS-1 and -2 have enigmatic roles, T3SS-3 is well-characterized and is required for escape from the endosome. In their review, Vander Broek and Steven discuss the current knowledge of *B. pseudomallei* T3SSs in the context of other well-characterized T3SSs.

Another bacterium highlighted in this issue, *Neisseria meningitidis*, can asymptotically reside in the nasopharynx of ∼10% of the human population, but can cause meningococcal meningitis with high mortality rate. It secretes numerous proteins through a T1SS and various T5SSs, and also presents lipoproteins to its surface. These secretion systems and surface-exposed proteins are known to play a crucial role in *N. meningitidis* pathogenic interactions with the host. In their review, Tommassen and Arenas discuss the role of these secretion systems with a particular focus on the functions of secreted proteins.

Furthermore, two reviews describe the current knowledge on two different secretion systems. First, the T5SS comprise diverse branches, such as autotransporter and two-partner secretion (TPS). TPS system utilizes a partner transporter named TpsB for the secretion of an effector protein named TpsA. Historically, TPS systems have been shown to secrete large effector proteins involved in interactions between the bacterial pathogen and their host. Recently though, two novel roles in inter-bacterial competition and cooperation have been uncovered for these TPS. In their review, Guérin et al. discuss the latest discoveries regarding the translocation through TPS, and their roles. Then, the T9SS is a recently discovered secretion system present only in the phylum *Bacteroidetes*. It is composed of at least 18 proteins, but this secretion mechanism is still largely enigmatic. Interestingly, T9SS has two very distinct roles in environmental and pathogenic bacteria. While in environmental bacteria, it is involved in gliding motility, it is used as a weapon by pathogens. In their review, Lasica et al. present an up-to-date review on this intriguing secretion system.

Finally, three outstanding reviews describe and discuss the tools available to the scientific community to study secretion systems, and their cognate effectors. In the review by Gunasinghe et al., they explore how advances in fluorescent microscopy allowed direct imaging of the process of secretion. Indeed, using super-resolution microscopy, researchers can now image the dynamics, distribution, and translocation of secretion systems and effectors. Then, Lien and Lai review the methodologies that have been used to specifically identify T6SS effectors, as well as the function of their known effectors. They further propose strategies to identify potential new T6SS effectors. Finally, Maffei et al. provide an overview of the tools that have been developed to track protein secretion. Briefly, they review the biochemical, genetic, and imaging tools available to study secreted proteins and illustrate their respective advantages and limitations.

Following these reviews, several original papers are included in this issue that highlight new discoveries in the area of bacterial secretion systems. For example, they uncover novel functions of several effectors, and develop new tools to better study secretion systems in general. A first paper discuss about Enterotoxigenic *Bacteroides fragilis*, a human pathogen associated with childhood diarrhea and colon cancer. Its genome encodes the *B. fragilis* toxin (BFT), whose secretion leads to cleavage of cadherin, loss of cell adherence, and inflammation. However, this secretion mechanism was a mystery. In this issue, Zakharzhevskaya et al. showed that it is associated with Outer Membrane Vesicles (OMVs). A better understanding of BFT secretion will certainly provide new perspectives for prevention of *B. fragilis* infections in the future.

As discussed above, *Neisseria meningitidis* can cause meningococcal meningitis. It produces eight autotransporters, also called T5SSb, seven of which have been extensively studied. In their study, Arenas et al. revealed the role of the eighth autotransporter, AutB, of this bacterium. AutB, which is widely distributed among pathogenic *Neisseria* spp, is secreted and exposed to the cell surface, where it promotes biofilm formation and delays transcytosis *in vitro*. They further hypothesize that AutB could facilitate microcolony formation.

In another study, Hooda et al. describe a new analytical tool to identify surface lipoproteins (SLPs), which can be present or displayed in the outer membrane of Gram-negative bacteria. In *Neisseria*, the display of SLPs require surface lipoprotein assembly modulators (Slam). Using *in silico* analyses, Hooda et al. identified 832 Slam related sequences in 638 Gram-negative species, including several human pathogens. They further validated the surface display of one predicted Slam-adjacent protein in *Pasteurella multocida*, a zoonotic pathogen. Together, this suggests that SLPs and their interaction partner Slam are found widely in Proteobacteria.

Then, another paper discusses about *Acinetobacter baumanii*, a nosocomial human pathogen of high concern, because it rapidly acquires antibiotic resistance. In their study, Waack et al. provide evidence for a role of the T2SS of *A. baumanii* in protecting the bacteria from human complement. They further develop and optimize a simple high-throughput screen to identify small molecule inhibitors of the T2SS. This high-throughput screening was performed with 6,400 molecules, and could be performed on larger libraries to develop new *A. baumanii* therapeutics.

Finally, Meuskens et al. discuss about Outer Membrane Proteins (OMPs), which are important for adherence, protein secretion, biofilm formation, and virulence. However, high production of such proteins in a heterologous host for further

characterization is usually challenging. In their study, the authors present a set of deletion mutants in *Escherichia coli* BL21 to specifically overproduce recombinant OMPs. The use of this engineered strain will facilitate future purification of OMPs. In addition, it will be useful for labeling experiments and biophysical measurements in the membrane environment.

Collectively, the reviews and original studies in this special issue explore a vast area of research, and describe new insights, new tools, and discusses several important aspects of protein secretion among bacterial pathogens.

## AUTHOR CONTRIBUTIONS

TS and SB wrote the manuscript with contribution from RV, DM, and BI.

## FUNDING

Work in SB laboratory was funded by the Excellence Initiative of Aix-Marseille University-A*Midex, a French Investissements d'Avenir program (Emergence and Innovation A-M-AAP-EI-17-139-170301-10.31-BLEVES-HLS).

**Conflict of Interest:** The authors declare that the research was conducted in the absence of any commercial or financial relationships that could be construed as a potential conflict of interest.

frontiers in Cellular and Infection Microbiology

ORIGINAL RESEARCH
published: 22 November 2016
doi: 10.3389/fcimb.2016.00162

# Expression of the Gene for Autotransporter AutB of *Neisseria meningitidis* Affects Biofilm Formation and Epithelial Transmigration

*Jesús Arenas[1]*, Fernanda L. Paganelli[2], Patricia Rodríguez-Castaño[1], Sara Cano-Crespo[1], Arie van der Ende[3], Jos P. M. van Putten[4] and Jan Tommassen[1]*

[1] Department of Molecular Microbiology and Institute of Biomembranes, Utrecht University, Utrecht, Netherlands, [2] Department of Medical Microbiology, University Medical Center Utrecht, Utrecht, Netherlands, [3] Department of Medical Microbiology, Academic Medical Center, Amsterdam, Netherlands, [4] Department of Infectious Diseases and Immunology, Faculty of Veterinary Medicine, Utrecht University, Utrecht, Netherlands

*Neisseria meningitidis* is a Gram-negative bacterium that resides as a commensal in the upper respiratory tract of humans, but occasionally, it invades the host and causes sepsis and/or meningitis. The bacterium can produce eight autotransporters, seven of which have been studied to some detail. The remaining one, AutB, has not been characterized yet. Here, we show that the *autB* gene is broadly distributed among pathogenic *Neisseria* spp. The gene is intact in most meningococcal strains. However, its expression is prone to phase variation due to slipped-strand mispairing at AAGC repeats located within the DNA encoding the signal sequence and is switched off in the vast majority of these strains. Moreover, various genetic disruptions prevent *autB* expression in most of the strains in which the gene is in phase indicating a strong selection against AutB synthesis. We observed that *autB* is expressed in two of the strains examined and that AutB is secreted and exposed at the cell surface. Functionality assays revealed that AutB synthesis promotes biofilm formation and delays the passage of epithelial cell layers in *vitro*. We hypothesize that this autotransporter is produced during the colonization process only in specific niches to facilitate microcolony formation, but its synthesis is switched off probably to evade the immune system and facilitate human tissue invasion.

**Keywords: autotransporters, protein secretion, biofilms, infection, *Neisseria meningitidis*, *Haemophilus influenzae*, pathogenesis**

OPEN ACCESS

***Edited by:***
*Romé Voulhoux, Aix-Marseille Université, France*

***Reviewed by:***
*Charlene Kahler, University of Western Australia, Australia*
*Laurent Aussel, Aix-Marseille Université, France*

****Correspondence:***
*Jesús Arenas*
*j.a.arenasbusto@uu.nl;*
*jesusarenasbust@yahoo.es*

***Received:*** *29 July 2016*
***Accepted:*** *07 November 2016*
***Published:*** *22 November 2016*

***Citation:***
*Arenas J, Paganelli FL, Rodríguez-Castaño P, Cano-Crespo S, van der Ende A, van Putten JPM and Tommassen J (2016) Expression of the Gene for Autotransporter AutB of Neisseria meningitidis Affects Biofilm Formation and Epithelial Transmigration. Front. Cell. Infect. Microbiol. 6:162. doi: 10.3389/fcimb.2016.00162*

## INTRODUCTION

The Gram-negative diplococcus *Neisseria meningitidis* is a common inhabitant of the human nasopharynx, but it is also the causative agent of meningococcal disease, a life-threatening infection characterized by fast development of septicemia and/or meningitis. The colonization and its persistence in the host involve the formation of microcolonies in the nasopharynx (Sim et al., 2000). Microcolonies are biofilm-like structures, which are defined as multicellular microbial communities often encased within a self-produced extracellular matrix (Costerton et al., 1995) and presumably help the bacteria to survive adverse circumstances, such as host defense mechanisms.

Amongst others, several autotransporters (ATs) have been demonstrated to play a role in biofilm formation in *N. meningitidis* (Arenas and Tommassen, 2016).

ATs are a class of proteins secreted by Gram-negative bacteria (Grijpstra et al., 2013). They contain an N-terminal signal sequence for transport across the inner membrane via the Sec machinery and a C-terminal translocator domain that inserts as a β-barrel in the outer membrane via the Bam complex and that assists in the translocation of an associated passenger domain across the outer membrane. Based on the structure of the translocator domain, two main types of ATs can be discriminated, the classical monomeric ATs and the trimeric ATs. In classical monomeric ATs, the C-terminal translocator domain forms a 12-stranded β-barrel, whilst in trimeric ATs, the translocator domain of each subunit contributes four β-strands to form a similar 12-stranded β-barrel as in the monomeric ATs. The passenger of classical ATs usually forms an extended β-helix on which smaller globular domains are displayed. The C-terminal part of these passengers often harbors a linker domain that, in some cases, has been demonstrated to contain autochaperone activity, i.e., it helps in the folding of the passenger after its secretion to the cell surface (Oliver et al., 2003; Peterson et al., 2010). After secretion, the passenger can remain attached to the cell surface or it can be released into the external medium by one of a variety of possible proteolytic mechanisms. Their functions can be very diverse, but they are often involved in virulence (Grijpstra et al., 2013).

Based on the analysis of genome sequences, it appears that *N. meningitidis* can produce up to eight different ATs, i.e., IgA1 protease, App, AusI, NalP, NhhA, NadA, AutA, and AutB (van Ulsen and Tommassen, 2006). Seven of them have been characterized to at least some extent. The passenger of IgA1 protease consists of two domains, the protease domain, which cleaves, amongst others, human immunoglobulin A1, the IgA subclass that predominates in the nasopharynx, and an α-peptide that can be released from the cell surface together with the protease domain, or it can remain attached to the cell surface where it is implicated in biofilm formation by binding extracellular DNA (eDNA) (Arenas et al., 2013a). Like IgA1 protease, App and AusI (a.k.a. MspA) are monomeric ATs with a protease domain, and both have been implicated in adhesion to epithelial cells (Serruto et al., 2003; Turner et al., 2006). Also NalP has protease activity; amongst others, it releases proteins from the bacterial cell surface, including the α-peptide of IgA1 protease and the neisserial heparin-binding antigen NHBA, a surface-exposed lipoprotein, which, like the α-peptide, is involved in biofilm formation by binding eDNA (van Ulsen et al., 2003; Serruto et al., 2010; Arenas et al., 2013a). Thus, NalP regulates biofilm formation. NhhA and NadA are cell-associated trimeric ATs with a role in adhesion to eukaryotic cells (Capecchi et al., 2005; Scarselli et al., 2006), whilst AutA is a monomeric AT involved in bacterial autoaggregation, a function that affects biofilm structure (Arenas et al., 2015). The remaining AT, AutB, has not been characterized yet. It is evolutionary related to a poorly characterized AT designated Lav, present in some strains of *Haemophilus influenzae*, another inhabitant of the nasopharynx, from which it was suggested to be acquired by horizontal gene transfer. Expression of its gene and its function remain enigmatic.

The expression of the genes for most ATs in *N. meningitidis* is prone to phase variation by slipped-strand mispairing at short nucleotide repeats (Turner et al., 2002; van Ulsen et al., 2006; Arenas et al., 2015). Besides, expression of several AT genes, e.g., *ausI* and *autA*, can be prevented in certain lineages by genetic disruptions, such as deletions or frame-shift mutations, possibly evolved by selection pressure imposed by the immune system (van Ulsen et al., 2006; Arenas et al., 2015). The expression of *autB* also seems to be prone to phase variation. The gene contains a variable number of AAGC nucleotide repeats immediately downstream of the start codon (Peak et al., 1999). These repeats are also present in the *autA* gene, where they were shown to be implicated in phase variation (Arenas et al., 2015). However, expression of *autB* has not been demonstrated so far. In fact, early studies suggested that *autB* is a pseudogene (Ait-Tahar et al., 2000). This conclusion was based on the lack of reactivity of two anti-AutB antisera against nine meningococcal and one gonococcal strains. However, the number of AAGC repeats and the presence of genetic disruptions in the *autB* genes of those strains were not evaluated. Therefore, the conclusion that *autB* is a pseudogene may be premature. The objective of the present work was to determine whether AutB can be produced in *N. meningitidis* and to elucidate its possible function.

# MATERIALS AND METHODS

## Bioinformatics Analysis

Amino-acid sequences encoded by the *autB* genes were predicted after alteration of the number of AAGC repeat units to create the correct reading frame and, in some cases, by removal of frameshift mutations and premature stop codons. The cleavage site of the N-terminal signal sequence was predicted using publicly available web tools (http://www.cbs.dtu.dk/services/SignalP/). The mature protein was then used for phylogenetic analysis using the neighbor-joining with bootstrap analysis (100 replications) considering distances based on p-distance with the available MEGA software version 6.0 (http://www.megasoftware.net/) (Tamura et al., 2013). For secondary and tertiary structure predictions, the public web-based programs PsiPred (Buchan et al., 2013) and PHYRE2 (http://www.sbg.bio.ic.ac.uk/phyre2/html/page.cgi?id=index), respectively, were used. Alignment of protein sequences was performed in MAFFT version 7 (http://mafft.cbrc.jp/alignment/server/). AutB variants were defined based on phylogeny of the N-terminal part of the passenger. Each variant was considered when the bootstrap value of the precedent node was 100, the distance within the group was lower than the overall distance for AutB, and the distance from other groups higher than the overall distance for AutB.

## Bacterial Strains and Growth Conditions

Meningococcal strains used in this study include reference strains MC58 (Tettelin et al., 2000), FAM18 (Bentley et al., 2007), α14

(Schoen et al., 2008), and α153 (Schoen et al., 2008). HB-1 (Bos and Tommassen, 2005) and BB-1 (Arenas et al., 2013a) are unencapsulated derivatives of H44/76 and B16B6, respectively. A panel of 102 meningococcal strains isolated from patients suffering from meningococcal disease in the Netherlands was already described (Arenas et al., 2015). All meningococcal strains were grown at 37°C on GC medium base (Difco) supplemented with IsovitaleX (Becton Dickinson) at 37°C in a candle jar overnight. To grow the bacteria in liquid cultures, bacteria were collected from GC plates and diluted in tryptic soy broth (TSB) (Beckton Dickinson) to an $OD_{550}$ of 0.1 and incubated in 25-$cm^2$ polystyrene cell culture flasks or 125-ml square media bottles with constant shaking at 110 rpm. *Escherichia coli* strains used in this study were DH5α and BL21(DE3) (Invitrogen), which were grown in Lysogeny broth (LB) or LB agar at 37°C.

For all strains, media were supplemented with the antibiotics kanamycin (100 μg $ml^{-1}$), chloramphenicol (25 μg $ml^{-1}$) or ampicillin (100 μg $ml^{-1}$) when required and with 0.1 mM of isopropyl-β-D-1-thiogalactopyranoside (IPTG) to induce gene expression.

## PCR Analysis and Sequencing of the *autB* Gene

Segments of *autB* were amplified by PCR from bacteria grown on plates with primers listed in Table S1 using High Fidelity Polymerase (Roche Diagnostics GmbH, Germany) or DreamTaq-DNA Polymerase (Fermentas, UK). PCR products were visualized in agarose gels stained with ethidium bromide. When required, they were purified with the PCR Clean-Up System (Promega Corporation) and sequenced at the Macrogen sequencing service (Amsterdam). Large sequences were assembled using the SeqMan II software (DNAstart) using at least two independent PCR reactions.

## Cloning and Transformation

For cloning, PCR fragments were obtained from DNA of strain HB-1 using primers described in Table S1. PCR fragments were purified and digested with restriction enzymes (Fermentas, UK) for which sites were included in the primers, to be subsequently cloned in appropriate vectors. To generate an *autB* knockout construct, PCR fragments from immediately upstream and downstream of the *autB* gene were cloned into pKO*nhbA-kan* (Arenas et al., 2013a). In the resulting plasmid, called pKO*autB-kan*, these segments flank a kanamycin-resistance cassette.

To generate a plasmid for the production of a part of the passenger domain of AutB of strain HB-1 in *E. coli*, the corresponding PCR product was cloned into pET16b (Invitrogen) resulting in plasmid pET16b-AutBp. To generate plasmids for expression of AutB variants in *N. meningitidis*, the entire *autB* genes from isolates 2081107 and α153 were amplified and cloned into plasmid $pFPIORF_1$ (Arenas et al., 2013b), resulting in $pENAutB_1$ and $pENAutB_2$, respectively. *N. meningitidis* and *E. coli* were transformed with intact or linearized plasmids following standard protocols (Arenas et al., 2015) and transformants were selected on solid medium supplemented with appropriate antibiotics. The proper generation of knockout mutants or the presence of the plasmid was verified by PCR. In addition, protein synthesis was confirmed by Western blotting or gene expression was confirmed by RT-PCR as described below.

## Purification of Recombinant AutB and Antiserum Production

A fragment of the AutB passenger domain of strain HB-1 was purified as described (Arenas et al., 2015). Briefly, the recombinant polypeptide, corresponding to amino-acid residues 151–278 of the mature AutB protein, with an N-terminal His-tag was produced in *E. coli* BL21(DE3) carrying pET16b-AutBp after induction with IPTG and purified as inclusion bodies. The protein band corresponding to the recombinant protein was excised from SDS-polyacrylamide gel electrophoresis (SDS-PAGE) gels and used for the production of rabbit antiserum at Eurogentec (Liège, Belgium). The concentration of the purified protein was determined with the BCA assay kit (Thermo Fisher Scientific, Rockford, IL, USA) and its purity was estimated in SDS-PAGE gels.

## RNA Purification and RT-PCR Assays

To obtain RNA, cells from exponentially growing cultures were collected by centrifugation for 10 min at 5000 rpm in an Eppendorf Centrifuge 5424, adjusted to an $OD_{550}$ of 4, and resuspended in trizol (Invitrogen, U.K.). Then, 200 μl of chloroform were added per ml of trizol, followed by centrifugation at 5000 rpm for 30 min. The resulting upper layer was mixed with an equal amount of ice-cold 75% ethanol. Next, RNA was isolated using the Nucleospin RNA II kit (Macherey-Nagel, U.S.A.) according to the manufacturer's instructions. The resulting solution was treated with Turbo DNA free (Ambion, Germany) for 1 h at 37°C to remove genomic DNA followed by inactivation of the DNase according to the recommendations of the manufacturer. The resulting pure RNA was used immediately to generate cDNA using the Transcriptor High Fidelity cDNA Synthesis Kit (Roche, The Netherlands). RNA, cDNA, and chromosomal DNA were used as templates in PCRs to determine the generation of specific transcripts with primers listed in Table S1. PCRs started with an incubation for 5 min at 95°C, followed by 30 cycles of 30 s at 95°C, 30 s at 65°C and 10 s at 72°C. Reactions ended with 10 min of incubation at 72°C.

## SDS-PAGE and Western Blotting

Whole cell lysates, supernatants and cell envelopes were prepared and adjusted as previously described (Arenas et al., 2015). Protein concentrations were determined with the BCA assay kit. Before SDS-PAGE, samples were diluted 1:1 in double-strength sample buffer and heated for 10 min at 100°C. Proteins separated on gels were stained with Coomassie brilliant blue G250 or transferred to nitrocellulose membranes. These membranes were next blocked with phosphate-buffered saline (PBS) containing 0.1% (v/v) Tween 20 and 0.5% (w/v) non-fat dried milk (PBS-T-M), and then incubated with primary antibodies and subsequently with horseradish peroxidase-conjugated goat anti-rabbit IgG or anti-mouse IgG antibodies (Biosource International), as previously described (Arenas et al., 2006). All incubations were performed

for 1 h and followed by three washes for 15 min with PBS-T-M. Blots were developed with the Pierce ECL Western Blotting Substrate. The monoclonal antibody MN2D6D directed against RmpM and the antiserum directed against fHbp were generously provided by the Netherlands Vaccine Institute (Bilthoven, The Netherlands) and by GlaxoSmithKline (Rixensart, Belgium), respectively. The antisera directed against the α-peptide and the translocator domain of IgA protease were from our laboratory collection (Roussel-Jazédé et al., 2014).

## Proteinase K Accessibility Assays

Proteinase K accessibility assays were performed as described (Arenas et al., 2015) with few modifications. Briefly, bacteria recovered from a culture grown for 4 h in TSB were adjusted to an optical density at 550 nm ($OD_{550}$) of 1 and incubated with 2 μg $ml^{-1}$ of proteinase K (Fermentas) for 1 h at 37°C, after which the protease was inactivated with 2 mM phenylmethylsulfonyl fluoride Sigma-Aldrich). Cells were harvested by centrifugation and protein degradation was examined by SDS-PAGE and Western blotting.

## Settling Experiments and Biofilm Formation

For biofilm formation and settling experiments, bacteria were initially grown in TSB with or without IPTG and adjusted to a similar $OD_{550}$. Settling experiments were performed as described (Arenas et al., 2015). Biofilm formation was analyzed under static conditions in polystyrene plates and in a flow-cell model as described before (Arenas et al., 2013a, 2015), with some modifications. Where indicated, 100 μg $ml^{-1}$ of DNase I was added to the cultures during biofilm formation. For the flow-cell model, pictures were taken at different time intervals during biofilm formation. After 16 h, biofilms were stained with LIVE/DEAD stain (Life Technologies Europe BV, the Netherlands) dissolved in Dulbecco's PBS (DPBS) (Lonza, USA) as suggested by the manufacturer. Structural parameters of the biofilms were analyzed using COMSTAT (Heydorn et al., 2000)/MATLAB R2010b software (The MathWorks) program, using eight image stacks randomly generated of each sample. For statistical analysis, data from at least three independent experiments performed in duplicate were used. Statistical comparisons of all biofilm parameters were calculated using an unpaired *t*-test with GRAPH PAD v 6.0 (Graph Pad Software, Inc).

## Infection Assays

The epithelial cell line NCI-H292 (ATCC CRL 1848) was cultured in RPMI 1640 medium supplemented with 5% fetal calf serum, which was heat inactivated before use (1 h at 56°C). All cell-culture medium components were purchased from Laboratories PAA. The cells were cultured at 37°C in a humidified atmosphere containing 5% $CO_2$ and maintained in 25-$cm^2$ tissue-culture flasks (Nunc) until ∼80% confluence was reached.

Bacterial adherence was determined as previously described (van Putten and Paul, 1995). In short, 2 days before the assays, NCI-H292 cells from 4 to 25 passages were seeded in 24-well plates. Bacteria grown overnight on plate were suspended in HEPES buffer (10 mM HEPES, 145 mM NaCl, 5 mM KCl, 5 mM glucose, 1 mM $CaCl_2$ and 1 mM $MgCl_2$, pH 7.2), washed by centrifugation (1500 *g*, 10 min) and incubated with cultured cells at a multiplicity of infection of 100 for 3 h. Non-adherent bacteria were removed by sequential washings with DPBS, and the viable adhering bacteria were counted by determining the colony-forming units (CFU) after disruption of the cell layer with 1% saponin diluted in DPBS for 15 min and subsequent mechanic homogenization.

Passage of cell layers was assayed as described previously (van Schilfgaarde et al., 1995) with modifications. In short, cells were grown on transparent tissue culture inserts with 1-μm pores (model no. 353104; Falcon) placed in 24-well plates (Falcon) containing 0.5 ml of medium. The culture medium was refreshed every 2 days. After 6 days, the transepithelial resistance of the cellular layers was measured with the Millicell-ERS Resistance system (Millipore, Bedford, Mass.), and the insert was moved to a new well containing 300 μl of RPMI in the basal compartment with 100 μg/ml of DNase I for avoid biofilm formation. Before starting the infection, the culture medium above the insert was replaced, and the cellular layers were then infected with $\sim 10^7$ CFU for in total 12 h. After 3 h, the medium in the upper compartment was replaced to avoid medium acidification, and the number of CFU in the basal compartment was determined at regular time intervals.

## Nucleic Acid Accession Numbers

The nucleotide sequences of the *autB* genes of disease isolates 2081107, 2061551, and 2070077 were deposited in GenBank ID (KT367782, KT367783, and KT367784, respectively).

# RESULTS

## Characterization and Distribution of the *autB* Gene

BLASTn searches identified the *autB* gene in available genome sequences of the pathogenic Neisseria spp. *N. meningitidis* and *N. gonorrhoeae* but not in those of non-pathogenic species, such as *N. lactamica* (**Table 1** and Table S2). The gene was also identified in some strains of Haemophilus spp. (**Table 1** and Table S2). **Figure 1** illustrates the position of the *autB* gene in representative genomes. The *autB* gene is ubiquitous in both pathogenic Neisseria spp. with the exception of one meningococcal strain, i.e., strain 053442. In this strain, as well as in *N. lactamica*, the flanking genes are preserved, but the *autB* gene is substituted by a 1415-bp sequence. Interestingly, the sequences flanking the *autB* gene in *H. influenzae* strains, including the 5′ end of the *holB* gene and the 3′ end of the *tmk* gene are also present as intergenic regions flanking *autB* in *N. meningitidis* and *N. gonorrhoeae* (**Figure 1**). This indicates that *autB* and the flanking regions may have been transferred en bloc from Haemophilus to Neisseria as suggested previously (Davis et al., 2001). However, many Haemophilus strains do neither contain the *autB* gene (**Table 1**), nor the alternative region found in *N. lactamica* (**Figure 1** and data not shown). Interestingly, a sequence containing the 3′ ends of the *autB* and *tmk* genes is

**TABLE 1 | Distribution of *autB* within available genome sequences of *Neisseria* and *Haemophilus* species.**

| Species | Strains analyzed | Presence *autB* | Intact[a] | In frame[b] |
|---|---|---|---|---|
| *N. meningitidis* | 118 | 117 | 104 | 2 |
| *N. gonorrhoeae* | 16 | 16 | 0 | 0 |
| *N. lactamica* | 4 | 0 | | |
| *N. flavescens* | 2 | 0 | | |
| *N. polysaccharea* | 2 | 0 | | |
| *N. sicca* | 4 | 0 | | |
| *H. influenzae* | 15 | 7 | 7 | 2 |
| *H. haemolyticus* | 9 | 2 | 2 | 2 |
| *H. parainfluenzae* | 2 | 1 | 1 | ? |
| *H. aegyptius* | 3 | 3 | 3 | 0 |

[a]*Strains having an intact autB gene that is either in or out of frame at the AAGC repeats.*
[b]*Strains having an intact autB gene that is in frame because of an appropriate number of AAGC repeats. In the case of the H. parainfluenzae strain, it cannot be determined whether the gene is in frame because the sequence upstream of the AAGC repeats is not available.*

tandem repeated in *H. haemolyticus* (**Figure 1**), indicating that this region is prone to genetic recombination.

The genetic characteristics of the *autB* gene in a panel of Neisseria and Haemophilus strains are listed in Table S2. **Table 1** summarizes the numbers of strains in which the gene can be expressed. The number of AAGC nucleotide repeats is considerably lower in Neisseria spp. (3–19) than in Haemophilus spp. (17–30 repeats). In the meningococcal *autA* gene, the same repeat is present, but the range of copies is considerably larger (6–40) (Arenas et al., 2015) than in meningococcal *autB*. In 12 of the 117 meningococcal strains examined (10.3%), the *autB* gene is in frame at these repeats, but in 10 of them the gene is disrupted further downstream of the repeats by frame-shift mutations, premature stop codons or insertion of a transposase element (Table S2). Thus, only two strains (1.7%), i.e., α153 and LNP27256, putatively express *autB* (**Table 1**). In stark contrast, in the 105 meningococcal strains, in which the *autB* gene is out of phase at the AAGC repeats, the gene is further intact with only three exceptions (Table S2). Hence, all these strains can potentially express the gene after phase variation occurs, but, apparently, this is prevented by a very strong selection pressure. Due to downstream disruptions, none of the gonococcal strains can express *autB*, independent of number or repeats. Such disruptions are not present in the *autB* genes of the Haemophilus strains examined, and the gene is in frame in 28% of them (Table S2), but all strains can potentially express *autB* after slipped-strand mispairing. To summarize, *autB* can be expressed, but expression seems to be prone to phase variation at the AAGC repeats and to different genetic disruptions. In addition, these data indicate a strong selection against *autB* expression in Neisseria, but not in Haemophilus spp.

## Structure and Variability of AutB

The *autB* gene from *N. meningitidis* reference strain MC58 is not expressed because the number of AAGC repeats renders the gene out of frame (Table S2). Deletion of two repeats results in an N-terminally extended ORF coding for a hypothetical protein of 674 amino-acid residues (aa). The signal peptide cleavage site in this protein was predicted between aa residues $A_{30}$ and $V_{31}$ resulting in a mature protein of 644 aa, which is similar to that of AutA (660 aa), and with a calculated molecular mass of 73.2 kDa. The passenger of AutB is constituted of two parts, a C-terminal linker domain (aa 231–338), which shows homology to the autochaperone domain of other ATs and could accordingly be modeled as a right-handed β-helix (data not shown), and an N-terminal domain. Secondary structure predictions indicate that this N-terminal part of the passenger contains two conserved α-helices (with approximate positions between aa 1–20 and 90–110 of the mature aa sequences) separated by a largely unstructured region of ∼80 aa and followed by a segment that is rich in β-sheet but occasionally also contains some α-helix prediction (Figure S1). Rather similar secondary structure was predicted for the corresponding fragment of AutA (Figure S1). The passengers of AutB proteins each contain one or two pairs of cysteines, which probably form a disulfide bond, but they are located at different positions in the sequence (Figure S2). The translocator domain of AutB (aa 360–644) is predicted to form a 12-stranded β-barrel that is connected via an α-helix (aa 337–354) to the passenger.

To determine sequence conservation, the predicted mature AutB proteins from several *Neisseria* and *Haemophilus* strains were aligned. The alignments (see Figure S2 for representatives) revealed that the sequence of the translocator domain was better conserved than that of the passenger. The translocator domain also showed considerable similarity to that of AutA of MC58 (not included in the alignments, but see below). However, the passenger domain showed high sequence diversity (see Figure S2 for examples). To investigate this variability in more detail, we performed independent phylogenetic analysis for the N-terminal part of the passenger, the linker and the translocator domain of representative AutB proteins and AutA of MC58 (**Figure 2**). Indeed, the translocator domain showed limited variability as compared with the other two domains (compare overall mean distances of the separate domains of the AutB proteins). Although similar to the translocator domain of the AutB proteins, the translocator domain of AutA clustered in a different branch, demonstrating that AutA is a different AT, which is consistent with its distinct genomic location. When the N-terminal domain of the passengers was analyzed, three major branches were identified, here designated AutB1, AutB2, and AutB3. The assignment of the AutB proteins in the different strains to these clusters is shown in Table S2. AutA again formed a separate branch. Interestingly, the phylogenic relationships of the AutB proteins do not parallel the boundaries of the species in which these proteins are found, suggesting that specific variants did not evolve in one specific organism, but that there is regular exchange of the genes between these species. AutB1 is the predominant variant in three species, i.e., *N. meningitidis*, *N. gonorrhoeae,* and *H. influenzae*. The AutB3 variant was found in three *Haemophilus* spp. and the AutB2 variant is present in all species except in *N. gonorrhoeae* and *H. parainfluenzae*. Variant AutB3 showed a larger diversity in the N-terminal domain of the passenger than the other variants and, interestingly, clustered with the passenger of AutA, suggesting the exchange of sequences

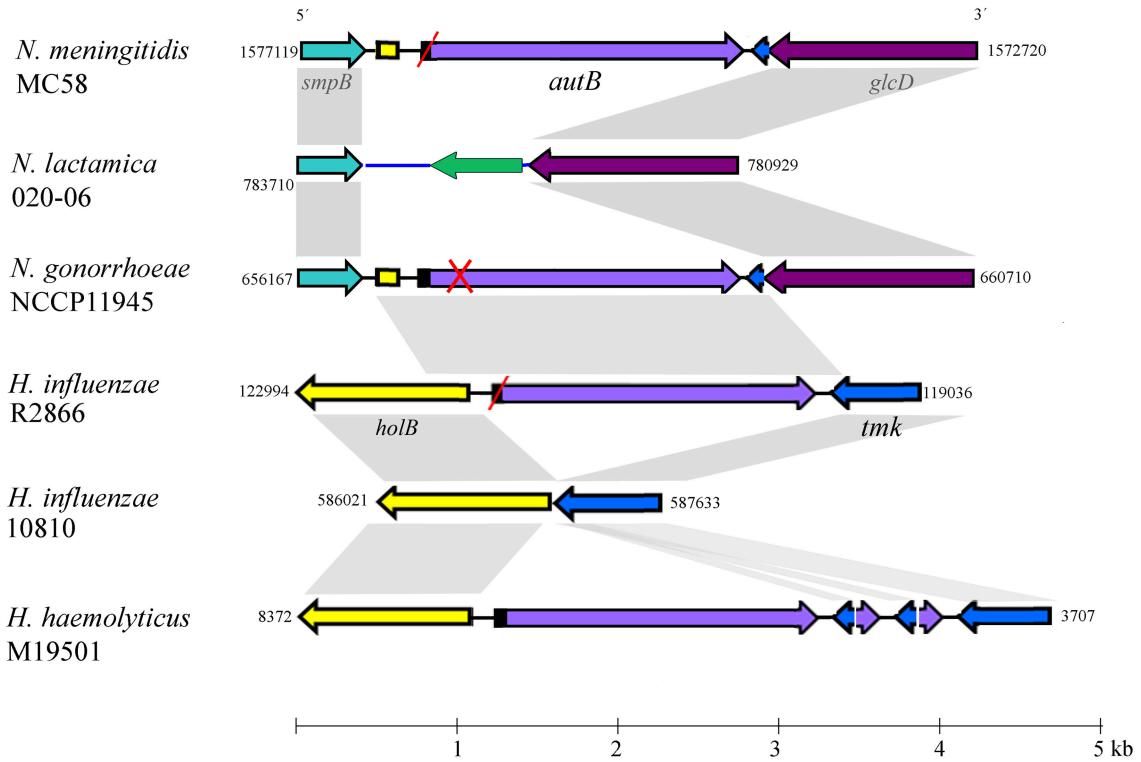


**FIGURE 1 | Genomic context of the *autB* gene.** The relevant part of the genome sequences of *N. meningitidis* strain MC58, *N. lactamica* strain 020-06, *N. gonorrhoeae* strain NCCP11945, *H. influenzae* strains R2866 and 10810, and *H. haemolyticus* strain M19501 are schematically depicted. Numbers at the side of each map indicate the first and last nucleotide position of the DNA fragment shown in accordance with genome annotations. The genes (arrows) and intergenic regions (lines) with high sequence similarity between different genome sequences are colored identically. Gray shadowing indicates regions with >85% of sequence identity. Red slashes indicate that the gene is out of phase at the AAGC repeats but can potentially be expressed after phase variation. A red cross indicates that the gene is disrupted and cannot be expressed even if it is in phase at the AAGC repeat region. The genes flanking *autB* are conserved in the *Neisseria* genomes. The upstream gene, *smpB*, encodes a protein of 148 amino-acid residues (aa), which is a component of the *trans*-translation system for releasing stalled ribosomes from damaged messenger RNAs. The downstream gene is a homolog of *glcD* of *E. coli*, which encodes the D subunit of glycolate oxidase. *N. lactamica* misses the *autB* gene and its flanking sequences; instead, it contains an alternative intergenic sequence (colored blue) and a gene encoding a hypothetical protein of 168 aa with a conserved DUF1877 domain (colored green). BLAST searches using this gene as query indicated that it is present in the genomes of other *Neisseria* spp. that lack *autB* as well as in many other bacteria. The *autB* gene is also present in some strains of *Haemophilus* spp. but in a different genomic context. In these species, the gene is located between the *holB* gene, which encodes the δ′ subunit of DNA polymerase III, and the *tmk* gene, which encodes thymidylate kinase. It is noteworthy that the intergenic region upstream of *autB* in the *Neisseria* genomes contains part of the 5′ end of the *holB* gene of *Haemophilus*; also downstream of *autB*, a part of the intergenic region and the 3′ end of the *tmk* gene is shared between *N. meningitidis* and *Haemophilus*, suggesting that a DNA segment containing *autB*, the flanking intergenic regions and parts of the *holB* and *tmk* genes from *Haemophilus* was inserted en bloc into a common ancestor of *N. meningitidis* and *N. gonorrhoeae*. Interestingly, a DNA fragment containing the 5′ ends of *autB* and *tmk* and their intergenic region is repeated several times downstream of *autB* in *H. haemolyticus* strain M19501.

between both AT, but limited to this domain. Cluster analysis of the linker domain also indicated the presence of the three main branches with AutA being a separate cluster. The groups were constituted of the same *autB* genes as for the N-terminal domain of the passenger; therefore, the same nomenclature is maintained. However, the relation between the groups varied notably. In this part of the protein, AutB1 was closely related to AutB3 and only distantly related to AutB2. This analysis confirmed that the passenger is rather variable as compared with the translocator domain, which is in agreement with its expected surface exposure and accessibility to the immune system. In addition, this analysis reflects shuffling of different domains within the passenger as suggested before (Davis et al., 2001).

To gain more insight in the evolution of *autB*, we calculated the GC content in the three regions in several *autB* genes. The GC content was similar in the regions encoding the N-terminal part of the passenger and the linker domain (35 ± 2%), but remarkably different for that encoding the translocator domain (44 ± 2%), which suggests that the passenger and the translocator domains have different evolutionary origins that are both different from the pathogenic *Neisseria* spp. with a GC content of 52% in their genome sequences. No differences were found in this respect between the three *autB* variants, suggesting that they evolved in the same species. In the *autA* gene, the GC content of the three regions was remarkably different, i.e., 40 ± 3, 52 ± 3, and 56 ± 1% for the N-terminal part of the passenger, the linker and the translocator domain, respectively. The two latter regions are closer to the average GC content in *Neisseria* genomes. Together, this analysis supports the hypothesis that both ATs have a different origin and suggests the exchange of

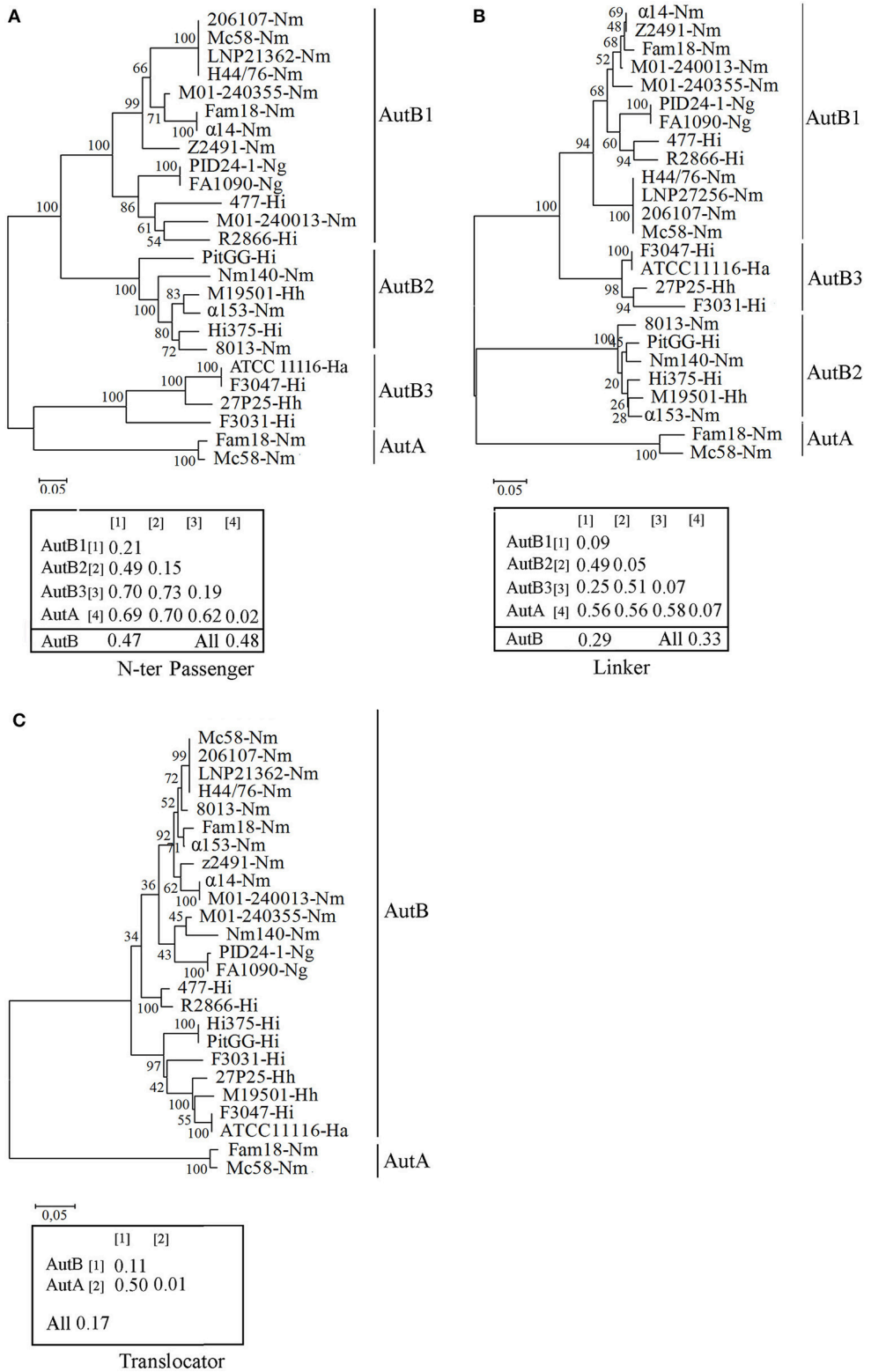


**FIGURE 2 | Phylogenetic trees of *autB* gene sequences.** Cluster analysis was performed on the N-terminal part of the passenger **(A)**, the linker **(B)**, and the translocator domain **(C)** of mature AutB and AutA proteins derived from representative genomes of *N. meningitidis* (*Nm*), *N. gonorrhoeae* (*Ng*), *H. influenzae* (*Hi*), *H. aegyptius* (*Ha*), and *H. haemolyticus (Hh)* strains. The *autB* genes from *H. influenzae* strain R2866 and *H. aegyptius* ATCC11116 were previously called *lav* and *las*, respectively (Davis et al., 2001). The bootstraps values are shown on the branches. Genetic distances within and between groups and overall mean distances for AutBs are included in the insets.

genetic material between genes of different ATs in the region encoding the passenger.

## Phase Variation of *autB* in Clinical Meningococcal Isolates

To study phase variation of *autB*, we analyzed large sets of meningococcal disease isolates from the same genetic origin. If phase variation indeed occurs frequently, different isolates of the same cc should contain different numbers of repeats and, in the absence of selection pressure, ∼33% should have the gene in the proper reading frame. We analyzed collections of cc213 and cc32 isolates, two hyper-invasive clonal complexes. The number of repeat units in the *autA* gene of these isolates was previously analyzed (Arenas et al., 2015) allowing us to compare phase variation in these two AT genes. In cc213 strain M01-240355, *autB* is in phase at the AAGC repeat but it is disrupted by a downstream frameshift mutation (Table S2). In the cc32 strains listed in Table S2 ($n = 17$), the *autB* gene is out of phase but it does not contain additional disruptions. All these genomes harbor an AutB1 variant (Table S2).

The repeat region of the *autB* gene was amplified by PCR and sequenced in a panel of 53 isolates of cc213 and 49 isolates of cc32 collected in The Netherlands between 2000 and 2010 from patients with meningococcal disease. The number of repeat units varied and ranged from 2 to 10 in *autB* and from 5 to 32 in *autA* (Table S3 and **Figure 3**). These results illustrate that slipped-strand mispairing at the AAGC repeats occurs in both genes and in both clonal complexes. However, in only 1 of the 49 cc32 isolates (2%), i.e., strain 2081107, and none of the 53 cc213 isolates the *autB* gene was in phase. This low frequency contrasts drastically with that observed for *autA*, where the gene was found to be in phase in 28% and 45% for cc213 and cc32 isolates, respectively (**Figure 3**), i.e., close to the 33% that would be expected in the absence of any selection pressure (Arenas et al., 2015). Thus, the results support the hypothesis that, although slipped-strand mispairing resulting in frameshifts does occur at the AAGC repeats in *autB*, there is a strong selection pressure against the occurrence of a number of repeats that would render the gene in frame in both clonal complexes. Further sequence examination revealed that cc213 isolates do not contain the same additional frameshift that disrupts the *autB* gene downstream of the AAGC repeats in strain M01-240355, suggesting that this feature is not conserved in cc213 strains. Therefore, the gene could potentially be expressed in this cc after slipped-strand mispairing. Interestingly, examination of the sequence after the repeats revealed that isolate 2041085 harbors an AutB2 variant, whilst all other cc213 isolates harbor an AutB1 variant, evidencing horizontal genetic transfer. The full-length *autB* gene was sequenced in three isolates of cc32, i.e., 2081107, which is in frame at the AAGC repeats, and 2061551 and 2070077, which are out of phase. All these isolates revealed only variation in the number of repeat units and no other genetic disruptions or amino-acid substitutions relative to that of strain MC58. Thus,

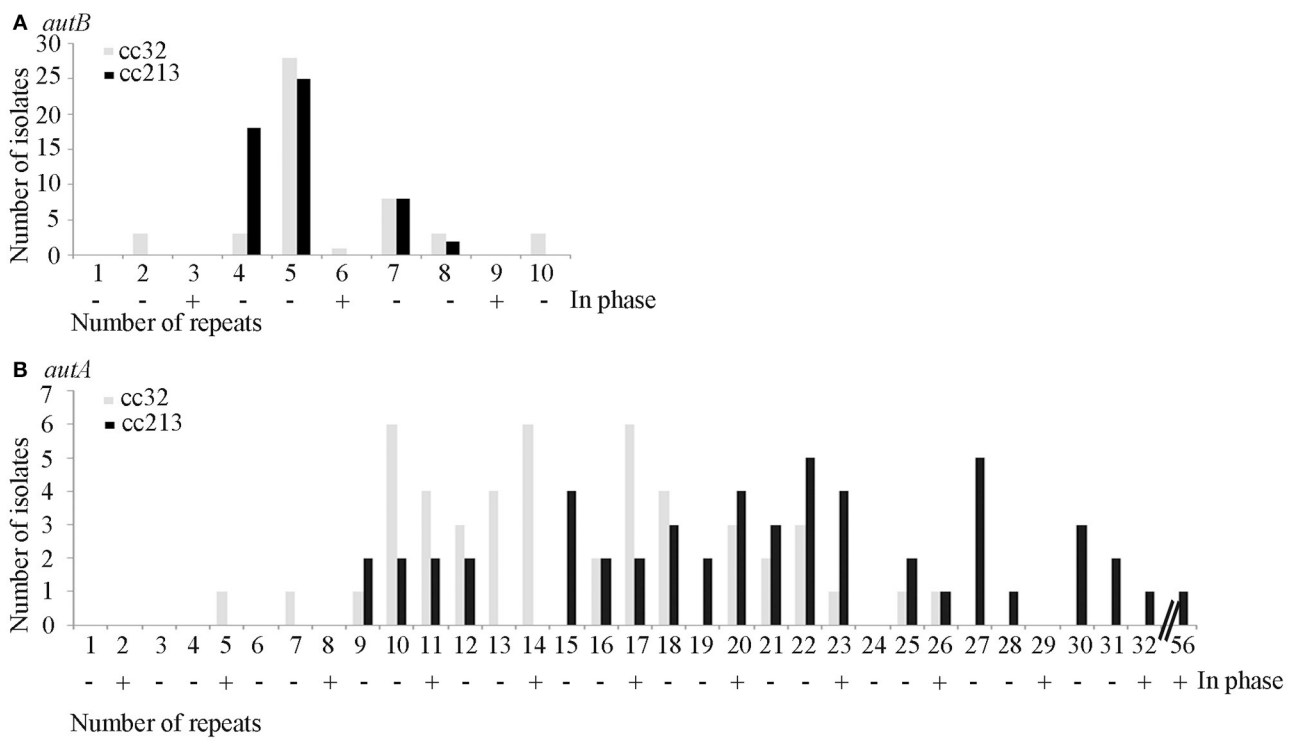


**FIGURE 3 | Variable numbers of AAGC repeats.** The numbers of AAGC repeats were determined in the *autB* **(A)** and *autA* **(B)** genes of 49 cc32 and 53 cc213 meningococcal strains isolated from patients with meningococcal disease. Data for AutA were taken from Arenas et al. (2015). The numbers of repeats that would render the gene in phase are indicated by a plus sign.

the *autB* gene of isolate 2081107 is intact and, therefore, probably expressed.

## Phase Variation of *autB* in Carriage Isolates

Since the vast majority of isolates analyzed in Tables S2, S3 are from patients with invasive meningococcal disease, our selection of strains may not be representative for those residing in the nasopharynx. Thus, we analyzed the *autB* gene in the genome sequences of a collection of carriage isolates available in a public data base (http://pubmlst.org/software/database/bigsdb/). A total of 207 strains was analyzed. The number of repeat units in the *autB* gene ranged from 2 to 22. In total, 10.6% of these isolates had 3, 6, or 12 repeats that render *autB* in frame. However, in the majority of these strains, the gene is disrupted by downstream-located single-nucleotide insertions and only 2.4% of isolates (28871, 28881, 28942, 28955, 28959) had an undisrupted *autB* gene in frame. Hence, these data do not show obvious differences in possible *autB* expression between carrier and disease isolates.

## Expression of Meningococcal AutB

We next analyzed whether AutB is indeed synthesized in strains where the gene is in phase at the AAGC repeats and has no other genetic disruptions. Plasmids encoding the *autB1* and *autB2* genes from strains 2081107 and α153, respectively, were introduced in HB-1Δ*autB*. Although the *autB* gene is phase off in HB-1 (Table S2), we deleted the chromosomal copy of the gene to avoid genetic exchange with the *autB* gene on the plasmids. Western blot analysis showed a band with an apparent molecular weight of ∼73 kDa in strain HB-1Δ*autB* carrying $pENAutB_1$ only when the strain was grown in the presence of IPTG (**Figure 4A**), thus identifying this band $AutB_1$. A band of similar size was detected in isolate 2081107, which contains an intact in-frame *autB* gene on the chromosome, but not in preparations of other strains where the *autB1* gene is out of phase (**Figure 4A**). This result demonstrates that AutB is synthesized in isolate 2081107. Unfortunately, an *autB* mutant of this strain could not be created, because the strain was not transformable. No reaction was observed in strains HB-1Δ*autB* carrying $pENAutB_2$ (data not shown) or α153, which is expected to express AutB2 from the chromosome (**Figure 4A**), presumably due to lack of cross-reactivity of the antiserum, which was raised against a part of AutB1 that shows little sequence similarity to AutB2 (Figure S2). The antiserum did also not react with a preparation of strain α14 (**Figure 4A**), which expresses AutA, confirming the specificity of the antiserum.

To investigate if *autB2* is expressed in α153, RT-PCR assays were done using primers targeting internal DNA fragments of *autB1* and *autB2*. With chromosomal DNA from HB-1 and α153 as templates, the amplicons for *autB1* and *autB2* were according the expected size, i.e., 100 and 150 bp, respectively (**Figure 4B**). No amplicons were obtained from RNA preparations as templates (data not shown), but they were obtained from cDNA preparations of strains HB-1Δ*autB* containing $pENAutB_1$ and grown in presence of IPTG and α153, but not of strains HB-1 and the α153Δ*autB* mutant (**Figure 4B**). Primers for *rmpM* yielded an amplicon in all preparations, evidencing that all contained similar amounts of cDNA. The lack of detection of

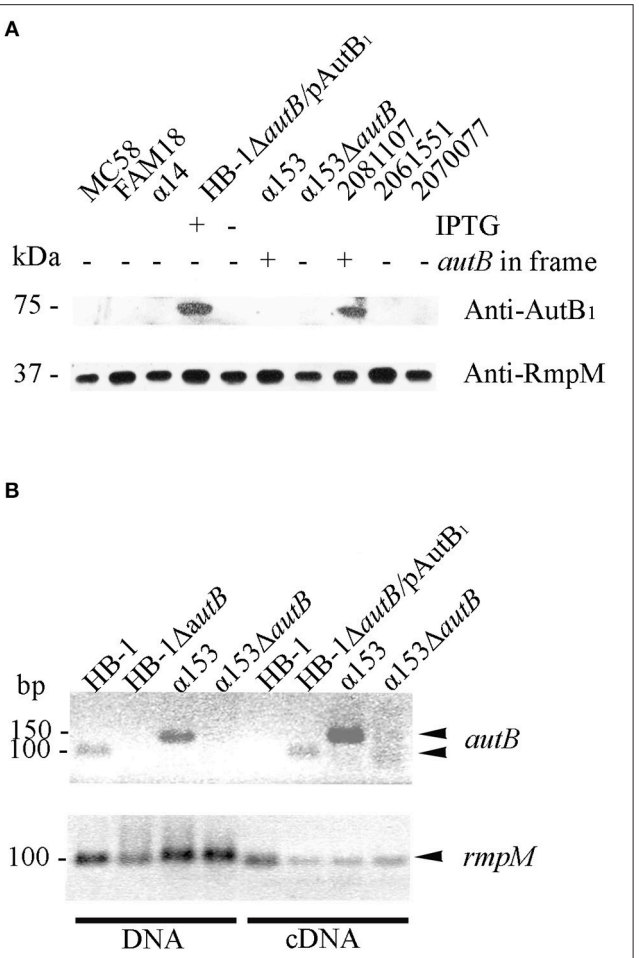


**FIGURE 4 | Expression of AutB. (A)** Western blots of cell envelope preparations of various *N. meningitidis* strains were probed with antisera directed against AutB1 and, as a loading control, against RmpM. HB-1Δ*autB* containing $pENAutB_1$ ($pAutB_1$) was grown in the presence or absence of IPTG as indicated. Also indicated is whether the chromosomal *autB* gene is in frame or not. Positions of molecular mass standards are shown at the left. Only the relevant parts of the blot are shown. **(B)** Agarose gels showing PCR products obtained with either chromosomal DNA or cDNA as templates as indicated at the bottom. The cDNA was generated from RNA, which was extracted from the *N. meningitidis* strains, using primers for *autB* or *rmpM* as indicated. HB-1Δ*autB* containing $pENAutB_1$ was grown in the presence of IPTG. Size standards are shown at the left. Only the relevant parts of the gels are shown.

*autB* transcripts in strain HB-1 could be due to degradation of the mRNA by the presence of a premature stop codon resulting from the frameshift at the AAGC repeat region. Together, these data show that *autB* is expressed in at least some meningococcal strains and confirm that its expression is determined by phase variation at the AAGC repeat units.

## Exposure of AutB at the Cell Surface

Our Western blotting analysis detected the full-length AutB in cell envelope preparations (**Figure 4A**). To determine whether the passenger domain may be released from a proportion of the AutB molecules into the extracellular medium, whole cell lysates, cell envelopes and supernatants of strain HB-1Δ*autB*

expressing AutB1 from pENAutB$_1$ were analyzed by SDS-PAGE and Western blotting. The expected 73-kDa band was detected in cell-envelope preparations but no band reacting with the antiserum was detected in supernatant preparations (**Figure 5A**). As a control, the secretion of IgA protease was also analyzed using specific antibodies against its translocator domain and the α-peptide, which is released into the milieu after cleavage by NalP (Roussel-Jazédé et al., 2014). As expected, the translocator domain and the α-peptide were detected in the cell envelope fraction and the culture supernatant, respectively (**Figure 5A**). Hence, the passenger of AutB is not released into the extracellular medium. To confirm its cell-surface exposition, we used proteinase K accessibility assays in intact bacteria (**Figure 5B**). The protease degraded AutB and fHbp, a surface-exposed lipoprotein that was analyzed as a positive control (Bos et al., 2014). In contrast, the periplasmically exposed outer membrane-associated protein RmpM remained unaffected, confirming the integrity of the outer membrane. Thus, the passenger of AutB is secreted but remains attached via the translocator domain to the cell surface.

## AutB Expression Impacts Biofilm Formation

Previously, we demonstrated that AutA has a role in autoaggregation and biofilm formation (Arenas et al., 2015). To investigate whether AutB also has a role in autoaggregation, settling assays were performed. These assays showed a clear effect of the of AutA production on bacterial autoaggregation (Figure S3A); however, such an effect was not observed when *autB1* was expressed from plasmid in HB-1Δ*autB*, and also no difference between α153 and its *autB* mutant derivative was observed (Figure S3A). Thus, in contrast to AutA, synthesis of AutB does not induce strong autoaggregation.

A possible role of AutB in biofilm formation was first studied under static conditions on polystyrene plates. The presence of a capsule is known to inhibit biofilm formation (Yi et al., 2004; Lappann et al., 2006), but α153 is a natural capsule null mutant. We also included the capsule-deficient reference strains HB-1 and BB-1, which were previously used in biofilm assays (Arenas et al., 2013a). After 1 h of incubation, α153 generated a biofilm mass intermediate between that of BB-1 and HB-1 (**Figure 6A**). Interestingly, deletion of *autB* drastically impaired biofilm formation to a level comparable with that of strain BB-1 (**Figure 6A**). This phenotype was complemented when either AutB1 or AutB2 was expressed *in trans* from plasmid (**Figure 6A**), demonstrating that both variants have a similar role.

*N. meningitidis* has two different strategies of biofilm formation, either dependent or independent of eDNA (Lappann et al., 2010). HB-1 and BB-1 follow the eDNA-dependent and -independent routes of biofilm formation, respectively (Arenas et al., 2013a). To investigate whether AutB-mediated biofilm formation is dependent on eDNA, biofilm formation of strain α153 and its *autB* mutant derivative was assessed in the presence of DNase I. This treatment considerably reduced biofilm mass in α153 to the level of the Δ*autB* mutant, but it did not impact on the residual biofilm formation of the mutant (**Figure 6A**, right panel). This data indicates that AutB-mediated biofilm formation is dependent on eDNA and suggests that the remaining biofilm formation in the *autB* mutant of α153 is eDNA independent. Presumably, AutB at the cell surface binds eDNA that acts as a glue facilitating interbacterial and bacterium-substratum interactions. Previously, the α-peptide of IgA protease and NHBA were reported to represent the main surface-exposed DNA-binding proteins involved in biofilm formation in strain HB-1 (Arenas et al., 2013a). Western blot analysis, however, revealed that the α-peptide of IgA protease is released into the medium in strain α153 (**Figure 5A**), whilst examination of the α153 genome sequence revealed that the *nhbA* gene is disrupted. Thus, probably, AutB is the main DNA-binding protein in α153 and, therefore, its inactivation has a drastic impact on biofilm formation. To investigate the DNA-binding capacities of AutB, we produced the entire passenger of AutB of strain HB-1 in *E. coli*. The protein formed inclusion bodies, which were purified, but we could not establish proper conditions to fold the protein *in vitro*.

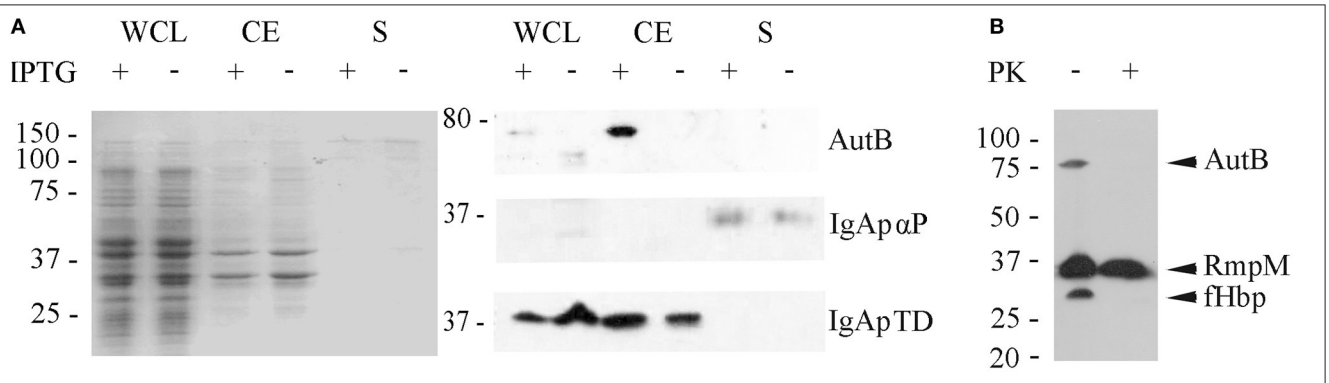


**FIGURE 5 | Localization of AutB. (A)** Strain HB-1Δ*autB* containing pENAutB1 was grown in the presence or absence of IPTG and whole cell lysates (WCL), cell envelopes (CE) and culture supernatants (S) were prepared and separated by SDS-PAGE. The left panel shows a Coomassie-stained gel, and corresponding Western blots with antisera directed against AutB1, and the α-peptide (αP) and the translocator domain (TD) of IgA protease (IgAp) are shown in the right panel. Only the relevant parts of the blots are shown. **(B)** Protease-accessibility assay. Cells of HB-1Δ*autB* containing pENAutB1 were grown in the presence of 0.1 mM IPTG and treated or not with 2 μg/ml of proteinase K (PK). The degradation of AutB, RmpM, and fHbp was analyzed by Western blotting using specific antibodies.

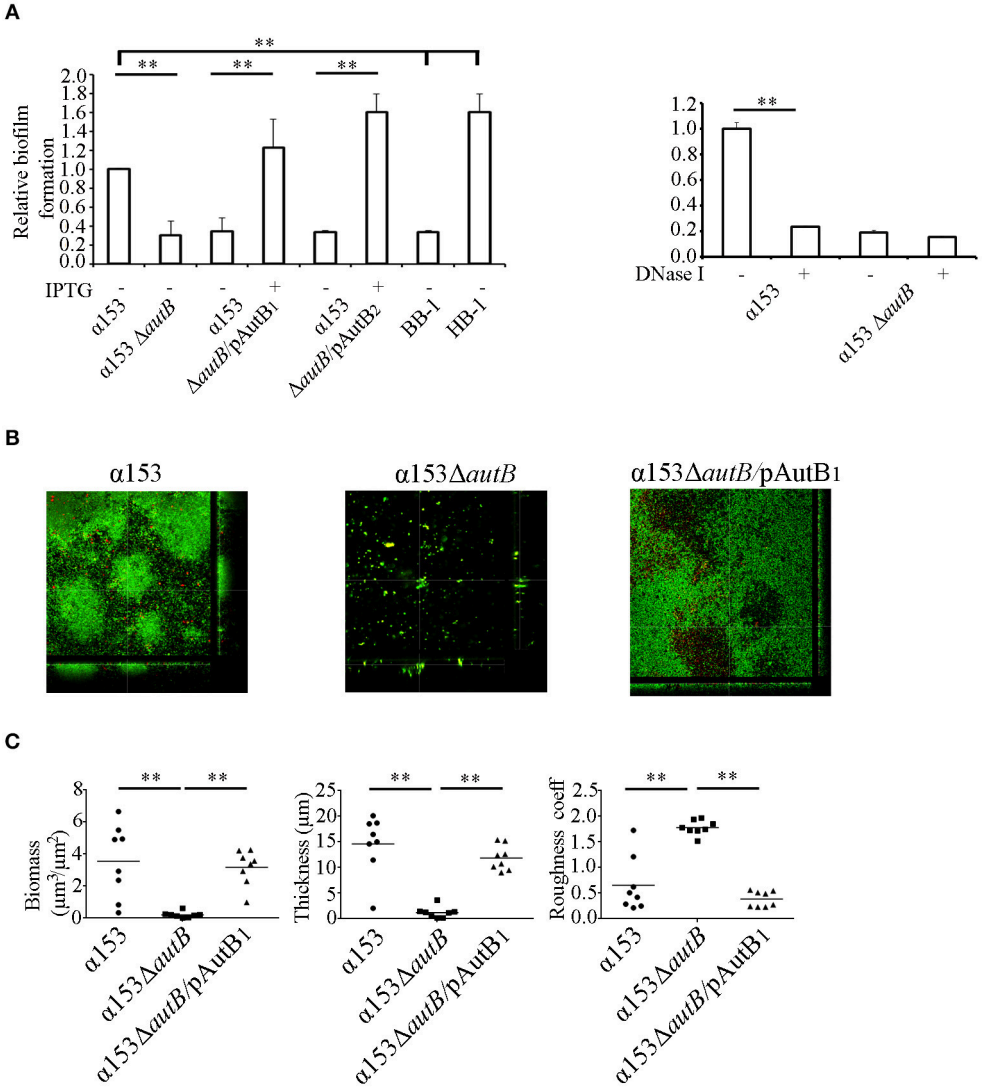


**FIGURE 6 | AutB mediates biofilm formation. (A)** Biofilm formation under static conditions. Bacteria were pre-cultured in TSB with or without 0.1 mM of IPTG and adjusted to an $OD_{550}$ of 1.0. Aliquots were then transferred into 24-well plates and incubated under static conditions for 1 h (left panel). The impact of DNase I on biofilm formation in α153 and its Δ*autB* mutant derivative is shown in the right panel. 100 μg/ml of DNase I was added to the cultures, which were subsequently incubated for 1 h under static conditions. Biofilms formed were quantified after staining with crystal violet by measuring the $OD_{630}$. The data represent means and standard deviations of at least three independent experiments, and values are given as relative to α153, which was set at 1.0. Statistically significant differences between groups are marked with two asterisks (unpaired *t*-test of $P < 0.01$). **(B)** Biofilm formation under flow conditions. Representative pictures are shown of structures of 16 h-old biofilms of α153, α153Δ*autB*, and α153Δ*autB* carrying pENAutB1 cultured in presence of 0.1 mM IPTG (α153Δ*autB*/$pAutB_1$). Bacteria were stained with Dead/Live staining for visualization. Green and red bacteria are live and dead cells, respectively. **(C)** Quantification of biomass, thickness, and roughness of 16 h-old biofilms under flow conditions. The biofilm parameters were determined with COMSTAT/MATLAB software. Asterisks indicate statistically significant differences ($P < 0.0005$) between groups calculated by unpaired *t*-test using GraphPad software.

To investigate the influence of AutB synthesis on biofilm formation in more detail, we used a flow-cell model. With this method, the flow in the nasopharynx or the bloodstream is mimicked, and biofilm development can continuously be monitored by microscopy. Biofilms formed by α153 were constituted of round aggregates of different sizes, which were surrounded by single cells (see representative pictures in **Figure 6B** and the development of the biofilm in Figure S3B). These aggregates fused into larger aggregates, which constituted the biomass of the biofilm (Figure S3B). These biofilm structures had a clearly different appearance than those reported previously for strains HB-1, BB-1, and α14 (Arenas et al., 2013a, 2015). Analysis of the α153Δ*autB* mutant did not reveal structured biofilms; instead, only few single cells or very small aggregates were randomly attached to the substratum (**Figure 6B**). COMSTAT analysis revealed a biomass and thickness significantly reduced as compared with the wild type (**Figure 6C**) in accordance with the results of the

biofilm assays under static conditions (**Figure 6A**). Furthermore, biofilm roughness, also determined by COMSTAT, increased significantly. All phenotypic differences were complemented when $AutB_1$ was expressed *in trans* from plasmid (**Figures 6B,C**). These data confirm that AutB is required for biofilm formation and architecture and demonstrate its biological relevance.

## AutB Synthesis Interferes with Meningococcal Translocation across Epithelial Cell Layers

To investigate whether the synthesis of AutB also affects the interaction of the bacteria with eukaryotic cells, we first determined the adherence of α153 and its *autB* mutant derivative to NCI-H292 cells by counting the number of cell-associated CFU 3 h after initiating infection. Although adherence of the mutant appeared slightly reduced (∼25%), a defect that was complemented when AutB was expressed *in trans* (**Figure 7A**), this difference was not statistically significant.

Next, we studied the ability of the strains to cross epithelial cell layers, a process necessary for host invasion. NCI-H292 cells were grown for 6 days on a permeable support to generate cellular junctions, as verified by a trans-epithelial resistance of $30 \pm 2$ $\Omega \times cm^2$, in accordance with values previously reported (van Schilfgaarde et al., 1995). The cell layers were then infected with bacteria and the numbers of bacteria that reached the basal compartment after passage of the cell layers were determined between 6 and 12 h post infection by counting CFU. Cells of the *autB* mutant reached the basal compartment faster than those of the parental strain as demonstrated, for example, by the significantly higher numbers of *autB* mutant bacteria than of wild-type bacteria in the basal compartment 10 h after infection (**Figure 7B**), a phenotype that was complemented by expression of a functional copy of *autB* from $pENAutB_1$. Clones of cells derived from the wild type that reached the trans-epithelial compartment early after infection were collected from different experiments and further analyzed. To investigate whether AutB synthesis and, consequently, their biofilm-formation capacity was altered, we tested biofilm formation under static conditions. Interestingly, all clones had a reduced biofilm-forming capacity like the *autB* mutant (see **Figure 7C** for representatives). Sequencing of the AAGC region in all clones did not show alterations, suggesting that phase variation was not the origin of such defect. To test whether *autB* expression was lost we analyzed one clone by RT-PCR assays and found no detectable *autB* expression (**Figure 7C**). Sequencing of the complete *autB* gene and flanking regions, however, did not reveal an obvious reason for this down-regulation, suggesting these clones had acquired a mutation in a regulatory gene. Together, these data demonstrate that *autB* expression negatively affects bacterial epithelial transmigration and suggests that biofilm formation is inversely correlated with invasion.

# DISCUSSION

The *autB* gene is present in bacteria colonizing the human mucosa and is restricted to certain species of the genera *Neisseria* and *Haemophilus*. This distribution was earlier explained by the transfer of the gene from an unidentified microorganism to *H. influenzae* and then to a recent ancestor of both *N. meningitidis* and *N. gonorrhoeae* (Davis et al., 2001). This hypothesis was mainly based on the observation that the gene is placed in *H. influenzae* between the *tmk* and *holB* genes, two genes that are contiguous in many gram-negative bacteria, whilst it is placed in a different context in *N. meningitidis* and *N. gonorrhoeae* but flanked by fragments of the *tmk* and *holB* genes from *H. influenzae* (**Figure 1**). These observations were made by the examination of the few genome sequences of *Neisseria* and *Haemophilus* strains that were available at that time (Davis et al., 2001). Now, many more genome sequences of both genera are available, and this allowed us to extend the earlier analysis. Indeed, our analysis confirms initial observations and adds new evidence about the evolution and expression of the gene.

First, the *autB* gene is not present in all *H. influenzae* isolates, indicating that the gene does not originate from this species. We found the gene in three other *Haemophilus* spp., i.e., *H. haemolytica*, *H. parainfluenzae,* and *H. aegyptius*, which are closely related to *H. influenzae*. Also in these species, the gene is found only in a limited number of isolates, indicating that they did not evolve from *autB*-containing *H. influenzae* strains but also acquired the gene by horizontal gene transfer. Second, the gene was ubiquitously present in *N. meningitidis* and *N. gonorrhoeae* genomes, but not in other *Neisseria* spp., consistent with the proposed acquisition of the gene by a recent ancestor of both pathogenic *Neisseria* spp. In agreement with its acquisition by horizontal gene transfer, the GC content of *autB* is substantially lower than that of *Neisseria* genomes. Third, our phylogenetic analysis revealed the existence of three main allelic variants of *autB*. Each variant was not restricted to one single species, but *N. meningitidis*, *H. influenzae*, *H. haemolyticus*, and *H. aegyptius* each contained several of these variants, a clear indication that they share a common pool of *autB* genes. In contrast, only *autB1* was detected in *N. gonorrhoeae*, indicating that this species does not participate in the exchange of *autB* variants which is consistent with its different niche. In the evolutionary context, it is also interesting to consider the origin of AutA, which is structurally related to AutB. In contrast to *autB*, *autA* is present in both pathogenic and commensal *Neisseria* species (Arenas et al., 2015). Therefore, it did not arise by gene duplication after introduction of *autB* into a common ancestor of the pathogenic *Neisseria* spp. Because it is ubiquitous among *Neisseria* spp., it may originate from a common ancestor of *Neisseria* spp. Its subsequent transfer to and evolution in other microorganisms may eventually have resulted in its return as *autB* in *Neisseria.* In agreement with the neisserial origin of *autA* is the GC content of the segments encoding the linker and translocator domains of the protein, which, in contrast to the corresponding domains of *autB*, are in accordance with those of neisserial genomes. However, the GC content of the segment encoding the N-terminal part of the AutA passenger is substantially lower indicating a different evolutionary origin of this part of the gene. Shuffling of domains is also suggested from the phylogenetic analysis of the *autB* genes. The translocator domain of AutB is well conserved, whilst the linker is more conserved than the N-terminal part of the

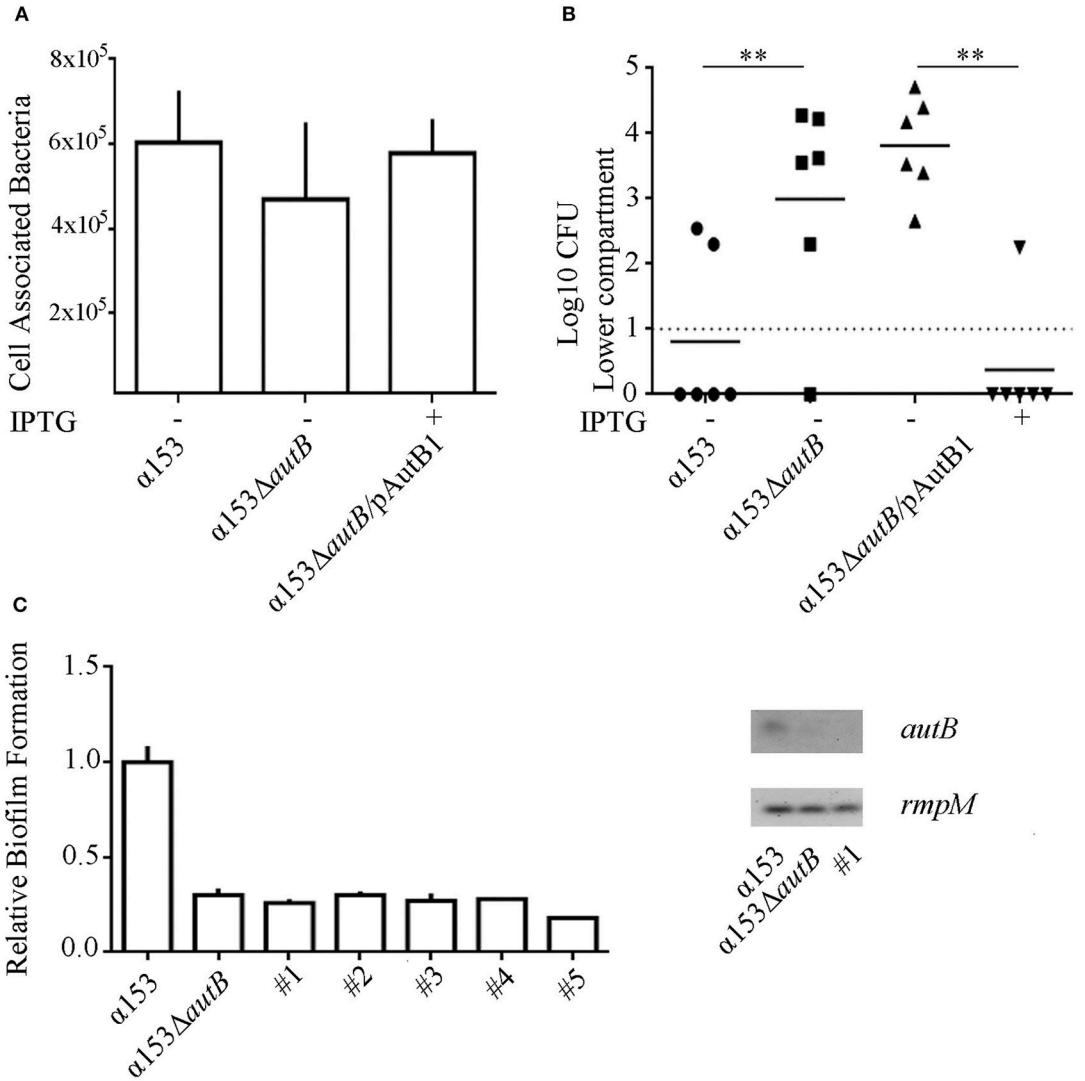


**FIGURE 7 | Inactivation of *autB* affects passage of NCI-H292 cell layers. (A)** Adherence of *N. meningitidis* strains α153, α153Δ*autB*, and α153Δ*autB* carrying pENAutB$_1$ to NCI-H292 cell layers. The complemented strain was grown in the presence of IPTG. The NCI-H292 cells were incubated with the bacteria for 3 h, washed, and cell-associated CFU were determined after lysing the cells with saponin. Means and standard deviations of three independent experiments performed in duplicate are shown. Differences observed were not statistically significant. **(B)** Passage of cells of strain α153, its Δ*autB* mutant derivative and the complemented mutant through NCI-H292 cell layers. The complemented mutant was grown with or without IPTG as indicated. The passage of bacteria through the cell layers was determined by counting CFUs from the basal compartment 10 h after inoculation. Results of three independent experiments performed in duplicate are shown. Asterisks show statistically significant differences between groups ($P < 0.001$, unpaired *t*-test). Before statistical analysis, CFUs were log10 converted. **(C)** Analysis of clones of cells of strain α153 that reached the trans-epithelial compartment. Several clones were recovered in independent infection experiments (#1–5). Their biofilm-forming capacity was determined as described for **Figure 6A** and is shown in the graft at the left. Expression of *autB* was determined by RT-PCR as described for **Figure 4B**, and agarose gels with PCR products obtained with cDNA as templates are shown in the right panel.

passenger. The N-terminal domain of AutB3 is only distantly related to the corresponding domains of AutB1 and AutB2. In contrast, its linker domain is closely related to that of AutB1, from which it probably evolved after having been linked to a different N-terminal domain.

In all *N. gonorrhoeae* strains examined, the *autB* gene cannot be expressed because of genetic disruptions downstream of the AAGC repeat region, indicating that AutB synthesis is not relevant in the particular niche of this species. In contrast, although phase off in most cases, an intact *autB* gene is preserved in the vast majority of *N. meningitidis* isolates, indicating that it is advantageous for this species to be able to synthesize AutB at some stage in the colonization process. However, it is also evident that it is important for the bacteria to be able to shut off the synthesis of AutB. With only very few exceptions, the number of AAGC repeats renders the gene phase off in meningococci with an intact *autB* gene (Tables S2, S3, **Figure 3**). Such an extreme preference for the off-phase of a phase-variable gene has, to the

best of our knowledge, not been reported before. As compared with *Haemophilus autB*, the number of AAGC repeats in *N. meningitidis autB* is generally lower. A lower number of repeats is expected to result in a reduced frequency of phase variation. However, the variable number of repeats observed in the *autB* gene of isolates of the same clonal complex demonstrates that loss and gain of these repeats through slipped-strand mispairing is still occurring in the meningococcus. When the number of these repeats is reduced to three, the gene is in the on phase and the frequency of phase variation is expected to be very low. In this case, the majority of the isolates have lost the possibility to express the *autB* gene through mutations further downstream in the gene, which accentuates the importance for the bacteria to switch off the expression of the gene.

Why is an intact *autB* gene retained in *N. meningitidis*, while its expression is shut off in the vast majority of the isolates? Like AutB, many other surface-exposed proteins of *N. meningitidis* show phase-variable expression (Saunders et al., 2000), most likely to escape from the immune system. As these proteins have important functions for colonization and persistence in the host, the functions of some of these proteins may be taken over by others when their expression is turned off. The *autB* gene has been considered to be a pseudogene because its expression could not be demonstrated in a limited set of meningococcal strains (Ait-Tahar et al., 2000). We demonstrate here that AutB is synthesized in at least some isolates and that it has a role in biofilm formation presumably by binding eDNA. This role would be equivalent to those of NHBA and the α-peptide of IgA protease (Arenas et al., 2013a). Although the expression of the genes for NHBA and IgA protease has not been reported to be phase variable, these proteins are cleaved from the cell surface by the AT protease NalP (Serruto et al., 2003; van Ulsen et al., 2003; Roussel-Jazédé et al., 2014), the expression of which is phase variable (Saunders et al., 2000). Thus, AutB may serve as a backup mechanism that enables biofilm formation if the amount of cell-surface-exposed NHBA and α-peptide is low.

Then, why is *autB* expression switched off in most isolates? Phase variation by slipped-strand mispairing is a random process and, with the AAGC repeats being located within the coding region, one would expect that 33% of the isolates are in phase on. Such a frequency was indeed found for the *autA* gene (Arenas et al., 2015), but *autB* was found to be in phase on in only ∼1% of the same set of isolates, indicating the existence of a strong selection pressure against expression of the gene. Possibly, AutB elicits a strong immune response. Consistent with this hypothesis is the high sequence variability we observed in the passenger domain of AutB, which may reflect antigenic variability due to immune pressure. However, another explanation for selection against *autB* expression in disease isolates is that biofilm formation, whilst presumably important in the colonization of the mucosal surfaces, may be hindering the passage of the epithelial layers to cause invasive disease. Indeed, we observed that AutB synthesis delays the passage of epithelial cell layers *in vitro*. It is noteworthy in this respect that no evidence for selection pressure against *autB* expression was observed in the limited number of *Haemophilus* genomes analyzed. The *H. influenzae* strains in which *autB* (*lav*) was found are nontypeable strains, which seldom cause invasive disease (Davis et al., 2001). Furthermore, *H. haemolyticus* is generally considered as a commensal in the nasopharynx, although also few cases of invasive disease by this bacterium have been reported (Jordan et al., 2011). Thus, these observations suggest a role for AutB during colonization of the nasopharynx and a negative effect of AutB synthesis on bacterial invasion. However, also the vast majority of strains isolated from carriers did not express *autB*. A possible explanation is that the isolation methods for carriage isolates selectively fail to collect AutB-expressing strains. Carriage strains are often isolated from healthy people using swabs. This method underestimates the number of carriers as was demonstrated by Sim et al. (2000), who reported that swabs allowed for the isolation of meningococci from 10% of the people examined whilst meningococci were detected in 45% of these people by immunohistochemistry. In addition, microcolonies were found with the latter technique below the epithelial surface, which could explain the observed underestimation of meningococcal carriage through swab isolation. Thus, it is possible that AutB facilitates microcolony formation in this specific niche.

In summary, we showed here for the first time the synthesis of AutB in some meningococcal isolates and the existence of strong selection pressure against *autB* expression. We also demonstrated the localization of AutB at the bacterial cell surface, its function in biofilm formation, and the negative consequences of its expression on the transit of the bacteria through epithelial cell layers. This work completes the initial characterization of the eight ATs identified so far in available meningococcal genome sequences and provides new insights in the commensal/virulence relationship of pathogenic *Neisseria* and *Haemophilus* species.

## AUTHOR CONTRIBUTIONS

JA, FP, JP, and JT conceived and designed the experiments; JA, SC, AE, and JT performed bioinformatics analysis; JA, FP, PR, and SC performed the experiments; JA, JT analyzed the data and wrote the paper. All authors have read and approved the manuscript.

## FUNDING

This work was partially supported by Utrecht University. PR, SC were supported by personal fellowships for student mobility (Spanish government) and by an Erasmus fellowship, respectively.

## ACKNOWLEDGMENTS

We would like to thank Tom van den Hoeven and Donia Tajouri for technical assistance and fruitful discussions.

## SUPPLEMENTARY MATERIAL

The Supplementary Material for this article can be found online at: http://journal.frontiersin.org/article/10.3389/fcimb.2016.00162/full#supplementary-material

## REFERENCES


Ait-Tahar, K., Wooldridge, K. G., Turner, D. P. J., Atta, M., Todd, I., and Ala'Aldeen, D. A. A. (2000). Auto-transporter A protein of *Neisseria meningitidis*: a potent CD4+ T-cell and B-cell stimulating antigen detected by expression cloning. *Mol. Microbiol.* 37, 1094–1105. doi: 10.1046/j.1365-2958.2000.02061.x

Arenas, J., Abel, A., Sánchez, S., Alcalá B., Criado, M. T., and Ferreirós, C. M. (2006). Locus NMB0035 codes for a 47-kDa surface-accessible conserved antigen in Neisseria. *Int. Microbiol.* 9, 273–280.

Arenas, J., Cano, S., Nijland, R., van Dongen, V., Rutten, L., van der Ende, A., et al. (2015). The meningococcal autotransporter AutA is implicated in autoaggregation and biofilm formation. *Environ. Microbiol.* 17, 1321–1337. doi: 10.1111/1462-2920.12581

Arenas, J., Nijland, R., Rodriguez, F. J., Bosma, T. N. P., and Tommassen, J. (2013a). Involvement of three meningococcal surface-exposed proteins, the heparin-binding protein NhbA, the α-peptide of IgA protease and the autotransporter protease NalP, in initiation of biofilm formation. *Mol. Microbiol.* 87, 254–268. doi: 10.1111/mmi.12097

Arenas, J., Schipper, K., van Ulsen, P., van der Ende, A., and Tommassen, J. (2013b). Domain exchange at the 3' end of the gene encoding the fratricide meningococcal two-partner secretion protein A. *BMC Genomics* 14:622. doi: 10.1186/1471-2164-14-622

Arenas, J., and Tommassen, J. (2016). Meningococcal biofilm formation: let's stick together. *Trends Microbiol.* doi: 10.1016/j.tim.2016.09.005. [Epub ahead of print].

Bentley, S. D., Vernikos, G. S., Snyder, L. A., Churcher, C., Arrowsmith, C., Chillingworth, T., et al. (2007). Meningococcal genetic variation mechanisms viewed through comparative analysis of serogroup C strain FAM18. *PLoS Genet.* 3:e23. doi: 10.1371/journal.pgen.0030023

Bos, M. P., Grijpstra, J., Tommassen-van Boxtel, R., and Tommassen, J. (2014). Involvement of *Neisseria meningitidis* lipoprotein GNA2091 in the assembly of a subset of outer membrane proteins. *J. Biol. Chem.* 289, 15602–15610. doi: 10.1074/jbc.M113.539510

Bos, M. P., and Tommassen, J. (2005). Viability of a capsule- and lipopolysaccharide-deficient mutant of *Neisseria meningitidis*. *Infect. Immun.* 73, 6194–6197. doi: 10.1128/IAI.73.9.6194-6197.2005

Buchan, D. W., Minneci, F., Nugent, T. C., Bryson, K., and Jones, D. T. (2013). Scalable web services for the PSIPRED protein analysis workbench. *Nucleic Acids Res.* 41, W349–W357. doi: 10.1093/nar/gkt381

Capecchi, B., Adu-Bobie, J., Di Marcello, F., Ciucchi, L., Masignani, V., Taddei, A., et al. (2005). *Neisseria meningitidis* NadA is a new invasin which promotes bacterial adhesion to and penetration into human epithelial cells. *Mol. Microbiol.* 55, 687–698. doi: 10.1111/j.1365-2958.2004.04423.x

Costerton, J. W., Lewandowski, Z., Caldwell, D. E., Korber, D. R., and Lappin-Scott, H. M. (1995). Microbial biofilms. *Annu. Rev. Microbiol.* 49, 711–745. doi: 10.1146/annurev.mi.49.100195.003431

Davis, J., Smith, A. L., Hughes, W. R., and Golomb, M. (2001). Evolution of an autotransporter: domain shuffling and lateral transfer from pathogenic *Haemophilus* to *Neisseria*. *J. Bacteriol.* 183, 4626–4635. doi: 10.1128/JB.183.15.000-000.2001

Grijpstra, J., Arenas, J., Rutten, L., and Tommassen, J. (2013). Autotransporter secretion: varying on a theme. *Res. Microbiol.* 164, 562–582. doi: 10.1016/j.resmic.2013.03.010

Heydorn, A., Nielsen, A. T., Hentzer, M., Sternberg, C., Givskov, M., Ersbøll, B. K., et al. (2000). Quantification of biofilm structures by the novel computer program COMSTAT. *Microbiology* 146, 2395–2407. doi: 10.1099/00221287-146-10-2395

Jordan, I. K., Conley, A. B., Antonov, I. V., Arthur, R. A., Cook, E. D., Cooper, G. P., et al. (2011). Genome sequences for five strains of the emerging pathogen *Haemophilus haemolyticus*. *J. Bacteriol.* 193, 5879–5880. doi: 10.1128/JB.05863-11

Lappann, M., Claus, H., van Alen, T., Harmsen, M., Elias, J., Molin, S., et al. (2010). A dual role of extracellular DNA during biofilm formation of *Neisseria meningitidis*. *Mol. Microbiol.* 75, 1355–1371. doi: 10.1111/j.1365-2958.2010.07054.x

Lappann, M., Haagensen, J. A., Claus, H., Vogel, U., and Molin, S. (2006). Meningococcal biofilm formation: structure, development and phenotypes in a standardized continuous flow system. *Mol. Microbiol.* 62, 1292–1309. doi: 10.1111/j.1365-2958.2006.05448.x

Oliver, D. C., Huang, G., Nodel, E., Pleasance, S., and Fernandez, R. C. (2003). A conserved region within the *Bordetella pertussis* autotransporter BrkA is necessary for folding of its passenger domain. *Mol. Microbiol* 47, 1367–1383. doi: 10.1046/j.1365-2958.2003.03377.x

Peak, I. R., Jennings, M. P., Hood, D. W., and Moxon, E. R. (1999). Tetranucleotide repeats identify novel virulence determinant homologues in *Neisseria meningitidis*. *Microb. Pathog.* 26, 13–23. doi: 10.1006/mpat.1998.0243

Peterson, J. H., Tian, P., Ieva, R., Dautin, N., and Bernstein, H. D. (2010). Secretion of a bacterial virulence factor is driven by the folding of a C-terminal segment. *Proc. Natl. Acad. Sci. U.S.A.* 107, 17739–17744. doi: 10.1073/pnas.1009491107

Roussel-Jazédé, V., Arenas, J., Langereis, J. D., Tommassen, J., and van Ulsen, P. (2014). Variable processing of the IgA protease autotransporter at the cell surface of *Neisseria meningitidis*. *Microbiology* 160, 2421–2431. doi: 10.1099/mic.0.082511-0

Saunders, N. J., Jeffries, A. C., Peden, J. F., Hood, D. W., Tettelin, H., Rappuoli, R., et al. (2000). Repeat-associated phase variable genes in the complete genome sequence of *Neisseria meningitidis* strain MC58. *Mol. Microbiol.* 37, 207–215. doi: 10.1046/j.1365-2958.2000.02000.x

Scarselli, M., Serruto, D., Montanari, P., Capecchi, B., Adu-Bobie, J., Veggi, D., et al. (2006). *Neisseria meningitidis* NhhA is a multifunctional trimeric autotransporter adhesin. *Mol. Microbiol.* 61, 631–644. doi: 10.1111/j.1365-2958.2006.05261.x

Schoen, C., Blom, J., Claus, H., Schramm-Glück, A., Brandt, P., Müller, T., et al. (2008). Whole-genome comparison of disease and carriage strains provides insights into virulence evolution in *Neisseria meningitidis*. *Proc. Natl. Acad. Sci. U.S.A.* 105, 3473–3478. doi: 10.1073/pnas.0800151105

Serruto, D., Adu-Bobie, J., Scarselli, M., Veggi, D., Pizza, M., Rappuoli, R., et al. (2003). *Neisseria meningitidis* App, a new adhesin with autocatalytic serine protease activity. *Mol. Microbiol.* 48, 323–334. doi: 10.1046/j.1365-2958.2003.03420.x

Serruto, D., Spadafina, T., Ciucchi, L., Lewis, L. A., Ram, S., Tontini, M., et al. (2010). *Neisseria meningitidis* GNA2132, a heparin-binding protein that induces protective immunity in humans. *Proc. Natl. Acad. Sci. U.S.A.* 23, 3770–3775. doi: 10.1073/pnas.0915162107

Sim, R. J., Harrison, M. M., Moxon, E. R., and Tang, C. M. (2000). Underestimation of meningococci in tonsillar tissue by nasopharyngeal swabbing. *Lancet* 356, 1653–1654. doi: 10.1016/S0140-6736(00)03162-7

Tamura, K., Stecher, G., Peterson, D., Filipski, A., and Kumar, S. (2013). MEGA6: molecular evolutionary genetics analysis version 6.0. *Mol. Biol. Evol.* 30, 2725–2729. doi: 10.1093/molbev/mst197

Tettelin, H., Saunders, N. J., Heidelberg, J., Jeffries, A. C., Nelson, K. E., Eisen, J. A., et al. (2000). Complete genome sequence of *Neisseria meningitidis* serogroup B strain MC58. *Science* 287, 1809–1815. doi: 10.1126/science.287.5459.1809

Turner, D. P. J., Marietou, A. G., Johnston, L., Ho, K. K. L., Rogers, A. J., Wooldridge, K. G., et al. (2006). Characterization of MspA, an immunogenic autotransporter protein that mediates adhesion to epithelial and endothelial cells in *Neisseria meningitidis*. *Infect. Immun.* 74, 2957–2964. doi: 10.1128/IAI.74.5.2957-2964.2006

Turner, D. P. J., Wooldridge, K. G., and Ala'Aldeen, D. A. A. (2002). Autotransported serine protease A of *Neisseria meningitidis*: an immunogenic, surface-exposed outer membrane, and secreted protein. *Infect. Immun.* 70, 4447–4461. doi: 10.1128/IAI.70.8.4447-4461.2002

van Putten, J. P. M., and Paul, S. M. (1995). Binding of syndecan-like cell surface proteoglycan receptors is required for *Neisseria gonorrhoeae* entry into human mucosal cells. *EMBO J.* 14, 2144–2154.

van Schilfgaarde, M., van Alphen, L., Eijk, P., Everts, V., and Dankert, J. (1995). Paracytosis of *Haemophilus influenzae* through cell layers of NCI-H292 lung epithelial cells. *Infect. Immun.* 63, 4729–4737.

van Ulsen, P., Adler, B., Fassler, P., Gilbert, M., van Schilfgaarde, M., van der Ley, P., et al. (2006). A novel phase-variable autotransporter serine protease, AusI, of *Neisseria meningitidis*. *Microbes Infect.* 8, 2088–2097. doi: 10.1016/j.micinf.2006.03.007

van Ulsen, P., and Tommassen, J. (2006). Protein secretion and secreted proteins in pathogenic *Neisseriaceae*. *FEMS Microbiol. Rev.* 30, 292–319. doi: 10.1111/j.1574-6976.2006.00013.x

van Ulsen, P., van Alphen, L., ten Hove, J., Fransen, F., van der Ley, P., and Tommassen, J. (2003). A *Neisserial* autotransporter NalP modulating the processing of other autotransporters. *Mol. Microbiol.* 50, 1017–1030. doi: 10.1046/j.1365-2958.2003.03773.x

Yi, K., Rasmussen, A. W., Gudlavalleti, S. K., Stephens, D. S., and Stojiljkovic, I. (2004). Biofilm formation by *Neisseria meningitidis*. *Infect. Immun.* 72, 6132–6138. doi: 10.1128/IAI.72.10.6132-6138.2004

**Conflict of Interest Statement:** The authors declare that the research was conducted in the absence of any commercial or financial relationships that could be construed as a potential conflict of interest.

frontiers in Cellular and Infection Microbiology

ORIGINAL RESEARCH
published: 17 January 2017
doi: 10.3389/fcimb.2017.00002

# Interaction of *Bacteroides fragilis* Toxin with Outer Membrane Vesicles Reveals New Mechanism of Its Secretion and Delivery

*Natalya B. Zakharzhevskaya[1]*, Vladimir B. Tsvetkov[1, 2, 3]*, Anna A. Vanyushkina[1], Anna M. Varizhuk[1], Daria V. Rakitina[1], Victor V. Podgorsky[1], Innokentii E. Vishnyakov[4, 5], Daria D. Kharlampieva[1], Valentin A. Manuvera[1], Fedor V. Lisitsyn[6], Elena A. Gushina[6], Vassili N. Lazarev[1, 7] and Vadim M. Govorun[1, 7, 8]*

[1] Federal Research and Clinical Centre of Physical-Chemical Medicine Federal Medical Biological Agency, Moscow, Russia, [2] Department of Polyelectrolytes and Surface-Active Polymers, Topchiev Institute of Petrochemical Synthesis, Moscow, Russia, [3] Department of Molecular Virology, FSBI Research Institute of Influenza, Ministry of Health of the Russian Federation, Saint Petersburg, Russia, [4] Lab of Genome Structural Organization, Institute of Cytology, Russian Academy of Sciences, Saint Petersburg, Russia, [5] Institute of Nanobiotechnologies, Peter the Great St. Petersburg Polytechnic University, Saint Petersburg, Russia, [6] N.F. Gamalei Federal Research Centre for Epidemiology and Microbiology, Ministry of Health Russian Federation, Moscow, Russia, [7] Lab of Systems Biology, Moscow Institute of Physics and Technology, Dolgoprudny, Russia, [8] Department of Proteomics, Shemyakin-Ovchinnikov Institute of Bioorganic Chemistry of the Russian Academy of Sciences, Moscow, Russia

OPEN ACCESS

**Edited by:**
*Thibault Géry Sana, Stanford University, USA*

**Reviewed by:**
*Anne-Marie Krachler, University of Texas Health Science Center at Houston, USA*
*Meta J. Kuehn, Duke University, USA*
*Lilian Lam, University of Oxford, UK*

***Correspondence:**
*Natalya B. Zakharzhevskaya*
*natazaha@gmail.com*
*Vladimir B. Tsvetkov*
*v.b.tsvetkov@gmail.com*

**Received:** *12 October 2016*
**Accepted:** *03 January 2017*
**Published:** *17 January 2017*

**Citation:**
*Zakharzhevskaya NB, Tsvetkov VB, Vanyushkina AA, Varizhuk AM, Rakitina DV, Podgorsky VV, Vishnyakov IE, Kharlampieva DD, Manuvera VA, Lisitsyn FV, Gushina EA, Lazarev VN and Govorun VM (2017) Interaction of Bacteroides fragilis Toxin with Outer Membrane Vesicles Reveals New Mechanism of Its Secretion and Delivery. Front. Cell. Infect. Microbiol. 7:2. doi: 10.3389/fcimb.2017.00002*

The only recognized virulence factor of enterotoxigenic *Bacteroides fragilis* (ETBF) that accompanies bloodstream infections is the zinc-dependent non-lethal metalloprotease *B. fragilis* toxin (BFT). The isolated toxin stimulates intestinal secretion, resulting in epithelial damage and necrosis. Numerous publications have focused on the interrelation of BFT with intestinal inflammation and colorectal neoplasia, but nothing is known about the mechanism of its secretion and delivery to host cells. However, recent studies of gram-negative bacteria have shown that outer membrane vesicles (OMVs) could be an essential mechanism for the spread of a large number of virulence factors. Here, we show for the first time that BFT is not a freely secreted protease but is associated with OMVs. Our findings indicate that only outer surface-exposed BFT causes epithelial cell contact disruption. According to our *in silico* models confirmed by Trp quenching assay and NMR, BFT has special interactions with outer membrane components such as phospholipids and is secreted during vesicle formation. Moreover, the strong cooperation of BFT with polysaccharides is similar to the behavior of lectins. Understanding the molecular mechanisms of BFT secretion provides new perspectives for investigating intestinal inflammation pathogenesis and its prevention.

**Keywords: toxin delivery, lipid protein interactions, shot gun lipidomics, Electron microscopy, fluorescence quenching, NMR**

## INTRODUCTION

Of the numerous microbial species that inhabit the gastrointestinal tract of mammals, Bacteroidetes is the most abundant gram-negative bacterial phylum (Ley et al., 2008). The anaerobe *Bacteroides fragilis* is a common colonic symbiont with an affinity for mucosal colonization, although it makes up only 1 to 2% of the cultured fecal flora (Huang et al., 2011). There are two molecular subtypes, non-toxigenic *B. fragilis* (NTBF) and enterotoxigenic *B. fragilis* (ETBF). ETBF is an intestinal

bacterium that has been associated with inflammatory bowel disease and colorectal cancer in humans (Prindiville et al., 2000; Toprak et al., 2006). The only well-studied virulence factor specific to ETBF is the secreted metalloprotease *B. fragilis* toxin (BFT) (Moncrief et al., 1995; Franco et al., 1997). BFT can affect zonula adherens and tight junctions in the intestinal epithelium by cleaving E-cadherin (Wu et al., 1998), resulting in rearrangements of the actin cytoskeleton of epithelial cells. BFT is synthesized as a 44.4-kDa precursor (pBFT), which is then processed into a 21-kDa mature BFT (mBFT) that is secreted into the supernatant of cultured cells (Kling et al., 1997). Three toxin isoforms have been described, BFT1, BFT2, and BFT3, with isoform BFT2 being the most common (Scotto d'Abusco et al., 2000). Although BFT is a secreted protease, nothing is known about the mechanisms of its secretion and transport to host cells. Gram-negative bacteria have evolved mechanisms to deliver virulence factors to the host (Koster et al., 2000). Well-studied examples include type III secretion systems (Galán et al., 2014), type IV secretion systems (Wallden et al., 2010), and type VI secretion systems, which are required for virulence factor transport to host cells (Hachani et al., 2016). Genomic studies of *B. fragilis* have not shown evidence of type III, IV, autotransporter, or two-partner secretion systems (Wilson et al., 2015). However, *B. fragilis* was shown to possess genes for Hly type I secretion systems, which are similar to the hemolysin type I secretion system HlyDb of *Escherichia coli* (Wang et al., 1991). Type VI secretion systems (T6SS) were recently discovered in a few Bacteroidetes strains, thereby extending the presence of these systems beyond Proteobacteria. Comprehensive analysis of all sequenced human gut Bacteroidales strains has shown that more than half contain T6SS loci (Coyne et al., 2016). T6SS as a multiprotein complex is specially organized into three distinct genetic architectures (GA) where GA1 and GA2 loci are present on conserved integrative conjugative elements (ICE) and are transferred and shared among diverse human gut Bacteroidales species. But GA3 loci are not contained on conserved ICE and are confined to *B. fragilis*. Thorough research has showed that GA3 loci of *B. fragilis* could be a source of numerous novel effector and immunity proteins (Chatzidaki-Livanis et al., 2016). But there is no evidence that T6SS may be used for *B. fragilis* toxin secretion.

Rather than secrete virulence factors into the surrounding milieu, where they could be degraded by host proteases, many gram-negative pathogens utilize outer membrane vesicles (OMVs) as a mechanism of delivering active proteins and other moieties into host cells (Kulp and Kuehn, 2010). Toxin delivery mediated by OMVs is recognized as a potent virulence mechanism for many pathogens (Ellis and Kuehn, 2010). It is now well known that both non-pathogenic and pathogenic gram-negative bacteria constitutively release OMVs (Kuehn and Kesty, 2005). OMVs are spherical proteoliposomes that have an average diameter ranging from 20 to 150 nm and that are enriched with outer membrane proteins, phospholipids, polysaccharides, and numerous proteins of a wide molecular mass range (Mashburn-Warren et al., 2008). Many periplasm-located virulence factors are enriched in OMVs, including Shiga toxin produced by *E. coli* and Cag toxin produced by *Helicobacter pylori* (Ismail et al., 2003; Kesty and Kuehn, 2004). The large number of enzyme-containing OMVs produced by *B. fragilis* suggests that OMV transport may be an important export pathway (Patrick et al., 1996; Cerdeño-Tárraga et al., 2005). Intracellular, periplasmic and outer membrane-bound proteases have been identified in *B. fragilis* (Elhenawy et al., 2014). Moreover, *B. fragilis* OMVs which contain surface located polysaccharide A have been shown to play an anti-inflammatory role by acting on regulatory T (Treg) cells (Shen et al., 2012). Many hydrolytic enzymes, which are generally considered pathogenic factors, may be bound to the membrane and/or secreted (Gibson and Macfarlane, 1988). Toxins secreted by enterotoxigenic *E. coli* and *V. cholerae* have been found to associate with LPS on the outer surface of OMVs (Horstman and Kuehn, 2002; Chatterjee and Chaudhuri, 2011), in a manner similar to lectins. Lectins are usually characterized by weak interactions between carbohydrates and proteins through hydrogen and coordinate bonds (Richards et al., 1979). Because the *B. fragilis* genome does not encode for known secretion system genes involved in BFT secretion and transport, we reasoned that BFT might be delivered to host cells by OMVs. Consequently, the toxin is incorporated in vesicle membranes during membrane formation due to interactions with outer membrane components, such as lipids and LPS. In the present study, we demonstrate that BFT is associated with OMV membranes through hydrophobic and electrostatic interactions and forms hydrogen and coordinate bonds with membrane components, similar to the behavior of lectins.

# RESULTS

## OMV Production by NTBF and ETBF and BFT2 Detection in Association with OMVs

To analyze the surface structure of both NTBF and ETBF strains, we examined the bacteria by TEM, which revealed the formation of OMVs on the cell surface (**Figure 1A**). It was observed that both strains (ETBF and NTBF) of *B. fragilis* produce vesicles (**Figures 1A,B** for ETBF and Supplementary Figures 2A,B for NTBF) with sizes ranging from 20 to 100 nm (**Figure 1C**). To avoid contamination with bacteria, small volume of OMV containing solution were cultivated on blood agar plates under anaerobic conditions for 2 days. *B. fragilis* colonies were not observed on blood agar plates.

After isolation of OMV containing fraction from 250 ml cultured cells, we measured the total protein concentration of the ETBF and NTBF OMV preparations, which was ∼40–60 μg in 50 μl. For toxin detection, we analyzed 40 μg ETBF and NTBF OMV preparations by western blot using polyclonal antibodies (anti-BFT2) specific to mBFT2 and pBFT2. As a result, we observed the association of mBFT2 with ETBF vesicles (**Figure 1D**). OMV-depleted medium was also used for toxin detection. Briefly, 100 ml OMV-free medium was lyophilized under reduced pressure by a rotary evaporator and analyzed by western blot with polyclonal antibodies (anti-BFT2). We did not detect any visible amount of free toxin. pBFT2 was not detected in the OMV fraction or in OMV-depleted medium. The cells fractions were also examined for toxin existence by

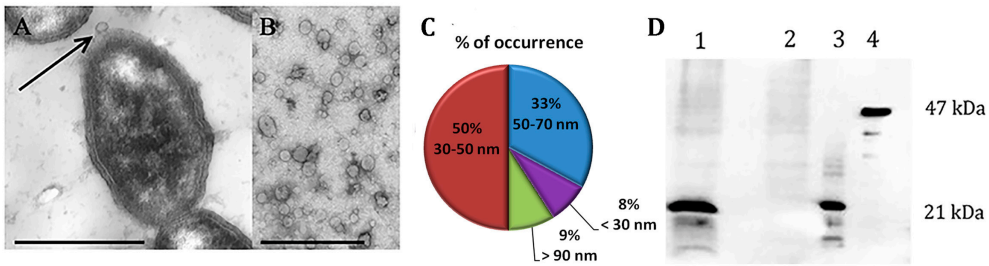


**FIGURE 1 | *B. fragilis* produces outer membrane vesicles (OMV), containing BFT.** TEM of thin section of ETBF cells during vesicle production **(A)** and isolated ETBF OMVs **(B)**, at magnification: x 10,000. Scale bars represent 1 μm for **(A)** and 300 nm for **(B)**. **(C)** OMV size distribution diagram determined from measurements of about 1000 OMVs from 10 samples **(D)**–5 μg of extracted OMV proteins of each strain (ETBF–1; NTBF–2) were run on 10% SDS-PAGE followed by western blot with antibody against BFT2. 100 ng of each recombinant forms of the toxin were also added (3–mBFT2 and 4–pBFT2).

western blot using polyclonal antibodies (anti-BFT2) specific to mBFT2 and pBFT2. As a result we detected major part of the pBFT2 in membrane fraction and small amount of pBFT2 in periplasm fraction of ETBF cells (Supplementary Figures 1A,B). We examined cells fractions by Q-TOF analysis (Supplementary Information 1).

To confirm the localization of the toxin in the bacterial membrane and in the OMV preparation, we performed immunoelectron microscopic analyses of thin sections using gold nanoparticles coupled with anti-BFT2 antibodies. We detected gold particles coupled with anti-BFT2 antibodies on the membrane and in the periplasm of ETBF (**Figures 2A,C**, **indicated by arrow**), which confirmed the previous results obtained by western blot analysis. There was no labeling of the same structure in NTBF cells (**Figure 2H** and Supplementary Figure 2A). We observed several labels located in the cytoplasm of bacterial cells, potentially indicating toxin formation (**Figures 2B–D**). Dynamics of OMV formation and release from the bacterial cell surface were monitored (**Figure 2B**, **indicated by arrow**). Importantly, we observed label predominantly located on the outer membrane (**Figure 2D**, **indicated by arrow**). ETBF and NTBF OMV samples were negatively stained and labeled with anti-BFT2 antibodies coupled with gold particles. We also examined freely isolated OMVs preparation for toxin localization by immunogold staining. We observed that the label was located on the surface of the ETBF OMV, indicating that the toxin was associated with the outer membrane (**Figures 2E–G**). There was no labeling of the same structure in NTBF OMVs (**Figure 2I** and Supplementary Figure 2B).

## Shot-Gun Lipidomics of the *B. fragilis* Outer Membrane

To detect the components of the *B. fragilis* membrane, which the toxin could potentially interact with, shot-gun mass spectrometric analysis of the isolated membrane lipids and LPS extracts was performed. In the fragmentation spectra of membrane lipids, we primarily detected characteristic ions of polar groups of phospholipids, variable fatty acid residues capable of forming different diacylglycerol esters, cycles, and other compounds with water loss. The full list of the identified ions is shown in Supplementary information 2 (Table 1). As expected, the most represented ions in the spectrum belonged to the classes of phosphatidylethanolamine (PE), phosphatidylcholine (PC), and diacylglycerol (DG) (**Figure 3**).

To determine the specific molecular structure of *B. fragilis* LPS, we performed comprehensive mass spectrometry analysis. We used the Tri-Reagent method to extract LPS from *B. fragilis* cell membranes (Elhenawy et al., 2014). To profile the extracted LPS, we used direct injection electrospray-time-of-flight mass spectrometry in negative ion mode as described in the **Materials and Methods** section. As a result, we identified 38 different LPS compounds in the *B. fragilis* LPS preparation [Supplementary information 2 (Table 2)]. Among the detected ions, we reliably identified lipid A-disaccharide-1-P, 3-deoxy-D-manno-octulosonyl-lipid IV(A), KDNalpha2-3Galbeta1-4Glcbeta-Cer[d18:1/24:1(15Z)] and numerous galactosylceramides and glucosylceramides (polysaccharide chains consisting of 4 to 8 carbohydrate units). The identified lipid A-disaccharide-1-P structure was the same as that previously described by Elhenawy et al. (Patrick et al., 1996). As expected, the most represented ions in the spectrum belonged to classes of cerebrosides that are normally produced by *B. fragilis* cells. The mass spectrometry metabolomic data have been deposited to UCSD Center for Computational Mass Spectrometry (MassIVE ID: MSV000080382).

## Modeling and Docking of Phospholipids (PC and PE), lipid A, Polysaccharide Chain, and BFT2 (mBFT2, pBFT2)

Two phospholipids of the most abundant classes represented in *B. fragilis* membranes (PC and PE) according to our shot-gun lipidomics data and the main components of LPS [lipid A and polysaccharide chain (PSC)] were docked to pBFT2 and mBFT2 surfaces. Modeling of the pBFT2 and mBFT2 surfaces according to hydrophobic potential distribution, cavities, and potential donors and acceptors of hydrogen bond distribution is shown in Supplementary Figures 3, 4.

The conformations of mBFT2 complexes with PE, PC, lipid A, and PSC with best values of binding energies are shown

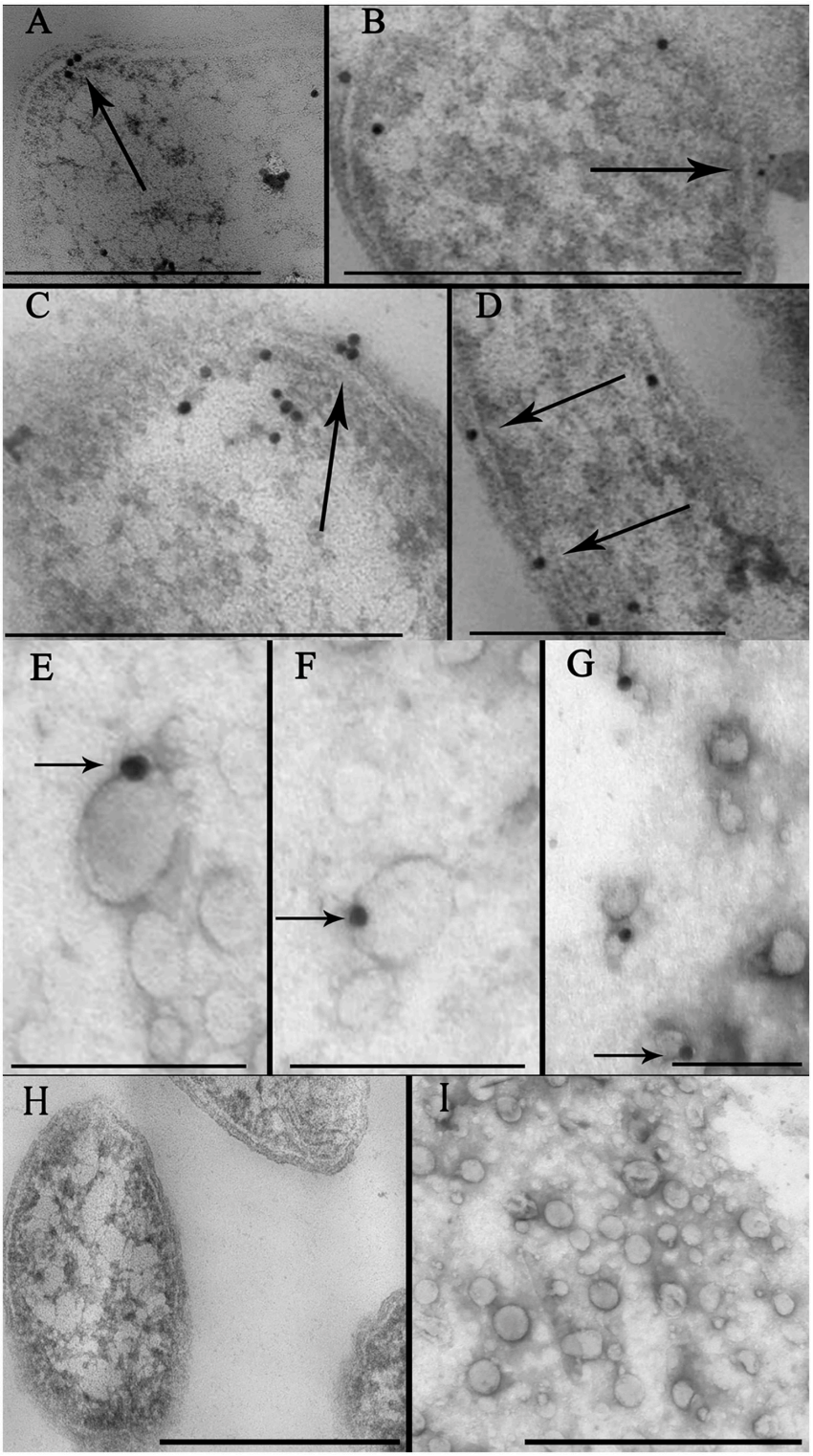


**FIGURE 2 | Identification of toxin cell and OMV localization via immune-microscopy with antibodies against BFT. (A–D)** Thin sections of ETBF cells analyzed by TEM contain some labels (black dots) coupled with antibodies against BFT fixed on periplasm and membrane (indicated by arrow). Several labels coupled with antibodies against BFT fixed on cytoplasm indicating probable toxin formation. Scale bars represent 300 nm for **(A)** and **(D)**, 500 nm for **(B)** and **(C)**. **(E–G)**—Negatively stained OMV preparations isolated from ETBF culture and coincubated with labels, (black dots indicated by arrow) coupled with antibodies against BFT were analyzed by TEM. Scale bars represent 100 nm for **(E,F)** and 150 nm for **(G). (H)** Thin section of NTBF cells analyzed by TEM contains no fixed labels coupled with antibodies against BFT. **(I)** Negatively stained OMV preparations isolated from NTBF culture contain no fixed labels coupled with antibodies against BFT. Scale bars represent 600 nm for **(H)** and 400 nm for **(I)**.

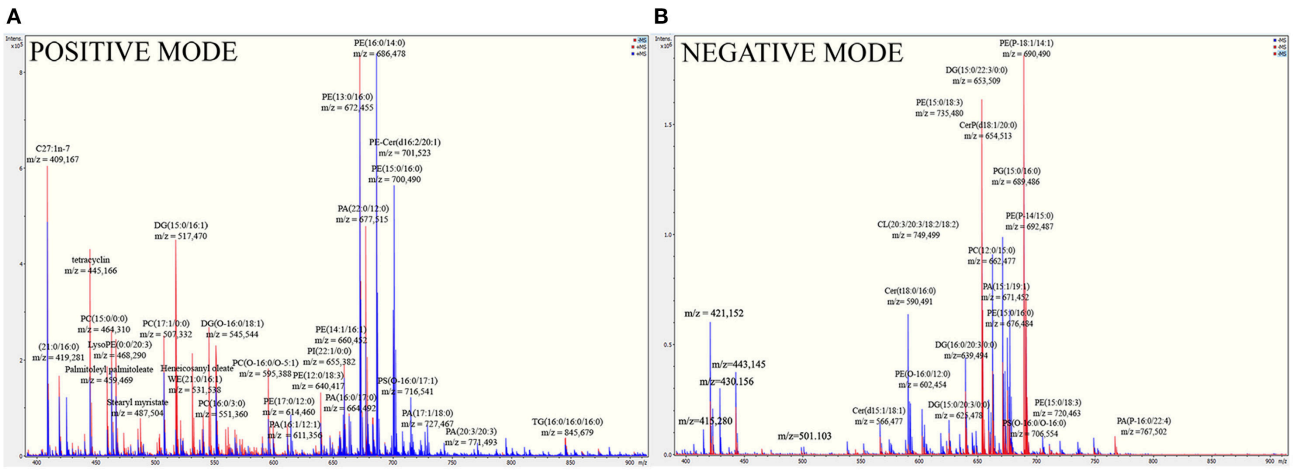


**FIGURE 3 | Full mass spectra of *B. fragilis* lipids show the most represented lipids of *B. fragilis* membrane. (A)** MS analysis of ETBF (colored in red) and NTBF (colored in blue) membrane in positive linear mode. **(B)** MS analysis of ETBF (colored in red) and NTBF (colored in blue) membrane in negative linear mode. *B. fragilis* cells membrane lipids were extracted by Folch method (see material and methods), dissolved in 200 μl ethanol and analyzed by quadruple time-of-flight tandem mass spectrometer. Mass spectrum of ETBF and NTBF in positive and negative linear mode showed the same cluster of peaks, indicating the most represented classes of lipids (PC, PE, DG, PA).

in **Figures 4**, **5**. As is evident from **S**upplementary information 2 (Table 3), hydrophobic interactions as well as electrostatic make a significant contribution ($\Delta G_{non-polar}$) to the binding energy upon complex formation for both proteins (mBFT2 and pBFT2). The Coulomb contribution ($\Delta G_{el}$) in the case of pBFT2 complex formation is insignificant ($\Delta G_{el}$ comparable to $\Delta G_{non-polar}$) compared with mBFT2 complex formation due to the latter's interaction with the zinc ion. Furthermore, the loss of conformational mobility during binding by the ligand as well as by the target leads to a decrease in entropy ($T\Delta S$) which reduces binding energy. Also note that electrostatic component of solvation energy ($\Delta G_{polar}$) significantly decreases binding energy.

Lipids can form H-bonds with amino acid residues on pBFT2/mBFT2 groove surfaces (Supplementary Figures 5, 6, PC acts as an acceptor, and PE can be either a donor or an acceptor).

Importantly, the nitrogen group of PE tends to form donor-acceptor bonds with amino acids located in the mBFT2 cavity (**Figure 4A**, **indicated by arrow**). In contrast, hydrophobic contributions are greater in the case of pBFT2 probably due to the larger size of the pBFT2 surface groove compared to that of mBFT2.

Lipid A, as a main component of LPS, also forms H-bonds with amino acid residues on the mBFT2 groove surface (**Figure 5A**). The lipid A molecule contains two-fold the amount of fatty acid residues compared to PE and PC and therefore makes a significant hydrophobic contribution to mBFT2-lipid A complex formation [(Supplementary information 2 (Table 3)]. In accordance with Elhenawy et al., the lipid A molecule contains a phosphate group, but PSC may exist without the phosphate group in an aqueous medium (Elhenawy et al., 2014). PSC is composed of long chains of monosaccharide units bound together by glycosidic linkages, which form multiple H-bonds with mBFT2 amino acids (**Figure 5C**). These interactions may have a significant impact on polysaccharide chain-mBFT2 complex formation.

Importantly, non-ester phosphate oxygen atoms of PC/PE (**Figures 4B,D**), lipid A (**Figure 5B**), and PSC (**Figure 5D**) tend to form coordinate bonds with the zinc ion in the active center of mBFT2. Carbonyl oxygen atoms of PC/PE might also form such bonds with the zinc ion. According to our data, electrostatic contributions are higher for the lipid-mBFT2 complex than for the lipid-pBFT2 complex, indicating possible coordinate bond formation [$\Delta Gel_{(PE+pBFT)}$; $\Delta Gel_{(PC+pBFT)} < \Delta Gel_{(PE+mBFT)}$; $\Delta Gel_{(PC+mBFT)}$] [(Supplementary information 2 (Table 3)].

## Trp Fluorescence Quenching Assay and 1H-NMR Spectroscopy of BFT-Lipid Complexes

In the above molecular modeling and docking experiments, we identified the most abundant classes of phospholipids of the *B. fragilis* membrane (PE and PC) and demonstrated their interaction with the mBFT2 and pBFT2 surfaces *in silico*. Next, the propensity of mBFT2 and pBFT2 to form complexes with PC was tested using 1H-NMR and Trp fluorescence quenching (**Figure 6**). Comparison of NMR spectra of PC alone and PC mixed with pBFT2/mBFT2 (**Figures 6A,B**) revealed changes in the chemical shifts and peak widths of the fatty acid signals (0—4 ppm), which indicated changes in PC conformation and mobility upon complex formation.

The Trp fluorescence quenching assay, a popular method for investigating lipid-protein interactions (Dua et al., 1995; Kraft et al., 2009), was chosen because BFT2 contains 4 Trp residues in its catalytic site. Proteinase K was used as a negative control, and BSA, which is known to bind lipids in the medium nanomolar range (Charbonneau and Tajmir-Riahi, 2010), was used as a positive control. Intrinsic protein fluorescence was monitored at the Trp/Tyr emission maximum upon excitation at 295 nm

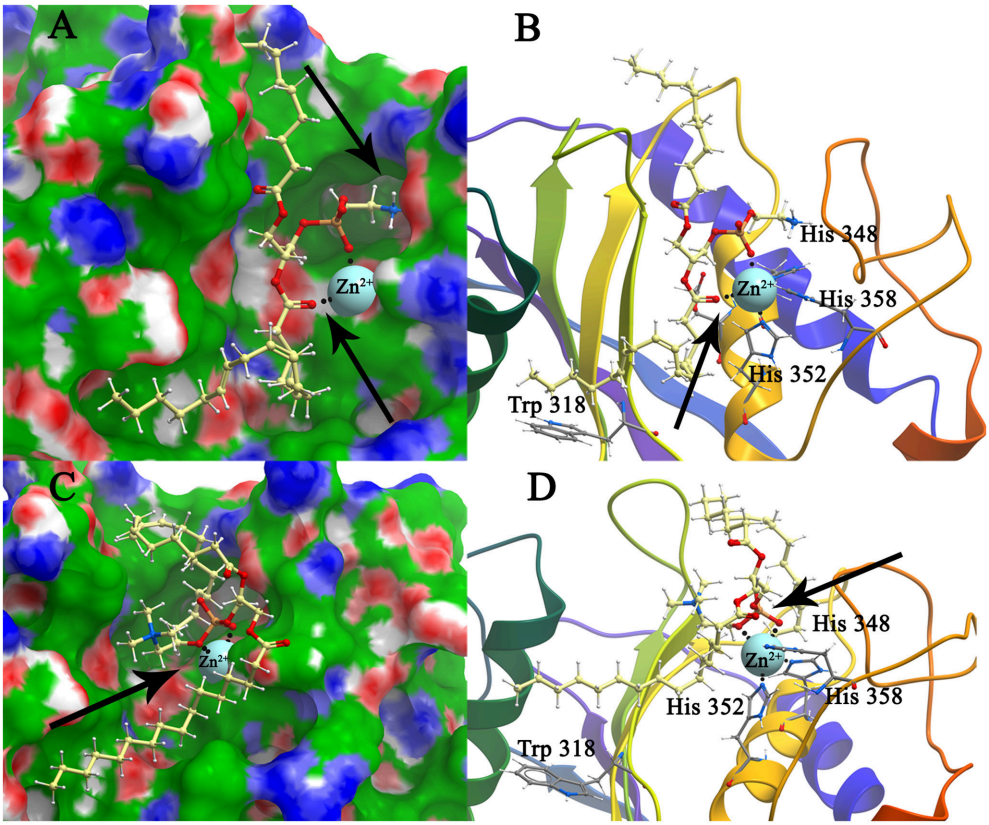


**FIGURE 4 | Structure model of mBFT and best (according to the binding energy) ligands (A)**—PC and **(C)**—PE location on the mBFT Conolly surface, painted depending on the values of the hydrophobic potential—green, donors—blue, acceptors—red, resulting docking via ICM. The atoms of the ligands are painted in the following colors: polar hydrogens—blue, nitrogen—dark blue, oxygen—red, phosphorus—orange, carbon—white. Zn ions are painted in blue. The non-polar hydrogens not shown. Black dot lines indicate hydrogen bonds. Oxygen of lipid phosphate group colored in red forming coordination bonds with zinc ion. Nitrogen group of PE forming donor-acceptor bounds with amino acids indicated by arrow. Detailed image of mBFT active center with PC **(B)** and PE **(D)**.

(Trp fluorescence, selectively, **Figures 6C,D**) or 280 nm (Trp and Tyr fluorescence, **Figures 6E,F**) in the presence of increasing concentrations of PC organized in liposomes by reverse-phase evaporation. The results suggest the formation of 1:1 protein-lipid complexes in a low ionic strength buffer and the formation of 3:1 mBFT2-lipid complexes in the standard PBS buffer. Importantly, the presence of larger aggregates with a different stoichiometry at high lipid concentrations cannot be excluded, as Trp fluorescence is likely only sensitive to initial saturation.

According to our docking models, non-ester phosphate oxygen atoms of the lipids tend to form coordinate bonds with the His-bound zinc ion in the active center of mBFT2. To test the model and the potential involvement of these coordinate bonds, we analyzed a BFT2 mutant with no His residues and, thus, no zinc ions in the active site. Both mutant forms (mBFT2-mut and pBFT2-mut) demonstrated enhanced affinity to PC, which may be attributed to their increased hydrophobicity, as the charged His residues had been replaced with polar but uncharged Tyr residues. The fact that mBFT2-mut bound with PC more efficiently than the wild-type protein argues against a major contribution by zinc to complex formation.

The Trp fluorescence quenching assay demonstrated that the most represented lipids of the *B. fragilis* cell membrane (PC and PE) form complexes with mBFT2, but to determine the lipid chemical groups capable of such interactions, NMR spectroscopy was performed. Similar to Trp fluorescence quenching assay results, constant values ($K_d$) calculated for PC-mBFT2 and PE-mBFT2 complexes had slight differences, confirming the specific nature of a protein-lipid interaction. Thus, PC was used as a model of protein-lipid complex formation. We used 5 μM of each form of BFT2 (pBFT2 and mBFT2) and 0.6 μM PC in a water solution to study complex formation. Common 1D proton (with WATERGATE water suppression) (**Figures 6A,B**) and 2D DOSY NMR spectra of PC, BFT2 forms and mixtures were obtained. L-α-phosphatidylcholine (P3556, Sigma Aldrich) was used as the model PC. We observed that PC formed a micelle suspension in the water solution. According to the diffusion NMR spectroscopy results, the micelles consisted of a rather large number of molecules (~10 molecules per micelle). This result corresponds to the literature on this topic (Mashburn-Warren et al., 2008). The diffusion coefficients of pBFT2 and mBFT2 in water solutions were $D = -8.4$ log($m^2$/s) and $D = -8.9$

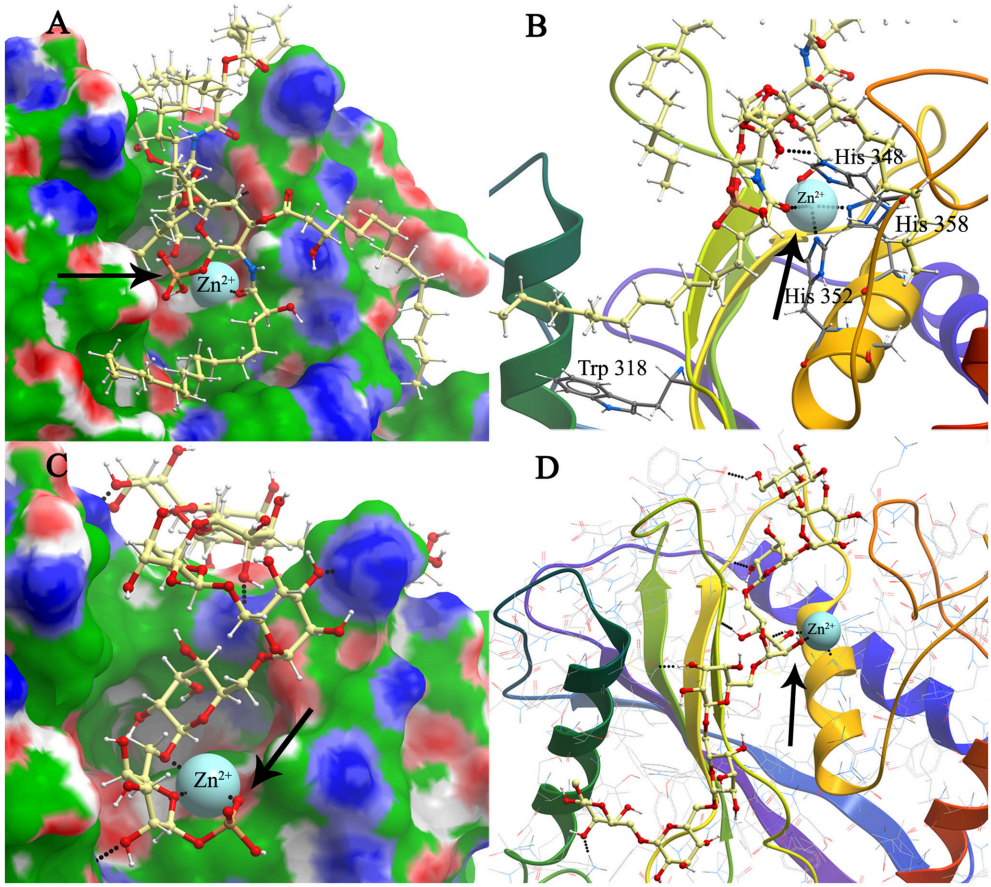


**FIGURE 5 | Modeling and docking of protein-lipid A and polysaccharide chain association.** Structure model of mBFT and best (according to the binding energy) ligand–lipid A **(A)** and polysaccharide chain **(C)** location on the mBFT Conolly surface, painted depending on the values of the hydrophobic potential—green, donors–blue, acceptors–red, resulting docking via ICM. Oxygen of lipid phosphate group colored in red forming coordination bonds with zinc ion (indicated by arrow). The atoms of the ligands are painted in the following colors: Polar hydrogens–blue, nitrogen–dark blue, oxygen–red, phosphorus–orange, carbon–white. Zn ions are painted in blue. The non-polar hydrogens not shown. Black dot lines indicate hydrogen bonds. Oxygen of lipid phosphate group colored in red forming coordination bonds with zinc ion. Detailed image of mBFT active center with lipid A **(B)** and polysaccharide chain **(D)**.

log($m^2$/s), respectively. The diffusion coefficient for PC in the water solution was D = −8.2 log($m^2$/s). The diffusion coefficients of PC and pBFT2 in the mixture were altered [D = −9.1 log($m^2$/s) and D = −8.6 log($m^2$/s), respectively] (**Figure 6A**) compared to the diffusion coefficients of each alone**.** The lipid molecules in the mixture were less mobile than in micelles in solution, and the protein molecules were also slightly less mobile in the mixture. In addition, the chemical shifts and peak widths of the fatty acid of PC in the mixture were slightly changed. Peak width changes in this case may be caused only by $T_2$ relaxation time, i.e., by PC mobility or conformation change. All these changes together may be explained by phospholipids-protein complex formation. Only one type of diffusion coefficient for PC and pBFT2 was present in the mixture, indicating that only one type of protein-phospholipid complex was present in the solution. The difference between the diffusion of free pBFT and pBFT2 in complex was not large. Consequently, complex formation probably causes only a protein conformation change. The results could be interpreted as the association of small lipid particles with the protein molecule core and PC shell. The results of NMR experiments with mBFT2 were similar to those described above (**Figure 6B**). mBFT2 also formed a complex in mixture with PC. However, the mBFT2 molecules were also partially self-aggregated, which was shown by 2D DOSY results. There were two fractions in the mBFT2 solution with diffusion coefficients D = −8.9 log ($m^2$/s) and D = −9.3 log ($m^2$/s). The mobility of the protein was also lower in the mixture with PC than individually, and PC in the mixture was less mobile as well. The diffusion coefficients of PC and mBFT2 in mixture were D = −8.7 log($m^2$/s) and D = −9 log($m^2$/s), respectively. The NMR data have been deposited to UCSD Center for Computational Mass Spectrometry (MassIVE ID: MSV000080385).

## OMV-Associated BFT Is Biologically Active

E-cadherin is a 120-kDa type I transmembrane protein essential to the intercellular adhesion of adjacent epithelial cells, which are the primary known substrate for BFT protease activity (Remacle et al., 2014). Given that mBFT2 was associated with OMVs,

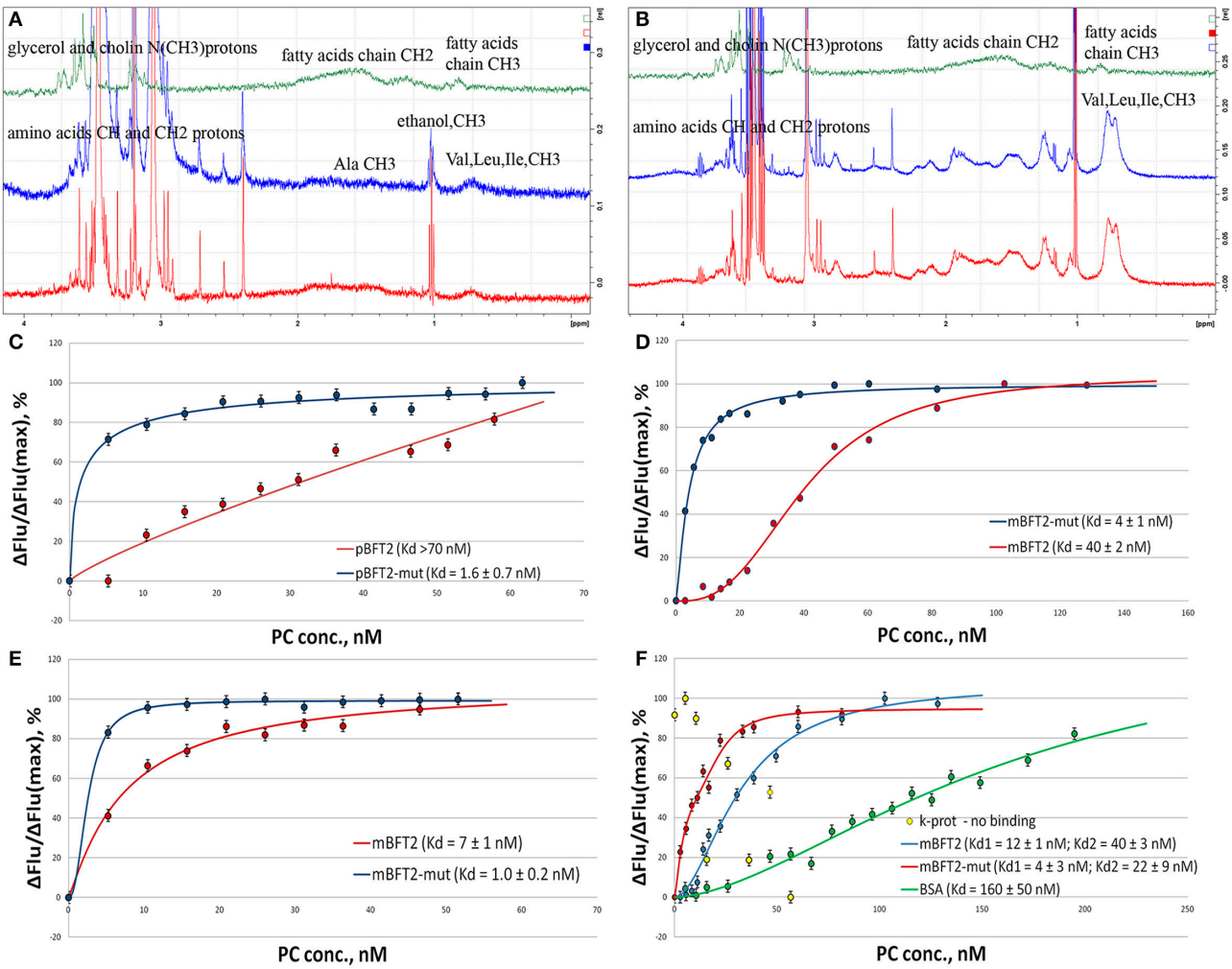


**FIGURE 6 | 500 MHz 1D proton.** NMR spectra of individual PC, pBFT2, and mBFT2 or their mixture **(A,B)** and fluorescence quenching assay**(C–F)**. **(A)** 500 MHz 1H-NMR spectra of PC (green), pBFT2 (blue), and their mixture (red), (0–4 ppm region). **(B)** 500 MHz 1H-NMR spectra of PC (green), mBFT2 (blue), and their mixture (red). **(C–F)** Trp fluorescence quenching. Conditions: The standard PBS buffer (**C–E**) or the low ionic strength buffer with Zn (**F**); excitation at 295 (**C,D**) or 280 nm (**E,F**) 20°C. Protein concentration was 3 nM. Error bars indicate standard deviation for three measurements.

vesicle treatment should promote E-cadherin degradation in HT-29 cells. Using western blot analysis (**Figure 7B**), we observed time-dependent degradation of the 120-kDa subunit E-cadherin and its complete cleavage after 2 h of treatment with ETBF OMV in HT-29 cells. To confirm the effect of mBFT2-containing OMVs of ETBF on E-cadherin degradation, we used NTBF OMV at the same time points, and there was no effect.

The effect of toxins on E-cadherin could be dependent on mBFT2 OMV localization. BFT2 can be located inside the vesicles, in the vesicle membrane, or on the OMV surface. We produced two types of liposomes that were reverse-phase constructed with PC. In the first case, the toxin was encapsulated into the liposomes by a reverse-phase evaporation method, while in the second case, mBFT2 was added to the prepared liposomes. We verified the encapsulation of BFT2 into liposomes and analyzed whether unbound BFT2 was present in the medium by western blot (**Figure 7C**). We found that all of the added BFT2 was associated with liposomes, as we did not observe free BFT2 in the medium after centrifugation. Two types of liposomes with mBFT2 and pBFT2 were used for E-cadherin degradation experiments.

We observed complete E-cadherin degradation in HT-29 cells after 2 h of treatment with liposomes with added mBFT2 (**Figure 7A**). The same effect was shown using mBFT2 without liposomes. There was no E-cadherin cleavage when HT-29 cells were incubated with mBFT2 encapsulated into the liposomes. As expected, we did not observe any effect of pBFT2 on E-cadherin.

As described previously, OMVs can be used for virulence factor delivery to host cells. OMVs isolated from ETBF (**Figure 7D**) and NTBF (**Figure 7E**) were labeled with the lipophilic dye DiI, and two forms of the toxin [mBFT2 (**Figure 7F**) and pBFT2 (**Figure 7G**)] were independently added

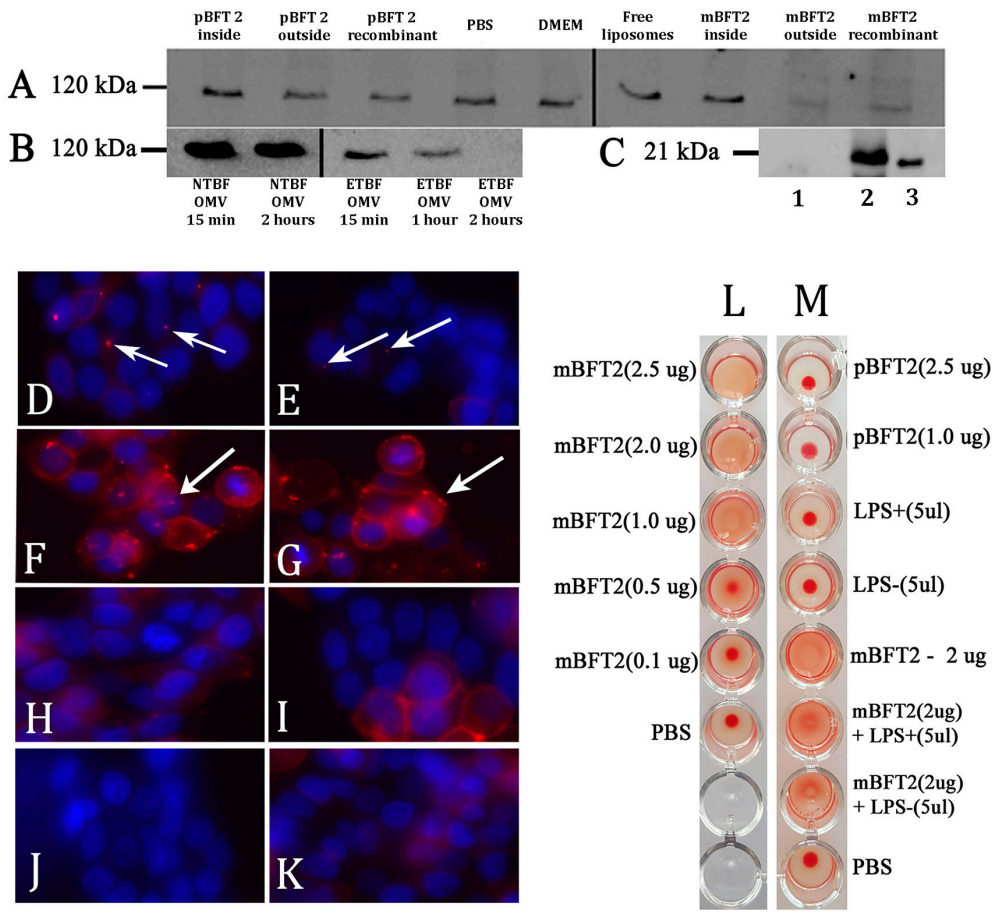


**FIGURE 7 | Toxin containing liposomes and OMVs show proteolytic activity against HT-29 cell line E-cadherin and form complexes (A–K).** Hemagglutination test **(L–M) (A)** Biological effects of the toxin to E-cadherin dependent of its localization. 12 nM pBFT2 and 14.2 nM mBFT2 encapsulated into liposome (pBFT2 inside and mBFT2 inside) or added to prepared liposomes—(pBFT2 outside and mBFT2 outside) were coincubated with HT-29 cells. Recombinant proteins were also coincubated with HT-29 cells (12 nM pBFT2–pBFT2 recombinant; 14.2 nM mBFT2–mBFT2 recombinant). PBS, DMEM and Free liposomes were used as negative controls. **(B)** Biological effect of the toxin containing OMVs to E-cadherin is time depended. 50 μg of total ETBF OMV proteins were coincubated with HT-29 cells for 15 min (ETBF OMV for 15 min), for 1 h (ETBF OMV for 1 h), for 2 h (ETBF OMV for 2 h). The same amounts of NTBF OMV proteins were coincubated with HT-29 cells for 15 min (NTBF OMV for 15 min) or for 2 h (NTBF OMV for 2 h). Extracted HT-29 cells proteins **(A,B)** were run on 10% SDS-PAGE followed by western blot with antibody against E-cadherin. **(C)** Toxin encapsulation and toxin-liposome association were examined by western blot. 14.2 nM mBFT2 with previously added prepared liposomes were dissolved in sterile culture media. After ultracentrifugation step supernatant was examined to unbound toxin—(lane 1), 14.2 nM mBFT2 encapsulated into the liposomes were treated with Proteinase K (20 ng/μl) and run on 10% SDS-PAGE followed by western blot with antibody against mBFT2–(lane 2). Recombinant protein—14.2 nM mBFT2—lane 3. **(D–K)** Complexes formation was examined by fluorescent microscopy. 3 μg OMVs, isolated from ETBF-**(D)** and NTBF-**(E)**; 12 nM pBFT2-**(F)** and 14.2 nM mBFT2-**(G)** were added to 100 μl prepared liposomes; 14.2 nM mBFT2-**(H)** and 12 nM pBFT2-**(I)** were encapsulated into the liposomes. **(J)**-10 μl VybrantDil were added to PBS and centrifuged at 100,000 g. **(K)**-100 μl liposomes. All samples **(D–I, K)** were labeled with VybrantDil (red) and coincubated with HT-29 cells for 1 h. Nuclei were stained with DAPI (blue). Arrows indicate protein-lipid complexes located on cells surfaces. **(L)**-Hemagglutination activity of mBFT2 depends on toxin concentration. **(M)**-Hemagglutination activity of mBFT2 and pBFT2 in a presence of LPS.

to the prepared liposomes and then incubated with HT-29 cells for 1 h. We also tested two forms of the toxin [mBFT2 (**Figure 7H**) and pBFT2 (**Figure 7I**)] encapsulated in liposomes for their ability to form complexes. As a control, we used free DiI-labeled liposomes that were also incubated with HT-29 cells for 1 h (**Figure 7J**). Moreover, to reduce possible false positive cell coloring, we dissolved 10 μl of stock DiI solution in PBS and centrifuged it at 100,000 × g; the resulting sediment dissolved in PBS was used for HT-29 cell labeling (**Figure 7K**). In agreement with our previous results, mBFT2 and pBFT2 added to the prepared liposomes formed complexes located on the cell surface (**Figure 7F,G**, **protein-lipid complexes indicated by arrows**). We observed ETBF OMVs and NTBF OMVs located on the cell surface, confirming that OMVs are used for protein delivery. Additionally, the relatively few NTBF OMVs located on the cell surface compared with ETBF OMVs may indicate that the toxin facilitates adherence between OMVs and cell membranes. We did not observe any labeled liposomes with encapsulated toxins on the cell surface, confirming the role of the toxin in complex formation.

## Hemagglutination Test

Since pBFT2 and mBFT2 tend to form H-bonds and coordinate bonds with membrane components, including LPS, we examined the hemagglutination and lectin activity for both types of the toxin. First, increasing concentrations (0.1–2.5 μg) of mBFT2 were tested for the ability to induce hemagglutination. We detected erythrocyte hemagglutination with mBFT2 at concentrations of 2.5 and 2 μg (**Figures 7L,M**). pBFT2 did not demonstrate hemagglutination activity. We also identified inhibition of hemagglutination when mBFT2 was premixed with LPS isolated from ETBF and NTBF. LPS alone did not demonstrate hemagglutination activity (**Figure 7M**).

# DISCUSSION

OMVs are considered to be one of the types of bacterial secretion system. Moreover, this secretion mechanism is well known in *B. fragilis* (Patrick et al., 1996; Elhenawy et al., 2014). Recently it has been described that *B. fragilis* contains T6SS, which is likely a source of numerous novel effector and immunity proteins (Coyne et al., 2016). But there is no evidence that this could be the mechanism for toxin secretion. In our study we hypotized that OMVs can be utilized for *B. fragilis* toxin secretion.

In our experiments, we demonstrated that both strains (ETBF and NTBF) of *B. fragilis* produce vesicles, and we detected mBFT2 in vesicles by western blot assay, suggesting that OMVs could be the mechanism of BFT secretion. As expected, microscopy assay results were in agreement with cells fractions and OMVs western blot results. We observed labeled antibodies against BFT2 in the periplasm, in membrane and in the vesicle membranes. Moreover, pBFT2 was detected primarily in membrane fraction but was not detected in OMVs suggesting possible toxin maturation in cells membrane. An NTBF cell fraction and OMVs isolated from NTBF culture were used as negative controls in all experiments.

The main visual biological effect of toxin exposure is that mBFT2 affects zonula adherens by cleaving E-cadherin. We used OMVs isolated from ETBF and NTBF to evaluate their biological activity against E-cadherin. As expected, we detected time-dependent E-cadherin degradation upon ETBF OMV treatment, but no degradation with NTBF OMV treatment, confirming that the toxin is active and associated with OMVs.

According to a recent publication, there is a special mechanism of OMV protein sorting. It was shown in *Campylobacter jejuni* that CDT toxin is not associated with membranes and is localized on the inner surface of the vesicles. This result was confirmed by OMV protease treatment, during which the toxin was not degraded because it was inside the vesicles (Lindmark et al., 2009). We used Proteinase K (20 ng/μl) treatment to determine possible toxin localization by western blot analysis and found that BFT2 was fully degraded within 10 min of Proteinase K treatment. These results indicate that the toxin is located on the OMV surface. To confirm surface-located toxin activity against E-cadherin, we prepared several types of liposomes with different localizations of the mBFT2. pBFT2 was used as a negative control because the immature toxin form does not contribute to E-cadherin degradation (Wu et al., 1998). In HT-29 cells treated with all liposome-toxin preparations, we observed E-cadherin degradation only when the toxin was added to the previously prepared liposomes, indicating that OMV-associated BFT2 is located on OMV surface. We observed toxin-liposome complexes labeled with the lipophilic dye DiI on the surface of HT-29 cells. Complex formation occurred only in the presence of toxin, which acted as an adhesive element. As expected, both types of OMV (isolated from ETBF and NTBF) were found on the HT-29 cell surface. Most likely, the ETBF and NTBF vesicle membranes contain adhesion proteins that facilitate OMV binding to the cell surface followed by internalization.

BFT could interact with a membrane protein receptor sensitive to depletion of membrane cholesterol (Wu et al., 2006). In this study, we hypothesized that BFTs interact with OMV membrane components, including phospholipids and LPS before binding with the potential receptor. First, we identified the *B. fragilis* membrane lipids and LPS using mass spectrometry. As expected, the most represented ions in the spectrum belonged to PE and PC classes, as they are prevalent lipid components of gram-negative bacteria membranes (Epand et al., 2007). Furthermore, we identified the lipid A and polysaccharide chain structures of *B. fragilis* LPS.

These results were further used for modeling and docking experiments. The mass spectrometric analysis results we obtained completely corresponded to data previously reported by Elhenawy et al. (2014). It should be noted that Elhenawy et al. previously characterized the same structure of lipid A and showed no difference between bacterial outer membrane and OMV lipid A structure. We identified that *B. fragilis* LPS consisted of a poly- and oligosaccharide region composed by monogalactosyl and -glucosyl units (up to 8 carbohydrate units in the chain) linked to lipid A-disaccharide.

We used the identified phospholipids, lipid A, and polysaccharide chain structures to model their interaction with mBFT2 and pBFT2. Polysaccharide chain and lipid A showed comparable binding energy values in docking with mBFT2. As expected, we observed the formation of multiple H-bonds between monosaccharide units of polysaccharide chain and amino acid residues of mBFT2, but an unusual effect was the coordinate bond formation between the oxygen of phosphate groups and zinc ion. This interaction is similar to the formation of non-covalent bonds in lectins, which have special binding sites for polysaccharides and form coordinate bonds with metal ions (Sharon, 1987; Abhilash et al., 2013). However, lectins are characterized by non-covalent interaction with sugars, not with lipids. The docking procedure for pBFT2 and LPS components was not performed because we did not expect the immature form of the protein to bind to LPS.

Despite the fact that mBFT2 is a soluble protease, we demonstrated, through the docking modeling that both mBFT2 and pBFT2 might hydrophobically interact with phospholipids. Carbonyl oxygen atoms of PC/PE (as it was shown for LPS components) formed coordinate bonds with the zinc ion located in the active center of mBFT2 after its processing. By diffusion NMR spectroscopy and Trp fluorescence quenching assays,

we evaluated the formation of pBFT2-lipid and mBFT2-lipid complexes. NMR data indicated that the fatty acid residues participate directly in these interactions. The mutant protein mBFT2-mut, which does not contain a zinc ion in the active site, demonstrated enhanced affinity for PC, which argues against a major role for the coordinate bonds. We also observed enhanced affinity of the mutant form of pBFT2 for PC, which could result from the conformational alterations caused by the mutation or somewhat increased hydrophobicity.

High lipid-protein tropism was also shown in cell culture experiments. The formation of mBFT2-lipid complexes associated with the cell surface was demonstrated by microscopic assay. It was also shown that labeled vesicles were located on the cell surface. Our microscopy results confirmed previous experiments reported by Sears et al. where labeled recombinant toxin was also located on the cell surface (Wu et al., 2006).

Based on the obtained results, we propose a mechanism of toxin secretion (**Figure 8**). pBFT2 interacts with cellular membrane lipids and accumulates in the inner membrane. In periplasm possibly it undergoes processing via proteolytic cleavage by a *B. fragilis* cysteine protease, forming the active version of the toxin (mBFT2) (Herrou et al., 2016). Oxygen atoms of lipid phosphate groups located on the inner surface of the outer membrane bilayer interact with the active center of mBFT2, simultaneously forming coordinate bonds with the zinc ion. Thermal motion of the protein leads to a local stretching of the lipid, facilitating the cessation of hydrophobic interactions with its membrane pair. Fatty acid tails of lipids tend to occupy the free grooves in mBFT2, resulting in the promotion of mBFT2 outside the outer membrane. At this point, vesicle formation could occur, and the toxin incorporated into the OMV membrane will be delivered to the host cell. However, the proposed model of toxin promotion through the membrane does not exclude the possibility of potential secretion system involvement.

The protein could also be promoted to the OMV surface, forming new, stronger electrostatic and hydrogen bonds with LPS components and disrupting previous focal and hydrophobic bonds between the lipid and protein. Further protein motion becomes impossible due to significant hydrogen bond formation between the LPS carbohydrate moiety and the toxin. The same protein-carbohydrate communication was demonstrated previously in numerous studies for lectins (Soult et al., 2014). Lectins and carbohydrates are linked by a number of relatively weak interactions that ensure specificity. The interactions between one cell surface with carbohydrates and another with lectins resemble the action of Velcro in that each interaction is relatively weak but the composite is strong. Today, the adhesins and toxins produced by *Vibrio cholerae*, *Shigella dysenteriae,* and *Bordetella pertussis* are the most significant microbial lectins (Sandros et al., 1994). To confirm the potential lectin activity of mBFT2, we tested the ability of the toxin to induce hemagglutination. Here, we show for the first time that mBFT2 has hemagglutination activity. However, lectin activity was determined by the ability of LPS to inhibit hemagglutination. We premixed mBFT2 with LPS isolated from ETBF and NTBF and demonstrated alteration of the hemagglutination activity of mBFT2. Erythrocytes tended to form pellets when LPS had been mixed with mBFT2. Of note, pBFT2 did not display hemagglutination activity. We suggest that pBFT2 does not have the ability to induce hemagglutination but acquires this property during processing. Two forms of the toxin that have different hemagglutination properties might also exhibit different interaction with lipids. Thus, we demonstrated that mBFT2 has strong lectin activity that could be necessary for its biological functions.

We believe that the strong lectin-like protein-membrane association identified here could be used in two potential mechanisms of toxin-host cell interaction. Toxin-lipid or toxin-LPS association leading to the local toxin concentration increasing on the surface of target cells may increase contact of the toxin with a corresponding substrate or receptor. Moreover, toxin associated with vesicles could be taken up via endocytosis by eukaryotic cells or undergo a membrane flip-flop mechanism and persist in the intracellular environment.

# MATERIALS AND METHODS

## Bacterial Strains and Growth Conditions

Enteropathogenic *B. fragilis* BOB25 (Nikitina et al., 2015) and non-toxigenic *B. fragilis* 323-J-86 (clinical isolates kindly provided from the Federal Research and Clinical Centre of Physical-Chemical Medicine Federal Medical Biological Agency, Moscow, Russia) were grown on blood agar plates containing either 5% defibrinated horse blood or brain heart infusion broth supplemented with hemin (5 g/ml) under anaerobic conditions.

## Cell Line Medium and Culture Conditions

Human colonic epithelial cells (HT-29) obtained from the American Type Culture Collection (ATCC Number HTB-38) were seeded in 25 $cm^2$ flasks at 37°C under 5% $CO_2$ in DMEM (Life Technologies, USA) containing 10% fetal bovine serum (FBS, Life Technologies, USA) and 2 mM GlutaMax (Life Technologies, USA).

## Recombinant Proteins and Antibodies

Immature and mature forms of recombinant toxins (mBFT2, pBFT2) were prepared as described previously (Kharlampieva et al., 2015). The mutant forms of BFT (mBFT2-mut, pBFT2-mut) were obtained by site-directed mutagenesis, where zinc-chelating histidine residues were mutated to tyrosine residues (H348Y, H352Y, and H358Y). Detailed information about how the mutant forms of the toxin have been described previously (Kharlampieva et al., 2015).

For BFT2-specific antibody preparation, 100 μg recombinant pBFT2 in 1x PBS was injected to rabbits four times at intervals of 3–4 weeks. Fourteen days after the final injection, 15 ml blood was collected. Immunoglobulin fraction separation from the serum was performed with protein A-sepharose.

## OMV Purification

Overnight-cultured *B. fragilis* (ETBF and NTBF) strains were centrifuged at 4500 × g at 4°C. To remove residual cells, the supernatant was filtered using a 0.45-μm pore membrane (Millex GV; Millipore). The filtrate was subjected to ultracentrifugation

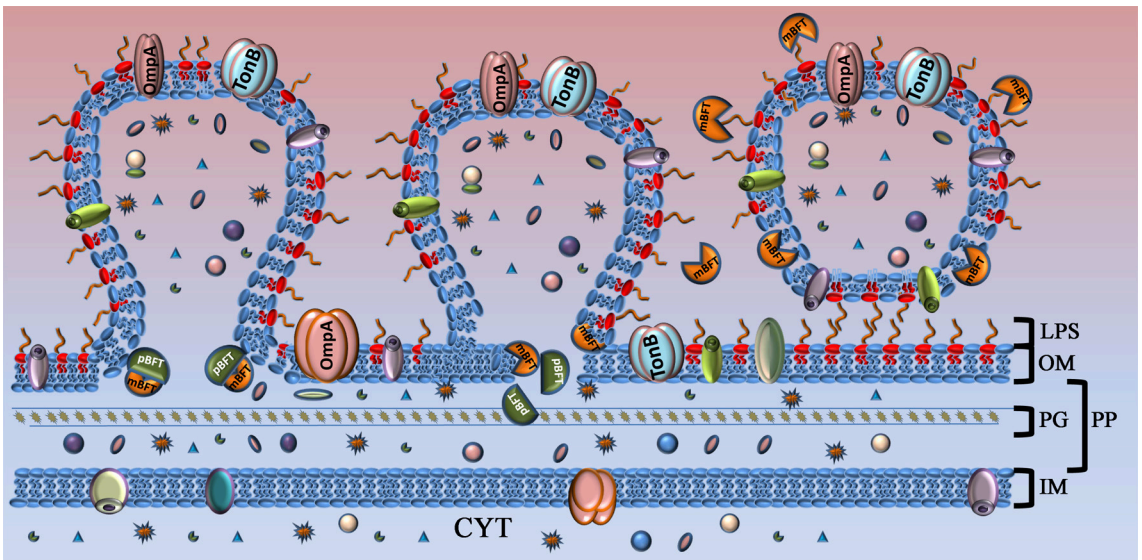


**FIGURE 8 | Model of toxin capture during vesicle formation.** Toxin is shown as complex of two subunits. Part of the toxin that will be processed (pBFT) and degraded is colored in dark green. Active part of the toxin (mBFT) colored in orange. OM, outer membrane; LPS, lipopolysaccharide; PG, peptidoglycan; PP, periplasm; IM, inner membrane; CYT, cytoplasma. At the beginning of vesicle formation, the major part of the toxin is not processed and could be found in membrane. During vesicle formation toxin could be processed by *B. fragilis* cysteine protease. Free grooves, located on the protein surface, formed during toxin processing interact with fatty acid residues of outer membrane lipids by hydrophobic interaction. Toxin promoted to the OMV surface where it interact with LPS. Incorporated or tightly binding toxin delivered to the target cell by OMVs.

at 100,000 × g for 2 h (Optima L-90K ultracentrifuge; Beckman Coulter). The supernatant was discarded, and the pellet was washed with sterile PBS and filtered through a 0.2-μm pore polyvinylidene difluoride (PVDF) membrane (Millex GV; Millipore). The ultracentrifugation step was repeated. The vesicle pellet was resuspended in 150 mM NaCl (pH 6.5). Protein concentration was quantified using a 2D-quant kit (GE Healthcare Life Sciences).

## Cell Fractionation

Cell fractionation was performed as described by Lindmark et al. (2009). Precipitated proteins from cell fractions were collected by centrifugation at 12,000 × g, washed with acetone, dried and dissolved in Laemmli sample buffer. Protein concentration was quantified using a 2D-quant kit (GE Healthcare Life Sciences). In total, 40–60 μg each extract sample was used for SDS-PAGE and western blot assay.

## Cells Fractions LC-MS/MS Analysis

Detail information about **SDS PAGE** and **In-gel trypsin digestion** of cell fractions proteins can be found in Supplemental information 2. LC-MS/MS analysis of tryptic peptides was carried out using Ultimate-3000 HPLC system (Thermo Scientific) coupled to a maXis qTOF after HDC-cell upgrade (Bruker) with a nano-electrospray source. Chromatographic separation of peptides was performed on a C-18 reversed phase column (Zorbax 300SB-C18, 150 mm x 75 um, particle diameter 3.5 um, Agilent). Gradient parameters were as follows: 5–35% acetonitrile in aqueous 0.1% (v/v) formic acid, duration 120 min, column flow 0.3 ul/min. Positive MS and MS/MS spectra were aquired using AutoMS/MS mode (capillary voltage 1700, curtain gas flow 4 l/min, curtain gas temperature 170 C, spectra rate 10 Hz, 4 precursors, m/z range 50–2200, active exclusion after 2 spectra, release after 0.5 min). Detail information about **Search Database Creation** and **Proteins and Peptides Identification** can be found in Supplemental information 2.

## SDS-PAGE and Western Blot Analysis

The isolated OMVs and different cellular extracts were mixed with Laemmli sample buffer (1:1) containing CHAPS and separated by SDS-PAGE. A total of 40 μg each (NTBF and ETBF) OMV sample and 40–60 μg periplasmic, cytoplasmic, and membrane fractions were used for SDS-PAGE and subsequent western blot analysis. We used BFT2-specific antibodies and horseradish peroxidase-linked anti-rabbit IgG (from sheep, dilution 1:10,000, GE Healthcare, USA). The membranes were processed with ECL Plus western blot detection reagents (GE Healthcare, USA) according to the manufacturer's guidelines. The signals were detected on a ChemiDoc MP (BioRad, USA).

## Electron Microscopy and Immunogold Labeling

Ultrathin sections of ETBF and NTBF cells were prepared as previously described (Farquhar, 1956). A volume of 5 μl of each OMV samples was negatively stained with 2% (wt/vol) uranyl acetate for 3 min and examined using a Zeiss Libra 120 electron microscope (Zeiss, Germany).

For immunogold labeling, cells were fixed by the addition of formaldehyde and glutaraldehyde to final concentrations of 4 and 0.1–0.2%, respectively, dehydrated with ethanol in increasing

concentrations (70, 96%) and embedded in LR-White resin (Polyscience, INC, USA). To visualize the distribution of the BFT protein in *B. fragilis* cells, BFT2-specific antibodies diluted 1:50 in PBS (1×) and conjugates of protein A with 15 nm colloid gold particles (Aurion, The Netherlands) were used. OMVs were adsorbed onto carbon-coated nickel grids for 2 min and coincubated with labels, coupled with antibodies against BFT, and then negatively stained. Immunogold labeled samples were examined using a Zeiss Libra 120 electron microscope (Zeiss, Germany).

## Lipid Extraction

For lipid extraction, 1 ml liquid culture (ETBF and NTBF) was used. Samples were incubated at –77°C for 15 min, then at room temperature for 3 min and centrifuged at 10,000 × g for 20 min. The resulting cell pellets were used for lipid extraction by a modified Folch protocol (Folch et al., 1957). LPS was isolated using the Tri-Reagent method described by Yi and Hackett (2000).

## Shot-Gun Lipidomics

Identification of extracted membrane lipids and LPS was performed using a quadrupole time-of-flight tandem mass spectrometer (Q-TOF Maxis, Bruker Daltonics, Germany) with an updated collision cell for electrospray ionization source. Metabolite identification was confirmed by the fragmentation of the detected parent ions. External phospholipid standards (choline, phosphatidylcholine, phosphatidylserine, phosphatidylethanolamine, phosphatidylglycerol, phosphatidic acid, and tetracycline; Sigma Aldrich) were used to optimize the MS/MS-acquisition conditions. We used the following databases for lipid identification: LIPID MAPS database (LIPID MAPS Lipidomics Gateway, a free resource sponsored by the National Institute of General Medical Sciences, USA; http://www.lipidmaps.org), Byrdwell G. Resources for Lipid Analysis in the twenty-first Century (http://www.byrdwell.com), Metlin (Scrips Center for Mass Spectrometry, USA; https://masspec.scripps.edu) and Galactosylceramides and Glucosylceramides (Cerebrosides) (http://www.lipidhome.co.uk/).

## Modeling and Docking

No BFT2 crystal structures have been reported thus far, so the atom coordinates for creating 3D models of this protein were taken from the XRD-based structure of its homolog BFT3 (PDB: 3p24 http://www.rcsb.org/pdb/explore/explore.do?structureId=3p24) by substituting several amino acid residues (see Supplemental information 2). The 3D models of the targets (PE, PC, Lipid A, and polysaccharide chain of LPS) were created with the Molsoft ICM version 3.8–3 application (Wesson and Eisenberg, 1992; Abagyan et al., 1994; Totrov and Abagyan, 2001a,b). Detailed information about the modeling and docking procedure can be found in Supplemental information 2.

## Trp Fluorescence Quenching Assay

Intrinsic fluorescence of the Trp and Tyr residues was measured after the addition of different amounts of vesicles constructed from PC to 3 nM mBFT, pBFT2, mBFT2, pBFT-mut, mBFT-mut, Proteinase K, or BSA solutions in the standard PBS buffer (Merck) or a low ionic strength buffer (1 nM $ZnSO_4$ in 1:50 diluted PBS). Each protein solution was mixed gently after the addition of the PC vesicles and stored at room temperature for 1–2 min prior to measurements. Fluorescence emission spectra were registered at 20°C using a Chirascan spectrometer (Applied Photophysics) equipped with a thermostatically controlled cuvette holder with slit widths of 4 and 6 nm upon excitation at 280 or 295 nm. Light scattering by liposomes was taken into account. The quenching curves were fitted with equation (1)

$$Y = \frac{Y_{\max} \times X^n}{X^n + K_d^n} \quad (1)$$

where Y is fluorescence quenching and $n$ is the Hill coefficient ($n = 1 \pm 0.3$ unless otherwise specified).

Fitting was performed using DataFit 9 software.

## NMR Analysis of Protein-Lipid Complexes

The samples for NMR spectroscopy [500 μg mBFT2, 500 μg phosphatidylcholine (Sigma Aldrich, USA)] were dissolved in water (100 μl $D_2O$ was added to each sample for the lock signal stabilization) and phosphate buffer (pH 7.4). All spectra were obtained on a Bruker Advance III 500 MHz NMR spectrometer (Bruker, USA) equipped with a Prodigy TCI cryogenic triple-channel probe. The sample temperature was kept at 300 K during the experiments. 2D DOSY (the stimulated echo pulse sequence with bipolar gradient pulses was used) and common 1D proton spectra were measured for the study of protein-lipid complex formation (Chou et al., 2004; Balayssac et al., 2009). The water peak in all experiments was suppressed by WATERGATE pulse sequence with five pairs of symmetric gradients (125 ms delay for binomial water suppression and 200 ms delay for gradient recovery). The NMR data processing and analysis were performed using Bruker TopSpin v.3.2 NMR.

## Preparation of Liposomes by Reverse-Phase (REV) Evaporation

To prepare liposomes, 30 μl phosphatidylcholine or phosphatidylethanolamine in chloroform solution (100 mg/ml) and 300 μl PBS with 1 ml diethyl ether were added to a 50 ml round-bottom flask with a long extension neck, and the solvent was removed under reduced pressure by a rotary evaporator. Prepared liposomes were dissolved in 200 μl PBS.

## Cell Culture Experiments

To examine the biological activity of BFT2-containing OMVs, HT-29 cells were co-incubated for 2 h with 40–60 μg total OMV proteins isolated from ETBF and NTBF. After co-incubation, cells were washed with 1x PBS buffer several times and mixed with 50 μl 1x Laemmli sample buffer containing CHAPS. To detect E-cadherin cleavage, western blot analysis with E-cadherin monoclonal mouse antibody (dilution 1:1000, Invitrogen, USA) and horseradish peroxidase-linked anti-mouse IgG (from sheep, dilution 1:10,000, GE Healthcare, USA) was performed. The membranes were processed with ECL Plus western blot detection

reagents (GE Healthcare, USA) according to the manufacturer's guidelines. The signals were detected on a ChemiDoc MP (BioRad, USA).

To determine mBFT2 localization (on the outer or inner surface of the OMV membrane) essential for biological activity against E-cadherin, two different types of liposomes were obtained by reverse-phase evaporation. For encapsulated toxin preparation, 14.2 ng mBFT2 and 12 nM pBFT2 were encapsulated into 30 μl (100 mg/ml) liposomes by reverse-phase evaporation method, described earlier ("Material and Methods"—"Preparation of liposomes by reverse-phase (REV) evaporation"). Proteolysis of unencapsulated mBFT2 was performed using Proteinase K (20 ng/μl) treatment. Toxin encapsulation was verified by western blot with BFT-specific antibodies. For the toxin added to the prepared liposomes, 14.2 ng mBFT2 and 12 nM pBFT2 were added to 30 μl previously prepared liposomes (100 mg/ml), and the mBFT2-liposome mix was purified by one ultracentrifugation step at 100,000 × g for 1 h. The amount of unbound mBFT2 in the medium was determined by western blot with BFT2-specific antibodies. Both types of liposomes were co-incubated with HT-29 cells for 1 h. After incubation, cells were washed several times with 1 × PBS and mixed with 50 μl 1x Laemmli sample buffer containing CHAPS. To detect E-cadherin cleavage, western blot analysis with anti E-cadherin antibody was performed.

For visual assessment of protein-lipid complexes (mBFT2/pBFT2-liposomes) and OMV fixed on the cell surface, fluorescence microscopy was performed. Briefly, isolated OMVs of NTBF and ETBF (40 μg each) and 50 μl prepared liposomes (100 mg/ml) were separately labeled with Vybrant DiI in a 30 min incubation and purified again by one step of ultracentrifugation at 100,000 × g for 1 h. Labeled OMVs, liposomes alone, prepared liposomes with added mBFT2 or pBFT2 and encapsulated toxin preparations were co-incubated with HT-29 cells for 1 h. The cells were then washed ∼three times, incubated with DAPI for nuclei labeling and observed with a Nikon Eclipse E800 microscope (Nikon, Japan) or an Olympus Live Cell Imaging System (Olympus IX51, Japan).

### Hemagglutination Assay

A hemagglutination assay was performed using red blood cells (RBCs) from humans. Blood was provided by volunteer donors (Lewis $O^{\alpha-\beta+}$). Written informed consent from participants was obtained and approved by the ethical committee of the Federal Research and Clinical Centre of Physical-Chemical Medicine Federal Medical Biological Agency, Moscow, Russia (approval number 1a/2016). Heparinized whole human blood erythrocytes were washed three times by centrifugation at 200 × g and resuspended to 1.5% packed cell volume in 1× PBS. mBFT2 in increasing concentrations (0.1–2.5 μg), 5 μl LPS (isolated from 20 ml ETBF and 20 ml NTBF) and pBFT (2.5 and 1 μg) were independently mixed with the erythrocyte suspension in a round-bottomed 96-well dish and agitated by hand. Separately, mBFT2 (2 μg) was premixed with ETBF LPS or NTBF LPS, and then prepared solutions were mixed with the erythrocyte suspension in a round-bottomed 96-well dish and agitated by hand. A positive result was recorded if hemagglutination occurred within 10 min.

## AUTHOR CONTRIBUTIONS

NZ, VT, AAV, AMV, and VP designed and performed experiments, analyzed data, and wrote the paper; DR, IV designed and performed experiments, FL, EG, DK, VM, and VL performed experiments; VG supervised the project.

## FUNDING

This research was supported by RSF grant 14-24-00159 and RSF 14-25-00013.

## ACKNOWLEDGMENTS

We thank Prof. Galina E. Pozmogova from Federal Research and Clinical Centre of Physical-Chemical Medicine of the Federal Medical Biological Agency for the critical review of the manuscript, Prof. Maria A. Lagarkova from Federal Research and Clinical Centre of Physical-Chemical Medicine of the Federal Medical Biological Agency for cell culture cultivation, Nina V. Seina, Ekaterina V. Surko, and Eskender Osmanov for TEM preparations.

## SUPPLEMENTARY MATERIAL

The Supplementary Material for this article can be found online at: http://journal.frontiersin.org/article/10.3389/fcimb.2017.00002/full#supplementary-material

## REFERENCES

Abagyan, R., Totrov, M., and Kuznetsov, D. (1994). ICM, a new method for protein modeling and design: applications to docking and structure prediction from the distorted native conformation. *J. Comput. Chem.* 15, 488–506. doi: 10.1002/jcc.540150503

Abhilash, J., Dileep, K. V., Palanimuthu, M., Geethanandan, K., Sadasivan, C., and Haridas, M. (2013). Metal ions in sugar binding, sugar specificity and structural stability of Spatholobus parviflorus seed lectin. *J. Mol. Model.* 19, 3271–3278. doi: 10.1007/s00894-013-1854-4

Balayssac, S., Delsuc, M. A., Gilard, V., Prigent, Y., and Malet-Martino, M. (2009). Two-dimensional DOSY experiment with excitation sculpting water suppression for the analysis of natural and biological media. *J. Magn. Reson.* 196, 78–83. doi: 10.1016/j.jmr.2008.09.022

Cerdeño-Tárraga, A. M., Patrick, S., Crossman, L. C., Blakely, G., Abratt, V., Lennard, N., et al. (2005). Extensive DNA inversions in the *B. fragilis* genome control variable gene expression. *Science* 307, 1463–1465. doi: 10.1126/science.1107008

Charbonneau, D. M., and Tajmir-Riahi, H. A. (2010). Study on the interaction of cationic lipids with bovine serum albumin. *J. Phys. Chem. B* 114, 1148–1155. doi: 10.1021/jp910077h

Chatterjee, D., and Chaudhuri, K. (2011). Association of cholera toxin with *Vibrio cholerae* outer membrane vesicles which are internalized by human intestinal epithelial cells. *FEBS Lett.* 585, 1357–1362. doi: 10.1016/j.febslet.2011.04.017

Chatzidaki-Livanis, M., Geva-Zatorsky, N., and Comstock, L. E. (2016). *Bacteroides fragilis* type VI secretion systems use novel effector and immunity proteins to antagonize human gut Bacteroidales species. *Proc. Natl. Acad. Sci. U.S.A.* 113, 3627–3632. doi: 10.1073/pnas.1522510113

Chou, J. J., Baber, J. L., and Bax, A. (2004). Characterization of phospholipid mixed micelles by translational diffusion. *J. Biomol. NMR* 29, 299–308. doi: 10.1023/B:JNMR.0000032560.43738.6a

Coyne, M. J., Roelofs, K. G., and Comstock, L. E. (2016). Type VI secretion systems of human gut Bacteroidales segregate into three genetic architectures, two of which are contained on mobile genetic elements. *BMC Genomics* 17:58. doi: 10.1186/s12864-016-2377-z

Dua, R., Wu, S. K., and Cho, W. (1995). A structure-function study of bovine pancreatic phospholipase A2 using polymerized mixed liposomes. *J. Biol. Chem.* 270, 263–268. doi: 10.1074/jbc.270.1.263

Elhenawy, W., Debelyy, M. O., and Feldman, M. F. (2014). Preferential packing of acidic glycosidases and proteases into Bacteroides outer membrane vesicles. *MBio* 5, e00909–e00914. doi: 10.1128/mBio.00909-14

Ellis, T. N., and Kuehn, M. J. (2010). Virulence and immunomodulatory roles of bacterial outer membrane vesicles. *Microbiol. Mol. Biol. Rev.* 74, 81–94. doi: 10.1128/MMBR.00031-09

Epand, R. F., Savage, P. B., and Epand, R. M. (2007). Bacterial lipid composition and the antimicrobial efficacy of cationic steroid compounds (Ceragenins). *Biochim. Biophys. Acta* 1768, 2500–2509. doi: 10.1016/j.bbamem.2007.05.023

Farquhar, M. G. (1956). Preparation of ultrathin tissue sections for electron microscopy review and compilation of procedures. *Lab. Invest.* 5, 317–337.

Folch, J., Lees, M., and Sloane Stanley, G. H. (1957). A simple method for the isolation and purification of total lipides from animal tissues. *J. Biol. Chem.* 226, 497–509.

Franco, A. A., Mundy, L. M., Trucksis, M., Wu, S., Kaper, J. B., and Sears, C. L. (1997). Cloning and characterization of the *Bacteroides fragilis* metalloprotease toxin gene. *Infect. Immun.* 65, 1007–1013.

Galán, J. E., Lara-Tejero, M., Marlovits, T. C., and Wagner, S. (2014). Bacterial type III secretion systems: specialized nanomachines for protein delivery into target cells. *Annu. Rev. Microbiol.* 68, 415–438. doi: 10.1146/annurev-micro-092412-155725

Gibson, S. A., and Macfarlane, G. T. (1988). Characterization of proteases formed by *Bacteroides fragilis*. *J. Gen. Microbiol.* 134, 2231–2240. doi: 10.1099/00221287-134-8-2231

Hachani, A., Wood, T. E., and Filloux, A. (2016). Type VI secretion and anti-host effectors. *Curr. Opin. Microbiol.* 29, 81–93. doi: 10.1016/j.mib.2015.11.006

Herrou, J., Choi, V. M., Bubeck Wardenburg, J., and Crosson, S. (2016). Activation mechanism of the *Bacteroides fragilis* cysteine peptidase, fragipain. *Biochemistry* 55, 4077–4084. doi: 10.1021/acs.biochem.6b00546

Horstman, A. L., and Kuehn, M. J. (2002). Bacterial surface association of heat-labile enterotoxin through lipopolysaccharide after secretion via the general secretory pathway. *J. Biol. Chem.* 277, 32538–32545. doi: 10.1074/jbc.M203740200

Huang, J. Y., Lee, S. M., and Mazmanian, S. K. (2011). The human commensal *Bacteroides fragilis* binds intestinal mucin. *Anaerobe* 17, 137–141. doi: 10.1016/j.anaerobe.2011.05.017

Ismail, S., Hampton, M. B., and Keenan, J. I. (2003). *Helicobacter pylori* outer membrane vesicles modulate proliferation and interleukin-8 production by gastric epithelial cells. *Infect. Immun.* 71, 5670–5675. doi: 10.1128/IAI.71.10.5670-5675.2003

Kesty, N. C., and Kuehn, M. J. (2004). Incorporation of heterologous outer membrane and periplasmic proteins into *Escherichia coli* outer membrane vesicles. *J. Biol. Chem.* 279, 2069–2076. doi: 10.1074/jbc.M307628200

Kharlampieva, D., Manuvera, V., Podgorny, O., Grafskaia, E., Kovalchuk, S., Pobeguts, O., et al. (2015). Recombinant fragilysin isoforms cause E-cadherin cleavage of intact cells and do not cleave isolated E-cadherin. *Microb. Pathog.* 83–84, 47–56. doi: 10.1016/j.micpath.2015.05.003

Kling, J. J., Wright, R. L., Moncrief, J. S., and Wilkins, T. D. (1997). Cloning and characterization of the gene for the metalloprotease enterotoxin of *Bacteroides fragilis*. *FEMS Microbiol. Lett.* 146, 279–284. doi: 10.1111/j.1574-6968.1997.tb10205.x

Koster, M., Bitter, W., and Tommassen, J. (2000). Protein secretion mechanisms in Gram-negative bacteria. *Int. J. Med. Microbiol.* 290, 325–331. doi: 10.1016/S1438-4221(00)80033-8

Kraft, C. A., Garrido, J. L., Leiva-Vega, L., and Romero, G. (2009). Quantitative analysis of protein-lipid interactions using tryptophan fluorescence. *Sci. Signal.* 2:pl4. doi: 10.1126/scisignal.299pl4

Kuehn, M. J., and Kesty, N. C. (2005). Bacterial outer membrane vesicles and the host-pathogen interaction. *Genes Dev.* 19, 2645–2655. doi: 10.1101/gad.1299905

Kulp, A., and Kuehn, M. J. (2010). Biological functions and biogenesis of secreted bacterial outer membrane vesicles. *Annu. Rev. Microbiol.* 64, 163–184. doi: 10.1146/annurev.micro.091208.073413

Ley, R. E., Hamady, M., Lozupone, C., Turnbaugh, P. J., Ramey, R. R., Bircher, J. S., et al. (2008). Evolution of mammals and their gut microbes. *Science* 320, 1647–1651. doi: 10.1126/science.1155725

Lindmark, B., Rompikuntal, P. K., Vaitkevicius, K., Song, T., Mizunoe, Y., Uhlin, B. E., et al. (2009). Outer membrane vesicle-mediated release of cytolethal distending toxin (CDT) from *Campylobacter jejuni*. *BMC Microbiol.* 9:220. doi: 10.1186/1471-2180-9-220

Mashburn-Warren, L., McLean, R. J., and Whiteley, M. (2008). Gram-negative outer membrane vesicles: beyond the cell surface. *Geobiology* 6, 214–219. doi: 10.1111/j.1472-4669.2008.00157.x

Moncrief, J. S., Obiso, R. Jr., Barroso, L. A., Kling, J. J., Wright, R. L., Van Tassell, R. L., et al. (1995). The enterotoxin of *Bacteroides fragilis* is a metalloprotease. *Infect. Immun.* 63, 175–181.

Nikitina, A. S., Kharlampieva, D. D., Babenko, V. V., Shirokov, D. A., Vakhitova, M. T., Manolov, A. I., et al. (2015). Complete genome sequence of an enterotoxigenic *Bacteroides fragilis* clinical isolate. *Genome Announc.* 3:e00450-15. doi: 10.1128/genomeA.00450-15

Patrick, S., McKenna, J. P., O'Hagan, S., and Dermott, E. (1996). A comparison of the haemagglutinating and enzymic activities of *Bacteroides fragilis* whole cells and outer membrane vesicles. *Microb. Pathog.* 20, 191–202. doi: 10.1006/mpat.1996.0018

Prindiville, T. P., Sheikh, R. A., Cohen, S. H., Tang, Y. J., Cantrell, M. C., Silva, J., et al. (2000). *Bacteroides fragilis* enterotoxin gene sequences in patients with inflammatory bowel disease. *Emerging Infect. Dis.* 6, 171–174. doi: 10.3201/eid0602.000210

Remacle, A. G., Shiryaev, S. A., and Strongin, A. Y. (2014). Distinct interactions with cellular E-cadherin of the two virulent metalloproteinases encoded by a *Bacteroides fragilis* pathogenicity island. *PLoS ONE* 9:e113896. doi: 10.1371/journal.pone.0113896

Richards, R. L., Moss, J., Alving, C. R., Fishman, P. H., and Brady, R. O. (1979). Choleragen (cholera toxin): a bacterial lectin. *Proc. Natl. Acad. Sci. U.S.A.* 76, 1673–1676. doi: 10.1073/pnas.76.4.1673

Sandros, J., Rozdzinski, E., Zheng, J., Cowburn, D., and Tuomanen, E. (1994). Lectin domains in the toxin of *Bordetella pertussis*: selectin mimicry linked to microbial pathogenesis. *Glycoconj. J.* 11, 501–506. doi: 10.1007/BF00731300

Scotto d'Abusco, A. S., Del Grosso, M., Censini, S., Covacci, A., and Pantosti, A. (2000). The alleles of the bft gene are distributed differently among enterotoxigenic *Bacteroides fragilis* strains from human sources and can be present in double copies. *J. Clin. Microbiol.* 38, 607–612.

Sharon, N. (1987). Bacterial lectins, cell-cell recognition and infectious disease. *FEBS Lett.* 217, 145–157. doi: 10.1016/0014-5793(87)80654-3

Shen, Y., Giardino Torchia, M. L., Lawson, G. W., Karp, C. L., Ashwell, J. D., and Mazmanian, S. K. (2012). Outer membrane vesicles of a human commensal mediate immune regulation and disease protection. *Cell Host Microbe* 12, 509–520. doi: 10.1016/j.chom.2012.08.004

Soult, M. C., Dobrydneva, Y., Wahab, K. H., Britt, L. D., and Sullivan, C. J. (2014). Outer membrane vesicles alter inflammation and coagulation mediators. *J. Surg. Res.* 192, 134–142. doi: 10.1016/j.jss.2014.05.007

Toprak, N. U., Yagci, A., Gulluoglu, B. M., Akin, M. L., Demirkalem, P., Celenk, T., et al. (2006). A possible role of *Bacteroides fragilis* enterotoxin in the aetiology of colorectal cancer. *Clin. Microbiol. Infect.* 12, 782–786. doi: 10.1111/j.1469-0691.2006.01494.x

Totrov, M., and Abagyan, R. (2001a). "Protein-Ligand docking as an energy optimization problem," in *Drug-Receptor Thermodynamics: Introduction and Applications,* ed R. B. Raffa (John Wiley & Sons), 603–624.

Totrov, M., and Abagyan, R. (2001b). Rapid boundary element solvation electrostatics calculations in folding simulations: successful folding of a 23-residue peptide. *Biopolymers* 60, 124–133. doi: 10.1002/1097-0282(2001)60:2<124::AID-BIP1008>3.0.CO;2-S

Wallden, K., Rivera-Calzada, A., and Waksman, G. (2010). Type IV secretion systems: versatility and diversity in function. *Cell. Microbiol.* 12, 1203–1212. doi: 10.1111/j.1462-5822.2010.01499.x

Wang, R. C., Seror, S. J., Blight, M., Pratt, J. M., Broome-Smith, J. K., and Holland, I. B. (1991). Analysis of the membrane organization of an *Escherichia coli* protein translocator, HlyB, a member of a large family of prokaryote and eukaryote surface transport proteins. *J. Mol. Biol.* 217, 441–454. doi: 10.1016/0022-2836(91)90748-U

Wesson, L., and Eisenberg, D. (1992). Atomic solvation parameters applied to molecular dynamics of proteins in solution. *Protein Sci.* 1, 227–235. doi: 10.1002/pro.5560010204

Wilson, M. M., Anderson, D. E., and Bernstein, H. D. (2015). Analysis of the outer membrane proteome and secretome of *Bacteroides fragilis* reveals a multiplicity of secretion mechanisms. *PLoS ONE* 10:e0117732. doi: 10.1371/journal.pone.0117732

Wu, S., Lim, K. C., Huang, J., Saidi, R. F., and Sears, C. L. (1998). *Bacteroides fragilis* enterotoxin cleaves the zonula adherens protein, E-cadherin. *Proc. Natl. Acad. Sci. U.S.A.* 95, 14979–14984. doi: 10.1073/pnas.95.25.14979

Wu, S., Shin, J., Zhang, G., Cohen, M., Franco, A., and Sears, C. L. (2006). The *Bacteroides fragilis* toxin binds to a specific intestinal epithelial cell receptor. *Infect. Immun.* 74, 5382–5390. doi: 10.1128/IAI.00060-06

Yi, E. C., and Hackett, M. (2000). Rapid isolation method for lipopolysaccharide and lipid A from gram-negative bacteria. *Analyst* 125, 651–656. doi: 10.1039/b000368i

**Conflict of Interest Statement:** The authors declare that the research was conducted in the absence of any commercial or financial relationships that could be construed as a potential conflict of interest.

frontiers in Cellular and Infection Microbiology

CORRECTION
published: 30 June 2017
doi: 10.3389/fcimb.2017.00308

# Corrigendum: Interaction of *Bacteroides fragilis* Toxin with Outer Membrane Vesicles Reveals New Mechanism of Its Secretion and Delivery

*Natalya B. Zakharzhevskaya[1]*, Vladimir B. Tsvetkov[1, 2, 3]*, Anna A. Vanyushkina[1], Anna M. Varizhuk[1], Daria V. Rakitina[1], Victor V. Podgorsky[1], Innokentii E. Vishnyakov[4, 5], Daria D. Kharlampieva[1], Valentin A. Manuvera[1], Fedor V. Lisitsyn[6], Elena A. Gushina[6], Vassili N. Lazarev[1, 7] and Vadim M. Govorun[1, 7, 8]*

[1] Federal Research and Clinical Centre of Physical-Chemical Medicine Federal Medical Biological Agency, Moscow, Russia, [2] Department of Polyelectrolytes and Surface-Active Polymers, Topchiev Institute of Petrochemical Synthesis, Moscow, Russia, [3] Department of Molecular Virology, FSBI Research Institute of Influenza, Ministry of Health of the Russian Federation, Saint Petersburg, Russia, [4] Lab of Genome Structural Organization, Institute of Cytology, Russian Academy of Sciences, Saint Petersburg, Russia, [5] Institute of Nanobiotechnologies, Peter the Great St. Petersburg Polytechnic University, Saint Petersburg, Russia, [6] N.F. Gamalei Federal Research Centre for Epidemiology and Microbiology, Ministry of Health Russian Federation, Moscow, Russia, [7] Lab of Systems Biology, Moscow Institute of Physics and Technology, Dolgoprudny, Russia, [8] Department of Proteomics, Shemyakin-Ovchinnikov Institute of Bioorganic Chemistry of the Russian Academy of Sciences, Moscow, Russia

**Keywords: toxin delivery, lipid protein interactions, shot gun lipidomics, electron microscopy, fluorescence quenching, NMR**

OPEN ACCESS

***Edited and reviewed by:***
*Thibault Géry Sana, Stanford University, United States*

****Correspondence:***
*Natalya B. Zakharzhevskaya*
*natazaha@gmail.com*
*Vladimir B. Tsvetkov*
*v.b.tsvetkov@gmail.com*

***Received:*** *02 June 2017*
***Accepted:*** *22 June 2017*
***Published:*** *30 June 2017*

***Citation:***
*Zakharzhevskaya NB, Tsvetkov VB, Vanyushkina AA, Varizhuk AM, Rakitina DV, Podgorsky VV, Vishnyakov IE, Kharlampieva DD, Manuvera VA, Lisitsyn FV, Gushina EA, Lazarev VN and Govorun VM (2017) Corrigendum: Interaction of Bacteroides fragilis Toxin with Outer Membrane Vesicles Reveals New Mechanism of Its Secretion and Delivery. Front. Cell. Infect. Microbiol. 7:308. doi: 10.3389/fcimb.2017.00308*

**A corrigendum on**

**Interaction of *Bacteroides fragilis* Toxin with Outer Membrane Vesicles Reveals New Mechanism of Its Secretion and Delivery**

*by Zakharzhevskaya, N. B., Tsvetkov, V. B., Vanyushkina, A. A., Varizhuk, A. M., Rakitinam, D. V., Podgorsky, V. V., et al. (2017). Front. Cell. Infect. Microbiol. 7:2. doi: 10.3389/fcimb.2017.00002*

There is an error in the Funding statement. The correct number for the Russian Science Foundation is 16-15-00258. The corrected Funding statement appears below. The authors apologize for this error and state that this does not change the scientific conclusions of the article in any way.

## FUNDING

This study was supported by Russian Science Foundation grant 16-15-00258, to DR and NZ. The docking and modeling and Fluorescence Quenching Assays were supported by Russian Science Foundation grant 14-25-00013 to AV.

**Conflict of Interest Statement:** The authors declare that the research was conducted in the absence of any commercial or financial relationships that could be construed as a potential conflict of interest.

frontiers in Cellular and Infection Microbiology

REVIEW
published: 09 May 2017
doi: 10.3389/fcimb.2017.00148

# Two-Partner Secretion: Combining Efficiency and Simplicity in the Secretion of Large Proteins for Bacteria-Host and Bacteria-Bacteria Interactions

*Jeremy Guérin[1], Sarah Bigot[2], Robert Schneider[3], Susan K. Buchanan[1] and Françoise Jacob-Dubuisson[4]**

[1] Laboratory of Molecular Biology, National Institute of Diabetes and Digestive and Kidney Diseases, National Institutes of Health, Bethesda, MD, USA, [2] Molecular Microbiology and Structural Biochemistry, Centre National de La Recherche Scientifique UMR 5086–Université Lyon 1, Institute of Biology and Chemistry of Proteins, Lyon, France, [3] NMR and Molecular Interactions, Université de Lille, Centre National de La Recherche Scientifique, UMR 8576–Unité de Glycobiologie Structurale et Fonctionnelle, Lille, France, [4] Université de Lille, Centre National de La Recherche Scientifique, Institut National de La Santé et de La Recherche Médicale, CHU Lille, Institut Pasteur de Lille, U1019–UMR 8204–Centre d'Infection et d'Immunité de Lille, Lille, France

OPEN ACCESS

**Edited by:**
*Sophie Bleves,*
*Aix-Marseille University, France*

**Reviewed by:**
*Raffaele Ieva,*
*UMR5100 Laboratoire de Microbiologie et Génétique Moléculaires, France*
*Dirk Linke,*
*University of Oslo, Norway*

***Correspondence:**
*Françoise Jacob-Dubuisson*
*francoise.jacob@ibl.cnrs.fr*

**Received:** *22 February 2017*
**Accepted:** *10 April 2017*
**Published:** *09 May 2017*

**Citation:**
*Guérin J, Bigot S, Schneider R, Buchanan SK and Jacob-Dubuisson F (2017) Two-Partner Secretion: Combining Efficiency and Simplicity in the Secretion of Large Proteins for Bacteria-Host and Bacteria-Bacteria Interactions. Front. Cell. Infect. Microbiol. 7:148. doi: 10.3389/fcimb.2017.00148*

Initially identified in pathogenic Gram-negative bacteria, the two-partner secretion (TPS) pathway, also known as Type Vb secretion, mediates the translocation across the outer membrane of large effector proteins involved in interactions between these pathogens and their hosts. More recently, distinct TPS systems have been shown to secrete toxic effector domains that participate in inter-bacterial competition or cooperation. The effects of these systems are based on kin vs. non-kin molecular recognition mediated by specific immunity proteins. With these new toxin-antitoxin systems, the range of TPS effector functions has thus been extended from cytolysis, adhesion, and iron acquisition, to genome maintenance, inter-bacterial killing and inter-bacterial signaling. Basically, a TPS system is made up of two proteins, the secreted TpsA effector protein and its TpsB partner transporter, with possible additional factors such as immunity proteins for protection against cognate toxic effectors. Structural studies have indicated that TpsA proteins mainly form elongated β helices that may be followed by specific functional domains. TpsB proteins belong to the Omp85 superfamily. Open questions remain on the mechanism of protein secretion in the absence of ATP or an electrochemical gradient across the outer membrane. The remarkable dynamics of the TpsB transporters and the progressive folding of their TpsA partners at the bacterial surface in the course of translocation are thought to be key elements driving the secretion process.

**Keywords: type V secretion, two-partner secretion, Omp85 transporter, gram-negative bacteria, outer membrane, contact-dependent growth inhibition**

## INTRODUCTION: AN OVERVIEW OF TYPE V SECRETION

Two-Partner secretion (TPS) represents a branch of so-called type V secretion. Widespread in Gram-negative bacteria, type V secretion encompasses several subtypes, identified a–e, that share several general features (**Figure 1**). The cores of type V systems are composed of one or two proteins. The effector ("passenger") proteins or domains are transported exclusively across the outer membrane, following Sec-dependent export to the periplasm. In subtypes Va, Vc, Vd, and Ve, the passenger domain is fused to the membrane domain. The latter is necessary and was once thought to be sufficient for secretion of the passenger domain, hence the generic name of "autotransporters" (Pohlner et al., 1987; Leyton et al., 2012). In subtype Vb (i.e., the TPS pathway), in contrast, the passenger protein generically called "TpsA" is separate from its cognate "TpsB" transporter. In the case of TPS systems, thus, a TpsB transporter can have more than one effector, but this does not generally seem to be the case.

The passenger proteins or domains secreted by the type V pathway are generally long and form fibrous structures, often β helices. They frequently contain repeated sequences determining repetitive folds that appear to be specific to the secretion subtype (see below). The transporter components form transmembrane β-barrel pores. In the available X-ray structures, the β barrels are plugged after secretion by one α helix for type Va and Vb systems, three α helices for type Vc systems and an extended polypeptide segment for type Ve systems (Oomen et al., 2004; Meng et al., 2006; Barnard et al., 2007; Clantin et al., 2007; van den Berg, 2010; Fairman et al., 2012; Shahid et al., 2012). No hydrolysable energy source or electrochemical gradient powers type V translocation, and the processes of secretion and folding are thought to be coupled. In line with the latter feature, general properties of the passenger domains include their slow intrinsic folding rate, paucity in Cys residues, high solubility and low propensity to aggregate prior to folding (Junker et al., 2006; Hartmann et al., 2009; Junker and Clark, 2010). Last but not least, a defining feature of the type V pathway is that protein secretion in all subtypes depends on transporters of the Omp85 superfamily (Webb et al., 2012; Heinz and Lithgow, 2014).

In classical autotransporters (ATs; type Va), the passenger domains are mainly adhesins, proteases, or esterases. The same polypeptide contains in succession the passenger domain and the 12-stranded, transmembrane β-barrel domain (**Figure 1**). Proteolytic processing between the two domains frequently occurs for classical ATs. The prototypical fold of the passenger domain is a β helix, but other structures also occur (Emsley et al., 1996; Otto et al., 2005; van den Berg, 2010). ATs have been the focus of most studies on type V secretion, and they were thoroughly reviewed in several recent articles (Leyton et al., 2012; Grijpstra et al., 2013; van Ulsen et al., 2014).

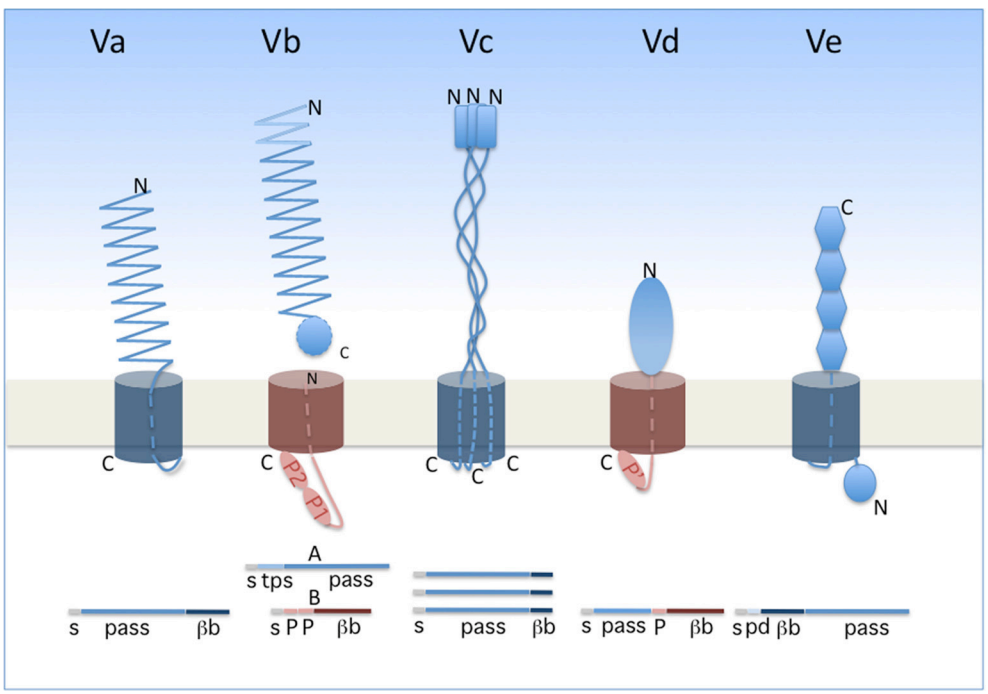


**FIGURE 1 | Type V secretion subtypes.** The proteins involved in each system are represented in their final form, i.e., after completion of secretion. A linear representation is shown underneath the schematics. The two types of β barrels are colored in dark blue (12-stranded barrel) and dark red (16-stranded barrel). The orientation of each protein is indicated by its N and C termini (denoted N and C). The POTRA domains (small ovals) are denoted P1, P2, and P' (the latter being a POTRA-like domain in PlpD). s, signal peptide; pass, passenger domain; βb, β-barrel domain; tps, TPS domain of TpsA proteins; pd, periplasmic domain of type Ve proteins.

Trimeric ATs (type Vc) are adhesins that may contribute to biofilm formation of pathogenic bacteria and have no known enzymatic activity (Hoiczyk et al., 2000; Cotter et al., 2005; Kim et al., 2006; Linke et al., 2006; Bentancor et al., 2012). They are homotrimers whose passenger domains assemble into long, rather rigid stalks with a "head," and harbor domains rich in β structure interspersed with helical coiled coils (reviewed in Fan et al., 2016). Each monomer contributes its four C-terminal β strands to the pore-forming transmembrane β barrel (Leo et al., 2012).

Type Ve proteins are intimins and invasins (Tsai et al., 2010; Leo et al., 2015b; Heinz et al., 2016). In these proteins, the 12-stranded transmembrane β barrel precedes the passenger domain, making them "reverse ATs" (Tsai et al., 2010; Fairman et al., 2012; Oberhettinger et al., 2012). Their modular passenger domains are composed of IgG-like and lectin-like domains. These proteins appear to also have periplasmic extensions involved in dimerization (Leo et al., 2015a).

The little studied type Vd proteins, of which PlpD of *P. aeruginosa* is the prototype, are hybrids between AT and TPS systems. Homologs of PlpD are restricted to specific lineages of Proteobacteria, Fusobacteria, Bacteroidetes, and Chlorobi, suggesting that they may have been acquired by horizontal transfer (Salacha et al., 2010). The passenger protein carries the four sequence blocks typical of patatin-like proteins (PLP) (da Mata Madeira et al., 2016) and has lipolytic activity. It is released into the milieu from the precursor by proteolytic cleavage. The transporter domain, which remains in the outer membrane after maturation of the precursor, is related to TpsB proteins (Salacha et al., 2010).

This short description of type V secretion suggests that new arrangements of the passenger and transporter moieties likely remain to be characterized, which might further expand this broad secretion pathway (Gal-Mor et al., 2008; Arnold et al., 2010; Jacob-Dubuisson et al., 2013). In this review devoted to type Vb secretion, we will first describe the basics of TPS systems. We will then develop functional aspects of the systems involved in contact-dependent growth inhibition (CDI), which thus far appear to be confined to the TPS pathway and are not found in other subtypes of type V secretion. We will cover the structural and mechanistic aspects of the TPS pathway, and to do so we will compare with other Type V systems where relevant. Earlier work will only be mentioned briefly, and thus readers are referred to previous reviews for more details (Jacob-Dubuisson et al., 2013; van Ulsen et al., 2014; Fan et al., 2016).

## TPS SYSTEMS: GENERALITIES

The term Two-Partner Secretion was initially coined to define a distinct secretion pathway exemplified by a handful of systems including ShlAB of *Serratia marcescens*, FhaBC of *Bordetella pertussis*, HpmAB of *Proteus mirabilis,* and HMW1ABC and HMW2ABC of non-typeable *Haemophilus influenzae* (Poole et al., 1988; Schiebel et al., 1989; Domenighini et al., 1990; Uphoff and Welch, 1990; Barenkamp and St Geme, 1994; Willems et al., 1994; Hertle et al., 1999; Jacob-Dubuisson et al., 2001). As implied by the name, the core of a TPS system consists of two proteins, the secretory passenger protein and its transporter across the outer membrane, generically called TpsA and TpsB partners, respectively. In most instances, the genes coding for a TPS system are part of the same operon, but other genetic arrangements have been found (Jacob-Dubuisson et al., 2013) (**Figure 2**). The degree of specificity of a TpsB transporter for its cognate partner varies between systems, and some TpsBs can secrete more than one TpsA (Julio and Cotter, 2005) or appear to be more promiscuous than others (van Ulsen et al., 2008; ur Rahman and van Ulsen, 2013).

The first TPS systems to be characterized were found to secrete cytolysins or adhesins in pathogenic bacteria (Jacob-Dubuisson et al., 2001, 2004). The list rapidly expanded to include other TPS systems with new or unknown functions in various bacterial genera (**Table 1**). Later, a whole new group of TPS systems were found to mediate inter-bacterial interactions involving molecular recognition of closely related bacteria and leading to collective—cooperative or competitive behaviors (Aoki et al., 2005, 2010; Willett et al., 2015b). These "contact-dependent growth inhibition" (CDI) systems will be described in more detail below. Insight into these new TPS functions has considerably boosted interest in the field.

Thus, more and more TPS systems have been characterized over the years, overwhelmingly in pathogens. Whether this reflects their actual distribution in Gram-negative bacteria is very much in doubt, as pathogenic bacteria are much more extensively studied than environmental bacteria. Actually, the discovery of CDI systems and of their roles in collective behaviors of bacteria rather suggests that TPS systems are likely to be widely distributed, well beyond bacterial pathogens (Jacob-Dubuisson et al., 2013).

## OLD AND NEW FUNCTIONS OF TPS SYSTEMS

### Functions of TPS Systems in Bacterial Pathogens

In pathogenic bacteria, TpsA cytolysins/hemolysins are probably rather common (**Table 1**). Orthologs of the prototypic ShlA and HpmA proteins have been found in various genera. In other cases the specific activities of the TpsA proteins have not necessarily been determined. In many instances, the TPS operons are up-regulated upon bacterial entry into the host, and experimental cellular and animal models of infection indicate their importance in host-pathogen interactions. Examples include the RscA protein of *Yersinia enterocolitica* that limits systemic dissemination (Nelson et al., 2001), and the TpsA proteins PfhB1 and B2 of *Pasteurella multocida* and PdtA of *P. aeruginosa* that were shown to contribute to virulence in models of mouse septicemia and *Caenorhabditis elegans* infection, respectively (Fuller et al., 2000; Faure et al., 2014).

Specific functions have nevertheless been ascribed to several TpsA proteins. Thus, some are involved in iron acquisition, including HxuA of *H. influenzae* (Fournier et al., 2011) and possibly HlpA in the root-colonizing bacterium *Pseudomonas*

**TABLE 1 | Diverse functions of TpsA proteins.**

| Class | Organism | Function | Reference |
|---|---|---|---|
| **CYTOLYSINS/HEMOLYSINS** | | | |
| ShlA | *Serratia marcescens* | Cytolysin, hemolysin, pore forming toxin, autophagy induction | Braun et al., 1992; Hertle et al., 1999; Konninger et al., 1999 |
| HpmA | *Proteus mirabilis* | Cytolysin, hemolysin | Uphoff and Welch, 1990; Zwihart and Welch, 1990 |
| EthA | *Edwardsiella tarda* | Cytolysin, hemolysin, host cell adherence, internalization process in fish | Hirono et al., 1997; Strauss et al., 1997; Wang et al., 2010 |
| HhdA | *Haemophilus ducreyi* | Hemolysin | Palmer and Munson, 1995 |
| PhlA | *Photorhabdus luminescens* | Hemolysin | Brillard et al., 2002 |
| ExlA | *Pseudomonas aeruginosa* | Exolysin, plasma membrane rupture of human cells, pore forming toxin | Elsen et al., 2014; Basso et al., 2017 |
| **PROTEASES** | | | |
| LepA | *Pseudomonas aeruginosa* | Induction of inflammatory responses trough human protease-activated receptors (PARs) | Kida et al., 2008, 2011 |
| **IRON ACQUISITION** | | | |
| HxuA | *Haemophilus influenzae* | Heme acquisition from hemopexin | Cope et al., 1994, 1995 |
| **ADHESINS** | | | |
| FHA | *Bordetella pertussis* | Adhesion to epithelial cells, biofilm formation, immunomodulation | Locht et al., 1993; Anderson et al., 2012; Serra et al., 2012 |
| HMW1/HMW2 | *Haemophilus influenzae* | Adhesion to epithelial cells | St Geme and Yeo, 2009 |
| EtpA | *Escherichia coli* | Intestinal colonization, adhesion to host cells by binding to the tip of flagella | Roy et al., 2009 |
| EtpB transporter | *Escherichia coli* | Adhesion to epithelial cells | Fleckenstein et al., 2006 |
| CdrA | *Pseudomonas aeruginosa* | Biofilm, binding to Psl exopolysaccharides | Borlee et al., 2010 |
| Ap58 (EnfA) transporter | *Escherichia coli* | Adhesion and hemagglutination activities | Monteiro-Neto et al., 2003 |
| **CDI SYSTEMS** | | | |
| CdiA | Enterobacteria species, *Pseudomonas aeruginosa* | Contact dependent growth inhibition, biofilm | Aoki et al., 2005; Ruhe et al., 2015; Mercy et al., 2016 |
| BcpA | *Burkholderia* species | Contact dependent growth inhibition, autoaggregation, biofilm, kin recognition, contact-dependent signaling | Anderson et al., 2012, 2014; Garcia et al., 2013, 2016 |
| HecA* | *Dickeya dadantii* | Adhesin, attachment and aggregation on leaves, killing of epidermal cells | Rojas et al., 2002 |
| HrpA* | *Neisseria meningitidis* | Adhesin, binding to epithelial cells, intracellular escape, immune evasion, biofilm formation | Schmitt et al., 2007; Tala et al., 2008; Neil and Apicella, 2009 |
| HxfA*, HxfB* | *Xylella fatidiosa* | Autoaggregation | Guilhabert and Kirkpatrick, 2005 |
| XacFhaB* | *Xanthomonas axonopodis* | Adhesin, biofilm formation | Gottig et al., 2009 |
| FhaB* | *Xanthomonas fuscans* | Vascular transmission to bean seeds | Darsonval et al., 2009 |
| MchA* | *Moraxella catarrhalis* | Adhesin, binding to epithelial cells | Plamondon et al., 2007 |
| MhaB* | *Moraxella catarrhalis* | Adhesin, binding to epithelial cells | Balder et al., 2007 |
| AbFhaB* | *Acinetobacter baumannii* | Adhesin, binding to epithelial cells and fibronectin | Perez et al., 2016 |
| **UNKNOWN FUNCTION** | | | |
| RscA | *Yersinia enterolitica* | Limitation of splenic dissemination | Nelson et al., 2001 |
| LspA1/LspA2 | *Haemophilus ducreyi* | Inhibition of phagocytosis | Dodd et al., 2014 |
| OtpA | *Escherichia coli* | Unknown | Choi et al., 2007 |
| PdtA | *Pseudomonas aeruginosa* | Virulence in nematode model | Faure et al., 2014 |
| BpaA | *Burkholderia pseudomallei* | Unknown | Brown et al., 2004 |
| HlpA | *Pseudomonas putida* | Seed and Root colonization | Molina et al., 2006 |
| PfhB1, PfhB2 | *Pasteurella multocida* | Virulence in septicemic mouse model | Fuller et al., 2000 |

**Predicted CDI system based on genetic analysis.*

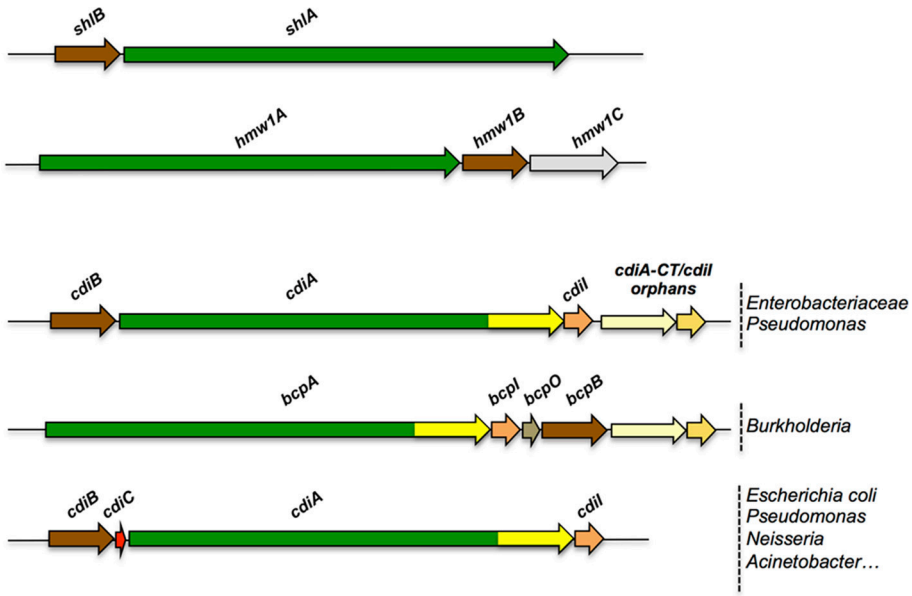


**FIGURE 2 | Organization of TPS operons.** Typical TPS operons are compared with operons coding for CDI systems found in various bacterial genera. Orphan variant *cdiA-CT/cdiI* cassettes are found downstream of some *cdi* operons that likely serve for homologous recombination with full-length *cdiA* genes, thus contributing to the polymorphism of the toxin moieties.

*putida* KT2440 (Molina et al., 2006). At the surface of the cell, HxuA interacts with hemopexin, a serum glycoprotein involved in heme recycling. This interaction causes release of the heme from hemopexin, making it available for import by the dedicated HxuC receptor (Fournier et al., 2011). In the case of enterotoxigenic *Escherichia coli* (ETEC), the TpsA protein EtpA is necessary for intestinal colonization. By binding to the tips of flagella, EtpA mediates bacterial adherence to intestinal cells (Roy et al., 2009). The TpsA proteins LspA1 and LspA2 of *H. ducreyi* are required for full virulence of this pathogen by inhibiting phagocytosis through the phosphorylation of the eukaryotic Src tyrosine kinase (Vakevainen et al., 2003; Ward et al., 2003; Dodd et al., 2014). In *P. aeruginosa,* the secreted TpsA protein LepA is a protease that activates the inflammatory response (Kida et al., 2008). Finally, the TpsB protein EtpB and its homolog EnfA, renamed Ap58, of enteroaggregative *E. coli* AEC O111H12 are involved in the adherence and hemagglutination activities of these isolates (Monteiro-Neto et al., 2003; Fleckenstein et al., 2006).

## CDI Systems

First described in the *E. coli* EC93 strain isolated from rats, bacterial growth inhibition of neighboring cells was revealed to occur by direct interactions and to imply a specific TPS system which was renamed CDI (Aoki et al., 2005). Growth inhibition is mediated by toxic activities associated with the last ∼300 C-terminal residues of the CdiA proteins, called CdiA-CT (**Figure 3A**). Upon cell contact, the surface-exposed CdiA binds the target cell, and its CdiA-CT is delivered, most likely after being cleaved off the rest of the protein, into the target bacterium. $CDI^+$ cells produce an immunity protein, CdiI, which protects them from fratricide by interacting with the cognate CdiA-CT and blocking its toxic activity. CDI systems are widespread among α, β, and γ Proteobacteria (Ruhe et al., 2013), but the genetic organization of those systems differs between species. Most of them share the classical *cdiBAI* locus found in *E. coli* EC93 (Aoki et al., 2005), but the *cdi* genes of *Burkholderia* species constitute a unique class with the distinct *bcp* (*Burkholderia* CDI proteins) nomenclature. This atypical *bcpAIB* gene organization can also comprise an accessory *bcpO* gene between *bcpI* and *bcpB* (Anderson et al., 2012) (**Figure 2**). Depending on the species, it codes for a predicted periplasmic lipoprotein or for a cytoplasmic protein of unknown function, which is necessary for the function of BcpA (Anderson et al., 2012). In addition, orphan variant *cdiA-CT/cdiI* cassettes are found downstream of the *cdi* operons in some species that likely serve for homologous recombination with full-length *cdiA* genes contributing to the variability of the CdiA-CT domain between CdiA proteins. Finally, several Proteobacteria contain a *cdiBCAI*-type operon, with *cdiC* encoding a protein predicted to belong to the toxin acyltransferase family (Ruhe et al., 2013; Ogier et al., 2016) (**Figure 2**). The function of the CdiC protein is unknown, but it might be involved in CdiBA biogenesis and/or post-translational modifications of CdiA.

Like TpsA proteins, CdiAs are composed of large regions rich in β structure, including the N-terminal TPS domain. They however differ from typical TpsA proteins in their C termini (**Figure 3A**). Sequence alignments have indicated that CdiA proteins share conserved C-proximal motifs of unknown function, such as (Q/E)LYN in *Burkholderia*, VENN in other bacteria or yet other motifs in some *Pseudomonas* (Aoki et al., 2005; Anderson et al., 2012; Mercy et al., 2016) (**Figure 3A**).

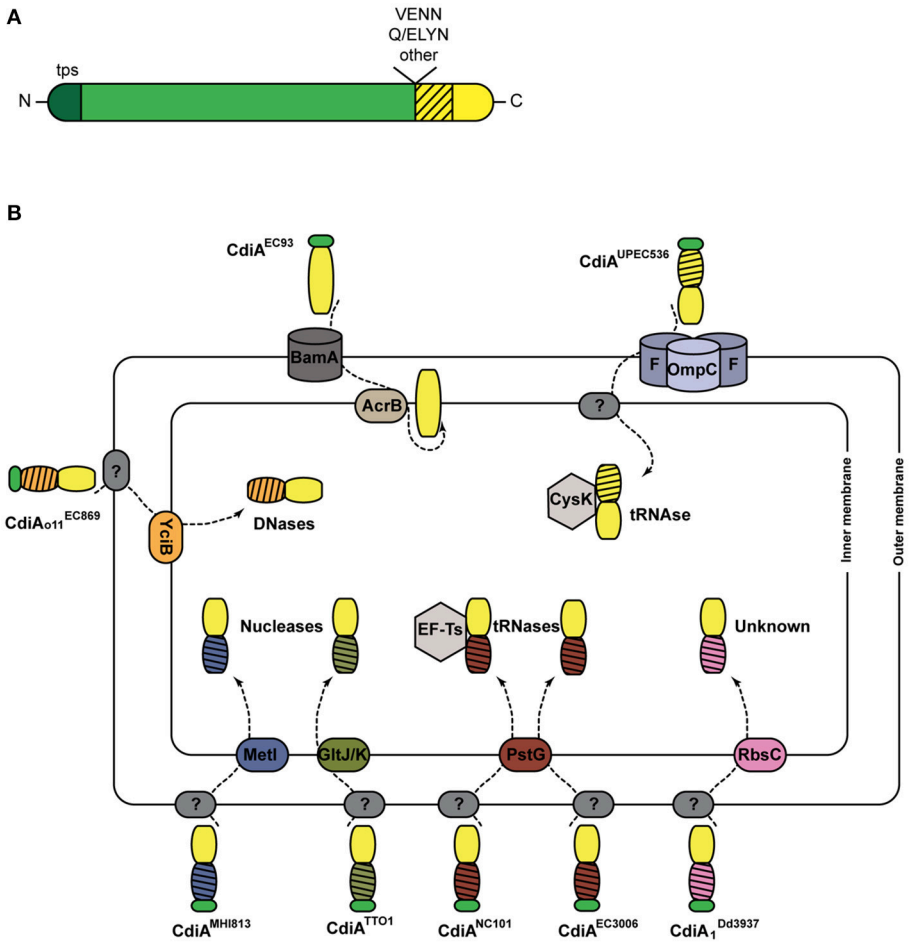


**FIGURE 3 | CDI systems. (A)** Linear representation of a typical CdiA protein. In addition to the TPS domain (in darker shade of green), found in all TpsA proteins and necessary for secretion, CdiA proteins also harbor specific sequence motifs such as VENN or (Q/E)LYN that separate the long central region from the CdiA-CT domain. The first part of the CT domain (hatched) is necessary for import into the target cell, while the second part carries the toxic activity of the protein. **(B)** Cell entry pathways of CdiA-CT. The pre-toxin motif that demarcates the variable CdiA-CT is represented in green. The receptors of CdiA-CT domains at the surface of the target bacteria remain unknown in most cases (indicated by ?). CdiA-CT$^{EC93}$ of *E. coli* EC93 is predicted to be a pore-forming domain that inserts into the inner membrane. For the other CdiA-CT domains, their N-terminal domains (hatched) are colored according to the membrane proteins putatively involved in their entry into the cytoplasm. The tRNase activities of CdiA-CT$^{UPEC536}$ and CdiA$^{NC101}$ are activated by the cytoplasmic cysteine synthase A CysK and the translational elongation factor EF-Ts, respectively. The CdiA toxin of *E. coli* EC869 is a DNase, and *E. coli* NC101 and EC3006 produce tRNases. The CdiA-CT moieties of *E. coli* MHI813 and *Photorhabdus luminescens* TTO1 harbor conserved nuclease_NS2 and endonuclease_VII domains, respectively. The toxic activity of CdiA produced by *Dickeya dadantii* 3937 is unknown.

The VENN motif of CdiA$^{UPEC536}$ was shown not to be required for toxin import in the target cell (Beck et al., 2014a). One hypothesis is that the conserved motifs might be involved in the proteolytic processing of the CdiA proteins to release their C-terminal domains, as for the bacterial intein-like (BIL) domain of CdiA of *P. syringae* (Amitai et al., 2003). Beyond the conserved motifs, the sequences diverge abruptly, and therefore the so-called "CdiA-CT" domains are highly variable. They have been identified as the toxic domains, carrying DNase, tRNase, or pore-forming activities (Aoki et al., 2010; Zhang et al., 2011; Ruhe et al., 2013; Webb et al., 2013).

The toxins need to reach the cytosol of target cells by crossing both bacterial membranes (**Figure 3B**). The study of their translocation pathways has revealed complex mechanisms that do not seem to be conserved among CDI systems. They have mostly been investigated in Enterobacteria, and a summary of these findings is depicted in **Figure 3B**. The CdiA proteins must bind outer membrane receptors before their CdiA-CT moieties are translocated into the target cells. Only two such receptors have been identified to date, BamA for CdiA$^{EC93}$ and heterotrimeric osmoporins composed of OmpC and OmpF for CdiA$^{UPEC536}$ (Aoki et al., 2008; Beck et al., 2016). The current model proposes that after recognition, proteolytic cleavage releases the CdiA-CT from the full CdiA protein through an unknown mechanism. The CdiA-CT is translocated into the periplasm, where it recognizes an inner membrane receptor. Import across the cytoplasmic membrane exploits specific membrane proteins, and the N-terminal part of the CdiA-CT

domain plays a crucial role in this step (Willett et al., 2015a) (**Figure 3B**). Once inside the cell, the CdiA-CT domains deploy their toxic activity, which is dictated by their sequences and their folds (Zhang et al., 2011). Activation of nuclease activity generally depends on host factors. The O-acetylserine sulfhydrylase CysK and the elongation factor Ts (Ef-Ts) are required for the activities of CdiA-CT$^{UPEC536}$ and CdiA$^{NC101}$, respectively (Diner et al., 2012; Kaundal et al., 2016; Jones et al., 2017).

The observations that CDI systems mostly target closely related species and that CdiA proteins preferentially bind kin receptors, thus allowing interactions between self-bacteria, suggest a role for CDI systems beyond competition in collective behaviors of bacteria. This hypothesis has recently been confirmed in *Burkholderia,* which use CDI proteins to establish signaling between CDI$^+$ neighbors and thus to affect gene expression in immune recipient bacteria (Garcia et al., 2016). This "contact-dependent signaling" (CDS) implies a functional CdiA-CT domain, but it is restricted to specific toxic domains. In line with signaling functions, some CDI systems help to retain genetic elements through a surveillance mechanism (Ruhe et al., 2016). This property is consistent with the fact that most *cdi* genes are typically found on genomic or pathogenicity islands (Klee et al., 2000; Dobrindt et al., 2002; Tuanyok et al., 2008; Tumapa et al., 2008; Siddaramappa et al., 2011; Willett et al., 2015b; Ruhe et al., 2016). The maintenance of genetic material by CDI is linked to toxin exchange between sibling cells and might serve to maintain the *cdi*-containing islands in a population.

Many TpsA adhesins have now been redefined as CdiA proteins (**Table 1**). Some of them contribute to the virulence of necrogenic bacterial phytopathogens, including *Dickeya dadantii* (Rojas et al., 2002), *Xylella fastidiosa* (Guilhabert and Kirkpatrick, 2005), and *Xanthomonas axonopodis* (Gottig et al., 2009), with activities ranging from adherence to biofilm formation to epidermal cell killing. Interestingly, some CdiA proteins appear to mediate biofilm formation, but in a CDI-independent manner (Garcia et al., 2013; Ruhe et al., 2015). Whether TpsA proteins might generally be multifunctional remains an open question, but this would be quite conceivable given their large sizes.

## REGULATION OF *TPS* EXPRESSION

Although *tps* genes appear to be expressed during infection and no specific regulatory pathways have been ascribed to this regulation, several factors modulating TPS production have been characterized (**Table 2**). To date, the two-component system BvgAS is the best-studied regulatory pathway, controlling *fhaB* and *fhaC* gene expression of *B. pertussis* (Scarlato et al., 1991). Other signal transduction systems have been identified as regulators of *tps* operons in several bacterial species. Quite frequently, the mechanism of production is closely related to the function of the TpsA protein. Thus, a large number of TPS systems are produced upon iron limitation, such as HxuABC involved in iron acquisition (Wong and Lee, 1994; Cope et al., 1995), or cytolysins/hemolysins whose production in low-iron conditions might be a means for the bacteria to release iron from eukaryotic cells or erythrocytes. In *P. aeruginosa*, the intracellular level of cyclic diguanylate monophosphate (c-di-GMP) controls the *cdrAB* operon (Borlee et al., 2010) through the transcriptional regulator FleQ (Baraquet and Harwood, 2015). In addition, the PhoBR two-component system and PUMA3 cell-surface signaling, both activated upon phosphate starvation, positively control the production of the PdtAB system (Llamas et al., 2009; Faure et al., 2014). Finally, two CDI systems are regulated by the post-transcriptional regulator RsmA (Mercy et al., 2016).

## ADDITIONS TO THE CORE: OTHER PROTEINS INVOLVED IN TPS SYSTEMS

A number of TPS systems comprise more than two partners (**Figure 2**). This is typically the case for the *cdiI, cdiO, cdiC* genes of CDI systems. In non-typeable *H. influenzae,* TPS systems are encoded by three-gene operons, *hmw1abc* and *hmw2abc* (Barenkamp and St Geme, 1994). *hmw1c* and *hmw2c* code for cytoplasmic glycosyltransferases. HMW1C covalently modifies Asn residues in repeated sequences of HMW1 with mono- and di-hexoses, which increases the stability of the adhesin against proteolytic degradation and antagonizes its release from the cell surface (Grass et al., 2003, 2010; Gross et al., 2008). Other TpsA proteins are also glycosylated (Fleckenstein et al., 2006), as are the passenger domains of a subset of proteins secreted by the type Va pathway (Benz and Schmidt, 2001; Moormann et al., 2002; Charbonneau et al., 2007; Charbonneau and Mourez, 2008; Côté et al., 2013). In addition to slowing down proteolytic degradation, these modifications appear to modify the properties of the adhesins and to modulate their secretion.

The hemopexin TpsA protein HxuA of *H. influenzae* is part of a three-gene operon, in which *hxuB* codes for the TpsB transporter and *hxuC* for a TonB-dependent transporter (Cope et al., 1995; Fournier et al., 2011). All three proteins are necessary to capture heme bound to hemopexin as an iron source. After binding hemopexin, HxuA would trigger heme release for its capture by HxuC (Zambolin et al., 2016).

Finally, some TpsA proteins undergo proteolytic maturation in the course of secretion, but the genes coding for their putative maturation proteases appear not to be part of the TPS-coding operons. Thus, the mature FHA adhesin of *B. pertussis* results from several proteolytic maturation steps (Coutte et al., 2001; Mazar and Cotter, 2006; Melvin et al., 2015). The protease involved in the release of the mature FHA protein from the cell surface is a subtilisin autotransporter called SphB1 (Coutte et al., 2001, 2003). Although no other substrates are known for SphB1, its gene does not belong to the locus encompassing *fhaB* and *fhaC*. Nevertheless, all three are regulated in a coordinated fashion, being part of the virulence regulon of *B. pertussis* (Antoine et al., 2000). In *P. aeruginosa*, the adhesin CdrA is a substrate of the periplasmic protease LapG whose activity is controlled by the intracellular level of c-di-GMP (Cooley et al., 2015; Rybtke et al., 2015). At low c-di-GMP level, LapG cleaves the periplasmic C-terminal tail of CdrA and releases this adhesin from the cell surface to prevent CdrA-dependent biofilm formation. Yet unidentified proteases are involved in the maturation of other TpsA proteins (Ward et al., 1998; Grass and St Geme, 2000; Schmitt et al., 2007).

**TABLE 2 | Factors involved in the regulation of TPS operons.**

| *tps* genes | Organism | Regulation | Reference |
|---|---|---|---|
| *hxuABC* | *Haemophilus influenzae* | Iron-limitation, Fur regulator | Wong and Lee, 1994; Cope et al., 1995 |
| *ethBA* | *Edwarsiella tarda* | Iron-limitation, Fur and EthR regulators, EsrAB two-component system | Hirono et al., 1997; Wang et al., 2009, 2010 |
| *phlBA* | *Photorhabdus luminescens* | Iron-limitation | Brillard et al., 2002 |
| *shlBA* | *Serratia marcescens* | Iron-limitation, RcsB regulator, RssAB two-component system | Poole and Braun, 1988; Lin et al., 2010; Di Venanzio et al., 2014 |
| *etpBAC* | *Escherichia coli* | Iron-limitation | Haines et al., 2015 |
| *rscBAC* | *Yersinia enterolitica* | RscR regulator | Nelson et al., 2001 |
| *cdrAB* | *Pseudomonas aeruginosa* | c-di-GMP level, FleQ regulator | Borlee et al., 2010; Baraquet and Harwood, 2015 |
| *fhaB-fhaC* | *Bordetella pertussis* | BvgAS two-component system | Scarlato et al., 1991 |
| *lspB-lspA2* | *Haemophilus ducreyi* | CpxRA two component system, Fis protein | Labandeira-Rey et al., 2009, 2013 |
| *pdtB-pdtA* | *Pseudomonas aeruginosa* | Phosphate limitation, PhoBR two-component system, PUMA3 system | Llamas et al., 2009; Faure et al., 2014 |
| *cdiBAI* | *Pseudomonas aeruginosa* | RsmA regulator | Mercy et al., 2016 |

# ANATOMY OF TPS SYSTEMS

## TpsA Proteins

TpsA proteins are large exoproteins (∼100–650 kDa) that progressively fold at the cell surface in the course of secretion across the outer membrane (see below). In spite of their different functions, all TpsA proteins harbor long stretches of imperfect repeats and are predicted to have high contents of β strand structure organized in fibrous, β-helix folds (Kajava and Steven, 2006a). First observed in pectate lyase (Yoder et al., 1993), the β-helix structure is a solenoid composed of long, parallel β sheets along the axis of the helix (Kajava et al., 2001; Kajava and Steven, 2006b). Its overall shape is provided by the stacking of coils, each of which is composed of three short β strands and forms a complete turn of the β helix. Each β strand interacts via hydrogen bonds with the closest β strands from previous and following coils, forming long parallel β sheets along the axis of the molecule. The interior of a β-helix protein is tightly packed with mostly hydrophobic residues, resulting in a very stable fold (Kajava and Steven, 2006a). Analysis of available structures has also highlighted structural elements that project out of the β-helical core and might carry out specific functions. The notion that the β helix serves as a scaffold to present functional loops or domains at a distance from the bacterial surface does not preclude the possibility that it also has specific functions of its own, such as mediating homotypic interactions that may contribute to biofilm formation (Menozzi et al., 1994; Ruhe et al., 2015).

The structural study of TpsA proteins is complicated by their large size and poor solubility. The fact that they must be secreted by their specific partners to acquire their native fold is a limiting factor for overexpression. Using X-ray crystallography, the majority of structures solved thus far are N-terminal TpsA fragments containing the "TPS" domain, or C-terminal fragments associated with toxin activities of CDI systems. One full-length TpsA structure has been solved, that of HxuA from *H. influenzae* (Zambolin et al., 2016).

All TpsA proteins share a conserved, ∼250-residue TPS domain, a.k.a. the secretion domain, corresponding to the minimal region needed for secretion. Located at the N terminus of the mature protein, this essential region mediates molecular recognition of the TpsB transporter in the periplasm, while coupling secretion and folding at the surface of the cell (see below) (Schönherr et al., 1993; Uphoff and Welch, 1994; Renauld-Mongénie et al., 1996; Jacob-Dubuisson et al., 1997; Grass and St Geme, 2000; Clantin et al., 2004; Surana et al., 2004; Hodak et al., 2006; Yeo et al., 2007; Weaver et al., 2009). Two subfamilies of TPS domains have been identified on the basis of sequence alignments (Yeo et al., 2007; Jacob-Dubuisson et al., 2009) and appear distinctly in the phylogenetic tree of TPS domains (**Figure 4**) (Yeo et al., 2007; Jacob-Dubuisson et al., 2009). In addition, subgroups can be defined based on TpsA functions, probably reflecting specificities in the steps of recognition and secretion initiation for these different groups. Thus far, four structures containing TPS domains are available, two of the first family, Fha30 of *B. pertussis* (Clantin et al., 2004) and HpmA265 of *P. mirabilis* (Weaver et al., 2009), and two of the second family, Hmw1-PP (*H. influenza;* Yeo et al., 2007), and HxuA of *H. influenzae* (Baelen et al., 2013; Zambolin et al., 2016).

TpsA proteins form right-handed β helices with three parallel β sheets, referred to as PB1, PB2, and PB3 (**Figure 5A**). The N-terminal β strands cap the β-helix tip by protecting the hydrophobic core from the solvent. The interior of the first β-helix coil is stabilized by a cluster of conserved aromatic residues from $\beta_4$, $\beta_5$, and $\beta_6$ (the nomenclature used here for strand numbering is that proposed in Baelen et al., 2013) (**Figure 5A**) (Clantin et al., 2004). Thereafter, the coils become more regular to eventually display a triangular-shaped cross-section in the C-terminal moiety of the TPS domain (**Figure 5B**). TPS domains present structural elements protruding from the β-helical core. Thus, in the middle of the TPS domain, an anti-parallel β sheet forms a β-sandwich structure with the core of the β helix (**Figure 5B**). In Hmw1-PP, the β sheet is formed by three β strands, with an α helix replacing the fourth one. TpsA proteins

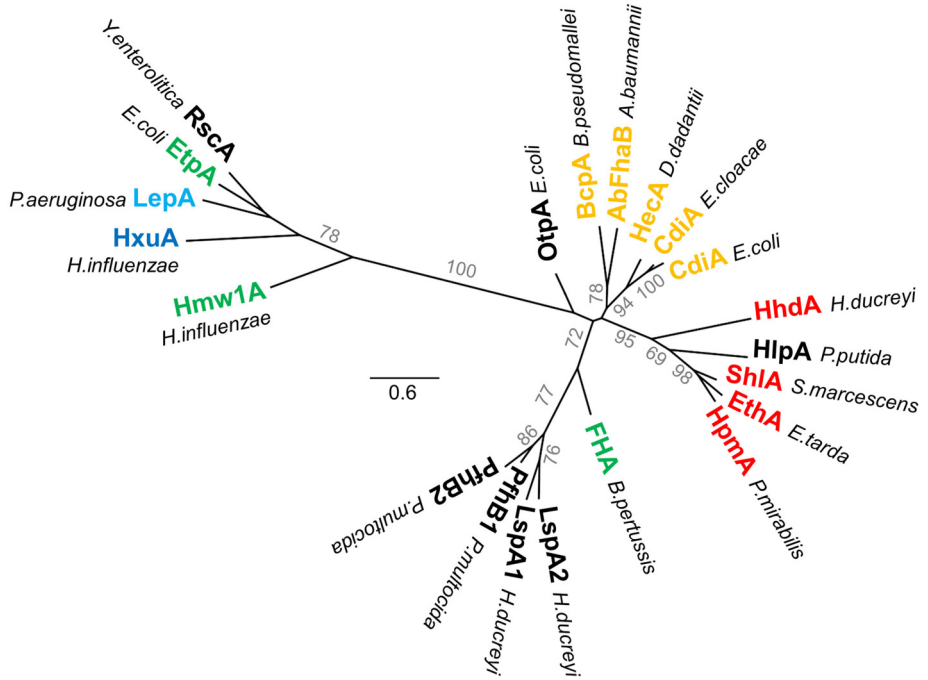


**FIGURE 4 | Phylogenetic tree of TPS domains.** Phylogenetic tree of TPS domains of TpsA proteins cited in this review. The tree shows the subdivision of TpsA proteins into two different families. The proteins also globally form clusters according to function (red for cytolysins/hemolysins, green for adhesins, orange for CDI systems, blue for proteases, dark blue for iron acquisition). The limits of the TPS domains included in the analysis were defined using both sequence similarities and secondary structure predictions, with available X-ray structures used as references. The amino acid sequences were aligned using Promals3D (Pei et al., 2008). PhyML implemented in Geneious v7.1.2 was used to generate an unrooted phylogenetic tree, where scale bars represent the number of substitutions per site, and bootstrap values above 50 (percentages of 1,000 replicates) are shown next to the branches.

also contain a highly conserved NPNG motif which forms a β turn between strands $\beta_{10}$ in PB2 and $\beta_{11}$ in PB3 and is crucial for folding and secretion (Jacob-Dubuisson et al., 1997; St Geme and Grass, 1998; Grass and St Geme, 2000; Hodak et al., 2006). Close to the N-terminus and only shared by Fha30 and HpmA265, a second anti-parallel β hairpin (denoted $\beta_{7/8}{}^{*}$) that harbors a conserved motif, NPNL, is also important for secretion (Schönherr et al., 1993; Jacob-Dubuisson et al., 1997; Hodak et al., 2006). As this anti-parallel β hairpin is absent from the second family of TPS domains, it is not essential for TpsA proteins in general but probably reflects specific secretion and/or folding properties of the TPS domains in the first family (**Figure 4**).

Due to their large size, little is known about the structural organization of full-length TpsA proteins beyond their TPS domains. Electron microscopy has been used to describe the global shape of 500-Å-long FHA (Makhov et al., 1994; Kajava et al., 2001). Based on electron microscopy and X-ray data, the most likely model for full-length FHA is that of a straight, elongated β helix formed from long regions of tandem repeats. The adherence functions of the protein likely map to extended loops and extra-helical motifs along the mature helix. A non-repeat domain of unknown structure that follows the β helix is also important for function (Kajava et al., 2001; Melvin et al., 2015). Folding of this domain requires the non-secreted C-terminal portion of the FHA precursor that is processed to form the mature protein and controls its release (Noel et al., 2012; Melvin et al., 2015).

The structure of the relatively small TpsA protein HxuA (96.3 kDa, 120 Å long) is shown in **Figure 5B**. HxuA is a right-handed β helix whose N-terminal and C-terminal moieties have different orientations because of a kink in PB1. This twist in the middle of the β helix divides the protein in two segments: the N-terminal moiety with the TPS domain, and the C-terminal moiety associated with HxuA function (**Figures 5A,B**). The latter is highly asymmetric due to α helices and long loops, including the essential M loop, that protrude from the β-helical core. The last residues resolved in the structure form an amphipathic α helix whose hydrophobic face interacts with PB1 while the other is solvent-exposed (**Figure 5B**).

Analysis of the HxuA-hemopexin complex by transmission electron microscopy and X-ray crystallography has revealed that hemopexin interacts only with the C-terminal moiety of HxuA (Zambolin et al., 2016). The interaction with hemopexin induces a large-scale motion of the M loop (**Figure 5B**) which then forms polar interactions with residues in the heme-binding pocket of hemopexin that trigger heme release.

In the HxuA structure, the 66 C-terminal amino acids are not detected in the electron density map. Similar to that of HMW1, the C terminus of HxuA is expected to remain in the periplasm. This anchor domain harbors a disulfide bond, which creates

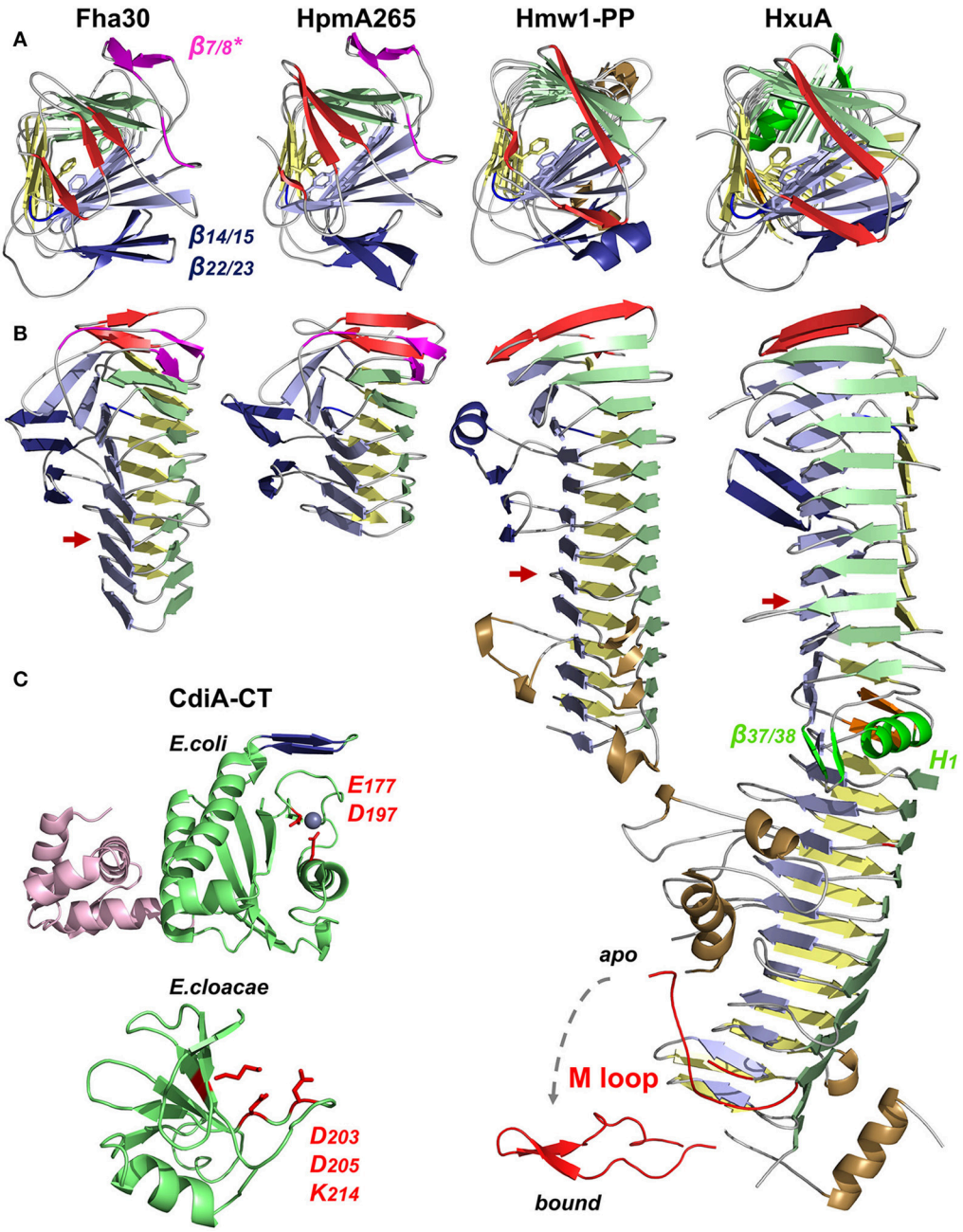


**FIGURE 5 | X-ray structures of TpsA proteins.** Cartoon representations of Fha30 (PDB entry 1rwr), HpmA265 (3fy3), Hmw1-PP (2odl), HxuA (4mr6 and 4rt6), CdiA-CT of *E. coli* EC869 (4g6u), and CdiA-CT of *E. cloacae* (4ntq). The parallel β sheets PB1, PB2, and PB3 are colored in light green, blue, and yellow, respectively. The first β strands corresponding to the N-terminal cap are represented in red. The NPNG motif and the extra-helical β-sheet $\beta_{14/15}$–$\beta_{22/23}$ conserved among TpsA proteins are in blue, and specific elements from the FHA subfamily (the NPNL motif and $\beta_{7/8}^{*}$) are in magenta. To harmonize the nomenclature between proteins, the numbers given to the structural elements may differ from those in the original publications. **(A)** Views from the N-terminal top of the β-helix axis. Residues of the aromatic cluster are shown in stick representation. **(B)** Side view of TpsA structures. Red arrows indicate the end of the TPS domain. Of note, $\beta_{14}$ is replaced by an α helix in Hmw1-PP, and part of that β sheet is missing in full-length HxuA. In these two structures, the extra-helical elements in the C-terminal moiety are in brown. For HxuA, structural elements responsible for the twist in the middle of the β helix are highlighted in green (α helix H1 in PB1, and β hairpin $\beta_{37}/\beta_{38}$). The M loop (in red) is represented in two conformations, with and without hemopexin, denoted bound and apo, respectively. **(C)** Structures of the CdiA-CT domains of CdiA proteins. The nuclease domain is highlighted in green, with the side chains of the active site residues in red. For the CdiA-CT of *E. coli*, the active-site $Zn^{2+}$ ion is shown as a sphere, and the N-terminal α-helical bundle is colored in pink. The β hairpin involved in forming β-sheet structure with the immunity protein is in blue. The structures of the toxins were solved in complex with their respective immunity proteins (not represented), arguing that the CdiA-CT moieties must be in inactive conformations.

a globular loop region that locks the TpsA C terminus in the pore of its TpsB partner (Buscher et al., 2006). Preventing HxuA release into the supernatant must be important to couple heme release and import. The presence or absence of this C-terminal anchor domain possibly reflects functional differences among TpsA proteins.

To date, no full structure has been reported of the very large CdiA proteins (180–650 kDa), but several structures of CdiA-CT domains have been obtained by producing the toxic domain in complex with its cognate CdiI immunity protein. For CdiA-CT of *E. coli* EC869, the structure starts ∼80 residues after the VENN motif. The N-terminal and C-terminal domains of CdiA-CT form a 4-helix bundle and a central β sheet sandwiched between four α helices, respectively (**Figure 5C**). The second domain is structurally similar to type IIS restriction endonucleases, with a $Zn^{2+}$ ion in the active site (Kachalova et al., 2008; Morse et al., 2012). Adjacent to the active site, a β hairpin interacts with the immunity protein by β augmentation, forming an anti-parallel β sheet (Morse et al., 2012). The structure of another CdiA-CT corresponding to the last 75 amino acids of the *E. cloacae* CdiA protein in interaction with its immunity protein shows a completely different fold, displaying structural homology with the nuclease domain of colicin E3. The toxin domain is folded into one α helix followed by a five-stranded anti-parallel β sheet and is expected to cleave 16S rRNA (**Figure 5C**) (Beck et al., 2014b). These two CdiA-CT moieties share no function, sequence or structural homologies, reflecting how bacteria use two-partner secretion and the modular organization of CdiA proteins to deliver various kinds of toxins into target cells.

## TpsB Transporters

The second partner in a TPS system is the TpsB protein. These proteins belong to the ubiquitous Omp85 superfamily, whose best-known members are the essential BamA transporters that assemble proteins in the outer membrane of Gram-negative bacteria (reviewed in Bos et al., 2007; Knowles et al., 2009; Hagan et al., 2011; Ricci and Silhavy, 2012). All the X-ray structures of Omp85 transporters thus far available show that these transporters share major structural features (Clantin et al., 2007; Gruss et al., 2013; Noinaj et al., 2013; Albrecht et al., 2014; Ni et al., 2014; Maier et al., 2015; Bakelar et al., 2016; Gu et al., 2016; Han et al., 2016). For TpsB transporters, the only structure reported thus far is that of FhaC (Clantin et al., 2007; Maier et al., 2015) (**Figure 6A**).

The C-terminal moiety of FhaC forms a 16-stranded, anti-parallel β barrel in the outer membrane, which has been shown to serve as the pore for the translocation of its FHA partner across the outer membrane (Baud et al., 2014). The β barrel is preceded by two periplasmic Polypeptide Transport-Associated (POTRA) domains in tandem, called POTRA1 and POTRA2. The POTRA domain fold is βααββ, with an anti-parallel β sheet flanked by two α helices on one side of the sheet. POTRA domains have been proposed to mediate protein-protein interactions, probably by β augmentation (Kim et al., 2007). The POTRA domains of several TpsB proteins have been shown to recognize the TPS domains of their respective TpsA partners (Surana et al., 2004; Hodak et al., 2006; Delattre et al., 2011; ur Rahman et al., 2014; Garnett et al., 2015; Grass et al., 2015). A major binding site for the FHA TPS domain in FhaC is a hydrophobic groove formed by the edge of the β sheet and the flanking α helix of the barrel-proximal POTRA2 domain (Delattre et al., 2011). This site appears to be well suited to accommodate amphipathic polypeptide segments of FHA, which interacts with FhaC in an extended, not-yet folded conformation (Hodak et al., 2006).

The β barrel of FhaC is occluded by the N-terminal α helix, H1, which crosses the barrel pore with its N terminus at the cell surface and its C terminus in the periplasm. Although not required for activity, similar helices are predicted in most TpsB proteins (Guérin et al., 2014). This N-terminal α helix might facilitate biogenesis as well as stabilize the "resting" form of the transporter (see below). The α helix H1 is followed by a 30-residue periplasmic linker in an extended conformation that joins H1 to the N terminus of the membrane-distal POTRA1 domain (Maier et al., 2015). Unlike H1, which is dispensable, the linker is necessary for FhaC secretion activity (Guédin et al., 2000; Clantin et al., 2007). The X-ray structure of FhaC has revealed that the linker occupies the FHA binding site along POTRA2. One of its functions might thus be to regulate accessibility of the binding site in a competitive mechanism (Guérin et al., 2014; Maier et al., 2015).

The β barrel of FhaC is also partially occluded by a long extracellular loop, L6, a hallmark feature of Omp85 transporters (Moslavac et al., 2005; Arnold et al., 2010). The Arg of the highly conserved VRGY/F motif at the tip of L6 forms a salt bridge with the Asp of another conserved motif, F/GxDxG, located on the β strand β13 of the barrel (Maier et al., 2015). This interaction thus positions L6 within the β barrel in a similar manner in all available Omp85 structures (Gruss et al., 2013; Noinaj et al., 2013; Albrecht et al., 2014; Ni et al., 2014; Bakelar et al., 2016; Gu et al., 2016; Han et al., 2016). Like the barrel-proximal POTRA domain, L6 is essential for the activity of Omp85 proteins. The functions of these critical pieces of the machinery remain unclear (Delattre et al., 2010; Leonard-Rivera and Misra, 2012; Rigel et al., 2013).

# PATHWAY OF TPSA PROTEINS ACROSS THE CELL ENVELOPE

The pathway of TpsA proteins from the cytoplasm to the cell surface has been reviewed in (Jacob-Dubuisson et al., 2004; van Ulsen et al., 2014). After an overview of current knowledge, we will spell out the unresolved questions on the transport mechanism.

## Export across the Inner Membrane and the Periplasm

TpsA proteins are synthesized as preproteins, and their N-terminal signal peptide determines Sec-dependent export across the cytoplasmic membrane (Grass and St Geme, 2000; Chevalier et al., 2004). Some of them have an extended signal peptide that harbors a semi-conserved N-terminal extension (Jacob-Dubuisson et al., 2004; van Ulsen et al., 2014), which is also found in subsets of classical and trimeric AT proteins (Peterson et al., 2006; Desvaux et al., 2007; Szczesny and Lupas, 2008). Among

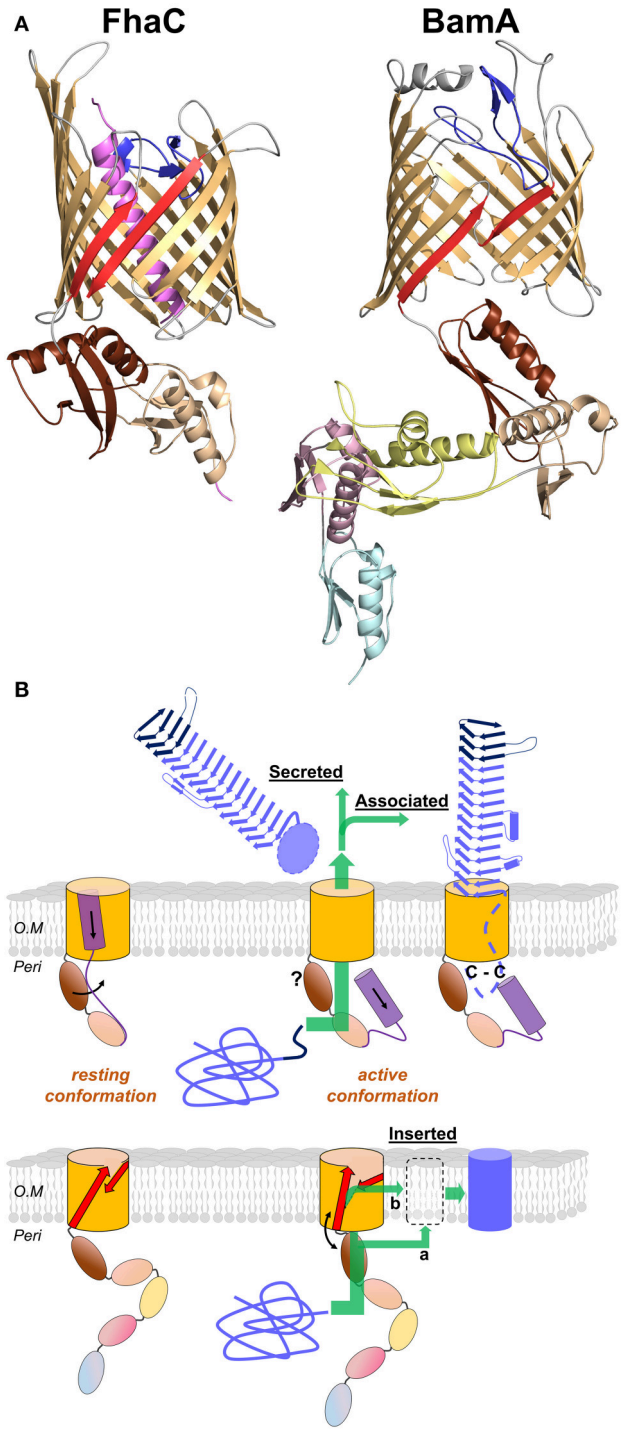


**FIGURE 6 | Omp85 transporters: X-ray structures to mechanistic models. (A)** Cartoon representations of FhaC from *B. pertussis* (PDB entry 4ql0) and BamA from *N. gonorrhoeae* (4k3b). The common structural features include the 16-strand barrel in gold, the L6 loop in blue and the last two POTRA domains in wheat and brown (POTRA1 and POTRA2 for FhaC). The $\beta_1$ and $\beta_{16}$ strands are shown in red. Specific elements include the N-terminal α helix of FhaC in purple, and the POTRA3-2-1 domains of BamA in yellow, pink, and cyan, respectively. **(B)** Mechanistic models for TpsB transporters and BamA proteins (upper and lower diagrams, respectively). The substrates *(Continued)*

**FIGURE 6 | Continued**
are colored blue, unfolded in the periplasm and folded in their final locations. For FhaC, the motions of the N-terminal α helix H1 and of the POTRA2 domain are shown with black arrows (see text). The TPS domain (dark blue) interacts with the POTRA domains, and the TpsA protein is translocated through the barrel pore (green arrow). The location of the POTRA domains at this stage remains to be determined. Depending on the subfamily, the TpsA is secreted into the milieu or remains associated with its transporter by a small globular periplasmic domain harboring a disulfide bond (C-C). For BamA, the available structures indicate at least two conformations, one in which POTRA5 is away from the β barrel and $\beta_1$ and $\beta_{16}$ are close to one another with H bonds formed between them, and another characterized by the occurrence of a lateral gate caused by the reorientation of $\beta_1$–$\beta_8$ and POTRA5. This gate might serve for progressive folding of the substrate through the formation of a hybrid barrel with BamA, before its release in the outer membrane (green arrow denoted b; BAM-budding model). Local destabilization of the bilayer close to the $\beta_1$–$\beta_{16}$ junction might also facilitate direct insertion of the prefolded substrate in the membrane (green arrow denoted a; BAM-assisted model). The L6 loop and the rest of the BAM complex are not represented.

TPS systems, the function of these extended signal peptides has been investigated only in the case of the TpsA preprotein FhaB, which is the precursor of FHA in *B. pertussis*. This study has revealed that the extension optimizes biogenesis by slowing down export and delaying signal peptide cleavage (Chevalier et al., 2004). The role of the extension has also been studied for several AT proteins, as reviewed in (Desvaux et al., 2006; van Ulsen et al., 2014). It was shown in the case of EspP that, by prolonging the association of the AT with the inner membrane, the extended signal peptide might prevent non-productive folding of the passenger domain in the periplasm (Szabady et al., 2005).

Following Sec-dependent export, the TpsA proteins reach the periplasm, where they remain in extended conformations for their interactions with their TpsB transporters. How the not-yet-folded TpsA secretion intermediates are protected from degradation, misfolding, or aggregation in the periplasm has been investigated in very few systems. Chaperone requirement by TpsA proteins might depend on their size, the proteolytic activity in the periplasm of the host bacterium, and the rates at which they tend to aggregate or to misfold. The proteins that form long β solenoids are generally slow to fold and do not have a strong tendency to aggregate, two properties favorable to Type V secretion (Hodak et al., 2006; Junker et al., 2006; Junker and Clark, 2010).

The time window during which TpsA periplasmic intermediates retain secretion competence markedly depends on the system. For the OtpAB system of *E. coli* O157:H7, expression of the OtpB transporter could be triggered after that of its TpsA partner with no detrimental effect on secretion, demonstrating that export across the cytoplasmic membrane and secretion across the outer membrane need not be temporally coupled (Choi and Bernstein, 2009). In contrast, periplasmic intermediates of FHA appeared to rapidly become secretion-incompetent *in vivo* (Guédin et al., 1998). Similarly, when secretion was reconstituted *in vitro*, delaying the addition of FhaC-containing proteoliposomes to FHA-producing spheroplasts strongly impaired translocation into the vesicles (Fan et al., 2012).

While *bona fide* periplasmic intermediates are detectable for some TpsA proteins, including ShlA, OtpA and a few others (Schiebel et al., 1989; van Ulsen et al., 2008; Choi and Bernstein, 2009), in other TPS systems, in contrast, they appear to be quickly degraded. Thus, HMW1 and FhaB were proteolyzed by the protease-chaperone DegP if their secretion was impeded, probably to limit the development of envelope stress (St Geme and Grass, 1998; Baud et al., 2009). On the other hand, in the case of FHA, DegP was also shown to facilitate secretion (Baud et al., 2009, 2011). In particular, a specific form of DegP associated with the cytoplasmic membrane was found to bind non-native FHA fragments with strong affinity, indicating that it might be a "holding chaperone" (Baud et al., 2009, 2011). The involvement of DegP has been shown in type Va, Vc, and Ve systems, suggesting that it might be general in the type V pathway (Mogensen and Otzen, 2005; Grosskinsky et al., 2007; Oberhettinger et al., 2012).

## Translocation across the Outer Membrane: Function of the TpsB Partner

Molecular recognition between the two partners is mediated by the TPS domain and the POTRA domains of the TpsA and TpsB proteins, respectively (Surana et al., 2004; Hodak et al., 2006; Delattre et al., 2011; Garnett et al., 2015). The TPS domain of the TpsA protein must be in an extended conformation for interaction with the POTRA domains of the TpsB transporter, as shown for the FHA/FhaC and HMW1/HMW1B pairs (Hodak et al., 2006; Grass et al., 2015). Surface plasmon resonance experiments with the FHA/FhaC pair have indicated interactions of micromolar affinity between the two proteins and suggested that association and dissociation occur very fast (Delattre et al., 2011). Similarly, NMR experiments on the LepAB system of *P. aeruginosa* have shown fast exchange between the bound and free forms, which also supports the idea that TpsA-TpsB interactions are dynamic (Garnett et al., 2015). While this may be expected from the fact that the partners must dissociate after secretion, this property is likely to have some bearing on the mechanisms of transport (see below). What constitutes the "secretion signal" of a TpsA protein is imperfectly defined but most likely involves a combination of conserved and non-conserved residues, as well as some extended amphipathic structure, likely for β augmentation of the POTRA β sheets (Hodak et al., 2006; Kim et al., 2007; Gatzeva-Topalova et al., 2010). Crystal structures of the soluble periplasmic domain of the Omp85 proteins BamA and TamA indicate that POTRA domains may generally interact with other proteins by β augmentation (Kim et al., 2007; Gruss et al., 2013).

Binding of the TPS domain to the POTRA domains is followed by the transport of the TpsA protein to the cell surface, most likely in an extended conformation, but a large gap persists in our understanding of the translocation step itself (**Figure 6B**). The path of translocation of FHA across the outer membrane has been investigated by *in vivo* cross-linking. This identified several regions of FhaC that interact with FHA: the surface of the POTRA domains, the inner lining of the β-barrel pore, and specific surface loops (Baud et al., 2014). Similarly, in particular two regions in the N-terminal and central parts of the TPS domain of FHA interact with FhaC. The interaction map reveals a funnel-like pathway, with the conformationally flexible TPS domain entering the channel in a non-exclusive manner and exiting along a specific four-stranded β sheet at the cell surface (Baud et al., 2014). Translocation initially appears to proceed in discrete steps, which is consistent with a repetitive, cyclic process (Baud et al., 2014).

Two models of translocation have been proposed. According to the first one, the TpsA protein forms a hairpin in the pore. Its TPS domain remains bound to the POTRA domains throughout the entire process, while the rest is progressively translocated and folds at the cell surface. In this scenario, the TPS domain is released at a late or final stage of translocation (Mazar and Cotter, 2006). In an alternative model, the TPS domain reaches the surface first and nucleates the folding of the rest of the protein (Hodak and Jacob-Dubuisson, 2007). Several pieces of evidence suggest that the latter mechanism is at play, notably the efficient secretion of N-terminal truncates of TpsA proteins (Jacob-Dubuisson et al., 2004), and the accessibility of the N-terminus of stalled FHA constructs at the cell surface (Guérin et al., 2014). In addition, the stable TPS fold and the observation that a TPS domain can initiate TpsA folding *in vitro* (Walker et al., 2004; Weaver et al., 2009) indicate that the TPS domain may have a similar role in initiating folding in two-partner secretion as that suggested for the stable C-terminal core of the passenger domain in autotransporter secretion (see below; Junker et al., 2006, 2009; Peterson et al., 2010; Renn et al., 2012; Besingi et al., 2013).

Irrespective of the model, the same basic questions arise: how is the TpsA protein pulled or pushed into the pore? What initiates the process and what drives it forward? Does the TpsB transporter cycle between different conformations in order to mediate the progressive transport of its substrate? It should be noted that no high-energy, hydrolyzable compounds such as ATP are available in the periplasm, and that the semi-permeable outer membrane cannot sustain an electrochemical gradient based on small ions, although a Donnan potential may exist (see below; Sen et al., 1988). The process should thus involve transitions between conformations separated by low energy barriers.

The dynamics of the FhaC transporter has been investigated using electron paramagnetic resonance (EPR), which provides information on the mobility of specific regions of the protein as well as the distances between them. These experiments revealed that FhaC exists in an equilibrium of several conformations. The first equilibrium concerns the N-terminal α helix H1 which spontaneously moves to the periplasm (Guérin et al., 2014). The movement of H1 breaks linker-POTRA interactions, thus allowing the TPS domain of the substrate protein to bind to the POTRA domains (**Figure 6B**). The equilibrium between the resting, closed conformation of FhaC and the open conformation of FhaC with H1 in the periplasm might thus be displaced by the binding of FHA (Guérin et al., 2014; Maier et al., 2015). Similarly, in the LepB transporter of *P. aeruginosa*, the linker may transiently interact with POTRA2 and be displaced by the substrate (Garnett et al., 2015).

The second equilibrium concerns the conserved loop L6 that is folded back inside the pore from the cell surface and interacts with the inner wall of the barrel (Guerin et al., 2015; Maier et al.,

2015). Although this loop, and in particular its VRGY hallmark motif, is essential for activity (Clantin et al., 2007; Delattre et al., 2010), its function remains obscure. It does not seem to have a direct role in substrate pulling (Baud et al., 2014) and appears relatively rigid in EPR experiments (Guerin et al., 2015). Notably, in BamA, attaching L6 to the barrel does not inhibit growth, so large-scale motion of L6 does not seem to be required for BamA function (Noinaj et al., 2014). Nevertheless, the position of L6 appears to change in the pore and to modulate channel opening (Guerin et al., 2015). Although these experiments have revealed that, overall, TpsB proteins are highly dynamic, they fall short of describing the full secretion cycle.

Secretion and folding are most likely coupled in the TPS pathway. This has long been proposed to explain how secretion could proceed in the absence of classical sources of energy. Thus, once a TpsA protein emerges at the cell surface and starts to fold into a β helix, the difference in free energy between the extended and the folded forms is thought to drive secretion (Jacob-Dubuisson et al., 2004). This model has been extensively probed for type Va AT proteins whose passenger domains also fold into long β solenoids. These β helices appear to unfold and fold in several steps, and many of them appear to have a stable core that initiates folding (Oliver et al., 2003; Renn and Clark, 2008). The passenger domain of a classical AT protein forms a hairpin in the pore in the course of secretion, and thus its C-terminal portion reaches the cell surface first (Bernstein, 2007; Junker et al., 2009; Zhai et al., 2011). In many cases the C-terminal region of the passenger has a greater thermostability than the rest of the protein, and this difference is thought to promote its vectorial folding, which may then drive secretion (Junker et al., 2006, 2009; Peterson et al., 2010; Renn et al., 2012; Besingi et al., 2013). The initiation of translocation, before passenger folding can occur, may then be linked to the energetically favorable folding and membrane insertion of the β barrel, with BamA lowering the kinetic barrier (Moon et al., 2013; Gessmann et al., 2014). Consistent with the hypothesis of folding-driven secretion, mutations that impair folding of the C-terminal passenger region or the β helix in general have been observed to reduce or abolish secretion (Peterson et al., 2010; Renn et al., 2012; Drobnak et al., 2015). However, it has been noted that the free energy typically associated with protein folding is orders of magnitude smaller than the energetic cost of protein transport across a membrane as it has been measured, for example, for translocation across the chloroplast envelope (Kang'ethe and Bernstein, 2013a). Nevertheless, the possibility of reconstituting type V secretion systems *in vitro* and obtaining translocation of TpsA proteins and AT passengers into liposomes demonstrates that, in these systems, protein translocation across a membrane is indeed possible without input of external energy (Norell et al., 2014). One solution that has been proposed to this apparent conundrum is a "Brownian ratchet"-type mechanism in which random thermal motion obtains directionality via an effectively irreversible step, here, the folding of the transport substrate on the extracellular side, which prevents backtracking of the protein chain (Peterson et al., 2010; Drobnak et al., 2015). Apart from the folding free energy, the required free energy for this process would be contributed by the mechanisms that keep secretion substrates unfolded in the periplasm, i.e., most likely chaperones (Baud et al., 2009; Jacob-Dubuisson et al., 2013). Such mechanisms have been described theoretically (Simon et al., 1992; Depperschmidt et al., 2013) and demonstrated experimentally e.g. for transport into the endoplasmatic reticulum (Matlack et al., 1999), suggesting that they may also be involved in bacterial type V secretion.

Still, it has been observed that, when engineered into an AT sequence, even a disordered domain that does not assume a stable structure could be secreted. This occurred even if the remaining passenger domain fragment was too short to fold (Kang'ethe and Bernstein, 2013b). A Brownian ratchet mechanism thus cannot be at play in this case. However, removal of negatively charged residues in the passenger was observed to inhibit secretion in this system. In this context, it is interesting to note that sizable Donnan potentials—with the periplasmic side negative—have been observed across the *E. coli* outer membrane and traced to the presence of negatively charged oligosaccharides (Sen et al., 1988). The observation that a disordered, negatively charged polypeptide can be secreted thus suggests that an electrochemical potential based on large, impermeable charged molecules may indeed be present across the bacterial OM and play a role in type V secretion. In addition, the process might also benefit from entropic effects due to the difference between the crowded periplasmic environment and the extracellular milieu (Fan et al., 2016); however, extracellular crowding agents have not been observed to affect AT secretion (Drobnak et al., 2015).

The same principles of differential stability between distinct regions of the secreted β helix and of vectorial folding observed in AT proteins likely apply to TPS systems as well, and therefore the region emerging first from the TpsB channel probably nucleates folding of the β helix at the cell surface. The conserved TPS domain is an obvious candidate for this function, and several data support the idea. Early studies have indicated that the TPS domain of ShlA was able to template the folding of the unfolded full-length protein to form the active toxin *in vitro* (Schiebel et al., 1989; Schönherr et al., 1993). Similar experiments with the TPS domain of HpmA have shown that cooperative β strand interactions mediate the folding of neighboring full-length proteins, a process called "template-assisted hemolysis" (Weaver et al., 2009). Two more recent pieces of work have addressed the unfolding properties of the TPS domains of FHA and HpmA, by using atomic force microscopy (Alsteens et al., 2013) or chemical denaturation (Wimmer et al., 2015), respectively. Both studies have shown that TPS domains unfold in several steps and harbor highly stable core subdomains. In the second case, the presence of the folded core subdomain allowed rapid folding of the rest of the TPS domain *in vitro*. It is tempting to speculate that these core regions of the TPS domain fold early in the course of secretion and nucleate folding of the rest by β augmentation concomitant with translocation, and that a Brownian ratchet-type of mechanism is at play in TPS secretion as well.

Translocation initiation in TPS systems cannot be linked to the free energy gained from β barrel folding and membrane insertion, as has been proposed for AT proteins (Moon et al., 2013), since the two processes are independent. Here, the specific but transient interactions observed between the TpsB transporter

and the TPS domain of its substrate likely play a role (Delattre et al., 2011).

The possibility that the TpsB transporter assists in the initial folding of its partner has been suggested by recent observations in two different TPS systems. Thus, specific interactions were shown to occur between parts of the FHA TPS domain and specific surface β strands and loops of FhaC (Baud et al., 2014). The edge of this small surface-exposed β sheet of FhaC might guide the secretion of the TPS domain and template its initial folding at the cell surface by β augmentation (Baud et al., 2014). Interestingly, the corresponding loops of HMW1B appear to tether the HMW1 adhesin at the cell surface of *H. influenzae* (Grass et al., 2015). Thus, specific structural features at the extracellular surface of the TpsB transporter might be involved in the secretion of the cognate TpsA partner and possibly also retain its N terminus close to the cell surface.

## What Can We Learn for the TPS Pathway from the Role of BamA in Type V Secretion?

TpsB transporters are Omp85 proteins specialized in the transport across the outer membrane of soluble protein substrates (Heinz and Lithgow, 2014). In parallel with the role of a specialized Omp85 transporter for type Vb secretion, there have been multiple demonstrations that another Omp85 transporter, BamA, and indeed the BAM complex, is involved in the folding and insertion of most outer membrane proteins, including classical ATs (type Va) (Jain and Goldberg, 2007; Ieva and Bernstein, 2009; Sauri et al., 2009; Ieva et al., 2011), trimeric ATs (Lehr et al., 2010) and type Ve intimins (Bodelón et al., 2009; Oberhettinger et al., 2012). Omp85 transporters thus form the mechanistic basis of type V secretion.

In spite of the many structures now available of BamA and the BAM complex (**Figure 6A**), our models for the molecular mechanisms of protein assembly in the outer membrane remain somewhat speculative (Hagan et al., 2011; Noinaj et al., 2015). Several studies have shown that BamA opens laterally between its first and last β strands in the outer membrane and that this opening is required for function (Noinaj et al., 2013, 2014; Albrecht et al., 2014; Iadanza et al., 2016). Another important feature common to all BamA structures is a decreased hydrophobic thickness where the first and last β strands meet, which causes a local thinning of the outer membrane (Noinaj et al., 2013, 2014). Two popular mechanistic models for BamA-mediated protein assembly are the BAM-assisted and BAM-budding models (**Figure 6B**). It should be noted that they have not been experimentally proven, and it is possible that different models apply to different classes of OMPs. The BAM-assisted model postulates that some OMPs can fold without help from accessory proteins and need only a locally destabilized outer membrane in which to insert the fully folded OMP. BamA locally disturbs the outer membrane where its first and last β strands meet, and it could serve as a folding catalyst by lowering the kinetic barrier to nascent OMP insertion (Burgess et al., 2008; Noinaj et al., 2013, 2015; Gessmann et al., 2014). The BAM-budding model takes into account the requirement for lateral opening of BamA and might explain how BAM helps to fold OMPs that do not spontaneously fold on their own. In this model, an unfolded OMP would be delivered to the BAM complex by periplasmic chaperones such as SurA and Skp. The nascent OMP would then be sequentially folded by pairing individual β strands with the first and last β strands of BamA separated by the lateral opening. In this model, β strands from the nascent OMP would be added to BamA, forming a hybrid BamA-OMP barrel, and eventually the new OMP would separate from BamA and move away laterally into the outer membrane (**Figure 6B**).

Classical AT proteins (type Va) are composed of both a β barrel moiety and a soluble passenger domain, and several pieces of work have indicated that the BAM complex is involved in both the insertion of the β barrel moiety into the membrane and the translocation of the passenger domain to the bacterial surface (Ieva et al., 2008; Ieva and Bernstein, 2009; Sauri et al., 2009). For the AT protein EspP, an assembly intermediate was detected in the periplasm whose topology resembled that of the assembled protein, with a segment preceding the barrel moiety embedded in a "proto-barrel" (Ieva et al., 2008). Interactions were detected between the BAM complex and both the barrel and the passenger domains of the AT substrate (Ieva and Bernstein, 2009). Formation of the β barrel domain thus appears to proceed to a certain extent in the periplasm, with a β hairpin that corresponds to a segment C-terminal of the passenger incorporated in its pore. According to these authors, the proto-barrel would then undergo a conformational change before translocation is initiated. The passenger domain would interact with the POTRA domains of BamA and progressively move through a channel, composed of BamA and/or the AT barrel (Pavlova et al., 2013). These observations are at odds with the model that the β barrel of the AT protein assembles progressively, hairpin by hairpin, in the outer membrane as suggested by the budding model, and they argue that the lateral opening of the BamA barrel might play another role in the assembly/secretion process of ATs.

What about TPS systems? TpsA proteins are soluble and have no transmembrane domain, and thus they represent "simpler" substrates than AT proteins. *In vitro* reconstitution of TPS secretion has shown that, while TpsB proteins are inserted into the OM by the BAM complex like most outer membrane proteins (Norell et al., 2014), they form autonomous secretion ports for their TpsA substrates (Fan et al., 2012). In other words, the translocation of a TpsA protein only requires its TpsB partner and does not proceed through a channel also involving BamA. A TpsB transporter thus mediates the translocation of its soluble TpsA substrate by itself.

The role of the POTRA domains in Omp85 transporters is likely to go beyond the recruitment of substrate proteins, as suggested by a point mutation in POTRA2 that affects the function of FhaC but not the binding of FHA (Delattre et al., 2011). This mutation changes a highly conserved Asp residue in the TpsB family that participates in periplasmic interactions between the POTRA2 domain, the linker and the barrel (Maier et al., 2015). The POTRA domains might thus contribute to addressing the TpsA protein to the pore of the TpsB transporter. Similar suggestions were made for the POTRA domains of HMW1B and LepB (Garnett et al., 2015; Grass et al., 2015).

Their role in shuttling the passenger to the barrel might explain why PlpD, the prototypic Vd protein, harbors a POTRA-like domain. Since the Patatin domains of the passenger are part of the same polypeptide as the TpsB-barrel-like transporter moiety, the POTRA-like domain is not necessary to recruit the substrate.

Both BamA and TpsB transporters most likely work in a cyclic manner and go through their "conformational cycle" several times in the course of secretion of their long substrates (**Figure 6B**). The conformational changes that they undergo remain to be described, but we propose that they involve concerted motions of the three conserved structural components essential for activity, i.e., the β barrel, the L6 loop and the barrel-proximal POTRA domain. A few observations support this hypothesis. It has been proposed that the L6 loop of BamA cycles between several conformations, and that its conformation is modulated by other Bam proteins via the POTRA5 domain (Rigel et al., 2013). A functional connection between the latter and L6 in BamA has also been found in a search for intragenic suppressors of a mutation that disrupts the L6-barrel interaction (Dwyer et al., 2013). Functional links between L6 and the barrel are clearly established. For instance, the FhaC channel becomes larger if the interaction between L6 and the wall of the barrel is disrupted (Guerin et al., 2015). Similarly, two conductance states have been recorded for the HMW1B transporter. The higher-conductance state is occasionally visited by the protein and likely corresponds to a more open channel (Duret et al., 2008).

Our current hypothesis for the mechanism of two-partner secretion is that the TpsB barrel cycles between narrow-channel and open-channel states. As seen with BamA, the conformational changes might induce a reorientation of β1 and POTRA2, with the formation of a lateral opening between the first and last strands of the β barrel. This lateral opening could be used to enlarge the β barrel with the insertion of amphipathic β hairpin(s) from periplasmic portions of the protein, thus hoisting a first portion of substrate bound to the POTRA domains toward the surface. After the substrate is released on the extracellular side of the outer membrane to initiate folding, possibly along a template provided by extracellular parts of the barrel, the inserted region switches back to the periplasm to repeat the cycle. We hypothesize also that L6 can stabilize these conformations by forming distinct interactions with specific regions of the β barrel in each of the two states. The TpsA protein might thus "hitch-hike" on spontaneous conformational changes of its transporter for translocation. Together with extracellular-only folding as required for a Brownian ratchet mechanism, and possibly a Donnan potential, our proposed mechanism accounts for the vectorial translocation of TpsA proteins across the bacterial OM.

## CONCLUSION

TPS systems are widespread among Gram-negative bacteria, both pathogenic and environmental. They serve many different functions that participate in the interactions of the bacteria with their environment, be it the host cell or bacterial competitors. The diversity of type V systems deployed by bacteria is probably yet larger than we have come to realize, with hybrid systems made up of parts borrowed from a variety of protein domains. The mechanisms of transport of such diverse and sometimes extremely long domains remain poorly understood. Endeavors to decipher those mechanisms will undoubtedly illuminate the inner workings of Omp85 transporters.

## AUTHOR CONTRIBUTIONS

All authors listed have made substantial, direct and intellectual contribution to the work, and approved it for publication.

## ACKNOWLEDGMENTS

We thank Maarten Ghequire for help with the Geneious software and phylogenetic trees. JG and SKB are supported by the Intramural Research Program of the NIH, the National Institute of Diabetes and Digestive and Kidney Diseases (NIDDK). SB is supported by a FINOVI grant and CNRS. The work of FJ has been supported over the years by the ANR (grant ANR-10-BLAN-1306), INSERM, CNRS, and Région Nord Pas de Calais. RS gratefully acknowledges funding via a "Projets exploratoires premier soutien" (PEPS) grant from the CNRS and the University of Lille. We also acknowledge support from TGE RMN THC (FR-3050, France) and FRABio (Univ. Lille, CNRS, FR 3688).

## REFERENCES

Albrecht, R., Schutz, M., Oberhettinger, P., Faulstich, M., Bermejo, I., Rudel, T., et al. (2014). Structure of BamA, an essential factor in outer membrane protein biogenesis. *Acta Crystallogr. D Biol. Crystallogr.* 70, 1779–1789. doi: 10.1107/S1399004714007482

Alsteens, D., Martinez, N., Jamin, M., and Jacob-Dubuisson, F. (2013). Sequential unfolding of beta helical protein by single-molecule atomic force microscopy. *PLoS ONE* 8:e73572. doi: 10.1371/journal.pone.0073572

Amitai, G., Belenkiy, O., Dassa, B., Shainskaya, A., and Pietrokovski, S. (2003). Distribution and function of new bacterial intein-like protein domains. *Mol. Microbiol.* 47, 61–73. doi: 10.1046/j.1365-2958.2003.03283.x

Anderson, M. S., Garcia, E. C., and Cotter, P. A. (2012). The *Burkholderia bcpAIOB* genes define unique classes of two-partner secretion and contact dependent growth inhibition systems. *PLoS Genet.* 8:e1002877. doi: 10.1371/journal.pgen.1002877

Anderson, M. S., Garcia, E. C., and Cotter, P. A. (2014). Kind discrimination and competitive exclusion mediated by contact-dependent growth inhibition systems shape biofilm community structure. *PLoS Pathog.* 10:e1004076. doi: 10.1371/journal.ppat.1004076

Antoine, R., Alonso, S., Raze, D., Coutte, L., Lesjean, S., Willery, E., et al. (2000). New virulence-activated and virulence-repressed genes identified by systematic gene inactivation and generation of transcriptional fusions in *Bordetella pertussis*. *J. Bacteriol.* 182, 5902–5905.

Aoki, S. K., Diner, E. J., de Roodenbeke, C. T., Burgess, B. R., Poole, S. J., Braaten, B. A., et al. (2010). A widespread family of polymorphic contact-dependent toxin delivery systems in bacteria. *Nature* 468, 439–442. doi: 10.1038/nature09490

Aoki, S. K., Malinverni, J. C., Jacoby, K., Thomas, B., Pamma, R., Trinh, B. N., et al. (2008). Contact-dependent growth inhibition requires the essential outer membrane protein BamA (YaeT) as the receptor and the inner membrane transport protein AcrB. *Mol. Microbiol.* 70, 323–340. doi: 10.1111/j.1365-2958.2008.06404.x

Aoki, S. K., Pamma, R., Hernday, A. D., Bickham, J. E., Braaten, B. A., and Low, D. A. (2005). Contact-dependent inhibition of growth in *Escherichia coli*. *Science* 309, 1245–1248. doi: 10.1126/science.1115109

Arnold, T., Zeth, K., and Linke, D. (2010). Omp85 from the thermophilic cyanobacterium *Thermosynechococcus elongatus* differs from proteobacterial Omp85 in structure and domain composition. *J. Biol. Chem.* 285, 18003–18015. doi: 10.1074/jbc.M110.112516

Baelen, S., Dewitte, F., Clantin, B., and Villeret, V. (2013). Structure of the secretion domain of HxuA from *Haemophilus influenzae*. *Acta Crystallogr. Sect. F Struct. Biol. Cryst. Commun.* 69, 1322–1327. doi: 10.1107/S174430911302962X

Bakelar, J., Buchanan, S. K., and Noinaj, N. (2016). The structure of the beta-barrel assembly machinery complex. *Science* 351, 180–186. doi: 10.1126/science.aad3460

Balder, R., Hassel, J., Lipski, S., and Lafontaine, E. R. (2007). *Moraxella catarrhalis* strain O35E expresses two filamentous hemagglutinin-like proteins that mediate adherence to human epithelial cells. *Infect. Immun.* 75, 2765–2775. doi: 10.1128/IAI.00079-07

Baraquet, C., and Harwood, C. S. (2015). FleQ DNA Binding consensus sequence revealed by studies of FleQ-dependent regulation of biofilm gene expression in *Pseudomonas aeruginosa*. *J. Bacteriol.* 198, 178–186. doi: 10.1128/JB.00539-15

Barenkamp, S. J., and St Geme, J. W. I. (1994). Genes encoding high-molecular-weight adhesion proteins of nontypeable *Haemophilus influenzae* are part of gene clusters. *Infect. Immun.* 62, 3320–3328.

Barnard, T. J., Dautin, N., Lukacik, P., Bernstein, H. D., and Buchanan, S. K. (2007). Autotransporter structure reveals intra-barrel cleavage followed by conformational changes. *Nat. Struct. Mol. Biol.* 14, 1214–1220. doi: 10.1002/0471140864.ps1709s47

Basso, P., Ragno, M., Elsen, S., Reboud, E., Golovkine, G., Bouillot, S., et al. (2017). *Pseudomonas aeruginosa* pore-forming exolysin and Type IV Pili Cooperate to induce host cell lysis. *MBio* 8, e02250–e02216. doi: 10.1128/mBio.02250-16

Baud, C., Guérin, J., Petit, E., Lesne, E., Dupre, E., Locht, C., et al. (2014). Translocation path of a substrate protein through its Omp85 transporter. *Nat. Commun.* 5:5271. doi: 10.1038/ncomms6271

Baud, C., Gutsche, I., Willery, E., de Paepe, D., Drobecq, H., Gilleron, M., et al. (2011). Membrane-associated DegP in *Bordetella* chaperones a repeat-rich secretory protein. *Mol. Microbiol.* 80, 1625–1636. doi: 10.1111/j.1365-2958.2011.07672.x

Baud, C., Hodak, H., Willery, E., Drobecq, H., Locht, C., Jamin, M., et al. (2009). Role of DegP for two-partner secretion in *Bordetella*. *Mol. Microbiol.* 74, 315–329. doi: 10.1111/j.1365-2958.2009.06860.x

Beck, C. M., Diner, E. J., Kim, J. J., Low, D. A., and Hayes, C. S. (2014a). The F pilus mediates a novel pathway of CDI toxin import. *Mol. Microbiol.* 93, 276–290. doi: 10.1111/mmi.12658

Beck, C. M., Morse, R. P., Cunningham, D. A., Iniguez, A., Low, D. A., Goulding, C. W., et al. (2014b). CdiA from *Enterobacter cloacae* delivers a toxic ribosomal RNase into target bacteria. *Structure* 22, 707–718. doi: 10.1016/j.str.2014.02.012

Beck, C. M., Willett, J. L., Cunningham, D. A., Kim, J. J., Low, D. A., and Hayes, C. S. (2016). CdiA effectors from uropathogenic *Escherichia coli* use heterotrimeric osmoporins as receptors to recognize target bacteria. *PLoS Pathog.* 12:e1005925. doi: 10.1371/journal.ppat.1005925

Bentancor, L. V., Camacho-Peiro, A., Bozkurt-Guzel, C., Pier, G. B., and Maira-Litran, T. (2012). Identification of Ata, a multifunctional trimeric autotransporter of *Acinetobacter baumannii*. *J. Bacteriol.* 194, 3950–3960. doi: 10.1128/JB.06769-11

Benz, I., and Schmidt, M. A. (2001). Glycosylation with heptose residues mediated by the *aah* gene product is essential for adherence of the AIDA-I adhesin. *Mol. Microbiol.* 40, 1403–1413.

Bernstein, H. D. (2007). Are bacterial 'autotransporters' really transporters? *Trends Microbiol.* 15, 441–447. doi: 10.1016/j.tim.2007.09.007

Besingi, R. N., Chaney, J. L., and Clark, P. L. (2013). An alternative outer membrane secretion mechanism for an autotransporter protein lacking a C-terminal stable core. *Mol. Microbiol.* 90, 1028–1045. doi: 10.1111/mmi.12414

Bodelón, G., Marín, E., and Fernandez, L. A. (2009). Role of periplasmic chaperones and BamA (YaeT/Omp85) in folding and secretion of intimin from enteropathogenic *Escherichia coli* strains. *J. Bacteriol.* 191, 5169–5179. doi: 10.1128/JB.00458-09

Borlee, B. R., Goldman, A. D., Murakami, K., Samudrala, R., Wozniak, D. J., and Parsek, M. R. (2010). *Pseudomonas aeruginosa* uses a cyclic-di-GMP-regulated adhesin to reinforce the biofilm extracellular matrix. *Mol. Microbiol.* 75, 827–842. doi: 10.1111/j.1365-2958.2009.06991.x

Bos, M. P., Robert, V., and Tommassen, J. (2007). Biogenesis of the gram-negative bacterial outer membrane. *Annu. Rev. Microbiol.* 61, 191–214. doi: 10.1146/annurev.micro.61.080706.093245

Braun, V., Hobbie, S., and Ondraczek, R. (1992). *Serratia marcescens* forms a new type of cytolysin. *FEMS Microbiol. Lett.* 100, 299–306.

Brillard, J., Duchaud, E., Boemare, N., Kunst, F., and Givaudan, A. (2002). The PhlA hemolysin from the entomopathogenic bacterium *Photorhabdus luminescens* belongs to the two-partner secretion family of hemolysins. *J. Bacteriol.* 184, 3871–3878.

Brown, N. F., Logue, C. A., Boddey, J. A., Scott, R., Hirst, R. G., and Beacham, I. R. (2004). Identification of a novel two-partner secretion system from *Burkholderia pseudomallei*. *Mol. Genet. Genomics* 272, 204–215. doi: 10.1007/s00438-004-1039-z

Burgess, N. K., Dao, T. P., Stanley, A. M., and Fleming, K. G. (2008). Beta-barrel proteins that reside in the *Escherichia coli* outer membrane *in vivo* demonstrate varied folding behavior *in vitro*. *J. Biol. Chem.* 283, 26748–26758. doi: 10.1074/jbc.M804231200

Buscher, A. Z., Grass, S., Heuser, J., Roth, R., and St Geme, J. W. III. (2006). Surface anchoring of a bacterial adhesin secreted by the two-partner secretion pathway. *Mol. Microbiol.* 61, 470–483. doi: 10.1111/j.1365-2958.2006.05236.x

Charbonneau, M. E., Girard, V., Nikolakakis, A., Campos, M., Berthiaume, F., Dumas, F., et al. (2007). O-linked glycosylation ensures the normal conformation of the autotransporter adhesin involved in diffuse adherence. *J. Bacteriol.* 189, 8880–8889. doi: 10.1128/JB.00969-07

Charbonneau, M. E., and Mourez, M. (2008). The *Escherichia coli* AIDA-I autotransporter undergoes cytoplasmic glycosylation independently of export. *Res. Microbiol.* 159, 537–544. doi: 10.1016/j.resmic.2008.06.009

Chevalier, N., Moser, M., Koch, H. G., Schimz, K. L., Willery, E., Locht, C., et al. (2004). Membrane targeting of a bacterial virulence factor harbouring an extended signal peptide. *J. Mol. Microbiol. Biotechnol.* 8, 7–18. doi: 10.1159/000082076

Choi, P. S., and Bernstein, H. D. (2009). Sequential translocation of an *Escherchia coli* two-partner secretion pathway exoprotein across the inner and outer membranes. *Mol. Microbiol.* 75, 440–451. doi: 10.1111/j.1365-2958.2009.06993.x

Choi, P. S., Dawson, A. J., and Bernstein, H. D. (2007). Characterization of a novel two-partner secretion system in *Escherichia coli* O157:H7. *J. Bacteriol.* 189, 3452–3461. doi: 10.1128/JB.01751-06

Clantin, B., Delattre, A. S., Rucktooa, P., Saint, N., Meli, A. C., Locht, C., et al. (2007). Structure of the membrane protein FhaC: a member of the Omp85-TpsB transporter superfamily. *Science* 317, 957–961. doi: 10.1126/science.1143860

Clantin, B., Hodak, H., Willery, E., Locht, C., Jacob-Dubuisson, F., and Villeret, V. (2004). The crystal structure of filamentous hemagglutinin secretion domain and its implications for the two-partner secretion pathway. *Proc. Natl. Acad. Sci. U.S.A.* 101, 6194–6199. doi: 10.1073/pnas.0400291101

Cooley, R. B., Smith, T. J., Leung, W., Tierney, V., Borlee, B. R., O'Toole, G. A., et al. (2015). Cyclic Di-GMP-regulated periplasmic proteolysis of a *Pseudomonas aeruginosa* type Vb secretion system substrate. *J. Bacteriol.* 198, 66–76. doi: 10.1128/JB.00369-15

Cope, L. D., Thomas, S. E., Latimer, J. L., Slaughter, C. A., Müller-Eberhard, U., and Hansen, E. J. (1994). The 100-kDa haem:hemopexin-binding protein of *Haemophilus influenzae*: structure and localization. *Mol. Microbiol.* 13, 863–873.

Cope, L. D., Yogev, R., Muller-Eberhard, U., and Hansen, E. J. (1995). A gene cluster involved in the utilization of both free heme and heme:hemopexin by *Haemophilus influenzae* type b. *J. Bacteriol.* 177, 2644–2653.

Côté, J. P., Charbonneau, M. E., and Mourez, M. (2013). Glycosylation of the *Escherichia coli* TibA self-associating autotransporter influences the conformation and the functionality of the protein. *PLoS ONE* 8:e80739. doi: 10.1371/journal.pone.0080739

Cotter, S. E., Surana, N. K., and St Geme, J. W. III. (2005). Trimeric autotransporters: a distinct subfamily of autotransporter proteins. *Trends Microbiol.* 13, 199–205. doi: 10.1016/j.tim.2005.03.004

Coutte, L., Antoine, R., Drobecq, H., Locht, C., and Jacob-Dubuisson, F. (2001). Subtilisin-like autotransporter serves as maturation protease in a bacterial secretion pathway. *EMBO J.* 20, 5040–5048. doi: 10.1093/emboj/20.18.5040

Coutte, L., Willery, E., Antoine, R., Drobecq, H., Locht, C., and Jacob-Dubuisson, F. (2003). Surface anchoring of bacterial subtilisin important for maturation function. *Mol. Microbiol.* 49, 529–539.

da Mata Madeira, P. V., Zouhir, S., Basso, P., Neves, D., Laubier, A., Salacha, R., et al. (2016). Structural basis of lipid targeting and destruction by the type V secretion system of *Pseudomonas aeruginosa*. *J. Mol. Biol.* 428, 1790–1803. doi: 10.1016/j.jmb.2016.03.012

Darsonval, A., Darrasse, A., Durand, K., Bureau, C., Cesbron, S., and Jacques, M. A. (2009). Adhesion and fitness in the bean phyllosphere and transmission to seed of *Xanthomonas fuscans* subsp. *fuscans*. *Mol. Plant Microbe Interact.* 22, 747–757. doi: 10.1094/MPMI-22-6-0747

Delattre, A. S., Clantin, B., Saint, N., Locht, C., Villeret, V., and Jacob-Dubuisson, F. (2010). Functional importance of a conserved sequence motif in FhaC, a prototypic member of the TpsB/Omp85 superfamily. *FEBS J.* 277, 4755–4765. doi: 10.1111/j.1742-4658.2010.07881.x

Delattre, A. S., Saint, N., Clantin, B., Willery, E., Lippens, G., Locht, C., et al. (2011). Substrate recognition by the POTRA domains of TpsB transporter FhaC. *Mol. Microbiol.* 81, 99–112. doi: 10.1111/j.1365-2958.2011.07680.x

Depperschmidt, A., Ketterer, N., and Pfaffelhuber, P. (2013). A Brownian ratchet for protein translocation including dissociation of ratcheting sites. *J. Math. Biol.* 66, 505–534. doi: 10.1007/s00285-012-0519-8

Desvaux, M., Cooper, L. M., Filenko, N. A., Scott-Tucker, A., Turner, S. M., Cole, J. A., et al. (2006). The unusual extended signal peptide region of the type V secretion system is phylogenetically restricted. *FEMS Microbiol. Lett.* 264, 22–30. doi: 10.1111/j.1574-6968.2006.00425.x

Desvaux, M., Scott-Tucker, A., Turner, S. M., Cooper, L. M., Huber, D., Nataro, J. P., et al. (2007). A conserved extended signal peptide region directs posttranslational protein translocation via a novel mechanism. *Microbiology* 153, 59–70. doi: 10.1099/mic.0.29091-0

Di Venanzio, G., Stepanenko, T. M., and García Véscosi, E. (2014). *Serratia marcescens* ShlA pore-forming toxin is responsible for early induction of autophagy in host cells and is transcriptionally regulated by RcsB. *Infect. Immun.* 82, 3542–3554. doi: 10.1128/IAI.01682-14

Diner, E. J., Beck, C. M., Webb, J. S., Low, D. A., and Hayes, C. S. (2012). Identification of a target cell permissive factor required for contact-dependent growth inhibition (CDI). *Genes Dev.* 26, 515–525. doi: 10.1101/gad.182345.111

Dobrindt, U., Blum-Oehler, G., Nagy, G., Schneider, G., Johann, A., Gottschalk, G., et al. (2002). Genetic structure and distribution of four pathogenicity islands (PAI I(536) to PAI IV(536)) of uropathogenic *Escherichia coli* strain 536. *Infect. Immun.* 70, 6365–6372.

Dodd, D. A., Worth, R. G., Rosen, M. K., Grinstein, S., van Oers, N. S., and Hansen, E. J. (2014). The *Haemophilus ducreyi* LspA1 protein inhibits phagocytosis by using a new mechanism involving activation of C-terminal Src kinase. *MBio* 5, e01178–e01114. doi: 10.1128/mBio.01178-14

Domenighini, M., Relman, D., Capiau, C., Falkow, S., Prugnola, A., Scarlato, V., et al. (1990). Genetic characterization of *Bordetella pertussis* filamentous hemagglutinin: a protein processed from an unusually large precursor. *Mol. Microbiol.* 4, 787–800.

Drobnak, I., Braselmann, E., and Clark, P. L. (2015). Multiple driving forces required for efficient secretion of autotransporter virulence proteins. *J. Biol. Chem.* 290, 10104–10116. doi: 10.1074/jbc.M114.629170

Duret, G., Szymanski, M., Choi, K. J., Yeo, H. J., and Delcour, A. H. (2008). The TpsB translocator HMW1B of *Haemophilus influenzae* forms a large conductance channel. *J. Biol. Chem.* 283, 15771–15778. doi: 10.1074/jbc.M708970200

Dwyer, R. S., Ricci, D. P., Colwell, L. J., Silhavy, T. J., and Wingreen, N. S. (2013). Predicting functionally informative mutations in *Escherichia coli* BamA using evolutionary covariance analysis. *Genetics* 195, 443–455. doi: 10.1534/genetics.113.155861

Elsen, S., Huber, P., Bouillot, S., Coute, Y., Fournier, P., Dubois, Y., et al. (2014). A type III secretion negative clinical strain of *Pseudomonas aeruginosa* employs a two-partner secreted exolysin to induce hemorrhagic pneumonia. *Cell Host Microbe* 15, 164–176. doi: 10.1016/j.chom.2014.01.003

Emsley, P., Charles, I. G., Fairweather, N. F., and Isaacs, N. W. (1996). Structure of *Bordetella pertussis* virulence factor P.69 pertactin. *Nature* 381, 90–92.

Fairman, J. W., Dautin, N., Wojtowicz, D., Liu, W., Noinaj, N., Barnard, T. J., et al. (2012). Crystal structures of the outer membrane domain of intimin and invasin from enterohemorrhagic *E. coli* and enteropathogenic *Y. pseudotuberculosis*. *Structure* 20, 1233–1243. doi: 10.1016/j.str.2012.04.011

Fan, E., Chauhan, N., Udatha, D. B., Leo, J. C., and Linke, D. (2016). Type V secretion systems in bacteria. *Microbiol. Spectr.* 4:VMBF-0009-2015. doi: 10.1128/microbiolspec.VMBF-0009-2015

Fan, E., Fiedler, S., Jacob-Dubuisson, F., and Müller, M. (2012). Two-partner secretion of gram-negative bacteria: a single beta-barrel protein enables transport across the outer membrane. *J. Biol. Chem.* 287, 2591–2599. doi: 10.1074/jbc.M111.293068

Faure, L. M., Garvis, S., de Bentzmann, S., and Bigot, S. (2014). Characterization of a novel two-partner secretion system implicated in the virulence of *Pseudomonas aeruginosa*. *Microbiology* 160, 1940–1952. doi: 10.1099/mic.0.079616-0

Fleckenstein, J. M., Roy, K., Fischer, J. F., and Burkitt, M. (2006). Identification of a two-partner secretion locus of enterotoxigenic *Escherichia coli*. *Infect. Immun.* 74, 2245–2258. doi: 10.1128/IAI.74.4.2245-2258.2006

Fournier, C., Smith, A., and Delepelaire, P. (2011). Haem release from haemopexin by HxuA allows *Haemophilus influenzae* to escape host nutritional immunity. *Mol. Microbiol.* 80, 133–148. doi: 10.1111/j.1365-2958.2011.07562.x

Fuller, T. E., Kennedy, M. J., and Lowery, D. E. (2000). Identification of *Pasteurella multocida* virulence genes in a septicemic mouse model using signature-tagged mutagenesis. *Microb. Pathog.* 29, 25–38. doi: 10.1006/mpat.2000.0365

Gal-Mor, O., Gibson, D. L., Baluta, D., Vallance, B. A., and Finlay, B. B. (2008). A novel secretion pathway of *Salmonella enterica* acts as an antivirulence modulator during salmonellosis. *PLoS Pathog.* 4:e1000036. doi: 10.1371/journal.ppat.1000036

Garcia, E. C., Anderson, M. S., Hagar, J. A., and Cotter, P. A. (2013). *Burkholderia* BcpA mediates biofilm formation independently of interbacterial contact-dependent growth inhibition. *Mol. Microbiol.* 89, 1213–1225. doi: 10.1111/mmi.12339

Garcia, E. C., Perault, A. I., Marlatt, S. A., and Cotter, P. A. (2016). Interbacterial signaling via *Burkholderia* contact-dependent growth inhibition system proteins. *Proc. Natl. Acad. Sci. U.S.A.* 113, 8296–8301. doi: 10.1073/pnas.1606323113

Garnett, J. A., Muhl, D., Douse, C. H., Hui, K., Busch, A., Omisore, A., et al. (2015). Structure-function analysis reveals that the *Pseudomonas aeruginosa* Tps4 two-partner secretion system is involved in CupB5 translocation. *Protein Sci.* 24, 670–687. doi: 10.1002/pro.2640

Gatzeva-Topalova, P. Z., Warner, L. R., Pardi, A., and Sousa, M. C. (2010). Structure and flexibility of the complete periplasmic domain of BamA: the protein insertion machine of the outer membrane. *Structure* 18, 1492–1501. doi: 10.1016/j.str.2010.08.012

Gessmann, D., Chung, Y. H., Danoff, E. J., Plummer, A. M., Sandlin, C. W., Zaccai, N. R., et al. (2014). Outer membrane beta-barrel protein folding is physically controlled by periplasmic lipid head groups and BamA. *Proc. Natl. Acad. Sci. U.S.A.* 111, 5878–5883. doi: 10.1073/pnas.1322473111

Gottig, N., Garavaglia, B. S., Garofalo, C. G., Orellano, E. G., and Ottado, J. (2009). A filamentous hemagglutinin-like protein of *Xanthomonas axonopodis* pv. citri, the phytopathogen responsible for citrus canker, is involved in bacterial virulence. *PLoS ONE* 4:e4358. doi: 10.1371/journal.pone.0004358

Grass, S., and St Geme, J. W. III. (2000). Maturation and secretion of the non-typable *Haemophilus influenzae* HMW1 adhesin: roles of the N-terminal and C-terminal domains. *Mol. Microbiol.* 36, 55–67.

Grass, S., Buscher, A. Z., Swords, W. E., Apicella, M. A., Barenkamp, S. J., Ozchlewski, N., et al. (2003). The *Haemophilus influenzae* HMW1 adhesin is glycosylated in a process that requires HMW1C and phosphoglucomutase, an enzyme involved in lipooligosaccharide biosynthesis. *Mol. Microbiol.* 48, 737–751.

Grass, S., Lichti, C. F., Townsend, R. R., Gross, J., and St Geme, J. W. III. (2010). The *Haemophilus influenzae* HMW1C protein is a glycosyltransferase that transfers hexose residues to asparagine sites in the HMW1 adhesin. *PLoS Pathog.* 6:e1000919. doi: 10.1371/journal.ppat.1000919

Grass, S., Rempe, K. A., and St Geme, J. W. III. (2015). Structural determinants of the interaction between the TpsA and TpsB proteins in the *Haemophilus influenzae* HMW1 two-partner secretion system. *J. Bacteriol.* 197, 1769–1780. doi: 10.1128/JB.00039-15

Grijpstra, J., Arenas, J., Rutten, L., and Tommassen, J. (2013). Autotransporter secretion: varying on a theme. *Res. Microbiol.* 164, 562–582. doi: 10.1016/j.resmic.2013.03.010

Gross, J., Grass, S., Davis, A. E., Gilmore-Erdmann, P., Townsend, R. R., and St Geme, J. W. III. (2008). The *Haemophilus influenzae* HMW1 adhesin is a glycoprotein with an unusual N-linked carbohydrate modification. *J. Biol. Chem.* 283, 26010–26015. doi: 10.1074/jbc.M801819200

Grosskinsky, U., Schütz, M., Fritz, M., Schmid, Y., Lamparter, M. C., Szczesny, P., et al. (2007). A conserved glycine residue of trimeric autotransporter domains plays a key role in *Yersinia adhesin* a autotransport. *J. Bacteriol.* 189, 9011–9019. doi: 10.1128/JB.00985-07

Gruss, F., Zähringer, F., Jakob, R. P., Burmann, B. M., Hiller, S., and Maier, T. (2013). The structural basis of autotransporter translocation by TamA. *Nat. Struct. Mol. Biol.* 20, 1318–1320. doi: 10.1038/nsmb.2689

Gu, Y., Li, H., Dong, H., Zeng, Y., Zhang, Z., Paterson, N. G., et al. (2016). Structural basis of outer membrane protein insertion by the BAM complex. *Nature* 531, 64–69. doi: 10.1038/nature17199

Guédin, S., Willery, E., Locht, C., and Jacob-Dubuisson, F. (1998). Evidence that a globular conformation is not compatible with FhaC-mediated secretion of the *Bordetella pertussis* filamentous haemagglutinin. *Mol. Microbiol.* 29, 763–774.

Guédin, S., Willery, E., Tommassen, J., Fort, E., Drobecq, H., Locht, C., et al. (2000). Novel topological features of FhaC, the outer membrane transporter involved in the secretion of the *Bordetella pertussis* filamentous hemagglutinin. *J. Biol. Chem.* 275, 30202–30210. doi: 10.1074/jbc.M005515200

Guérin, J., Baud, C., Touati, N., Saint, N., Willery, E., Locht, C., et al. (2014). Conformational dynamics of protein transporter FhaC: large-scale motions of plug helix. *Mol. Microbiol.* 92, 1164–1176. doi: 10.1111/mmi.12585

Guerin, J., Saint, N., Baud, C., Meli, A. C., Etienne, E., Locht, C., et al. (2015). Dynamic interplay of membrane-proximal POTRA domain and conserved loop L6 in Omp85 transporter FhaC. *Mol. Microbiol.* 98, 490–501. doi: 10.1111/mmi.13137

Guilhabert, M. R., and Kirkpatrick, B. C. (2005). Identification of *Xylella fastidiosa* antivirulence genes: hemagglutinin adhesins contribute a biofilm maturation to *X. fastidios* and colonization and attenuate virulence. *Mol. Plant Microbe Interact.* 18, 856–868. doi: 10.1094/MPMI-18-0856

Hagan, C. L., Silhavy, T. J., and Kahne, D. (2011). beta-Barrel membrane protein assembly by the Bam complex. *Annu. Rev. Biochem.* 80, 189–210. doi: 10.1146/annurev-biochem-061408-144611

Haines, S., Arnaud-Barbe, N., Poncet, D., Reverchon, S., Wawrzyniak, J., Nasser, W., et al. (2015). IscR regulates synthesis of colonization factor antigen I fimbriae in response to iron starvation in enterotoxigenic *Escherichia coli*. *J. Bacteriol.* 197, 2896–2907. doi: 10.1128/JB.00214-15

Han, L., Zheng, J., Wang, Y., Yang, X., Liu, Y., Sun, C., et al. (2016). Structure of the BAM complex and its implications for biogenesis of outer-membrane proteins. *Nat. Struct. Mol. Biol.* 23, 192–196. doi: 10.1038/nsmb.3181

Hartmann, M. D., Ridderbusch, O., Zeth, K., Albrecht, R., Testa, O., Woolfson, D. N., et al. (2009). A coiled-coil motif that sequesters ions to the hydrophobic core. *Proc. Natl. Acad. Sci. U.S.A.* 106, 16950–16955. doi: 10.1073/pnas.0907256106

Heinz, E., and Lithgow, T. (2014). A comprehensive analysis of the Omp85/TpsB protein superfamily structural diversity, taxonomic occurrence, and evolution. *Front. Microbiol.* 5:370. doi: 10.3389/fmicb.2014.00370

Heinz, E., Stubenrauch, C. J., Grinter, R., Croft, N. P., Purcell, A. W., Strugnell, R. A., et al. (2016). Conserved features in the structure, mechanism, and biogenesis of the inverse autotransporter protein family. *Genome Biol. Evol.* 8, 1690–1705. doi: 10.1093/gbe/evw112

Hertle, R., Hilger, M., Weingardt-Kocher, S., and Walev, I. (1999). Cytotoxic action of *Serratia marcescens* hemolysin on human epithelial cells. *Infect. Immun.* 67, 817–825.

Hirono, I., Tange, N., and Aoki, T. (1997). Iron-regulated haemolysin from *Edwardsiella tarda*. *Mol. Microbiol.* 24, 851–856.

Hodak, H., and Jacob-Dubuisson, F. (2007). Current challenges in autotransport and two-partner protein secretion pathways. *Res. Microbiol.* 158, 631–637. doi: 10.1016/j.resmic.2007.08.001

Hodak, H., Clantin, B., Willery, E., Villeret, V., Locht, C., and Jacob-Dubuisson, F. (2006). Secretion signal of the filamentous haemagglutinin, a model two-partner secretion substrate. *Mol. Microbiol.* 61, 368–382. doi: 10.1111/j.1365-2958.2006.05242.x

Hoiczyk, E., Roggenkamp, A., Reichenbecher, M., Lupas, A., and Heesemann, J. (2000). Structure and sequence analysis of *Yersinia* YadA and *Moraxella* UspAs reveal a novel class of adhesins. *EMBO J.* 19, 5989–5999. doi: 10.1093/emboj/19.22.5989

Iadanza, M. G., Higgins, A. J., Schiffrin, B., Calabrese, A. N., Brockwell, D. J., Ashcroft, A. E., et al. (2016). Lateral opening in the intact beta-barrel assembly machinery captured by cryo-EM. *Nat. Commun.* 7:12865. doi: 10.1038/ncomms12865

Ieva, R., and Bernstein, H. D. (2009). Interaction of an autotransporter passenger domain with BamA during its translocation across the bacterial outer membrane. *Proc. Natl. Acad. Sci. U.S.A.* 106, 19120–19125. doi: 10.1073/pnas.0907912106

Ieva, R., Skillman, K. M., and Bernstein, H. D. (2008). Incorporation of a polypeptide segment into the beta-domain pore during the assembly of a bacterial autotransporter. *Mol. Microbiol.* 67, 188–201. doi: 10.1111/j.1365-2958.2007.06048.x

Ieva, R., Tian, P., Peterson, J. H., and Bernstein, H. D. (2011). Sequential and spatially restricted interactions of assembly factors with an autotransporter beta domain. *Proc. Natl. Acad. Sci. U.S.A.* 108, E383–E391. doi: 10.1073/pnas.1103827108

Jacob-Dubuisson, F., Buisine, C., Willery, E., Renauld-Mongenie, G., and Locht, C. (1997). Lack of functional complementation between *Bordetella pertussis* filamentous hemagglutinin and *Proteus mirabilis* HpmA hemolysin secretion machineries. *J. Bacteriol.* 179, 775–783.

Jacob-Dubuisson, F., Fernandez, R., and Coutte, L. (2004). Protein secretion through autotransporter and two-partner pathways. *Biochim. Biophys. Acta* 1694, 235–257. doi: 10.1016/j.bbamcr.2004.03.008

Jacob-Dubuisson, F., Guerin, J., Baelen, S., and Clantin, B. (2013). Two-partner secretion: as simple as it sounds? *Res. Microbiol.* 164, 583–595. doi: 10.1016/j.resmic.2013.03.009

Jacob-Dubuisson, F., Locht, C., and Antoine, R. (2001). Two-partner secretion in Gram-negative bacteria: a thrifty, specific pathway for large virulence proteins. *Mol. Microbiol.* 40, 306–313.

Jacob-Dubuisson, F., Villeret, V., Clantin, B., Delattre, A. S., and Saint, N. (2009). First structural insights into the TpsB/Omp85 superfamily. *Biol. Chem.* 390, 675–684. doi: 10.1515/BC.2009.099

Jain, S., and Goldberg, M. B. (2007). Requirement for YaeT in the outer membrane assembly of autotransporter proteins. *J. Bacteriol.* 189, 5393–5398. doi: 10.1128/JB.00228-07

Jones, A. M., Garza-Sanchez, F., So, J., Hayes, C. S., and Low, D. A. (2017). Activation of contact-dependent antibacterial tRNase toxins by translation elongation factors. *Proc. Natl. Acad. Sci. U.S.A.* 114, E1951–E1957. doi: 10.1073/pnas.1619273114

Julio, S. M., and Cotter, P. A. (2005). Characterization of the filamentous hemagglutinin-like protein FhaS in *Bordetella bronchiseptica*. *Infect. Immun.* 73, 4960–4971. doi: 10.1128/IAI.73.8.4960-4971.2005

Junker, M., and Clark, P. L. (2010). Slow formation of aggregation-resistant beta-sheet folding intermediates. *Proteins* 78, 812–824. doi: 10.1002/prot.22609

Junker, M., Besingi, R. N., and Clark, P. L. (2009). Vectorial transport and folding of an autotransporter virulence protein during outer membrane secretion. *Mol. Microbiol.* 71, 1323–1332. doi: 10.1111/j.1365-2958.2009.06607.x

Junker, M., Schuster, C. C., McDonnell, A. V., Sorg, K. A., Finn, M. C., Berger, B., et al. (2006). Pertactin beta-helix folding mechanism suggests common themes for the secretion and folding of autotransporter proteins. *Proc. Natl. Acad. Sci. U.S.A.* 103, 4918–4923. doi: 10.1073/pnas.0507923103

Kachalova, G. S., Rogulin, E. A., Yunusova, A. K., Artyukh, R. I., Perevyazova, T. A., Matvienko, N. I., et al. (2008). Structural analysis of the heterodimeric type IIS restriction endonuclease R.BspD6I acting as a complex between a

monomeric site-specific nickase and a catalytic subunit. *J. Mol. Biol.* 384, 489–502. doi: 10.1016/j.jmb.2008.09.033

Kajava, A. V., and Steven, A. C. (2006a). The turn of the screw: variations of the abundant beta-solenoid motif in passenger domains of Type V secretory proteins. *J. Struct. Biol.* 155, 306–315. doi: 10.1016/j.jsb.2006.01.015

Kajava, A. V., and Steven, A. C. (2006b). Beta-rolls, beta-helices, and other beta-solenoid proteins. *Adv. Protein Chem.* 73, 55–96. doi: 10.1016/S0065-3233(06)73003-0

Kajava, A. V., Cheng, N., Cleaver, R., Kessel, M., Simon, M. N., Willery, E., et al. (2001). Beta-helix model for the filamentous haemagglutinin adhesin of *Bordetella pertussis* and related bacterial secretory proteins. *Mol. Microbiol.* 42, 279–292.

Kang'ethe, W., and Bernstein, H. D. (2013a). Stepwise folding of an autotransporter passenger domain is not essential for its secretion. *J. Biol. Chem.* 288, 35028–35038. doi: 10.1074/jbc.M113.515635

Kang'ethe, W., and Bernstein, H. D. (2013b). Charge-dependent secretion of an intrinsically disordered protein via the autotransporter pathway. *Proc. Natl. Acad. Sci. U.S.A.* 110, E4246–E4255. doi: 10.1073/pnas.1310345110

Kaundal, S., Uttam, M., and Thakur, K. G. (2016). Dual role of a biosynthetic enzyme, CysK, in contact dependent growth inhibition in bacteria. *PLoS ONE* 11:e0159844. doi: 10.1371/journal.pone.0159844

Kida, Y., Higashimoto, Y., Inoue, H., Shimizu, T., and Kuwano, K. (2008). A novel secreted protease from *Pseudomonas aeruginosa* activates NF-kappaB through protease-activated receptors. *Cell. Microbiol.* 10, 1491–1504. doi: 10.1111/j.1462-5822.2008.01142.x

Kida, Y., Shimizu, T., and Kuwano, K. (2011). Cooperation between LepA and PlcH contributes to the *in vivo* virulence and growth of *Pseudomonas aeruginosa* in mice. *Infect. Immun.* 79, 211–219. doi: 10.1128/IAI.01053-10

Kim, D. S., Chao, Y., and Saier, M. H. Jr. (2006). Protein-translocating trimeric autotransporters of gram-negative bacteria. *J. Bacteriol.* 188, 5655–5667. doi: 10.1128/JB.01596-05

Kim, S., Malinverni, J. C., Sliz, P., Silhavy, T. J., Harrison, S. C., and Kahne, D. (2007). Structure and function of an essential component of the outer membrane protein assembly machine. *Science* 317, 961–964. doi: 10.1126/science.1143993

Klee, S. R., Nassif, X., Kusecek, B., Merker, P., Beretti, J. L., Achtman, M., et al. (2000). Molecular and biological analysis of eight genetic islands that distinguish *Neisseria meningitidis* from the closely related pathogen *Neisseria gonorrhoeae*. *Infect. Immun.* 68, 2082–2095.

Knowles, T. J., Scott-Tucker, A., Overduin, M., and Henderson, I. R. (2009). Membrane protein architects: the role of the BAM complex in outer membrane protein assembly. *Nat. Rev. Microbiol.* 7, 206–214. doi: 10.1038/nrmicro2069

Konninger, U. W., Hobbie, S., Benz, R., and Braun, V. (1999). The haemolysin-secreting ShlB protein of the outer membrane of *Serratia marcescens*: determination of surface-exposed residues and formation of ion-permeable pores by ShlB mutants in artificial lipid bilayer membranes. *Mol. Microbiol.* 32, 1212–1225.

Labandeira-Rey, M., Dodd, D. A., Brautigam, C. A., Fortney, K. R., Spinola, S. M., and Hansen, E. J. (2013). The *Haemophilus ducreyi* Fis protein is involved in controlling expression of the lspB-lspA2 operon and other virulence factors. *Infect. Immun.* 81, 4160–4170. doi: 10.1128/IAI.00714-13

Labandeira-Rey, M., Mock, J. R., and Hansen, E. J. (2009). Regulation of expression of the *Haemophilus ducreyi* LspB and LspA2 proteins by CpxR. *Infect. Immun.* 77, 3402–3411. doi: 10.1128/IAI.00292-09

Lehr, U., Schutz, M., Oberhettinger, P., Ruiz-Perez, F., Donald, J. W., Palmer, T., et al. (2010). C-terminal amino acid residues of the trimeric autotransporter adhesin YadA of *Yersinia enterocolitica* are decisive for its recognition and assembly by BamA. *Mol. Microbiol.* 78, 932–946. doi: 10.1111/j.1365-2958.2010.07377.x

Leo, J. C., Grin, I., and Linke, D. (2012). Type V secretion: mechanism(s) of autotransport through the bacterial outer membrane. *Philos. Trans. R. Soc. Lond. B Biol. Sci.* 367, 1088–1101. doi: 10.1098/rstb.2011.0208

Leo, J. C., Oberhettinger, P., Chaubey, M., Schutz, M., Kuhner, D., Bertsche, U., et al. (2015a). The Intimin periplasmic domain mediates dimerisation and binding to peptidoglycan. *Mol. Microbiol.* 95, 80–100. doi: 10.1111/mmi.12840

Leo, J. C., Oberhettinger, P., Schutz, M., and Linke, D. (2015b). The inverse autotransporter family: intimin, invasin and related proteins. *Int. J. Med. Microbiol.* 305, 276–282. doi: 10.1016/j.ijmm.2014.12.011

Leonard-Rivera, M., and Misra, R. (2012). Conserved residues of the putative L6 Loop of *Escherichia coli* BamA play a critical role in the assembly of beta-barrel outer membrane proteins, including that of BamA itself. *J. Bacteriol.* 194, 4662–4668. doi: 10.1128/JB.00825-12

Leyton, D. L., Rossiter, A. E., and Henderson, I. R. (2012). From self sufficiency to dependence: mechanisms and factors important for autotransporter biogenesis. *Nat. Rev. Microbiol.* 10, 213–225. doi: 10.1038/nrmicro2733

Lin, C. S., Horng, J. T., Yang, C. H., Tsai, Y. H., Su, L. H., Wei, C. F., et al. (2010). RssAB-FlhDC-ShlBA as a major pathogenesis pathway in *Serratia marcescens*. *Infect. Immun.* 78, 4870–4881. doi: 10.1128/IAI.00661-10

Linke, D., Riess, T., Autenrieth, I. B., Lupas, A., and Kempf, V. A. (2006). Trimeric autotransporter adhesins: variable structure, common function. *Trends Microbiol.* 14, 264–270. doi: 10.1016/j.tim.2006.04.005

Llamas, M. A., van der Sar, A., Chu, B. C., Sparrius, M., Vogel, H. J., and Bitter, W. (2009). A novel extracytoplasmic function (ECF) sigma factor regulates virulence in *Pseudomonas aeruginosa*. *PLoS Pathog.* 5:e1000572. doi: 10.1371/journal.ppat.1000572

Locht, C., Bertin, P., Menozzi, F. D., and Renauld, G. (1993). The filamentous haemagglutinin, a multifaceted adhesin produced by virulent *Bordetella* spp. *Mol. Microbiol.* 9, 653–660.

Maier, T., Clantin, B., Gruss, F., Dewitte, F., Delattre, A. S., Jacob-Dubuisson, F., et al. (2015). Conserved Omp85 lid-lock structure and substrate recognition in FhaC. *Nat. Commun.* 6:7452. doi: 10.1038/ncomms8452

Makhov, A. M., Hannah, J. H., Brennan, M. J., Trus, B. L., Kocsis, E., Conway, J. F., et al. (1994). Filamentous hemagglutinin of *Bordetella pertussis*. A bacterial adhesin formed as a 50-nm monomeric rigid rod based on a 19-residue repeat motif rich in beta strands and turns. *J. Mol. Biol.* 241, 110–124.

Matlack, K. E., Misselwitz, B., Plath, K., and Rapoport, T. A. (1999). BiP acts as a molecular ratchet during posttranslational transport of prepro-alpha factor across the ER membrane. *Cell* 97, 553–564.

Mazar, J., and Cotter, P. A. (2006). Topology and maturation of filamentous haemagglutinin suggest a new model for two-partner secretion. *Mol. Microbiol.* 62, 641–654. doi: 10.1111/j.1365-2958.2006.05392.x

Melvin, J. A., Scheller, E. V., Noel, C. R., and Cotter, P. A. (2015). New insight into filamentous hemagglutinin secretion reveals a role for full-length FhaB in *Bordetella* virulence. *mBio* 6:e01189-15. doi: 10.1128/mBio.01189-15

Meng, G., Surana, N. K., St Geme, J. W. III, and Waksman, G. (2006). Structure of the outer membrane translocator domain of the *Haemophilus influenzae* Hia trimeric autotransporter. *EMBO J.* 25, 2297–2304. doi: 10.1038/sj.emboj.7601132

Menozzi, F. D., Boucher, P. E., Riveau, G., Gantiez, C., and Locht, C. (1994). Surface-associated filamentous hemagglutinin induces autoagglutination of *Bordetella pertussis*. *Infect. Immun.* 62, 4261–4269.

Mercy, C., Ize, B., Salcedo, S. P., de Bentzmann, S., and Bigot, S. (2016). Functional characterization of *Pseudomonas* contact dependent growth inhibition (CDI) systems. *PLoS ONE* 11:e0147435. doi: 10.1371/journal.pone.0147435

Mogensen, J. E., and Otzen, D. E. (2005). Interactions between folding factors and bacterial outer membrane proteins. *Mol. Microbiol.* 57, 326–346. doi: 10.1111/j.1365-2958.2005.04674.x

Molina, M. A., Ramos, J. L., and Espinosa-Urgel, M. (2006). A two-partner secretion system is involved in seed and root colonization and iron uptake by *Pseudomonas putida* KT2440. *Environ. Microbiol.* 8, 639–647. doi: 10.1111/j.1462-2920.2005.00940.x

Monteiro-Neto, V., Bando, S. Y., Moreira-Filho, C. A., and Giron, J. A. (2003). Characterization of an outer membrane protein associated with haemagglutination and adhesive properties of enteroaggregative *Escherichia coli* O111:H12. *Cell. Microbiol.* 5, 533–547.

Moon, C. P., Zaccai, N. R., Fleming, P. J., Gessmann, D., and Fleming, K. G. (2013). Membrane protein thermodynamic stability may serve as the energy sink for sorting in the periplasm. *Proc. Natl. Acad. Sci. U.S.A.* 110, 4285–4290. doi: 10.1073/pnas.1212527110

Moormann, C., Benz, I., and Schmidt, M. A. (2002). Functional substitution of the TibC protein of enterotoxigenic *Escherichia coli* strains for the autotransporter adhesin heptosyltransferase of the AIDA system. *Infect. Immun.* 70, 2264–2270.

Morse, R. P., Nikolakakis, K. C., Willett, J. L., Gerrick, E., Low, D. A., Hayes, C. S., et al. (2012). Structural basis of toxicity and immunity in contact-dependent growth inhibition (CDI) systems. *Proc. Natl. Acad. Sci. U.S.A.* 109, 21480–21485. doi: 10.1073/pnas.1216238110

Moslavac, S., Mirus, O., Bredemeier, R., Soll, J., von Haeseler, A., and Schleiff, E. (2005). Conserved pore-forming regions in polypeptide-transporting proteins. *FEBS J.* 272, 1367–1378. doi: 10.1111/j.1742-4658.2005.04569.x

Neil, R. B., and Apicella, M. A. (2009). Role of HrpA in biofilm formation of *Neisseria meningitidis* and regulation of the hrpBAS transcripts. *Infect. Immun.* 77, 2285–2293. doi: 10.1128/IAI.01502-08

Nelson, K. M., Young, G. M., and Miller, V. L. (2001). Identification of a locus involved in systemic dissemination of *Yersinia enterocolitica*. *Infect. Immun.* 69, 6201–6208. doi: 10.1128/IAI.69.10.6201-6208.2001

Ni, D., Wang, Y., Yang, X., Zhou, H., Hou, X., Cao, B., et al. (2014). Structural and functional analysis of the beta-barrel domain of BamA from *Escherichia coli*. *FASEB J.* 28, 2677–2685. doi: 10.1096/fj.13-248450

Noel, C. R., Mazar, J., Melvin, J. A., Sexton, J. A., and Cotter, P. A. (2012). The prodomain of the *Bordetella* two-partner secretion pathway protein FhaB remains intracellular yet affects the conformation of the mature C-terminal domain. *Mol. Microbiol.* 86, 988–1006. doi: 10.1111/mmi.12036

Noinaj, N., Kuszak, A. J., Balusek, C., Gumbart, J. C., and Buchanan, S. K. (2014). Lateral opening and exit pore formation are required for BamA function. *Structure* 22, 1055–1062. doi: 10.1016/j.str.2014.05.008

Noinaj, N., Kuszak, A. J., Gumbart, J. C., Lukacik, P., Chang, H., Easley, N. C., et al. (2013). Structural insight into the biogenesis of beta-barrel membrane proteins. *Nature* 501, 385–390. doi: 10.1038/nature12521

Noinaj, N., Rollauer, S. E., and Buchanan, S. K. (2015). The beta-barrel membrane protein insertase machinery from Gram-negative bacteria. *Curr. Opin. Struct. Biol.* 31, 35–42. doi: 10.1016/j.str.2014.05.008

Norell, D., Heuck, A., Tran-Thi, T. A., Gotzke, H., Jacob-Dubuisson, F., Clausen, T., et al. (2014). Versatile *in vitro* system to study translocation and functional integration of bacterial outer membrane proteins. *Nat. Commun.* 5:5396. doi: 10.1038/ncomms6396

Oberhettinger, P., Schutz, M., Leo, J. C., Heinz, N., Berger, J., Autenrieth, I. B., et al. (2012). Intimin and invasin export their C-terminus to the bacterial cell surface using an inverse mechanism compared to classical autotransport. *PLoS ONE* 7:e47069. doi: 10.1371/journal.pone.0047069

Ogier, J. C., Duvic, B., Lanois, A., Givaudan, A., and Gaudriault, S. (2016). A new member of the growing family of contact-dependent growth inhibition systems in *Xenorhabdus doucetiae*. *PLoS ONE* 11:e0167443. doi: 10.1371/journal.pone.0167443

Oliver, D. C., Huang, G., Nodel, E., Pleasance, S., and Fernandez, R. C. (2003). A conserved region within the *Bordetella pertussis* autotransporter BrkA is necessary for folding of its passenger domain. *Mol. Microbiol.* 47, 1367–1383.

Oomen, C. J., Van Ulsen, P., Van Gelder, P., Feijen, M., Tommassen, J., and Gros, P. (2004). Structure of the translocator domain of a bacterial autotransporter. *EMBO J.* 23, 1257–1266. doi: 10.1038/sj.emboj.7600148

Otto, B. R., Sijbrandi, R., Luirink, J., Oudega, B., Heddle, J. G., Mizutani, K., et al. (2005). Crystal structure of hemoglobin protease, a heme binding autotransporter protein from pathogenic *Escherichia coli*. *J. Biol. Chem.* 280, 17339–17345. doi: 10.1074/jbc.M412885200

Palmer, K. L., and Munson, R. S. J. (1995). Cloning and characterization of the genes encoding the haemolysin of *Haemophilus ducreyi*. *Mol. Microbiol.* 18, 821–830.

Pavlova, O., Peterson, J. H., Ieva, R., and Bernstein, H. D. (2013). Mechanistic link between beta barrel assembly and the initiation of autotransporter secretion. *Proc. Natl. Acad. Sci. U.S.A.* 110, E938–E947. doi: 10.1073/pnas.1219076110

Pei, J., Kim, B. H., and Grishin, N. V. (2008). PROMALS3D: a tool for multiple protein sequence and structure alignments. *Nucleic Acids Res.* 36, 2295–2300. doi: 10.1093/nar/gkn072

Perez, A., Merino, M., Rumbo-Feal, S., Alvarez-Fraga, L., Vallejo, J. A., Beceiro, A., et al. (2016). The FhaB/FhaC two-partner secretion system is involved in adhesion of *Acinetobacter baumannii* AbH12O-A2 strain. *Virulence* 18, 1–16. doi: 10.1080/21505594.2016.1262313

Peterson, J. H., Szabady, R. L., and Bernstein, H. D. (2006). An unusual signal peptide extension inhibits the binding of bacterial presecretory proteins to the signal recognition particle, trigger factor, and the SecYEG complex. *J. Biol. Chem.* 281, 9038–9048. doi: 10.1074/jbc.M508681200

Peterson, J. H., Tian, P., Ieva, R., Dautin, N., and Bernstein, H. D. (2010). Secretion of a bacterial virulence factor is driven by the folding of a C-terminal segment. *Proc. Natl. Acad. Sci. U.S.A.* 107, 17739–17744. doi: 10.1073/pnas.1009491107

Plamondon, P., Luke, N., and Campagnari, A. (2007). Identification of a novel two-partner secretion locus in *Moraxella catarrhalis*. *Infect. Immun.* 75, 2929–2936. doi: 10.1128/IAI.00396-07

Pohlner, J., Halter, R., Beyreuther, K., and Meyer, T. F. (1987). Gene structure and extracellular secretion of *Neisseria gonorrheae* IgA protease. *Nature* 325, 458–462.

Poole, K., and Braun, V. (1988). Iron regulation of *Serratia marcescens* hemolysin gene expression. *Infect. Immun.* 56, 2967–2971.

Poole, K., Schiebel, E., and Braun, V. (1988). Molecular characterization of the hemolysin determinant of *Serratia marcescens*. *J. Bacteriol.* 170, 3177–3188.

Renauld-Mongénie, G., Cornette, J., Mielcarek, N., Menozzi, F. D., and Locht, C. (1996). Distinct roles of the N-terminal and the C-terminal precursor domains in the biogenesis of the *Bordetella pertussis* filamentous hemagglutinin. *J. Bacteriol.* 178, 1053–1060.

Renn, J. P., and Clark, P. L. (2008). A conserved stable core in the passenger domain beta-helix of autotransporter virulence proteins. *Biopolymers* 89, 420–427. doi: 10.1002/bip.20924

Renn, J. P., Junker, M., Besingi, R. N., Braselmann, E., and Clark, P. L. (2012). ATP-independent control of autotransporter virulence protein transport via the folding properties of the secreted protein. *Chem. Biol.* 19, 287–296. doi: 10.1016/j.chembiol.2011.11.009

Ricci, D. P., and Silhavy, T. J. (2012). The Bam machine: a molecular cooper. *Biochim. Biophys. Acta* 1818, 1067–1084. doi: 10.1016/j.bbamem.2011.08.020

Rigel, N. W., Ricci, D. P., and Silhavy, T. J. (2013). Conformation-specific labeling of BamA and suppressor analysis suggest a cyclic mechanism for beta-barrel assembly in *Escherichia coli*. *Proc. Natl. Acad. Sci. U.S.A.* 110, 5151–5156. doi: 10.1073/pnas.1302662110

Rojas, C. M., Ham, J. H., Deng, W. L., Doyle, J. J., and Collmer, A. (2002). HecA, a member of a class of adhesins produced by diverse pathogenic bacteria, contributes to the attachment, aggregation, epidermal cell killing, and virulence phenotypes of *Erwinia chrysanthemi* EC16 on *Nicotiana clevelandii* seedlings. *Proc. Natl. Acad. Sci. U.S.A.* 99, 13142–13147. doi: 10.1073/pnas.202358699

Roy, K., Hilliard, G. M., Hamilton, D. J., Luo, J., Ostmann, M. M., and Fleckenstein, J. M. (2009). Enterotoxigenic *Escherichia coli* EtpA mediates adhesion between flagella and host cells. *Nature* 457, 594–598. doi: 10.1038/nature07568

Ruhe, Z. C., Low, D. A., and Hayes, C. S. (2013). Bacterial contact-dependent growth inhibition. *Trends Microbiol.* 21, 230–237. doi: 10.1016/j.tim.2013.02.003

Ruhe, Z. C., Nguyen, J. Y., Chen, A. J., Leung, N. Y., Hayes, C. S., and Low, D. A. (2016). CDI Systems are stably maintained by a cell-contact mediated surveillance mechanism. *PLoS Genet.* 12:e1006145. doi: 10.1371/journal.pgen.1006145

Ruhe, Z. C., Townsley, L., Wallace, A. B., King, A., Van der Woude, M. W., Low, D. A., et al. (2015). CdiA promotes receptor-independent intercellular adhesion. *Mol. Microbiol.* 98, 175–192. doi: 10.1111/mmi.13114

Rybtke, M., Berthelsen, J., Yang, L., Hoiby, N., Givskov, M., and Tolker-Nielsen, T. (2015). The LapG protein plays a role in *Pseudomonas aeruginosa* biofilm formation by controlling the presence of the CdrA adhesin on the cell surface. *Microbiologyopen* 4, 917–930. doi: 10.1002/mbo3.301

Salacha, R., Kovacic, F., Brochier-Armanet, C., Wilhelm, S., Tommassen, J., Filloux, A., et al. (2010). The *Pseudomonas aeruginosa* patatin-like protein PlpD is the archetype of a novel Type V secretion system. *Environ. Microbiol.* 12, 1498–1512. doi: 10.1111/j.1462-2920.2010.02174.x

Sauri, A., Soprova, Z., Wickstrom, D., de Gier, J. W., Van der Schors, R. C., Smit, A. B., et al. (2009). The Bam (Omp85) complex is involved in secretion of the autotransporter haemoglobin protease. *Microbiology* 155, 3982–3991. doi: 10.1099/mic.0.034991-0

Scarlato, V., Arico, B., Prugnola, A., and Rappuoli, R. (1991). Sequential activation and environmental regulation of virulence genes in *Bordetella pertussis*. *EMBO J.* 10, 3971–3975.

Schiebel, E., Schwarz, H., and Braun, V. (1989). Subcellular localization and unique secretion of the hemolysin of *Serratia marcescens*. *J. Biol. Chem.* 264, 16311–16320.

Schmitt, C., Turner, D., Boesl, M., Abele, M., Frosch, M., and Kurzai, O. (2007). A functional two-partner secretion system contributes to adhesion of *Neisseria meningitidis* to epithelial cells. *J. Bacteriol.* 189, 7968–7976. doi: 10.1128/JB.00851-07

Schönherr, R., Tsolis, R., Focareta, T., and Braun, V. (1993). Amino acid replacements in the *Serratia marcescens* haemolysin ShlA define sites involved in activation and secretion. *Mol. Microbiol.* 9, 1229–1237.

Sen, K., Hellman, J., and Nikaido, H. (1988). Porin channels in intact cells of *Escherichia coli* are not affected by Donnan potentials across the outer membrane. *J. Biol. Chem.* 263, 1182–1187.

Serra, D. O., Conover, M. S., Arnal, L., Sloan, G. P., Rodriguez, M. E., Yantorno, O. M., et al. (2012). FHA-mediated cell-substrate and cell-cell adhesions are critical for *Bordetella pertussis* biofilm formation on abiotic surfaces and in the mouse nose and the trachea. *PLoS ONE* 6:e28811. doi: 10.1371/journal.pone.0028811

Shahid, S. A., Bardiaux, B., Franks, W. T., Krabben, L., Habeck, M., van Rossum, B. J., et al. (2012). Membrane-protein structure determination by solid-state NMR spectroscopy of microcrystals. *Nat. Methods* 9, 1212–1217. doi: 10.1038/nmeth.2248

Siddaramappa, S., Challacombe, J. F., Duncan, A. J., Gillaspy, A. F., Carson, M., Gipson, J., et al. (2011). Horizontal gene transfer in *Histophilus somni* and its role in the evolution of pathogenic strain 2336, as determined by comparative genomic analyses. *BMC Genomics* 12:570. doi: 10.1186/1471-2164-12-570

Simon, S. M., Peskin, C. S., and Oster, G. F. (1992). What drives the translocation of proteins? *Proc. Natl. Acad. Sci. U.S.A.* 89, 3770–3774.

St Geme, J. W. III, and Grass, S. (1998). Secretion of the *Haemophilus influenzae* HMW1 and HMW2 adhesins involves a periplasmic intermediate and requires the HMWB and HMWC proteins. *Mol. Microbiol.* 27, 617–630.

St Geme, J. W. III, and Yeo, H. J. (2009). A prototype two-partner secretion pathway: the *Haemophilus influenzae* HMW1 and HMW2 adhesin systems. *Trends Microbiol.* 17, 355–360. doi: 10.1016/j.tim.2009.06.002

Strauss, E. J., Ghori, N., and Falkow, S. (1997). An *Edwardsiella tarda* strain containing a mutation in a gene with homology to *shlB* and *hpmB* is defective for entry into epithelial cells in culture. *Infect. Immun.* 65, 3924–3932.

Surana, N. K., Grass, S., Hardy, G. G., Li, H., Thanassi, D. G., and Geme, J. W. III. (2004). Evidence for conservation of architecture and physical properties of Omp85-like proteins throughout evolution. *Proc. Natl. Acad. Sci. U.S.A.* 101, 14497–14502. doi: 10.1073/pnas.0404679101

Szabady, R. L., Peterson, J. H., Skillman, K. M., and Bernstein, H. D. (2005). An unusual signal peptide facilitates late steps in the biogenesis of a bacterial autotransporter. *Proc. Natl. Acad. Sci. U.S.A.* 102, 221–226. doi: 10.1073/pnas.0406055102

Szczesny, P., and Lupas, A. (2008). Domain annotation of trimeric autotransporter adhesins–daTAA. *Bioinformatics* 24, 1251–1256. doi: 10.1093/bioinformatics/btn118

Tala, A., Progida, C., De Stefano, M., Cogli, L., Spinosa, M. R., Bucci, C., et al. (2008). The HrpB-HrpA two-partner secretion system is essential for intracellular survival of *Neisseria meningitidis*. *Cell. Microbiol.* 10, 2461–2482. doi: 10.1111/j.1462-5822.2008.01222.x

Tsai, J. C., Yen, M. R., Castillo, R., Leyton, D. L., Henderson, I. R., and Saier, M. H. Jr. (2010). The bacterial intimins and invasins: a large and novel family of secreted proteins. *PLoS ONE* 5:e14403. doi: 10.1371/journal.pone.0014403

Tuanyok, A., Leadem, B. R., Auerbach, R. K., Beckstrom-Sternberg, S. M., Beckstrom-Sternberg, J. S., Mayo, M., et al. (2008). Genomic islands from five strains of *Burkholderia pseudomallei*. *BMC Genomics* 9:566. doi: 10.1186/1471-2164-9-566

Tumapa, S., Holden, M. T., Vesaratchavest, M., Wuthiekanun, V., Limmathurotsakul, D., Chierakul, W., et al. (2008). *Burkholderia pseudomallei* genome plasticity associated with genomic island variation. *BMC Genomics* 9:190. doi: 10.1186/1471-2164-9-190

Uphoff, T. S., and Welch, R. A. (1990). Nucleotide sequencing of the *Proteus mirabilis* calcium-independent hemolysin genes (*hpmA* and *hpmB*) reveals sequence similarity with the *Serratia marcescens* hemolysin genes (*shlA* and *shlB*). *J. Bacteriol.* 172, 1206–1216.

Uphoff, T. S., and Welch, R. A. (1994). "Structural and functional analysis of HpmA hemolysin of *Proteus mirabilis*," in *Molecular Mechanisms of Bacterial Virulence*, eds C. I. Kado and J. H. Crosa (Kluwer Academics Publishers), 283–292.

ur Rahman, S., and van Ulsen, P. (2013). System specificity of the TpsB transporters of coexpressed two-partner secretion systems of *Neisseria meningitidis*. *J. Bacteriol.* 195, 788–797. doi: 10.1128/JB.01355-12

ur Rahman, S., Arenas, J., Ozturk, H., Dekker, N., and van Ulsen, P. (2014). The polypeptide transport-associated (POTRA) domains of TpsB transporters determine the system specificity of two-partner secretion systems. *J. Biol. Chem.* 289, 19799–19809. doi: 10.1074/jbc.M113.544627

Vakevainen, M., Greenberg, S., and Hansen, E. J. (2003). Inhibition of phagocytosis by *Haemophilus ducreyi* requires expression of the LspA1 and LspA2 proteins. *Infect. Immun.* 71, 5994–6003.

van den Berg, B. M. (2010). Crystal structure of a full-length autotransporter. *J. Mol. Biol.* 396, 627–633. doi: 10.1016/j.jmb.2009.12.061

van Ulsen, P., Rahman, S., Jong, W., Daleke-Schermerhorn, M., and Luirink, J. (2014). Type V secretion: from biogenesis to biotechnology. *Biochim. Biophys. Acta* 1843, 1592–1611. doi: 10.1016/j.bbamcr.2013.11.006

van Ulsen, P., Rutten, L., Feller, M., Tommassen, J., and van der Ende, A. (2008). Two-partner secretion systems of *Neisseria meningitidis* associated with invasive clonal complexes. *Infect. Immun.* 76, 4649–4658. doi: 10.1128/IAI.00393-08

Walker, G., Hertle, R., and Braun, V. (2004). Activation of *Serratia marcescens* hemolysin through a conformational change. *Infect. Immun.* 72, 611–614.

Wang, F., Zhang, M., Hu, Y., Zhang, W., and Sun, L. (2009). Regulation of the *Edwardsiella tarda* hemolysin gene and luxS by EthR. *J. Microbiol. Biotechnol.* 19, 765–773.

Wang, X., Wang, Q., Xiao, J., Liu, Q., Wu, H., and Zhang, Y. (2010). Hemolysin EthA in *Edwardsiella tarda* is essential for fish invasion *in vivo* and *in vitro* and regulated by two-component system EsrA-EsrB and nucleoid protein HhaEt. *Fish Shellfish Immunol.* 29, 1082–1091. doi: 10.1016/j.fsi.2010.08.025

Ward, C. K., Latimer, J. L., Nika, J., Vakevainen, M., Mock, J. R., Deng, K., et al. (2003). Mutations in the lspA1 and lspA2 genes of *Haemophilus ducreyi* affect the virulence of this pathogen in an animal model system. *Infect. Immun.* 71, 2478–2486.

Ward, C. K., Lumbley, S. R., Latimer, J. L., Cope, L. D., and Hansen, E. J. (1998). *Haemophilus ducreyi* secretes a filamentous hemagglutinin-like protein. *J. Bacteriol.* 180, 6013–6022.

Weaver, T. M., Hocking, J. M., Bailey, L. J., Wawrzyn, G. T., Howard, D. R., Sikkink, L. A., et al. (2009). Structural and functional studies of truncated hemolysin a from *Proteus mirabilis*. *J. Biol. Chem.* 284, 22297–22309. doi: 10.1074/jbc.M109.014431

Webb, C. T., Heinz, E., and Lithgow, T. (2012). Evolution of the beta-barrel assembly machinery. *Trends Microbiol.* 20, 612–620. doi: 10.1016/j.tim.2012.08.006

Webb, J. S., Nikolakakis, K. C., Willett, J. L., Aoki, S. K., Hayes, C. S., and Low, D. A. (2013). Delivery of CdiA nuclease toxins into target cells during contact-dependent growth inhibition. *PLoS ONE* 8:e57609. doi: 10.1371/journal.pone.0057609

Willems, R. J., Geuijen, C., van der Heide, H. G., Renauld, G., Bertin, P., van den Akker, W. M., et al. (1994). Mutational analysis of the *Bordetella pertussis fim/fha* gene cluster: identification of a gene with sequence similarities to haemolysin accessory genes involved in export of FHA. *Mol. Microbiol.* 11, 337–347.

Willett, J. L., Gucinski, G. C., Fatherree, J. P., Low, D. A., and Hayes, C. S. (2015a). Contact-dependent growth inhibition toxins exploit multiple independent cell-entry pathways. *Proc. Natl. Acad. Sci. U.S.A.* 112, 11341–11346. doi: 10.1073/pnas.1512124112

Willett, J. L., Ruhe, Z. C., Goulding, C. W., Low, D. A., and Hayes, C. S. (2015b). Contact-dependent growth inhibition (CDI) and CdiB/CdiA two-partner secretion proteins. *J. Mol. Biol.* 427, 3754–3765. doi: 10.1016/j.jmb.2015.09.010

Wimmer, M. R., Woods, C. N., Adamczak, K. J., Glasgow, E. M., Novak, W. R., Grilley, D. P., et al. (2015). Sequential unfolding of the hemolysin two-partner secretion domain from *Proteus mirabilis*. *Protein Sci.* 24, 1841–1855. doi: 10.1002/pro.2791

Wong, H. C., and Lee, Y. S. (1994). Regulation of iron on bacterial growth and production of thermostable direct hemolysin by *Vibrio parahaemolyticus* in intraperitoneal infected mice. *Microbiol. Immunol.* 38, 367–371.

Yeo, H. J., Yokoyama, T., Walkiewicz, K., Kim, Y., Grass, S., and St Geme, J. W. III. (2007). The structure of the *Haemophilus influenzae*

HMW1 pro-piece reveals a structural domain essential for bacterial two-partner secretion. *J. Biol. Chem.* 282, 31076–31084. doi: 10.1074/jbc.M705750200

Yoder, M. D., Keen, N. T., and Jurnak, F. (1993). New domain motif: the structure of pectate lyase C, a secreted plant virulence factor. *Science* 260, 1503–1507.

Zambolin, S., Clantin, B., Chami, M., Hoos, S., Haouz, A., Villeret, V., et al. (2016). Structural basis for haem piracy from host haemopexin by *Haemophilus influenzae*. *Nat. Commun.* 7:11590. doi: 10.1038/ncomms11590

Zhai, Y., Zhang, K., Huo, Y., Zhu, Y., Zhou, Q., Lu, J., et al. (2011). Autotransporter passenger domain secretion requires a hydrophobic cavity at the extracellular entrance of the beta-domain pore. *Biochem. J.* 435, 577–587. doi: 10.1042/BJ20101548

Zhang, D., Iyer, L. M., and Aravind, L. (2011). A novel immunity system for bacterial nucleic acid degrading toxins and its recruitment in various eukaryotic and DNA viral systems. *Nucleic Acids Res.* 39, 4532–4552. doi: 10.1093/nar/gkr036

Zwihart, K., and Welch, R. (1990). Cytotoxic activity of the *Proteus* hemolysin HpmA. *Infect. Immun.* 58, 1861–1869.

**Conflict of Interest Statement:** The authors declare that the research was conducted in the absence of any commercial or financial relationships that could be construed as a potential conflict of interest.

frontiers in Cellular and Infection Microbiology

REVIEW
published: 26 May 2017
doi: 10.3389/fcimb.2017.00215

# The Type IX Secretion System (T9SS): Highlights and Recent Insights into Its Structure and Function

*Anna M. Lasica*[1,2]*, *Miroslaw Ksiazek*[1,3], *Mariusz Madej*[3] and *Jan Potempa*[1,3]*

[1] Department of Oral Immunology and Infectious Diseases, University of Louisville School of Dentistry, Louisville, KY, United States, [2] Department of Bacterial Genetics, Faculty of Biology, Institute of Microbiology, University of Warsaw, Warsaw, Poland, [3] Department of Microbiology, Faculty of Biochemistry, Biophysics, and Biotechnology, Jagiellonian University, Krakow, Poland

Protein secretion systems are vital for prokaryotic life, as they enable bacteria to acquire nutrients, communicate with other species, defend against biological and chemical agents, and facilitate disease through the delivery of virulence factors. In this review, we will focus on the recently discovered type IX secretion system (T9SS), a complex translocon found only in some species of the *Bacteroidetes* phylum. T9SS plays two roles, depending on the lifestyle of the bacteria. It provides either a means of movement (called gliding motility) for peace-loving environmental bacteria or a weapon for pathogens. The best-studied members of these two groups are *Flavobacterium johnsoniae*, a commensal microorganism often found in water and soil, and *Porphyromonas gingivalis*, a human oral pathogen that is a major causative agent of periodontitis. In *P. gingivalis* and some other periodontopathogens, T9SS translocates proteins, especially virulence factors, across the outer membrane (OM). Proteins destined for secretion bear a conserved C-terminal domain (CTD) that directs the cargo to the OM translocon. At least 18 proteins are involved in this still enigmatic process, with some engaged in the post-translational modification of T9SS cargo proteins. Upon translocation across the OM, the CTD is removed by a protease with sortase-like activity and an anionic LPS is attached to the newly formed C-terminus. As a result, a cargo protein could be secreted into the extracellular milieu or covalently attached to the bacterial surface. T9SS is regulated by a two-component system; however, the precise environmental signal that triggers it has not been identified. Exploring unknown systems contributing to bacterial virulence is exciting, as it may eventually lead to new therapeutic strategies. During the past decade, the major components of T9SS were identified, as well as hints suggesting the possible mechanism of action. In addition, the list of characterized cargo proteins is constantly growing. The actual structure of the translocon, situated in the OM of bacteria, remains the least explored area; however, new technical approaches and increasing scientific attention have resulted in a growing body of data. Therefore, we present a compact up-to-date review of this topic.

**Keywords: secretion, T9SS, *Porphyromonas gingivalis*, pathogenesis, gliding motility, proteins, virulence**

OPEN ACCESS

***Edited by:***
*Thibault Géry Sana,*
*Stanford University, United States*

***Reviewed by:***
*Eric Cascales,*
*Aix-Marseille University, France*
*Koji Nakayama,*
*Nagasaki University, Japan*
*Mark J. McBride,*
*University of Wisconsin–Milwaukee, United States*

***Correspondence:**
*Anna M. Lasica*
*alasica@biol.uw.edu.pl*
*Jan Potempa*
*jan.potempa@louisville.edu*

***Received:*** *02 March 2017*
***Accepted:*** *11 May 2017*
***Published:*** *26 May 2017*

***Citation:***
*Lasica AM, Ksiazek M, Madej M and Potempa J (2017) The Type IX Secretion System (T9SS): Highlights and Recent Insights into Its Structure and Function. Front. Cell. Infect. Microbiol. 7:215. doi: 10.3389/fcimb.2017.00215*

## INTRODUCTION

Secretion of hemolysin A by *E. coli*, described four decades ago, was the first protein secretion system discovered in Gram-negative bacteria (diderm bacteria; Goebel and Hedgpeth, 1982). Since then, eight other protein secretion pathways have been characterized in these prokaryotes, which have a cell envelope consisting of the inner membrane (IM) and the outer membrane (OM) separated by the periplasm. They are now referred to as type *x* secretion systems (T1SS–T9SS; reviewed in Abdallah et al., 2007; Gerlach and Hensel, 2007; Remaut et al., 2008; Desvaux et al., 2009; Goyal et al., 2014; Costa et al., 2015; Abby et al., 2016). Secretion systems in diderm bacteria are considered gateways through the OM that transport cargo with the help of either dedicated IM and periplasmic proteins or the Sec, Tat, and holins systems that first transport cargo to the periplasm. In fact, the Sec, Tat, and holins pathways, which transport proteins across the cytoplasmic membrane, are universal among bacteria, eukaryotes, and even archaea (Hutcheon and Bolhuis, 2003; Denks et al., 2014; Berks, 2015; Saier and Reddy, 2015). Therefore, secretion may be either a single-step process in which substrates (proteins or DNA) are translocated through a designated cell envelope-spanning structure (T1SS, T3SS, T4SS, and T6SS) or a two-step process in which the substrates first cross the IM into the periplasm using the Sec/Tat/holins systems, then are directed to the OM translocon. The final destinations of secreted cargos are diverse: they may stay attached to the surface of the OM, be released into the extracellular milieu, or be injected into the cytoplasm of a target cell (Costa et al., 2015; Abby et al., 2016).

Secretion systems perform numerous physiological functions essential for cell propagation and fitness within a specific ecological niche. They facilitate nutrient acquisition, communication with the environment, attachment to various surfaces, defense against host antimicrobial systems, and delivery of virulence factors at a precise location such as a eukaryotic cell (Letoffe et al., 1994; Henke and Bassler, 2004; Gerlach and Hensel, 2007; Rondelet and Condemine, 2013; Gaytan et al., 2016; Hachani et al., 2016; Majerczyk et al., 2016). However, none of the above adaptations can be assigned solely to one type of secretion.

The presence of protein secretion systems varies among phylogenetic lineages of diderm bacteria. *Proteobacteria* encode the broadest range of described secretion types, whereas other clades have a strong preference for only one or two types (e.g., *Fusobacteria* possess only T5SS; *Chlamydiae*, T3SS and T5SS). The most widespread systems are T1SS and T5SS; conversely, T2SS is rarely detected outside *Proteobacteria* (Abby et al., 2016).

In this review, we will cover the current knowledge regarding the recently discovered type IX secretion system (T9SS), also known as the Por secretion system (PorSS) or PerioGate. T9SS is exclusively present in the *Bacteroidetes* phylum, in a majority of its species (62% out of 97 genomes available; Sato et al., 2010; McBride and Zhu, 2013; Abby et al., 2016).

## DISCOVERY OF T9SS

Uncovering and characterizing this unique secretion system was a gradual process over the last two decades and originated from studies of the Gram-negative, non-motile, anaerobic bacterium *Porphyromonas gingivalis*. *P. gingivalis* is a human oral pathogen that is a major causative agent of periodontitis, and, along with two other bacteria, *Tannerella forsythia* and *Treponema denticola*, forms the so-called red complex (Hajishengallis, 2015). Besides being a key pathogen in periodontitis, *P. gingivalis* is implicated in many systemic illnesses such as atherosclerosis (Kebschull et al., 2010), aspiration pneumonia (Benedyk et al., 2016), rheumatoid arthritis (RA; Laugisch et al., 2016), and even cancer (Whitmore and Lamont, 2014; Gao et al., 2016).

An important initial finding was that *P. gingivalis* produces potent proteolytic enzymes called gingipains (Kgp, RgpA, and RgpB; discussed in more detail later in this review; Pike et al., 1994; Pavloff et al., 1995; Curtis et al., 1999). Gingipains are essential virulence factors responsible for corrupting host innate defense mechanisms (Potempa et al., 2003; Hajishengallis, 2015). They are secreted in large amounts and are mainly attached to the surface of the OM, but are also partially released in a soluble form into the extracellular milieu (Pike et al., 1994; Rangarajan et al., 1997). Because none of the genes associated with known protein secretion systems could be found in the *P. gingivalis* genome, it was suspected that this bacterium had developed a unique OM translocon.

The search for this novel secretion system was greatly facilitated by the observation that colonies of *P. gingivalis* deficient in gingipain activity lack black pigmentation while growing on blood agar plates (**Figure 1**; Okamoto et al., 1998; Shi et al., 1999). Colony pigmentation results from the accumulation of heme on the surface of *P. gingivalis* cells, a process dependent on the proteolytic activity and hemagglutinin- and heme/hemoglobin-binding activity of gingipains (Smalley et al., 1998; Sroka et al., 2001). Spontaneous white/beige mutants were occasionally observed, and this phenotype was associated with, among other things, decreased cell surface-associated proteolytic activity (McKee et al., 1988; Shah et al., 1989). The discovery of the essential role of secreted, cell-bound gingipains in heme acquisition meant that pigmentation could be used as an easy screening tool for mutations blocking gingipain secretion. Of note, as potent virulence factors, gingipains were of particular interest for elucidating the role of *P. gingivalis* in the development of periodontitis.

Several high-throughput transposon mutagenesis studies were performed, resulting in the characterization of various pigment-less clones. Early studies associated this phenotype with the impaired activity of trypsin-like proteases and diminished hemagglutination and heme acquisition by mutants (Hoover and Yoshimura, 1994; Genco et al., 1995). Later investigations found aberrations in polysaccharide synthesis and disruption of *kgp* (one of the gingipains; Simpson et al., 1999; Chen et al., 2000; Abaibou et al., 2001; Shoji et al., 2002). Finally, Sato et al. (2005) identified in their transposon study *porT* (PG0751/PGN_0778), the first gene encoding a protein involved in the secretion of

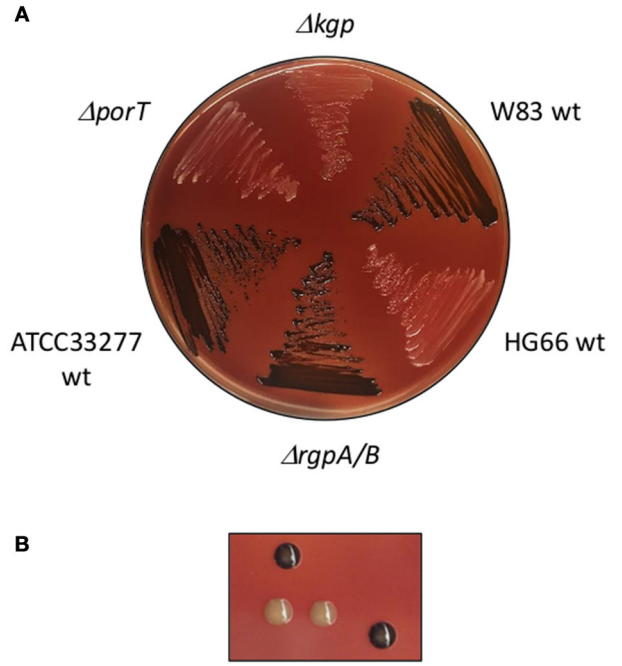


**FIGURE 1 | Pigmentation of various *P. gingivalis* W83 strains. (A)** The wild-type *P. gingivalis* W83 and ATCC33277 strains grown anaerobically on blood agar plates present brown/black pigmentation due to heme accumulation. This phenotype is in a great part dependent on Kgp gingipain activity on the cell surface. *P. gingivalis* strains deficient in Kgp activity yield beige colonies which darken over the time. Arginine gingipains (RgpA/B) are not involved in this process and their deletion does not influence pigmentation. Strains impaired in T9SS e.g., Δ*porT* lack pigmentation which is never restored. Due to the absence of A-LPS in the *P. gingivalis* HG66 strain all gingipains and other T9SS cargo proteins are not associated with the cell membrane, but secreted into extracellular milieu resulting in white phenotype. **(B)** Single colonies of *P. gingivalis* strains grown for 7 days showing black or white pigmentation.

gingipains. Their mutated, non-pigmented strain had impaired gingipain activity. Moreover, gingipains accumulated in the periplasm as enzymatically inactive proenzymes instead of being exported outside the cell. A database search (BLASTP) found that PorT is present only in some species of the *Bacteroidetes* phylum, such as *Porphyromonas gingivalis*, *Cytophaga hutchinsonii*, and *Prevotella intermedia*, and absent from many other phylum proteomes like *Bacteroides thetaiotaomicron* and *Bacteroides fragilis* (Sato et al., 2005). Two years later, another gene, *sov* (PG0809/PGN_0832), was implicated in the secretion of gingipains, showing a mutation phenotype identical to the one observed for the *porT* mutation (Saiki and Konishi, 2007).

Finally, the 2010 comparison of the *porT*-positive proteomes/genomes of *C. hutchinsonii* and *P. gingivalis* with the *porT*-negative species *B. thetaiotaomicron* resulted in a list of 55 genes (in addition to *porT*) potentially involved in the secretion mechanism. Subsequent isogenic mutagenesis of all selected genes resulted in the identification of 11 genes (including *porT* and *sov*) associated with gingipain transport across the OM and gingipain activation. Because these proteins do not have sequence similarity to components of any other known secretion system, it was assumed to be a novel secretion system and was originally called the Por secretion system (PorSS; Sato et al., 2010; Nakayama, 2015). To be consistent with the existing nomenclature of secretion systems in diderm bacteria, the system was later designated the type IX secretion system or T9SS.

## NEW SECRETION SYSTEM: A DEADLY WEAPON OR A PEACEFUL TOOL?

The comparative analysis of genomes carried out in a search for *porT* homologs revealed that T9SS is exclusively present in the *Bacteroidetes* phylum (Sato et al., 2005). Numerous studies on *P. gingivalis* show that T9SS is involved in virulence factor secretion, which damages human tissues and dysregulates immune responses (Potempa et al., 2003; Yoshimura et al., 2008; Sato et al., 2013; Bielecka et al., 2014; Taguchi et al., 2015). In addition, *T. forsythia* and *Prevotella intermedia* (another oral pathogenic bacteria) use this secretion pathway to disseminate their effector proteins (Nguyen et al., 2007; Veith et al., 2013; Narita et al., 2014; Tomek et al., 2014; Ksiazek et al., 2015b). Consequently, it is plausible that more pathogens from the *Bacteroidetes* phylum carrying *porT* homologs are utilizing this mechanism for virulence factor secretion. Although no experimental data are available to support this, it is likely that T9SS is a molecular weapon aimed at various host cells, similar to many other secretion systems (especially T3SS and T6SS).

Among *Bacteroidetes*' *porT*-positive species, there are many non-pathogenic environmental microorganisms such as *C. hutchinsonii* and *F. johnsoniae*. Both bacteria are aerobes ubiquitously distributed in soil and are capable of digesting macromolecules such as cellulose and chitin, respectively (Stanier, 1942, 1947). They are motile microorganisms that use a movement mechanism called gliding motility (Jarrell and McBride, 2008; Nakane et al., 2013). Surprisingly, the core T9SS genes are a subset of those necessary for gliding (*gldK: ortholog of P. gingivalis porK*, *gldL/porL*, *gldM/porM*, *gldN/porN*, *sprA/sov*, *sprE/porW*, and *sprT/porT*; Sato et al., 2010; McBride and Zhu, 2013; Shrivastava et al., 2013; McBride and Nakane, 2015). Moreover, secretion of chitinase and cellulase requires T9SS, meaning the system functions as a non-invasive tool used for movement and food acquisition in these bacteria (Kharade and McBride, 2014; Zhu and McBride, 2014; Yang et al., 2016).

The detailed mechanisms and regulation of T9SS in gliding motility and food scavenging are still under investigation and may reveal additional functions (even in non-gliding species).

## STRUCTURAL AND FUNCTIONAL COMPONENTS OF *P. gingivalis* T9SS

Presently, 18 genes from a total of 29 candidates have been proven essential for proper T9SS function in *P. gingivalis* by deletion mutagenesis studies (Heath et al., 2016). Deletion of any of these genes results in the white pigmentation phenotype and accumulation of cargos (e.g., gingipains) in the periplasm. Some

of these proteins build the core structures in the IM and OM, some play regulatory or accessory roles, and others are involved in post-translationally modifying cargo proteins (**Table 1**). Many aspects of their functions have yet to be discovered.

Genes encoding T9SS components are scattered around the *P. gingivalis* genome. The exception is a group of five genes, *porP-porK-porL-porM-porN*, that are co-transcribed (Vincent et al., 2016). In many other *Bacteroidetes* species, the operon structure of these genes is conserved [databases: STRING (Snel et al., 2000), DOOR (Dam et al., 2007; Mao et al., 2009), ProOpDB (Taboada et al., 2012), OperonDB (Pertea et al., 2009)]. Orthologs of the *porP* gene (*sprP* in some gliding motility bacteria) show the most variation, as the gene can be located in different genomic loci (e.g., *F. johnsoniae Fjoh_3477* vs. *gldK/Fjoh_1853*), and, even if they precede *porK*, they remain as separate transcriptional units (e.g., *C. hutchinsonii sprP/CHU_0170* and *gldK/CHU_0171*; Zhu and McBride, 2014). The rest of the *P. gingivalis* T9SS genes are either single units or predicted to be in 2–5 gene operons (**Figure 2**) with genes unrelated to T9SS structure and function. In addition, none of the adjacent genes encode T9SS cargo proteins.

## Cytoplasmic and IM Components

Presently, there is only one known T9SS-related protein residing entirely in the cytoplasm: PorX (PG0928/PGN_1019). It is a response regulator (RR) of a two-component system (TCS) involved in regulating the expression of several T9SS genes. Its sensor kinase partner, PorY (PG0052/PGN_2001), is an IM-anchored protein containing two transmembrane (TM) helices and a large cytoplasmic domain (∼222 aa; Sato et al., 2010; Vincent et al., 2016). Both proteins will be discussed in more detail in the Regulation Section.

Two other essential components of T9SS, PorL (*PG0289 /PGN_1675*) and PorM (*PG0290/PGN_1674*), are also anchored in the IM. PorL possesses two TM helices located between residues 17–48 and 48–74, with both N- and C-termini in the cytoplasm. The precise locations of the helices (the exact amino acids) have not been determined (Vincent et al., 2017). The large cytoplasmic C-terminal domain (∼236 residues) interacts *in vitro* with PorX (Vincent et al., 2016); thus it may be involved in regulating T9SS function. Moreover, PorL cytoplasmic domain forms a homotrimer in *E. coli* cells and the full-length protein was found in a complex with PorM both *in vitro* (Gorasia et al., 2016; Vincent et al., 2017) and *in vivo* (Sato et al., 2010). PorM is anchored in the IM by a single TM helix at its N-terminus (between residues 9 and 41), with the remaining residues (475) forming a domain facing the periplasm. In *E. coli* cells, the periplasmic part of PorM dimerizes and interacts with two other core T9SS proteins: PorK and PorN (Vincent et al., 2017). The recombinant periplasmic domain (amino acid residues 36–516) was crystallized, presenting with tetragonal crystals, but automatic model building failed to provide a realistic structure, thus leaving the nature of interactions unknown (Stathopulos et al., 2015). Nevertheless, a possible function for PorL/PorM, apart from the regulatory implications for PorL, has been suggested.

It was proposed that the two proteins form an energy transducer complex to provide energy for T9SS assembly and substrate translocation. The idea came from *F. johnsoniae*, which utilizes a proton-motive force for gliding motility (Nakane et al., 2013; Gorasia et al., 2016). It was further noted that the hydrophobic TM helixes of GldL (PorL ortholog), PorL, and PorM possess conserved glutamate residues characteristic of known energy transducers (Shrivastava et al., 2013; Vincent et al., 2017). These assumptions need experimental verification; nevertheless, they are compatible with mechanisms used by other secretion systems to provide the energy needed to drive substrate transport such as hydrolysis of ATP, proton-motive force, low-energy assembly, and entropy gradient (Costa et al., 2015).

## Periplasmic Components

Four T9SS proteins are located in the periplasm: PorN (PG0291/PGN_1673), PorK (PG0288/PGN_1676), PorW (PG1947/PGN_1877), and PG1058/PGN_1296. All but one (PorN) are predicted or proven to be lipoproteins associated with membranes (Sato et al., 2010). PorW is the least investigated protein among the periplasmic elements of *P. gingivalis* secretion. Experimental work on PorW has only been performed on the *F. johnsoniae* PorW ortholog, SprE (Fjoh_1051), which is a predicted lipoprotein that localizes to a membrane fraction (most likely the OM). A mutant with a deleted *sprE* gene exhibits phenotypes in gliding bacteria typical of other T9SS function-deficient mutants, such as non-spreading colonies, defective gliding, and blocked secretion of chitinase (Rhodes et al., 2011; Kharade and McBride, 2015). Its subcellular localization and the effects of its mutation on the secretory/gliding phenotype suggest that SprE/PorW is yet another structural component of T9SS.

PG1058 is a multidomain protein necessary for T9SS function. The phenotype of *P. gingivalis* with an inactivated *PG1058* gene is typical of other T9SS mutants: colonies on blood agar lack pigmentation and inactive, unprocessed gingipains accumulate in the periplasm. The PG1058 protein is anchored by its lipid modification to the periplasmic surface of the OM. The predicted structure suggests the presence of four structural domains: a tetratricopeptide repeat (TPR) domain, a β-propeller domain, a carboxypeptidase regulatory domain-like fold (CRD), and an OmpA_C-like putative peptidoglycan-binding domain. TPR and β-propeller domains are involved in protein-protein interactions; hence, together with the *PG1058* mutant phenotype, it is plausible that PG1058 supports the T9SS translocon structure (Heath et al., 2016). Further, experiments are needed to verify this hypothesis.

PorN is a periplasmic protein that forms dimers *in vitro* and has the propensity to interact both *in vitro* and *in vivo* with IM protein PorM and periplasmic lipoprotein PorK (Gorasia et al., 2016; Vincent et al., 2017). The nature of the interaction with PorK is interesting, as both proteins form a ring-shaped structure with an external and internal diameter of 50 and 35 nm, respectively. It was proposed that they form a large complex in which PorN interacts in an almost 1:1 fashion (32–36 total subunits) with the PorK lipoprotein. The ring structure is anchored into the OM through the fatty acids of PorK. Consistent with detected interactions, PorN has a crucial role in stabilizing both PorL–PorM and PorN–PorK complexes, as deletion of the

**TABLE 1 | T9SS components.**

| Locus Tag | | | *Porphyromonas gingivalis* W83 | | | | | |
|---|---|---|---|---|---|---|---|---|
| **W83 NC_002950.2** | | **ATCC33277 NC_010729.1** | **Protein accession number** | **Protein description** | **Mol weight (kDa)[a]** | **Interactions [b]*in vitro* [c]*in vivo*** | **Homologs *T. forsythia* ATCC 43037–Tanf *F. johnsoniae* UW101-Fjoh** | **References[d]** |
| **CYTOPLASMIC AND INNER MEMBRANE COMPONENTS** | | | | | | | | |
| PG_RS04080 | PG0928 | PGN_1019 | WP_005875211.1 | PorX; chemotaxis protein CheY, cytoplasmic protein | 60.6 | PorY[b], SigP[b], PorL[b] | Tanf_12330 Fjoh_2906 | Sato et al., 2010; Kadowaki et al., 2016; Vincent et al., 2016 |
| PG_RS00240 | PG0052 | PGN_2001 | WP_005873974.1 | PorY; sensor histidine kinase, inner membrane protein | 44.6 | PorX[b] | Tanf_13050 Fjoh_1592 | |
| PG_RS01295 | PG0289 | PGN_1675 | WP_012458450.1 | PorL, inner membrane protein | 34.8 | PorM[b,c] | Tanf_02365 Fjoh_1854 (GldL) | Sato et al., 2010; Gorasia et al., 2016; Kadowaki et al., 2016; Vincent et al., 2016, 2017 |
| PG_RS01300 | PG0290 | PGN_1674 | WP_005874203.1 | PorM, inner membrane protein | 56.4 | PorL/K/N[c] | Tanf_02370 Fjoh_1855 (GldM) | Sato et al., 2010; Gorasia et al., 2016; Kadowaki et al., 2016; Vincent et al., 2017 |
| **PERIPLASMIC COMPONENTS** | | | | | | | | |
| PG_RS01305 | PG0291 | PGN_1673 | WP_005874243.1 | PorN | 41.3 | PorP[b], PorK/L/M[c] PG0189[c] | Tanf_02375 Fjoh_1856 (GldN) | Sato et al., 2010; Gorasia et al., 2016; Kadowaki et al., 2016; Vincent et al., 2017 |
| PG_RS01290 | PG0288 | PGN_1676 | WP_043876477.1 | PorK; lipoprotein | 54.1 | PorN[c], PorM/P[b]PG0189[c] | Tanf_02360 Fjoh_1853 (GldK) | Sato et al., 2010; Gorasia et al., 2016; Kadowaki et al., 2016; Vincent et al., 2017 |
| PG_RS08590 | PG1947 | PGN_1877 | WP_005873869.1 | PorW; lipoprotein | 132.1 | n.d.[e] | Tanf_00060 Fjoh_1051 (SprE) | Sato et al., 2010 |
| PG_RS04660 | PG1058 | PGN_1296 | WP_005873448.1 | Lipoprotein; TPRd, WD40d, CRDd, OmpA Family domain | 74.9 | n.d. | Tanf_02260 Fjoh_1647[f] | Heath et al., 2016 |
| **OUTER MEMBRANE AND SURFACE COMPONENTS** | | | | | | | | |
| PG_RS03550 | PG0809 | PGN_0832 | WP_012457811.1[g] | Sov; β-barrel protein | 281.1 | n.d. | Tanf_04410 Fjoh_1653 (SprA) | Saiki and Konishi, 2007, 2010b; Sato et al., 2010; Kadowaki et al., 2016 |
| PG_RS02670 | PG0602 | PGN_0645 | WP_010956079.1 | PorQ; β-barrel protein | 37.9 | n.d. | Tanf_12465 Fjoh_2755 | Sato et al., 2010 |
| PG_RS01285 | PG0287 | PGN_1677 | WP_005874180.1 | PorP; β-barrel protein | 35.0 | PorN/K[b] | Tanf_02355 Fjoh_3477[h] | Sato et al., 2010; Kadowaki et al., 2016; Vincent et al., 2017 |
| PG_RS03295 | PG0751 | PGN_0778 | WP_039417575.1 | PorT; β-barrel protein | 26.7 | n.d. | Tanf_10520 Fjoh_1466 (SprT) | Sato et al., 2005, 2010; Nguyen et al., 2007; Kadowaki et al., 2016 |
| PG_RS00125 | PG0027 | PGN_0023 | WP_004583425.1 | PorV (LptO); β-barrel protein | 43.1 | PorU[c] | Tanf_04220 Fjoh_1555 | Ishiguro et al., 2009; Sato et al., 2010; Chen et al., 2011; Glew et al., 2012; Saiki and Konishi, 2014 |
| PG_RS00870 | PG0189 | PGN_0297 | WP_005874727.1 | β-barrel protein | 25.6 | PorK/N[c] | Tanf_09815 Fjoh_1692 | Gorasia et al., 2016 |
| PG_RS02385 | PG0534 | PGN_1437 | WP_005875072.1 | TonB-dependent receptor; β-barrel protein | 92.3 | n.d. | Tanf_07980 Fjoh_0118 | Saiki and Konishi, 2010a |
| PG_RS00885 | PG0192 | PGN_300 | WP_043876475.1 | Omp17; OmpH-like | 19.6 | n.d. | Tanf_09800 Fjoh_1689[i] | Taguchi et al., 2015 |

*(Continued)*

**TABLE 1 | Continued**

| Locus Tag | | | *Porphyromonas gingivalis* W83 | | | | |
|---|---|---|---|---|---|---|---|
| **W83 NC_002950.2** | **ATCC33277 NC_010729.1** | **Protein accession number** | **Protein description** | **Mol weight (kDa)[a]** | **Interactions [b]*in vitro* [c]*in vivo*** | **Homologs *T. forsythia* ATCC 43037–Tanf *F. johnsoniae* UW101-Fjoh** | **References[d]** |
| PG_RS00120 | PG0026 | PGN_0022 | WP_005874469.1 | PorU; surface C-terminal signal peptidase | 128.2 | PorV (LptO)[c] | Tanf_02580<br>Fjoh_1556 | Sato et al., 2010; Glew et al., 2012; Saiki and Konishi, 2014; Gorasia et al., 2015 |
| PG_RS07070 | PG1604 | PGN_0509 | WP_010956350.1 | PorZ; surface B-propeller protein | 83.6 | n.d. | Tanf_12435<br>Fjoh_0707 | Glew et al., 2014; Lasica et al., 2016 |

*[a]Calculated from amino acid sequence including a signal peptide.*
*[b]In vitro experiments.*
*[c]In vivo experiments.*
*[d]References to original papers pertinent only to P. gingivalis T9SS. Proteomic papers are not cited in the table but they are referred in the text.*
*[e]Not determined.*
*[f]F. johnsoniae possesses 5 proteins homologous to PG1058, the one with the highest score is given in the table. All 5 F. johnsoniae proteins (Fjoh_1647, Fjoh_4540, Fjoh_3950, Fjoh_3973, Fjoh_3476) range between 26–29% identities with 90-98% coverage comparing to PG1058 (assessed by NCBI BLAST).*
*[g]Accession number given in the table is for the Sov protein from P. gingivalis ATCC33277 due to miss-annotation in W83 genome as two separate ORFs (PG0809/PG0810; Saiki and Konishi, 2007).*
*[h]F. johnsoniae possesses numerous homologous proteins to PG0287 (PorP), the one with the highest score is given in the table. Five proteins with the highest overall score (Fjoh_3477, Fjoh_3951, Fjoh_1646, Fjoh_4539, Fjoh_2274) range between 25–29% identities with 86–93% coverage and gaps 3–9% comparing to PG0287 (PorP). The most explored PorP-like protein of F. johnsoniae is Fjoh_0978 (SprF; Rhodes et al., 2011) however, it has lower scores comparing to the proteins mentioned above (22% identities, 83% coverage, 18% gaps) as assessed by NCBI BLAST.*
*[i]The closest homolog in F. johnsoniae proteome is Fjoh_1689 is much larger protein than its equivalent in P. gingivalis (341 residues vs. 174; 32% identities, 95% PG0192 coverage assessed by NCBI BLAST).*

*porN* gene resulted in the degradation of PorL, PorM, and PorK in *P. gingivalis* cells. By contrast, deletion of either *porL* or *porM* does not interfere with the stability of the PorN/K complex (Gorasia et al., 2016).

Further, studies on PorK,L,M,N interactions suggest the existence of a $PorK_2L_3M_2N_2$ complex that likely oligomerizes to form a superstructure with a final molecular mass of over 1.2 MDa (Gorasia et al., 2016; Vincent et al., 2017). Such a large complex was originally reported by Sato and colleagues, who identified all four proteins in a single spot on a blue-native electrophoresis gel (Sato et al., 2010). However, additional elements of the complex were recently identified: PG0189 and PorP (PG0287/PGN_1677). Because they are predicted to be integral OM β-barrel proteins, they are discussed in more detail in the following section.

## OM and Surface Components

The vast majority of T9SS components are confined to the OM. In addition to the peripheral OM-associated and periplasmic proteins delineated above, seven others (Sov, PorQ, PorP, PorT, PorV, PG0189, and PG0534) are predicted to be integral OM β-barrel proteins. Furthermore, two proteins, PorU and PorZ, are associated with the bacterial surface. In addition, PG0192 was found in a membrane fraction, but its association with the OM needs further verification.

PorT and Sov were the first proteins found to be essential for *P. gingivalis* protein secretion, and the discovery led to intense research on T9SS (see Discovery Section; Sato et al., 2005, 2010; Saiki and Konishi, 2007). Despite this, we still know very little about the structure and function of these proteins a decade later. PorT is predicted to have eight anti-parallel, membrane-traversing β-strands, with four large loops facing the environment, and this topology has been experimentally confirmed (Nguyen et al., 2009). Sov was also described as an integral OM protein with its C-terminal region likely exposed to the extracellular milieu (Saiki and Konishi, 2007, 2010b). However, the precise roles of both proteins in T9SS structure and function remain unknown. Even less information is available concerning PorQ (PG0602/PGN_0645) as a T9SS component (Sato et al., 2010). In the genome annotation, it is described as a hypothetical protein with a β-barrel structure belonging to the porin superfamily (Nelson et al., 2003); thus it is assumed to localize to the OM.

Similarly, little is known about PG0534/PGN_1437 as a protein essential for T9SS function (Saiki and Konishi, 2010a). Interestingly, *PG0534* is upregulated in human gingival epithelial cells, suggesting its contribution to *P. gingivalis* eukaryotic cell invasion and/or intracellular survival (Park et al., 2004). *In silico* predictions run on the RaptorX server (Kallberg et al., 2012) modeled PG0534 as a β-barrel OM protein, with the pyochelin OM receptor FptA from *Pseudomonas aeruginosa* (Cobessi et al., 2005) as the best template (PDB: 1xkwA; *p*-value: 1.82e-23).

The next T9SS OM component, PG0192/PGN_300 (annotated as an OmpH-like protein), was found in the total membrane fraction. Due to its 17 kDa molecular mass, the protein is referred to as Omp17 (Taguchi et al., 2015). The best template prediction by the RaptorX server is a putative

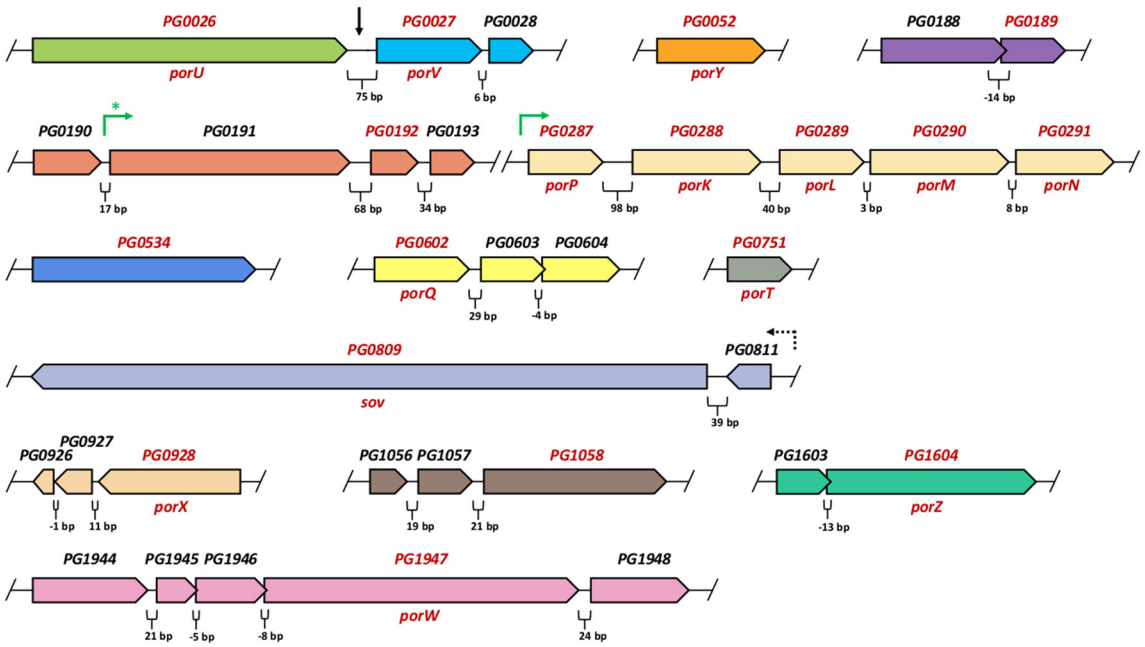


**FIGURE 2 | Arrangement of *P. gingivalis* W83 genes encoding T9SS components.** Genes are grouped according to *in silico* operon predictions, reflecting direction of transcripts (Dam et al., 2007; Mao et al., 2009; Pertea et al., 2009; Taboada et al., 2012). Gaps in the genome are indicated by the slashes. Intervals between adjacent genes or overlapping regions (in base pairs-bp) are marked below each section. Each transcription unit is shown in different color. Genes encoding T9SS components are depicted in red font. Black vertical arrow shows continuous region (75 bp) between *PG0026* (*porU*) and *PG0027* (*porV*) but the two genes were predicted to transcribe independently. Green arrows indicate operons that were confirmed experimentally (Taguchi et al., 2015; Vincent et al., 2017). Green asterisk denotes proved single transcription unit for the *PG0191-PG0192-PG0193* genes (in *P. gingivalis* ATCC33277 strain), however co-transcription of preceding the *PG0190* gene (17 bp interval) was not investigated (Taguchi et al., 2015). The *PG0809* (*Sov*) gene was re-sequenced and confirmed to consist of the two combined genes *PG0809* and *PG0810*, mis-annotated in W83 genome as separate ORFs (Saiki and Konishi, 2007). A dashed arrow denotes indirect evidence that *PG0809* (*Sov*) and *PG0811* may be co-transcribed. It was shown that sigma factor SigP (regulator of other *por* genes) binds to the region preceding *PG0811* but not the one before *PG0809* (Kadowaki et al., 2016).

OM chaperone (OmpH-like) from *Caulobacter crescentus* (PDB: 4kqtA; *p*-value: 6.78e-04). The phenotypic effects of *omp17* mutation are typical of other T9SS-defective mutants but with an interesting exception. The mutant is still able to secrete unprocessed T9SS cargo proteins, including pro-gingipains and CPG70, which accumulate in the periplasm in other secretion mutants (Taguchi et al., 2015). Of note, in the wild-type *P. gingivalis*, T9SS cargos remain attached to the bacterial surface through anionic lipopolysaccharide (A-LPS) anchoring (Shoji et al., 2002; Shoji and Nakayama, 2016). This modification is added by the surface-located PorU protein (Gorasia et al., 2015; for more details see the Mechanism Section). Taguchi and colleagues showed that A-LPS synthesis in the *omp17* mutant was not affected, suggesting the impairment of PorU function. Consistent with that, PorU was not detected in the *omp17*$^{-}$ cell envelope fraction, but was found in the cytoplasm/periplasm fraction. Moreover, the *omp17* mutant was less virulent than the wild type in the mouse subcutaneous model, which is consistent with the lack of gingipain activity (Taguchi et al., 2015).

As previously mentioned, PG0189 and PorP (a part of the *porPKLMN* operon) were detected in association with the PorKLMN complex. Specifically, a periplasmic loop of PG0189 interacts with both PorK and PorN, as shown by cross-linking experiments. Due to its low abundance, PG0189 is proposed to play an accessory role in secretion (Gorasia et al., 2016). The nature of the interaction of PorP with PorK and PorM is still enigmatic. The proteins co-precipitate *in vitro*; however, all tested proteins were produced in *E. coli* cells, and, so far, have not been detected in the native complex (Vincent et al., 2017).

Currently, the only OM β-barrel protein with an assigned function is PorV (PG0027/PGN_0023/LptO). The PorV-mutated strain retains inactive, unprocessed gingipains in the periplasm (Ishiguro et al., 2009) and fails to O-deacylate LPS, which might be a necessary step in post-translational processing during the secretion of cargo proteins (Chen et al., 2011; Glew et al., 2012). Yet another study indicated that PorV interacts *in vivo* with PorU (PG0026/PGN_0022), and it was proposed that PorV serves as an OM anchor for PorU (Saiki and Konishi, 2014). Indeed, PorU localizes to the surface of *P. gingivalis* cells and is involved in T9SS cargo processing (see the next section; Glew et al., 2012; Gorasia et al., 2015). Despite this relative abundance of knowledge on PorV, it remains unknown whether PorV is directly involved in LPS processing or if it is only an accessory protein for an unknown LPS O-deacylase. The secretion-deficient phenotype of the PorV mutant might be related to the lack of PorU immobilization on its surface.

The last known component of T9SS is a surface-located PorZ protein (PG1604/PGN_0509) recently characterized by our group (Lasica et al., 2016). The non-pigmented phenotype of the PorZ-mutant strain and its accumulation of unprocessed, inactive gingipains confirmed that PorZ is essential for the system. Interestingly, it was shown (through proteomics and mutagenesis studies) that PorZ is itself a cargo of T9SS and has the conserved C-terminal domain (CTD) (Glew et al., 2014; Lasica et al., 2016). The CTD works as a signal, directing T9SS cargo proteins to the OM translocon (see the next section; Shoji et al., 2011). However, unlike other cargos, the CTD of PorZ is not cleaved off upon secretion and the protein is not anchored in the OM in the same manner as other secreted proteins (Lasica et al., 2016). This phenomenon was observed for only one other protein, PorU, which is also both a functionally essential element and a cargo of T9SS (Glew et al., 2012). PorZ is currently the sole Por protein with a solved atomic structure. It is composed of two large β-propeller domains and a CTD, conforming to canonical β-sandwich architecture (de Diego et al., 2016; Lasica et al., 2016). Although the precise role of PorZ remains to be revealed, β-propeller domains are a good platform for protein-protein interactions and provide binding areas for small molecules (e.g., saccharides; Hunt et al., 1987; Zhang et al., 2014). Considering the structure and processing, we hypothesize that, like PorU, PorZ may be involved in post-translational maturation of T9SS cargo proteins during their translocation across the OM.

## MECHANISM OF SECRETION

Protein secretion using T9SS is a two-step process. First, the cargo proteins are guided by a classical signal peptide to the Sec machinery in the IM. During translocation, the signal peptide is cleaved off by type I signal peptidase, and the cargo is released into the periplasm. Although, the Sec pathway has not been experimentally analyzed in *P. gingivalis*, the screening of *Bacteroidetes* genomes confirmed that the system is mostly conserved (McBride and Zhu, 2013). In the periplasm, transported proteins fold into a stable conformation, as indicated from the accumulation of their soluble forms in the periplasm of T9SS secretory mutants. Whether the cargo proteins require a chaperone(s) to assist in folding and/or guiding them to the OM translocon is still unknown.

A common feature of all T9SS cargo proteins is the conserved CTD that targets T9SS cargo proteins to the OM translocon. The function of the CTD was first recognized while studying the secretion and processing of the RgpB (PG0506/PGN_1466) gingipain. The protein without the C-terminal Ig-like domain of 72 amino acid residues was not secreted, but accumulated in the periplasm of the mutated *P. gingivalis* strain in its truncated form (Seers et al., 2006). A parallel study confirmed this observation, showing that the integrity of the CTD is essential for RgpB secretion, as even truncating the C-terminal by two residues hinders transport across the OM. The same effect is caused by mutating the highly conserved residues at the C-terminus of the CTD (Nguyen et al., 2007). The elegant follow-up investigations with CTDs from different *P. gingivalis* T9SS cargo proteins (HBP35/PG0616/PGN_0659, CPG70/PG0232/PGN_0335, P27/PG1795/no PGN, and RgpB) genetically fused to GFP found that GFP was secreted and post-translationally modified by *P. gingivalis* in the same way as the native T9SS cargos. The secretion/modification signal was narrowed down to the last 22 residues of the CTD domain (Shoji et al., 2011), and proteomic analysis revealed cleaved CTDs in the culture medium (Veith et al., 2013).

Taken together, these findings suggested the existence of a C-terminal-sorting peptidase responsible for the proteolytic removal of the CTD during the cargos' translocation across the OM. The postulated sortase was identified in *P. gingivalis* as PorU, a surface-located cysteine peptidase that shares significant sequence similarity with gingipains (see previous section; Glew et al., 2012). Analysis of the cleavage sites of T9SS cargos in *P. gingivalis* revealed a PorU preference toward polar or acidic amino acid residues (Ser, Thr, Asn, Asp) at the carbonyl site (P1′ position) and small amino acid residues (such as Gly, Ser, Ala) at the amide site (P1 position; Glew et al., 2012; Veith et al., 2013). This low specificity of PorU was confirmed when the amino acids surrounding the cleavage site (P1–P1′) in RgpB were mutated. Of note, this did not affect the secretion of the gingipain (Zhou et al., 2013).

### Secretion Signal for T9SS Substrates Is Embedded in the Secondary Structure

Bioinformatic analysis of 21 fully sequenced genomes from the *Bacteroidetes* phylum revealed the presence of 663 predicted CTD-containing proteins (Veith et al., 2013). Alignment of the amino acid sequence of identified CTDs revealed up to five conserved sequential motifs (A–E) in different T9SS cargo proteins (Seers et al., 2006; Nguyen et al., 2007; Slakeski et al., 2011). Out of these, two sequential motifs, PxGxYVV and KxxxK, that reside in the last 22 amino acids of CTDs are the most conserved. This conservation is consistent with this fragment being sufficient for secretion in *P. gingivalis* (Shoji et al., 2011; Veith et al., 2013). Cumulatively, however, the limited sequence identity of CTDs suggests that the signal recognized by the T9SS machinery is not imprinted in the amino acid sequence but is formed by a specific fold of the CTD. This contention was confirmed by the atomic structure of the CTD from two *P. gingivalis* T9SS cargo proteins: RgpB and PorZ (de Diego et al., 2016; Lasica et al., 2016). Their CTDs consist of seven β-strands of similar length, generating a compact, sandwich-like fold typical of an immunoglobulin-superfamily (IgSF) domain. Analysis of the CTD of RgpB revealed a propensity of the protein to dimerize by swapping the last β-strand (de Diego et al., 2016). Of note, the last two β-strands overlap perfectly with the 22 amino acid residues essential for secretion of CTD proteins (Shoji et al., 2011). Despite the differences within the loops and the low amino acid sequence similarity, the PorZ-derived CTD structure is topologically equivalent to that of RgpB. This conclusion likely extends to the majority of identified CTDs, which share the fold of the IgSF domain. Therefore, the tertiary structure of the CTD, especially its two terminal β-strands, likely contains the signal recognized by the T9SS translocon (Lasica et al., 2016).

### Secretion-Associated Modifications of T9SS Cargo Proteins

The characteristic feature of T9SS function is the retention of cargo proteins on the bacterial surface. SDS-PAGE analysis of OM-associated proteins produced diffuse bands about 20 kDa larger than that predicted from the primary structure of T9SS-secreted proteins (Veith et al., 2002). The difference is due to the presence of an A-LPS (Paramonov et al., 2005; Rangarajan et al., 2008) covalently attached to the cargo proteins imbedded into the OM, as indicated by western blot using specific antibodies (Abs). By contrast, the molecular mass of proteins accumulating in the periplasm of secretion mutants correlates well with the predicted molecular mass, and the proteins have no reactivity with anti-A-LPS Abs (Shoji et al., 2014). In addition, electron microscopy revealed that CTD-containing proteins (especially gingipains) form the electron-dense surface layer (EDSL) encapsulating *P. gingivalis* cells (Chen et al., 2011). Gorasia et al. (2015) found that the *wbaP* (PG1964/PGN_1896) mutant of *P. gingivalis*, which is defective in A-LPS synthesis, completely lacks the EDSL and releases T9SS cargos in soluble form into culture fluid. The proteins lack CTDs, suggesting normal PorU sortase activity, but are not A-LPS modified and therefore cannot be incorporated into the OM (Gorasia et al., 2015).

The mechanism of A-LPS attachment to CTD-containing proteins during secretion by T9SS is still unknown. The analysis of CTD proteins isolated from the growth media of the *wbaP* mutant revealed that peptides/amino acids derived from growth medium or glycine (if added in excess to the broth) were added to the proteins' C-termini via peptide bond. On the other hand, a 648 Da linker attached to C-termini by an isopeptide bond was identified in CTDs derived from the wild-type *P. gingivalis* strain (Gorasia et al., 2015). Such modification is reminiscent of a sortase-like mechanism of protein binding to peptidoglycan in Gram-positive bacteria. Sortases are cysteine proteases (C60 family) that have a catalytic Cys/His dyad, characteristic for many cysteine proteases, and possess a conserved Arg residue essential for sorting activity (Marraffini et al., 2004). This Arg is absent in gingipains, but is found in PorU sortase (Gorasia et al., 2015). All these findings suggest that PorU is a sortase, the first identified among Gram-negative bacteria. It cleaves the CTD and simultaneously attaches the A-LPS moiety to the newly generated C-terminus of a cargo protein via a linker of unknown structure. In this context, the T9SS mechanism resembles the covalent attachment of proteins to the cell wall in Gram-positive bacteria such as *S. aureus* (Schneewind and Missiakas, 2012).

## REGULATION

Essential T9SS genes, including *porT*, *porV*, *sov*, *porP*, *porK*, *porL*, *porM*, and *porN*, are regulated at the transcriptional level by a signaling pathway composed of the PorXY two-component system (TCS) and an extracytoplasmic function (ECF) sigma factor (SigP/PG0162/PGN_0274; Kadowaki et al., 2016). In contrast to the majority of TCSs, in which the components are encoded within the same operon, the *porX* and *porY* genes occur at separate loci within the *P. gingivalis* chromosome. Despite this unusual genomic organization, the activation of the PorXY TCS is canonical. PorY has a modular architecture typical for a histidine kinase (HK) and undergoes autophosphorylation at His193, as shown by radiolabeled [$^{32}$P-$\gamma$]ATP. The phosphate group is then transferred to the conserved Asp58 residue in the receiver domain of PorX, which functions as the response regulator (RR). To compensate for the lack of a DNA-binding domain in the RR, PorX interacts with SigP, which directly binds the promotor regions of T9SS genes. The SigP protein level is very low in the *porX*-deletion mutant, suggesting a stabilizing function for PorX on SigP (Kadowaki et al., 2016). Disruption of the PorXY TCS results in the dysfunction of T9SS, which manifests as the decrease of Rgp and Kgp activity, as well as the impaired processing of gingipains (Sato et al., 2010).

PorX can also modulate the T9SS architecture directly by interacting with the cytoplasmic domain of PorL (Vincent et al., 2016). The N-terminal domain of PorX is similar to RRs belonging to the CheY family, which are involved in chemotaxis. After phosphorylation, the CheY protein binds to the C-ring of flagella, which changes the direction of flagellar movement (Roman et al., 1992; Sagi et al., 2003). Due to the fact that T9SS was proposed to be a rotary apparatus enabling the rotary movement of SprB adhesin in gliding bacteria (Shrivastava et al., 2015), it has been speculated that the PorX mechanism might be similar to that of CheY (Vincent et al., 2016). However, its role in *P. gingivalis* cells will likely be different as this bacterium is non-motile.

There are other studies reporting the changes in a T9SS protein's expression profile under specific circumstances. In a PorZ-deletion strain, some of the T9SS genes (including *porT*, *porV*, and *porN*), together with genes encoding CTD-cargo peptidases (RgpB, Kgp, and CPG70), are upregulated, whereas the expression of other T9SS genes (such as *porQ*, *porW*, *sov*, and *porU*) is not changed (Lasica et al., 2016). Additionally, the gliding motility protein GldN (orthologous of *P. gingivalis* PorN) of *Flavobacterium psychrophilum* is significantly upregulated under iron-limited growth conditions and *in vivo* (LaFrentz et al., 2009). The expression of T9SS proteins must be strictly regulated to fine-tune the energy-absorbing secretion of proteins into the environment. However, a precise environmental signal has not been identified and our knowledge about T9SS regulation is still limited.

## PROTEIN EFFECTORS IN *P. gingivalis*

Only a few secretion systems are dedicated to carrying a single cargo protein; examples are HlyA in *E. coli* and HasA in *S. marcescens* for T1SS (Kanonenberg et al., 2013), and PulA in *K. oxytoca* and LT toxin in *E. coli* for T2SS (Rondelet and Condemine, 2013). The majority of secretion systems translocate many proteins of similar or diverse functions [e.g., T3SS; Gaytan et al., 2016]. In many respects, T9SS is one of the most robust secretion systems, which, in *P. gingivalis* alone, facilitates secretion of up to 35 cargos bearing the CTD (see **Table 2**), many of which are implicated in bacterial pathogenicity. In fact, experiments conducted to characterize the important virulence factors (the gingipains RgpA, RgpB, and Kgp) contributed to

**TABLE 2 | T9SS cargo proteins.**

| *Porphyromonas gingivalis*[a] | | | | | |
|---|---|---|---|---|---|
| Locus Tag | | | | | |
| **W83 NC_002950.2** | | **ATCC33277 NC_010729.1** | **Protein accession number** | **Protein description** | **References** |
| PG_RS00120 | PG0026 | PGN_0022 | WP_005874469.1 | PorU; surface C-terminal sortase | Glew et al., 2012; Veith et al., 2013; Gorasia et al., 2015 |
| PG_RS00835 | PG0182 | PGN_0291 | WP_010955943.1 | Mfa5; VWA domain-containing protein [von Willebrand factor (vWF) type A domain] | Hasegawa et al., 2016 |
| PG_RS00840 | PG0183 | no PGN | WP_043876389.1 | Hypothetical protein containing VWA domain identical to that in PG0182 (circa 430 residues); lipoprotein | Found only by proteomic analysis[a] |
| PG_RS01060 | PG0232 | PGN_0335 | WP_005873522.1 | CPG70; zinc carboxypeptidase | Veith et al., 2004; Shoji et al., 2011; Zhou et al., 2013 |
| PG_RS01560 | PG0350 | PGN_1611 | WP_005873799.1 | Internalin; hypothetical protein; leucine-rich repeats (x8) | Found only by proteomic analysis[a] |
| PG_RS01820 | PG0410 | no PGN | WP_005873803.1 | Hypothetical gingipain-like peptidase C25 | |
| PG_RS01825 | PG0411 | PGN_1556 | WP_010956006.1 | T9SS C-terminal target domain-containing protein | Found only by proteomic analysis[a] |
| PG_RS02195 | PG0495 | PGN_1476 | WP_010956042.1 | T9SS C-terminal target domain-containing protein | Found only by proteomic analysis[a] |
| PG_RS02240 | PG0506 | PGN_1466 | WP_010956050.1 | RgpB; arginine specific gingipain B, cysteine protease | Pike et al., 1994; Seers et al., 2006; Guo et al., 2010; de Diego et al., 2016 |
| PG_RS02455 | PG0553 | PGN_1416 | WP_010956068.1 | PepK; lysine specific serine endopeptidase | Sato et al., 2013; Nonaka et al., 2014; Veith et al., 2014 |
| PG_RS02700 | PG0611 | PGN_0654 | WP_043876409.1 | Hypothetical protein | Found only by proteomic analysis[a] |
| PG_RS02710 | PG0614 | PGN_0657 | WP_005874506.1 | Hypothetical protein | Found only by proteomic analysis[a] |
| PG_RS02720 | PG0616 | PGN_0659 | WP_005874521.1 | HBP35 (hemin binding protein 35) | Shoji et al., 2010, 2011 |
| PG_RS02765 | PG0626 | no PGN | WP_005874512.1 | T9SS C-terminal target domain-containing protein | Found only by proteomic analysis[a] |
| PG_RS02890 | PG0654 | PGN_0693 | WP_005873571.1 | T9SS C-terminal target domain-containing protein | Found only by proteomic analysis[a]; Glew et al., 2012 |
| PG_RS03370 | PG0769 | PGN_0795 | WP_010956121.1 | Fibronectin; hypothetical protein[b] | Found only by proteomic analysis[a]; Sato et al., 2013 |
| PG_RS03450 | PG0787 | PGN_0810 | WP_005873930.1 | T9SS C-terminal target domain-containing protein[c] | Found only by proteomic analysis[a] |
| PG_RS04535 | PG1030 | PGN_1321 | WP_005874101.1 | T9SS C-terminal target domain-containing protein | Found only by proteomic analysis[a] |
| PG_RS05835 | PG1326 | PGN_1115 | WP_005875446.1 | Hemagglutinin | Found only by proteomic analysis[a] |
| PG_RS06055 | PG1374 | PGN_0852 | WP_005874331.1 | T9SS C-terminal target domain-containing protein, leucine-rich repeats (x7) | Found only by proteomic analysis[a]; Glew et al., 2012 |
| PG_RS06255 | PG1424 | PGN_0898 | WP_005873463.1 | PPAD; peptidylarginine deiminase | Sato et al., 2013; Koziel et al., 2014; Goulas et al., 2015 |
| PG_RS06260 | PG1427 | PGN_0900 | WP_005873781.1 | Periodontain; peptidase C10; PrtT-related | Nelson et al., 1999 |
| PG_RS06835 | PG1548 | PGN_0561 | WP_043876505.1 | PrtT; cystein protease (domain peptidase C10) | Madden et al., 1995; Gorasia et al., 2015 |
| PG_RS07070 | PG1604 | PGN_0509 | WP_010956350.1 | PorZ; surface B-propeller protein | Lasica et al., 2016 |
| PG_RS07920 | PG1795 | PGN_1770 | WP_005874140.1 | Hypothetical protein | Found only by proteomic analysis[a] |
| PG_RS07930 | PG1798 | PGN_1767 | WP_005874135.1 | T9SS C-terminal target domain-containing protein | Found only by proteomic analysis[a] |
| PG_RS08090 | PG1837 | PGN_1733 | WP_043876452.1 | HagA (hemagglutinin A, 8 HA domains) | Shi et al., 1999; Glew et al., 2012; Saiki and Konishi, 2014 |
| PG_RS08105 | PG1844 | PGN_1728 | WP_043876454.1 | Kgp; lysine specific gingipain, cysteine protease | Pike et al., 1994; Veith et al., 2002 |
| PG_RS08700 | PG1969[d] | no PGN | WP_010956456.1 | T9SS C-terminal target domain-containing protein | Found only by proteomic analysis[a] |
| PG_RS08940 | PG2024 | PGN_1970 | WP_010956476.1 | RgpA; arginine specific gingipain A; cysteine protease | Pike et al., 1994; Veith et al., 2002; Glew et al., 2012 |
| PG_RS09310 | PG2100 | no PGN | WP_005873768.1 | T9SS C-terminal target domain-containing protein; TapC | Kondo et al., 2010; Sato et al., 2013 |
| PG_RS09320 | PG2102 | PGN_0152 | WP_005873754.1 | T9SS C-terminal target domain-containing protein; TapA | Kondo et al., 2010; Glew et al., 2012; Sato et al., 2013 |
| PG_RS09640 | PG2172 | PGN_0123 | WP_005874973.1 | Hypothetical protein | Found only by proteomic analysis[a]; Glew et al., 2012 |
| PG_RS09755 | PG2198 | PGN_2065 | WP_005874281.1 | Hypothetical protein; peptidase | Found only by proteomic analysis[a] |

*(Continued)*

**TABLE 2 | Continued**

| *Porphyromonas gingivalis*[a] | | | | | |
|---|---|---|---|---|---|
| Locus Tag | | | | | |
| **W83 NC_002950.2** | | **ATCC33277 NC_010729.1** | **Protein accession number** | **Protein description** | **References** |
| PG_RS09850 | PG2216 | PGN_2080 | WP_010956525.1 | Hypothetical protein | Found only by proteomic analysis[a]; Glew et al., 2012 |
| ***Tannerella forsythia* ATCC43037** | | | | | |
| Tanf_03370 | | | WP_046824918.1 | TfsA (surface layer protein A), classical CTD | Tomek et al., 2014 |
| Tanf_03375 | | | WP_046824919.1 | TfsB (surface layer protein B), classical CTD | Tomek et al., 2014 |
| Tanf_04820 | | | WP_046825062.1 | BspA, cell surface antigen, leucine rich protein, classical CTD | Veith et al., 2009; Friedrich et al., 2015 |
| Tanf_06225 | | | WP_046825275.1 | Forsilysin, metalloprotease, KLIKK-type CTD | Narita et al., 2014 |
| Tanf_00450 | | | WP_070098098.1 | Mirolysin, metalloprotease, KLIKK-type CTD | Karim et al., 2010; Ksiazek et al., 2015a,b; Koneru et al., 2017 |
| Tanf_06550 | | | D0EM77.2 | Karilysin, metalloprotease, KLIKK-type CTD | Karim et al., 2010; Narita et al., 2014; Ksiazek et al., 2015a; Koneru et al., 2017 |
| Tanf_00440 | | | AIZ49398.1 | Mirolase, serine protease, KLIKK-type CTD | Karim et al., 2010; Ksiazek et al., 2015a,b; Koneru et al., 2017 |
| Tanf_09450, Tanf_06530 (not merged in one contig) | | | AKG97061.1 | Miropsin-1, serine protease, KLIKK-type CTD | Ksiazek et al., 2015b |
| Tanf_06530 | | | WP_046825306.1 | Miropsin-2, serine protease KLIKK-type CTD | Narita et al., 2014 |
| ***F. johnsoniae* UW101[e]** | | | | | |
| Fjoh_4555 | | | WP_012026520.1 | ChiA, chitinase | Rhodes et al., 2010; Kharade and McBride, 2014 |
| Fjoh_0979 | | | WP_012023065.1 | SprB, surface adhesin, necessary for gliding motility | Rhodes et al., 2010; Shrivastava et al., 2013 |
| Fjoh_0808 | | | WP_052295174.1 | RemA, mobile surface adhesin, necessary for gliding motility | Shrivastava et al., 2012, 2013 |

[a] *All P. gingivalis cargo proteins excluding PG0410 (no PGN) and PG1548 (PGN_0561) were originally found by Veith et al. (2013).*
[b] *PG0769 (PGN_0795) processing is unclear. Protein is devoid of N-terminal cleavage signal for periplasm transport (searched with SignalP and LipoP servers) as well as T9SS CTD domain.*
[c] *PG0787 (PGN_0810) is a very small peptide (80 aa) devoid of N-terminal cleavage signal for periplasm transport (searched in SignalP and LipoP servers), however its last 66 aa constitute a classical T9SS CTD domain.*
[d] *PG1969 processing is unclear. Protein is devoid of N-terminal cleavage signal for periplasm transport (searched with SignalP and LipoP servers) but contains T9SS CTD domain.*
[e] *Proteins listed are the best studied among other identified T9SS cargos of F. johnsoniae. For more information please see Kharade and McBride (2015).*

the discovery of T9SS. Below, we briefly describe only the most important cargos from the point of view of *P. gingivalis* virulence. References to other cargo proteins can be found in **Table 2**.

## Gingipains and CPG70

There are three enzymes collectively termed gingipains: RgpA (PG2024/PGN_1970), RgpB (PG0506/PGN_1466), and Kgp (PG1844/PGN_1728). They are cysteine proteases that hydrolyze peptide bonds at the carboxyl group of arginine (RgpA/B: Arg–Xaa) or lysine residues (Kgp: Lys–Xaa; Pike et al., 1994). They are exported into the periplasm as inactive zymogens, with the N-terminal prodomain (NTP) functioning as a chaperone and maintaining the latency of the proteases (Mikolajczyk et al., 2003; Pomowski et al., 2017). After folding in the periplasm, they are transported to the bacterial surface, where they are subjected to extensive post-translational processing. The CTD is cleaved by PorU sortase during translocation, with the concomitant covalent attachment of A-LPS via an isopeptide bond to the newly formed carbonyl group (Glew et al., 2012; Gorasia et al., 2015). Then, the OM-anchored gingipains activate themselves by cleaving off the NTP. For RgpB, this is the end of processing, but the polypeptide chains of RgpA and Kgp are further fragmented to form a large, non-covalent complex of catalytic and hemagglutinin domains on the bacterial surface (Bhogal et al., 1997; Veith et al., 2002; Sztukowska et al., 2012). The activation and further processing are still not well-understood, and, in addition to trans- and cis-autoproteolysis, they also involve the removal of the C-terminal Arg and Lys residues by the Arg/Lys-specific carboxypeptidase CPG70 (PG0232/PGN_0335; Chen et al., 2002). Interestingly, CPG70 is a T9SS substrate itself (Veith et al., 2004; Zhou et al., 2013). Of note, the retention of gingipains, CPG70, and other T9SS cargos on the bacterial surface depends on the synthesis of A-LPS. The *P. gingivalis* strain HG66, which lacks the activity of an enzyme in the A-LPS synthesis pathway, secretes soluble gingipains into the media (Pike et al., 1994; Shoji et al., 2014; Siddiqui et al., 2014).

Gingipains are the most powerful weapon within the *P. gingivalis* arsenal of virulence factors, as they are responsible for nearly 85% of the total proteolytic activity (Potempa et al.,

1997). They are responsible for a variety of pathogenic functions such as colonization, nutrition, neutralization of host defenses, and alteration of the inflammatory response, which all lead to massive oral tissue destruction called periodontitis during prolonged infection (reviewed in Guo et al., 2010; Bostanci and Belibasakis, 2012; Hajishengallis, 2015). However, gingipains are not only directed against host proteins, but are also involved in processing other *P. gingivalis* proteins [e.g., long fimbriae (FimA)] (Nakayama et al., 1996; Xu et al., 2016). Interestingly, gingipains' activities rely on their local concentration, resulting in either activation of some pathways at low concentrations (specifically human complement) or destroying them upon accumulation (Krauss et al., 2010). Moreover, despite the cleavage specificity to a single C-terminal Arg or Lys residue, they can act in a precise and fastidious manner or as unlimited shredders (Potempa et al., 2000; Sroka et al., 2001; Goulet et al., 2004).

Considering the broad range of activities combined with cell surface localization, it is not surprising that gingipains are a tempting target for designing periodontitis treatments as well as preventive strategies (inhibitors and vaccines; Olsen and Potempa, 2014; Inaba et al., 2016; Wilensky et al., 2016).

## Porphyromonas Peptidylarginine Deiminase (PPAD)

Porphyromonas peptidylarginine deiminase (PPAD), encoded by PG1424/PGN_0898, is a unique enzyme among prokaryotes. It is the first and only bacterial peptidylarginine deiminase (PAD) identified, and, moreover, its presence is limited to a single species: *P. gingivalis* (McGraw et al., 1999; Gabarrini et al., 2015).

PADs are well-described eukaryotic enzymes functioning in vertebrates as post-translational modifiers of proteins. Specifically, they citrullinate internal arginine residues, which changes the fold, function, and half-life of proteins and peptides (Vossenaar et al., 2003; Gyorgy et al., 2006). Dysregulation of this process, particularly the accumulation of citrullinated proteins, leads to inflammatory disorders and has been associated with numerous diseases such as Alzheimer's disease, multiple sclerosis, psoriasis, fibrosis, cancer, and rheumatoid arthritis (RA) (Vossenaar et al., 2003; Chang and Han, 2006; Baka et al., 2012; Gudmann et al., 2015). The latter develops through an autoimmune response against citrullinated proteins and is enhanced by a combination of environmental and genetic factors (MacGregor et al., 2000; McInnes and Schett, 2011). Currently, periodontal disease is an acknowledged RA risk factor, and the discovery of PPAD uncovered a missing mechanistic link between the two illnesses (Wegner et al., 2010; Koziel et al., 2014; Quirke et al., 2015; Laugisch et al., 2016).

PPAD was identified as a T9SS substrate through proteomics studies of a *porT* mutant (Sato et al., 2013); however, the enzyme was characterized mostly in relation to its function rather than secretion. It citrullinates C-terminal arginine residues in a calcium-independent manner, whereas eukaryotic PADs are $Ca^{2+}$-dependent (Takahara et al., 1986; McGraw et al., 1999; Abdallah et al., 2007; Wegner et al., 2010; Bielecka et al., 2014). Moreover, the C-terminal specificity of PPAD plays into the cleavage activities of RgpA/B (after Arg), which greatly enlarge the pool of citrullinated substrates from both bacterial and host origins as gingipains cleave numerous human proteins (Guo et al., 2010). Gingipain-null mutants (RgpA/B) are almost devoid of endogenous citrullination (Wegner et al., 2010). Furthermore, even the presence of PPAD (not only its activity) may elevate anti-citrullination immune responses, as it undergoes autocitrullination. Only this form triggers specific Abs in mice and was recognized by RA patients' sera (reviewed in Koziel et al., 2014).

Analysis of PPAD structure revealed that the enzyme is composed of four elements: a profragment, a catalytic domain (CD), an IgSF domain, and a CTD, resembling domains observed in gingipains. The CD has a flat 5-fold α/β-propeller architecture and includes a catalytic triad ($C^{351}$-$H^{236}$-$N^{297}$) also conserved in human PADs (Goulas et al., 2015; Montgomery et al., 2016). The crystal structure of substrate-free and substrate-bound forms confirmed that PPAD is efficient in accommodating and processing C-terminally situated Arg residues regardless of total chain length (peptide or protein; Goulas et al., 2015).

The surface location of PPAD and the availability of its detailed structure, combined with its important role in two prevalent human diseases (periodontitis and RA), should make PPAD a good target for therapeutic strategies; however, no such experiments have been reported.

## T9SS IN *T. forsythia*

The mechanism of protein secretion by T9SS was mostly studied in *P. gingivalis* and gliding bacteria. Apart from a different subset of secreted proteins reflecting bacterial habitats, the mechanism of action is the same. Briefly, T9SS cargo proteins are directed to the T9SS machinery by the CTD, which is removed during secretion. Then, secreted proteins may be modified and attached to the surface by A-LPS (*P. gingivalis*), stay associated with the cell through polysaccharides, or be released (gliding bacteria; McBride and Nakane, 2015; Nakayama, 2015). However, analysis of T9SS in another member of the red complex, *T. forsythia*, revealed some interesting differences.

*T. forsythia* is covered with a two-dimensional crystalline surface (S-) layer that is thought to function as a protective coat, working as an external sieve and ion trap (Sleytr and Beveridge, 1999; Messner et al., 2010). It also mediates adhesion and subsequent invasion into human gingival epithelial cells (Sakakibara et al., 2007) and delays recognition of the bacterium by the host innate immune system (Sekot et al., 2012). The S-layer is composed of the glycosylated proteins TfsA (Tanf_03370) and TfsB (Tanf_03375). Deleting *porU* (Tanf_02580), *porT* (Tanf_10520), *sov* (Tanf_04410), or *porK* (Tanf_02360) results in the lack of an S-layer, which can be observed by transmission electron microscope (Narita et al., 2014; Tomek et al., 2014). In those mutants, both components of the S-layer are trapped within the periplasm, but, unlike in *P. gingivalis*, they are modified by O-glycosylation through the addition of multiple copies of a complex oligosaccharide using a general glycosylation pathway operating in *Bacteroidetes* (Coyne et al., 2013; Posch et al., 2013;

Tomek et al., 2014). Nevertheless, TfsA and TfsB trapped in the periplasm are much smaller than both proteins in the wild-type cells, indicating that, upon secretion, both proteins are modified by a second glycan attachment in a manner different than O-glycosylation. It is speculated that, as in *P. gingivalis*, it could be a variant of LPS (Tomek et al., 2014).

T9SS cargo proteins in *T. forsythia* have two different types of CTD. The "classical" CTD associated with proteins from other *Bacteroidetes* species is found in TfsA, TfsB, and leucine rich protein BspA (Veith et al., 2009; Tomek et al., 2014). By contrast, a family of six proteases, three metalloproteases (karilysin, mirolysin, and forsilysin) and three serine proteases (mirolase, miropsin-1, and miropsin-2), bear a nearly identical CTD that shares very limited sequence similarity with the classical CTD. Because these six CTDs end with a KLIKK sequential motif, the enzymes are referred to as KLIKK proteases (Ksiazek et al., 2015b). The KLIKK proteases possess a unique structure and undergo extensive autoproteolytic processing (Cerda-Costa et al., 2011; Lopez-Pelegrin et al., 2015). Their activities, such as degrading complement proteins and LL-37 (the crucial antimicrobial peptide in the human oral cavity), may contribute to *T. forsythia* virulence through evading innate immunity (Jusko et al., 2015; Koneru et al., 2017).

In stark contrast to the other CTD proteins of *T. forsythia*, KLIKK proteases seem to be secreted directly into the extracellular medium, as shown for miropsin-2 (Tanf_06530), karilysin (Tanf_06550), and forsilysin (Tanf_06225) (Narita et al., 2014). Supporting this, proteomic analysis of the *T. forsythia* OM identified 13 of 26 proteins bearing the classical CTD, including TfsA, TfsB, and BspA (Tanf_04820), but none of the KLIKK proteases (Veith et al., 2009). Conversely, four KLIKK proteases, forsilysin, miropsin-2 (Friedrich et al., 2015), mirolase (Tanf_00440), and karilysin (Veith et al., 2015), were found in outer membrane vesicles (OMVs), although with a low Mascot score. This discrepancy could be explained by the transient presence of these proteases in the periplasm before they enter the OM translocon of T9SS. Interestingly, all three of the KLIKK proteases characterized thus far (karilysin, mirolase, and mirolysin) can remove the CTD during autoprocessing (Karim et al., 2010; Ksiazek et al., 2015a; Koneru et al., 2017). Collectively, the available data suggest that the KLIKK proteases are secreted into the extracellular milieu without removal of the CTD. This finding is similar to the secretion of PorU and PorZ from *P. gingivalis*, where the CTD is also not removed during secretion, although proteins stay associated with the cell surface (Lasica et al., 2016).

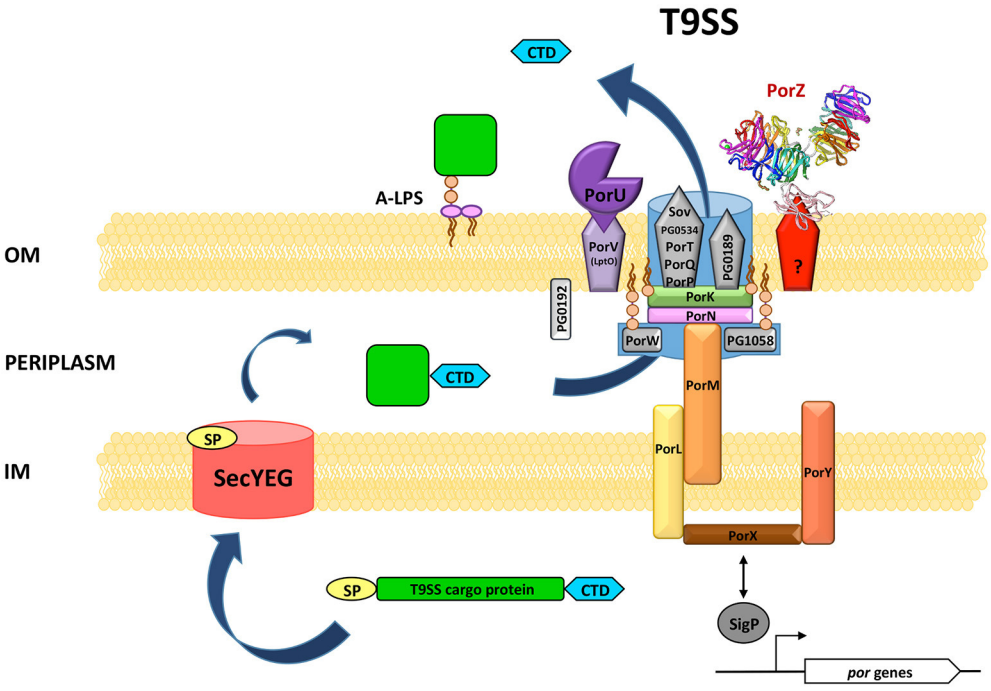


**FIGURE 3 | Hypothetical model of the structure and function of *P. gingivalis* T9SS.** The overall translocon structure and the protein(s) forming a pore in the OM (outer membrane) have not yet been characterized. Therefore, it is shown as a background blue shape accommodating known components. Interacting proteins are situated in close proximity. OM β-barrel proteins are depicted as pentagons. PorZ is presently the only T9SS protein with the known atomic structure. The mode of its association with the translocon is not yet defined. PorK, PorW, and PG1058 are lipoproteins anchored into the inner surface of the OM. PG0192 protein precise localization and possible interactions are not known. A T9SS cargo protein is equipped with two sorting signals: N-terminal signal peptide (SP) directing the protein to the general secretion system SecYEG and conserved C-terminal domain (CTD) recognized by T9SS. After translocation through the IM (inner membrane) most proteins acquire their proper fold in the periplasm. Next, CTD directs the protein for further translocation across the OM through T9SS. Finally, CTD is cleaved off by PorU sortase and a secreted protein is modified by attachment of A-LPS resulting in the anchorage of cargo protein to the cell surface. Two component system PorX/PorY and sigma factor SigP have regulatory effect on *por* genes. Although, they are not physical elements of T9SS, PorX was shown *in vitro* to interact with PorL.

## CONCLUDING REMARKS

In this review, we summarized the biochemical and structural data concerning the recently discovered T9SS identified in a majority of the bacterial species belonging to the *Bacteroidetes* phylum (Sato et al., 2010; McBride and Zhu, 2013). The system has been investigated predominantly in human oral pathogens, such as *P. gingivalis* and *T. forsythia*, and environmental saprophytes, such as *F. johnsoniae* and *C. hutchinsonii*. It seems to be a major mechanism of protein secretion in these bacteria however, some families from *Bacteroidetes* were reported to possess other secretion systems e.g., T1SS or T6SS (Russell et al., 2014; Wilson et al., 2015; Abby et al., 2016; Chatzidaki-Livanis et al., 2016; Wexler et al., 2016; Ibrahim et al., 2017). Notably, both systems allow for direct substrate translocation from bacterial cytoplasm to the cell exterior, while T9SS cargos do not omit the periplasmic space during their secretion.

The role of T9SS is to ensure cell survival and fitness in response to the microorganisms' habitat by providing transportation of proteins necessary for, among other things, virulence, nutrition, and movement (gliding motility). Hence, the variety of secreted proteins even within a single species is large and comprises numerous adhesins and hydrolytic enzymes used for attachment and degradation of large organic compounds such as proteins, cellulose, and chitin (Guo et al., 2010; McBride and Nakane, 2015).

The cargo proteins of this system (**Table 2**) are equipped with the classical signal peptide for Sec-dependent translocation to the IM and the conserved CTD that directs them further to the secretion machinery in the OM. The recognition signal is mostly embedded within the IgSF-like tertiary structure of the CTD (de Diego et al., 2016; Lasica et al., 2016) and likely located within the 22 amino acid residues composing the sequential motifs of PxGxYVV and KxxxK in the two most C-terminal β-strands (Shoji et al., 2011; Veith et al., 2013).

Currently, for *P. gingivalis* cells, there are 16 proteins recognized as the structural and/or functional components of the translocon and two additional elements involved in T9SS regulation (**Table 1**). None of these proteins are fully characterized, so their structure, mode of reciprocal interactions, and precise roles in secretion are still obscure. Nevertheless, a contemporary general concept of T9SS structure and function based on available data is presented in **Figure 3**. Verification of this model requires extensive structural and functional investigations to elucidate the mechanism of CTD recognition and cleavage, passage of cargos though the OM translocon, attachment of a glucan moiety, and anchoring of cargos onto the cell surface, their release into the environment, or their assembly into gliding motility machinery.

## AUTHOR CONTRIBUTIONS

AL analyzed literature, wrote the paper (excluding MK and MM sections), prepared the figures and tables. MK wrote the Mechanism of secretion and T9SS *T. forsythia* sections. MM wrote the Regulation section. JP edited the manuscript. All authors read and approved the full manuscript.

## FUNDING

This work was supported by National Science Centre (NCN)—2012/04/A/NZ1/00051 to JP and UMO-2015/19/N/NZ1/00322 to MM; Polish Ministry of Science and Higher Education—1306/MOB/IV/2015/0 (Mobilnosc Plus) to MK and K/DSC/003690 to MM and National Institutes of Health (NIH)—DE 022597 to AL and JP.

## REFERENCES

Abaibou, H., Chen, Z., Olango, G. J., Liu, Y., Edwards, J., and Fletcher, H. M. (2001). vimA gene downstream of recA is involved in virulence modulation in *Porphyromonas gingivalis* W83. *Infect. Immun.* 69, 325–335. doi: 10.1128/IAI.69.1.325-335.2001

Abby, S. S., Cury, J., Guglielmini, J., Neron, B., Touchon, M., and Rocha, E. P. (2016). Identification of protein secretion systems in bacterial genomes. *Sci. Rep.* 6:23080. doi: 10.1038/srep23080

Abdallah, A. M., Gey van Pittius, N. C., Champion, P. A., Cox, J., Luirink, J., Vandenbroucke-Grauls, C. M., et al. (2007). Type VII secretion–mycobacteria show the way. *Nat. Rev. Microbiol.* 5, 883–891. doi: 10.1038/nrmicro1773

Baka, Z., Gyorgy, B., Geher, P., Buzas, E. I., Falus, A., and Nagy, G. (2012). Citrullination under physiological and pathological conditions. *Joint Bone Spine* 79, 431–436. doi: 10.1016/j.jbspin.2012.01.008

Benedyk, M., Mydel, P. M., Delaleu, N., Plaza, K., Gawron, K., Milewska, A., et al. (2016). Gingipains: critical factors in the development of aspiration pneumonia caused by *Porphyromonas gingivalis*. *J. Innate Immun.* 8, 185–198. doi: 10.1159/000441724

Berks, B. C. (2015). The twin-arginine protein translocation pathway. *Annu. Rev. Biochem.* 84, 843–864. doi: 10.1146/annurev-biochem-060614-034251

Bhogal, P. S., Slakeski, N., and Reynolds, E. C. (1997). A cell-associated protein complex of *Porphyromonas gingivalis* W50 composed of Arg- and Lys-specific cysteine proteinases and adhesins. *Microbiology* 143(Pt 7), 2485–2495. doi: 10.1099/00221287-143-7-2485

Bielecka, E., Scavenius, C., Kantyka, T., Jusko, M., Mizgalska, D., Szmigielski, B., et al. (2014). Peptidyl arginine deiminase from *Porphyromonas gingivalis* abolishes anaphylatoxin C5a activity. *J. Biol. Chem.* 289, 32481–32487. doi: 10.1074/jbc.C114.617142

Bostanci, N., and Belibasakis, G. N. (2012). *Porphyromonas gingivalis*: an invasive and evasive opportunistic oral pathogen. *FEMS Microbiol. Lett.* 333, 1–9. doi: 10.1111/j.1574-6968.2012.02579.x

Cerda-Costa, N., Guevara, T., Karim, A. Y., Ksiazek, M., Nguyen, K. A., Arolas, J. L., et al. (2011). The structure of the catalytic domain of *Tannerella forsythia* karilysin reveals it is a bacterial xenologue of animal matrix metalloproteinases. *Mol. Microbiol.* 79, 119–132. doi: 10.1111/j.1365-2958.2010.07434.x

Chang, X., and Han, J. (2006). Expression of peptidylarginine deiminase type 4 (PAD4) in various tumors. *Mol. Carcinog.* 45, 183–196. doi: 10.1002/mc.20169

Chatzidaki-Livanis, M., Geva-Zatorsky, N., and Comstock, L. E. (2016). Bacteroides fragilis type VI secretion systems use novel effector and immunity proteins to antagonize human gut Bacteroidales species. *Proc. Natl. Acad. Sci. U.S.A.* 113, 3627–3632. doi: 10.1073/pnas.1522510113

Chen, T., Dong, H., Yong, R., and Duncan, M. J. (2000). Pleiotropic pigmentation mutants of *Porphyromonas gingivalis*. *Microb. Pathog.* 28, 235–247. doi: 10.1006/mpat.1999.0338

Chen, Y. Y., Cross, K. J., Paolini, R. A., Fielding, J. E., Slakeski, N., and Reynolds, E. C. (2002). CPG70 is a novel basic metallocarboxypeptidase with C-terminal polycystic kidney disease domains from *Porphyromonas gingivalis*. *J. Biol. Chem.* 277, 23433–23440. doi: 10.1074/jbc.M200811200

Chen, Y. Y., Peng, B., Yang, Q., Glew, M. D., Veith, P. D., Cross, K. J., et al. (2011). The outer membrane protein LptO is essential for the O-deacylation of LPS and the co-ordinated secretion and attachment of A-LPS and CTD proteins in *Porphyromonas gingivalis*. *Mol. Microbiol.* 79, 1380–1401. doi: 10.1111/j.1365-2958.2010.07530.x

Cobessi, D., Celia, H., and Pattus, F. (2005). Crystal structure at high resolution of ferric-pyochelin and its membrane receptor FptA from *Pseudomonas aeruginosa*. *J. Mol. Biol.* 352, 893–904. doi: 10.1016/j.jmb.2005.08.004

Costa, T. R., Felisberto-Rodrigues, C., Meir, A., Prevost, M. S., Redzej, A., Trokter, M., et al. (2015). Secretion systems in Gram-negative bacteria: structural and mechanistic insights. *Nat. Rev. Microbiol.* 13, 343–359. doi: 10.1038/nrmicro3456

Coyne, M. J., Fletcher, C. M., Chatzidaki-Livanis, M., Posch, G., Schaffer, C., and Comstock, L. E. (2013). Phylum-wide general protein O-glycosylation system of the Bacteroidetes. *Mol. Microbiol.* 88, 772–783. doi: 10.1111/mmi.12220

Curtis, M. A., Kuramitsu, H. K., Lantz, M., Macrina, F. L., Nakayama, K., Potempa, J., et al. (1999). Molecular genetics and nomenclature of proteases of *Porphyromonas gingivalis*. *J. Periodont. Res.* 34, 464–472. doi: 10.1111/j.1600-0765.1999.tb02282.x

Dam, P., Olman, V., Harris, K., Su, Z., and Xu, Y. (2007). Operon prediction using both genome-specific and general genomic information. *Nucleic Acids Res.* 35, 288–298. doi: 10.1093/nar/gkl1018

de Diego, I., Ksiazek, M., Mizgalska, D., Koneru, L., Golik, P., Szmigielski, B., et al. (2016). The outer-membrane export signal of *Porphyromonas gingivalis* type IX secretion system (T9SS) is a conserved C-terminal β-sandwich domain. *Sci. Rep.* 6:23123. doi: 10.1038/srep23123

Denks, K., Vogt, A., Sachelaru, I., Petriman, N. A., Kudva, R., and Koch, H. G. (2014). The Sec translocon mediated protein transport in prokaryotes and eukaryotes. *Mol. Membr. Biol.* 31, 58–84. doi: 10.3109/09687688.2014.907455

Desvaux, M., Hebraud, M., Talon, R., and Henderson, I. R. (2009). Secretion and subcellular localizations of bacterial proteins: a semantic awareness issue. *Trends Microbiol.* 17, 139–145. doi: 10.1016/j.tim.2009.01.004

Friedrich, V., Gruber, C., Nimeth, I., Pabinger, S., Sekot, G., Posch, G., et al. (2015). Outer membrane vesicles of *Tannerella forsythia*: biogenesis, composition, and virulence. *Mol. Oral Microbiol.* 30, 451–473. doi: 10.1111/omi.12104

Gabarrini, G., de Smit, M., Westra, J., Brouwer, E., Vissink, A., Zhou, K., et al. (2015). The peptidylarginine deiminase gene is a conserved feature of *Porphyromonas gingivalis*. *Sci. Rep.* 5:13936. doi: 10.1038/srep13936

Gao, S., Li, S., Ma, Z., Liang, S., Shan, T., Zhang, M., et al. (2016). Presence of *Porphyromonas gingivalis* in esophagus and its association with the clinicopathological characteristics and survival in patients with esophageal cancer. *Infect. Agents Cancer* 11, 3. doi: 10.1186/s13027-016-0049-x

Gaytan, M. O., Martinez-Santos, V. I., Soto, E., and Gonzalez-Pedrajo, B. (2016). Type three secretion system in attaching and effacing pathogens. *Front. Cell. Infect. Microbiol.* 6:129. doi: 10.3389/fcimb.2016.00129

Genco, C. A., Simpson, W., Forng, R. Y., Egal, M., and Odusanya, B. M. (1995). Characterization of a Tn4351-generated hemin uptake mutant of *Porphyromonas gingivalis*: evidence for the coordinate regulation of virulence factors by hemin. *Infect. Immun.* 63, 2459–2466.

Gerlach, R. G., and Hensel, M. (2007). Protein secretion systems and adhesins: the molecular armory of Gram-negative pathogens. *Int. J. Med. Microbiol.* 297, 401–415. doi: 10.1016/j.ijmm.2007.03.017

Glew, M. D., Veith, P. D., Chen, D., Seers, C. A., Chen, Y. Y., and Reynolds, E. C. (2014). Blue native-PAGE analysis of membrane protein complexes in *Porphyromonas gingivalis*. *J. Proteomics* 110, 72–92. doi: 10.1016/j.jprot.2014.07.033

Glew, M. D., Veith, P. D., Peng, B., Chen, Y. Y., Gorasia, D. G., Yang, Q., et al. (2012). PG0026 is the C-terminal signal peptidase of a novel secretion system of *Porphyromonas gingivalis*. *J. Biol. Chem.* 287, 24605–24617. doi: 10.1074/jbc.M112.369223

Goebel, W., and Hedgpeth, J. (1982). Cloning and functional characterization of the plasmid-encoded hemolysin determinant of *Escherichia coli*. *J. Bacteriol.* 151, 1290–1298.

Gorasia, D. G., Veith, P. D., Chen, D., Seers, C. A., Mitchell, H. A., Chen, Y. Y., et al. (2015). *Porphyromonas gingivalis* Type IX Secretion substrates are cleaved and modified by a sortase-like mechanism. *PLoS Pathog.* 11:e1005152. doi: 10.1371/journal.ppat.1005152

Gorasia, D. G., Veith, P. D., Hanssen, E. G., Glew, M. D., Sato, K., Yukitake, H., et al. (2016). Structural insights into the PorK and PorN components of the *Porphyromonas gingivalis* Type IX secretion system. *PLoS Pathog.* 12:e1005820. doi: 10.1371/journal.ppat.1005820

Goulas, T., Mizgalska, D., Garcia-Ferrer, I., Kantyka, T., Guevara, T., Szmigielski, B., et al. (2015). Structure and mechanism of a bacterial host-protein citrullinating virulence factor, *Porphyromonas gingivalis* peptidylarginine deiminase. *Sci. Rep.* 5:11969. doi: 10.1038/srep11969

Goulet, V., Britigan, B., Nakayama, K., and Grenier, D. (2004). Cleavage of human transferrin by *Porphyromonas gingivalis* gingipains promotes growth and formation of hydroxyl radicals. *Infect. Immun.* 72, 4351–4356. doi: 10.1128/IAI.72.8.4351-4356.2004

Goyal, P., Krasteva, P. V., Van Gerven, N., Gubellini, F., Van den Broeck, I., Troupiotis-Tsailaki, A., et al. (2014). Structural and mechanistic insights into the bacterial amyloid secretion channel CsgG. *Nature* 516, 250–253. doi: 10.1038/nature13768

Gudmann, N. S., Hansen, N. U., Jensen, A. C., Karsdal, M. A., and Siebuhr, A. S. (2015). Biological relevance of citrullinations: diagnostic, prognostic and therapeutic options. *Autoimmunity* 48, 73–79. doi: 10.3109/08916934.2014.962024

Guo, Y., Nguyen, K. A., and Potempa, J. (2010). Dichotomy of gingipains action as virulence factors: from cleaving substrates with the precision of a surgeon's knife to a meat chopper-like brutal degradation of proteins. *Periodontol. 2000* 54, 15–44. doi: 10.1111/j.1600-0757.2010.00377.x

Gyorgy, B., Toth, E., Tarcsa, E., Falus, A., and Buzas, E. I. (2006). Citrullination: a posttranslational modification in health and disease. *Int. J. Biochem. Cell Biol.* 38, 1662–1677. doi: 10.1016/j.biocel.2006.03.008

Hachani, A., Wood, T. E., and Filloux, A. (2016). Type VI secretion and anti-host effectors. *Curr. Opin. Microbiol.* 29, 81–93. doi: 10.1016/j.mib.2015.11.006

Hajishengallis, G. (2015). Periodontitis: from microbial immune subversion to systemic inflammation. *Nat. Rev. Immunol.* 15, 30–44. doi: 10.1038/nri3785

Hasegawa, Y., Iijima, Y., Persson, K., Nagano, K., Yoshida, Y., Lamont, R. J., et al. (2016). Role of Mfa5 in expression of Mfa1 fimbriae in *Porphyromonas gingivalis*. *J. Dent. Res.* 95, 1291–1297. doi: 10.1177/0022034516655083

Heath, J. E., Seers, C. A., Veith, P. D., Butler, C. A., Nor Muhammad, N. A., Chen, Y. Y., et al. (2016). PG1058 is a novel multidomain protein component of the bacterial Type IX secretion system. *PLoS ONE* 11:e0164313. doi: 10.1371/journal.pone.0164313

Henke, J. M., and Bassler, B. L. (2004). Quorum sensing regulates type III secretion in *Vibrio harveyi* and *Vibrio parahaemolyticus*. *J. Bacteriol.* 186, 3794–3805. doi: 10.1128/JB.186.12.3794-3805.2004

Hoover, C. I., and Yoshimura, F. (1994). Transposon-induced pigment-deficient mutants of *Porphyromonas gingivalis*. *FEMS Microbiol. Lett.* 124, 43–48. doi: 10.1111/j.1574-6968.1994.tb07259.x

Hunt, L. T., Barker, W. C., and Chen, H. R. (1987). A domain structure common to hemopexin, vitronectin, interstitial collagenase, and a collagenase homolog. *Protein Seq. Data Anal.* 1, 21–26.

Hutcheon, G. W., and Bolhuis, A. (2003). The archaeal twin-arginine translocation pathway. *Biochem. Soc. Trans.* 31(Pt 3), 686–689. doi: 10.1042/bst0310686

Ibrahim, M., Subramanian, A., and Anishetty, S. (2017). Comparative pan genome analysis of oral *Prevotella* species implicated in periodontitis. *Funct. Integr. Genomics.* doi: 10.1007/s10142-017-0550-3. [Epub ahead of print]. Available online at: http://link.springer.com/journal/10142/onlineFirst/page/1

Inaba, H., Tagashira, M., Kanda, T., Murakami, Y., Amano, A., and Matsumoto-Nakano, M. (2016). Apple- and Hop-polyphenols inhibit *Porphyromonas gingivalis*-mediated precursor of matrix metalloproteinase-9 activation and invasion of oral squamous cell carcinoma cells. *J. Periodontol.* 87, 1103–1111. doi: 10.1902/jop.2016.160047

Ishiguro, I., Saiki, K., and Konishi, K. (2009). PG27 is a novel membrane protein essential for a *Porphyromonas gingivalis* protease secretion system. *FEMS Microbiol. Lett.* 292, 261–267. doi: 10.1111/j.1574-6968.2009.01489.x

Jarrell, K. F., and McBride, M. J. (2008). The surprisingly diverse ways that prokaryotes move. *Nat. Rev. Microbiol.* 6, 466–476. doi: 10.1038/nrmicro1900

Jusko, M., Potempa, J., Mizgalska, D., Bielecka, E., Ksiazek, M., Riesbeck, K., et al. (2015). A metalloproteinase mirolysin of tannerella forsythia inhibits all pathways of the complement system. *J. Immunol.* 195, 2231–2240. doi: 10.4049/jimmunol.1402892

Kadowaki, T., Yukitake, H., Naito, M., Sato, K., Kikuchi, Y., Kondo, Y., et al. (2016). A two-component system regulates gene expression of the type IX secretion component proteins via an ECF sigma factor. *Sci. Rep.* 6:23288. doi: 10.1038/srep23288

Kallberg, M., Wang, H., Wang, S., Peng, J., Wang, Z., Lu, H., et al. (2012). Template-based protein structure modeling using the RaptorX web server. *Nat. Protoc.* 7, 1511–1522. doi: 10.1038/nprot.2012.085

Kanonenberg, K., Schwarz, C. K., and Schmitt, L. (2013). Type I secretion systems - a story of appendices. *Res. Microbiol.* 164, 596–604. doi: 10.1016/j.resmic.2013.03.011

Karim, A. Y., Kulczycka, M., Kantyka, T., Dubin, G., Jabaiah, A., Daugherty, P. S., et al. (2010). A novel matrix metalloprotease-like enzyme (karilysin) of the periodontal pathogen *Tannerella forsythia* ATCC 43037. *Biol. Chem.* 391, 105–117. doi: 10.1515/bc.2010.009

Kebschull, M., Demmer, R. T., and Papapanou, P. N. (2010). "Gum bug, leave my heart alone!"–epidemiologic and mechanistic evidence linking periodontal infections and atherosclerosis. *J. Dent. Res.* 89, 879–902. doi: 10.1177/0022034510375281

Kharade, S. S., and McBride, M. J. (2014). *Flavobacterium johnsoniae* chitinase ChiA is required for chitin utilization and is secreted by the type IX secretion system. *J. Bacteriol.* 196, 961–970. doi: 10.1128/JB.01170-13

Kharade, S. S., and McBride, M. J. (2015). *Flavobacterium johnsoniae* PorV is required for secretion of a subset of proteins targeted to the type IX secretion system. *J. Bacteriol.* 197, 147–158. doi: 10.1128/JB.02085-14

Kondo, Y., Ohara, N., Sato, K., Yoshimura, M., Yukitake, H., Naito, M., et al. (2010). Tetratricopeptide repeat protein-associated proteins contribute to the virulence of *Porphyromonas gingivalis*. *Infect. Immun.* 78, 2846–2856. doi: 10.1128/IAI.01448-09

Koneru, L., Ksiazek, M., Waligorska, I., Straczek, A., Lukasik, M., Madej, M., et al. (2017). Mirolysin, a LysargiNase from *Tannerella forsythia*, proteolytically inactivates the human cathelicidin, LL-37. *Biol Chem.* 398, 395–409. doi: 10.1515/hsz-2016-0267

Koziel, J., Mydel, P., and Potempa, J. (2014). The link between periodontal disease and rheumatoid arthritis: an updated review. *Curr. Rheumatol. Rep.* 16, 408. doi: 10.1007/s11926-014-0408-9

Krauss, J. L., Potempa, J., Lambris, J. D., and Hajishengallis, G. (2010). Complementary Tolls in the periodontium: how periodontal bacteria modify complement and Toll-like receptor responses to prevail in the host. *Periodontol. 2000* 52, 141–162. doi: 10.1111/j.1600-0757.2009.00324.x

Ksiazek, M., Karim, A. Y., Bryzek, D., Enghild, J. J., Thogersen, I. B., Koziel, J., et al. (2015a). Mirolase, a novel subtilisin-like serine protease from the periodontopathogen *Tannerella forsythia*. *Biol. Chem.* 396, 261–275. doi: 10.1515/hsz-2014-0256

Ksiazek, M., Mizgalska, D., Eick, S., Thogersen, I. B., Enghild, J. J., and Potempa, J. (2015b). KLIKK proteases of *Tannerella forsythia*: putative virulence factors with a unique domain structure. *Front. Microbiol.* 6:312. doi: 10.3389/fmicb.2015.00312

LaFrentz, B. R., LaPatra, S. E., Call, D. R., Wiens, G. D., and Cain, K. D. (2009). Proteomic analysis of *Flavobacterium psychrophilum* cultured *in vivo* and in iron-limited media. *Dis. Aquat. Org.* 87, 171–182. doi: 10.3354/dao02122

Lasica, A. M., Goulas, T., Mizgalska, D., Zhou, X., de Diego, I., Ksiazek, M., et al. (2016). Structural and functional probing of PorZ, an essential bacterial surface component of the type-IX secretion system of human oral-microbiomic *Porphyromonas gingivalis*. *Sci. Rep.* 6:37708. doi: 10.1038/srep37708

Laugisch, O., Wong, A., Sroka, A., Kantyka, T., Koziel, J., Neuhaus, K., et al. (2016). Citrullination in the periodontium–a possible link between periodontitis and rheumatoid arthritis. *Clin. Oral Investig.* 20, 675–683. doi: 10.1007/s00784-015-1556-7

Letoffe, S., Ghigo, J. M., and Wandersman, C. (1994). Secretion of the *Serratia marcescens* HasA protein by an ABC transporter. *J. Bacteriol.* 176, 5372–5377. doi: 10.1128/jb.176.17.5372-5377.1994

Lopez-Pelegrin, M., Ksiazek, M., Karim, A. Y., Guevara, T., Arolas, J. L., Potempa, J., et al. (2015). A novel mechanism of latency in matrix metalloproteinases. *J. Biol. Chem.* 290, 4728–4740. doi: 10.1074/jbc.M114.605956

MacGregor, A. J., Snieder, H., Rigby, A. S., Koskenvuo, M., Kaprio, J., Aho, K., et al. (2000). Characterizing the quantitative genetic contribution to rheumatoid arthritis using data from twins. *Arthritis Rheum* 43, 30–37. doi: 10.1002/1529-0131(200001)43:1<30::AID-ANR5>3.0.CO;2-B

Madden, T. E., Clark, V. L., and Kuramitsu, H. K. (1995). Revised sequence of the *Porphyromonas gingivalis* prtT cysteine protease/hemagglutinin gene: homology with streptococcal pyrogenic exotoxin B/streptococcal proteinase. *Infect. Immun.* 63, 238–247.

Majerczyk, C., Schneider, E., and Greenberg, E. P. (2016). Quorum sensing control of Type VI secretion factors restricts the proliferation of quorum-sensing mutants. *Elife* 5:e14712. doi: 10.7554/eLife.14712

Mao, F., Dam, P., Chou, J., Olman, V., and Xu, Y. (2009). DOOR: a database for prokaryotic operons. *Nucleic Acids Res.* 37, D459–D463. doi: 10.1093/nar/gkn757

Marraffini, L. A., Ton-That, H., Zong, Y., Narayana, S. V., and Schneewind, O. (2004). Anchoring of surface proteins to the cell wall of *Staphylococcus aureus*. A conserved arginine residue is required for efficient catalysis of sortase A. *J. Biol. Chem.* 279, 37763–37770. doi: 10.1074/jbc.M405282200

McBride, M. J., and Nakane, D. (2015). Flavobacterium gliding motility and the type IX secretion system. *Curr. Opin. Microbiol.* 28, 72–77. doi: 10.1016/j.mib.2015.07.016

McBride, M. J., and Zhu, Y. (2013). Gliding motility and Por secretion system genes are widespread among members of the phylum bacteroidetes. *J. Bacteriol.* 195, 270–278. doi: 10.1128/JB.01962-12

McGraw, W. T., Potempa, J., Farley, D., and Travis, J. (1999). Purification, characterization, and sequence analysis of a potential virulence factor from *Porphyromonas gingivalis*, peptidylarginine deiminase. *Infect. Immun.* 67, 3248–3256.

McInnes, I. B., and Schett, G. (2011). The pathogenesis of rheumatoid arthritis. *N. Engl. J. Med.* 365, 2205–2219. doi: 10.1056/NEJMra1004965

McKee, A. S., McDermid, A. S., Wait, R., Baskerville, A., and Marsh, P. D. (1988). Isolation of colonial variants of Bacteroides gingivalis W50 with a reduced virulence. *J. Med. Microbiol.* 27, 59–64. doi: 10.1099/00222615-27-1-59

Messner, P., Schaffer, C., Egelseer, E. M., and Sleytr, U. B. (2010). "Occurrence, structure, chemistry, genetics, morphogenesis, and functions of s-layers," in *Prokaryotic Cell Wall Compounds, Structure and Biochemistry*, eds H. König, H. Claus, and A. Varma (Berlin: Springer-Verlag), 53–109.

Mikolajczyk, J., Boatright, K. M., Stennicke, H. R., Nazif, T., Potempa, J., Bogyo, M., et al. (2003). Sequential autolytic processing activates the zymogen of Arg-gingipain. *J. Biol. Chem.* 278, 10458–10464. doi: 10.1074/jbc.M210564200

Montgomery, A. B., Kopec, J., Shrestha, L., Thezenas, M. L., Burgess-Brown, N. A., Fischer, R., et al. (2016). Crystal structure of *Porphyromonas gingivalis* peptidylarginine deiminase: implications for autoimmunity in rheumatoid arthritis. *Ann. Rheum. Dis.* 75, 1255–1261. doi: 10.1136/annrheumdis-2015-207656

Nakane, D., Sato, K., Wada, H., McBride, M. J., and Nakayama, K. (2013). Helical flow of surface protein required for bacterial gliding motility. *Proc. Natl. Acad. Sci. U.S.A.* 110, 11145–11150. doi: 10.1073/pnas.1219753110

Nakayama, K. (2015). *Porphyromonas gingivalis* and related bacteria: from colonial pigmentation to the type IX secretion system and gliding motility. *J. Periodont. Res.* 50, 1–8. doi: 10.1111/jre.12255

Nakayama, K., Yoshimura, F., Kadowaki, T., and Yamamoto, K. (1996). Involvement of arginine-specific cysteine proteinase (Arg-gingipain) in fimbriation of *Porphyromonas gingivalis*. *J. Bacteriol.* 178, 2818–2824. doi: 10.1128/jb.178.10.2818-2824.1996

Narita, Y., Sato, K., Yukitake, H., Shoji, M., Nakane, D., Nagano, K., et al. (2014). Lack of a surface layer in *Tannerella forsythia* mutants deficient in the type IX secretion system. *Microbiology* 160(Pt 10), 2295–2303. doi: 10.1099/mic.0.080192-0

Nelson, D., Potempa, J., Kordula, T., and Travis, J. (1999). Purification and characterization of a novel cysteine proteinase (periodontain) from Porphyromonas gingivalis. Evidence for a role in the inactivation of human alpha1-proteinase inhibitor. *J. Biol. Chem.* 274, 12245–12251. doi: 10.1074/jbc.274.18.12245

Nelson, K. E., Fleischmann, R. D., DeBoy, R. T., Paulsen, I. T., Fouts, D. E., Eisen, J. A., et al. (2003). Complete genome sequence of the oral pathogenic Bacterium *porphyromonas gingivalis* strain W83. *J. Bacteriol.* 185, 5591–5601. doi: 10.1128/JB.185.18.5591-5601.2003

Nguyen, K. A., Travis, J., and Potempa, J. (2007). Does the importance of the C-terminal residues in the maturation of RgpB from *Porphyromonas gingivalis*

reveal a novel mechanism for protein export in a subgroup of Gram-Negative bacteria? *J. Bacteriol.* 189, 833–843. doi: 10.1128/JB.01530-06

Nguyen, K. A., Zylicz, J., Szczesny, P., Sroka, A., Hunter, N., and Potempa, J. (2009). Verification of a topology model of PorT as an integral outer-membrane protein in *Porphyromonas gingivalis*. *Microbiology* 155(Pt 2), 328–337. doi: 10.1099/mic.0.024323-0

Nonaka, M., Shoji, M., Kadowaki, T., Sato, K., Yukitake, H., Naito, M., et al. (2014). Analysis of a Lys-specific serine endopeptidase secreted via the type IX secretion system in *Porphyromonas gingivalis*. *FEMS Microbiol. Lett.* 354, 60–68. doi: 10.1111/1574-6968.12426

Okamoto, K., Nakayama, K., Kadowaki, T., Abe, N., Ratnayake, D. B., and Yamamoto, K. (1998). Involvement of a lysine-specific cysteine proteinase in hemoglobin adsorption and heme accumulation by *Porphyromonas gingivalis*. *J. Biol. Chem.* 273, 21225–21231. doi: 10.1074/jbc.273.33.21225

Olsen, I., and Potempa, J. (2014). Strategies for the inhibition of gingipains for the potential treatment of periodontitis and associated systemic diseases. *J. Oral Microbiol.* 6:24800. doi: 10.3402/jom.v6.24800

Paramonov, N., Rangarajan, M., Hashim, A., Gallagher, A., Aduse-Opoku, J., Slaney, J. M., et al. (2005). Structural analysis of a novel anionic polysaccharide from *Porphyromonas gingivalis* strain W50 related to Arg-gingipain glycans. *Mol. Microbiol.* 58, 847–863. doi: 10.1111/j.1365-2958.2005.04871.x

Park, Y., Yilmaz, O., Jung, I. Y., and Lamont, R. J. (2004). Identification of *Porphyromonas gingivalis* genes specifically expressed in human gingival epithelial cells by using differential display reverse transcription-PCR. *Infect. Immun.* 72, 3752–3758. doi: 10.1128/IAI.72.7.3752-3758.2004

Pavloff, N., Potempa, J., Pike, R. N., Prochazka, V., Kiefer, M. C., Travis, J., et al. (1995). Molecular cloning and structural characterization of the Arg-gingipain proteinase of *Porphyromonas gingivalis*. Biosynthesis as a proteinase-adhesin polyprotein. *J. Biol. Chem.* 270, 1007–1010. doi: 10.1074/jbc.270.3.1007

Pertea, M., Ayanbule, K., Smedinghoff, M., and Salzberg, S. L. (2009). OperonDB: a comprehensive database of predicted operons in microbial genomes. *Nucleic Acids Res.* 37, D479–D482. doi: 10.1093/nar/gkn784

Pike, R., McGraw, W., Potempa, J., and Travis, J. (1994). Lysine- and arginine-specific proteinases from *Porphyromonas gingivalis*. Isolation, characterization, and evidence for the existence of complexes with hemagglutinins. *J. Biol. Chem.* 269, 406–411.

Pomowski, A., Uson, I., Nowakowska, Z. M., Veillard, F., Sztukowska, M. N., Guevara, T., et al. (2017). Structural insights unravel the zymogenic mechanism of the virulence factor gingipain K from *Porphyromonas gingivalis*, a causative agent of gum disease from the human oral microbiome. *J. Biol. Chem.* 292, 5724–5735. doi: 10.1074/jbc.M117.776724

Posch, G., Andrukhov, O., Vinogradov, E., Lindner, B., Messner, P., Holst, O., et al. (2013). Structure and immunogenicity of the rough-type lipopolysaccharide from the periodontal pathogen *Tannerella forsythia*. *Clin. Vaccine Immunol.* 20, 945–953. doi: 10.1128/CVI.00139-13

Potempa, J., Banbula, A., and Travis, J. (2000). Role of bacterial proteinases in matrix destruction and modulation of host responses. *Periodontol. 2000* 24, 153–192. doi: 10.1034/j.1600-0757.2000.2240108.x

Potempa, J., Pike, R., and Travis, J. (1997). Titration and mapping of the active site of cysteine proteinases from *Porphyromonas gingivalis* (gingipains) using peptidyl chloromethanes. *Biol. Chem.* 378, 223–230. doi: 10.1515/bchm.1997.378.3-4.223

Potempa, J., Sroka, A., Imamura, T., and Travis, J. (2003). Gingipains, the major cysteine proteinases and virulence factors of *Porphyromonas gingivalis*: structure, function and assembly of multidomain protein complexes. *Curr. Protein Pept. Sci.* 4, 397–407. doi: 10.2174/1389203033487036

Quirke, A. M., Lundberg, K., Potempa, J., Mikuls, T. R., and Venables, P. J. (2015). PPAD remains a credible candidate for inducing autoimmunity in rheumatoid arthritis: comment on the article by Konig et al. *Ann. Rheum. Dis.* 74, e7. doi: 10.1136/annrheumdis-2014-206665

Rangarajan, M., Aduse-Opoku, J., Paramonov, N., Hashim, A., Bostanci, N., Fraser, O. P., et al. (2008). Identification of a second lipopolysaccharide in *Porphyromonas gingivalis* W50. *J. Bacteriol.* 190, 2920–2932. doi: 10.1128/JB.01868-07

Rangarajan, M., Smith, S. J., Sally, U., and Curtis, M. A. (1997). Biochemical characterization of the arginine-specific proteases of *Porphyromonas gingivalis* W50 suggests a common precursor. *Biochem. J.* 323(Pt 3), 701–709. doi: 10.1042/bj3230701

Remaut, H., Tang, C., Henderson, N. S., Pinkner, J. S., Wang, T., Hultgren, S. J., et al. (2008). Fiber formation across the bacterial outer membrane by the chaperone/usher pathway. *Cell* 133, 640–652. doi: 10.1016/j.cell.2008.03.033

Rhodes, R. G., Samarasam, M. N., Shrivastava, A., van Baaren, J. M., Pochiraju, S., Bollampalli, S., et al. (2010). *Flavobacterium johnsoniae* gldN and gldO are partially redundant genes required for gliding motility and surface localization of SprB. *J. Bacteriol.* 192, 1201–1211. doi: 10.1128/JB.01495-09

Rhodes, R. G., Samarasam, M. N., Van Groll, E. J., and McBride, M. J. (2011). Mutations in *Flavobacterium johnsoniae* sprE result in defects in gliding motility and protein secretion. *J. Bacteriol.* 193, 5322–5327. doi: 10.1128/JB.05480-11

Roman, S. J., Meyers, M., Volz, K., and Matsumura, P. (1992). A chemotactic signaling surface on CheY defined by suppressors of flagellar switch mutations. *J. Bacteriol.* 174, 6247–6255. doi: 10.1128/jb.174.19.6247-6255.1992

Rondelet, A., and Condemine, G. (2013). Type II secretion: the substrates that won't go away. *Res. Microbiol.* 164, 556–561. doi: 10.1016/j.resmic.2013.03.005

Russell, A. B., Wexler, A. G., Harding, B. N., Whitney, J. C., Bohn, A. J., Goo, Y. A., et al. (2014). A type VI secretion-related pathway in Bacteroidetes mediates interbacterial antagonism. *Cell Host Microbe* 16, 227–236. doi: 10.1016/j.chom.2014.07.007

Sagi, Y., Khan, S., and Eisenbach, M. (2003). Binding of the chemotaxis response regulator CheY to the isolated, intact switch complex of the bacterial flagellar motor: lack of cooperativity. *J. Biol. Chem.* 278, 25867–25871. doi: 10.1074/jbc.M303201200

Saier, M. H. Jr., and Reddy, B. L. (2015). Holins in bacteria, eukaryotes, and archaea: multifunctional xenologues with potential biotechnological and biomedical applications. *J. Bacteriol.* 197, 7–17. doi: 10.1128/JB.02046-14

Saiki, K., and Konishi, K. (2007). Identification of a *Porphyromonas gingivalis* novel protein sov required for the secretion of gingipains. *Microbiol. Immunol.* 51, 483–491. doi: 10.1111/j.1348-0421.2007.tb03936.x

Saiki, K., and Konishi, K. (2010a). Identification of a novel *Porphyromonas gingivalis* outer membrane protein, PG534, required for the production of active gingipains. *FEMS Microbiol. Lett.* 310, 168–174. doi: 10.1111/j.1574-6968.2010.02059.x

Saiki, K., and Konishi, K. (2010b). The role of Sov protein in the secretion of gingipain protease virulence factors of *Porphyromonas gingivalis*. *FEMS Microbiol. Lett.* 302, 166–174. doi: 10.1111/j.1574-6968.2009.01848.x

Saiki, K., and Konishi, K. (2014). *Porphyromonas gingivalis* C-terminal signal peptidase PG0026 and HagA interact with outer membrane protein PG27/LptO. *Mol. Oral Microbiol.* 29, 32–44. doi: 10.1111/omi.12043

Sakakibara, J., Nagano, K., Murakami, Y., Higuchi, N., Nakamura, H., Shimozato, K., et al. (2007). Loss of adherence ability to human gingival epithelial cells in S-layer protein-deficient mutants of *Tannerella forsythensis*. *Microbiology* 153(Pt 3), 866–876. doi: 10.1099/mic.0.29275-0

Sato, K., Naito, M., Yukitake, H., Hirakawa, H., Shoji, M., McBride, M. J., et al. (2010). A protein secretion system linked to bacteroidete gliding motility and pathogenesis. *Proc. Natl. Acad. Sci. U.S.A.* 107, 276–281. doi: 10.1073/pnas.0912010107

Sato, K., Sakai, E., Veith, P. D., Shoji, M., Kikuchi, Y., Yukitake, H., et al. (2005). Identification of a new membrane-associated protein that influences transport/maturation of gingipains and adhesins of *Porphyromonas gingivalis*. *J. Biol. Chem.* 280, 8668–8677. doi: 10.1074/jbc.M413544200

Sato, K., Yukitake, H., Narita, Y., Shoji, M., Naito, M., and Nakayama, K. (2013). Identification of *Porphyromonas gingivalis* proteins secreted by the Por secretion system. *FEMS Microbiol. Lett.* 338, 68–76. doi: 10.1111/1574-6968.12028

Schneewind, O., and Missiakas, D. M. (2012). Protein secretion and surface display in Gram-positive bacteria. *Philos. Trans. R. Soc. Lond. B Biol. Sci.* 367, 1123–1139. doi: 10.1098/rstb.2011.0210

Seers, C. A., Slakeski, N., Veith, P. D., Nikolof, T., Chen, Y. Y., Dashper, S. G., et al. (2006). The RgpB C-terminal domain has a role in attachment of RgpB to the outer membrane and belongs to a novel C-terminal-domain family found in *Porphyromonas gingivalis*. *J. Bacteriol.* 188, 6376–6386. doi: 10.1128/JB.00731-06

Sekot, G., Posch, G., Oh, Y. J., Zayni, S., Mayer, H. F., Pum, D., et al. (2012). Analysis of the cell surface layer ultrastructure of the oral pathogen *Tannerella forsythia*. *Arch. Microbiol.* 194, 525–539. doi: 10.1007/s00203-012-0792-3

Shah, H. N., Seddon, S. V., and Gharbia, S. E. (1989). Studies on the virulence properties and metabolism of pleiotropic mutants of *Porphyromonas gingivalis* (Bacteroides gingivalis) W50. *Oral Microbiol. Immunol.* 4, 19–23. doi: 10.1111/j.1399-302X.1989.tb00401.x

Shi, Y., Ratnayake, D. B., Okamoto, K., Abe, N., Yamamoto, K., and Nakayama, K. (1999). Genetic analyses of proteolysis, hemoglobin binding, and hemagglutination of *Porphyromonas gingivalis*. Construction of mutants with a combination of rgpA, rgpB, kgp, and hagA. *J. Biol. Chem.* 274, 17955–17960. doi: 10.1074/jbc.274.25.17955

Shoji, M., and Nakayama, K. (2016). Glycobiology of the oral pathogen *Porphyromonas gingivalis* and related species. *Microb. Pathog.* 94, 35–41. doi: 10.1016/j.micpath.2015.09.012

Shoji, M., Ratnayake, D. B., Shi, Y., Kadowaki, T., Yamamoto, K., Yoshimura, F., et al. (2002). Construction and characterization of a nonpigmented mutant of *Porphyromonas gingivalis*: cell surface polysaccharide as an anchorage for gingipains. *Microbiology* 148(Pt 4), 1183–1191. doi: 10.1099/00221287-148-4-1183

Shoji, M., Sato, K., Yukitake, H., Kondo, Y., Narita, Y., Kadowaki, T., et al. (2011). Por secretion system-dependent secretion and glycosylation of *Porphyromonas gingivalis* hemin-binding protein 35. *PLoS ONE* 6:e21372. doi: 10.1371/journal.pone.0021372

Shoji, M., Sato, K., Yukitake, H., Naito, M., and Nakayama, K. (2014). Involvement of the Wbp pathway in the biosynthesis of *Porphyromonas gingivalis* lipopolysaccharide with anionic polysaccharide. *Sci. Rep.* 4:5056. doi: 10.1038/srep05056

Shoji, M., Shibata, Y., Shiroza, T., Yukitake, H., Peng, B., Chen, Y. Y., et al. (2010). Characterization of hemin-binding protein 35 (HBP35) in *Porphyromonas gingivalis*: its cellular distribution, thioredoxin activity and role in heme utilization. *BMC Microbiol.* 10:152. doi: 10.1186/1471-2180-10-152

Shrivastava, A., Johnston, J. J., van Baaren, J. M., and McBride, M. J. (2013). *Flavobacterium johnsoniae* GldK, GldL, GldM, and SprA are required for secretion of the cell surface gliding motility adhesins SprB and RemA. *J. Bacteriol.* 195, 3201–3212. doi: 10.1128/JB.00333-13

Shrivastava, A., Lele, P. P., and Berg, H. C. (2015). A rotary motor drives Flavobacterium gliding. *Curr. Biol.* 25, 338–341. doi: 10.1016/j.cub.2014.11.045

Shrivastava, A., Rhodes, R. G., Pochiraju, S., Nakane, D., and McBride, M. J. (2012). *Flavobacterium johnsoniae* RemA is a mobile cell surface lectin involved in gliding. *J. Bacteriol.* 194, 3678–3688. doi: 10.1128/JB.00588-12

Siddiqui, H., Yoder-Himes, D. R., Mizgalska, D., Nguyen, K. A., Potempa, J., and Olsen, I. (2014). Genome sequence of *Porphyromonas gingivalis* strain HG66 (DSM 28984). *Genome Announc.* 2:e00947-14. doi: 10.1128/genomeA.00947-14

Simpson, W., Wang, C. Y., Mikolajczyk-Pawlinska, J., Potempa, J., Travis, J., Bond, V. C., et al. (1999). Transposition of the endogenous insertion sequence element IS1126 modulates gingipain expression in *Porphyromonas gingivalis*. *Infect. Immun.* 67, 5012–5020.

Slakeski, N., Seers, C. A., Ng, K., Moore, C., Cleal, S. M., Veith, P. D., et al. (2011). C-terminal domain residues important for secretion and attachment of RgpB in *Porphyromonas gingivalis*. *J. Bacteriol.* 193, 132–142. doi: 10.1128/JB.00773-10

Sleytr, U. B., and Beveridge, T. J. (1999). Bacterial S-layers. *Trends Microbiol.* 7, 253–260. doi: 10.1016/S0966-842X(99)01513-9

Smalley, J. W., Silver, J., Marsh, P. J., and Birss, A. J. (1998). The periodontopathogen *Porphyromonas gingivalis* binds iron protoporphyrin IX in the mu-oxo dimeric form: an oxidative buffer and possible pathogenic mechanism. *Biochem. J.* 331(Pt 3), 681–685. doi: 10.1042/bj3310681

Snel, B., Lehmann, G., Bork, P., and Huynen, M. A. (2000). STRING: a web-server to retrieve and display the repeatedly occurring neighbourhood of a gene. *Nucleic Acids Res.* 28, 3442–3444. doi: 10.1093/nar/28.18.3442

Sroka, A., Sztukowska, M., Potempa, J., Travis, J., and Genco, C. A. (2001). Degradation of host heme proteins by lysine- and arginine-specific cysteine proteinases (gingipains) of *Porphyromonas gingivalis*. *J. Bacteriol.* 183, 5609–5616. doi: 10.1128/JB.183.19.5609-5616.2001

Stanier, R. Y. (1942). The cytophaga group: a contribution to the biology of myxobacteria. *Bacteriol. Rev.* 6, 143–196.

Stanier, R. Y. (1947). Studies on nonfruiting myxobacteria; Cytophaga johnsonae, n. sp., a chitindecomposing myxobacterium. *J. Bacteriol.* 53, 297–315.

Stathopulos, J., Cambillau, C., Cascales, E., Roussel, A., and Leone, P. (2015). Crystallization and preliminary X-ray analysis of the C-terminal fragment of PorM, a subunit of the *Porphyromonas gingivalis* type IX secretion system. *Acta Crystallogr. F. Struct. Biol. Commun.* 71(Pt 1), 71–74. doi: 10.1107/S2053230X1402559X

Sztukowska, M., Veillard, F., Potempa, B., Bogyo, M., Enghild, J. J., Thogersen, I. B., et al. (2012). Disruption of gingipain oligomerization into non-covalent cell-surface attached complexes. *Biol. Chem.* 393, 971–977. doi: 10.1515/hsz-2012-0175

Taboada, B., Ciria, R., Martinez-Guerrero, C. E., and Merino, E. (2012). ProOpDB: prokaryotic operon database. *Nucleic Acids Res.* 40, D627–D631. doi: 10.1093/nar/gkr1020

Taguchi, Y., Sato, K., Yukitake, H., Inoue, T., Nakayama, M., Naito, M., et al. (2015). Involvement of an Skp-Like Protein, PGN_0300, in the type IX secretion system of *Porphyromonas gingivalis*. *Infect. Immun.* 84, 230–240. doi: 10.1128/IAI.01308-15

Takahara, H., Okamoto, H., and Sugawara, K. (1986). Calcium-dependent properties of peptidylarginine deiminase from rabbit skeletal muscle *Agric. Biol. Chem.* 50, 2899–2904.

Tomek, M. B., Neumann, L., Nimeth, I., Koerdt, A., Andesner, P., Messner, P., et al. (2014). The S-layer proteins of *Tannerella forsythia* are secreted via a type IX secretion system that is decoupled from protein O-glycosylation. *Mol. Oral Microbiol.* 29, 307–320. doi: 10.1111/omi.12062

Veith, P. D., Chen, Y. Y., Chen, D., O'Brien-Simpson, N. M., Cecil, J. D., Holden, J. A., et al. (2015). *Tannerella forsythia* outer membrane vesicles are enriched with substrates of the type IX secretion system and tonb-dependent receptors. *J. Proteome Res.* 14, 5355–5366. doi: 10.1021/acs.jproteome.5b00878

Veith, P. D., Chen, Y. Y., Gorasia, D. G., Chen, D., Glew, M. D., O'Brien-Simpson, N. M., et al. (2014). *Porphyromonas gingivalis* outer membrane vesicles exclusively contain outer membrane and periplasmic proteins and carry a cargo enriched with virulence factors. *J. Proteome Res.* 13, 2420–2432. doi: 10.1021/pr401227e

Veith, P. D., Chen, Y. Y., and Reynolds, E. C. (2004). *Porphyromonas gingivalis* RgpA and Kgp proteinases and adhesins are C terminally processed by the carboxypeptidase CPG70. *Infect. Immun.* 72, 3655–3657. doi: 10.1128/IAI.72.6.3655-3657.2004

Veith, P. D., Nor Muhammad, N. A., Dashper, S. G., Likic, V. A., Gorasia, D. G., Chen, D., et al. (2013). Protein substrates of a novel secretion system are numerous in the Bacteroidetes phylum and have in common a cleavable C-terminal secretion signal, extensive post-translational modification, and cell-surface attachment. *J. Proteome Res.* 12, 4449–4461. doi: 10.1021/pr400487b

Veith, P. D., O'Brien-Simpson, N. M., Tan, Y., Djatmiko, D. C., Dashper, S. G., and Reynolds, E. C. (2009). Outer membrane proteome and antigens of *Tannerella forsythia*. *J. Proteome Res.* 8, 4279–4292. doi: 10.1021/pr900372c

Veith, P. D., Talbo, G. H., Slakeski, N., Dashper, S. G., Moore, C., Paolini, R. A., et al. (2002). Major outer membrane proteins and proteolytic processing of RgpA and Kgp of *Porphyromonas gingivalis* W50. *Biochem. J.* 363(Pt 1), 105–115. doi: 10.1042/bj3630105

Vincent, M. S., Canestrari, M. J., Leone, P., Stathopoulos, J., Ize, B., Zoued, A., et al. (2017). Characterization of the *Porphyromonas gingivalis* type IX secretion trans-envelope PorKLMNP core complex. *J. Biol. Chem.* 292, 3252–3261. doi: 10.1074/jbc.M116.765081

Vincent, M. S., Durand, E., and Cascales, E. (2016). The PorX response regulator of the *Porphyromonas gingivalis* PorXY two-component system does not directly regulate the type IX secretion genes but binds the PorL subunit. *Front. Cell. Infect. Microbiol.* 6:96. doi: 10.3389/fcimb.2016.00096

Vossenaar, E. R., Zendman, A. J., van Venrooij, W. J., and Pruijn, G. J. (2003). PAD, a growing family of citrullinating enzymes: genes, features and involvement in disease. *Bioessays* 25, 1106–1118. doi: 10.1002/bies.10357

Wegner, N., Wait, R., Sroka, A., Eick, S., Nguyen, K. A., Lundberg, K., et al. (2010). Peptidylarginine deiminase from *Porphyromonas gingivalis* citrullinates human fibrinogen and alpha-enolase: implications for autoimmunity in rheumatoid arthritis. *Arthritis Rheum.* 62, 2662–2672. doi: 10.1002/art.27552

Wexler, A. G., Bao, Y., Whitney, J. C., Bobay, L. M., Xavier, J. B., Schofield, W. B., et al. (2016). Human symbionts inject and neutralize antibacterial toxins to persist in the gut. *Proc. Natl. Acad. Sci. U.S.A.* 113, 3639–3644. doi: 10.1073/pnas.1525637113

Whitmore, S. E., and Lamont, R. J. (2014). Oral bacteria and cancer. *PLoS Pathog.* 10:e1003933. doi: 10.1371/journal.ppat.1003933

Wilensky, A., Potempa, J., Houri-Haddad, Y., and Shapira, L. (2016). Vaccination with recombinant RgpA peptide protects against *Porphyromonas gingivalis*-induced bone loss. *J. Periodontal. Res.* 52, 285–291. doi: 10.1111/jre.12393

Wilson, M. M., Anderson, D. E., and Bernstein, H. D. (2015). Analysis of the outer membrane proteome and secretome of *Bacteroides fragilis* reveals a multiplicity of secretion mechanisms. *PLoS ONE* 10:e0117732. doi: 10.1371/journal.pone.0117732

Xu, Q., Shoji, M., Shibata, S., Naito, M., Sato, K., Elsliger, M. A., et al. (2016). A distinct type of pilus from the human microbiome. *Cell* 165, 690–703. doi: 10.1016/j.cell.2016.03.016

Yang, T., Bu, X., Han, Q., Wang, X., Zhou, H., Chen, G., et al. (2016). A small periplasmic protein essential for *Cytophaga hutchinsonii* cellulose digestion. *Appl. Microbiol. Biotechnol.* 100, 1935–1944. doi: 10.1007/s00253-015-7204-y

Yoshimura, M., Ohara, N., Kondo, Y., Shoji, M., Okano, S., Nakano, Y., et al. (2008). Proteome analysis of *Porphyromonas gingivalis* cells placed in a subcutaneous chamber of mice. *Oral Microbiol. Immunol.* 23, 413–418. doi: 10.1111/j.1399-302X.2008.00444.x

Zhang, Z., Liu, Q., and Hendrickson, W. A. (2014). Crystal structures of apparent saccharide sensors from histidine kinase receptors prevalent in a human gut symbiont. *FEBS J.* 281, 4263–4279. doi: 10.1111/febs.12904

Zhou, X. Y., Gao, J. L., Hunter, N., Potempa, J., and Nguyen, K. A. (2013). Sequence-independent processing site of the C-terminal domain (CTD) influences maturation of the RgpB protease from *Porphyromonas gingivalis*. *Mol. Microbiol.* 89, 903–917. doi: 10.1111/mmi.12319

Zhu, Y., and McBride, M. J. (2014). Deletion of the *Cytophaga hutchinsonii* type IX secretion system gene sprP results in defects in gliding motility and cellulose utilization. *Appl. Microbiol. Biotechnol.* 98, 763–775. doi: 10.1007/s00253-013-5355-2

**Conflict of Interest Statement:** The authors declare that the research was conducted in the absence of any commercial or financial relationships that could be construed as a potential conflict of interest.

frontiers in Cellular and Infection Microbiology

REVIEW
published: 29 May 2017
doi: 10.3389/fcimb.2017.00220

# Super-Resolution Imaging of Protein Secretion Systems and the Cell Surface of Gram-Negative Bacteria

*Sachith D. Gunasinghe[1], Chaille T. Webb[1], Kirstin D. Elgass[2], Iain D. Hay[1] and Trevor Lithgow[1]**

[1] Infection and Immunity Program, Department of Microbiology, Biomedicine Discovery Institute, Monash University, Clayton, VIC, Australia, [2] Monash Micro Imaging, Monash University, Clayton, VIC, Australia

Gram-negative bacteria have a highly evolved cell wall with two membranes composed of complex arrays of integral and peripheral proteins, as well as phospholipids and glycolipids. In order to sense changes in, respond to, and exploit their environmental niches, bacteria rely on structures assembled into or onto the outer membrane. Protein secretion across the cell wall is a key process in virulence and other fundamental aspects of bacterial cell biology. The final stage of protein secretion in Gram-negative bacteria, translocation across the outer membrane, is energetically challenging so sophisticated nanomachines have evolved to meet this challenge. Advances in fluorescence microscopy now allow for the direct visualization of the protein secretion process, detailing the dynamics of (i) outer membrane biogenesis and the assembly of protein secretion systems into the outer membrane, (ii) the spatial distribution of these and other membrane proteins on the bacterial cell surface, and (iii) translocation of effector proteins, toxins and enzymes by these protein secretion systems. Here we review the frontier research imaging the process of secretion, particularly new studies that are applying various modes of super-resolution microscopy.

**Keywords: protein secretion, outer membrane, lipopolysaccharide, BAM complex**

OPEN ACCESS

***Edited by:***
*Bérengère Ize, Centre National de la Recherche Scientifique (CNRS), France*

***Reviewed by:***
*Andreas Diepold, Max Planck Institute for Terrestrial Microbiology, Germany*
*William D. Picking, University of Kansas, United States*

***Correspondence:**
*Trevor Lithgow*
*trevor.lithgow@monash.edu*

***Received:*** *05 April 2017*
***Accepted:*** *12 May 2017*
***Published:*** *29 May 2017*

***Citation:***
*Gunasinghe SD, Webb CT, Elgass KD, Hay ID and Lithgow T (2017) Super-Resolution Imaging of Protein Secretion Systems and the Cell Surface of Gram-Negative Bacteria. Front. Cell. Infect. Microbiol. 7:220. doi: 10.3389/fcimb.2017.00220*

Fluorescence microscopy has proven to be a powerful tool for cell biologists, given the wide array of fluorescent probes available (fluorescent fusion proteins, reactive tags, and fluorescent antibodies) to specifically label and detect sub-cellular components in a cellular context. Together with increasingly higher quality optics, sensitive detectors and coherent light sources, the resolution capacity of fluorescence microscopy has now been extended to generate superior images with finer details than ever before. Until these recent developments, microbiologists were unable to fully capitalize on fluorescence microscopy, since the diffraction limit of light means only objects larger than ~250 nm in lateral dimension and ~500 nm in axial dimension could be resolved: any objects smaller than these limits are merely blurred spots (Patterson et al., 2010). Many of the structures of interest in microbes are much smaller than this classical limit, with bacteria themselves only 1–10 μm in length (Koch, 1996).

The advent of super-resolution microscopy extended the classical limit imposed by conventional light microscopy (Hell, 2007, 2009; Huang et al., 2009, 2010). There are two general classes of super-resolution microscopy. The first class of imaging modalities utilizes spatially patterned fluorescence excitation beams to achieve the sub-diffraction level of resolution. The most notable examples of this technique are stimulated emission depletion (STED) microscopy (Hell and Wichmann, 1994; Klar and Hell, 1999), reversible saturable optical fluorescence transitions (RESOLFT) microscopy (Hell and Wichmann, 1994; Hofmann et al., 2005) and structured illumination microscopy (SIM) (Gustafsson, 2000, 2005).

The second class circumvents the diffraction barrier through actively controlling the fluorescence emitter (fluorescent proteins, antibodies or tags) concentrations by stochastic photo-activation or by stochastic photo-switching (Heilemann et al., 2009; Lippincott-Schwartz and Patterson, 2009; Kamiyama and Huang, 2012), thereby enabling spatio-temporal resolution of emitter localizations. This class includes photoactivation localization microscopy (PALM) (Betzig et al., 2006) and stochastic optical reconstruction microscopy (STORM), collectively known as single molecule localization microscopy (SMLM) (Rust et al., 2006). These techniques are documented to reach 10–25 nm of lateral resolution (Kamiyama and Huang, 2012), a scale that allows visualization of macromolecules in small cellular systems (**Figure 1**).

In order to exploit their environmental niches, bacteria undertake vital tasks such as sensing the external milieu, cell to cell communication, nutrient uptake against concentration gradients, cell-cell warfare and the secretion of macromolecules into the environment. Gram-negative bacteria have a highly evolved cell wall with two membranes composed of a complex array of integral and peripheral proteins, as well as phospholipids and glycolipids. The outer membrane is an asymmetric bilayer, with an inner leaflet of phospholipids and an outer leaflet of lipopolysaccharide (LPS). As discussed herein, we are beginning to appreciate that this asymmetric lipid environment promotes spatial heterogeneity of membrane constituents and impedes the sort of lateral mobility that is common for the proteins integrated in phospholipid bilayers. Super resolution microscopy is being applied to dissect diverse aspects of bacterial cell biology, including membrane protein structure and dynamics (Xie et al., 2008). In this review, we highlight the advances that have been made in understanding spatial-temporal characteristics of bacterial surface proteins, particularly protein secretion systems, that the recent advances in microscopy have allowed. To date, model bacterial systems like *Escherichia coli* and *Caulobacter cresentus* have been the subject for the majority of single molecule localization studies (Gahlmann and Moerner, 2014).

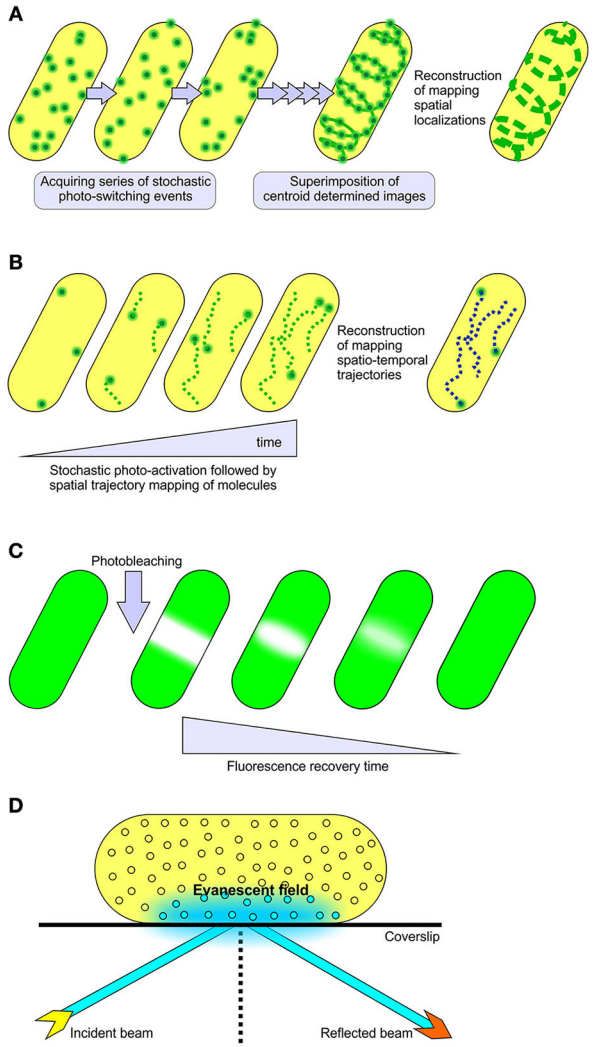


**FIGURE 1 |** Methods for single molecule localization and tracking. **(A)** STORM and **(B)** PALM super-resolution microscopy, collectively referred to as single molecule localization microscopy methods (SMLM). These modalities utilize stochastic photo-switching or photo-activation of a subset of fluorescence emitters to achieve sub-diffraction resolution of 10–25 nm in lateral dimensions. PALM is well known for live cell imaging and mapping spatiotemporal trajectories of individual fluorescently labeled molecules (Manley et al., 2008). STORM is documented for its use in determining the localized positioning of fluorescently labeled molecules in both live and fixed samples (Kamiyama and Huang, 2012). The mobility of fluorescent fusion proteins in live cells can also be surveyed through **(C)** FRAP and **(D)** TIRF microscopy techniques. In FRAP experiments, a relatively small area within the cell is irreversibly photo-bleached by a high intensity laser beam, followed by subsequent monitoring of the redistribution of non-bleached fluorescence molecules into the photo-bleached region under low laser power. TIRFM relies upon the generation of a rapidly decaying evanescent field at the interface of sample and coverslip to sparsely excite fluorophores, providing a high signal to background noise ratio in single particle tracking studies (Toomre and Bewersdorf, 2010).

## FLUORESCENCE IMAGING OF OUTER MEMBRANE STRUCTURE AND BIOGENESIS

Most bacterial outer membrane proteins (OMPs) have a β-barrel architecture (De Geyter et al., 2016; Plummer and Fleming, 2016; Noinaj et al., 2017; Slusky, 2017) and, of these, the channels that allow for selective permeability of small molecules across the outer membrane are referred to as porins (Hancock, 1987). Some of these porins display surface exposed extracellular domains, often simply loops of polypeptide between adjacent β-strands, which none the less provide the means to fluorescently label them for mobility assessment studies on live cells (Gibbs et al., 2004; Spector et al., 2010; Rassam et al., 2015). With the aid of fluorescent recovery after photo-bleaching (FRAP) and single particle tracking using total internal reflection fluorescence microscopy (TIRFM), we are now beginning to understand time-resolved spatial movements of these outer membrane proteins (Gibbs et al., 2004; Spector et al., 2010; Rothenberg et al., 2011; Rassam et al., 2015).

LamB is a trimeric porin responsible for maltose uptake in *E. coli* (Schirmer et al., 1995). LamB also serves as the

receptor for certain bacteriophage (Chatterjee and Rothenberg, 2012), and has been extensively studied in terms of diffusion dynamics. Using various labeling techniques and different imaging modalities, LamB mobility has been described using parametric measurements such as the short-time diffusion coefficient. In essence, this quantifies the area a molecule inhabits in a per second measurement. LamB displays a short-time diffusion coefficient of 0.15 – 0.06 $\mu m^2 s^{-1}$, with each molecule therefore being confined to a space of ∼20 nm at the outer membrane (Oddershede et al., 2002; Gibbs et al., 2004; Rothenberg et al., 2011). Similar results have come from study of other porins. OmpF, for example, was reported to have short-time diffusion coefficients of 0.006 $\mu m^2 s^{-1}$ (Spector et al., 2010). Similarly, a short-time diffusion coefficient of 0.05 $\mu m^2 s^{-1}$ was reported for the TonB-dependent receptor BtuB, which facilitates cobalamin uptake (Spector et al., 2010). For both OmpF and BtuB, recent work has suggested that their distribution and relative immobility may be due to non-specific, protein-protein interactions (Rassam et al., 2015). OmpA functions to lock the outer membrane to the under-lying peptidoglycan layer, and it had been expected that this feature alone would dictate the relative immobility predicted for OmpA (Samsudin et al., 2016). However, deletion of peptidoglycan binding domain of OmpA, did not affect the diffusion coefficient measurements for the β-barrel domain of OmpA (Verhoeven et al., 2013). These and other studies have led to the understanding that, compared to inner membrane proteins, OMPs generally display orders of magnitude slower diffusion dynamics whether or not they are tethered to other cellular structures (Oddershede et al., 2002; Gibbs et al., 2004; Spector et al., 2010; Rothenberg et al., 2011; Ritchie et al., 2013; Verhoeven et al., 2013; Rassam et al., 2015).

In this emerging paradigm of membrane spatial rigidity, it has become clear that the distribution of LPS is also greatly constrained. By fluorescently labeling LPS via the α-mannose moiety of its O-antigen, distinct helical ribbon-like geometric arrangements were observed for LPS on live *E.coli* (Ghosh and Young, 2005). Very low diffusion coefficients reported by FRAP experiments showed that LPS molecules were practically immobile by comparison with the (already very low) OMP diffusion rates (Mühlradt et al., 1973; Schindler et al., 1980). The current hypothesis is that LPS helical ribbons may represent a geometric arrangement important for staging outer membrane biogenesis. Given the high abundance yet constrained spatial distribution of LPS, it is becoming clear that any model for protein transport into or across the outer membrane will need to take into account this spatial information.

Few studies have yet to directly address the spatio-temporal aspects of the process of β-barrel assembly into the outer membrane. In one, temporal labeling of LamB appearance on the bacterial cell surface has been studied in elegant work, using detailed computational analysis to reconstruct the first spatio-temporal distribution of OMP biogenesis (Ursell et al., 2012). Employing site specific protein labeling strategy using Sfp phosphopantetheinyl transferase to covalently label emergent loops of nascent LamB molecules, the appearance and mobility of LamB molecules was monitored through time-lapse fluorescence microscopy. Inducible pulse-chase expression of LamB revealed an initial emergence of fluorescent punctae which represents a heterogeneous distribution of fluorescent spots per bacterium. The heterogeneous localization of LamB was due to discrete bursts of insertion of new material at discrete sites throughout the outer membrane. This presumably relates to the number and location of active β-barrel assembly machinery (BAM) complexes, which serve to catalyse β-barrel protein assembly into the outer membrane (De Geyter et al., 2016; Plummer and Fleming, 2016; Noinaj et al., 2017). The numbers of these punctae is similar to the number of sites estimated in an early EM-based study that captured porin insertion sites in *Salmonella* Typhimurium using ferritin-conjugated OMP-specific antibodies (Smit and Nikaido, 1978). Importantly, FRAP experiments showed that any laterally measurable movement of the OMPs across the bacterial cell surface was dependent on membrane growth and was not diffusional (Ursell et al., 2012). Since LamB also serves as receptor for several bacteriophage (Hancock and Reeves, 1976), fluorescently labeled λ phage tails have also been used to monitor the endogenous distribution of LamB—without plasmid-borne over-expression—and these studies too find it to be driven by cell growth and elongation (Gibbs et al., 2004).

The process of outer membrane biogenesis also depends on OMP turn-over through generational change in an *E. coli* population. A recent study using covalently modified colicins to fluorescently label two OMPs, BtuB and Cir, elegantly followed this process through TIRFM (Rassam et al., 2015). BtuB and Cir were observed to be clustered together in "OMP islands," huge rafts with an average size of ∼ 0.5 μm (hundreds to thousands of proteins molecules would be encompassed in this island, with little or no interstitial lipid present). Unlike the LamB studies, where new material was delivered at points all across the cell surface, Rassam et al. suggested that the insertion of new BtuB and Cir into these rafts was only observed in the mid-cell region (Rassam et al., 2015). Irrespective of the site of new material deposition, computer modeling studies (Wang et al., 2008; Ursell et al., 2012; Rassam et al., 2015) have demonstrated that in either scenario, pre-existent OMPs and LPS will always tend to be forced toward poles, and that cell division will ultimately yield an unequal partitioning of membrane materials to create distinct subpopulations of cells, ones having mixed set of old and new material and others with predominantly or exclusively "young" OMPs. Within a bacterial population this then creates a range of phenotypes in the outer membrane proteome, and a range of adaptive advantages for individual bacteria to survive and replicate in that environment. In various ways, other studies have demonstrated how "older" elements of the other major cell envelope constituents, LPS and peptidoglycan, are also ultimately retained at cell poles (Kato et al., 1990, 2000; De Pedro et al., 2003; Thiem et al., 2007; Thiem and Sourjik, 2008). *In silico* models have predicted this type of protein clustering and binary partitioning of membrane proteins. For example, this temporal positioning has been observed to be important in resolving protein aggregates associated with bacterial cell aging, but is also important in positioning chemoreceptor arrays and regulation of cell division (Janakiraman and Goldberg, 2004;

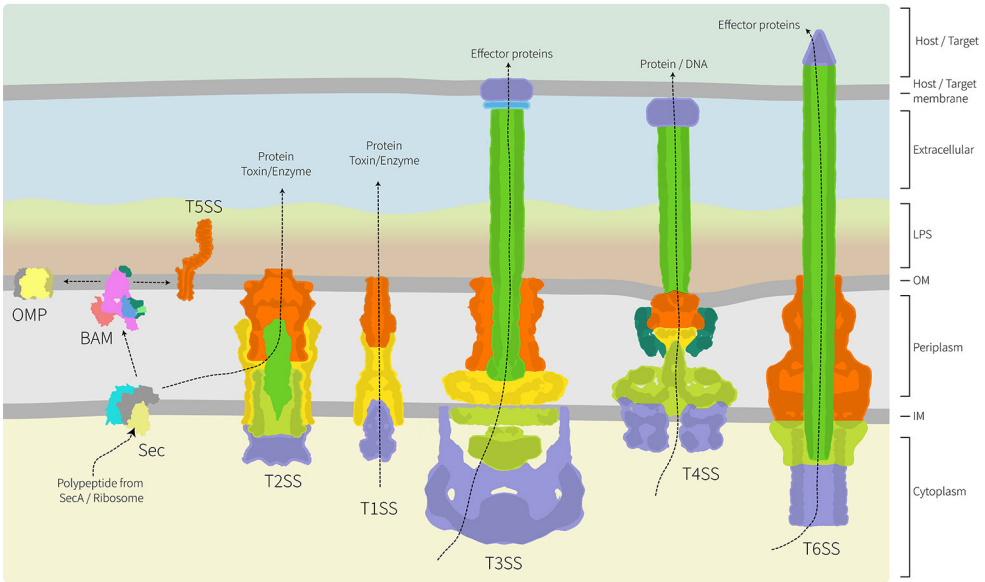


**FIGURE 2 |** Architecture of the major protein secretion systems found in Gram-negative bacteria. Of the six major protein secretion systems, five span the inner and outer membranes and the periplasm. These nanomachines are thereby trapped in the peptidoglycan layer. The T1SS, T3SS, T4SS, and T6SS collect substrate proteins directly from the cytoplasm for secretion across both membranes, while the T2SS collects substrate proteins from the periplasm with their delivery there being via the Sec translocon (shown) or Tat transport system (not shown). While informed artistic license was taken with the placement, orientation and shape of some proteins/complexes, wherever possible relative structural information was used. The structural data used as a basis in the preparation of this figure are: PDB 1ek9, 5l22, 5mg3, 5d0o, 1mal, 5ksr, 5wq8, 3fpp, 4ksr, 5l22, 3fpp, 4kh3, 4mee; and EMD-2927, EMD-2667, EMD-2567, EMD-1875. The structure and function of these various protein translocation systems are detailed elsewhere in this special volume.

Thiem et al., 2007; Lindner et al., 2008; Thiem and Sourjik, 2008).

## FLUORESCENCE-BASED IMAGING OF BACTERIAL SECRETION SYSTEMS

A frontier area of research in bacterial cell biology concerns the assembly and distribution of protein secretion machines. Bacteria have evolved numerous mechanisms to efficiently secrete proteins into the environment and characterization of several protein secretion systems is yielding exciting advances in understanding their structure and function (Dalbey and Kuhn, 2012; Costa et al., 2015). Because these systems are detailed elsewhere in this special edition, we have focused our review on studies where spatial distribution appears to be important either to the biogenesis of the secretion system, or to its function. As highlighted in **Figure 2**, the architecture of these secretion nanomachines can differ from single component systems, to relatively simple systems composed of only 3 subunits, to multicomponent systems containing over 20 protein subunits and spanning all four compartments of the bacterial cell (Dalbey and Kuhn, 2012; Campos et al., 2013; Galán et al., 2014; Ho et al., 2014; Thomas et al., 2014; Trokter et al., 2014; van Ulsen et al., 2014; Zoued et al., 2014; Basler, 2015; Costa et al., 2015; Fan et al., 2016; Notti and Stebbins, 2016).

## TYPE 1 SECRETION SYSTEM (T1SS)

Effector proteins secreted through T1SS have been characterized in a number of bacterial pathogens including in uropathogenic *E. coli*, *Bordetella pertussis* and more recently through effector protein RtxA in *Legionella pneumophila* (Brooks et al., 1980; Shrivastava and Miller, 2009; Fuche et al., 2015). Using deletion mutants and fluorescence protein fusion constructs of RtxA (photoactivatable mCherry-RtxA), secretion was monitored through the course of infection. *Legionella* were internalized by host cells into the endoplasmic reticulum-like compartment, the *Legionella*-containing vacuole, where bacterial replication takes place inside the host. With the versatility of genetically-encoded, reactive tags (Halo-tag and SNAP-tag), Barlag et al. imaged subunits of T1SS in *Salmonella enterica* at a nanoscopic level (Barlag et al., 2016). Diffusion coefficients reported for SiiF, the inner membrane component the T1SS were $0.008\,\mu m^2 s^{-1}$ and the secretion machine was confined into 3–4 localized punctae. This very low diffusion coefficient for an inner membrane protein is perhaps predictable, given that T1SS include a TolC-type protein integrated into the outer membrane (Thomas et al., 2014), and in consideration that by spanning the periplasm the T1SS would be trapped within the peptidoglycan meshwork. This peptidoglycan trap would likely apply equally in constraining the movement of other protein secretion systems too (**Figure 2**). Together, these studies illustrate the resourcefulness of fluorescent fusion and enzyme tags and how these can be utilized in super resolution imaging of the secretion

machines and their substrates, without altering the functionality of either.

## TYPE 2 SECRETION SYSTEM (T2SS)

The T2SS has been identified in a number of bacterial pathogens, and is particularly well known in *Vibrio cholerae* as the system responsible for cholera toxin secretion (Sandkvist et al., 1997; Connell et al., 1998; Lybarger et al., 2009; Sikora et al., 2011). Elements required for the assembly of this T2SS are encoded by the extracellular protein secretion (*eps*) genes (Overbye et al., 1993; Sandkvist et al., 1997; Marsh and Taylor, 1998; Fullner and Mekalanos, 1999) and the localization of fluorescently labeled protein subunits in *V. cholerae* has revealed insight into the assembly and spatial dynamics. Using chromosomal and plasmid borne GFP fusions with the EpsM, EspG and EpsC subunits of the T2SS the subcellular localization of each components was assessed in *Vibrio cholerae* (Lybarger et al., 2009). When chromosomally-expressed (to produce endogenous steady-state levels of protein), GFP-EpsM formed distinct fluorescent foci that were not concentrated at cell poles. Conversely, when plasmid-borne over-expression of GFP-EpsM was instituted, the protein displayed a polar localization.

This discernible effect on protein subcellular localization under differential gene expression is a concern that needs careful consideration. The impact of overexpression on physiologically-relevant vs. non-physiological localizations is equally of concern in studies on other protein secretion systems (and all subcellular structures) too. As mentioned previously, protein aggregates tend to be deposited in polar locations (Janakiraman and Goldberg, 2004; Thiem et al., 2007; Lindner et al., 2008; Thiem and Sourjik, 2008).

Type 4 pili are a locomotional appendage that are ancestrally and structurally related to the T2SS (Peabody et al., 2003). The distribution of T4 pili has been followed using fluorescent protein fusions. An mCherry fusion tag was attached to the BfpB subunit in the Type 4 pili of enteropathogenic *E. coli* (Lieberman et al., 2012). PALM was used to capture single molecule localization events of BfpB-PAmCherry, providing evidence for a largely non-polar distribution pattern in Type 4 pili biogenesis, as is likely in T2SS biogenesis. Conversely, studies in *Pseudomonas aeruginosa* suggest that Type 4 pili biogenesis occurs at sites of cell division: that is, that the nanomachines are pre-installed at what will become a cell pole (after cell division concludes) (Carter et al., 2017). Taken together these exciting studies highlight the complex spatio-temporal scenarios that exist in the cell biology of bacteria, and caution against concluding that what is true in *E. coli* is necessarily true in other bacterial species.

## TYPE 3 SECRETION SYSTEM (T3SS)

The T3SS has been identified in several bacterial pathogens including *Yersinia enterocolitica*, *E. coli*, *Shigella flexneri*, and *Salmonella* Typhimurium. While electron microscopy and electron tomography have provided exquisite detail in the structure of these complicated nanomachines (Spreter et al., 2009; Carleton et al., 2013; Radics et al., 2014; Hu et al., 2015, 2017), a number of different fluorescence microscopy imaging studies on live cells have provided in-depth analysis on different stages of T3SS assembly and effector protein secretion into host cells. Time-lapse fluorescence microscopy has monitored the T3SS during *S.* Typhimurium infection of epithelial cells (Schlumberger et al., 2005). A fluorescently-labeled substrate of the T3SS, SipA, was monitored for its emergence into the host cells, and its concomitant depletion from the bacterial cytoplasm. At the event of infection, it was estimated via fluorescence measurements that *S.* Typhimurium was able to deliver $6 \pm 3 \times 10^3$ molecules of SipA to the host cell within 100–600 s, and the effector protein ejection starts ∼16–25 s after docking on to the host. In terms of the nanomachine itself, subunits of the T3SS in *S.* Typhimurium have been visualized too (Diepold et al., 2010, 2015; Kudryashev et al., 2015; Notti et al., 2015; Barlag et al., 2016). The diffusion coefficient for SpaS, an inner membrane component of the T3SS, was measured to be $0.055\,\mu m^2 s^{-1}$, which is a similar scale to the diffusion coefficients measured for outer membrane proteins LamB and OmpF. While not directly tested, this level of immobility of the inner membrane elements of the T3SS is consistent with them being constrained in their diffusional movements by the outer membrane components of the nanomachine and the peptidoglycan trap. The same would be true of the T1SS (Barlag et al., 2016), where SiiF is found in the inner membrane but would be constrained in its diffusional movement by its spanning the peptidoglycan and attached to the TolC-homolog SiiC in the outer membrane (Kiss et al., 2007). In these studies, the localization of the T3SS was distributed relatively evenly across the bacterial cell. It would be of great interest to monitor the T3SS distribution in pathogens such as enteropathogenic *E. coli* during the initial events of host cell encounter, when only a single surface of the bacterium engages the epithelial cell surface to initiate pathogen attachment and effacement (Wong et al., 2011; Gaytán et al., 2016). Is there a random engagement of only some T3SS with the host cell? Or does the pathogen control the spatial arrangement of T3SS to ensure maximal engagement on the "host side" of its surface?

## TYPE 4 SECRETION SYSTEM (T4SS)

The T4SS functions to transfer proteins and/or DNA in bacterial conjugation encounters or during infection (Ding et al., 2003; Trokter et al., 2014). The Dot/Icm machinery is the T4SS in *Legionella* spp. and is responsible for hundreds of effector proteins throughout the infection cycle (So et al., 2015). Epitope-tagging one of these effectors, LncP, enabled fluorescence imaging of infected macrophages and showed that the protein was secreted from the bacterial cytoplasm by the T4SS and ultimately translocated across a remarkable five membranes in order to be assembled into the mitochondrial inner membrane of the host cell (Dolezal et al., 2012). An equivalent T4SS is found in *Coxiella burnetii*, and has been reported to be exclusively located at one pole of the bacterium (Morgan et al., 2010). It has been suggested that in these species, bacteria-host membrane contact might be required to initiate secretion into the host cell cytoplasm (Voth and Heinzen, 2007). That being the case, a unique localization of

the T4SS nanomachines would promote the efficiency of effector protein secretion.

The T4SS has been well characterized in the plant pathogen *Agrobacterium tumefaciens* (Zupan et al., 2000), where it is composed of 12 subunits (Das and Xie, 2000; Ward et al., 2002; Jakubowski et al., 2003; Low et al., 2014; Trokter et al., 2014; Chandran Darbari and Waksman, 2015; Costa et al., 2015) and facilitates the delivery of tumor inducing pTi plasmid to plant cells, causing overproduction of certain plant growth hormones and leading to a resultant tumor (Dessaux et al., 1993). Initial spatial location studies on the T4SS in *A. tumefaciens* suggested that the VirD4 and VirB6 components were located at cell poles (Kumar and Das, 2002; Judd et al., 2005). Using deconvolution fluorescence microscopy and antibodies to specifically label the T4SS in *A. tumefaciens*, multiple clustered regions were observed along the cell periphery, i.e., not at the cell poles, in a majority of bacterial cells (Aguilar et al., 2011). Based on these finding, the authors proposed a lateral attachment model providing a more effective means for contact between pathogen and host during *A. tumefaciens* infection compared to a cell pole mediated attachment.

## TYPE 5 SECRETION SYSTEM (T5SS)

There are several sub-types of T5SS, including autotransporters, inverse autotransporters, two-partner secretion systems and others (Fan et al., 2016; Heinz et al., 2016). Fluorescence microscopy studies on autotransporters derived from a variety of bacteria, including AIDA-I from *E. coli*, IcsA and SepA from *Shigella flexneri*, BrkA from *Bordetella pertussis*, and BimA from *Burkholderia thailandensis*, were shown to be directly localized to bacterial cell poles when translocated to the cell surface (Charles et al., 2001; Jain et al., 2006; Lu et al., 2015). Indeed, when IcsA, SepA, and BrkA were expressed in *E. coli* systems, they still migrated to the poles, suggesting that intrinsic features in the autotransporters programmes this polar localization (Jain et al., 2006). Conversely, at least one autotransporter, Ag43, was localized as covering the whole cell surface without any concentration toward poles (Danese et al., 2000; Kjærgaard et al., 2000). It is important to note that none of these studies have addressed where the integration event took place, nor any dynamics of movement of the autotransporters, but rather visualized their steady-state positioning. In addition to the effects of cell division or LPS leading to polar localization, the location at which a protein is translocated across the cytoplasmic membrane, through processes collectively considered as "transertion" (Bakshi et al., 2014; Matsumoto et al., 2015), may be important in determining how a protein achieves polar localization.

## TYPE 6 SECRETION SYSTEM (T6SS)

While being the most recently discovered of the major protein secretion systems in Gram-negative bacteria, predictions suggest the T6SS to be present in ∼25% of species (Basler et al., 2012). Characterization studies show that the T6SS functions in virulence for several pathogens including *B. thailandensis, Pseudomonas aeruginosa*, *Serratia marcescens* and *V. cholerae* (Mougous et al., 2006; Pukatzki et al., 2006, 2007; Schwarz et al., 2014). Structural elucidation of the T6SS from *V. cholerae* revealed startling similarities to bacteriophage tails. In general, T6SSs are assembled to contain a contractible sheath, baseplate and a membrane puncturing spike to mediate effector protein secretion into host cells (Basler et al., 2012; Filloux, 2013). Using a super-folder green fluorescent protein (sfGFP) fusion to VipA, one of the two protein components that makeup the contractile sheath, long straight tubular structures were localized in the cytoplasm extending along the width or length of the bacterium (Basler et al., 2012). Time-lapse fluorescence microscopy revealed these sub-cellular structures were highly dynamic in nature. They assemble at 20–30 s $\mu m^{-1}$, rapidly contracted to about 50% from their original length within $\leq$5 ms, and finally disassembled over a 30–60 s period (Basler et al., 2012). Recent studies using a similar fluorescent protein fusion tag approach captured the baseplate protein TssA joining the sheath component's polymerization in *E. coli* (Zoued et al., 2016).

T6SSs are often used in inter-species warfare, in order to outcompete bacterial neighbors (Hood et al., 2010; MacIntyre et al., 2010; Schwarz et al., 2010; Murdoch et al., 2011; Zoued et al., 2014; Journet and Cascales, 2016). Time-lapse fluorescence microscopy quantitatively demonstrated this antibacterial activity through predator-prey cell dynamics on live cells (Brunet et al., 2013). Co-culturing a pathogenic, "predator" *E. coli* strain expressing TssB-sfGFP (TssB is alternatively known as VipA) and a non-pathogenic, "prey" *E. coli* strain devoid of T6SS expressing fluorescent protein mCherry, showed that only upon contact with the prey was the contraction of the sheath structure triggered in predator cells. Conversely, in *S. marcescens* equivalent experimental strategies showed that the bacteria does not wait to encounter prey (or enemy) cells, but behaves aggressively and fires the T6SS irrespective of any provocation by cell-cell contact (Gerc et al., 2015). These studies again highlight the diverse behaviors that different bacterial species have evolved to deploy against their neighbors and enemies, and provide fascinating insight into the dynamics of how T6SS effector proteins are secreted to target other bacteria.

## CONCLUSION

It is early in the application of super resolution microscopy techniques to capture the cellular events in the biogenesis and action of protein secretion systems in bacteria. Already, studies have challenged our preconceptions on bacterial cell envelope organization and protein dynamics. For example, the outer membrane is not a fluid mosaic, but a turgid structure that constrains membrane protein movement. Selective deployment of a protein secretion system is thereby possible at highly precise locations. High resolution imaging modalities will be tremendously useful in answering long-standing questions in bacterial cell biology, such as what mechanisms drive the biogenesis of outer membrane vesicles (Turnbull et al.,

2016), questions which until recently have largely been experimentally intractable. A further example is the extent to which transertion—the coupling of transcription, translation, and translocation—provides a mechanism for highly localized distributions of membrane proteins. This review has indicated the uses for the growing number of versatile fluorescent probes, which can be used in the distinct cellular environments, and how they promise to extend fluorescence microscopy applications even further. Examining host-pathogen interactions, detailing the nanoscale organization of protein secretion systems and studying the dynamic nature of sub-cellular compartments in live bacteria is now possible through super resolution microscopy. In the future, no doubt, these imaging techniques will be applied to understand the cell biology of the grand diversity of bacterial species, beyond characteristic model bacteria.

## AUTHOR CONTRIBUTIONS

SG read the literature and wrote the manuscript. CW read the literature and wrote the manuscript. KE read the literature and wrote the manuscript. IH read the literature and wrote the manuscript. TL read the literature and wrote the manuscript.

## ACKNOWLEDGMENTS

We thank Dr. Alex Fulcher for comments on the manuscript. SG thanks Dr. Toby Bell for training and critical discussions in single molecule imaging. The authors' work in this area is supported by NHMRC Program Grant 1092262 and the Australian Research Council (ARC; FL130100038). SG is supported by an ARC Laureate Scholarship, IH and CW are ARC Laureate Postdoctoral Fellows, and TL is an ARC Australian Laureate Fellow.

## REFERENCES

Aguilar, J., Cameron, T. A., Zupan, J., and Zambryski, P. (2011). Membrane and core periplasmic *Agrobacterium tumefaciens* virulence Type IV secretion system components localize to multiple sites around the bacterial perimeter during lateral attachment to plant cells. *MBio* 2, e00218–e00211. doi: 10.1128/mBio.00218-11

Bakshi, S., Choi, H., Mondal, J., and Weisshaar, J. C. (2014). Time-dependent effects of transcription- and translation-halting drugs on the spatial distributions of the *Escherichia coli* chromosome and ribosomes. *Mol. Microbiol.* 94, 871–887. doi: 10.1111/mmi.12805

Barlag, B., Beutel, O., Janning, D., Czarniak, F., Richter, C. P., Kommnick, C., et al. (2016). Single molecule super-resolution imaging of proteins in living *Salmonella enterica* using self-labelling enzymes. *Sci. Rep.* 6:31601. doi: 10.1038/srep31601

Basler, M., Pilhofer, M., Henderson, G. P., Jensen, G. J., and Mekalanos, J. J. (2012). Type VI secretion requires a dynamic contractile phage tail-like structure. *Nature* 483, 182–186. doi: 10.1038/nature10846

Basler, M. (2015). Type VI secretion system: secretion by a contractile nanomachine. *Philos. Trans. R. Soc. B* 370:20150021. doi: 10.1098/rstb.2015.0021

Betzig, E., Patterson, G. H., Sougrat, R., Lindwasser, O. W., Olenych, S., Bonifacino, J. S., et al. (2006). Imaging intracellular fluorescent proteins at nanometer resolution. *Science* 313, 1642–1645. doi: 10.1126/science.1127344

Brooks, H. J., O'Grady, F., McSherry, M. A., and Cattell, W. (1980). Uropathogenic properties of *Escherichia coli* in recurrent urinary-tract infection. *J. Med. Microbiol.* 13, 57–68. doi: 10.1099/00222615-13-1-57

Brunet, Y. R., Espinosa, L., Harchouni, S., Mignot, T., and Cascales, E. (2013). Imaging type VI secretion-mediated bacterial killing. *Cell Rep.* 3, 36–41. doi: 10.1016/j.celrep.2012.11.027

Campos, M., Cisneros, D. A., Nivaskumar, M., and Francetic, O. (2013). The type II secretion system–a dynamic fiber assembly nanomachine. *Res. Microbiol.* 164, 545–555. doi: 10.1016/j.resmic.2013.03.013

Carleton, H. A., Lara-Tejero, M., Liu, X., and Galan, J. E. (2013). Engineering the type III secretion system in non-replicating bacterial minicells for antigen delivery. *Nat. Commun.* 4:1590. doi: 10.1038/ncomms2594

Carter, T., Buensuceso, R. N., Tammam, S., Lamers, R. P., Harvey, H., Howell, P. L., et al. (2017). The type IVa pilus machinery is recruited to sites of future cell division. *MBio* 8:e02103-16. doi: 10.1128/mBio.02103-16

Chandran Darbari, V., and Waksman, G. (2015). Structural biology of bacterial type IV secretion systems. *Annu. Rev. Biochem.* 84, 603–629. doi: 10.1146/annurev-biochem-062911-102821

Charles, M., Pérez, M., Kobil, J. H., and Goldberg, M. B. (2001). Polar targeting of *Shigella* virulence factor IcsA in *Enterobacteriacae* and *Vibrio*. *Proc. Natl. Acad. Sci. U.S.A.* 98, 9871–9876. doi: 10.1073/pnas.171310498

Chatterjee, S., and Rothenberg, E. (2012). Interaction of bacteriophage λ with its *E. coli* receptor, LamB. *Viruses* 4, 3162–3178. doi: 10.3390/v4113162

Connell, T. D., Metzger, D. J., Lynch, J., and Folster, J. P. (1998). Endochitinase is transported to the extracellular milieu by the eps-encoded general secretory pathway of *Vibrio cholerae*. *J. Bacteriol.* 180, 5591–5600.

Costa, T. R., Felisberto-Rodrigues, C., Meir, A., Prevost, M. S., Redzej, A., Trokter, M., et al. (2015). Secretion systems in Gram-negative bacteria: structural and mechanistic insights. *Nat. Rev. Microbiol.* 13, 343–359. doi: 10.1038/nrmicro3456

Dalbey, R. E., and Kuhn, A. (2012). Protein traffic in Gram-negative bacteria–how exported and secreted proteins find their way. *FEMS Microbiol. Rev.* 36, 1023–1045. doi: 10.1111/j.1574-6976.2012.00327.x

Danese, P. N., Pratt, L. A., Dove, S. L., and Kolter, R. (2000). The outer membrane protein, Antigen 43, mediates cell-to-cell interactions within *Escherichia coli* biofilms. *Mol. Microbiol.* 37, 424–432. doi: 10.1046/j.1365-2958.2000.02008.x

Das, A., and Xie, Y. H. (2000). The *Agrobacterium* T-DNA transport pore proteins VirB8, VirB9, and VirB10 interact with one another. *J. Bacteriol.* 182, 758–763. doi: 10.1128/JB.182.3.758-763.2000

De Geyter, J., Tsirigotaki, A., Orfanoudaki, G., Zorzini, V., Economou, A., and Karamanou, S. (2016). Protein folding in the cell envelope of *Escherichia coli*. *Nat. Microbiol.* 1:16107. doi: 10.1038/nmicrobiol.2016.107

De Pedro, M. A., Schwarz, H., and Koch, A. L. (2003). Patchiness of murein insertion into the sidewall of *Escherichia coli*. *Microbiology* 149, 1753–1761. doi: 10.1099/mic.0.26125-0

Dessaux, Y., Petit, A., and Tempe, J. (1993). Chemistry and biochemistry of opines, chemical mediators of parasitism. *Phytochemistry* 34, 31–38. doi: 10.1016/S0031-9422(00)90778-7

Diepold, A., Amstutz, M., Abel, S., Sorg, I., Jenal, U., and Cornelis, G. R. (2010). Deciphering the assembly of the *Yersinia type* III secretion injectisome. *EMBO J.* 29, 1928–1940. doi: 10.1038/emboj.2010.84

Diepold, A., Kudryashev, M., Delalez, N. J., Berry, R. M., and Armitage, J. P. (2015). Composition, formation, and regulation of the cytosolic c-ring, a dynamic component of the type III secretion injectisome. *PLoS Biol.* 13:e1002039. doi: 10.1371/journal.pbio.1002039

Ding, Z., Atmakuri, K., and Christie, P. J. (2003). The outs and ins of bacterial type IV secretion substrates. *Trends Microbiol.* 11, 527–535. doi: 10.1016/j.tim.2003.09.004

Dolezal, P., Aili, M., Tong, J., Jiang, J. H., Marobbio, C. M., Lee, S. F., et al. (2012). *Legionella pneumophila* secretes a mitochondrial carrier protein during infection. *PLoS Pathog.* 8:e1002459. doi: 10.1371/journal.ppat.1002459

Fan, E., Chauhan, N., Udatha, D. G., Leo, J. C., and Linke, D. (2016). Type V secretion systems in bacteria. *Microbiol. Spectr.* 4:VMBF-0009-2015. doi: 10.1128/microbiolspec.VMBF-0009-2015

Filloux, A. (2013). Microbiology: a weapon for bacterial warfare. *Nature* 500, 284–285. doi: 10.1038/nature12545

Fuche, F., Vianney, A., Andrea, C., Doublet, P., and Gilbert, C. (2015). Functional type 1 secretion system involved in *Legionella pneumophila* virulence. *J. Bacteriol.* 197, 563–571. doi: 10.1128/JB.02164-14

Fullner, K. J., and Mekalanos, J. J. (1999). Genetic characterization of a new type IV-A pilus gene cluster found in both classical and El Tor biotypes of *Vibrio cholerae*. *Infect. Immun.* 67, 1393–1404.

Gahlmann, A., and Moerner, W. (2014). Exploring bacterial cell biology with single-molecule tracking and super-resolution imaging. *Nature Rev. Microbiol.* 12, 9–22. doi: 10.1038/nrmicro3154

Galán, J. E., Lara-Tejero, M., Marlovits, T. C., and Wagner, S. (2014). Bacterial type III secretion systems: specialized nanomachines for protein delivery into target cells. *Annu. Rev. Microbiol.* 68, 415–438. doi: 10.1146/annurev-micro-092412-155725

Gaytán, M. O., Martínez-Santos, V. I., Soto, E., and González-Pedrajo, B. (2016). Type three secretion system in attaching and effacing pathogens. *Front. Cell. Infect. Microbiol.* 6:129. doi: 10.3389/fcimb.2016.00129

Gerc, A. J., Diepold, A., Trunk, K., Porter, M., Rickman, C., Armitage, J. P., et al. (2015). Visualization of the *Serratia* type vi secretion system reveals unprovoked attacks and dynamic assembly. *Cell Rep.* 12, 2131–2142. doi: 10.1016/j.celrep.2015.08.053

Ghosh, A. S., and Young, K. D. (2005). Helical disposition of proteins and lipopolysaccharide in the outer membrane of *Escherichia coli*. *J. Bacteriol.* 187, 1913–1922. doi: 10.1128/JB.187.6.1913-1922.2005

Gibbs, K. A., Isaac, D. D., Xu, J., Hendrix, R. W., Silhavy, T. J., and Theriot, J. A. (2004). Complex spatial distribution and dynamics of an abundant *Escherichia coli* outer membrane protein, LamB. *Mol. Microbiol.* 53, 1771–1783. doi: 10.1111/j.1365-2958.2004.04242.x

Gustafsson, M. G. (2000). Surpassing the lateral resolution limit by a factor of two using structured illumination microscopy. *J. Microsc.* 198, 82–87. doi: 10.1046/j.1365-2818.2000.00710.x

Gustafsson, M. G. (2005). Nonlinear structured-illumination microscopy: wide-field fluorescence imaging with theoretically unlimited resolution. *Proc. Natl. Acad. Sci. U.S.A.* 102, 13081–13086. doi: 10.1073/pnas.0406877102

Hancock, R. (1987). Role of porins in outer membrane permeability. *J. Bacteriol.* 169, 929. doi: 10.1128/jb.169.3.929-933.1987

Hancock, R. E., and Reeves, P. (1976). Lipopolysaccharide-deficient, bacteriophage-resistant mutants of *Escherichia coli* K-12. *J. Bacteriol.* 127, 98–108.

Heilemann, M., Dedecker, P., Hofkens, J., and Sauer, M. (2009). Photoswitches: key molecules for subdiffraction-resolution fluorescence imaging and molecular quantification. *Laser Photon. Rev.* 3, 180–202. doi: 10.1002/lpor.200810043

Heinz, E., Stubenrauch, C. J., Grinter, R., Croft, N. P., Purcell, A. W., Strugnell, R. A., et al. (2016). Conserved features in the structure, mechanism, and biogenesis of the inverse autotransporter protein family. *Genome Biol. Evol.* 8, 1690–1705. doi: 10.1093/gbe/evw112

Hell, S. W. (2007). Far-field optical nanoscopy. *Science* 316, 1153–1158. doi: 10.1126/science.1137395

Hell, S. W. (2009). Microscopy and its focal switch. *Nat. Methods* 6, 24–32. doi: 10.1038/nmeth.1291

Hell, S. W., and Wichmann, J. (1994). Breaking the diffraction resolution limit by stimulated emission: stimulated-emission-depletion fluorescence microscopy. *Opt. Lett.* 19, 780–782. doi: 10.1364/OL.19.000780

Ho, B. T., Dong, T. G., and Mekalanos, J. J. (2014). A view to a kill: the bacterial type VI secretion system. *Cell Host Microbe* 15, 9–21. doi: 10.1016/j.chom.2013.11.008

Hofmann, M., Eggeling, C., Jakobs, S., and Hell, S. W. (2005). Breaking the diffraction barrier in fluorescence microscopy at low light intensities by using reversibly photoswitchable proteins. *Proc. Natl. Acad. Sci. U.S.A.* 102, 17565–17569. doi: 10.1073/pnas.0506010102

Hood, R. D., Singh, P., Hsu, F., Güvener, T., Carl, M. A., Trinidad, R. R., et al. (2010). A type VI secretion system of *Pseudomonas aeruginosa* targets a toxin to bacteria. *Cell Host Microbe* 7, 25–37. doi: 10.1016/j.chom.2009.12.007

Hu, B., Lara-Tejero, M., Kong, Q., Galan, J. E., and Liu, J. (2017). *In situ* molecular architecture of the *Salmonella* type III secretion machine. *Cell* 168, 1065–1074.e1010. doi: 10.1016/j.cell.2017.02.022

Hu, B., Margolin, W., Molineux, I. J., and Liu, J. (2015). Structural remodeling of bacteriophage T4 and host membranes during infection initiation. *Proc. Natl. Acad. Sci. U.S.A.* 112, E4919–E4928. doi: 10.1073/pnas.1501064112

Huang, B., Babcock, H., and Zhuang, X. (2010). Breaking the diffraction barrier: super-resolution imaging of cells. *Cell* 143, 1047–1058. doi: 10.1016/j.cell.2010.12.002

Huang, B., Bates, M., and Zhuang, X. (2009). Super-resolution fluorescence microscopy. *Annu. Rev. Biochem.* 78, 993–1016. doi: 10.1146/annurev.biochem.77.061906.092014

Jain, S., van Ulsen, P., Benz, I., Schmidt, M. A., Fernandez, R., Tommassen, J., et al. (2006). Polar localization of the autotransporter family of large bacterial virulence proteins. *J. Bacteriol.* 188, 4841–4850. doi: 10.1128/JB.00326-06

Jakubowski, S. J., Krishnamoorthy, V., and Christie, P. J. (2003). *Agrobacterium tumefaciens* VirB6 protein participates in formation of VirB7 and VirB9 complexes required for type IV secretion. *J. Bacteriol.* 185, 2867–2878. doi: 10.1128/JB.185.9.2867-2878.2003

Janakiraman, A., and Goldberg, M. B. (2004). Evidence for polar positional information independent of cell division and nucleoid occlusion. *Proc. Natl. Acad. Sci. U.S.A.* 101, 835–840. doi: 10.1073/pnas.0305747101

Journet, L., and Cascales, E. (2016). The type VI secretion system in *Escherichia coli* and related species. *EcoSal Plus* 7:ESP-0009-2015. doi: 10.1128/ecosalplus.ESP-0009-2015

Judd, P. K., Kumar, R. B., and Das, A. (2005). The type IV secretion apparatus protein VirB6 of *Agrobacterium tumefaciens* localizes to a cell pole. *Mol. Microbiol.* 55, 115–124. doi: 10.1111/j.1365-2958.2004.04378.x

Kamiyama, D., and Huang, B. (2012). Development in the STORM. *Dev. Cell* 23, 1103–1110. doi: 10.1016/j.devcel.2012.10.003

Kato, N., Ohta, M., Kido, N., Ito, H., Naito, S., Hasegawa, T., et al. (1990). Crystallization of R-form lipopolysaccharides from *Salmonella minnesota* and *Escherichia coli*. *J. Bacteriol.* 172, 1516–1528. doi: 10.1128/jb.172.3.1516-1528.1990

Kato, N., Sugiyama, T., Naito, S., Arakawa, Y., Ito, H., Kido, N., et al. (2000). Molecular structure of bacterial endotoxin (*Escherichia coli* Re lipopolysaccharide): implications for formation of a novel heterogeneous lattice structure. *Mol. Microbiol.* 36, 796–805. doi: 10.1046/j.1365-2958.2000.01893.x

Kiss, T., Morgan, E., and Nagy, G. (2007). Contribution of SPI-4 genes to the virulence of *Salmonella enterica*. *FEMS Microbiol. Lett.* 275, 153–159. doi: 10.1111/j.1574-6968.2007.00871.x

Kjærgaard, K., Schembri, M. A., Hasman, H., and Klemm, P. (2000). Antigen 43 from *Escherichia coli* induces inter-and intraspecies cell aggregation and changes in colony morphology of *Pseudomonas fluorescens*. *J. Bacteriol.* 182, 4789–4796. doi: 10.1128/JB.182.17.4789-4796.2000

Klar, T. A., and Hell, S. W. (1999). Subdiffraction resolution in far-field fluorescence microscopy. *Opt. Lett.* 24, 954–956. doi: 10.1364/OL.24.000954

Koch, A. L. (1996). What size should a bacterium be? A question of scale. *Annu. Rev. Microbiol.* 50, 317–348. doi: 10.1146/annurev.micro.50.1.317

Kudryashev, M., Diepold, A., Amstutz, M., Armitage, J. P., Stahlberg, H., and Cornelis, G. R. (2015). *Yersinia enterocolitica* type III secretion injectisomes form regularly spaced clusters, which incorporate new machines upon activation. *Mol. Microbiol.* 95, 875–884. doi: 10.1111/mmi.12908

Kumar, R. B., and Das, A. (2002). Polar location and functional domains of the *Agrobacterium tumefaciens* DNA transfer protein VirD4. *Mol. Microbiol.* 43, 1523–1532. doi: 10.1046/j.1365-2958.2002.02829.x

Lieberman, J. A., Frost, N. A., Hoppert, M., Fernandes, P. J., Vogt, S. L., Raivio, T. L., et al. (2012). Outer membrane targeting, ultrastructure, and single molecule localization of the enteropathogenic *Escherichia coli* type IV pilus secretin BfpB. *J. Bacteriol.* 194, 1646–1658. doi: 10.1128/JB.06330-11

Lindner, A. B., Madden, R., Demarez, A., Stewart, E. J., and Taddei, F. (2008). Asymmetric segregation of protein aggregates is associated with cellular aging and rejuvenation. *Proc. Natl. Acad. Sci. U.S.A.* 105, 3076–3081. doi: 10.1073/pnas.0708931105

Lippincott-Schwartz, J., and Patterson, G. H. (2009). Photoactivatable fluorescent proteins for diffraction-limited and super-resolution imaging. *Trends Cell Biol.* 19, 555–565. doi: 10.1016/j.tcb.2009.09.003

Low, H. H., Gubellini, F., Rivera-Calzada, A., Braun, N., Connery, S., Dujeancourt, A., et al. (2014). Structure of a type IV secretion system. *Nature* 508, 550–553. doi: 10.1038/nature13081

Lu, Q., Xu, Y., Yao, Q., Niu, M., and Shao, F. (2015). A polar-localized iron-binding protein determines the polar targeting of *Burkholderia* BimA autotransporter and actin tail formation. *Cell Microbiol.* 17, 408–424. doi: 10.1111/cmi.12376

Lybarger, S. R., Johnson, T. L., Gray, M. D., Sikora, A. E., and Sandkvist, M. (2009). Docking and assembly of the type II secretion complex of *Vibrio cholerae*. *J. Bacteriol.* 191, 3149–3161. doi: 10.1128/JB.01701-08

MacIntyre, D. L., Miyata, S. T., Kitaoka, M., and Pukatzki, S. (2010). The *Vibrio cholerae* type VI secretion system displays antimicrobial properties. *Proc. Natl. Acad. Sci. U.S.A.* 107, 19520–19524. doi: 10.1073/pnas.1012931107

Manley, S., Gillette, J. M., Patterson, G. H., Shroff, H., Hess, H. F., Betzig, E., et al. (2008). High-density mapping of single-molecule trajectories with photoactivated localization microscopy. *Nat. Methods* 5, 155–157. doi: 10.1038/nmeth.1176

Marsh, J. W., and Taylor, R. K. (1998). Identification of the *Vibrio cholerae* type 4 prepilin peptidase required for cholera toxin secretion and pilus formation. *Mol. Microbiol.* 29, 1481–1492. doi: 10.1046/j.1365-2958.1998.01031.x

Matsumoto, K., Hara, H., Fishov, I., Mileykovskaya, E., and Norris, V. (2015). The membrane: transertion as an organizing principle in membrane heterogeneity. *Front. Microbiol.* 6:572. doi: 10.3389/fmicb.2015.00572

Morgan, J. K., Luedtke, B. E., and Shaw, E. I. (2010). Polar localization of the *Coxiella burnetii* type IVB secretion system. *FEMS Microbiol. Lett.* 305, 177–183. doi: 10.1111/j.1574-6968.2010.01926.x

Mougous, J. D., Cuff, M. E., Raunser, S., Shen, A., Zhou, M., Gifford, C. A., et al. (2006). A virulence locus of *Pseudomonas aeruginosa* encodes a protein secretion apparatus. *Science* 312, 1526–1530. doi: 10.1126/science.1128393

Mühlradt, P. F., Menzel, J., Golecki, J. R., and Speth, V. (1973). Outer membrane of *Salmonella*. *Eur. J. Biochem.* 35, 471–481.

Murdoch, S. L., Trunk, K., English, G., Fritsch, M. J., Pourkarimi, E., and Coulthurst, S. J. (2011). The opportunistic pathogen *Serratia marcescens* utilizes type VI secretion to target bacterial competitors. *J. Bacteriol.* 193, 6057–6069. doi: 10.1128/JB.05671-11

Noinaj, N., Gumbart, J. C., and Buchanan, S. K. (2017). The β-barrel assembly machinery in motion. *Nat. Rev. Microbiol.* 15, 197–204. doi: 10.1038/nrmicro.2016.191

Notti, R. Q., Bhattacharya, S., Lilic, M., and Stebbins, C. E. (2015). A common assembly module in injectisome and flagellar type III secretion sorting platforms. *Nat. Commun.* 6:7125. doi: 10.1038/ncomms8125

Notti, R. Q., and Stebbins, C. E. (2016). The structure and function of type III secretion systems. *Microbiol. Spectr.* 4:VMBF-0004-2015. doi: 10.1128/microbiolspec.VMBF-0004-2015

Oddershede, L., Dreyer, J. K., Grego, S., Brown, S., and Berg-Sørensen, K. (2002). The motion of a single molecule, the λ-receptor, in the bacterial outer membrane. *Biophys. J.* 83, 3152–3161. doi: 10.1016/S0006-3495(02)75318-6

Overbye, L. J., Sandkvist, M., and Bagdasarian, M. (1993). Genes required for extracellular secretion of enterotoxin are clustered in *Vibrio cholerae*. *Gene* 132, 101–106. doi: 10.1016/0378-1119(93)90520-D

Patterson, G., Davidson, M., Manley, S., and Lippincott-Schwartz, J. (2010). Superresolution imaging using single-molecule localization. *Annu. Rev. Phys. Chem.* 61, 345–367. doi: 10.1146/annurev.physchem.012809.103444

Peabody, C. R., Chung, Y. J., Yen, M.R., Vidal-Ingigliardi, D., Pugsley, A. P., and Saier, M. H. (2003). Type II protein secretion and its relationship to bacterial type IV pili and archaeal flagella. *Microbiology* 149, 3051–3072. doi: 10.1099/mic.0.26364-0

Plummer, A. M., and Fleming, K. G. (2016). From chaperones to the membrane with a BAM! *Trends Biochem. Sci.* 41, 872–882. doi: 10.1016/j.tibs.2016.06.005

Pukatzki, S., Ma, A. T., Revel, A. T., Sturtevant, D., and Mekalanos, J. J. (2007). Type VI secretion system translocates a phage tail spike-like protein into target cells where it cross-links actin. *Proc. Natl. Acad. Sci. U.S.A.* 104, 15508–15513. doi: 10.1073/pnas.0706532104

Pukatzki, S., Ma, A. T., Sturtevant, D., Krastins, B., Sarracino, D., Nelson, W. C., et al. (2006). Identification of a conserved bacterial protein secretion system in *Vibrio cholerae* using the *Dictyostelium* host model system. *Proc. Natl. Acad. Sci. U.S.A.* 103, 1528–1533. doi: 10.1073/pnas.0510322103

Radics, J., Konigsmaier, L., and Marlovits, T. C. (2014). Structure of a pathogenic type 3 secretion system in action. *Nat. Struct. Mol. Biol.* 21, 82–87. doi: 10.1038/nsmb.2722

Rassam, P., Copeland, N. A., Birkholz, O., Tóth, C., Chavent, M., Duncan, A. L., et al. (2015). Supramolecular assemblies underpin turnover of outer membrane proteins in bacteria. *Nature* 523, 333–336. doi: 10.1038/nature14461

Ritchie, K., Lill, Y., Sood, C., Lee, H., and Zhang, S. (2013). Single-molecule imaging in live bacteria cells. *Phil. Trans. R. Soc. B* 368:20120355. doi: 10.1098/rstb.2012.0355

Rothenberg, E., Sepúlveda, L. A., Skinner, S. O., Zeng, L., Selvin, P. R., and Golding, I. (2011). Single-virus tracking reveals a spatial receptor-dependent search mechanism. *Biophys. J.* 100, 2875–2882. doi: 10.1016/j.bpj.2011.05.014

Rust, M. J., Bates, M., and Zhuang, X. (2006). Sub-diffraction-limit imaging by stochastic optical reconstruction microscopy (STORM). *Nat. Methods* 3, 793–796. doi: 10.1038/nmeth929

Samsudin, F., Ortiz-Suarez, M. L., Piggot, T. J., Bond, P. J., and Khalid, S. (2016). OmpA: a flexible clamp for bacterial cell wall attachment. *Structure* 24, 2227–2235. doi: 10.1016/j.str.2016.10.009

Sandkvist, M., Michel, L. O., Hough, L. P., Morales, V. M., Bagdasarian, M., Koomey, M., et al. (1997). General secretion pathway (eps) genes required for toxin secretion and outer membrane biogenesis in *Vibrio cholerae*. *J. Bacteriol.* 179, 6994–7003. doi: 10.1128/jb.179.22.6994-7003.1997

Schindler, M., Osborn, M. J., and Koppel, D. E. (1980). Lateral diffusion of lipopolysaccharide in the outer membrane of *Salmonella typhimurium*. *Nature* 285, 261–263. doi: 10.1038/285261a0

Schirmer, T., Keller, T. A., Wang, Y.-F., and Rosenbusch, J. P. (1995). Structural basis for sugar translocation through maltoporin channels at 3.1 angstrom resolution. *Science* 267:512. doi: 10.1126/science.7824948

Schlumberger, M. C., Müller, A. J., Ehrbar, K., Winnen, B., Duss, I., Stecher, B., et al. (2005). Real-time imaging of type III secretion: *Salmonella* SipA injection into host cells. *Proc. Natl. Acad. Sci. U.S.A.* 102, 12548–12553. doi: 10.1073/pnas.0503407102

Schwarz, S., Singh, P., Robertson, J. D., LeRoux, M., Skerrett, S. J., Goodlett, D. R., et al. (2014). VgrG-5 is a *Burkholderia* type VI secretion system-exported protein required for multinucleated giant cell formation and virulence. *Infect. Immun.* 82, 1445–1452. doi: 10.1128/IAI.01368-13

Schwarz, S., West, T. E., Boyer, F., Chiang, W.-C., Carl, M. A., Hood, R. D., et al. (2010). *Burkholderia* type VI secretion systems have distinct roles in eukaryotic and bacterial cell interactions. *PLoS Pathog.* 6:e1001068. doi: 10.1371/journal.ppat.1001068

Shrivastava, R., and Miller, J. F. (2009). Virulence factor secretion and translocation by *Bordetella* species. *Curr. Opin. Microbiol.* 12, 88–93. doi: 10.1016/j.mib.2009.01.001

Sikora, A. E., Zielke, R. A., Lawrence, D. A., Andrews, P. C., and Sandkvist, M. (2011). Proteomic analysis of the *Vibrio cholerae* type II secretome reveals new proteins, including three related serine proteases. *J. Biol. Chem.* 286, 16555–16566. doi: 10.1074/jbc.M110.211078

Slusky, J. S. (2017). Outer membrane protein design. *Curr. Opin. Struct. Biol.* 45, 45–52. doi: 10.1016/j.sbi.2016.11.003

Smit, J., and Nikaido, H. (1978). Outer membrane of gram-negative bacteria. XVIII. Electron microscopic studies on porin insertion sites and growth of cell surface of *Salmonella typhimurium*. *J. Bacteriol.* 135, 687–702.

So, E. C., Mattheis, C., Tate, E. W., Frankel, G., and Schroeder, G. N. (2015). Creating a customized intracellular niche: subversion of host cell signaling by *Legionella* type IV secretion system effectors 1. *Can. J. Microbiol.* 61, 617–635. doi: 10.1139/cjm-2015-0166

Spector, J., Zakharov, S., Lill, Y., Sharma, O., Cramer, W. A., and Ritchie, K. (2010). Mobility of BtuB and OmpF in the *Escherichia coli* outer membrane: implications for dynamic formation of a translocon complex. *Biophys. J.* 99, 3880–3886. doi: 10.1016/j.bpj.2010.10.029

Spreter, T., Yip, C. K., Sanowar, S., Andre, I., Kimbrough, T. G., Vuckovic, M., et al. (2009). A conserved structural motif mediates formation of the periplasmic rings in the type III secretion system. *Nat. Struct. Mol. Biol.* 16, 468–476. doi: 10.1038/nsmb.1603

Thiem, S., Kentner, D., and Sourjik, V. (2007). Positioning of chemosensory clusters in *E. coli* and its relation to cell division. *EMBO J.* 26, 1615–1623. doi: 10.1038/sj.emboj.7601610

Thiem, S., and Sourjik, V. (2008). Stochastic assembly of chemoreceptor clusters in *Escherichia coli*. *Mol. Microbiol.* 68, 1228–1236. doi: 10.1111/j.1365-2958.2008.06227.x

Thomas, S., Holland, I. B., and Schmitt, L. (2014). The type 1 secretion pathway—the hemolysin system and beyond. *Biochim. Biophys. Acta* 1843, 1629–1641. doi: 10.1016/j.bbamcr.2013.09.017

Toomre, D., and Bewersdorf, J. (2010). A new wave of cellular imaging. *Annu. Rev. Cell Dev. Biol.* 26, 285–314. doi: 10.1146/annurev-cellbio-100109-104048

Trokter, M., Felisberto-Rodrigues, C., Christie, P. J., and Waksman, G. (2014). Recent advances in the structural and molecular biology of type IV secretion systems. *Curr. Opin. Struct. Biol.* 27, 16–23. doi: 10.1016/j.sbi.2014.02.006

Turnbull, L., Toyofuku, M., Hynen, A. L., Kurosawa, M., Pessi, G., Petty, N. K., et al. (2016). Explosive cell lysis as a mechanism for the biogenesis of bacterial membrane vesicles and biofilms. *Nat Commun.* 7:11220. doi: 10.1038/ncomms11220

Ursell, T. S., Trepagnier, E. H., Huang, K. C., and Theriot, J. A. (2012). Analysis of surface protein expression reveals the growth pattern of the gram-negative outer membrane. *PLoS Comput. Biol.* 8:e1002680. doi: 10.1371/journal.pcbi.1002680

van Ulsen, P., ur Rahman, S. U., Jong, W. S., Daleke-Schermerhorn, M. H., and Luirink, J. (2014). Type V secretion: from biogenesis to biotechnology. *Biochim. Biophys. Acta* 1843, 1592–1611. doi: 10.1016/j.bbamcr.2013.11.006

Verhoeven, G. S., Dogterom, M., and den Blaauwen, T. (2013). Absence of long-range diffusion of OmpA in *E. coli* is not caused by its peptidoglycan binding domain. *BMC Microbiol.* 13:66. doi: 10.1186/1471-2180-13-66

Voth, D. E., and Heinzen, R. A. (2007). Lounging in a lysosome: the intracellular lifestyle of *Coxiella burnetii*. *Cell. Microbiol.* 9, 829–840. doi: 10.1111/j.1462-5822.2007.00901.x

Wang, H., Wingreen, N. S., and Mukhopadhyay, R. (2008). Self-organized periodicity of protein clusters in growing bacteria. *Phys. Rev. Lett.* 101:218101. doi: 10.1103/PhysRevLett.101.218101

Ward, D. V., Draper, O., Zupan, J. R., and Zambryski, P. C. (2002). Peptide linkage mapping of the *Agrobacterium tumefaciens* vir-encoded type IV secretion system reveals protein subassemblies. *Proc. Natl. Acad. Sci. U.S.A.* 99, 11493–11500. doi: 10.1073/pnas.172390299

Wong, A. R., Pearson, J. S., Bright, M. D., Munera, D., Robinson, K. S., Lee, S. F., et al. (2011). Enteropathogenic and enterohaemorrhagic *Escherichia coli*: even more subversive elements. *Mol. Microbiol.* 80, 1420–1438. doi: 10.1111/j.1365-2958.2011.07661.x

Xie, X. S., Choi, P. J., Li, G. W., Lee, N. K., and Lia, G. (2008). Single-molecule approach to molecular biology in living bacterial cells. *Annu. Rev. Biophys.* 37, 417–444. doi: 10.1146/annurev.biophys.37.092607.174640

Zoued, A., Brunet, Y. R., Durand, E., Aschtgen, M.S., Logger, L., Douzi, B., et al. (2014). Architecture and assembly of the Type VI secretion system. *Biochim. Biophys. Acta* 1843, 1664–1673. doi: 10.1016/j.bbamcr.2014.03.018

Zoued, A., Durand, E., Brunet, Y. R., Spinelli, S., Douzi, B., Guzzo, M., et al. (2016). Priming and polymerization of a bacterial contractile tail structure. *Nature* 531, 59–63. doi: 10.1038/nature17182

Zupan, J., Muth, T. R., Draper, O., and Zambryski, P. (2000). The transfer of DNA from *Agrobacterium tumefaciens* into plants: a feast of fundamental insights. *Plant J.* 23, 11–28. doi: 10.1046/j.1365-313x.2000.00808.x

**Conflict of Interest Statement:** The authors declare that the research was conducted in the absence of any commercial or financial relationships that could be construed as a potential conflict of interest.

frontiers in Cellular and Infection Microbiology

ORIGINAL RESEARCH
published: 31 May 2017
doi: 10.3389/fcimb.2017.00207

# Identification of a Large Family of Slam-Dependent Surface Lipoproteins in Gram-Negative Bacteria

*Yogesh Hooda, Christine C. L. Lai and Trevor F. Moraes* *

*Department of Biochemistry, University of Toronto, Toronto, ON, Canada*

The surfaces of many Gram-negative bacteria are decorated with soluble proteins anchored to the outer membrane via an acylated N-terminus; these proteins are referred to as surface lipoproteins or SLPs. In *Neisseria meningitidis*, SLPs such as transferrin-binding protein B (TbpB) and factor-H binding protein (fHbp) are essential for host colonization and infection because of their essential roles in iron acquisition and immune evasion, respectively. Recently, we identified a family of outer membrane proteins called Slam (Surface lipoprotein assembly modulator) that are essential for surface display of neisserial SLPs. In the present study, we performed a bioinformatics analysis to identify 832 Slam related sequences in 638 Gram-negative bacterial species. The list included several known human pathogens, many of which were not previously reported to possess SLPs. Hypothesizing that genes encoding SLP substrates of Slams may be present in the same gene cluster as the Slam genes, we manually curated neighboring genes for 353 putative Slam homologs. From our analysis, we found that 185 (~52%) of the 353 putative Slam homologs are located adjacent to genes that encode a protein with an N-terminal lipobox motif. This list included genes encoding previously reported SLPs in *Haemophilus influenzae* and *Moraxella catarrhalis*, for which we were able to show that the neighboring Slams are necessary and sufficient to display these lipoproteins on the surface of *Escherichia coli*. To further verify the authenticity of the list of predicted SLPs, we tested the surface display of one such Slam-adjacent protein from *Pasteurella multocida*, a zoonotic pathogen. A robust Slam-dependent display of the *P. multocida* protein was observed in the *E. coli* translocation assay indicating that the protein is a Slam-dependent SLP. Based on multiple sequence alignments and domain annotations, we found that an eight-stranded beta-barrel domain is common to all the predicted Slam-dependent SLPs. These findings suggest that SLPs with a TbpB-like fold are found widely in *Proteobacteria* where they exist with their interaction partner Slam. In the future, SLPs found in pathogenic bacteria can be investigated for their role in virulence and may also serve as candidates for vaccine development.

**Keywords: gram-negative bacteria, surface lipoproteins, outer membrane transporters, bacterial gene clusters, protein translocation pathways, flow cytometry**

OPEN ACCESS

***Edited by:***
*Romé Voulhoux, Centre National de la Recherche Scientifique UMR7255 IMM Aix Marseille University, France*

***Reviewed by:***
*Françoise Jacob-Dubuisson, Centre National de la Recherche Scientifique (CNRS), France*
*Trevor Lithgow, Monash University, Australia*
*Jan Tommassen, Utrecht University, Netherlands*

***Correspondence:**
*Trevor F. Moraes*
*trevor.moraes@utoronto.ca*

***Received:*** *14 March 2017*
***Accepted:*** *09 May 2017*
***Published:*** *31 May 2017*

***Citation:***
*Hooda Y, Lai CC and Moraes TF (2017) Identification of a Large Family of Slam-Dependent Surface Lipoproteins in Gram-Negative Bacteria. Front. Cell. Infect. Microbiol. 7:207. doi: 10.3389/fcimb.2017.00207*

## INTRODUCTION

Gram-negative bacteria contain an asymmetric outer membrane that protects the bacteria from environmental stress and acts as a shield from harmful chemicals (Silhavy et al., 2010). However, this creates a logistic challenge for the transport of various biomolecules to and from the extracellular milieu and across the outer membrane of the bacteria (Pagès et al., 2008; Delcour, 2009). Toward this end, Gram-negative bacteria have developed dedicated translocation systems that deliver various families of proteins and other biomolecules across the outer membrane (Nikaido, 2003; Costa et al., 2015; Geyter et al., 2016). The mechanism for this transport is distinct from translocation systems found in the inner membrane owing to the lack of ATP in the periplasm and is an active field of research (Karuppiah et al., 2011).

Surface lipoproteins or SLPs are a class of soluble proteins that are present on the surface of Gram-negative bacteria. They are anchored to the outer membrane via three fatty acyl chains that are post-translationally attached to their N-termini (Wilson and Bernstein, 2016). The first reported SLP was TraT, a protein of the F sex factor in *E. coli* (Manning et al., 1980). Several other SLPs were identified soon after within a few Gram-negative bacterial families including *Klebsiella* (Pugsley et al., 1986), *Neisseria* (Schryvers and Morris, 1988), and *Spirochetes* (Chamberlain et al., 1989; Brandt et al., 1990). Recently, there has been an increase in the number of reports of SLPs from different bacterial species with distinct structural folds and surface topologies (Konovalova and Silhavy, 2015). SLPs are involved in several important cellular pathways for nutrient acquisition, cellular adhesion and stress response (Zückert, 2014; Szewczyk and Collet, 2016; Wilson and Bernstein, 2016).

The discovery of SLPs in different bacteria has raised questions regarding the biosynthetic pathway used by these proteins for their synthesis and transport to the surface. SLPs are synthesized in the cytoplasm and transported to the periplasm by the Sec or Tat machinery based on the signal sequence present on the SLPs (Chatzi et al., 2013). Once in the periplasm, three enzymes in the inner membrane process the SLPs by cleaving the signal sequence and attaching three fatty acyl chains to the N-terminal cysteine residue (Szewczyk and Collet, 2016). Upon lipidation, most SLPs are transported across the periplasm to the inner leaflet of the outer membrane through the Lol system (Okuda and Tokuda, 2011). However, there are a few exceptions to this rule, including pullulanase that avoids the Lol system and moves to the surface through the Type-II secretion system (D'Enfert et al., 1987). Additionally, in *Borrelia* sp., SLPs are proposed to require a periplasmic "holding" chaperone that prevents premature folding of SLPs before reaching the outer membrane (Chen and Zückert, 2011; Zückert, 2014).

Upon insertion into the outer membrane, the translocation systems required for the movement of SLPs across the outer membrane remain poorly characterized. The first SLP for which the export pathway was characterized was pullulanase in *Klebsiella* sp. that utilizes the Type II secretion system (D'Enfert et al., 1987). More recent studies have shown that NalP (a neisserial SLP) functions as a Type Va "autotransporter" secretion system (Van Ulsen et al., 2003), while BamC (Webb et al., 2012) and RscF (Cho et al., 2014; Konovalova et al., 2014) in *E. coli* use the Bam complex to move across the outer membrane. Functional and mutagenesis studies in *Borrelia* sp. (Schulze et al., 2010; Chen and Zückert, 2011) and *Bacteroides* sp. (Lauber et al., 2016) have shown that the sorting rules used by these SLPs are distinct from other SLPs, indicating that different bacterial species may possess different translocation systems for the delivery of SLPs. Additionally, within *Neisseria* sp., *two* distinct SLP export pathways have been reported (Hooda et al., 2017), suggesting that multiple systems for the export of SLPs may exist in a single bacterial species.

The SLPs found in the genus *Neisseria* are amongst the most extensively studied SLPs. *N. meningitidis* and *N. gonorrhoeae* encode multiple SLPs that are involved in a variety of cellular pathways critical for survival of neisserial pathogens in humans (Hooda et al., 2017). In *N. meningitidis*, eight SLPs have been well-characterized, of which three [transferrin-binding protein B (TbpB) (Schryvers and Morris, 1988), lactoferrin-binding protein B (LbpB) (Pettersson et al., 1998) and hemoglobin-haptoglobin utilization protein (HpuA) (Lewis et al., 1997)] are involved in iron acquisition while two others: factor-H binding protein (fHbp) (Madico et al., 2006) and neisserial heparin binding antigen (NHBA) (Serruto et al., 2010) are involved in immune evasion. Other neisserial SLPs include *Neisseria* autotransporter protease (NalP) (Van Ulsen et al., 2003), anaerobically induced protein A (AniA) (Hoehn and Clark, 1992) and macrophage infectivity potentiator (MIP) (Leuzzi et al., 2005) which play roles in extracellular proteolysis, anaerobic growth and intracellular survival respectively. These SLPs have been shown to bind to different human factors and atomic resolution full-length or partial structures of these SLPs have aided in understanding their mechanism of action (Hooda et al., 2017). Recently, we described a family of outer membrane proteins called Slam or Surface lipoprotein assembly modulator that is essential for surface display of a subset of neisserial SLPs (Hooda et al., 2016). *N. meningitidis* contains two Slam proteins: Slam1 is necessary for the display of TbpB, LbpB, and fHbp, whereas Slam2 is specifically required for the SLP HpuA. Furthermore, Slam have been shown to potentiate the functional display of neisserial SLPs on the surface of laboratory strains of *E. coli* that do not possess any Slam or SLP homologs (Hooda et al., 2016). This work suggested that a subset of neisserial SLPs utilize a unique mechanism to get to the cell surface that is dependent on the Slam family of outer membrane proteins.

In our previous work, we discovered that genes encoding Slam2 and HpuA are adjacent to each other in multiple neisserial genomes (Hooda et al., 2016). Based on this observation, we searched and annotated genes upstream and downstream of 353 putative Slam homologs found in other proteobacterial species. This dataset showed that a large number of Slam related sequences are located adjacent to genes that encode putative lipoproteins with TbpB-like folds suggesting a genetic linkage between these two families of proteins. The bioinformatics analysis allowed us to identify TbpB-like SLPs in many bacterial species that were previously not known to possess SLPs, including the human pathogens

*Acinetobacter baumannii* and *Salmonella enterica* subsp. *arizonae*.

# MATERIALS AND METHODS

## Identification of Slam Homologs

To generate a database of Slam related sequences, iterative psi-blast searches were performed (March 4, 2016) against a non-redundant database containing all partial and complete bacterial genome sequences using the sequence of Slam1 protein (NMB0313) from *Neisseria meningitidis* strain MC58 as the query. Four independent psi-blast searches were performed for different clades of proteobacteria (alpha-, beta-, gamma-, and delta/epsilon/zeta-proteobacteria). The lists of putative Slam genes obtained from these four psi-blast searches were pooled and only unique representative Slam sequences were kept from a given bacterial species. The list was manually checked to remove the following: (i) partial sequences (containing premature stop codons or with partial gene sequence coverage), and (ii) sequences coding for only the N-terminal domain (Ntd) of Slam. This gave a final list (Supplementary Data 1) of 832 Slam sequences spanning 638 bacterial species.

To understand the distribution of Slam related sequences, a phylogenetic tree of different proteobacterial species was made using the 16S-RNA sequences obtained from the database Greengenes (DeSantis et al., 2006). One representative member was kept from each family of bacteria. In total 52 species (8: alpha-, 10: beta-, 23: gamma-, 5: delta-, 5: epsilon-, and 1: zeta-proteobacteria) were selected for the final tree. The tree was made using the PhyML plugin in the software Geneious (Kearse et al., 2012) with 100 bootstraps. The nodes were kept if they appeared in 60% of the bootstrap runs. The presence of Slam related sequences was mapped on the phylogenetic tree.

## Analysis of Gene Neighborhoods Around Putative Slam Homologs

The list of 353 Slam related sequences generated in our previous study (Hooda et al., 2016) was used to further investigate the neighboring genes in the Slam gene clusters. This number is more than a third of the total Slam related sequences and covers all major bacterial phyla that possess Slam related sequences, except for epsilon- and zeta-proteobacteria (Supplementary Data 1). In selecting genomes for a given bacterial species, fully sequenced reference genomes were given preference. For each of the Slam related genes present in these species, the corresponding genomic record (NCBI genome) was used to identify genes upstream and downstream along with their corresponding functional annotations (NCBI protein database, Ensembl bacteria). In a few of the cases, no genes were predicted upstream or downstream as the Slam related genes were close to the beginning or the end of the contig respectively and these sequences were ignored.

Within the Slam related gene clusters, a number of the neighboring genes were predicted to encode lipoproteins (predicted by an N-terminal lipobox motif using LipoP and/or SignalP) and we also found many examples of genes encoding TonB dependent transporters (IPR000531). The putative lipoproteins were annotated as either GNA1870-related lipoproteins, TBP-like solute-binding proteins or pagP-beta barrel proteins (InterPro signature; IPR01490; IPR001677; IPR011250 respectively). All the genes with one of the above-mentioned annotations are included in Supplementary Data 2.

## Bacterial Strains and Growth Conditions

Strains used in this study are summarized in Supplementary Table 1. *E. coli* were grown in LB media containing antibiotics when necessary (50 μg/mL kanamycin and 100 μg/mL ampicillin). Cloning procedures were carried out using *E. coli* MM294 competent cells. Protein expression was performed using *E. coli* C43 (DE3) cells for all the flow-cytometry and western blot analysis.

## Generation of Plasmids for Expression of Slams and SLPs

For flow cytometry experiments, the three SLPs (*Haemophilus influenzae* TbpB, *Moraxella catarrhalis* TbpB and *Pasteurella multocida* PM1514) were cloned into pET52b (to make pET52b *Hinf* TbpB, *Mcat* TbpB or *Pmul* SLP) using the restriction-free (RF) cloning strategy (van den Ent and Löwe, 2006). The *tbpb* genes were amplified from the genomes of *H. influenzae* strain 86-028NP and *M. catarrhalis* strain O35E, and the *pm1514* gene was amplified from *P. multocida* strain h48. A FLAG tag was inserted on the C-terminus of *M. catarrhalis tbpb* using FastCloning (Li et al., 2011) to make pET52b Mcat TbpB-flag. pET52b PmSLP-flag and pET52b PmSLP-flag-Slam was cloned by replacing the *catarrhalis tbpb* gene with *pm1514* and *pm1515-pm1514* respectively in frame with the FLAG tag using RF cloning.

The corresponding Slams were inserted into pET26b (pET26 *Hinf* Slam1, *Mcat* Slam1, and *Pmul* Slam) using RF cloning (van den Ent and Löwe, 2006). A 6xHis-tag was inserted between the *pelB* and the mature Slam sequences.

## Flow Cytometry

For the *E. coli* translocation assays, the display of an SLP was determined using flow cytometry. Pairs of SLP and Slam plasmids (shown in Supplementary Table 1) were transformed into C43 (DE3) cells and grown in 1 mL of auto-induction media (Studier, 2005) for 18 h at 37°C. *H. influenzae* Slam showed poor expression when grown overnight in autoinduction media. Hence, for *H. influenzae* TbpB flow cytometry assays were performed by growing cells at 37°C to an $OD_{600}$ ∼ 0.6 and then inducing protein expression by the addition of 1 mM isopropyl β-D-1-thiogalactopyranoside (IPTG). Upon induction, cells were grown at 18°C for 16–18 h. Cells were harvested, washed twice in PBS containing 1 mM $MgCl_2$, and incubated with α-Flag antibodies (1:200, Sigma), or biotinylated human transferrin (0.05 mg/ml, Sigma) for 1 h at 4°C. The cells were then washed twice with PBS containing 1 mM $MgCl_2$ and then labeled with R-phycoerythrin (R-PE) conjugated Streptavidin (0.5 mg/ml, Cedarlane) or R-PE conjugated α-mouse IgG (25 μg/mL, Thermo Fisher Scientific) for 1 h at 4°C. Following staining, cells were fixed in 2% formaldehyde for 20 min and further washed with PBS containing 1 mM

$MgCl_2$. Flow cytometry was performed with a Becton Dickinson FACSCalibur and the results were analyzed using FLOWJO software. Mean fluorescence intensity (MFI) from at least three biological replicates were used to compare surface exposure of a given SLP between different samples. Statistical significance was calculated by comparing MFI between different samples using the one-way ANOVA test available in the software Prism 6.

Western blots were used to test the expression levels of each of the constructs used for the flow cytometry experiments. α-Flag (1:5,000, Sigma) and α-His (1:5,000, Thermo Fisher Scientific) antibodies were used to test expression of the SLP and Slam constructs respectively. α-GroEL (1:10,000) antibodies were used as loading controls.

## Sucrose Density Ultracentrifugation

*E. coli* C43(DE3) cells expressing pET52b PmSLP-flag and pET26b empty or pET26 PmSlam were grown overnight and then used to inoculate 50 ml LB with the appropriate antibiotic. The cells were grown to an $OD_{600} \sim 0.6$, induced with 1 mM IPTG and then grown for an additional 18 h. The cells were pelleted, resuspended in 20 mM Tris pH 8.0, 200 mM NaCl with fresh lysozyme (1 mg/ml), 2 mM PMSF and DNase I (0.05 mg/ml), lysed by sonication and then centrifuged at 10,000 r.c.f. to remove cell debris. The supernatant was centrifuged at 125,000 r.c.f. for 1 h to collect the cellular membranes. The membrane pellet was resuspended in 1 ml of 20 mM Tris pH 8.0, 200 mM NaCl using a micro-glass homogenizer.

The inner and the outer membrane of *E. coli* were separated using a modified sucrose density ultracentrifugation protocol that was previously described (Hooda et al., 2016). For this assay, 100 µl of the membrane pellet was applied on top of a 13.2 ml thin-wall polypropylene tube containing step gradients of 3 ml of 2.02 M, 6 ml of 1.44 M and 3 ml of 0.77 M sucrose. The tubes were centrifuged at 83,000 r.c.f. for 16 h. The outer membrane and inner membranes partitioned to the interface of the 2 M and 1.44 M sucrose cushions and 1.44 M and 0.77 M sucrose layers, respectively. Twelve 1 ml fractions were collected and subjected to SDS–PAGE followed by western blotting with α-Flag (1:10,000), α-LepB (1:10,000), and α-OmpA (1:40,000) antibodies.

# RESULTS

## Identification of Putative Slam Homologs in Gram-Negative Bacteria

In a previous study, we had used the *N. meningitidis* Slam1 sequence to perform psi-blast searches (Altschul et al., 1997) and identified 353 putative Slam homologs in 225 Gram-negative bacteria (Hooda et al., 2016). All identified Slam related sequences possessed an N-terminal domain (Ntd) predicted to contain tetratricopeptide repeats(TPR) and a C-terminal beta-barrel domain annotated as a DUF560 domain (**Figure 1A**). Since that study, a large number of bacterial genomes have been sequenced by next-generation sequencing techniques. Hence, we performed updated psi-blast searches and were able to identify 832 Slam related sequences in 638 Gram-negative bacteria (Supplementary Data 1). The Slam1 gene (*nmb0313*) was used as the search template and we manually analyzed the list to remove genes for which only partial sequences were available. We also removed several hits that contained a large single domain with TPR repeats that are similar to the TPR repeats found in Slam-Ntd. As was previously observed, all Slam sequences obtained in our dataset contained both the Ntd and DUF560 domains and no sequences containing only the DUF560 were obtained. With these additional genomic sequences, we were able to identify Slam related sequences in all clades of the phylum *Proteobacteria* (**Figure 1B**). Slam related sequences were identified in bacterial species living in diverse environments including free-living, commensal and/or pathogenic bacteria. Slam-like proteins are predicted to be found in many human pathogens such as *Vibrio cholerae*, *Salmonella enterica* subsp. *arizonae,* and *Acinetobacter baumannii*.

## Slams Adjacent to TbpB in *M. catarrhalis* and *H. influenzae* Translocate Their Respective TbpBs to the Surface in *E. coli*

A number of potential Slam homologs identified in this study were found in bacterial species that colonize the upper respiratory tract of mammals. Human respiratory tract bacteria that contain Slam sequences include *N. meningitidis, M. catarrhalis* and the HACEK (*Haemophilus, Aggregatibacter, Cardiobacterium, Eikenella, Kingella*) group of bacteria (Nørskov-Lauritsen, 2014). Slam sequences were also identified in bacteria that colonize the upper respiratory tract of cattle (*Moraxella bovis*, *Mannheimia haemolytica,* and *Histophilus somni*) and pigs (*Actinobacillus pleuropneumoniae*). Many of these species have been reported to contain transferrin-binding surface lipoproteins that are homologs of TbpB in *N. meningitidis* (Gray-Owen and Schyvers, 1996). Not surprisingly, two TbpB homologs in *M. catarrhalis* (Yu and Schryvers, 1993) and *H. influenzae* (Gray-Owen et al., 1995) were found to be adjacent to putative Slam genes (**Figure 2A**). Both *M. catarrhalis* and *H. influenzae* are human pathogens and their TbpBs have been previously shown to bind to human transferrin. The presence of TbpB genes adjacent to a Slam gene in their genome strongly suggests that these bacteria use a Slam-dependent translocation system to deliver TbpBs to the bacterial cell surface.

To confirm that these TbpBs depend on their adjacent Slam for translocation to the cell surface, we introduced the gene encoding TbpB in *M. catarrhalis* in laboratory strains of *E. coli* with and without its neighboring Slam. To monitor the expression of *M. catarrhalis* TbpB, we introduced a FLAG-tag at the C-terminus of TbpB. We labeled the cells with biotinylated human transferrin or α-Flag antibodies (**Figure 2B**). Flow cytometry was used to quantify the amount of *M. catarrhalis* TbpB on the surface of the cell. An increase in *M. catarrhalis* TbpB was observed only in the presence of its neighboring Slam and was quantified using mean fluorescence intensity (MFI) (**Figure 2C**). Western blots with α-Flag and by α-His antibodies were used to test the expression of *M. catarrhalis* TbpB & Slam respectively (**Figure 2C**, lower panel). *M. catarrhalis* TbpB was robustly displayed on the surface of *E. coli* in the presence of Slam

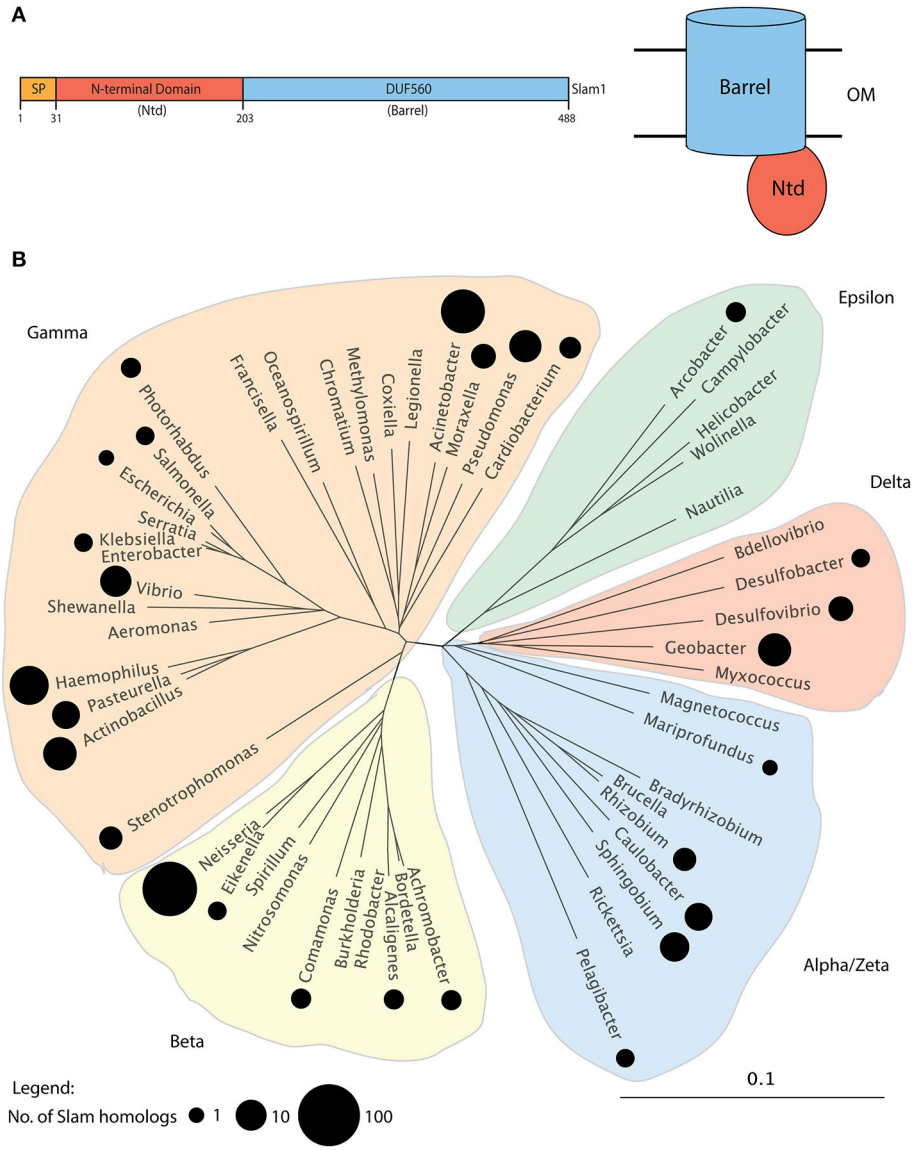


**FIGURE 1 | Putative Slam family of proteins in Gram-negative bacteria. (A)** Domain architecture of *N. meningitidis* Slam1. Slams possess 2 domains: a periplasmic N-terminal domain (Ntd) containing tetratricopeptide repeats and a predicted membrane bound 14-stranded barrel domain referred to as DUF560. **(B)** Distribution of Slam related sequences in *Proteobacteria*. A family tree of *Proteobacteria* was made using 16S-RNA sequences from 52 species representing the major bacterial families within *Proteobacteria*. The families containing at least 1 species with a Slam related sequence containing both the Ntd and DUF560 domains are highlighted by black circles. The size of the circle represents the number of Slams identified in a given bacterial family. Slams were found within all clades of *Proteobacteria*.

confirming that this TbpB homolog also uses a Slam-dependent system to reach the cell surface.

To verify that the FLAG-tag did not affect the Slam-dependent display of *M. catarrhalis* TbpB, we also tested the surface display of *M. catarrhalis* TbpB without the FLAG-tag in laboratory strains of *E. coli*. We labeled the cells using biotinylated human transferrin to test the functional display of the TbpB. Flow cytometry was used to quantify the amount of TbpB located on the surface of the cell. Similar to the results obtained for the FLAG-tagged construct, an increase in signal was obtained only in the presence of the neighboring Slam gene suggesting that the FLAG-tag does not affect translocation (**Figure 2D**). Additionally, we also tested the surface display of *H. influenzae* TbpB with or without its neighboring Slam using biotinylated human transferrin. In this case, a signal increase was obtained on the surface of *E. coli* in the presence of Slam, however the signal was weaker compared to *M. catarrhalis* TbpB. Westerns blot analysis using α-His antibody suggested that *M. catarrhalis* Slam (**Figure 2D**, lower panel) is expressed much more strongly in comparison to *H. influenzae* Slam (**Figure 2E**,

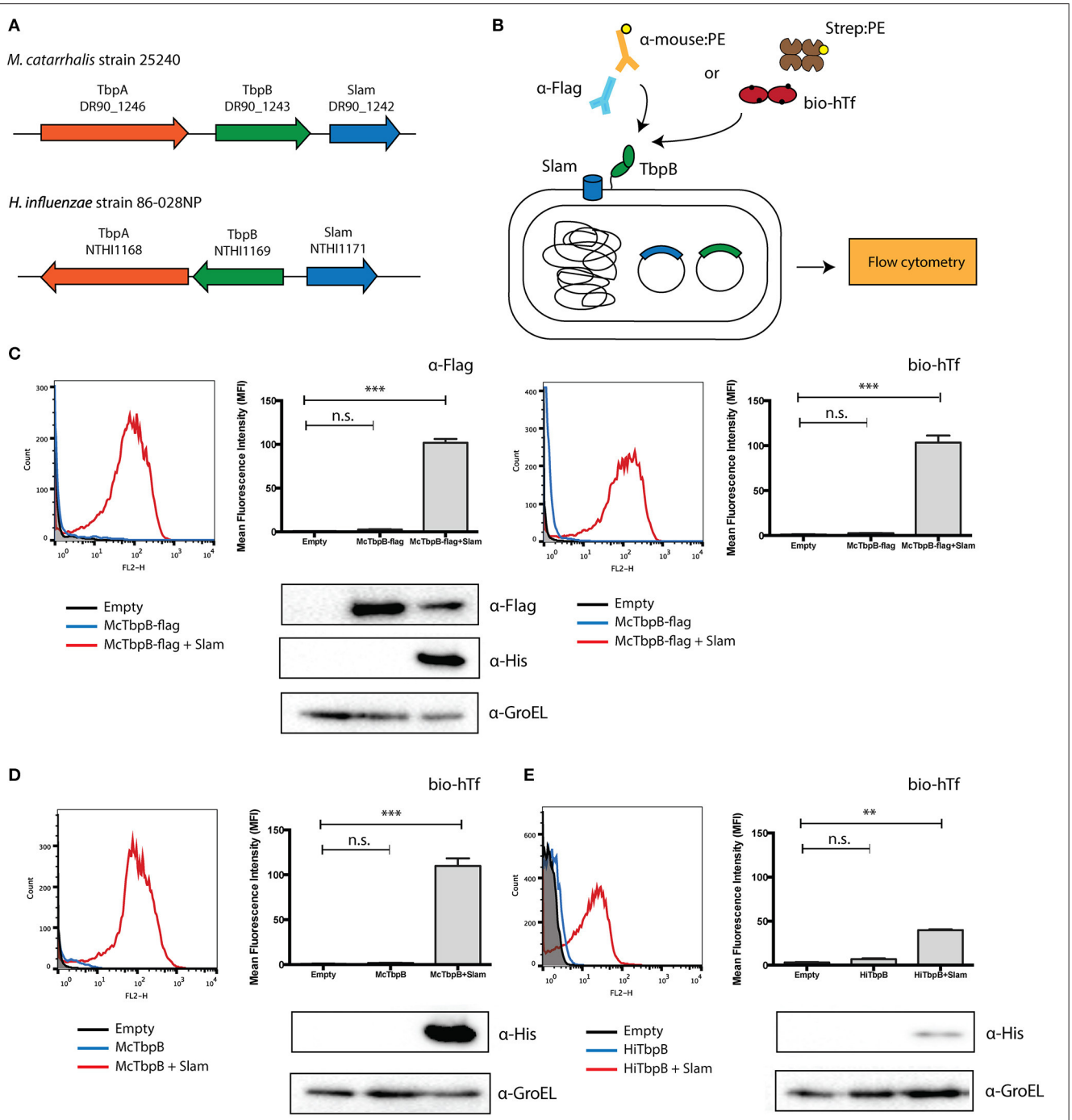


**FIGURE 2 | Translocation assay with Slam and TbpB pairs from *Moraxella catarrhalis* and *Haemophilus influenzae*. (A)** Slam and TbpB gene cluster in *M. catarrhalis* and *H. influenzae*. From the bioinformatics analysis, Slam genes were found adjacent to the known transferrin binding surface lipoprotein TbpB in the human pathogens *M. catarrhalis* and *H. influenzae*. **(B)** *E. coli* translocation assay used in this study. The Slam and TbpB genes were expressed in *E. coli* C43 (DE3) cells. The cells were labeled with either biotinylated human transferrin and streptavidin linked to R-PE, or mouse α-Flag antibody and α-mouse linked to R-PE. Surface display of TbpB was quantified using flow cytometry. **(C)** Flow cytometry profiles of C43 cells transformed with empty plasmid (black), *M. catarrhalis* TbpB-flag (blue), *M. catarrhalis* TbpB-flag + Slam (red) were obtained using α-Flag (left panel) and biotinylated human transferrin (right panel). An increase in fluorescence intensity was observed in the presence of Slam for both α-Flag and biotinylated human transferrin. Surface TbpB was quantified using mean fluorescence intensity. Western blots using α-Flag and α-His were used to quantify McTbpB and McSlam. α-GroEL is used as the loading control **(D)** Flow cytometry profile of TbpB homologs from *M. catarrhalis* (McTbpB) and **(E)** flow cytometry profile of *H. influenzae* (HiTbpB) using biotinylated human transferrin. Scatter plots of cell counts (Count) vs. R-PE fluorescence (FL2-H) in the presence (shown in red) or absence (shown in blue) of Slam are illustrated in the left panels. C43 cells transformed with empty plasmid (shown in black) were used as negative controls. Surface TbpB was quantified using mean fluorescence intensity (right panels). Western blots were done with α-His to examine Slam expression and α-GroEL was used as the loading control. Statistical significance was determined using one-way ANOVA. $^{***}p \leq 0.001$, $^{**}p \leq 0.01$, n.s. $p > 0.05$.

lower panel), which may contribute to the lower signal obtained for *H. influenzae* TbpB.

## Predicted SLP Genes Are Found Adjacent to Slam Genes in a Number of Gram-Negative Bacteria

For 353 of the 832 Slam related genes identified, a list of neighboring genes was analyzed using InterProScan (Jones et al., 2014) to identify Slam related gene clusters that also contain lipoprotein-encoding genes. From our analysis, 185 of the 353 (∼52% of the clusters examined) Slam related genes contained lipoprotein-encoding genes in their gene clusters. This list of putative lipoproteins contained three experimentally confirmed SLPs (**Figure 3A**). These include two HpuA homologs in *Neisseria gonorrhoeae* and *Kingella denitrificans* that were functionally and structurally characterized by Wong et al. (2015). We also identified a putative human factor H binding protein from *H. influenzae,* referred to as protein H (PH) (Fleury et al., 2014) that has sequence homology to the Slam-dependent SLPs in *N. meningitidis*.

The 185 predicted lipoproteins were found in 129 different species distributed throughout *Proteobacteria*. One such lipoprotein was identified in the nematode pathogen *Xenorhabdus nematophila* that has not been previously shown to contain SLPs (**Figure 3B**). This lipoprotein, named NilC has been previously shown to be lipidated *in vivo*, present in the outer membrane and is important for host colonization (Cowles and Goodrich-Blair, 2004). The gene encoding NilB, a putative Slam homolog, is present next to the gene encoding NilC, and is shown to be required for host colonization (Bhasin et al., 2012). Our analysis suggests that NilC is a surface lipoprotein (SLP) that is dependent on the Slam homolog, NilB, for surface display.

Studying other genes in the Slam related gene clusters, we uncovered that 120 of the 185 clusters also possessed genes that encode proteins annotated as TonB-dependent receptors (TonBDR). This is not surprising as in *Neisseria* sp., three Slam-dependent SLPs (TbpB, LbpB, and HpuA) work in conjunction with a TonBDR to acquire iron (Hooda et al., 2017). The presence of TonBDRs gene in proximity to these putative SLPs supports their potential roles in nutrient acquisition. Furthermore, a small subset of Slam gene clusters (nine) contained multiple lipoprotein-encoding genes suggesting that they may be responsible for the display of multiple target SLPs.

## A Putative SLP Gene in *Pasteurella multocida* Is Displayed on the Surface of *E. coli* in a Slam-Dependent Manner

To further confirm the hypothesis that we have identified a large family of Slam-dependent SLPs, we sought to characterize the surface display of some of the remaining lipoproteins that were identified in this study for which no other functional data could be found. One such predicted lipoprotein was found in *P. multocida,* a zoonotic pathogen that resides in the normal respiratory microbiota of mammals. We identified the gene of the putative Slam (PM1515) adjacent to the predicted lipoprotein (PM1514) in all the sequenced strains of *P. multocida*

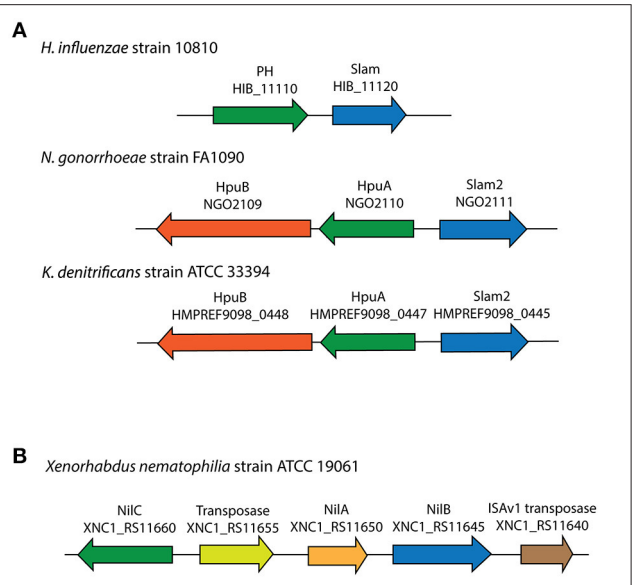


**FIGURE 3 | Slam related gene clusters identified in this study with known lipoproteins. (A)** Three SLP-containing Slam gene clusters were found in *Neisseria gonorrhoeae*, *Kingella denitrificans* and *Haemophilus influenzae*. **(B)** Lipoprotein-containing Slam gene cluster in *Xenorhabdus nematophilia*.

(**Figure 4A**). The Slam displayed 32% identity to *N. meningitidis* Slam1 while the putative SLP showed no sequence similarity to any of the known Slam-dependent neisserial SLPs. Interestingly, the Slam gene cluster also included two other SLPs, PM1517 (PlpD), and PM1518 (PlpE) that have been investigated as potential vaccine antigens against *Pasteurella* infections (Nardini et al., 1998; Wu et al., 2007).

To test if this *pm1514* gene encoded a Slam-dependent SLP, we cloned the predicted Slam and lipoprotein genes into *E. coli* expression vectors (**Figure 4B**). We transformed *E. coli* cells with FLAG-tagged *P. multocida* lipoprotein and Slam, and used the FLAG-epitope to detect the SLP on the surface. As predicted, we saw an increase in FLAG signal upon expression of Slam as seen in flow cytometry profiles (**Figure 4C**) and quantified in mean fluorescence intensity (MFI) plots (**Figure 4D**). Furthermore, to confirm the translocation pathway used by the *P. multocida* SLP, we examined its outer membrane localization in the presence or absence of Slam by sucrose density ultracentrifugation (**Figure 4E**). Collectively, these findings suggest that PM1514 is a putative Slam-dependent SLP and that many other Slam-dependent SLPs on our list (Supplementary Data 2) likely use a similar translocation pathway as *N. meningitidis* TbpB to reach the surface (Hooda et al., 2016).

## Comparison of Putative SLP Proteins Revealed a Conserved Structural Domain

With this dataset of putative Slam-dependent SLPs, we were interested in identifying structural features that are shared by this family of proteins. Structures for four neisserial Slam-dependent SLPs have been solved by X-ray crystallography

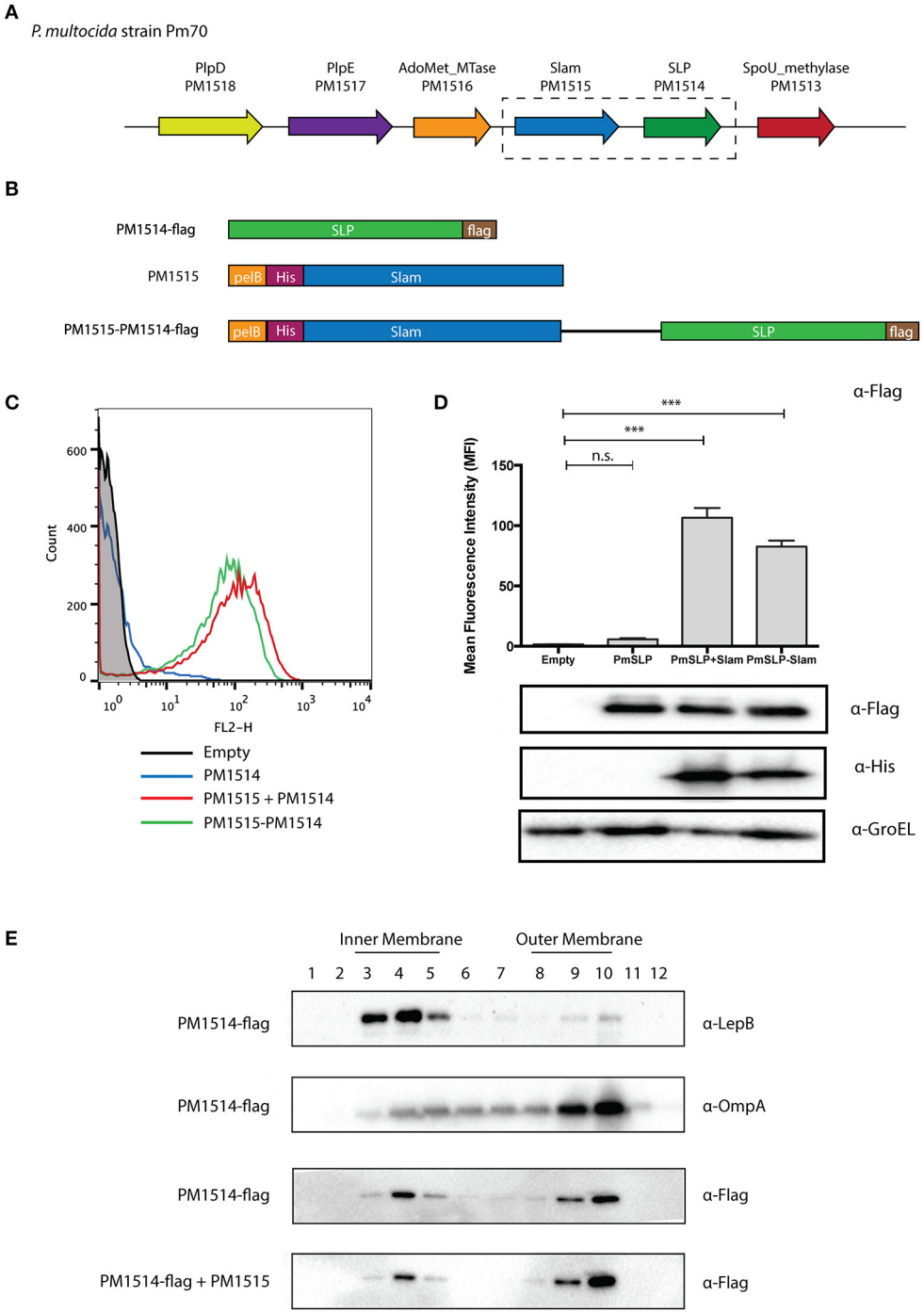


**FIGURE 4 | Identification of a putative Slam-dependent surface lipoprotein in *Pasteurella multocida*. (A)** Slam gene cluster in *P. multocida* strain Pm70. PM1515 (shown in blue) was identified as a putative Slam homolog in our bioinformatics search. PM1514 (shown in green) was annotated as a hypothetical protein with a predicted signal peptidase II cleavage site located within a putative lipobox motif. **(B)** *P. multocida* constructs utilized in an *E. coli* reconstituted translocation assay. To investigate if PM1514 is a Slam-dependent SLP, we cloned the following: PM1514 with a C-terminal FLAG-tag (PM1514-flag), PM1515 with an N-terminal His-tag and pelB signal sequence, and PM1515-PM1514-flag construct with both PM1515 and PM1514 region. **(C)** Flow cytometry profiles of *P. multocida* constructs. The 3 constructs were expressed in *E. coli* C43 (DE3) cells and labeled with α-Flag antibody and a secondary antibody directed against mouse IgG and linked to R-PE. Flow cytometry profiles of empty plasmid (black), PM1514-flag (blue), PM1515+PM1514-flag (red) and PM1515-PM1514-flag (green) are shown. **(D)** Mean fluorescence intensity plots for *P. multocida* constructs. Surface PM1514 was quantified using mean fluorescence intensity (MFI). Statistical significance was determined using one-way ANOVA. *** $p \leq 0.001$, n.s. $p > 0.05$. **(E)** Localization of *P. multocida* SLP using sucrose density ultracentrifugation. To test the localization of *P. multocida* SLP in *E. coli,* cells expressing PM1514-flag with or without PM1515 were harvested. Cell membranes were then isolated and layered on a sucrose gradient to separate the inner and outer membrane. Westerns blots were performed on different fractions with α-Flag, α-LepB, and α-OmpA antibodies to detect PmSLP, LepB (inner membrane control) and OmpA (outer membrane control) respectively.

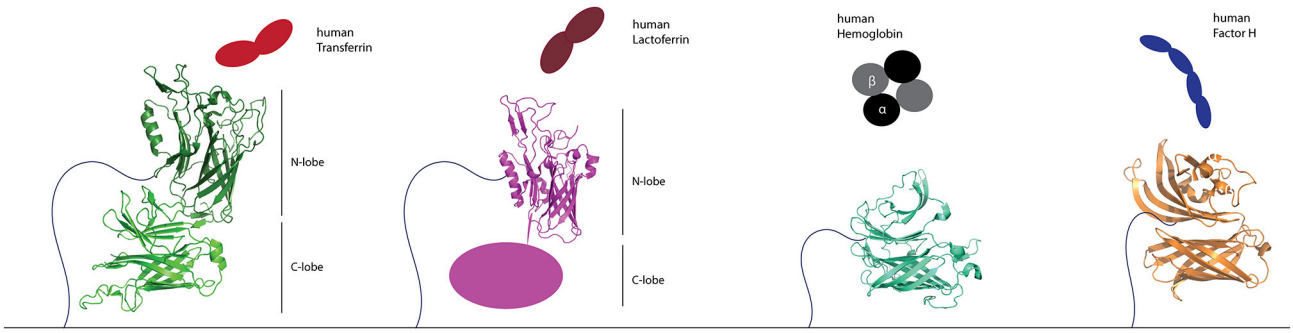


| Species | PDB ID |
|---|---|
| *Neisseria meningitidis* | 4QQ1, 3VE1, 3VE2, 3V8U |
| *Actinobacillus suis* | 4O3W |
| *Actinobacillus pleuropneumoniae* | 4O3X, 4O3Y, 4O3Z, 4O49, 3PQU, 3PQS, 3HOE, 3HOL |
| *Haemophilus parasuis* | 4O4U, 4O4X |

| Species | PDB ID |
|---|---|
| *Neisseria meningitidis* | 4U9C |
| *Moraxella bovis* | 3UAQ |

| Species | PDB ID |
|---|---|
| *Neisseria gonorrhoeae* | 5EE2 |
| *Kingella denitrificans* | 5EC6, 5EE4 |

| Species | PDB ID |
|---|---|
| *Neisseria meningitidis* | 4Z3T, 4AYD, 4AYE, 4AYI, 4AYM, 4AYN, 2Y7S, 3KVD, 2KC0, 2W80, 2W81 |

**FIGURE 5 | Structures of known Slam-dependent SLPs.** Structures of TbpB (green), LbpB N-lobe (magenta) HpuA (cyan) and fHbp (orange) are shown. The binding partner for each of the SLPs [human transferrin (red), lactoferrin (brown), hemoglobin (black), and Factor H (blue)] is also shown. Table below lists the accession numbers for all Slam-dependent SLP structures deposited to the Protein Data Bank (PDB). Primary references for TbpB (Moraes et al., 2009; Calmettes et al., 2011, 2012; Noinaj et al., 2012; Adamiak et al., 2015; Frandoloso et al., 2015), LbpB N-lobe (Arutyunova et al., 2012; Brooks et al., 2014), HpuA (Wong et al., 2015), and fHbp (Cantini et al., 2009; Schneider et al., 2009; Cendron et al., 2011; Scarselli et al., 2011; Johnson et al., 2012; Konar et al., 2015) structures are also included.

and NMR (**Figure 5**). While these proteins share no sequence similarity, they do share a protein domain composed of a flexible handle domain followed by an eight-stranded barrel domain. *N. meningitidis* TbpB and LbpB contain two lobes of the conserved domain, while fHbp and HpuA contain only one lobe.

To gain insight into the structure of Slam-dependent SLPs, we compared the predicted domains (InterProScan) on our list of putative Slam-dependent SLPs. We found that 58 contain either a lipoprotein GNA1870-related (InterPro signature: IPR014902) or a solute-binding protein, TBP-like (InterPro signature: IPR001677) domain. These domains are found on fHbp and TbpB respectively, both of which are Slam-dependent SLPs, and contain an eight-stranded beta barrel at their C-terminus. Further, 127 were predicted to encode a PagP-beta barrel (InterPro signature: IPR011250). PagP is an outer membrane enzyme that forms an eight-stranded barrel and is involved in catalyzing palmitate transfer from a phospholipid to a glucosamine unit of lipid A (Cuesta-Seijo et al., 2010). While PagP is an integral outer membrane protein, several soluble proteins are also predicted to contain an eight-stranded PagP-beta barrel. Most of the predicted Slam-adjacent lipoproteins also had a variable N-terminal region preceding the eight-stranded barrel that could form a handle-like domain seen in the representative three-dimensional structures of Slam-dependent SLPs.

## DISCUSSION

With the increase in the number of bacterial genomic sequences, it has become evident that surface lipoproteins (or SLPs) are widespread in Gram-negative bacteria. One family of SLPs is characterized by a common structural architecture composed of an eight-stranded beta-barrel domain and a beta rich handle domain (TbpB, LbpB, HpuA, and fHbp). These proteins require a member of a unique family of proteins to traverse the outer membrane named Slam (Hooda et al., 2016). While we still do not know the exact role played by Slams, these proteins are specific for TbpB-like SLPs and may represent a novel class of outer membrane translocon or chaperone dedicated to the transport of SLPs from the inner leaflet of the outer membrane to the surface.

In this study, we performed a bioinformatic analysis of putative Slam homologs and identified a number of Slam-dependent SLPs in many different species of *Proteobacteria*. To our knowledge, this is the first systematic study to look at the distribution of SLPs in different Gram-negative bacteria. Previous attempts to look at TbpB-like lipoproteins have been stymied by the degree of variation that is found in these proteins. Since Slam sequences are more conserved, we were able to identify a large number of SLP homologs owing to the genetic linkage between Slams and TbpB-like SLPs. We have extended the number of bacteria that are now predicted to possess SLPs and also provide a framework to systematically search for these proteins. Based on this work, Slam-dependent SLPs represent the largest sub-family of SLPs reported thus far. However, our approach also has some limitations. To date, we have only identified genes for putative SLPs located in the immediate vicinity of genes for Slams. Using this method, we would have overlooked many known Slam-dependent SLPs in pathogenic *Neisseria* sp., which are transported in a Slam1-dependent manner but are encoded

by genes not located in the vicinity of the gene for Slam1 (e.g., NmTbpB and NmLbpB). Therefore, our list of Slam-dependent SLPs is certainly incomplete; the bacterial species containing Slam homologs but no Slam-adjacent lipoproteins may also contain SLPs elsewhere in the genome.

Our analysis allowed the identification of a previously uncharacterized protein PM1514 in *Pasteurella multocida* as a putative SLP. Using localization assays we confirmed PM1514 is present in the outer membrane but is only detected on the surface of *E. coli* when co-expressed with the putative Slam PM1515. Taken together, these findings suggest that PM1515 is a Slam homolog and PM1514 is a Slam-dependent SLP. Additional work is required to further investigate this putative SLP, including a $^{3}$H-palmitoyl labeling assay to confirm the lipidation of PM1514 in both *E. coli* and *P. multocida*. Flow cytometry and proteinase K shaving assay should be performed in *P. multocida* to test the surface display of PM1514 in its endogenous host. PM1514 is found in most sequenced strains of *P. multocida*, indicating that it may play an important role in the survival of *P. multocida* in its host organisms.

In our present search, we identified that Slam related sequences are found in *Proteobacteria* and not found in *Bacteroides*, *Borrelia,* and *Campylobacter*. Interestingly, we investigated the gene neighborhoods of four other known SLPs namely, JlpA in *Campylobacter* (Jin et al., 2001), HmuY (Wójtowicz et al., 2009) and SusD (Shipman et al., 2000) in *Bacteroides* and OspA/C in *Borrelia* (Schulze et al., 2010). Upon inspection none of these SLPs showed genetic linkage with any known/predicted outer membrane protein (data not shown) nor were any Slam related sequences found in *Bacteroides* or *Borrelia*. Coupled with the mechanistic studies completed on the SLP translocation pathways for *Bacteroides* (Lauber et al., 2016) and *Borrelia* (Chen and Zückert, 2011), it is likely that other translocation systems are used by *Bacteroides* and *Borrelia* to facilitate translocation of these SLPs to the cell surface.

Using the list of putative Slam-dependent SLPs, we have found that all these proteins contain a predicted eight-stranded barrel domain. All Slam-dependent SLPs contain either one or two copies of this barrel domain. Hence, we predict that the barrel domain may contain the translocation motif that is recognized by Slam. However, further experiments are required to tease apart the translocation motif present on these SLPs. Toward this end, the dataset generated by this study will be a valuable tool to identify secretion motif that is common amongst Slam-dependent SLPs.

The ability of Slam proteins to robustly potentiate the display of TbpB-like SLPs from a diverse set of bacteria in *E. coli* provides further evidence of their direct involvement in translocation. While more work is required to understand the mechanism of Slam function, the work done so far shows the efficacy of using Slam as a system to deliver proteins to the surface of Gram-negative bacteria and has potential applications in development of bacterial surface display technology (Ståhl and Uhlén, 1997). Taken together with our previous study (Hooda et al., 2016), our work suggests that TbpB-like SLPs and Slams form a "plug-and-play" cassette, reminiscent of the two-partner secretion systems (TPSS) or Type Vb secretion system (Jacob-Dubuisson et al., 2013). To date, we believe that Slams are specific for the delivery of lipidated proteins to the surface of Gram-negative bacteria. However, it will be interesting to see if they represent a more generalized secretion system. Finally, this study furthers the argument that SLPs are an important and yet under-appreciated family of proteins and their investigation may lead to identification of novel mechanisms utilized by many different bacteria to interact with their environmental surroundings and/or their hosts.

## AUTHOR CONTRIBUTIONS

YH and TM designed the experiments and wrote the manuscript. YH did the bioinformatics analysis. YH and CL. performed the experiments. YH, CL, and TM. analyzed the data.

## FUNDING

This work was supported by a Canadian Institutes of Health Research (CIHR) grants (PJT-148795 to TM), as well as with instrumentation and infrastructure support provided by Canadian Foundation for Innovation (CFI), and Ontario Ministry of Education and Innovation. TM is a Canada Research Chair in the Structural Biology of Membrane Proteins.

## ACKNOWLEDGMENTS

We thank Drs. A.B. Schryvers (University of Calgary), Scott Gray-Owen (University of Toronto), JW de Gier (Stockholm University) and Walid Houry (University of Toronto) for plasmids, strains and antibodies. We also thank the members of the Moraes Lab for technical assistance and discussions.

## SUPPLEMENTARY MATERIAL

The Supplementary Material for this article can be found online at: http://journal.frontiersin.org/article/10.3389/fcimb.2017.00207/full#supplementary-material

## REFERENCES

Adamiak, P., Calmettes, C., Moraes, T. F., and Schryvers, A. B. (2015). Patterns of structural and sequence variation within isotype lineages of the *Neisseria meningitidis* transferrin receptor system. *Microbiologyopen* 4, 491–504. doi: 10.1002/mbo3.254

Altschul, S. F., Madden, T. L., Schäffer, A. A., Zhang, J., Zhang, Z., Miller, W., et al. (1997). Gapped BLAST and PSI-BLAST: a new generation of protein database search programs. *Nucleic Acids Res.* 25, 3389–3402. doi: 10.1093/nar/25.17.3389

Arutyunova, E., Brooks, C. L., Beddek, A., Mak, M. W., Schryvers, A. B., and Lemieux, M. J. (2012). Crystal structure of the N-lobe of lactoferrin binding protein B from *Moraxella bovis*. *Biochem. Cell Biol. Biochim. Biol. Cell.* 90, 351–361. doi: 10.1139/o11-078

Bhasin, A., Chaston, J. M., and Goodrich-Blair, H. (2012). Mutational analyses reveal overall topology and functional regions of NilB, a bacterial

outer membrane protein required for host association in a model of animal-microbe mutualism. *J. Bacteriol.* 194, 1763–1776. doi: 10.1128/JB.06711-11

Brandt, M. E., Riley, B. S., Radolf, J. D., and Norgard, M. V. (1990). Immunogenic integral membrane proteins of *Borrelia burgdorferi* are lipoproteins. *Infect. Immun.* 58, 983–991.

Brooks, C. L., Arutyunova, E., and Lemieux, M. J. (2014). The structure of lactoferrin-binding protein B from *Neisseria meningitidis* suggests roles in iron acquisition and neutralization of host defences. *Acta Crystallogr. Sect. F Struct. Biol. Commun.* 70, 1312–1317. doi: 10.1107/S2053230X14019372

Calmettes, C., Alcantara, J., Yu, R.-H., Schryvers, A. B., and Moraes, T. F. (2012). The structural basis of transferrin sequestration by transferrin-binding protein B. *Nat. Struct. Mol. Biol.* 19, 358–360. doi: 10.1038/nsmb.2251

Calmettes, C., Yu, R., Silva, L. P., Curran, D., Schriemer, D. C., Schryvers, A. B., et al. (2011). Structural variations within the transferrin binding site on transferrin-binding protein B, TbpB. *J. Biol. Chem.* 286, 12683–12692. doi: 10.1074/jbc.M110.206102

Cantini, F., Veggi, D., Dragonetti, S., Savino, S., Scarselli, M., Romagnoli, G., et al. (2009). Solution structure of the factor H-binding protein, a survival factor and protective antigen of *Neisseria meningitidis*. *J. Biol. Chem.* 284, 9022–9026. doi: 10.1074/jbc.C800214200

Cendron, L., Veggi, D., Girardi, E., and Zanotti, G. (2011). Structure of the uncomplexed *Neisseria meningitidis* factor H-binding protein fHbp (rLP2086). *Acta Crystallograph. Sect. F Struct. Biol. Cryst. Commun.* 67, 531–535. doi: 10.1107/S1744309111006154

Chamberlain, N. R., Brandt, M. E., Erwin, A. L., Radolf, J. D., and Norgard, M. V. (1989). Major integral membrane protein immunogens of *Treponema pallidum* are proteolipids. *Infect. Immun.* 57, 2872–2877.

Chatzi, K. E., Sardis, M. F., Karamanou, S., and Economou, A. (2013). Breaking on through to the other side: protein export through the bacterial sec system. *Biochem. J.* 449, 25–37. doi: 10.1042/BJ20121227

Chen, S., and Zückert, W. R. (2011). Probing the *Borrelia burgdorferi* surface lipoprotein secretion pathway using a conditionally folding protein domain. *J. Bacteriol.* 193, 6724–6732. doi: 10.1128/JB.06042-11

Cho, S.-H., Szewczyk, J., Pesavento, C., Zietek, M., Banzhaf, M., Roszczenko, P., et al. (2014). Detecting envelope stress by monitoring β-barrel assembly. *Cell* 159, 1652–1664. doi: 10.1016/j.cell.2014.11.045

Costa, T. R. D., Felisberto-Rodrigues, C., Meir, A., Prevost, M. S., Redzej, A., Trokter, M., et al. (2015). Secretion systems in Gram-negative bacteria: structural and mechanistic insights. *Nat. Rev. Microbiol.* 13, 343–359. doi: 10.1038/nrmicro3456

Cowles, C. E., and Goodrich-Blair, H. (2004). Characterization of a lipoprotein, NilC, required by *Xenorhabdus nematophila* for mutualism with its nematode host. *Mol. Microbiol.* 54, 464–477. doi: 10.1111/j.1365-2958.2004.04271.x

Cuesta-Seijo, J. A., Neale, C., Khan, M. A., Moktar, J., Tran, C. D., Bishop, R. E., et al. (2010). PagP crystallized from SDS/cosolvent reveals the route for phospholipid access to the hydrocarbon ruler. *Structure* 18, 1210–1219. doi: 10.1016/j.str.2010.06.014

D'Enfert, C., Chapon, C., and Pugsley, A. P. (1987). Export and secretion of the lipoprotein Pullulanase by *Klebsiella pneumoniae*. *Mol. Microbiol.* 1, 107–116.

Delcour, A. H. (2009). Outer membrane permeability and antibiotic resistance. *Biochim. Biophys. Acta* 1794, 808–816. doi: 10.1016/j.bbapap.2008.11.005

DeSantis, T. Z., Hugenholtz, P., Larsen, N., Rojas, M., Brodie, E. L., Keller, K., et al. (2006). Greengenes, a chimera-checked 16S rRNA gene database and workbench compatible with ARB. *Appl. Environ. Microbiol.* 72, 5069–5072. doi: 10.1128/AEM.03006-05

Fleury, C., Su, Y.-C., Hallström, T., Sandblad, L., Zipfel, P. F., and Riesbeck, K. (2014). Identification of a *Haemophilus influenzae* factor H-Binding lipoprotein involved in serum resistance. *J. Immunol.* 192, 5913–5923. doi: 10.4049/jimmunol.1303449

Frandoloso, R., Martínez-Martínez, S., Calmettes, C., Fegan, J., Costa, E., Curran, D., et al. (2015). Nonbinding site-directed mutants of transferrin binding protein B exhibit enhanced immunogenicity and protective capabilities. *Infect. Immun.* 83, 1030–1038. doi: 10.1128/IAI.02572-14

Geyter, J. D., Tsirigotaki, A., Orfanoudaki, G., Zorzini, V., Economou, A., and Karamanou, S. (2016). Protein folding in the cell envelope of *Escherichia coli*. *Nat. Microbiol.* 1:16107. doi: 10.1038/nmicrobiol.2016.107

Gray-Owen, S. D., Loosmore, S., and Schryvers, A. B. (1995). Identification and characterization of genes encoding the human transferrin-binding proteins from *Haemophilus influenzae*. *Infect. Immun.* 63, 1201–1210.

Gray-Owen, S. D., and Schyvers, A. B. (1996). Bacterial transferrin and lactoferrin receptors. *Trends Microbiol.* 4, 185–191. doi: 10.1016/0966-842X(96)10025-1

Hoehn, G. T., and Clark, V. L. (1992). The major anaerobically induced outer membrane protein of *Neisseria gonorrhoeae*, Pan 1, is a lipoprotein. *Infect. Immun.* 60, 4704–4708.

Hooda, Y., Lai, C. C.-L., Judd, A., Buckwalter, C. M., Shin, H. E., Gray-Owen, S. D., et al. (2016). Slam is an outer membrane protein that is required for the surface display of lipidated virulence factors in Neisseria. *Nat. Microbiol.* 1:16009. doi: 10.1038/nmicrobiol.2016.9

Hooda, Y., Shin, H. E., Bateman, T. J., and Moraes, T. F. (2017). Neisserial surface lipoproteins: structure, function and biogenesis. *Pathog. Dis.* 75:ftx010. doi: 10.1093/femspd/ftx010

Jacob-Dubuisson, F., Guérin, J., Baelen, S., and Clantin, B. (2013). Two-partner secretion: as simple as it sounds? *Res. Microbiol.* 164, 583–595. doi: 10.1016/j.resmic.2013.03.009

Jin, S., Joe, A., Lynett, J., Hani, E. K., Sherman, P., and Chan, V. L. (2001). JlpA, a novel surface-exposed lipoprotein specific to *Campylobacter jejuni*, mediates adherence to host epithelial cells. *Mol. Microbiol.* 39, 1225–1236. doi: 10.1111/j.1365-2958.2001.02294.x

Johnson, S., Tan, L., Veen, S., van der, Caesar, J., Jorge, E. G. D., Harding, R. J., et al. (2012). Design and evaluation of meningococcal vaccines through structure-based modification of host and pathogen molecules. *PLoS Pathog.* 8:e1002981. doi: 10.1371/journal.ppat.1002981

Jones, P., Binns, D., Chang, H.-Y., Fraser, M., Li, W., McAnulla, C., et al. (2014). InterProScan 5: genome-scale protein function classification. *Bioinformatics* 30, 1236–1240. doi: 10.1093/bioinformatics/btu031

Karuppiah, V., Berry, J.-L., and Derrick, J. P. (2011). Outer membrane translocons: structural insights into channel formation. *Trends Microbiol.* 19, 40–48. doi: 10.1016/j.tim.2010.10.006

Kearse, M., Moir, R., Wilson, A., Stones-Havas, S., Cheung, M., Sturrock, S., et al. (2012). Geneious basic: an integrated and extendable desktop software platform for the organization and analysis of sequence data. *Bioinformatics* 28, 1647–1649. doi: 10.1093/bioinformatics/bts199

Konar, M., Pajon, R., and Beernink, P. T. (2015). A meningococcal vaccine antigen engineered to increase thermal stability and stabilize protective epitopes. *Proc. Natl. Acad. Sci. U.S.A.* 112, 14823–14828. doi: 10.1073/pnas.1507829112

Konovalova, A., Perlman, D. H., Cowles, C. E., and Silhavy, T. J. (2014). Transmembrane domain of surface-exposed outer membrane lipoprotein RcsF is threaded through the lumen of β-barrel proteins. *Proc. Natl. Acad. Sci. U.S.A.* 111, E4350–E4358. doi: 10.1073/pnas.1417138111

Konovalova, A., and Silhavy, T. J. (2015). Outer membrane lipoprotein biogenesis: lol is not the end. *Phil. Trans. R. Soc. B* 370:20150030. doi: 10.1098/rstb.2015.0030

Lauber, F., Cornelis, G. R., and Renzi, F. (2016). Identification of a new lipoprotein export signal in gram-negative bacteria. *MBio* 7:01216. doi: 10.1128/mbio.01232-16

Leuzzi, R., Serino, L., Scarselli, M., Savino, S., Fontana, M. R., Monaci, E., et al. (2005). Ng-MIP, a surface-exposed lipoprotein of *Neisseria gonorrhoeae*, has a peptidyl-prolyl cis/trans isomerase (PPIase) activity and is involved in persistence in macrophages. *Mol. Microbiol.* 58, 669–681. doi: 10.1111/j.1365-2958.2005.04859.x

Lewis, L. A., Gray, E., Wang, Y. P., Roe, B. A., and Dyer, D. W. (1997). Molecular characterization of hpuAB, the haemoglobin-haptoglobin-utilization operon of *Neisseria meningitidis*. *Mol. Microbiol.* 23, 737–749. doi: 10.1046/j.1365-2958.1997.2501619.x

Li, C., Wen, A., Shen, B., Lu, J., Huang, Y., and Chang, Y. (2011). FastCloning: a highly simplified, purification-free, sequence- and ligation-independent PCR cloning method. *BMC Biotechnol.* 11:92. doi: 10.1186/1472-6750-11-92

Madico, G., Welsch, J. A., Lewis, L. A., McNaughton, A., Perlman, D. H., Costello, C. E., et al. (2006). The meningococcal vaccine candidate GNA1870 binds the complement regulatory protein factor H and enhances serum resistance. *J. Immunol. Baltim.* 177, 501–510. doi: 10.4049/jimmunol.177.1.501

Manning, P. A., Beutin, L., and Achtman, M. (1980). Outer membrane of *Escherichia coli*: properties of the F sex factor traT protein which is involved in surface exclusion. *J. Bacteriol.* 142, 285–294.

Moraes, T. F., Yu, R., Strynadka, N. C. J., and Schryvers, A. B. (2009). Insights into the bacterial transferrin receptor: the structure of transferrin-binding protein B from *Actinobacillus pleuropneumoniae*. *Mol. Cell* 35, 523–533. doi: 10.1016/j.molcel.2009.06.029

Nardini, P. M., Mellors, A., and Lo, R. Y. (1998). Characterization of a fourth lipoprotein from *Pasteurella haemolytica* A1 and its homology to the OmpA family of outer membrane proteins. *FEMS Microbiol. Lett.* 165, 71–77. doi: 10.1111/j.1574-6968.1998.tb13129.x

Nikaido, H. (2003). Molecular basis of bacterial outer membrane permeability revisited. *Microbiol. Mol. Biol. Rev.* 67, 593–656. doi: 10.1128/MMBR.67.4.593-656.2003

Noinaj, N., Easley, N. C., Oke, M., Mizuno, N., Gumbart, J., Boura, E., et al. (2012). Structural basis for iron piracy by pathogenic Neisseria. *Nature* 483, 53–58. doi: 10.1038/nature10823

Nørskov-Lauritsen, N. (2014). Classification, identification, and clinical significance of *Haemophilus* and *Aggregatibacter* species with host specificity for humans. *Clin. Microbiol. Rev.* 27, 214–240. doi: 10.1128/CMR.00103-13

Okuda, S., and Tokuda, H. (2011). Lipoprotein sorting in bacteria. *Annu. Rev. Microbiol.* 65, 239–259. doi: 10.1146/annurev-micro-090110-102859

Pagès, J.-M., James, C. E., and Winterhalter, M. (2008). The porin and the permeating antibiotic: a selective diffusion barrier in Gram-negative bacteria. *Nat. Rev. Microbiol.* 6, 893–903. doi: 10.1038/nrmicro1994

Pettersson, A., Prinz, T., Umar, A., Van Der Biezen, J., and Tommassen, J. (1998). Molecular characterization of LbpB, the second lactoferrin-binding protein of *Neisseria meningitidis*. *Mol. Microbiol.* 27, 599–610. doi: 10.1046/j.1365-2958.1998.00707.x

Pugsley, A. P., Chapon, C., and Schwartz, M. (1986). Extracellular pullulanase of Klebsiella pneumoniae is a lipoprotein. *J. Bacteriol.* 166, 1083–1088. doi: 10.1128/jb.166.3.1083-1088.1986

Scarselli, M., Aricò, B., Brunelli, B., Savino, S., Marcello, F. D., Palumbo, E., et al. (2011). Rational design of a meningococcal antigen inducing broad protective immunity. *Sci. Transl. Med.* 3, 91ra62–91ra62. doi: 10.1126/scitranslmed.3002234

Schneider, M. C., Prosser, B. E., Caesar, J. J. E., Kugelberg, E., Li, S., Zhang, Q., et al. (2009). *Neisseria meningitidis* recruits factor H using protein mimicry of host carbohydrates. *Nature* 458, 890–893. doi: 10.1038/nature07769

Schryvers, A. B., and Morris, L. J. (1988). Identification and characterization of the transferrin receptor from *Neisseria meningitidis*. *Mol. Microbiol.* 2, 281–288. doi: 10.1111/j.1365-2958.1988.tb00029.x

Schulze, R. J., Chen, S., Kumru, O. S., and Zückert, W. R. (2010). Translocation of *Borrelia burgdorferi* surface Lipoprotein OspA through the outer membrane requires an unfolded conformation and can initiate at the C-terminus. *Mol. Microbiol.* 76, 1266–1278. doi: 10.1111/j.1365-2958.2010.07172.x

Serruto, D., Spadafina, T., Ciucchi, L., Lewis, L. A., Ram, S., Tontini, M., et al. (2010). Neisseria meningitidis GNA2132, a heparin-binding protein that induces protective immunity in humans. *Proc. Natl. Acad. Sci. U.S.A.* 107, 3770–3775. doi: 10.1073/pnas.0915162107

Shipman, J. A., Berleman, J. E., and Salyers, A. A. (2000). Characterization of Four Outer membrane proteins involved in binding starch to the cell surface of *Bacteroides thetaiotaomicron*. *J. Bacteriol.* 182, 5365–5372. doi: 10.1128/JB.182.19.5365-5372.2000

Silhavy, T. J., Kahne, D., and Walker, S. (2010). The bacterial cell envelope. *Cold Spring Harb. Perspect. Biol.* 2:a000414. doi: 10.1101/cshperspect.a000414

Ståhl, S., and Uhlén, M. (1997). Bacterial surface display: trends and progress. *Trends Biotechnol.* 15, 185–192. doi: 10.1016/S0167-7799(97)01034-2

Studier, F. W. (2005). Protein production by auto-induction in high density shaking cultures. *Protein Expr. Purif.* 41, 207–234. doi: 10.1016/j.pep.2005.01.016

Szewczyk, J., and Collet, J.-F. (2016). "Chapter One - the journey of lipoproteins through the cell: one birthplace, multiple destinations," in *Advances in Microbial Physiology*, ed R. K. Poole (Academic Press), 1–50. Available online at: http://www.sciencedirect.com/science/article/pii/S0065291116300248 (Accessed October 24, 2016).

van den Ent, F., and Löwe, J. (2006). RF cloning: a restriction-free method for inserting target genes into plasmids. *J. Biochem. Biophys. Methods* 67, 67–74. doi: 10.1016/j.jbbm.2005.12.008

Van Ulsen, P., Van Alphen, L., Ten Hove, J., Fransen, F., Van Der Ley, P., and Tommassen, J. (2003). A *Neisserial autotransporter* NalP modulating the processing of other autotransporters. *Mol. Microbiol.* 50, 1017–1030. doi: 10.1046/j.1365-2958.2003.03773.x

Webb, C., Selkrig, J., Perry, A., Noinaj, N., Buchanan, S. K., and Lithgow, T. (2012). Dynamic association of BAM complex modules includes surface exposure of the lipoprotein BamC. *J. Mol. Biol.* 422, 545–555. doi: 10.1016/j.jmb.2012.05.035

Wilson, M. M., and Bernstein, H. D. (2016). Surface-Exposed Lipoproteins: an emerging secretion phenomenon in gram-negative bacteria. *Trends Microbiol.* 24, 198–208. doi: 10.1016/j.tim.2015.11.006

Wójtowicz, H., Guevara, T., Tallant, C., Olczak, M., Sroka, A., Potempa, J., et al. (2009). Unique structure and stability of HmuY, a novel heme-binding protein of *Porphyromonas gingivalis*. *PLoS Pathog.* 5:e1000419. doi: 10.1371/journal.ppat.1000419

Wong, C. T., Xu, Y., Gupta, A., Garnett, J. A., Matthews, S. J., and Hare, S. A. (2015). Structural analysis of haemoglobin binding by HpuA from the Neisseriaceae family. *Nat. Commun.* 6:10172. doi: 10.1038/ncomms10172

Wu, J.-R., Shien, J.-H., Shieh, H. K., Chen, C.-F., and Chang, P.-C. (2007). Protective immunity conferred by recombinant *Pasteurella multocida* lipoprotein E (PlpE). *Vaccine* 25, 4140–4148. doi: 10.1016/j.vaccine.2007.03.005

Yu, R., and Schryvers, A. B. (1993). The interaction between human transferrin and transferrin binding protein 2 from Moraxella (Branhamella) catarrhalis differs from that of other human pathogens. *Microb. Pathog.* 15, 433–445. doi: 10.1006/mpat.1993.1092

Zückert, W. R. (2014). Secretion of bacterial Lipoproteins: through the cytoplasmic membrane, the periplasm and beyond. *Biochim. Biophys. Acta* 1843, 1509–1516. doi: 10.1016/j.bbamcr.2014.04.022

**Conflict of Interest Statement:** The authors declare that the research was conducted in the absence of any commercial or financial relationships that could be construed as a potential conflict of interest. However, a patent titled "Slam polynucleotides and polypetides and uses thereof" CA2017050160 has been filed.

The reviewer FJD and handling Editor declared their shared affiliation, and the handling Editor states that the process nevertheless met the standards of a fair and objective review.

frontiers in Cellular and Infection Microbiology

REVIEW
published: 31 May 2017
doi: 10.3389/fcimb.2017.00221

# Tracking Proteins Secreted by Bacteria: What's in the Toolbox?

*Benoit Maffei*[1,2], *Olivera Francetic*[3,4]* *and Agathe Subtil*[1,2]*

[1] Unité de Biologie Cellulaire de l'Infection Microbienne, Institut Pasteur, Paris, France, [2] Centre National de la Recherche Scientifique UMR3691, Paris, France, [3] Unité de Biochimie des Interactions Macromoléculaires, Institut Pasteur, Paris, France, [4] Centre National de la Recherche Scientifique ERL6002, Paris, France

Bacteria have acquired multiple systems to expose proteins on their surface, release them in the extracellular environment or even inject them into a neighboring cell. Protein secretion has a high adaptive value and secreted proteins are implicated in many functions, which are often essential for bacterial fitness. Several secreted proteins or secretion machineries have been extensively studied as potential drug targets. It is therefore important to identify the secretion substrates, to understand how they are specifically recognized by the secretion machineries, and how transport through these machineries occurs. The purpose of this review is to provide an overview of the biochemical, genetic and imaging tools that have been developed to evaluate protein secretion in a qualitative or quantitative manner. After a brief overview of the different tools available, we will illustrate their advantages and limitations through a discussion of some of the current open questions related to protein secretion. We will start with the question of the identification of secreted proteins, which for many bacteria remains a critical initial step toward a better understanding of their interactions with the environment. We will then illustrate our toolbox by reporting how these tools have been applied to better understand how substrates are recognized by their cognate machinery, and how secretion proceeds. Finally, we will highlight recent approaches that aim at investigating secretion in real time, and in complex environments such as a tissue or an organism.

**Keywords: reporter, secretion signal, exoproteome, secretion machinery, live imaging**

OPEN ACCESS

***Edited by:***
*Bérengère Ize, Centre National de la Recherche Scientifique (CNRS), France*

***Reviewed by:***
*Suzana P. Salcedo, MMSB-Lyon, France*
*Cammie Lesser, Massachusetts General Hospital, United States*
*Aoife Boyd, NUI Galway, Ireland*

***Correspondence:**
*Olivera Francetic*
*ofrancet@pasteur.fr*
*Agathe Subtil*
*asubtil@pasteur.fr*

***Received:*** *30 March 2017*
***Accepted:*** *15 May 2017*
***Published:*** *31 May 2017*

***Citation:***
*Maffei B, Francetic O and Subtil A (2017) Tracking Proteins Secreted by Bacteria: What's in the Toolbox? Front. Cell. Infect. Microbiol. 7:221. doi: 10.3389/fcimb.2017.00221*

Secretion refers to the capacity, shared by all cells, to release a selected subset of the proteins they produce beyond the membrane that defines them as individual entities. In bacteria, secreted proteins are implicated in many essential functions such as nutrient uptake and catabolism, biodegradation of polymers, respiration, motility, cell attachment to the substratum or to other cells to allow beneficial or detrimental contacts, and biofilm formation. In pathogenic bacteria, the major virulence factors are typically secreted into the milieu or injected into neighboring target or host cells to change their integrity or function. These multiple roles are often essential for bacterial fitness, and several secreted proteins have been studied as potential drug targets. Optimization of the secretion process is also key for the production of many bioengineered products. Protein secretion, which allows communication with the external world, is also a fascinating biological problem for which numerous mechanisms have evolved, each one adapted to different, and often multiple, biological functions.

The purpose of this review is to provide an overview of the available biochemical, genetic and imaging tools that have been developed to evaluate protein secretion in a qualitative or quantitative manner. The different secretion machineries in bacteria are briefly presented in **Figure 1** and we

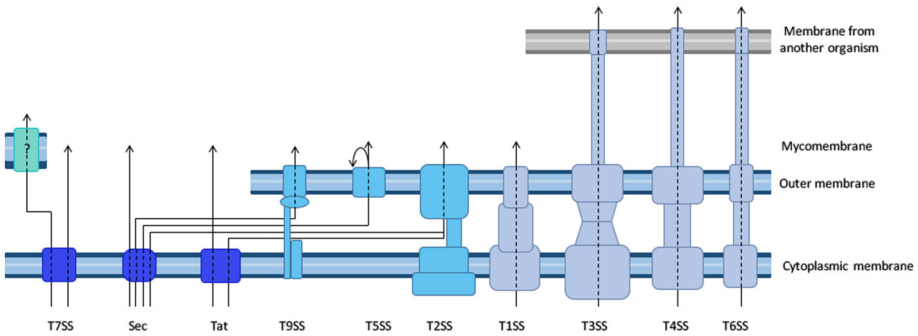


**FIGURE 1 |** Diversity of the bacterial secretion systems. Schematic representation of the secretion systems identified in bacteria, partially based on structural data. In monoderm bacteria **(left)**, protein export (synonymous for secretion in that case) follows the Sec or Tat pathway, or the signal peptide independent T7SS. In diderm-non-LPS bacteria such as *Mycobacteria* or *Corynebacteria* **(far-left)**, it is unknown whether the T7SS system results in protein secretion in one or two steps (question mark). In diderm-LPS bacteria **(center and right)**, secreted proteins can reach the external environment through a one-step process via T1SS, T3SS, T4SS, or T6SS. Other secreted proteins are first exported to the periplasm via the Sec system (T2SS, T5SS, or T9SS) or the Tat system (for T2SS only).

refer the reader to several excellent reviews for mechanical insight on these processes (Desvaux et al., 2009; Korotkov et al., 2012; Leyton et al., 2012; Lycklama A Nijeholt and Driessen, 2012; Palmer and Berks, 2012; Kanonenberg et al., 2013; Christie et al., 2014; Ho et al., 2014; Basler, 2015; Costa et al., 2015; Ates et al., 2016; Green and Mecsas, 2016). Importantly, different tools are applicable to different secretion systems, and the choice of tools is oriented by the question asked. Therefore, after a brief overview of the different tools available, we will illustrate their advantages and limitations through a discussion of some of the current open questions related to protein secretion. We will start with the question of the identification of secreted proteins, which for many bacteria remains a critical initial step toward a better understanding of their interactions with the environment. We will then illustrate our toolbox by describing how these tools have been applied to better understand how substrates are recognized by their cognate machinery, and how secretion proceeds. Finally, we will highlight recent technical developments that aim at investigating secretion in real time and in complex environments such as a tissue or an organism. For space limitations, we will not discuss here the tools to study pilus assembly systems, wherein secretion is coupled to polymerization of protein subunits into fibers, and which include type I pili (Remaut et al., 2008), type IV pili (Berry and Pelicic, 2015), or curli (Van Gerven et al., 2015).

To discuss protein transport across bacterial membranes, we need to clarify the terminology, as the term "protein secretion" is commonly used to describe three distinct processes. We will use the term "export" to describe the translocation of proteins across the cytoplasmic membrane (also called inner membrane (IM) in diderm bacteria). In monoderm bacteria, exported proteins are surface exposed, thus export is equivalent to "secretion." However, in diderm bacteria, exported proteins typically remain intracellular, and are therefore not "secreted," unless another machinery takes them across the outer membrane (OM). Several trans-envelope machineries (classified by numbers, often reflecting the order of their discovery) can perform this second translocation step, including the Type 2, 5, 7, and 9 secretion systems (T2SS, T5SS, T7SS, and T9SS). Other secretion machineries that span the entire envelope of diderm bacteria promote protein secretion in a single step directly from the cytoplasm (T1SS, T3SS, T4SS, and T6SS). Note that some secreted proteins may remain associated with cell surface, and are therefore not synonymous with the "exoproteome" that describes the subset of proteins present in the extracellular medium (Desvaux et al., 2009). Finally, the third process commonly covered by the term "secretion" leads to the injection of the protein beyond a third membrane, that of a neighboring cell, so that the translocated protein becomes inserted in this membrane or is released in the cytoplasm of the neighboring cell. While this process is more accurately described by the word "injection," the term secretion is also suitable.

## OVERVIEW OF THE TOOLBOX

The different methods to investigate protein secretion follow two main strategies. In the first, secreted proteins are identified after a fractionation step that isolates the compartment into which they are targeted. The second strategy is to keep cells intact, and use assays based on accessibility to probes, or on the activity of the secreted proteins, to monitor secretion. This second category includes several microscopy-based assays, and is amenable to the study of secretion in living cells. It also includes genetic or chemical screens aimed at the identification of components of secretion machineries and of secretion signals (see Identification of components of secretion machineries and secretion signals). Complementary to these approaches, bioinformatics tools are being used to identify putative secretion substrates based on their sequence (see Bioinformatics tools).

### Fractionation-Based Assays

Fractionation-based assays are most appropriate to study proteins that are released from the bacteria, either free in the extracellular medium, or injected into a host cell. However, coupled to strategies to purify the OM, such assays can also be used to study proteins that remain associated with the bacteria after secretion.

The fractionation step can be very straightforward, like separating bacteria from the culture medium by centrifugation, or more complicated, for instance in the case of a protein translocated into a given eukaryotic compartment, that will require isolation of that compartment. The readout for secretion after the fractionation step depends on the protein of interest (detection with antibodies, detection of localized enzymatic activity, use of an engineered chimera with a readily-detectable reporter protein etc.), if the strategy is used to follow a given protein. Progress in protein identification by mass spectrometry now enables the use of fractionation-based strategies to characterize bacterial exoproteomes and to detect protein modifications after secretion, without prior information on the secretion mechanism involved. One limitation of this strategy is that setting up the appropriate protocol for the isolation of the compartment of interest to limit contamination by proteins from other compartments can be time-consuming. The high sensitivity of the technique raises the issue of false-positives and requires further experimental validation. For example, a bacterial protein can only be considered as secreted if most of it is found in an extra-cytoplasmic compartment or environment and if such a location is compatible with its function. Furthermore, identification of membrane proteins by mass spectrometry remains technically challenging, and the approach is therefore best suited for soluble secreted proteins.

## Whole-Cell Based Assays

Identification and characterization of secretion system components usually starts with genetic analyses such as deletion or insertion mutagenesis that can define the roles of individual components in more or less complex secretion machineries. Ideally, secretion should be specifically linked to a phenotype to allow for screening or selection; for example, secretion of an amylase is required for growth on starch, while secretion of a hemolysin produces a halo on blood agar plates (see Analysis of protein secretion signals and machineries for examples of genetic and chemical screens). Other, more complex phenotypes can be studied *in vitro*, such as killing of target bacteria *via* the T6SS effectors in mixed bacterial cultures (Brunet et al., 2013) (see When is protein injection activated?). Appearance of a given protein on the bacterial surface can sometimes be assessed directly using antibodies or reporter systems, as illustrated below. For proteins secreted into the extracellular medium, or translocated into a neighboring cell, use of a reporter system is usually the method of choice, in particular when secretion is measured using microscopy to achieve spatial and temporal resolution.

# IDENTIFICATION OF SECRETED PROTEINS

Secreted proteins are ambassadors, mediating most of the interactions of a bacterium with its surrounding environment. Cataloguing the secreted proteins is often an obligatory step toward a comprehensive understanding of how a given bacterium deals with its environment. Some of the tools that can be used to identify secreted proteins, like the bioinformatics approaches described below, are specific to a given secretion machinery. Others, like proteomics-based approaches, or phage display, do not require information on the secretion mechanism. The tools illustrated below are complementary. Typically, global approaches generate lists of secreted proteins candidates, which are later validated using targeted secretion assays, often based on reporter fusion systems.

## Bioinformatics Tools

Type 1 to type 6 secretion systems (**Figure 1**) are sufficiently well documented and conserved to predict the secretion machinery repertoire in newly sequenced bacterial genomes. One recent study built online and standalone computational tools to predict protein secretion systems and related appendages accurately in bacteria with an OM containing lipopolysaccharide, retrieving ∼10,000 candidate systems amongst which T1SS and T5SS were by far the most abundant and widespread (Abby et al., 2016). The identification of the substrates of these secretion machineries is more difficult, and novel secretion substrates generally cannot be identified unambiguously from genomic sequence alone. However, in many cases, sequence similarity with a known secretion substrate, and/or the presence of a "signal peptide" (see below), and/or genomic localization in proximity to genes coding for a secretion machinery, provide strong indications of novel secretion substrates. This is often not sufficient, especially for secretion substrates of pathogenic bacteria that are tailored for a very specific target, and are therefore often specific to a single bacterial species. To identify these elusive secretion substrates, machine-learning approaches have been implemented for use with T3SS and T4SS, for which the data base is sufficiently large. Globally, secretion substrates fall into two categories, depending on the presence or absence of a so-called signal peptide.

### First Scenario: Presence of a Signal Peptide

Two machineries export proteins across the IM: the Sec translocon and the twin-arginine translocation (Tat) machinery. Proteins that are targeted to these export machineries have N-terminal extensions called signal peptides. Canonical signal peptides have a tripartite structure with a basic region at the N-terminus, a central hydrophobic region and a polar carboxyl terminus with a consensus cleavage site (AXA) (von Heijne, 1990). The Tat signal peptides differ somewhat from the Sec-targeting signals in that they possess an extended N-terminal region with a conserved twin-arginine motif TRRxFLK that is crucial for targeting to Tat export pathway (Palmer and Berks, 2012). Importantly, the Tat pathway is capable of transporting folded proteins and protein complexes; therefore, proteins that lack a signal peptide but form complexes with partner subunits that have twin-arginine signal peptides can also be exported in a "piggy-back fashion" through this pathway. Furthermore, it is important to note that some bacterial genomes have a strong base compositional bias and, consequently, encode Sec-dependent proteins with non-canonical signal peptides (Payne et al., 2012).

Several bioinformatics programs can be used to predict the presence of cleavable Sec or Tat signal peptides, such as SignalP (http://www.cbs.dtu.dk/services/SignalP) (Petersen et al., 2011),

PSort (http://www.psort.org), which conveniently also provides a list of links toward other subcellular prediction programs, Pred-Tat, TatP or TatFind (see Berks, 2015, for comparison). Lipoprotein signal peptides are a distinct class of Sec dependent signal peptides characterized by a C-terminal consensus sequence, the lipobox, which ends with an absolutely conserved cysteine residue that, after fatty acylation, becomes the first residue of the mature protein (www.cbs.dtu.dk/services/LipoP/) (Juncker et al., 2003). Experimental validation is necessary, however, to demonstrate a tentatively-identified secreted protein uses a given transport pathway to exit the producing cell, as illustrated in parts Analysis of protein secretion signals and machineries and Resolution of secretion in time and space.

As explained earlier, protein transport across the IM by the Sec or Tat pathways in monoderm bacteria results in protein secretion. However, in diderm bacteria, proteins face an additional barrier, the OM that, together with the IM, defines the periplasmic compartment with distinct properties, composition and content. While the periplasm is the final destination for many proteins, others are inserted into the OM or cross it entirely to reach the bacterial surface using specialized transport systems. Protein secretion pathways that include a periplasmic intermediate are called two-step pathways.

The T2SS is a typical two-step pathway that takes up specific periplasmic substrates in a folded state. T2SS substrates can therefore be recognized by the presence of an N-terminal signal sequence in their precursors. However, despite many extensive analyses, the recognition events and signals that mediate the second transport step have not been elucidated and appear to vary between different bacterial species and substrates (Korotkov et al., 2012).

T5SS substrates, formerly called auto-transporters, are made of a translocator and passenger domain; these domains are usually encoded by a single gene, but can also be separate polypeptides in the so-called two-partner secretion systems (Leyton et al., 2012). The conserved and mandatory C-proximal translocator domain with characteristics typical of most outer beta-barrel membrane proteins, following a large N-proximal domain with a signal sequence is usually sufficient to predict the latter as the passenger (secreted) domain (Abby et al., 2016).

Another two-step secretion pathway is the recently discovered T9SS, found exclusively in the Bacteroidetes phylum. Substrates of this pathway are secreted in a folded state, and, in addition to the signal sequence, share a conserved C-terminal domain harboring the secretion signal (Sato et al., 2010; de Diego et al., 2016).

### Second Scenario: Absence of a Signal Peptide

Proteins that are not made as precursors with an amino terminal signal peptide can still be secreted, by T1SS, T3SS, T4SS, T6SS, or T7SS. It proved difficult or impossible to identify sequence features in secretion substrates that indicate that they will use one or other of these pathways. Several machine-learning techniques have been developed recently for this purpose based on datasets of known T3SS and T4SS secretion substrates. They differ in terms of the machine learning methods, the curated data sets and the features used, and reach different levels of prediction performance. Several, but not all (Meyer et al., 2013), of these tools were recently compared (An et al., 2016). All predictors are flawed, to various degrees, with false positives (secretion signal identified in non-secreted proteins) and false negatives (documented secretion substrates not predicted as such), so while they can be precious in orienting research, experimental validation is required.

T1SS substrates also contain a Sec-independent secretion sequence, which is either located at the N-terminus (certain bacteriocins or colicins) or at the C-terminus (all other systems) of the substrate. Like in T3SS and T4SS substrates, these sequences lack recognizable features, so T1SS substrates cannot be identified based on the recognition of a characteristic secretion signal (Kanonenberg et al., 2013). However, prediction tools cannot yet be developed, because the data base is too small to build training sets. The same is true for T6SS substrates for which some properties (size, isoelectric point, operon structure) have been used to orient genome searches, but robust bioinformatics based methods do not exist (Ho et al., 2014).

Finally, the T7SS, initially identified in mycobacteria, is still poorly understood. Mycobacteria and related genera have an external membrane composed of unique and complex lipids and are therefore diderm, despite the fact that, like monoderms, they stain Gram-positive. They secrete several proteins by a Sec-independent mechanism, and it is not known whether protein secretion occurs in one or two steps. Substrates of this secretion machinery share a loosely defined C-terminal secretion signal, which includes the consensus motif YxxxD/E (Ates et al., 2016). The T7SS is also present in a few monoderm bacteria such as *Staphylococcus aureus*, where it promotes secretion of proteins with antibacterial activities (Cao et al., 2016).

## Identification of Secreted Proteins through Proteomics

One method of choice to identify new secreted proteins in the extracellular medium, irrespective of the secretion mechanism, is mass spectrometry. Combined with the use of mutant strains, or specific culture conditions, it can also identify the substrates of a given secretion machinery. For instance, comparison of the exoproteome of *Pseudomonas aeruginosa* in conditions where one T6SS machinery was on or off allowed the identification of three novel T6SS secretion substrates (Hood et al., 2010).

Quantitative proteomics not only can lead to identification of novel effectors, but also provide information on the regulation of secretion, as was recently shown with a focused exoproteome analysis of the T3SS in *Ralstonia*. The use of secretion mutants revealed that secretion is finely tuned and identified specific subsets of effectors with different secretion patterns (Lonjon et al., 2016).

Combined with a fractionation method to isolate a specific compartment of a target cell, proteomics can also identify novel translocated proteins in their target location. For example, this approach was used to draw up a list of putative nuclear effectors of *Anaplasma phagocytophilum* (Sinclair et al., 2015), and to identify *Chlamydia trachomatis* proteins associated to lipid droplets (Saka et al., 2015). Obviously, the method is

not sufficiently sensitive if the effector is present in minute amounts and is overwhelmed by eukaryotic proteins. One way to circumvent this limitation is to enrich for bacterial proteins using non-canonical amino acid tagging (Mahdavi et al., 2014). Selective labeling of bacterial proteins is accomplished via translational incorporation of a methionine surrogate. The technique requires the introduction of a gene coding for a mutant form of the methionyl-tRNA synthetase into the bacterium. During mixed culture with the bacterium, the host cells do not produce the altered methionyl-tRNA synthetase and do not incorporate the methionine surrogate, whereas the bacteria do. Bacterial proteins with the methionine surrogate are then enriched from the eukaryotic cells and identified by mass-spectrometry. This approach was used to identify *Yersinia* proteins that were secreted into the medium and translocated into cells (Mahdavi et al., 2014). In addition, pulse labeling with the methionine surrogate can be used to achieve temporal resolution (see Resolution of secretion in time and space).

Integral membrane proteins are notoriously difficult to detect by mass spectrometry because detergents interfere with the analyses. In a pioneering work in which alkaline sodium carbonate was used instead of detergent, Molloy et al identified the majority of integral *Escherichia coli* OM proteins and several diacyl-glyceride attached lipoproteins (Molloy et al., 2000). Proteomics is currently the method of choice to obtain an overall view of the secretion capacity of a given bacterium. For instance, it was recently applied to characterize the OM proteome and the exoproteome of *Bacteroides fragilis*, highlighting striking differences with *Proteobacteria*, from which most of the current information on bacterial secretion was derived so far (Wilson et al., 2015).

## Reporter-Based Assays

A large part of the "secretion toolbox" relies on reporter-based assays, which use genetic tools to tag a given secretion substrate with a readily detectable but otherwise neutral reporter and follow its secretion through a dedicated assay. In most cases, these assays are applied with a specific secretion machinery in mind, which orients the choice of the tag and the tagging strategy. A few rules are listed below, and most tags currently in use are briefly described in **Table 1**, with examples of their application.

### Tag Flexibility

For each new tag, one prerequisite is to ensure that the tag itself is neutral with regard to the secretion capacity of the machinery under inspection. Some secretion processes require the secretion substrate to unfold, and proteins that fold very rapidly upon synthesis are inappropriate as tags. For instance, green fluorescence protein (GFP) (Jaumouille et al., 2008) and glutathione S-transferase (Riordan et al., 2008), which fold rapidly block T3SS. Although GFP-tagged proteins are successfully exported through the Sec pathway, GFP fluorophore

**TABLE 1 |** Reporter systems to track protein secretion.

| Tag | Read-out | Tested for | Examples of application |
|---|---|---|---|
| Calmodulin-dependent adenylate cyclase (Cya) | cAMP production, Western-blot | T3S, T4S | Defining components and signals required for secretion (Sory and Cornelis, 1994)<br>Genome wide screens for T3S and T4S effectors candidates (Subtil et al., 2005; Carey et al., 2011) |
| Alkaline phosphatase (PhoA) | Enzymatic assay | | Protein export reporter (Manoil and Beckwith, 1985). |
| Amino-peptidase (AP) | Enzymatic assay | Sec dependent export (Gram+ bacteria) | Optimization of secretion (Guan et al., 2016) |
| β-1,4-mannanase (ManB) | Enzymatic assay | Sec dependent export (Gram+ bacteria) | Optimization of secretion (Lin et al., 2015) |
| staphylococcal nuclease (NucA) | Enzymatic assay | Sec dependent export (Gram+ bacteria) | Validation of predicted signal peptides and optimization of secretion (Mathiesen et al., 2009) |
| Green fluorescent protein (GFP) | fluorescence | T2S | Assembly pathway of the T2S complex (Lybarger et al., 2009) |
| Split GFP | fluorescence | T3S | Localization of secreted effectors in eukaryotic host (Van Engelenburg and Palmer, 2010) |
| Tetracysteine motif | fluorescence | T3S | Kinetics of effector translocation (Enninga et al., 2005) |
| LOV | fluorescence | T3S | Detection of effector translocation (Gawthorne et al., 2016) |
| Glutamyl carboxypeptidase | fluorescence | T3S | Detection of protein secretion (Yount et al., 2010) |
| TEM-1 β-lactamase | fluorescence (FRET) | T3S, T4S | Genome wide screen for T4S effector candidates (Zhu et al., 2011), study of translocation dynamics (Mills et al., 2013) |
| Gaussia princeps luciferase (Gluc) | luminescence | T1S | Detection of secreted fusion protein in culture supernatant (Wille et al., 2012) |
| Bacteriophage P1 Cre recombinase | luminescence/ fluorescence | T3S, T4S | Detection of effector translocation (Luo and Isberg, 2004; Briones et al., 2006) |
| Phosphorylation target | Western blot: detection of phosphorylated tag | T3S, T4S | Detection of effector translocation (Day et al., 2003; Garcia et al., 2006) |
| Nucleoskeletal-like protein (Nsp) | Western-blot | Flagellar secretion apparatus | Identification of export signal (Wang et al., 2016) |

is inefficiently folded in the periplasm (Feilmeier et al., 2000). On the other hand, GFP is an ideal reporter for the Tat system, since it can be exported in a folded form (Thomas et al., 2001). The GFP re-folding problems have been solved using superfolder GFP variant (Choi et al., 2017) or monomeric red fluorescent protein (mRFP) and its derivatives (Shaner et al., 2004). Several strategies were developed to find alternatives to GFP to facilitate the tracking of effector injection into a host cell with fluorescence (**Figure 2**, and see part Resolution of secretion in time and space for live imaging with temporal resolution).

### Tag Position

The position at which the tag is fused to the secreted protein is important because the tag can compromise the recognition of the secretion signal. For instance, T3SS substrates have an amino-terminal signal that must remain unaltered in the tagged construct. Typically, C-terminal tags are used for proteins with an N-terminal signal sequence.

### Secretion Readout

Many tags are associated with an enzymatic activity, which provides quantitative data on secretion. Tags that are enzymatically active only in a given environment facilitate quantification. For example, alkaline phosphatase and beta-lactamase are active only in the periplasm, and have been used extensively to probe IM protein topology and to identify periplasmic proteins by gene fusion approaches. The membrane impermeable beta-lactamase substrate nitrocephin is a useful probe for surface exposed beta-lactamase fusions that remain cell associated upon secretion (Sauvonnet and Pugsley, 1996). One widely used reporter of protein injection (via T3SS or T4SS) into a host cell is the calmodulin-dependent adenylyl cyclase of *Bordetella pertussis*. Since bacteria do not produce calmodulin, whereas eukaryotic cells do, accumulation of cyclic AMP marks the injection of the reporter in the cytoplasmic compartment of the target cell (Sory and Cornelis, 1994). Reporter tags that become phosphorylated in the eukaryotic cytosol have also been used (Day et al., 2003; Garcia et al., 2006). In the last ten years, the development of fluorogenic beta lactamase substrates allowed to follow injection of effectors fused with beta lactamase (TEM1), and this enzymatic-based assay has also largely been used, including very recently, *in vivo* (see Resolution of secretion in time and space).

In contrast to global approaches using bioinformatics or proteomics described above, reporter-based assays are only amenable in genetically tractable microorganisms. However, secretion machineries and secretion signals are well conserved, allowing the use of heterologous secretion systems to identify secretion substrates in non-genetically tractable bacteria (Subtil et al., 2001).

Reporter-based assays are mostly used for candidate-based approaches, because they require the generation of genetically modified organisms. They are typically used to validate candidates indicated by secretion signal predictors or by proteomic approaches. However, high-throughput cloning strategies and simplification of the read-outs have allowed the application of these assays to screen for novel secretion substrates in genome wide approaches (Subtil et al., 2005; Carey et al., 2011; Zhu et al., 2011).

## Functional Screens in Yeast

Many proteins injected into a eukaryotic host cell target proteins and pathways that are highly conserved in all eukaryotic cells. Based on this observation, expression libraries of bacterial genes under inducible promoters have been screened in yeast. Most screens selected bacterial genes that inhibited yeast growth (Campodonico et al., 2005; Slagowski et al., 2008), but atypical localization of bacterial proteins (for instance in the nucleus)

| Reporter system | Before effector translocation | During/after effector translocation | Sensitivity | Resolution in time | Resolution in space | Quantitative | Versatility | Endogenous effector tracking |
|---|---|---|---|---|---|---|---|---|
| CCF2/4 [47, 113] |  | | ☑ | ☑ | ✗ | ✗ | ☑ | ✗ |
| GFP-chaperone [108] |  | | ☑ | ☑ | ☑ | ☑ | ✗ | ☑ |
| Tetracysteine motif [109] |  | | ☑ | ☑ | ✗ | ☑ | ☑ | ✗ |
| Cre/LoxP [132] |  | | ☑ | ✗ | ✗ | ✗ | ☑ | ✗ |
| Split-GFP [128] |  | | ☑ | ✗ | ☑ | ✗ | ☑ | ✗ |
| LOV [129] |  | | ☑ | ☑ | ✗ | ✗ | ☑ | ✗ |

**FIGURE 2 |** Comparison of the different tools to image effector secretion into living cells. Illustrations reflect different experimental set-ups, please refer to the indicated reference for description of the bacterium, effector and time scale. Bacteria are represented by an oval, cells by a rectangle. Colors represent the fluorescent signal recorded before **(left)** and after **(right)** the effector translocation has started. Discussion on the pros and cons of some of these assays can be found in Ehsani et al. (2009) and Zuverink and Barbieri (2015).

(Sisko et al., 2006) or other particular phenotypes such as interference with the secretory pathway can also be screened for (Heidtman et al., 2009). The ease of manipulating yeast genome, and conservation of the molecular pathways with higher eukaryotes, can then facilitate the identification of specific targets of the bacterial effectors identified by this approach.

### Phage Display Technology

Jacobsson and Frykberg were the first to take advantage of the power of shot-gun filamentous bacteriophage display (display of random fragments of bacterial genomic DNA) to identify *S. aureus* proteins that interact with components of the extracellular matrix and immunoglobulins (Jacobsson and Frykberg, 1996). Since then, many genes encoding proteins involved in host-microbial interactions have been identified using this technology. Coupled to next generation sequencing, it can also be applied to the identification of secretomes, in particular in mixed microbial populations. This powerful technology was recently reviewed in detail and will not be discuss further (Gagic et al., 2016).

## ANALYSIS OF PROTEIN SECRETION SIGNALS AND MACHINERIES

### Identification of Components of Secretion Machineries and Secretion Signals

#### Genetic and Chemical Screens

The first protein export signals identified were the cleavable N-terminal signal peptides that target proteins to the endoplasmic reticulum in eukaryotic cells (Jackson and Blobel, 1977). In *E. coli*, studies of genes involved in maltose and lactose transport or catabolism have provided a wealth of genetic tools to study protein export (**Figure 3**). Powerful genetic approaches have been designed based on special properties of beta-galactosidase (LacZ) fusions (Shuman and Silhavy, 2003). Selections devised to identify mutations that affect protein export were based on the Lac- phenotype of strains producing fusions of the periplasmic maltose-binding protein MalE with the cytoplasmic LacZ. These fusions, which target beta-galactosidase to the export pathway, are enzymatically inactive and confer a Lac- phenotype to bacteria, allowing for selection of Lac+ export-defective mutants. The mutations frequently mapped to the proximal region of gene fusions coding for the signal peptide (Bedouelle et al., 1980), introducing charged residues in their hydrophobic segment. Importantly, Lac+ selection also yielded several classes of mutants with pleiotropic export defects. Many of those were conditional lethal mutations in genes encoding novel protein export factors, including the preprotein translocase SecA, or the translocation channel SecY (Ito et al., 1983). Suppressor (*prl*) mutations that restored export of proteins with defective signal sequences also mapped in the *secA* and *secY* genes, strongly suggesting that signal sequences interacted with their gene products. Indeed, this was confirmed by many studies and by structural data that revealed how signal sequences bind to SecA (Gelis et al., 2007) or SecY and the lipid bilayer (Li et al., 2016). Although they do not share sequence homology and appear to be interchangeable between proteins, signal sequences differ in their ability to promote efficient export, as illustrated in a genome-wide

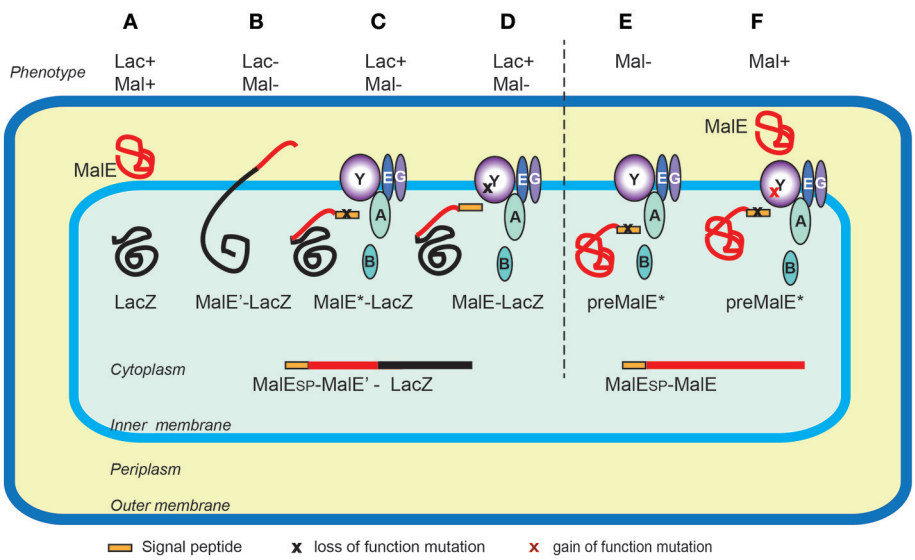


**FIGURE 3 |** Genetic selections of export-defective mutants based of MalE-LacZ fusions. In wild type *E. coli* the correct localization of LacZ (cytoplasmic) and MalE (periplasmic) allows lactose catabolism and maltose uptake, respectively, conferring the ability to ferment these sugars, and the red colony phenotype on MacConkey indicator plates **(A)**. The MalE-LacZ fusion proteins directed to the periplasm confer a Lac- phenotype **(B)**, which served as a basis for selection of spontaneous Lac+ mutants on lactose tetrazolium plates. These strains either contained mutations in MalE signal sequence (MalE*) **(C)**, or the loss-of- function mutations in the *sec* genes encoding export factors, five of which, (SecA, B, Y, E and G) are depicted **(D)**. Bacteria producing the full-length MalE precursor with a signal sequence mutation are export defective and Mal- **(E)**, allowing for selection of Mal+ suppressor mutations (gain-of-function *prl* alleles) mapping in several *sec* genes, (e.g., *secY*) that promote export of MalE* variants with signal sequence mutations **(F)**. Note that the MalE signal sequence (yellow rectangle) is absent from periplasmic MalE-LacZ or MalE, as it is cleaved and degraded upon export across the IM.

study of *Lactobacillus* signal peptides that assessed their ability to promote export of nuclease reporter (Mathiesen et al., 2009). Successful approaches to improve signal sequence efficiency have been reported. For example, combinatorial mutagenesis of the signal sequence-coding region resulted in variants with increased export and production of beta-lactamase, probably due to an overlap of export signals with elements of translational or post-translational regulation (Heggeset et al., 2013).

The Tat signal was also largely investigated through genetic screens. Although a native Sec substrate, MalE was successfully used to monitor the activity of the Tat-dependent signal peptide of TorA, by following maltose utilization on pH indicator media (indicating maltose fermentation) or by growth on minimal maltose plates (Kreutzenbeck et al., 2007). This allowed the use of powerful genetic approaches to identify suppressors of Tat signal sequence changes that restored MalE export, affecting genes encoding the TatB and TatC export machinery components (Lausberg et al., 2012). In a genome-wide screen for Tat-dependent exo-proteins of *P. aeruginosa*, the authors used the *E. coli* amidase AmiA as a reporter to validate the functionality of a newly identified Tat signal peptide (Ball et al., 2016). Tat-mediated AmiA export is required for the correct separation of daughter cells during cell division, and defects in this process render *E. coli* hypersensitive to detergents, providing a simple plate test.

In monoderm bacteria, surface proteins of the "LPxTG" family are anchored to the cell wall in a process mediated by the sortase enzymes (Schneewind and Missiakas, 2014). Since sortase substrates include major virulence factors, small molecule screening has been used to identify sortase inhibitors (Maresso et al., 2007). In *S. aureus*, transposon mutagenesis was used to look for mutants with defective surface anchoring of the protein A (SpA), using detection of fluorescently labeled Anti-SpA antibodies and flow cytometry (Frankel et al., 2010).

## Assays of Protein Export to the Periplasm or Secretion across the OM

### *Signal pepides and the Sec system*

Measuring the rate of signal peptide processing can serve as a good quantitative indicator of protein export, as the signal peptidase cleavage takes place in the periplasm. Radioactively labeled amino acids (usually $^{35}S$ - labeled methionine and cysteine) are incorporated into the newly synthesized proteins during a short "pulse" labeling period. Addition of an excess of unlabeled amino acids and an inhibitor of protein synthesis during a "chase" period allows one to follow precursor cleavage with precision and to establish the time course characteristic for a given strain (**Figure 4**; Kumamoto and Gannon, 1988). In addition, strong export defects, such as those caused by signal sequence mutations, can be observed in steady state by the presence of precursor forms of a protein by denaturing SDS-PAGE and immuno-detection. Fractionation in steady state can reveal partitioning of the precursors with the cell fraction and mature forms to the periplasm (Francetic et al., 2007). This approach has been used to characterize the strongly hydrophobic signal sequences that direct proteins like thioredoxin or DsbA to the co-translational export *via* the signal recognition particle (SRP) (Huber et al., 2005). All of these assays are target-based and rely on the availability of specific antibodies or antigen tags for immuno-precipitation of radioactively labeled protein or for immuno-detection.

### *Lipoproteins*

Lipoproteins are exported proteins that undergo fatty acylation during biogenesis and remain anchored in membranes (Zückert, 2014). Lipoprotein signal peptides can be predicted by bioinformatics approaches, mostly thanks to the presence of a conserved lipobox motif with a consensus LAGC. This motif probably interacts with Lgt (Pallier et al., 2012), the first component of the biogenesis pathway that adds the diacyl-glycerol moiety to the invariant Cys residue. In the next step, the signal peptide is removed by a dedicated lipoprotein signal peptidase, Lsp. Accumulation of unprocessed precursors in the presence of globomycin, an Lsp inhibitor, can serve as a tool for experimental validation of predicted lipoproteins, at least in *E. coli*. Another method frequently used to demonstrate protein fatty-acylation *in vivo* is metabolic labeling with radioactive fatty acids, usually palmitate (Jackowski and Rock, 1986).

In *E. coli* and related bacteria, lipoproteins either remain anchored in the IM or are taken to the OM *via* the Lol sorting machinery (Zückert, 2014). The sorting signals that determine retention in the IM or extraction and transport to the OM typically reside within the four N-terminal residues of the mature lipoprotein. Systematic analysis of model lipoproteins in an *in vitro* membrane release assay allowed Hara and co-workers to characterize these signals in *E. coli* providing the basis for bioinformatics predictions (Hara et al., 2003). However, the sorting rules are not valid for all bacteria and there are many exceptions, even in well-studied enterobacterial species. Membrane fractionation in sucrose density gradients followed by immuno-detection is a reliable tool to determine *in vivo* localization of lipoproteins, as for integral membrane proteins. This method relies on differences in composition and density of the *E. coli* IM and OM, allowing good separation using equilibrium centrifugation in flotation sucrose density gradients, where the total membranes are deposited on the bottom and float upon ultra-centrifugation to their equilibrium density. Relative positions of specific proteins in gradient fractions can be analyzed by immunodetection, as in the systematic analysis of +2 residue substitutions in a model lipoprotein lipoMalE (Seydel et al., 1999). In addition, lipoMalE conferred a Mal+ phenotype to *E. coli* when localized in the IM but not in the OM, providing a plate assay for lipoprotein localization based on utilization of maltose as a carbon source. As a different approach, *in vivo* analysis of lipoproteins fused to the monomeric fluorescent protein mCherry can be performed following plasmolysis, which swells the periplasm and facilitates direct visualization of IM or OM lipoprotein association: while OM lipoproteins follow the contours of the bacterial cell, the irregularly shaped plasmolysis bays are decorated with IM associated lipoproteins (Lewenza et al., 2006).

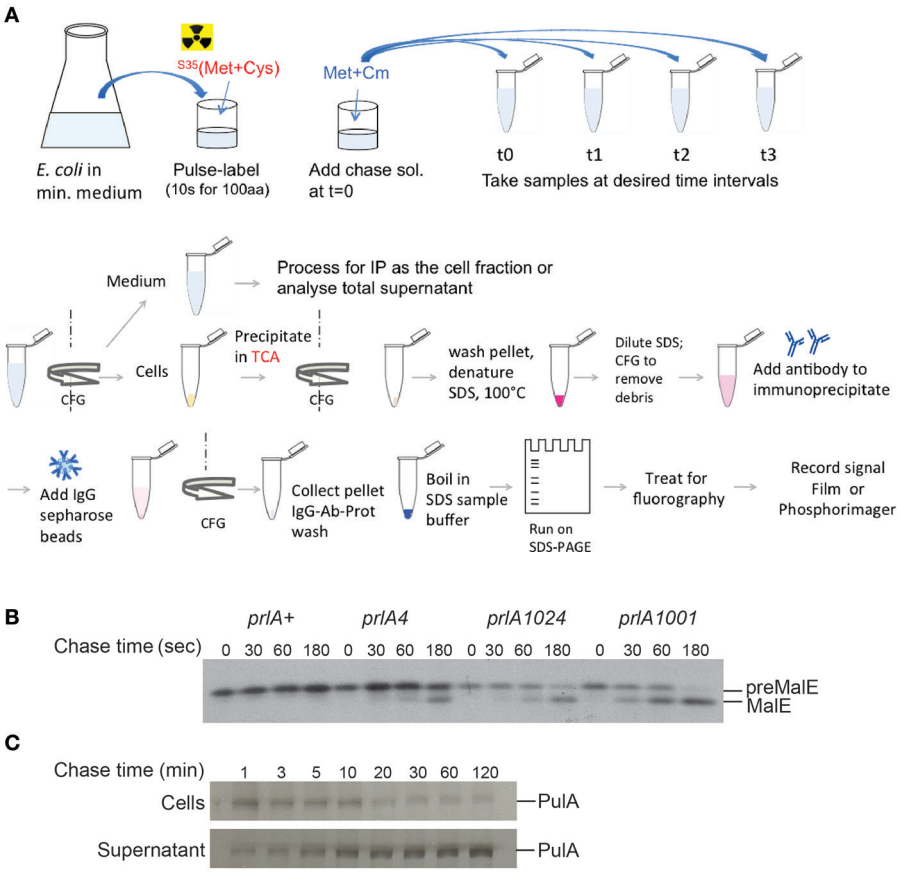


**FIGURE 4 |** Pulse-chase assay to analyze protein export or secretion rates. **(A)** Bacteria are grown in minimal medium in conditions inducing the expression of the gene of interest and pulse labeled with $^{35}$S-methionine and cysteine for a short period (30 s–2 min, depending on the size of the protein under study), followed by addition of cold methionine and chloramphenicol (Cm) to stop protein synthesis. Samples are collected at indicated times and bacterial cultures are either precipitated with TCA or separated from the medium prior to precipitation of each fraction. The collected precipitates are washed with acetone, dissolved in SDS buffer and boiled to denature proteins. Upon the removal of cell debris by centrifugation and dilution of SDS, antibodies are added for immuno-precipitation. Antigen-antibody complexes are adsorbed on protein A-sepharose beads, washed and eluted in SDS sample buffer for analysis by SDS-gel electrophoresis and fluorography. **(B)** Kinetics of signal sequence processing in preMalE variant carrying a signal sequence mutation, reflecting the kinetics of MalE export. While the preMalE export and processing are blocked in wild type *E. coli* (*prlA*+), they are partially restored in strains carrying different suppressor *prlA* alleles of the *secY* gene encoding the translocation channel. Bacteria were labeled for 20 s with radioactive methionine and a chase with excess cold methionine was performed for the indicated times. After immuno-precipitation of total cell extracts with anti-MalE antibodies, proteins were separated on SDS-PAGE, and analyzed by fluorography (modified from Francetic et al., 1993). **(C)** Pulse-chase and fractionation were used to follow the kinetics of pullulanase (PulA) secretion *via* the T2SS. The bacteria were cultured as in **(A)** and pulse-labeled for 3 min. Samples were collected after the indicated times of chase with cold methionine, and cell and supernatant fractions were separated by centrifugation, prior to immunoprecipitation and SDS-PAGE analysis as in **(A)** (modified from Francetic and Pugsley, 2005).

While lipoproteins represent an important group of surface proteins in monoderm bacteria, in diderms they generally reside in the periplasmic membrane leaflets. However, recent investigations have revealed lipoproteins that are fully or partially surface-exposed, either through known secretion systems (T2SS, T5SS) (Leyton et al., 2012; Rondelet and Condemine, 2013), or by novel mechanisms (Wilson and Bernstein, 2016). In the Lyme disease agent *Borrelia burgdorferi* many lipoproteins that play a role in virulence are exposed on the cell surface. Their localization has been studied using mRFP as a fluorescent reporter. Using the model lipoprotein OspA-mRFP, a cell-sorting based mutant screen led to identification of residues required for the surface exposure presumably participating in a flipping step whose cellular determinants remain to be identified (Kumru et al., 2010). Some *E. coli* lipoproteins, including Lpp (Cowles et al., 2011) and RcsF, are partially exposed on the bacterial surface. This unusual feature has been tested using the so-called epitope walking approach of the OM lipoprotein RcsF. The FLAG tag was inserted at multiple positions in the RcsF sequence, and a dot blot analysis of whole and lysed cells using monoclonal anti-FLAG antibody allowed for identification of protein regions that are accessible in intact cells. The FLAG appears to be a useful and neutral tag that does not seem to interfere with transport across membranes (Konovalova et al., 2014). This approach revealed how RcsF uses OM proteins as portals for surface exposure, and how this mechanism allows the bacteria to monitor the functional state of their Beta-barrel Assembly Machinery (BAM) (Konovalova et al., 2014).

*Surface exposed and associated proteins*

A subset of exported proteins is inserted in the outer membrane and partially exposed on the cell surface to perform diverse functions, including solute uptake, macromolecule transport or proteolysis. The OM insertion generally relies on the signals encoded in the mature protein, notably the propensity to form beta-barrels, and is generally mediated by the BAM complex (Voulhoux et al., 2003; Wu et al., 2005). The BAM machinery is probably responsible for OM insertion of the beta-barrel domain of T5SSs, which provide the portal for secretion of so-called "passenger domains" (Leyton et al., 2012; Bernstein, 2015). Although the passenger domains can be cleaved and released into the medium to perform diverse extracellular functions, many of them remain surface bound. The surface exposure of specific proteins or protein domains can be assessed through analysis of non-permeabilized cells by immunofluorescence or by analyzing protease accessibility in whole cells, with a comparative assessment of general protease susceptibility of the same substrate in lysed bacteria (Besingi and Clark, 2015). For enzymes that degrade biopolymers, plate assays for protease, lipase, cellulase or chitinase activities, to name a few, rely on the visualization of a halo zone of substrate degradation surrounding the secreting colonies. Secretion of one of the first identified T2SS substrates, the lipoprotein pullulanase (d'Enfert et al., 1987), has been assessed by growth on minimal media containing pullulan as the sole carbon source, through degradation of chromogen-tagged pullulan, or by semi-quantitative enzymatic assays that determine the fraction of hydrolytic activity present in intact compared to the lysed bacteria by measuring the reducing sugar as the reaction product. All these methods are semi-quantitative, end-point assays, which do not provide kinetic information on protein secretion.

Similar approaches have been used to study surface protein secretion via T5SS or the recently discovered T9SS. In *Porphyromonas gingivalis* the T9SS is required for the black pigment of colonies on blood agar, linked to heme acquisition mediated by secreted proteases gingipains. Substrates of this pathway are exported to the periplasm via the Sec pathway and their N-terminal signal peptide. Their secretion in a folded state requires a C-terminal signal within a specific beta-sandwich domain, which is able to promote secretion of folded GFP (de Diego et al., 2016).

## Mechanistic Approaches

Understanding a secretion mechanism requires detailed structural knowledge of the secretion machinery, its composition, biogenesis and dynamics during interactions with the secreted substrate. A few assays have been designed to understand how secretion proceeds. They are complementary to microscopic observations of secretion machineries, itself an expanding field of research (Costa et al., 2015; Li et al., 2016). The question concerning energy requirements for the process has been addressed by depleting ATP or by dissipating the proton motive force, two main energy sources required for membrane transport (e.g., Possot et al., 1997). Many secretion systems use at least one ATPase as an essential component, and ATP hydrolysis as a mechanical force generator (Costa et al., 2015).

### Capture of Protein Interactions and of Intermediate States in the Secretion Process

In many systems, a bacterial two-hybrid approach is an excellent tool to map protein-protein interactions between dynamic components in secretion systems, in particular membrane embedded elements in trans-envelope complexes (Karimova et al., 1998). Fusions to cytoplasmic fragments of the CyaA reporter can effectively block some transport intermediates in the membrane and allow assessment of interactions that are transient in the native system. Examples include studies of complexes in T2SS (Nivaskumar et al., 2016) and T6SS (Logger et al., 2016).

Specific inhibitors of secretion can also be used to block secretion at a specific step (Moir et al., 2011). Chemical libraries have been used to identify compounds that specifically inhibit elastase and Plc secretion in *Pseudomonas* T2SS using a colorimetric enzymatic screen of culture supernatants (Moir et al., 2011). Once such inhibitors are identified, the major challenge is to identify their specific protein targets and modes of inhibition.

In T1SS and T3SS, substrates are secreted in an unfolded state and bulky domains fused to the substrate might block secretion, potentially providing important clues about intermediates in the secretion process. In T3SS, blocking the secretion using a GFP fusion with a secretion substrate revealed that secretion occurs at a cell pole (Jaumouille et al., 2008). A bulky "knot" region fused to different T3SS substrate allowed Dohlich and coworkers to demonstrate that the substrate passes through the T3SS channel (Dohlich et al., 2014).

In many cases substrates of blocked or incomplete secretion systems are degraded *in vivo* due to the absence of specific partners, chaperones or cellular structures. In T6SS, for example, the component of an inner tube HCP binds specific folded substrates in the bacterial cytoplasm and is required for their stability (Silverman et al., 2013). Folded substrate PulA of the T2SS (East et al., 2016) or TcpF secreted by the assembly system of TCP pili (Kirn et al., 2003) are also prone to degradation if their secretion is compromised. Since protein secretion efficiency is typically assessed in steady state by combining fractionation and substrate detection using antibodies or activity assays, it is important to keep in mind that proteolysis of non-secreted substrate may skew quantification of secretion efficiency. While the bulk of secretion-defective variants will be degraded, a small amount of extracellular protein that escapes degradation might give an impression of full secretion efficiency. The use of radiolabeling in pulse-chase assays coupled to fractionation might help overcome this problem (**Figure 4C**). Radioactive labeling is a powerful tool in secretion analysis due to its unsurpassed sensitivity. Selective labeling of bacterial proteins in cell culture has helped to identify proteins from enteropathogenic *E. coli* injected into eukaryotic cells *via* T3SS (Kenny and Finlay, 1995).

A number of gene fusion and mutagenesis approaches have been employed using different T2SS substrates to elucidate the molecular nature of the secretion signal and the component of the secretion machinery with which they interact. As already discussed, the sequence diversity of exoproteins, including those using the same secretion system, and systems makes

this task difficult, however. In view of their heterogeneity, it is reasonable to assume that T2SS components that are interchangeable between systems do not make specific contacts with secretion substrates. A site-directed *in vivo* cross-linking approach has been used to identify secretion motifs in PelI and their interactions with the T2SS of the plant pathogen *Dickeya dadantii*. The unnatural photo-cross-linkable amino acid pBPA incorporated at specific sites in exoproteins was used as a tool to capture transient complexes *in vivo,* providing evidence for PelI binding to OutD forming the OM channel of the T2SS, and to OutC, which interacts with OutD (Pineau et al., 2014). A similar approach has been used to track secretion intermediates in T5SS (Ieva et al., 2011).

### *In vitro* Reconstitution

In an advanced stage of analysis, secretion systems could be reconstituted *in vitro* to gain insights into the transport process. With the notable exception of the Sec system that has been functionally reconstituted *in vitro* (Duong and Wickner, 1997), few other systems have been studied at this level, due to their complexity and difficulties to extract them from the bacterial envelope in a functional state. Nevertheless, *in vitro* transcription-translation systems have been used successfully to study biogenesis of specific transport components including the OM channel called secretin that self-assembles and insert into liposomes (Guilvout et al., 2008) or the IM prepilin peptidase, both components of the T2SS (Aly et al., 2013).

## RESOLUTION OF SECRETION IN TIME AND SPACE

Several tools have been developed in the last two decades to improve the spatio-temporal resolution of techniques aimed at tracking secretion. They have mostly been applied to effector injection into a neighboring cell through the T3SS and T4SS, and to some extent to the T6SS.

### When Is Protein Injection Activated?

Protein injection in a neighboring cell is a highly regulated process that is typically constitutively turned off and only activated by specific signals. In many cases, activation occurs at least in part at the transcriptional level (Mavris et al., 2002; Urbanowski et al., 2005), so the activity of promoters has been used as a read-out for secretion activity. Monteiro et al. (2012) used the luciferase reporter under the control of the promoter of *hrpB*, the transcriptional regulator that controls the expression of *Ralstonia solanacearum* T3SS genes, in order to track the activity of the T3SS *in planta*. This approach revealed that T3SS activation was important not only for the first stages of infection, to manipulate host plant defenses, but also during late stages of infection (Monteiro et al., 2012). In a somewhat different set-up using a fast-maturing GFP under the control of the transcription activator MxiE, Campbell-Valois and collaborators provided evidence that *Shigella flexneri* T3SS goes through two waves of activation: one upon cell contact, during the invasion process, and a second, concomitant with the motile stage of the infection cycle, when bacteria move throughout the cytoplasm through actin cytoskeleton remodeling. The T3SS was switched off between these two phases (Campbell-Valois et al., 2014).

Another readout of active protein injection can be found in the effects on the target, when this effect is rapid and easy to detect. The T6SS functions as a contractile nanomachine, called the molecular crossbow, that punctures target cells to deliver lethal effectors. Time-lapse fluorescence microscopy of cocultures demonstrated that prey cells were killed upon contact with predator cells, and that prey lysis occurred within minutes after sheath contraction (Brunet et al., 2013). A killing assay was designed to understand how *Proteus mirabilis* coordinates multicellular swarming behavior and discriminates itself from another *Proteus* species during swarming. This assay, together with live-cell microscopy, demonstrated that T6SS-mediated lethality is unique to morphologically distinct swarmer cells, and that it requires direct cell-cell contact (Alteri et al., 2013).

The strategies illustrated above aim at measuring the activation of a given secretion machinery. They do not provide information on the nature of translocated effectors, or on the kinetics of secretion of a given effector, questions that are addressed below.

### How Fast Does Protein injection Take Place and What Is the Hierarchy of Substrate Secretion?

Highly sensitive and time-resolutive tools were needed to answer these questions in order to focus on the very early secreted effectors, typically during the first 15 min following the attachment of a bacterium to its target cell. The current tools are mostly microscopy-based, allowing for single-cell measurements.

A pioneering work in the field focused on the secretion of SipA, an early effector of *Salmonella* Typhimurium (Schlumberger et al., 2005). The kinetics of secretion of this effector were measured by two complementary approaches. First, using live microscopy and a GFP-tagged version of the SipA chaperone, InvB, produced by a genetically engineered eukaryotic host cell, the secretion kinetics were determined by monitoring and quantifying InvB-GFP recruitment to contact sites between *Salmonella* and the cell. This elegant approach can not be applied to all effectors, since it requires the identification of a high-affinity partner (here the chaperone). As the second readout, the redistribution of SipA from the bacterial cytoplasm to its periphery was measured, on samples fixed at various times after live microscopy, from the moment of contact between the bacteria and the cell. Although this could in theory be automated to some extent, it requires very clean antibodies and extensive image acquisition. Another disadvantage was that detection of SipA with antibodies required sample fixation, preventing live imaging and analysis of later events.

In a different approach, two early effectors of *S. flexneri*, IpaB, and IpaC, were tagged with a tetracysteine tag. By loading the bacteria with fluorescent FlAsH probes, it was demonstrated that both effectors were secreted instantly after contact with host cells, with a half maximal rate of 4 min in both cases (Enninga et al., 2005). FlAsH labeling yields a somewhat poor signal-to-noise ratio, and is probably not appropriate for effectors of moderate

or low abundance. The signal was only poorly detectable in the host cell, and loss of effector from the bacteria was recorded.

One current limitation of all the live imaging techniques is that they allow tracking of only one effector at a time. In order to gain insight into the hierarchy of secretion of different effectors, it is therefore necessary to compare the kinetics of secretion measured separately. For instance, the rate of secretion of tetracysteine-tagged SopE2 was found to be about 2-fold faster than that of SptP, another *Salmonella* effector, explaining how two effectors with antagonistic effects on the host cell could cooperate during the infectious process (Van Engelenburg and Palmer, 2008).

Currently, the most widely used assay is based on the development of fluorogenic substrates of beta-lactamase, and has been extensively applied to monitor secretion in T3SS and T4SS. Effector proteins are fused to beta-lactamase, while host cells are pre-loaded with the membrane-permeable substrate coumarin cephalosporin fluorescein (CCF2 or CCF4). The injection of the effector/beta-lactamase fusion protein into the host cytosol is detected by the loss of FRET upon cleavage of the fluorogenic substrate, inducing a switch in the fluorescence from green to blue (Charpentier and Oswald, 2004; Zuverink and Barbieri, 2015; **Figure 5**). This system has for instance been used with the beta-lactamase reporter encoded chromosomally in fusion to twenty different enteropathogenic *E. coli* (EPEC) effectors (Mills et al., 2013). Changes in the fluorescence of the CCF2 were monitored at 90 s intervals, and the secretion kinetics of ten different effectors was determined through this approach.

Although less resolutive in time, measurements on whole populations can provide information as to the order of effector secretion under some circumstances. *Chlamydia trachomatis* secretes several effectors, e.g., TarP and TepP, upon contact with the host cell. Once in the cytosol, TarP and TepP are tyrosine phosphorylated by host kinases. TarP phosphorylation was detectable as early as 5 min post infection whereas TepP phosphorylation occurred only between 5 and 15 min post infection, indicating that TarP injection occurs first (Chen et al., 2014). A similar strategy, combined with the addition of tags that become phosphorylated in the eukaryotic environment (Day et al., 2003; Garcia et al., 2006), could, in theory, be applied to several effectors, provided that they differ in size. Using an identical tag for each effector would limit the possibility that a difference in phosphorylation rates only reflects substrate preference by the host kinases involved.

On a larger scale, bio-orthogonal non-canonical amino acid tagging (BONCAT), combined with pulse labeling of the methionine surrogate, introduced the possibility to track the injection of endogenous proteins. Using this elegant strategy, Mahdavi and collaborators were able to characterize the order and pace of secretion, over 3 h of infection, of 11 Yop effectors from *Yersinia enterocolitica* (Mahdavi et al., 2014).

## When Does Secretion Occur in a Complex Environment?

Although the complexity of secretion has been explored experimentally *in vitro* at a single cell level, fewer studies have tried to unravel the secretion complexity in more complex systems such as a population of cells and bacteria or even during infection in animal models.

The heterogeneity in secretion rates between different effectors led Mills and collaborators to pay attention not only to effectors but also to the target cells. By single cell tracking in cultures loaded with CCF2 and infected with either *Salmonella*

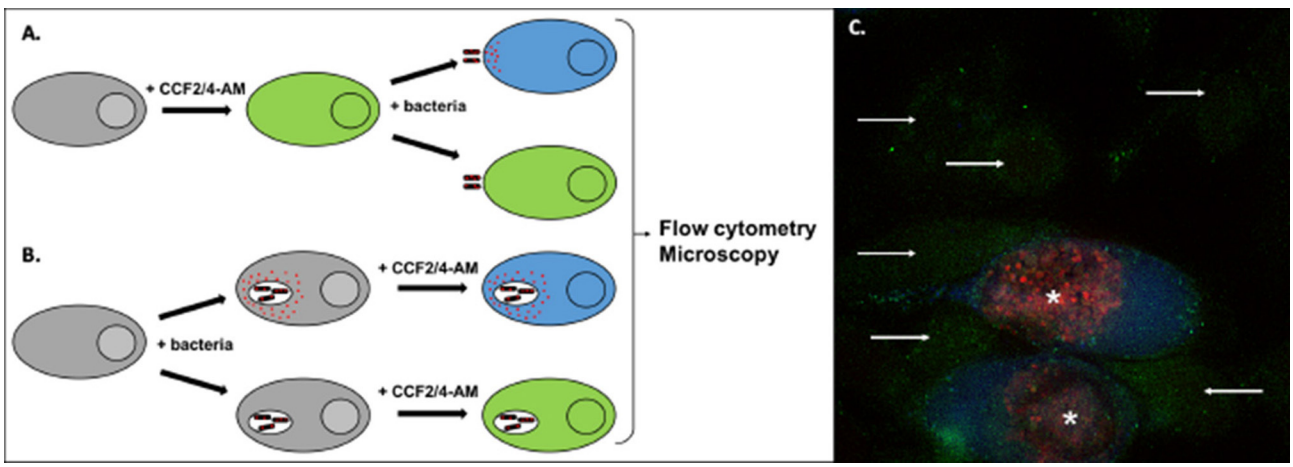


**FIGURE 5 |** Detection of effector translocation using the beta-lactamase/CCF2/4-AM system. **(A,B)** Schematic view of the experimental set-up to test the translocation of a bacterial protein fused to beta-lactamase (red dots). To monitor secretion from extracellular bacteria, or from intracellular bacteria at an early stage of infection, cells are usually pre-loaded with the CCF2/4-AM **(A)**. Alternatively, the probe can be added to cells after infection, to monitor secretion events that occur later in infection **(B)**. Conversion of the fluorescent probe can be measured by microscopy or by flow cytometry. **(C)** Illustration of the analysis using microscopy. HeLa cells were infected for 40 h with *Chlamydia trachomatis* stably transformed with a plasmid expressing the translocated protein TarP in fusion with beta-lactamase and mCherry (Mueller and Fields, 2015). In the last 2 h of incubation the cells were loaded with CCF4-AM probe, before fixation. In uninfected cells the probe emits green fluorescence (arrows). In infected cells (bacteria in red, asterisks) translocation of the beta-lactamase activity into the cytosol is revealed by the appearance of a blue fluorescent signal, corresponding to the cleaved probe.

Typhimurium or EPEC producing effectors fused to beta-lactamase, they identified a population of cells that were resistant to secretion, for which, despite the contact with bacteria, the fluorescence of the CCF2 remained unchanged even a couple of hours after infection. Whether this resistance to secretion is conferred by the host cell or is due to heterogeneities in the bacterial population remains unclear (Mills et al., 2013).

Only few studies have analyzed bacterial protein secretion in whole organisms. One example is the study of the activation of T3SS in whole plants, as was mentioned above (Monteiro et al., 2012). The early production of the T3S effector ExoU of *P. aeruginosa* and its secretion were shown to be critical for the development of the pathology in the lung of infected mice, using inducible production of the protein and immunolabelling on histological sections with a specific antibody to ExoU (Howell et al., 2013).

In a more complex system, Rolán and collaborators tackled the challenge of identifying the targets of the *Yersinia* effector YopH *in vivo* in mice, the main difficulty being the isolation of the few neutrophils targeted by the bacteria. In order to achieve this, they fused the beta-lactamase reporter to the first 100 amino acids of YopE. The splenocytes were then purified and loaded with CCF4 *ex vivo*, and the neutrophils injected with YopE were sorted from non-targeted cells on the basis of their fluorescence profile. This strategy allowed the authors to identify YopH-targeted signal transduction pathways that impair neutrophil responses *in vivo* (Hortensia Rolán et al., 2013).

Very recently, a genome-wide method, named EXIT (exported *in vivo* technology), was developed to identify proteins that are exported by bacteria during infection (Perkowski et al., 2017). EXIT utilizes the TEM beta-lactamase reporter lacking its native signal peptide, which, when fused in-frame to an export signal (i.e., signal peptide or transmembrane domain) confers beta-lactam resistance. By combining a comprehensive library of in-frame TEM fusions with the ability to select bacteria exporting fusion proteins *in vivo* and next-generation sequencing en masse of the recovered fusions, EXIT identified 593 proteins exported by *Mycobacterium tuberculosis* during infection in mice (Perkowski et al., 2017). Fifty-seven percent of these hits were predicted integral membrane proteins and 38% contained a predicted signal peptide. EXIT also identified 32 proteins (5%) lacking *in silico* predicted export signals.

## CONCLUDING REMARKS

In the last decade, the repertoires of bacteria known to secrete proteins and of secreted proteins have expanded, and several novel secretion machineries have been discovered. These findings were mostly driven by technological advances, such as the discovery of secretion substrates through phage display coupled to next generation sequencing or through proteomics, independently of the secretion mechanism used, or by the development of probes that allowed sensitive detection of effector injection into a neighboring cell. Machine learning approaches have also pointed to new potential secretion substrates, and, with the expansion of the training sets (i.e., validated substrates and characterized secretion machineries) these approaches will likely be applicable to more secretion systems. In parallel, remarkable progress has been made in the exploration of the structure of the multicomponent secretion machineries using cryo-electron microscopy and tomography that should allow us in the future to understand their molecular mechanisms and their dynamic behavior. Still, very fundamental questions regarding the specificity of these machines remain unanswered. In many cases, the nature of the signal(s) that designate a protein as a secretion substrate and its recognition by the given machinery are still poorly understood. Insights into substrate recognition require detailed structural knowledge of a dynamic process that likely involves a series of intermediates. Capturing these intermediates has been extremely challenging, and their structure was resolved in part only in the Sec system. Cross-linking or mutagenesis approaches might enable one to stabilize and study these intermediate states. Computational approaches, including structural modeling and molecular dynamics have the potential to predict the details of these transient interactions and, combined with other validation tools, improve our understanding of transport processes. Finally, recent developments in high-resolution microscopy and tomography have provided important information on the architecture of secretion systems *in situ*, as a valuable basis for future studies (Chang et al., 2016; Hu et al., 2017). More studies are needed to understand how the secretion of different substrates by the same machinery is regulated. The design of probes that would allow one to track the secretion of two proteins simultaneously in living cells would certainly also help in addressing this question. Some of the tools described in this review are amenable to single-cell studies, and might reveal heterogeneity in the secretory behavior of bacteria, which has not been addressed so far. However, the next main challenge seems to be to probe bacterial secretion in complex environments such as biofilms, mixed microbial populations or within living hosts. Only a few of the approaches described here can be used in complex environments: our toolbox needs yet more new tools.

## AUTHOR CONTRIBUTIONS

BM, OF, and AS conceived and wrote the manuscript.

## ACKNOWLEDGMENTS

We thank Tony Pugsley for critical reading of the manuscript. This work was supported by the European Research Council Starting Grant NUChLEAR N°282046 to AS, the Institut Pasteur and the Centre National de la Recherche Scientifique. The OF group is funded by the French ANR grant FiberSpace N°ANR-14-CE09-0004.

## REFERENCES


Abby, S. S., Cury, J., Guglielmini, J., Neron, B., Touchon, M., and Rocha, E. P. (2016). Identification of protein secretion systems in bacterial genomes. *Sci. Rep.* 6:23080. doi: 10.1038/srep23080

Alteri, C. J., Himpsl, S. D., Pickens, S. R., Lindner, J. R., Zora, J. S., Miller, J. E., et al. (2013). Multicellular bacteria deploy the Type VI secretion system to preemptively strike neighboring cells. *PLoS Path.* 9:e1003608. doi: 10.1371/journal.ppat.1003608

Aly, K. A., Beebe, E. T., Chan, C. H., Goren, M. A., Sepulveda, C., Makino, S., et al. (2013). Cell-free production of integral membrane aspartic acid proteases reveals zinc-dependent methyltransferase activity of the *Pseudomonas aeruginosa* prepilin peptidase PilD. *Microbiologyopen* 2, 94–104. doi: 10.1002/mbo3.51

An, Y., Wang, J., Li, C., Leier, A., Marquez-Lago, T., Wilksch, J., et al. (2016). Comprehensive assessment and performance improvement of effector protein predictors for bacterial secretion systems III, IV and VI. *Brief. Bioinformat.* doi: 10.1093/bib/bbw100. [Epub ahead of print].

Ates, L. S., Houben, E. N., and Bitter, W. (2016). Type VII secretion: a highly versatile secretion system. *Microbiol. Spectr.* 4. doi: 10.1128/microbiolspec.VMBF-0011-2015

Ball, G., Antelmann, H., Imbert, P. R., Gimenez, M. R., Voulhoux, R., and Ize, B. (2016). Contribution of the Twin Arginine Translocation system to the exoproteome of *Pseudomonas aeruginosa*. *Sci. Rep.* 6:27675. doi: 10.1038/srep27675

Basler, M. (2015). Type VI secretion system: secretion by a contractile nanomachine. *Philos. Trans. R. Soc. Lond. B. Biol. Sci.* 370: 20150021. doi: 10.1098/rstb.2015.0021

Bedouelle, H., Bassford P. J. Jr., Fowler, A. V., Zabin, I., Beckwith, J., and Hofnung, M. (1980). Mutations which alter the function of the signal sequence of the maltose binding protein of *Escherichia coli*. *Nature* 285, 78–81. doi: 10.1038/285078a0

Berks, B. C. (2015). The twin-arginine protein translocation pathway. *Annu. Rev. Biochem.* 84, 843–864. doi: 10.1146/annurev-biochem-060614-034251

Bernstein, H. D. (2015). Looks can be deceiving: recent insights into the mechanism of protein secretion by the autotransporter pathway. *Mol. Microbiol.* 97, 205–215. doi: 10.1111/mmi.13031

Berry, J. L., and Pelicic, V. (2015). Exceptionally widespread nanomachines composed of type IV pilins: the prokaryotic Swiss Army knives. *FEMS Microbiol. Rev.* 39, 134–154. doi: 10.1093/femsre/fuu001

Besingi, R. N., and Clark, P. L. (2015). Extracellular protease digestion to evaluate membrane protein cell surface localization. *Nat. Protoc.* 10, 2074–2080. doi: 10.1038/nprot.2015.131

Briones, G., Hofreuter, D., and Galan, J. E. (2006). Cre reporter system to monitor the translocation of type III secreted proteins into host cells. *Infect. Immun.* 74, 1084–1090. doi: 10.1128/IAI.74.2.1084-1090.2006

Brunet, Y. R., Espinosa, L., Harchouni, S., Mignot, T., and Cascales, E. (2013). Imaging type VI secretion-mediated bacterial killing. *Cell Rep.* 3, 36–41. doi: 10.1016/j.celrep.2012.11.027

Campbell-Valois, F. X., Schnupf, P., Nigro, G., Sachse, M., Sansonetti, P. J., and Parsot, C. (2014). A Fluorescent Reporter Reveals On/Off Regulation of the Shigella Type III Secretion Apparatus during Entry and Cell-to-Cell Spread. *Cell Host Microbe* 15, 177–189. doi: 10.1016/j.chom.2014.01.005

Campodonico, E. M., Chesnel, L., and Roy, C. R. (2005). A yeast genetic system for the identification and characterization of substrate proteins transferred into host cells by the *Legionella pneumophila* Dot/Icm system. *Mol. Microbiol.* 56, 918–933. doi: 10.1111/j.1365-2958.2005.04595.x

Cao, Z., Casabona, M. G., Kneuper, H., Chalmers, J. D., and Palmer, T. (2016). The type VII secretion system of *Staphylococcus aureus* secretes a nuclease toxin that targets competitor bacteria. *Nat. Microbiol.* 2, 1–11. doi: 10.1038/nmicrobiol.2016.183

Carey, K. L., Newton, H. J., Lührmann, A., and Roy, C. R. (2011). The Coxiella burnetii Dot/Icm System Delivers a Unique Repertoire of Type IV Effectors into Host Cells and Is Required for Intracellular Replication. *PLoS Path.* 7:e1002056. doi: 10.1371/journal.ppat.1002056

Chang, Y. W., Rettberg, L. A., Treuner-Lange, A., Iwasa, J., Sogaard-Andersen, L., and Jensen, G. J. (2016). Architecture of the type IVa pilus machine. *Science* 351:aad2001. doi: 10.1016/j.bpj.2015.11.2509

Charpentier, X., and Oswald, E. (2004). Identification of the secretion and translocation domain of the enteropathogenic and enterohemorrhagic *Escherichia coli* effector Cif, using TEM-1 beta-lactamase as a new fluorescence-based reporter. *J. Bacteriol.* 186, 5486–5495. doi: 10.1128/JB.186.16.5486-5495.2004

Chen, Y. S., Bastidas, R. J., Saka, H. A., Carpenter, V. K., Richards, K. L., Plano, G. V., et al. (2014). The *Chlamydia trachomatis* type III secretion chaperone Slc1 engages multiple early effectors, including TepP, a tyrosine-phosphorylated protein required for the recruitment of CrkI-II to nascent inclusions and innate immune signaling. *PLoS Pathog.* 10:e1003954. doi: 10.1371/journal.ppat.1003954

Choi, J. Y., Jang, T. H., and Park, H. H. (2017). The mechanism of folding robustness revealed by the crystal structure of extra-superfolder GFP. *FEBS Lett.* 591, 442–447. doi: 10.1002/1873-3468.12534

Christie, P. J., Whitaker, N., and Gonzalez-Rivera, C. (2014). Mechanism and structure of the bacterial type IV secretion systems. *Biochim. Biophys. Acta* 1843, 1578–1591. doi: 10.1016/j.bbamcr.2013.12.019

Costa, T. R., Felisberto-Rodrigues, C., Meir, A., Prevost, M. S., Redzej, A., Trokter, M., et al. (2015). Secretion systems in Gram-negative bacteria: structural and mechanistic insights. *Nat. Rev. Microbiol.* 13, 343–359. doi: 10.1038/nrmicro3456

Cowles, C. E., Li, Y., Semmelhack, M. F., Cristea, I. M., and Silhavy, T. J. (2011). The free and bound forms of Lpp occupy distinct subcellular locations in *Escherichia coli*. *Mol. Microbiol.* 79, 1168–1181. doi: 10.1111/j.1365-2958.2011.07539.x

Day, J. B., Ferracci, F., and Plano, G. V. (2003). Translocation of YopE and YopN into eukaryotic cells by *Yersinia pestis* yopN, tyeA, sycN, yscB and lcrG deletion mutants measured using a phosphorylatable peptide tag and phosphospecific antibodies. *Mol. Microbiol.* 47, 807–823. doi: 10.1046/j.1365-2958.2003.03343.x

de Diego, I., Ksiazek, M., Mizgalska, D., Koneru, L., Golik, P., Szmigielski, B., et al. (2016). The outer-membrane export signal of *Porphyromonas gingivalis* type IX secretion system (T9SS) is a conserved C-terminal beta-sandwich domain. *Sci. Rep.* 6:23123. doi: 10.1038/srep23123

d'Enfert, C., Chapon, C., and Pugsley, A. P. (1987). Export and secretion of the lipoprotein pullulanase by *Klebsiella pneumoniae*. *Mol. Microbiol.* 1, 107–116. doi: 10.1111/j.1365-2958.1987.tb00534.x

Desvaux, M., Hebraud, M., Talon, R., and Henderson, I. R. (2009). Secretion and subcellular localizations of bacterial proteins: a semantic awareness issue. *Trends Microbiol.* 17, 139–145. doi: 10.1016/j.tim.2009.01.004

Dohlich, K., Zumsteg, A. B., Goosmann, C., and Kolbe, M. (2014). A substrate-fusion protein is trapped inside the Type III secretion system channel in *Shigella flexneri*. *PLoS Path.* 10:e1003881. doi: 10.1371/journal.ppat.1003881

Duong, F., and Wickner, W. (1997). Distinct catalytic roles of the SecYE, SecG and SecDFyajC subunits of preprotein translocase holoenzyme. *EMBO J.* 16, 2756–2768. doi: 10.1093/emboj/16.10.2756

East, A., Mechaly, A. E., Huysmans, G. H., Bernarde, C., Tello-Manigne, D., Nadeau, N., et al. (2016). Structural basis of pullulanase membrane binding and secretion revealed by X-Ray crystallography, molecular dynamics and biochemical analysis. *Structure* 24, 92–104. doi: 10.1016/j.str.2015.10.023

Ehsani, S., Rodrigues, C. D., and Enninga, J. (2009). Turning on the spotlight - using light to monitor and characterize bacterial effector secretion and translocation. *Curr. Opin. Microbiol.* 12, 24–30. doi: 10.1016/j.mib.2008.11.007

Enninga, J., Mounier, J., Sansonetti, P., and and, G., Tran Van Nhieu (2005). Secretion of type III effectors into host cells in real time. *Nat. Methods* 2, 959–965. doi: 10.1038/nmeth804

Feilmeier, B. J., Iseminger, G., Schroeder, D., Webber, H., and Phillips, G. J. (2000). Green fluorescent protein functions as a reporter for protein localization in *Escherichia coli*. *J. Bacteriol.* 182, 4068–4076. doi: 10.1128/JB.182.14.4068-4076.2000

Francetic, O., Buddelmeijer, N., Lewenza, S., Kumamoto, C. A., and Pugsley, A. P. (2007). Signal recognition particle-dependent inner membrane targeting of the PulG Pseudopilin component of a type II secretion system. *J. Bacteriol.* 189, 1783–1793. doi: 10.1128/JB.01230-06

Francetic, O., Hanson, M. P., and Kumamoto, C. A. (1993). prlA suppression of defective export of maltose-binding protein in secB mutants of *Escherichia coli*. *J. Bacteriol.* 175, 4036–4044. doi: 10.1128/jb.175.13.4036-4044.1993

Francetic, O., and Pugsley, A. P. (2005). Towards the identification of type II secretion signals in a nonacylated variant of pullulanase from *Klebsiella oxytoca*. *J. Bacteriol.* 187, 7045–7055. doi: 10.1128/JB.187.20.7045-7055.2005

Frankel, M. B., Wojcik, B. M., DeDent, A. C., Missiakas, D. M., and Schneewind, O. (2010). ABI domain-containing proteins contribute to surface protein display and cell division in *Staphylococcus aureus*. *Mol. Microbiol.* 78, 238–252. doi: 10.1111/j.1365-2958.2010.07334.x

Gagic, D., Ciric, M., Wen, W. X., Ng, F., and Rakonjac, J. (2016). Exploring the secretomes of microbes and microbial communities using filamentous phage display. *Front. Microbiol.* 7:429. doi: 10.3389/fmicb.2016.00429

Garcia, J. T., Ferracci, F., Jackson, M. W., Joseph, S. S., Pattis, I., Plano, L. R., et al. (2006). Measurement of effector protein injection by type III and type IV secretion systems by using a 13-residue phosphorylatable glycogen synthase kinase tag. *Infect. Immun.* 74, 5645–5657. doi: 10.1128/IAI.00690-06

Gawthorne, J. A., Audry, L., McQuitty, C., Dean, P., Christie, J. M., Enninga, J., et al. (2016). Visualizing the translocation and localization of bacterial Type III effector proteins by using a genetically encoded reporter system. *Appl. Environ. Microbiol.* 82, 2700–2708. doi: 10.1128/AEM.03418-15

Gelis, I., Bonvin, A. M., Keramisanou, D., Koukaki, M., Gouridis, G., Karamanou, S., et al. (2007). Structural basis for signal-sequence recognition by the translocase motor SecA as determined by NMR. *Cell* 131, 756–769. doi: 10.1016/j.cell.2007.09.039

Green, E. R., and Mecsas, J. (2016). Bacterial secretion systems: an overview. *Microbiol. Spectr.* 4. doi: 10.1128/microbiolspec.VMBF-0012-2015

Guan, C. R., Cui, W. J., Cheng, J. T., Liu, R., Liu, Z. M., Zhou, L., et al. (2016). Construction of a highly active secretory expression system via an engineered dual promoter and a highly efficient signal peptide in *Bacillus subtilis*. *N. Biotechnol.* 33, 372–379. doi: 10.1016/j.nbt.2016.01.005

Guilvout, I., Chami, M., Berrier, C., Ghazi, A., Engel, A., Pugsley, A. P., et al. (2008). *in vitro* multimerization and membrane insertion of bacterial outer membrane secretin PulD. *J. Mol. Biol.* 382, 13–23. doi: 10.1016/j.jmb.2008.06.055

Hara, T., Matsuyama, S., and Tokuda, H. (2003). Mechanism underlying the inner membrane retention of *Escherichia coli* lipoproteins caused by Lol avoidance signals. *J. Biol. Chem.* 278, 40408–40414. doi: 10.1074/jbc.M307836200

Heggeset, T. M., Kucharova, V., Naerdal, I., Valla, S., Sletta, H., Ellingsen, T. E., et al. (2013). Combinatorial mutagenesis and selection of improved signal sequences and their application for high-level production of translocated heterologous proteins in *Escherichia coli*. *Appl. Environ. Microbiol.* 79, 559–568. doi: 10.1128/AEM.02407-12

Heidtman, M., Chen, E. J., Moy, M. Y., and Isberg, R. R. (2009). Large-scale identification of *Legionella pneumophila* Dot/Icm substrates that modulate host cell vesicle trafficking pathways. *Cell. Microbiol.* 11, 230–248. doi: 10.1111/j.1462-5822.2008.01249.x

Ho, B. T., Dong, T. G., and Mekalanos, J. J. (2014). A view to a kill: the bacterial type VI secretion system. *Cell Host Microbe* 15, 9–21. doi: 10.1016/j.chom.2013.11.008

Hood, R. D., Singh, P., Hsu, F., Guvener, T., Carl, M. A., Trinidad, R. R., et al. (2010). A type VI secretion system of *Pseudomonas aeruginosa* targets a toxin to bacteria. *Cell Host Microbe* 7, 25–37. doi: 10.1016/j.chom.2009.12.007

Hortensia Rolán, G., Enrique Durand, A., and Mecsas, J. (2013). Identifying Yersinia YopH-Targeted signal transduction pathways that impair neutrophil responses during *in vivo* murine infection. *Cell Host Microbe* 14, 306–317. doi: 10.1016/j.chom.2013.08.013

Howell, H. A., Logan, L. K., and Hauser, A. R. (2013). Type III secretion of ExoU is critical during early *Pseudomonas aeruginosa* pneumonia. *mBio* 4:e00032-13. doi: 10.1128/mBio.00032-13

Hu, B., Lara-Tejero, M., Kong, Q., Galán, J. E., and Liu, J. (2017). *In situ* molecular architecture of the salmonella Type III secretion machine. *Cell* 168, 1065–1074.e10. doi: 10.1016/j.cell.2017.02.022

Huber, D., Boyd, D., Xia, Y., Olma, M. H., Gerstein, M., and Beckwith, J. (2005). Use of thioredoxin as a reporter to identify a subset of *Escherichia coli* signal sequences that promote signal recognition particle-dependent translocation. *J. Bacteriol.* 187, 2983–2991. doi: 10.1128/JB.187.9.2983-2991.2005

Ieva, R., Tian, P., Peterson, J. H., and Bernstein, H. D. (2011). Sequential and spatially restricted interactions of assembly factors with an autotransporter beta domain. *Proc. Natl. Acad. Sci. U.S.A.* 108, E383–E391. doi: 10.1073/pnas.1103827108

Ito, K., Wittekind, M., Nomura, M., Shiba, K., Yura, T., Miura, A., et al. (1983). A temperature-sensitive mutant of *E. coli* exhibiting slow processing of exported proteins. *Cell* 32, 789–797. doi: 10.1016/0092-8674(83)90065-X

Jackowski, S., and Rock, C. O. (1986). Transfer of fatty acids from the 1-position of phosphatidylethanolamine to the major outer membrane lipoprotein of *Escherichia coli*. *J. Biol. Chem.* 261, 11328–11333.

Jackson, R. C., and Blobel, G. (1977). Post-translational cleavage of presecretory proteins with an extract of rough microsomes from dog pancreas containing signal peptidase activity. *Proc. Natl. Acad. Sci. U.S.A.* 74, 5598–5602. doi: 10.1073/pnas.74.12.5598

Jacobsson, K., and Frykberg, L. (1996). Phage display shot-gun cloning of ligand-binding domains of prokaryotic receptors approaches 100% correct clones. *Biotechniques* 20, 1070-6, 1078, 1080–1081.

Jaumouille, V., Francetic, O., Sansonetti, P. J., and Tran Van Nhieu, G. (2008). Cytoplasmic targeting of IpaC to the bacterial pole directs polar type III secretion in Shigella. *EMBO J.* 27, 447–457. doi: 10.1038/sj.emboj.7601976

Juncker, A. S., Willenbrock, H., Von Heijne, G., Brunak, S., Nielsen, H., and Krogh, A. (2003). Prediction of lipoprotein signal peptides in Gram-negative bacteria. *Protein Sci.* 12, 1652–1662. doi: 10.1110/ps.0303703

Kanonenberg, K., Schwarz, C. K., and Schmitt, L. (2013). Type I secretion systems - a story of appendices. *Res. Microbiol.* 164, 596–604. doi: 10.1016/j.resmic.2013.03.011

Karimova, G., Pidoux, J., Ullmann, A., and Ladant, D. (1998). A bacterial two-hybrid system based on a reconstituted signal transduction pathway. *Proc. Natl. Acad. Sci. U.S.A.* 95, 5752–5756. doi: 10.1073/pnas.95.10.5752

Kenny, B., and Finlay, B. B. (1995). Protein secretion by enteropathogenic *Escherichia coli* is essential for transducing signals to epithelial cells. *Proc. Natl. Acad. Sci. U.S.A.* 92, 7991–7995. doi: 10.1073/pnas.92.17.7991

Kirn, T. J., Bose, N., and Taylor, R. K. (2003). Secretion of a soluble colonization factor by the TCP type 4 pilus biogenesis pathway in *Vibrio cholerae*. *Mol. Microbiol.* 49, 81–92. doi: 10.1046/j.1365-2958.2003.03546.x

Konovalova, A., Perlman, D. H., Cowles, C. E., and Silhavy, T. J. (2014). Transmembrane domain of surface-exposed outer membrane lipoprotein RcsF is threaded through the lumen of beta-barrel proteins. *Proc. Natl. Acad. Sci. U.S.A.* 111, E4350–E4358. doi: 10.1073/pnas.1417138111

Korotkov, K. V., Sandkvist, M., and Hol, W. G. (2012). The type II secretion system: biogenesis, molecular architecture and mechanism. *Nat. Rev. Microbiol.* 10, 336–351. doi: 10.1038/nrmicro2762

Kreutzenbeck, P., Kroger, C., Lausberg, F., Blaudeck, N., Sprenger, G. A., and Freudl, R. (2007). *Escherichia coli* twin arginine (Tat) mutant translocases possessing relaxed signal peptide recognition specificities. *J. Biol. Chem.* 282, 7903–7911. doi: 10.1074/jbc.M610126200

Kumamoto, C. A., and Gannon, P. M. (1988). Effects of *Escherichia coli* secB mutations on pre-maltose binding protein conformation and export kinetics. *J. Biol. Chem.* 263, 11554–11558.

Kumru, O. S., Schulze, R. J., Slusser, J. G., and Zuckert, W. R. (2010). Development and validation of a FACS-based lipoprotein localization screen in the Lyme disease spirochete *Borrelia burgdorferi*. *BMC Microbiol.* 10:277. doi: 10.1186/1471-2180-10-277

Lausberg, F., Fleckenstein, S., Kreutzenbeck, P., Frobel, J., Rose, P., Muller, M., et al. (2012). Genetic evidence for a tight cooperation of TatB and TatC during productive recognition of twin-arginine (Tat) signal peptides in *Escherichia coli*. *PLoS ONE* 7:e39867. doi: 10.1371/journal.pone.0039867

Lewenza, S., Vidal-Ingigliardi, D., and Pugsley, A. P. (2006). Direct visualization of red fluorescent lipoproteins indicates conservation of the membrane sorting rules in the family Enterobacteriaceae. *J. Bacteriol.* 188, 3516–3524. doi: 10.1128/JB.188.10.3516-3524.2006

Leyton, D. L., Rossiter, A. E., and Henderson, I. R. (2012). From self sufficiency to dependence: mechanisms and factors important for autotransporter biogenesis. *Nat. Rev. Microbiol.* 10, 213–225. doi: 10.1038/nrmicro2733

Li, L., Park, E., Ling, J., Ingram, J., Ploegh, H., and Rapoport, T. A. (2016). Crystal structure of a substrate-engaged SecY protein-translocation channel. *Nature* 531, 395–399. doi: 10.1038/nature17163

Lin, J., Zou, Y., Ma, C., She, Q., Liang, Y., Chen, Z., et al. (2015). Heterologous expression of mannanase and developing a new reporter gene system in *Lactobacillus casei* and *Escherichia coli*. *PLoS ONE* 10:e0142886. doi: 10.1371/journal.pone.0142886

Logger, L., Aschtgen, M. S., Guerin, M., Cascales, E., and Durand, E. (2016). Molecular dissection of the interface between the Type VI secretion TssM

cytoplasmic domain and the TssG baseplate component. *J. Mol. Biol.* 428, 4424–4437. doi: 10.1016/j.jmb.2016.08.032

Lonjon, F., Turner, M., Henry, C., Rengel, D., Lohou, D., van de Kerkhove, Q., et al. (2016). Comparative secretome analysis of *Ralstonia solanacearum* Type 3 secretion-associated mutants reveals a fine control of effector delivery, essential for bacterial pathogenicity. *Mol. Cell. Proteomics* 15, 598–613. doi: 10.1074/mcp.M115.051078

Luo, Z. Q., and Isberg, R. R. (2004). Multiple substrates of the *Legionella pneumophila* Dot/Icm system identified by interbacterial protein transfer. *Proc. Natl. Acad. Sci. U.S.A.* 101, 841–846. doi: 10.1073/pnas.0304916101

Lybarger, S. R., Johnson, T. L., Gray, M. D., Sikora, A. E., and Sandkvist, M. (2009). Docking and assembly of the type II secretion complex of *Vibrio cholerae*. *J. Bacteriol.* 191, 3149–3161. doi: 10.1128/JB.01701-08

Lycklama A Nijeholt, J. A., and Driessen, A. J. (2012). The bacterial Sec-translocase: structure and mechanism. *Philos. Trans. R. Soc. Lond. B. Biol. Sci.* 367, 1016–1028. doi: 10.1098/rstb.2011.0201

Mahdavi, A., Szychowski, J., Ngo, J. T., Sweredoski, M. J., Graham, R. L., Hess, S., et al. (2014). Identification of secreted bacterial proteins by noncanonical amino acid tagging. *Proc. Natl. Acad. Sci. U.S.A.* 111, 433–438. doi: 10.1073/pnas.1301740111

Manoil, C., and Beckwith, J. (1985). TnphoA: a transposon probe for protein export signals. *Proc. Natl. Acad. Sci. U.S.A.* 82, 8129–8133. doi: 10.1073/pnas.82.23.8129

Maresso, A. W., Wu, R., Kern, J. W., Zhang, R., Janik, D., Missiakas, D. M., et al. (2007). Activation of inhibitors by sortase triggers irreversible modification of the active site. *J. Biol. Chem.* 282, 23129–23139. doi: 10.1074/jbc.M701857200

Mathiesen, G., Sveen, A., Brurberg, M. B., Fredriksen, L., Axelsson, L., and Eijsink, V. G. (2009). Genome-wide analysis of signal peptide functionality in Lactobacillus plantarum WCFS1. *BMC Genomics* 10:425. doi: 10.1186/1471-2164-10-425

Mavris, M., Page, A. L., Tournebize, R., Demers, B., Sansonetti, P., and Parsot, C. (2002). Regulation of transcription by the activity of the *Shigella flexneri* type III secretion apparatus. *Mol. Microbiol.* 43, 1543–1553. doi: 10.1046/j.1365-2958.2002.02836.x

Meyer, D. F., Noroy, C., Moumene, A., Raffaele, S., Albina, E., and Vachiery, N. (2013). Searching algorithm for type IV secretion system effectors 1.0: a tool for predicting type IV effectors and exploring their genomic context. *Nucleic Acids Res.* 41, 9218–9229. doi: 10.1093/nar/gkt718

Mills, E., Baruch, K., Aviv, G., Nitzan, M., and Rosenshine, I. (2013). Dynamics of the Type III secretion system activity of enteropathogenic *Escherichia coli*. *mBio* 4:e00303-13. doi: 10.1128/mBio.00303-13

Moir, D. T., Di, M., Wong, E., Moore, R. A., Schweizer, H. P., Woods, D. E., et al. (2011). Development and application of a cellular, gain-of-signal, bioluminescent reporter screen for inhibitors of Type II secretion in *Pseudomonas aeruginosa* and *Burkholderia pseudomallei*. *J. Biomol. Screen.* 16, 694–705. doi: 10.1177/1087057111408605

Molloy, M. P., Herbert, B. R., Slade, M. B., Rabilloud, T., Nouwens, A. S., Williams, K. L., et al. (2000). Proteomic analysis of the *Escherichia coli* outer membrane. *Eur. J. Biochem.* 267, 2871–2881. doi: 10.1046/j.1432-1327.2000.01296.x

Monteiro, F., Genin, S., van Dijk, I., and Valls, M. (2012). A luminescent reporter evidences active expression of Ralstonia solanacearum type III secretion system genes throughout plant infection. *Microbiol. Sgm* 158, 2107–2116. doi: 10.1099/mic.0.058610-0

Mueller, K. E., and Fields, K. A. (2015). Application of β-lactamase reporter fusions as an indicator of effector protein secretion during infections with the obligate intracellular pathogen *Chlamydia trachomatis*. *PLoS ONE* 10:e0135295. doi: 10.1371/journal.pone.0135295

Nivaskumar, M., Santos-Moreno, J., Malosse, C., Nadeau, N., Chamot-Rooke, J., Tran Van Nhieu, G., et al. (2016). Pseudopilin residue E5 is essential for recruitment by the type 2 secretion system assembly platform. *Mol. Microbiol.* 101, 924–941. doi: 10.1111/mmi.13432

Pallier, J., Aucher, W., Pires, M., and Buddelmeijer, N. (2012). Phosphatidyllycerol::prolipoprotein diacylglyceryl transferase (Lgt) of *Escherichia coli* has seven transmembrane segments and its essential residues are embedded in the membrane. *J. Bacteriol.* 194, 2142–2151. doi: 10.1128/JB.06641-11

Palmer, T., and Berks, B. C. (2012). The twin-arginine translocation (Tat) protein export pathway. *Nat. Rev. Microbiol.* 10, 483–496. doi: 10.1038/nrmicro2814

Payne, S. H., Bonissone, S., Wu, S., Brown, R. N., Ivankov, D. N., Frishman, D., et al. (2012). Unexpected diversity of signal peptides in prokaryotes. *mBio* 3: e00339-12. doi: 10.1128/mBio.00339-12

Perkowski, E. F., Zulauf, K. E., Weerakoon, D., Hayden, J. D., Ioerger, T. R., Oreper, D., et al. (2017). The EXIT strategy: an approach for identifying bacterial proteins exported during host infection. *mBio* 8:e00333-17. doi: 10.1128/mBio.00333-17

Petersen, T. N., Brunak, S., von Heijne, G., and Nielsen, H. (2011). SignalP 4.0: discriminating signal peptides from transmembrane regions. *Nat. Methods* 8, 785–786. doi: 10.1038/nmeth.1701

Pineau, C., Guschinskaya, N., Robert, X., Gouet, P., Ballut, L., and Shevchik, V. E. (2014). Substrate recognition by the bacterial type II secretion system: more than a simple interaction. *Mol. Microbiol.* 94, 126–140. doi: 10.1111/mmi.12744

Possot, O. M., Letellier, L., and Pugsley, A. P. (1997). Energy requirement for pullulanase secretion by the main terminal branch of the general secretory pathway. *Mol. Microbiol.* 24, 457–464. doi: 10.1046/j.1365-2958.1997.3451726.x

Remaut, H., Tang, C., Henderson, N. S., Pinkner, J. S., Wang, T., Hultgren, S. J., et al. (2008). Fiber formation across the bacterial outer membrane by the chaperone/usher pathway. *Cell* 133, 640–652. doi: 10.1016/j.cell.2008.03.033

Riordan, K. E., Sorg, J. A., Berube, B. J., and Schneewind, O. (2008). Impassable YscP substrates and their impact on the *Yersinia enterocolitica* type III secretion pathway. *J. Bacteriol.* 190, 6204–6216. doi: 10.1128/JB.00467-08

Rondelet, A., and Condemine, G. (2013). Type II secretion: the substrates that won't go away. *Res. Microbiol.* 164, 556–561. doi: 10.1016/j.resmic.2013.03.005

Saka, H. A., Thompson, J. W., Chen, Y. S., Dubois, L. G., Haas, J. T., Moseley, A., et al. (2015). *Chlamydia trachomatis* infection leads to defined alterations to the lipid droplet proteome in epithelial cells. *PLoS ONE* 10:e0124630. doi: 10.1371/journal.pone.0124630

Sato, K., Naito, M., Yukitake, H., Hirakawa, H., Shoji, M., McBride, M. J., et al. (2010). A protein secretion system linked to bacteroidete gliding motility and pathogenesis. *Proc. Natl. Acad. Sci. U.S.A.* 107, 276–281. doi: 10.1073/pnas.0912010107

Sauvonnet, N., and Pugsley, A. P. (1996). Identification of two regions of *Klebsiella oxytoca* pullulanase that together are capable of promoting beta-lactamase secretion by the general secretory pathway. *Mol. Microbiol.* 22, 1–7. doi: 10.1111/j.1365-2958.1996.tb02650.x

Schlumberger, M. C., Muller, A. J., Ehrbar, K., Winnen, B., Duss, I., Stecher, B., et al. (2005). Real-time imaging of type III secretion: Salmonella SipA injection into host cells. *Proc. Natl. Acad. Sci. U.S.A.* 102, 12548–12553. doi: 10.1073/pnas.0503407102

Schneewind, O., and Missiakas, D. (2014). Sec-secretion and sortase-mediated anchoring of proteins in Gram-positive bacteria. *Biochim. Biophys. Acta* 1843, 1687–1697. doi: 10.1016/j.bbamcr.2013.11.009

Seydel, A., Gounon, P., and Pugsley, A. P. (1999). Testing the '+2 rule' for lipoprotein sorting in the *Escherichia coli* cell envelope with a new genetic selection. *Mol. Microbiol.* 34, 810–821. doi: 10.1046/j.1365-2958.1999.01647.x

Shaner, N. C., Campbell, R. E., Steinbach, P. A., Giepmans, B. N., Palmer, A. E., and Tsien, R. Y. (2004). Improved monomeric red, orange and yellow fluorescent proteins derived from Discosoma sp. red fluorescent protein. *Nat. Biotechnol.* 22, 1567–1572. doi: 10.1038/nbt1037

Shuman, H. A., and Silhavy, T. J. (2003). The art and design of genetic screens: *Escherichia coli*. *Nat. Rev. Genet.* 4, 419–431. doi: 10.1038/nrg1087

Silverman, J. M., Agnello, D. M., Zheng, H., Andrews, B. T., Li, M., Catalano, C. E., et al. (2013). Haemolysin coregulated protein is an exported receptor and chaperone of type VI secretion substrates. *Mol. Cell* 51, 584–593. doi: 10.1016/j.molcel.2013.07.025

Sinclair, S. H., Garcia-Garcia, J. C., and Dumler, J. S. (2015). Bioinformatic and mass spectrometry identification of *Anaplasma phagocytophilum* proteins translocated into host cell nuclei. *Front. Microbiol.* 6:55. doi: 10.3389/fmicb.2015.00055

Sisko, J. L., Spaeth, K., Kumar, Y., and Valdivia, R. H. (2006). Multifunctional analysis of *Chlamydia*-specific genes in a yeast expression system. *Mol. Microbiol.* 60, 51–66. doi: 10.1111/j.1365-2958.2006.05074.x

Slagowski, N. L., Kramer, R. W., Morrison, M. F., LaBaer, J., and Lesser, C. F. (2008). A functional genomic yeast screen to identify pathogenic bacterial proteins. *PLoS Pathog.* 4:e9. doi: 10.1371/journal.ppat.0040009

Sory, M. P., and Cornelis, G. R. (1994). Translocation of a hybrid YopE-adenylate cyclase from *Yersinia enterocolitica* into HeLa cells. *Mol. Microbiol.* 14, 583–594. doi: 10.1111/j.1365-2958.1994.tb02191.x

Subtil, A., Delevoye, C., Bala,-á, M. E., Tastevin, L., Perrinet, S., and Dautry-Varsat, A. (2005). A directed screen for chlamydial proteins secreted by a type III mechanism identifies a translocated protein and numerous other new candidates. *Mol. Microbiol.* 56, 1636–1647. doi: 10.1111/j.1365-2958.2005.04647.x

Subtil, A., Parsot, C., and Dautry-Varsat, A. (2001). Secretion of predicted Inc proteins of *Chlamydia pneumoniae* by a heterologous type III machinery. *Mol. Microbiol.* 39, 792–800. doi: 10.1046/j.1365-2958.2001.02272.x

Thomas, J. D., Daniel, R. A., Errington, J., and Robinson, C. (2001). Export of active green fluorescent protein to the periplasm by the twin-arginine translocase (Tat) pathway in *Escherichia coli*. *Mol. Microbiol.* 39, 47–53. doi: 10.1046/j.1365-2958.2001.02253.x

Urbanowski, M. L., Lykken, G. L., and Yahr, T. L. (2005). A secreted regulatory protein couples transcription to the secretory activity of the *Pseudomonas aeruginosa* type III secretion system. *Proc. Natl. Acad. Sci. U.S.A.* 102, 9930–9935. doi: 10.1073/pnas.0504405102

Van Engelenburg, S. B., and Palmer, A. E. (2008). Quantification of real-time Salmonella effector type III secretion kinetics reveals differential secretion rates for SopE2 and SptP. *Chem. Biol.* 15, 619–628. doi: 10.1016/j.chembiol.2008.04.014

Van Engelenburg, S. B., and Palmer, A. E. (2010). Imaging type-III secretion reveals dynamics and spatial segregation of Salmonella effectors. *Nat. Methods* 7, 325–330. doi: 10.1038/nmeth.1437

Van Gerven, N., Klein, R. D., Hultgren, S. J., and Remaut, H. (2015). Bacterial amyloid formation: structural insights into curli biogensis. *Trends Microbiol.* 23, 693–706. doi: 10.1016/j.tim.2015.07.010

von Heijne, G. (1990). The signal peptide. *J. Membr. Biol.* 115, 195–201. doi: 10.1007/BF01868635

Voulhoux, R., Bos, M. P., Geurtsen, J., Mols, M., and Tommassen, J. (2003). Role of a highly conserved bacterial protein in outer membrane protein assembly. *Science* 299, 262–265. doi: 10.1126/science.1078973

Wang, G. Q., Xia, Y. J., Xiong, Z. Q., Zhang, H., and Ai, L. Z. (2016). Use of a novel report protein to study the secretion signal of Flagellin in *Bacillus subtilis*. *Curr. Microbiol.* 73, 242–247. doi: 10.1007/s00284-016-1054-4

Wille, T., Blank, K., Schmidt, C., Vogt, V., and Gerlach, R. G. (2012). Gaussia princeps luciferase as a reporter for transcriptional activity, protein secretion, and protein-protein interactions in *Salmonella enterica* Serovar Typhimurium. *Appl. Environ. Microbiol.* 78, 250–257. doi: 10.1128/AEM.06670-11

Wilson, M. M., Anderson, D. E., and Bernstein, H. D. (2015). Analysis of the outer membrane proteome and secretome of *Bacteroides fragilis* reveals a multiplicity of secretion mechanisms. *PLoS ONE* 10:e0117732. doi: 10.1371/journal.pone.0117732

Wilson, M. M., and Bernstein, H. D. (2016). Surface-Exposed Lipoproteins: an emerging secretion phenomenon in gram-negative bacteria. *Trends Microbiol.* 24, 198–208. doi: 10.1016/j.tim.2015.11.006

Wu, T., Malinverni, J., Ruiz, N., Kim, S., Silhavy, T. J., and Kahne, D. (2005). Identification of a multicomponent complex required for outer membrane biogenesis in *Escherichia coli*. *Cell* 121, 235–245. doi: 10.1016/j.cell.2005.02.015

Yount, J. S., Tsou, L. K., Dossa, P. D., Kullas, A. L., van der Velden A. W., and Hang, H. C. (2010). Visible fluorescence detection of type III protein secretion from bacterial pathogens. *J. Am. Chem. Soc.* 132, 8244–8245. doi: 10.1021/ja102257v

Zhu, W., Banga, S., Tan, Y., Zheng, C., Stephenson, R., Gately, J., et al. (2011). Comprehensive identification of protein substrates of the Dot/Icm Type IV Transporter of *Legionella pneumophila*. *PLoS ONE* 6:e17638. doi: 10.1371/journal.pone.0017638

Zückert, W. (2014). Secretion of bacterial lipoproteins: through the cytoplasmic membrane, the periplasm and beyond. *Biochem. Biophys. Acta Mol. Cell Res.* 1843, 1509–1516. doi: 10.1016/j.bbamcr.2014.04.022

Zuverink, M., and Barbieri, J. T. (2015). From GFP to β-lactamase: advancing intact cell imaging for toxins and effectors. *Pathog. Dis.* 73:ftv097. doi: 10.1093/femspd/ftv097

**Conflict of Interest Statement:** The authors declare that the research was conducted in the absence of any commercial or financial relationships that could be construed as a potential conflict of interest.

frontiers in Cellular and Infection Microbiology

REVIEW
published: 15 June 2017
doi: 10.3389/fcimb.2017.00255

# Type III Secretion in the Melioidosis Pathogen *Burkholderia pseudomallei*

*Charles W. Vander Broek and Joanne M. Stevens* *

*The Roslin Institute and Royal (Dick) School of Veterinary Studies, University of Edinburgh, Midlothian, United Kingdom*

*Burkholderia pseudomallei* is a Gram-negative intracellular pathogen and the causative agent of melioidosis, a severe disease of both humans and animals. Melioidosis is an emerging disease which is predicted to be vastly under-reported. Type III Secretion Systems (T3SSs) are critical virulence factors in Gram negative pathogens of plants and animals. The genome of *B. pseudomallei* encodes three T3SSs. T3SS-1 and -2, of which little is known, are homologous to Hrp2 secretion systems of the plant pathogens *Ralstonia* and *Xanthomonas*. T3SS-3 is better characterized and is homologous to the Inv/Mxi-Spa secretion systems of *Salmonella* spp. and *Shigella flexneri*, respectively. Upon entry into the host cell, *B. pseudomallei* requires T3SS-3 for efficient escape from the endosome. T3SS-3 is also required for full virulence in both hamster and murine models of infection. The regulatory cascade which controls T3SS-3 expression and the secretome of T3SS-3 have been described, as well as the effect of mutations of some of the structural proteins. Yet only a few effector proteins have been functionally characterized to date and very little work has been carried out to understand the hierarchy of assembly, secretion and temporal regulation of T3SS-3. This review aims to frame current knowledge of *B. pseudomallei* T3SSs in the context of other well characterized model T3SSs, particularly those of *Salmonella* and *Shigella*.

**Keywords: T3SS, effector, translocator, *Burkholderia pseudomallei*, melioidosis**

OPEN ACCESS

***Edited by:***
*Sophie Bleves,*
*Aix-Marseille University, France*

***Reviewed by:***
*Erin J. Van Schaik,*
*Texas A&M Health Science Center, United States*
*Erin C. Garcia,*
*University of Kentucky College of Medicine, United States*
*Brian H. Kvitko,*
*University of Georgia, United States*

***Correspondence:**
*Joanne M. Stevens*
*jo.stevens@roslin.ed.ac.uk*

***Received:*** *20 March 2017*
***Accepted:*** *31 May 2017*
***Published:*** *15 June 2017*

***Citation:***
*Vander Broek CW and Stevens JM (2017) Type III Secretion in the Melioidosis Pathogen Burkholderia pseudomallei. Front. Cell. Infect. Microbiol. 7:255. doi: 10.3389/fcimb.2017.00255*

## INTRODUCTION

Bacteria are required to adapt to and survive in constantly changing and harsh environments. In order to respond to and alter their environment, secretion systems have evolved in bacteria to export proteins into the surrounding milieu (reviewed in Costa et al., 2015). One secretion system in Gram-negative bacteria that has been the focus of much research in the last three decades is the Type III secretion system (T3SS) (reviewed in Galán et al., 2014). Type III Secretion Systems (T3SSs) have been shown to be important for virulence in many Gram-negative bacterial pathogens of animals and plants; including *Pseudomonas syringae*, *Xanthomonas*, *Ralstonia solanacearum*, *Erwinia*, pathogenic *Escherichia coli*, *Salmonella*, *Shigella*, *Yersinia*, and *Burkholderia* (Gemski et al., 1980; Maurelli et al., 1985; Galán and Curtiss, 1989; Jarvis et al., 1995; Stevens et al., 2002; Büttner and He, 2009). T3SSs span the bacterial inner and outer membranes forming a "molecular syringe" which allows bacteria to export proteins, called effectors, from the bacterial cytoplasm into a target eukaryotic cell (reviewed in Galán et al., 2014).

The focus of this review is T3SSs in the pathogenic bacterium *Burkholderia pseudomallei*, and to some extent the closely related species *B. mallei* and *B. thailandensis*. Originally described in drug addicts in Rangoon in the early twentieth century by Alfred Whitmore (Whitmore, 1913), *Burkholderia pseudomallei* is a facultative intracellular pathogen (Pruksachartvuthi et al., 1990)

that is the causative agent of melioidosis, or Whitmore's disease. Melioidosis is a severe disease of humans and animals, causing an estimated 165,000 cases of human melioidosis per year resulting in a predicted 89,000 deaths (Limmathurotsakul et al., 2016). Infection with *B. pseudomallei* is usually associated with environmental exposure and can occur through breaks in the skin, inhalation or ingestion (reviewed in Cheng and Currie, 2005). In the majority of cases, the incubation period for melioidosis is between 1 and 21 days following infection (Ngauy et al., 2005). About 50% of melioidosis cases affect people with diabetes and other important risk factors include lung disease, cystic fibrosis and excessive alcohol consumption (Currie et al., 2010). There are varied clinical presentations of *B. pseudomallei* infection ranging from skin infections to pneumonia and septic shock, which hampers accurate diagnosis in a clinical setting (Currie et al., 2010). *B. pseudomallei* is reported to be able to reactivate after remaining latent following a primary infection. The longest reported period between infection and reactivation occurred in a World War II veteran who manifested symptoms 62 years after exposure (Ngauy et al., 2005). *B. pseudomallei* has been classified as a bioterrorism agent by both the UK government and the US Centres for Disease Control and Prevention (reviewed in Rotz et al., 2002; Cheng and Currie, 2005).

*B. mallei*, the causative agent of glanders in horses and other solipeds, is a zoonotic pathogen with restricted host range (Yabuuchi et al., 1992; Srinivasan et al., 2001). In humans, *B. mallei* causes a disease similar to melioidosis and has been similarly classified as a potential bioterrorism agent in the UK and US (Rotz et al., 2002; Van Zandt et al., 2013). The soil saprophyte *B. thailandensis* is non-pathogenic and present in high numbers in the soils and standing waters of endemic areas. This species is commonly used as an alternative model system for *B. pseudomallei* and *B. mallei* studies as its genome encodes many homologs of virulence factors from these pathogenic species (Brett et al., 1998; Moore et al., 2004; Yu et al., 2006; Haraga et al., 2008).

## TYPE THREE SECRETION SYSTEMS IN *B. PSEUDOMALLEI*

The *B. pseudomallei* genome encodes three T3SSs which are referred to as T3SS-1, T3SS-2, and T3SS-3. The genome of *B. pseudomallei* consists of two circular chromosomes, with all three T3SSs residing on chromosome 2 (Holden et al., 2004). T3SS-2 and T3SS-3 are present in the genomes of *B. mallei* and *B. thailandensis*, whereas T3SS-1 is absent from both (Rainbow et al., 2002). T3SS-1 and T3SS-2 are relatively poorly characterized and share homology with the Hrp2 family of T3SSs found in plant pathogens (Winstanley et al., 1999; Rainbow et al., 2002). The best characterized of the *B. pseudomallei* T3SSs, T3SS-3, is also known as the *Burkholderia* secretion apparatus (Bsa) T3SS. It is a member of the Inv-Mxi-Spa family of T3SSs from *Salmonella* spp. (SPI-1) and *Shigella flexneri* (Attree and Attree, 2001; Stevens et al., 2002; Egan et al., 2014).

*Burkholderia pseudomallei* T3SS-1 (BPSS1390-BPSS1410) and T3SS-2 (BPSS1610-BPSS1629) show closest homology to the Hrp2 T3SS of the plant pathogen *Ralstonia solanacearum* (Angus et al., 2014). *B. pseudomallei* T3SS-2 expression is activated by the AraC-type regulator HrpB (BPSS1610) (Lipscomb and Schell, 2011). HrpB also regulates the expression of a type IV pilus encoded directly upstream of T3SS-2, but does not appear to regulate the other T3SSs in *B. pseudomallei* (Lipscomb and Schell, 2011). In order to investigate the role that T3SS-1 and T3SS-2 play in plants, a tomato plant infection model was established for *B. pseudomallei* and *B. thailandensis* (Lee et al., 2010). *B. pseudomallei* KHW T3SS-1 and T3SS-2 mutants were reported to be attenuated in tomato plants (Lee et al., 2010). However, in a more recent study, *B. thailandensis* did not display phytopathogenic activity in tomato plants which were treated identically to those in Lee et al. (2010), Lipscomb and Schell (2011). The question of whether *B. pseudomallei* is capable of infecting plants, and what if any role T3SS-1 and -2 have in this process, remain important unanswered questions.

The function of T3SS-1 and -2 in mammalian systems has also been investigated to some extent. T3SSs-1 and -2 do not appear to be required for vacuole escape of the bacterium into the cytoplasm of infected macrophages (Burtnick et al., 2008), and are dispensable in a Syrian hamster model of infection (Warawa and Woods, 2005). However, a *B. pseudomallei* T3SS-1 mutant displayed increased co-localisation with the autophagy marker LC3 and a reduction in intracellular survival in RAW264.7 cells (D'Cruze et al., 2011). In the same study, T3SS-1 was required for full virulence in a respiratory murine model of melioidosis (D'Cruze et al., 2011). Both earlier studies inactivated T3SS-1 by mutating the structural auto-protease component (BpscU, **Table 1**) (Warawa and Woods, 2005; Burtnick et al., 2008) while the latter study generated a system knockout by mutation of the ATPase (BpscN, **Table 1**), which may account for the different phenotypes observed.

### T3SS-3

The best characterized of the three T3SSs, T3SS-3 (BPSS1516-BPSS1552, **Figure 1**) is a member of the Inv/Mxi-Spa family of T3SSs (Egan et al., 2014) of which the prototypic systems are found in *Salmonella* Spp. and *Shigella flexneri*. The *Salmonella* and *Shigella* prototypic systems are required in these bacteria for host cell invasion and escape from the endocytic vacuole into the cytosol, respectively (reviewed in Galán et al., 2014). *B. pseudomallei* is a facultative intracellular pathogen capable of survival in both phagocytic and non-phagocytic cell lines (Jones et al., 1996). T3SS-3 is required for *B. pseudomallei* to efficiently escape the endocytic vesicle (Stevens et al., 2002). The T3SS-3 is also required for full virulence in both murine and Syrian hamster models of infection (Stevens et al., 2004; Warawa and Woods, 2005; Gutierrez et al., 2015a). T3SS-3 deficient mutants are also impaired in their ability to disseminate from the lungs of mice infected intra-nasally (Gutierrez et al., 2015a). A recent study used Tn-seq to identify genes required for respiratory melioidosis in mice and identified the following T3SS-3 genes as being required: *bprA* (BPSS1530), *bipC* (BPSS1531), *bipB* (BPSS1532), *bicA* (BPSS1533), *bsaZ* (BPSS1534), *bsaW* (BPSS1537), *bsaV* (BPSS1538), *bsaO* (BPSS1545), *bsaM* (BPSS1547), *bsaL* (BPSS1548), *bsaK* (BPSS1549), and *bsaJ*

**TABLE 1 |** *B. pseudomallei* T3SS-1 and -2 genes, corresponding proteins and predicted functions.

| ***B. pseudomallei* K96243** | | ***B. pseudomallei* K96243** | | ***R. solanacearum*** | **Universal Nomenclature** | **Predicted function** |
|---|---|---|---|---|---|---|
| **T3SS-1** | | **T3SS-2** | | **Hrp2** | **Protein name** | |
| **Locus tag** | **Protein name** | **Locus tag** | **Protein name** | **Protein name** | | |
| BPSS1388 | Similar to Hrpk1 from *P. syringae* | | | | | Translocator |
| BPSS1390 | BpscC | BPSS1592 | BpscC2 | HrcC | SctC | Outer membrane ring / secretin |
| BPSS1391 | BpspB | BPSS1610 | BpspB2 | HrpB | | T3SS Regulator |
| BPSS1392 | BpscT | BPSS1629 | BpscT2 | HrcT | SctT | Inner membrane export apparatus |
| BPSS1393 | BpspD | BPSS1628 | BpspD2 | HrpD | SctO | Stalk protein |
| BPSS1394 | BpscN | BPSS1627 | BpscN2 | HrcN | SctN | ATPase |
| BPSS1395 | BpscL | BPSS1626 | BpscL2 | HrcL | SctL | Stator protein |
| BPSS1396 | BpspH | BPSS1625 | BpspH2 | HrpH | | Inner membrane component |
| BPSS1397 | BpscJ | BPSS1624 | BpscJ2 | HrcJ | SctJ | Inner membrane ring component |
| BPSS1398 | BpspJ | BPSS1623 | BpspJ2 | HrpJ | | Inner rod component |
| BPSS1399 | BpspK | BPSS1622 | BpspK2 | HrpK | | Inner rod component |
| BPSS1400 | BpscU | BPSS1621 | BpscU2 | HrcU | SctU | Autoprotease, early/middle substrate switch |
| BPSS1401 | BpscV | BPSS1620 | BpscV2 | HrcV | SctV | Export gate |
| BPSS1402 | BpsaP | BPSS1619 | BpsaP2 | HpaP | SctP | Regulates needle length / translocator secretion |
| BPSS1403 | BpscQ | BPSS1618 | BpscQ2 | HrcQ | SctQ | Cytoplasmic ring |
| BPSS1404 | BpscR | BPSS1617 | BpscR2 | HrcR | SctR | Inner membrane export apparatus |
| BPSS1405 | BpscS | BPSS1616 | BpscS2 | HrcS | SctS | Inner membrane export apparatus |
| BPSS1406 | BpspV | BPSS1615 | BpspV2 | HrpV | | Secreted regulator |
| BPSS1407 | BpscD | BPSS1614 | BpscD2 | HrcD | SctD | Inner membrane ring component |
| BPSS1410 | BpsaB | BPSS1611 | BpsaB2 | HpaB | | Chaperone |

*Homologs from R. solanacearum Hrp2 T3SS are given for reference. Where applicable, the universal nomenclature for T3SS structural proteins is also listed to allow for comparison to genes from T3SS-3 listed in* ***Table 2****.*

(BPSS1550) (Gutierrez et al., 2015b). This highlights the importance of T3SS-3 in melioidosis.

## TRANSCRIPTIONAL REGULATION OF T3SS-3

The transcriptional regulation of T3SS-3 has been elucidated (Sun et al., 2010). At the top of the regulatory hierarchy is the gene *bspR* (BPSL1105), which, when disrupted led to a reduced level of expression of genes in the T3SS-3 locus as shown by microarray and real time PCR (Sun et al., 2010). *bspR* signals through the membrane bound regulator *bprP* (BPSS1553) which controls expression levels of both structural and secreted components of T3SS-3 (Sun et al., 2010). *bprP* further signals through *bsaN* (BPSS1546) and its co-activator, the chaperone *bicA* (BPSS1533), controlling transcription of the known effectors *bopC, bopE* and *bopA*, as well as the chaperone *bicP* (BPSS1523) and the regulators *bprB-D* (BPSS1520-22) (Sun et al., 2010; Chen et al., 2014). *bsaN* also relays the regulation signal to the virulence-associated Type 6 secretion system and virulence factors such as *bimA* and *virAG* (Sun et al., 2010; Chen et al., 2014).

The presence of genes allowing for arabinose assimilation was one of the first methods used to differentiate between virulent *B. pseudomallei* and avirulent *B. thailandensis* (Smith et al., 1997; Moore et al., 2004). Expressing the *B. thailandensis* arabinose assimilation operon in *B. pseudomallei* causes a down-regulation of expression of the T3SS-3 genes, notably the T3SS regulator *bsaN,* and also results in a reduction in virulence in a Syrian hamster model of infection (Moore et al., 2004). This suggests that loss of the arabinose assimilation operon may account for some of the differential virulence observed between these two species of *Burkholderia* (Moore et al., 2004).

## STRUCTURE OF T3SS-3

The structure of the T3SS is well conserved and is similar to that of the bacterial flagella system (Kubori et al., 1998; Young et al., 1999; Gophna et al., 2003). It is thought that the flagella and the T3SS evolved from a similar ancestor, but the T3SS has been the product of a large amount of horizontal gene transfer (Gophna et al., 2003). T3SSs are separated into seven different families named after the archetype system in each family, each with slight differences in structure and host cell target, with multiple types of T3SS present in some bacterial species (e.g., plant or animal) (reviewed by Büttner, 2012). In recent years the structure of the *Salmonella* T3SS has been solved using cryo-EM (Schraidt and Marlovits, 2011) and cryo-ET (Hu et al., 2017). The structure of the *Salmonella* T3SS (reviewed by Galán et al., 2014) consists of inner and outer membrane rings connected by a rod, the extracellular needle and a secreted translocation pore which

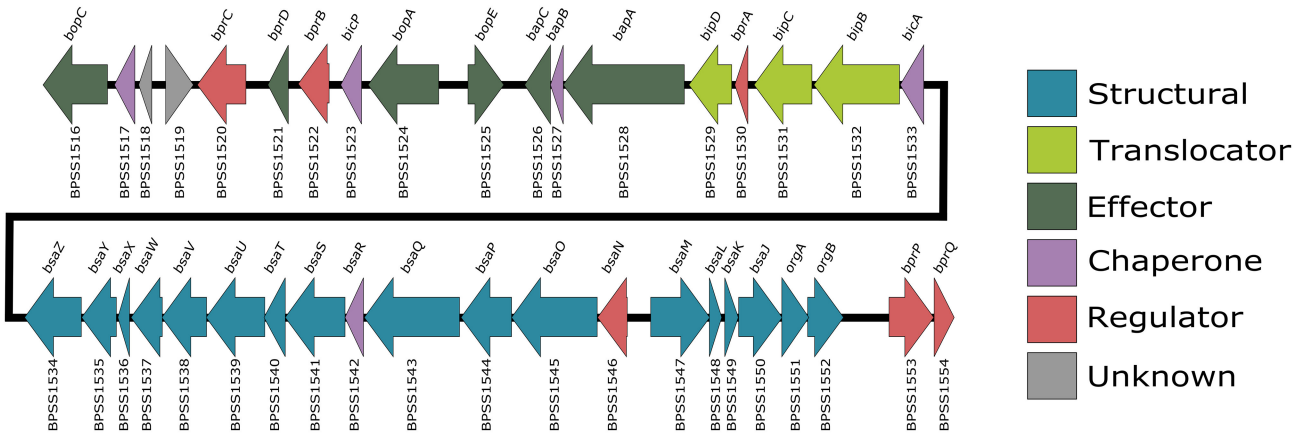


**FIGURE 1 |** *B. pseudomallei* K96243 T3SS-3 gene locus. Also known as the *bsa* locus, the T3SS-3 genes are encoded by chromosome 2 (BPSS1516-BPSS1554). Arrows which point right represent genes encoded on the forward strand and arrows which point left represent genes encoded on the reverse strand**.** Gene locus tags are listed below each arrow and gene names are listed above. The arrows are color coded according to their predicted function.

spans the target cell membrane. Assembly of the T3SS appears to be hierarchical and is the subject of multiple recent reviews (Büttner, 2012; Diepold and Wagner, 2014). Based on evidence from *Yersinia* and *Salmonella*, it appears construction of the T3SS begins with the formation of the outer-membrane/structural ring (Secretin) and independently the inner membrane export machinery, which are then linked by YscJ (*Yersinia*) or PrgK (*Salmonella*), followed by assembly of the ATPase/C-ring and the formation of the mature needle complex (Diepold et al., 2010, 2011; Wagner et al., 2010). The structural proteins in the *B. pseudomallei* T3SS-3 (**Figure 2**) that have been studied specifically are described below.

## Components of the Export Apparatus

### BsaZ (BPSS1534)

BsaZ (BPSS1534) is a structural component with homology to SpaS of *Salmonella* (Stevens et al., 2002). SpaS is a component of the export apparatus and has been shown to undergo auto-cleavage causing a switch between secretion of structural components (early substrates) to secretion of the needle complex and translocator proteins (intermediate substrates) (Zarivach et al., 2008). *B. pseudomallei bsaZ* mutants are unable to secrete effector and translocator proteins (Stevens et al., 2003; Muangman et al., 2011; Vander Broek et al., 2015). Mutations in *bsaZ* result in a significant delay in escape from the phagosome and reduced intracellular survival in J774.2 cells (Stevens et al., 2002; Burtnick et al., 2008). *bsaZ* mutants are also attenuated in murine (Stevens et al., 2004; Burtnick et al., 2008) and Syrian hamster (Warawa and Woods, 2005) models of melioidosis. *bsaZ* mutants have proven to be a useful tool in understanding the role of T3SS-3 in *B. pseudomallei* pathogenesis, however, the effect of these mutations other than an inability to secrete effector proteins is not well understood. For example, it is unclear if BsaZ undergoes auto-cleavage and is involved in secretion hierarchy in a similar manner to SpaS. It has also not been determined if *bsaZ* mutants still assemble the external needle appendage, or at what stage in formation of the mature T3SS complex they are impaired.

### BsaQ (BPSS1543)

Another component of the export apparatus of the *B. pseudomallei* T3SS-3 that has been described is BsaQ (BPSS1543), which is homologous to InvA from *Salmonella* (Sun et al., 2005). InvA is required for the formation of the mature T3SS in *Salmonella* as well as secretion of effector proteins (Kubori et al., 2000). *bsaQ* mutants display a similar phenotype to other T3SS-3 structural mutants in that they are delayed in phagosome escape, resulting in reduced intracellular survival (Muangsombut et al., 2008). The *bsaQ* mutants are unable to secrete the effector protein BopE or translocator tip protein BipD, and show significant defects in cell invasion (Muangsombut et al., 2008). Similarly to BsaZ, there is a gap in our knowledge of whether BsaQ truly functions in a manner similar to InvA.

## Inner Membrane Ring

### BsaM (BPSS1547)

The inner membrane component BsaM (BPSS1547) is homologous to *Salmonella* PrgH, which forms the inner membrane ring of the *Salmonella* T3SS and is required for secretion of effector proteins (Kubori et al., 2000; Marlovits et al., 2004). A *B. pseudomallei bsaM* mutant induced lower levels of NF-κB signaling in HEK 293T cells when compared to the isogenic parent strain (Teh et al., 2014). The *bsaM* mutant activated NF-κB at time points corresponding to a delayed escape from the phagosome, suggesting it has similar effects to the other T3SS-3 structural knockouts (Teh et al., 2014).

## Needle Components

### BsaL (BPSS1548)

A crystal structure of the protein BsaL (BPSS1548) demonstrated significant structural similarity with MxiH (*Shigella*) and PrgI (*Salmonella*), which form the external needle structure (major needle subunit) of the T3SS (Zhang et al., 2006; Wang et al., 2007; Barrett et al., 2008). BsaL is recognized by the host cell neuronal inhibitory protein (NAIP) leading to activation of the NLRC4 inflammasome (Yang et al., 2013). NLRC4 has been shown to

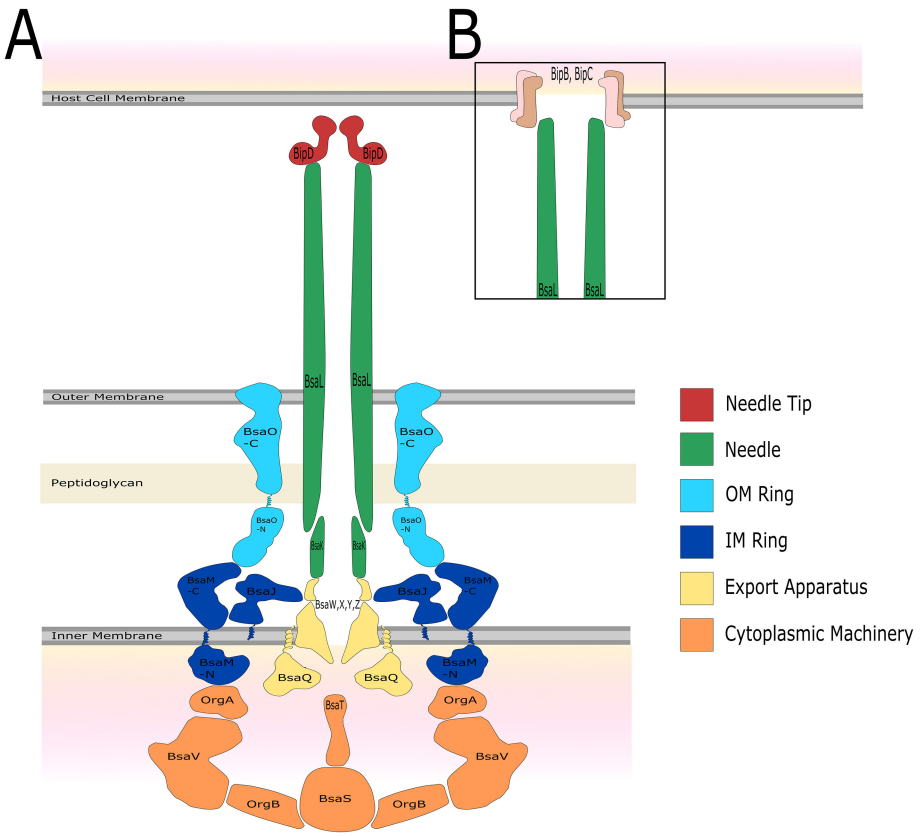


**FIGURE 2 |** The predicted structure of the *B.* pseudo*mallei* K96243 T3SS-3 based on *Salmonella* SPI-1. The name of the protein which is predicted to constitute each structural component, as well as colors to represent different portions of the T3SS structure, are shown. **(A)** Before host cell contact, the T3SS is fully assembled spanning both the inner and outer bacterial membrane. The needle forms a channel extending out of the bacterium which is capped by the needle tip protein. **(B)** After contact with the host cell, a signal is relayed through the T3SS and translocator proteins form a pore in the host cell membrane allowing for injection of bacterial effector proteins.

be important in a murine model of respiratory melioidosis and a human *NLRC4* polymorphism is associated with survival in melioidosis patients (West et al., 2014).

### BsaK (BPSS1549)

The cellular protein Nod-like receptor NLRC4 recognizes T3SS minor needle component proteins from a range of Gram-negative bacteria, including BsaK (BPSS1549) from *B. pseudomallei*, activating an innate immune response through casapase-1 (Miao et al., 2010; Zhao et al., 2011; Bast et al., 2014). A *B. pseudomallei bsaK* mutant was highly attenuated in an intranasal murine model of melioidosis (Bast et al., 2014).

## Non-structural Proteins

### BsaU (BPSS1539)

BsaU (BPSS1539) is homologous to InvJ from *Salmonella* which is the "molecular ruler" which determines the length of the T3SS needle (Kubori et al., 2000). Mutation of *bsaU* in *B. pseudomallei* resulted in delay in phagosome escape and reduced virulence in a BALB/c intranasal mouse infection model (Pilatz et al., 2006). The mutant was also deficient in its ability to secrete the effector protein BopE and the translocator tip protein BipD (Pilatz et al., 2006). It can be hypothesized that without BsaU, the needle complex of T3SS-3 forms incorrectly, accounting for the lack of effector and translocator secretion.

### BsaP (BPSS1544)

A family of T3SS proteins called the "gatekeeper" proteins (InvE/MxiC/SepL/YopN-TyeA) are involved in the control of effector and translocator protein secretion and the switch from intermediate to late substrates for secretion in *Salmonella*/*Shigella*/*E. coli*/*Yersinia*, respectively (reviewed in Büttner, 2012). These proteins are involved in the temporal regulation of their respective T3SSs and deletion of all of these proteins causes an increase in levels of secreted effectors, but has differing effects on the secretion of translocators. For example deletion of *invE* (Kubori and Galán, 2002) and *sepL* (Kresse et al., 2000; Deng et al., 2004, 2005) causes a reduction in translocator secretion, deletion of *mxiC* (Botteaux et al., 2009) has no effect on translocator secretion, and deletion of *yopN* (Forsberg et al., 1991; Iriarte et al., 1998) increases levels of secreted translocators. The closest homolog to this family of proteins in *B. pseudomallei* is BsaP (BPSS1544), which we have demonstrated functions as

a gatekeeper protein for effectors in a manner most similar to *Salmonella invE* (Vander Broek et al., 2015). Deletion of *bsaP* creates a phenotype in which effector proteins are hyper-secreted with a concomitant decrease in translocator secretion (Vander Broek et al., 2015). Further studies are warranted to determine the molecular interactions of BsaP with other components of the T3SS-3, in order to fully understand BsaP in the context of the other members of the gatekeeper family of proteins.

### Structural Components for Which No Data Is Available

Proteins for which no published work is available are OrgA (BPSS1551), OrgB (BPSS1552), BsaJ (BPSS1550), BsaO (BPSS1545), BsaT (BPSS1540), BsaV (BPSS1538), BsaW (BPSS1537), BsaX (BPSS1536), and BsaY (BPSS1535). The putative function of these proteins can be found in **Table 2** and their predicted location in the structure of T3SS-3 is shown in **Figure 2**.

T3SS-3 has been well studied in terms of its role in virulence however very little has been reported on the structure and the molecular interactions between individual components of the T3SS itself. Determining the finer points of structure and hierarchy of assembly represent a major unanswered research question in terms of understanding T3SS-3 in the context of other well studied T3SSs.

## ENERGIZING SECRETION AND UNFOLDING OF SUBSTRATES

Proteins are secreted in an unfolded state due to the narrow width of the needle channel which is 2–3 nm in S. *flexneri* (Blocker et al., 2001; Radics et al., 2014). This was proven by cryo-EM imaging of a substrate which was engineered to become trapped in the secretion channel (Radics et al., 2014). The ATPase at the base of the secretion system has been shown to dissociate proteins from their chaperones and is also thought to be involved in unfolding of the protein (Akeda and Galán, 2005). The source of energy for exporting proteins is the subject of some debate. In the flagellar T3SS of *Yersinia* and *Salmonella*, secretion can take place in the absence of the ATPase (Wilharm et al., 2004; Erhardt et al., 2014). This evidence, combined with a study which showed flagellar T3S was halted in the absence of a proton gradient, has led to the hypothesis that the ATPase is primarily required for protein unfolding and that proton motive force energizes secretion of the unfolded substrate (Paul et al., 2008).

The *B. pseudomallei* T3SS-3 ATPase is BsaS (BPSS1541). A *B. pseudomallei bsaS* mutant was unable to secrete the known effector protein BopE, demonstrated a defect in intracellular survival in RAW264.7 cells and was attenuated in BALB/c mice infected intra-nasally, demonstrating that the ATPase is required for T3S of effector proteins and has a similar phenotype to other T3SS-3 structural mutants (Gong et al., 2015). This agrees with a previous study in which *B. pseudomallei* and *B. thailandensis* containing in-frame deletions in *bsaS,* were impaired in their ability to escape the endosomal compartment and form plaques in host cell monolayers as a result of cell-to-cell spread (French et al., 2011). *Salmonella* lacking a functional ATPase will still assemble a mature T3SS, and will still secrete effector proteins, though at a reduced level (Erhardt et al., 2014). The effect that a *bsaS* mutation in *B. pseudomallei* T3SS-3 may have on either assembly of the T3SS apparatus or the secretion of early/middle substrates, such as the major needle component (BsaL) and the needle tip protein (BipD) remains an interesting open question.

## NEEDLE TIP AND TRANSLOCATOR PROTEINS-SENSING HOST CONTACT

Upon host cell contact, the translocators of the T3SS are inserted into the host cell membrane forming a pore through which effector proteins may pass. *Shigella* is able to lyse red blood cells by inserting the translocators IpaB and IpaC into the RBC membrane forming a 25 angstrom pore (Blocker et al., 1999). Secretion of the translocator proteins is controlled by the needle tip protein. A *Shigella* needle tip protein mutant (*ipaD*), constitutively secreted the translocators IpaB and IpaC (Picking et al., 2005). Immunofluorescence microscopy demonstrated the presence of the *Shigella* IpaD protein on the surface of the bacteria in the absence of a host cell membrane, a finding that was further confirmed by electron microscopy (Espina et al., 2006). The needle tip protein probably acts to sense host cell contact, inhibiting premature secretion of translocators (Espina et al., 2006). In the same study it was shown that antibodies to the tip protein disrupted the haemolysis of sheep erythrocytes indicating the functional importance of IpaD in the insertion of the translocator complex into eukaryotic cell membranes, as well as regulating effector protein secretion (Espina et al., 2006). Next, the T3SS senses host cell contact when IpaD binds to bile salts causing IpaB to be exposed at the needle tip (Olive et al., 2007; Stensrud et al., 2008).

The final step in secretion of the translocation pore is dependent on *Shigella* interacting with host cell lipids to induce IpaC secretion (Epler et al., 2009). When cultured in the presence of liposomes, IpaC localizes to the bacterial surface and is secreted (Epler et al., 2009). This agrees with earlier evidence that cholesterol is bound by translocation components (*Salmonella* SipB and *Shigella* IpaB), is important for entry into host cells and is required for efficient translocation of effector proteins into host cells (Lafont et al., 2002; Hayward et al., 2005). There is some evidence to suggest that the translocator proteins, along with the needle tip and a functional T3SS, may be sufficient to determine the intracellular niche of *Salmonella* and *Shigella* in the absence of any of the effector proteins (Du et al., 2016).

### BipD (BPSS1529)

BipD (BPSS1529) is the needle tip protein of the *B. pseudomallei* T3SS-3. It is homologous to SipD (*Salmonella*), IpaD (*Shigella*), and LcrV (*Yersinia*). BipD has been confirmed to be secreted by the *B. pseudomallei* T3SS-3 (Stevens et al., 2003; Vander Broek et al., 2015). The crystal structure of BipD was solved (Erskine et al., 2006; Knight et al., 2006; Roversi et al., 2006; Johnson et al., 2007; Pal et al., 2010) and the 3-dimensional

**TABLE 2 |** *B. pseudomallei* T3SS-3 genes, corresponding proteins and predicted functions.

| ***B. pseudomallei* K96243** | | **Homologs** | | **Universal nomenclature** | **Function** |
|---|---|---|---|---|---|
| **T3SS-3** | | ***Salmonella* SPI-1** | ***Shigella*** | **Protein name** | |
| **Locus tag** | **Protein name** | **Protein name** | **Protein name** | | |
| BPSS1516 | BopC | | | | Effector |
| BPSS1517 | — | | | | Chaperone of BopC |
| BPSS1518 | — | | | | |
| BPSS1519 | — | | | | |
| BPSS1520 | BprC | | | | Regulator of T6SS-1 |
| BPSS1521 | BprD | | | | Effector/Regulator |
| BPSS1522 | BprB | | | | Putative regulator |
| BPSS1523 | BicP | SicP | | | Chaperone, shown to bind to BapA |
| BPSS1524 | BopA | SptP | IcsB | | Effector protein |
| BPSS1525 | BopE | SopE | | | Effector protein |
| BPSS1526 | BapC | IagB | IpgF | | Effector protein |
| BPSS1527 | BapB | IacP | | | Negative regulator, predicted chaperone |
| BPSS1528 | BapA | | | | Effector protein |
| BPSS1529 | BipD | SipD | IpaD | SctA | Needle tip |
| BPSS1530 | BprA | | | | Putative regulator |
| BPSS1531 | BipC | SipC | IpaC | SctB | Minor translocator |
| BPSS1532 | BipB | SipB | IpaB | SctE | Major translocator |
| BPSS1533 | BicA | SicA | IpgC | | Chaperone/Co-activator of BsaN |
| BPSS1534 | BsaZ | SpaS | Spa40 | SctU | Autoprotease, early/middle substrate switch |
| BPSS1535 | BsaY | SpaR | Spa29 | SctT | Inner membrane export apparatus |
| BPSS1536 | BsaX | SpaQ | Spa9 | SctS | Inner membrane export apparatus |
| BPSS1537 | BsaW | SpaP | Spa24 | SctR | Inner membrane export apparatus |
| BPSS1538 | BsaV | SpaO | Spa33 | SctQ | Cytoplasmic ring |
| BPSS1539 | BsaU | InvJ | Spa32 | SctP | Needle length control protein |
| BPSS1540 | BsaT | InvI | Spa13 | SctO | Stalk protein |
| BPSS1541 | BsaS | InvC | Spa47 | SctN | ATPase |
| BPSS1542 | BsaR | InvB | Spa15 | | Chaperone, predicted to bind BopE |
| BPSS1543 | BsaQ | InvA | MxiA | SctV | Export gate |
| BPSS1544 | BsaP | InvE | MxiC | SctW | Middle/late substrate switch |
| BPSS1545 | BsaO | InvG | MxiD | SctC | Outer membrane ring / secretin |
| BPSS1546 | BsaN | InvF | MxiE | | Regulator of T3SS-3 effector proteins |
| BPSS1547 | BsaM | PrgH | MxiG | SctD | Inner membrane ring component |
| BPSS1548 | BsaL | PrgI | MxiH | SctF | Outer rod/ major needle component |
| BPSS1549 | BsaK | PrgJ | MxiI | SctI | Inner rod/minor needle component |
| BPSS1550 | BsaJ | PrgK | MxiJ | SctJ | Inner membrane ring component |
| BPSS1551 | OrgA | OrgA | MxiK | SctK | ATPase cofactor |
| BPSS1552 | OrgB | OrgB | MxiN | SctL | Stator protein |
| BPSS1553 | BprP | | | | Regulator of T3SS-3 |
| BPSS1554 | BprQ | | | | Regulator of T3SS-3 |

*Homologs from Salmonella SPI-1 and Shigella are given for reference. Where applicable, the universal nomenclature for T3SS structural proteins is also listed.*

structure is highly similar to IpaD of *Shigella* (Johnson et al., 2007) and *Salmonella* SipD (Espina et al., 2007), but *bipD* cannot functionally complement *sipD* in *Salmonella* (Klein et al., 2017). It was demonstrated that the structure of BipD, as well as IpaD and SipD, is dependent on pH changes (Markham et al., 2008). Interestingly when cultured in a more acidic pH of 4.5, *B. thailandensis* secretes increased amounts of BipD as well as BopE (Jitprasutwit et al., 2010), though the study also described amino acid differences between BipD of *B. pseudomallei* and *B. thailandensis* (Jitprasutwit et al., 2010), raising the question as to what effect pH may have on T3SS-3 in *B. pseudomallei.*

In a *B. pseudomallei bipD* mutant, the levels of both translocators and effectors secreted into the culture supernatant

are increased (Stevens et al., 2003; Vander Broek et al., 2015), in agreement with data published for the homologous *Shigella* protein IpaD (Parsot et al., 1995; Picking et al., 2005). IpaD blocks secretion of effector proteins until host cell contact has taken place (Roehrich et al., 2013), and because of its similarity in both sequence and structure (Erskine et al., 2006) it is perhaps unsurprising that BipD would function in a similar manner. More recent evidence suggests that *Shigella* IpaD may be involved in controlling the secretion of translocator and effector proteins through an interaction with the gatekeeper protein MxiC (Roehrich et al., 2016). This would suggest an interaction between BipD and BsaP in *B. pseudomallei* which may have a similar activity.

Needle tip proteins are of particular interest because of their potential use as subunit vaccines. Most notably the *Yersinia pestis* needle tip protein LcrV (V antigen), especially when combined with the Fraction 1 (F1) protein, is an effective vaccine that has been tested in human clinical trials (reviewed by Williamson, 2009). Vaccination of mice with the *Shigella* needle tip protein IpaD, along with the translocator IpaB, induced high levels of protection upon subsequent challenge (Martinez-Becerra et al., 2012, 2013; Heine et al., 2013). Some 15 years ago, it was described that convalescent serum from a melioidosis patient reacted specifically with a recombinant GST-tagged BipD protein (Stevens et al., 2002). CD4+ T cells taken from mice infected with an attenuated strain of *B. pseudomallei* showed specificity for BipD (Haque et al., 2006). Similarly, human monocyte-derived dendritic cells from healthy *B. pseudomallei* seropositive donors were pulsed with purified BipD after which CD4+ T cells were able to recognize the recombinant protein (Tippayawat et al., 2011). A *B. pseudomallei bipD* mutant was significantly attenuated in a BALB/c intranasal murine infection model, demonstrating the importance of this protein *in vivo* (Stevens et al., 2004). Attempts have been made to use BipD as a recombinant subunit vaccine in a BALB/c murine intraperitoneal model of infection, but in both studies the vaccine showed no protection upon subsequent challenge (Stevens et al., 2004; Druar et al., 2008).

## BipB (BPSS1532)

BipB (BPSS1532) shares 46% amino acid identity with the *Salmonella* translocator protein SipB, and is secreted by T3SS-3 in a *bsaZ* dependant manner (Vander Broek et al., 2015). In a *Salmonella sipB* mutant, *bipB* is unable to complement *sipB* demonstrating evolutionary separation of these proteins (Klein et al., 2017). This is an important reminder that although T3SSs are similar in structure, T3SS proteins do not always function identically.

A *B. pseudomallei* K96243 *bipB* insertion mutant showed reduced invasion and cell-to-cell spread in HeLa cells, and a reduced ability to form multi-nucleated giant cells in J774 cells (Suparak et al., 2005). *In vivo*, in BALB/c mice infected intranasally, the *bipB* mutant was greatly attenuated and showed a phenotype similar to that of the *bipD* translocator mutant (Stevens et al., 2004; Suparak et al., 2005). This is likely due to the inability of the T3SS to function correctly without the formation of the translocation pore, and any proposed secondary function would require further investigation. The N-terminal region of BipB has been tested as a protective antigen in a murine model of melioidosis, but as with BipD, showed no protection upon subsequent challenge (Druar et al., 2008).

## BipC (BPSS1521)

BipC (BPSS1531) is a homolog of the *Salmonella* SipC and *Shigella* IpaC translocator proteins. The *Salmonella* SipC protein has been shown to interact with SipB to form the translocon pore (Myeni et al., 2013). Beyond their role as a translocator protein, SipC and IpaC also function as effector proteins within the eukaryotic cell. SipC has actin nucleation activity and bundles F-actin (Hayward and Koronakis, 1999). The ability of SipC to nucleate and bundle F-actin as well as form the translocation pore, are all dependant on the C-terminal 209 amino acids of the 409 amino acid protein (Hayward and Koronakis, 1999; Chang et al., 2005; Myeni and Zhou, 2010). Actin bundling appears to be important for cell invasion, as *Salmonella* containing a *sipC* mutation abolishing its actin bundling activity, but not translocator function, was less invasive than the parental strain (Myeni and Zhou, 2010). Internalization of *B. pseudomallei* can be blocked by the actin polymerization inhibitor cytochalasin D (Jones et al., 1996), indicating the importance of actin cytoskeletal rearrangements in the uptake of *B. pseudomallei*. Similarly to SipC, BipC is also able to polymerise actin *in vitro* and stabilizes F-actin indicating possible actin bundling activity (Kang et al., 2016a and our own unpublished observations). Interestingly, *Salmonella* SipA protein enhances the ability of SipC to nucleate and bundle F-actin (McGhie et al., 2001), but a homolog of SipA is not encoded by the genome of *B. pseudomallei*. SipC has also been shown to bind to host Syntaxin 6 and thereby recruit LAMP1 to the *Salmonella* containing vacuole (SCV), helping to stabilize its membrane (Madan et al., 2012). The functional relevance of the actin-binding activity of BipC and whether it binds any other host cell proteins requires further study.

In *Salmonella* and *Shigella*, the SipC/IpaC family of translocator/effector proteins may play a crucial role in determining the intracellular niche of the bacteria. There is evidence to suggest that *sipC* and *ipaC* cannot fully complement each other (Osiecki et al., 2001; Klein et al., 2017). The authors suggest the proteins, while both translocators, may have some divergent functions which may parallel the different intracellular lifestyles of the pathogens, with *Salmonella* residing within the vacuole and *Shigella* rapidly escaping into the cytosol (Osiecki et al., 2001). This is supported by a recent study in which *Salmonella* expressing *ipaC*, was shown to be capable of vacuole escape (Du et al., 2016). Because of closer parallels between the intracellular lifestyles of *B. pseudomallei* and *Shigella*, we would predict that BipC would function in a manner more similar to IpaC than SipC, mediating the exit of the bacterium from the endocytic compartment into the host cell cytosol. In a *Salmonella sipC* mutant, *bipC* is unable to complement *sipC* (Klein et al., 2017), further supporting a possible difference in accessory function of these proteins.

The C-terminal and N-terminal regions of BipC have previously been separately tested as a protective antigen in mice, but neither antigen showed any protection upon challenge with

*B. pseudomallei* (Druar et al., 2008). In another study, a *B. pseudomallei bipC* mutant showed reduced cell adhesion and invasion of A549 cells (Kang et al., 2015). This *bipC* mutant also showed a delay in escape from the phagosome, leading to a delay in formation of actin tails in the host cell cytoplasm and intracellular replication (Kang et al., 2015). The mutant was also attenuated in BALB/c mice infected intraperitoneally (Kang et al., 2015). The transcriptome of livers of mice infected with the *bipC* mutant showed a lower expression of genes involved in actin cytoskeleton signaling, MAPK signaling, integrin signaling and TNF when compared to mice infected with the parental *B. pseudomallei* strain (Kang et al., 2016b). While this shows the importance of BipC in virulence, both *in vivo* and *in vitro*, it does not separate the role of BipC as a translocator necessary for a functional T3SS and rapid escape from the endosome, from its role as an effector protein.

## SECRETION SIGNALS AND CHAPERONES

Type III secretion signals are located at the N-terminus of a protein, are not cleaved and do not share primary sequence identity with each other (Michiels and Cornelis, 1991; Schesser et al., 1996). In *Yersinia*, it was demonstrated that as little as 15 amino acids of the N-terminus of YopE were required for secretion (Sory et al., 1995). Interestingly, substituting the alanines at position 2 and 15 in the YopE secretion signal with glutamic acid, did not affect secretion (Anderson and Schneewind, 1997). Even shifting the reading frame did not prevent the secretion of YopE, which the authors suggested may indicate a secretion signal located in the mRNA encoding the effector protein (Anderson and Schneewind, 1997).

A second important signal in the N-terminal region of T3SS effector proteins is the chaperone binding domain (CBD) which is required for the specific secretion of effector proteins (Abe et al., 1999; Ehrbar et al., 2003, 2006; Lee and Galán, 2003, 2004) as well as for their stability in the bacterial cytoplasm (Frithz-Lindsten et al., 1995; Abe et al., 1999). By determining the crystal structure of an effector protein bound to its chaperone, it is known that T3SS chaperones in *Yersinia* and *Salmonella* bind the N-terminal amino acids of their effector protein, just after the T3S signal, but before any functional domains, and maintain the bound effector protein in a partially unfolded state that may be more competent for secretion (Birtalan and Ghosh, 2001; Stebbins and Galán, 2001).

The T3S signal also appears to be promiscuous between systems, allowing secretion of effector proteins from bacteria in an unrelated host bacterium containing a T3SS (Rossier et al., 1999; Hovis et al., 2013). This is even true of less similar T3SSs, as demonstrated by the ability of the Hrp Plant T3SS of *Xanthomonas* to secrete the mammalian effector protein *Yersinia* YopE (Rossier et al., 1999). Perhaps because of the similarity between the two, virulence-associated T3SS effectors can be secreted by the bacterial flagellar T3SS system in *Yersinia* and *Salmonella* (Young and Young, 2002; Lee and Galán, 2004; Warren and Young, 2005; Ehrbar et al., 2006). It is only through interaction with the appropriate chaperone that specific secretion through a single system is achieved. Inhibition of the ability of *Salmonella* SopE to bind its chaperone InvB, caused secretion through both the flagellar and SPI-1 virulence associated T3SS (Lee and Galán, 2004; Ehrbar et al., 2006). The genome of *B. pseudomallei* encodes five putative T3SS-3 chaperones, though little work concerning their function has yet been described.

### BPSS1517

The protein encoded by the gene BPSS1517 is predicted to be a putative chaperone (Panina et al., 2005) and has been shown to interact with the downstream effector protein BopC (BPSS1516) (Muangman et al., 2011).

### BicP (BPSS1523)

BicP (BPSS1523) shares homology with *Salmonella* SicP, a specific chaperone for the effector protein SptP (Fu and Galán, 1998). The closest homolog to SptP in *B. pseudomallei* is BopA (BPSS1524) which was predicted to be the binding partner for BicP (Panina et al., 2005), but the interaction between the two proteins has not formally been demonstrated.

### BapB (BPSS1526)

BapB (BPSS1526) is homologous to *Salmonella* IacP (Stevens et al., 2002). IacP is important for *Salmonella* invasion into host cells by playing a role in regulating SopA, SopB and SopD secretion (Kim et al., 2011). Formerly considered a possible candidate effector protein, BapB was not found to be secreted by T3SS-3 (Treerat et al., 2015; Vander Broek et al., 2015). Deletion of *bapB* caused an increase in the transcription and secretion of BopE, indicating it may be a negative regulator of effector transcription (Treerat et al., 2015). In the same study the authors performed a phylogenetic analysis which suggested that BapB may be closely related to the *Salmonella* FliT chaperone protein (Treerat et al., 2015).

### BicA (BPSS1533)

BicA (BPSS1533) is homologous to the *Salmonella* chaperone SicA. SicA binds to and prevents the association and resulting degradation of SipC and SipB in the bacterial cytoplasm (Tucker and Galán, 2000). As SipC is secreted by a mature needle complex, SicA is freed and interacts with the transcriptional regulator InvF to increase the expression of effector proteins (Tucker and Galán, 2000; Darwin and Miller, 2001). *B. pseudomallei* BicA is required for the secretion of the known effector proteins BopE and BopA (Sun et al., 2010), and BicA along with the regulator BsaN activate transcription of T3SS-3 effector proteins, translocators and chaperones (Chen et al., 2014). The *bicA* gene is also able to partially complement a *Salmonella sicA* mutant (Klein et al., 2017), further supporting a homologous function. BicA is required for respiratory melioidosis in mice (Gutierrez et al., 2015b).

### BsaR (BPSS1542)

BsaR (BPSS1542) is homologous to the *Salmonella* chaperone InvB which has been shown to be required for secretion of the effector proteins SopE and SopA (Ehrbar et al., 2003, 2004; Lee and Galán, 2003). BsaR is predicted to be the chaperone for BopE using a computational screen for chaperones in *B. pseudomallei*

K96243 (Panina et al., 2005), although this has not yet been experimentally validated.

## T3SS-3 EFFECTOR PROTEINS

The role of the T3SS is to deliver an array of effector proteins into the target cell to subvert host cell functions. The function of different effector proteins is extremely varied, ranging from blocking apoptosis (*E. coli* NleH) (Hemrajani et al., 2010), prevention of phagocytosis (*Yersinia* YopH) (Persson et al., 1997), cytotoxic activity (*Pseudomonas aeruginosa* ExoU) (Sato et al., 2003) and disruption of the actin cytoskeleton (*Salmonella* SopE) (Hardt et al., 1998). *B. pseudomallei* encodes seven effector proteins known to be secreted by T3SS-3 (CHBP, BopC, BopA, BapA, BprD, BapC, and BopE), as well as one hypothetical T3SS effector BopB (Pumirat et al., 2014; Vander Broek et al., 2015).

### CHBP/Cif (BPSS1385)

CHBP (BPSS1385) is a homolog of *E. coli* cell cycle inhibiting factor (Cif) and is the only identified T3SS-3 effector protein that is encoded outside of the T3SS-3 locus. Cif and CHBP are able to deamidate cellular NEDD8 causing cell cycle arrest (Nougayrède et al., 2001; Cui et al., 2010) and CHBP causes cell cycle arrest when expressed in *B. thailandensis* (Cui et al., 2010). CHBP has also been shown to activate the cellular kinase ERK independent of its ability to deamidate NEDD8 (Ng et al., 2017).

The gene encoding CHBP is present in ∼76% of the available *B. pseudomallei* genomes and a Western blot assay used to probe for the presence of the CHBP protein in *B. pseudomallei* clinical isolates from the endemic region detected CHBP in 47% of isolates tested (Pumirat et al., 2014). Interestingly, CHBP is not secreted under standard growth conditions, but *B. pseudomallei* secretes CHBP in U937 cells in a *bsaQ*–dependent manner (Pumirat et al., 2014). A *B. pseudomallei* K96243 *chbP* insertion mutant was impaired in its ability to form plaques in HeLa cells at 24 h and demonstrated lower cytotoxicity at 6 h as assessed by LDH release assays (Pumirat et al., 2014). Both phenotypes could be complemented by expression of *chbP in trans* indicating that these phenotypes were due to disruption of the *chbP* gene and not due to unexpected polar effects of the insertion mutation (Pumirat et al., 2014).

### BopB/FolE (BPSS1514)

BopB (BPSS1514) or FolE, is annotated to be a GTP cyclohydrolase I and was thought to be a candidate effector protein (Stevens et al., 2004). Yet a *bopB* mutant did not display a significantly reduced time to death in a BALB/c intraperitoneal infection model (Stevens et al., 2004). Similarly, mutation of *bopB* did not affect invasion and intracellular replication of host cells (Chen et al., 2014). Expression of *bopB* is co-regulated with the other T3SS-3 effectors by BsaN, but the role BopB plays in infection is still unknown (Chen et al., 2014).

### BopC (BPSS1516)

BopC (BPSS1516) is a 509 amino acid protein with no significant sequence homology to proteins from other species besides *B. mallei*. It is encoded just before the T3SS-3 locus along with BPSS1517, its chaperone (Muangman et al., 2011). BopC was detected in the culture supernatants of WT *B. pseudomallei* 10276, but not in supernatants of a *bsaZ* insertion mutant, indicating that BopC is secreted by T3SS-3 (Muangman et al., 2011; Vander Broek et al., 2015). The first 20 amino acids of BopC fused to the β-lactamase gene TEM1, was sufficient for translocation into HeLa cells in a T3SS-dependant manner (Muangman et al., 2011). A *B. pseudomallei* K96243 *bopC* mutant was hindered in its ability to invade A549 cells (Muangman et al., 2011) and displayed reduced levels of intracellular survival (Srinon et al., 2013). The *bopC* mutant also demonstrated delayed phagosome escape in J774A.1 cells as shown by staining for co-localisation of the bacteria with the cellular lysosomal marker protein LAMP–1, which likely explains the defect in intracellular survival (Srinon et al., 2013).

### BprD (BPSS1521)

BprD (BPSS1521) has no known homology to proteins outside of *B. pseudomallei* and the closely related *Burkholderia* species. It is labeled as a putative regulator of T3SS-3, though a knockout of the *bpr* operon (*bprB-D*) showed no effect on the expression of T3SS-3 genes (Sun et al., 2010). Its expression is regulated by BsaN along with the known effector proteins BopA, BopC and BopE (Sun et al., 2010; Chen et al., 2014) and *bipD* gene expression is significantly up-regulated in tissues of infected mice (Chirakul et al., 2014). The same study demonstrated attenuation of the *bprD* mutant in BALB/c mice infected intraperitoneally, which the authors speculate may be due to the up-regulation of the T6SS-1 through effects on *bprC* (Chirakul et al., 2014).

Our own work has demonstrated that BprD is secreted into the supernatant in a T3SS-3 *bsaZ*-dependant manner (Vander Broek et al., 2015). While this may seem surprising, it is not without precedent that a regulator of the T3SS is also a substrate for secretion, for example, *Yersinia* LcrQ (Cambronne et al., 2000). It is thought that LcrQ acts as a feedback inhibitor of the expression of *Yersinia* effectors (Cambronne et al., 2000). When LcrQ is secreted into host cells and the levels of LcrQ in the bacterium are depleted, inhibition is relieved and T3S can progress (Cambronne et al., 2000). Whether BprD is secreted into host cells, whether it acts as a true effector protein and the mechanisms by which it regulates virulence and T6S present interesting research questions for the field.

### BopA (BPSS1524)

BopA (BPSS1524) shares 23% amino acid identity with *Shigella* IcsB (Cullinane et al., 2008). It has been predicted to contain a Rho GTPase inactivation domain (RID) similar to that found in *Vibrio cholerae* VcRtxA and other MARTX toxins which indirectly inactivate Rho GTPases (Pei and Grishin, 2009). IcsB, along with its chaperone IpgA, are important for *Shigella*'s ability to escape LC3-positive autophagosomes once inside the host cell, and this activity is dependent on the IcsB cholesterol-binding domain (Kayath et al., 2010; Campbell-Valois et al., 2015). BopA also contains a functional cholesterol-binding domain (Kayath et al., 2010). The *B. pseudomallei* homolog of IpgA is BicP, which co-purifies with BopA and helps to prevent its degradation, indicating that it is the chaperone for BopA (Kayath et al., 2010).

BopA is secreted by T3SS-3 in a *bsaZ*-dependant manner (Vander Broek et al., 2015) and the first 58 amino acids of *B. mallei* BopA fused to the *Yersinia enterolitica* phospholipase YplA, has been shown to be secreted in a surrogate enteropathogenic *E. coli* host (Whitlock et al., 2008).

BopA is important for the intracellular survival of *B. pseudomallei* in phagocytic cells (Cullinane et al., 2008). A *B. pseudomallei* K96243 *bopA* mutant displayed reduced intracellular survival and an increased localisation with GFP-LC3, an indicator of autophagy stimulation, in RAW 264.7 cells (Cullinane et al., 2008). This reduction in intracellular survival was overcome when cells were treated with the autophagy inhibitor wortmannin (Cullinane et al., 2008). Another study demonstrated that BopA is important for escape of the bacterium from the phagosome (Gong et al., 2011). A *B. mallei* ATCC 23344 *bopA* mutant demonstrated reduced intracellular survival in J774A.1 cells (Whitlock et al., 2008). Interestingly, in the murine alveolar macrophage cell line MH-S, the same *B. mallei bopA* mutant exhibited increased intracellular survival when compared to the isogenic parental strain, indicating that different cell types may rely on different mechanisms to control intracellular *B. mallei* (Whitlock et al., 2009). BALB/c mice infected intraperitoneally with a *B. pseudomallei* 576 *bopA* insertion mutant were significantly delayed in time to death when compared to the parental strain (Stevens et al., 2004). Similarly, BALB/c mice infected intra-nasally with a *B. mallei* ATCC 23344 *bopA* insertion mutant also showed a delayed time to death. No bacteria were recovered from the lung tissue of animals infected with the *bopA* mutant while $10^8$ bacteria were recovered from the lungs of animals infected with *B. mallei* (Whitlock et al., 2009). In mice immunized with recombinant BopA and challenged intra-nasally with *B. mallei* ATCC23344 or *B. pseudomallei* 1026b, the BopA vaccine protected 100 and 60%, respectively of animals 21 days post infection (Whitlock et al., 2010).

## BopE (BPSS1525)

BopE (BPSS1525) is the best characterized of the *B. pseudomallei* effector proteins and is commonly used as a readout for the ability of the T3SS-3 to secrete effector proteins. BopE is 27% identical over a region of 168 amino acids to the *Salmonella* guanine nucleotide exchange factor (GEF) SopE (Stevens et al., 2003). BopE is secreted by *B. pseudomallei* in a manner dependent on the T3SS-3 (Stevens et al., 2003; Muangsombut et al., 2008; Vander Broek et al., 2015) and is required for efficient invasion of non-phagocytic cells (Stevens et al., 2003). Also, ectopic expression of BopE in HeLa cells causes significant actin cytoskeletal rearrangements with similarity to ectopic SipC expression (Stevens et al., 2003). Using fluorescence spectrometry, it was demonstrated that purified BopE, similar to SopE, is a functional GEF for both Rac1 and Cdc42, but with about 10 fold lower activity than SopE (Stevens et al., 2003). This lower activity may be explained by differences in the catalytic domains, as the SopE catalytic domain stays in an open conformation, while BopE adopts a closed conformation which requires interaction with Cdc42 to allow for GEF activity (Upadhyay et al., 2008). HEK 293T cells transfected with plasmids expressing BopE and caspase–1, resulted in increased activation of caspase–1 and –7 (Bast et al., 2014). When the active site of the transfected BopE was mutated, levels of activation of caspase–1 and –7 returned to basal levels indicating BopE's GEF activity is required for the activation of caspase–1 and –7 (Bast et al., 2014).

BopE is a potent T cell antigen in mice (Haque et al., 2006) and in sero-positive recovered melioidosis patients (Tippayawat et al., 2009). However, in an intraperitoneal BALB/c murine model of melioidosis, ablation of the *bopE* gene did not affect the median time to death of the animals when compared to the parental strain (Stevens et al., 2004).

## BapC (BPSS1527)

BapC (BPSS1526) is homologous to *Salmonella* IagB (Stevens et al., 2002). IagB is thought to be a lytic transglycosylase involved in the breakdown of the bacterial peptidoglycan layer, allowing connection of the inner and outer membrane components of the secretion system, though this function has not been formally demonstrated (Zahrl et al., 2005). BapC is secreted by T3SS-3 in a manner dependant on *bsaS* (Treerat et al., 2015). A *B. pseudomallei* K96243 *bapC* mutant showed a slight attenuation in a competitive growth assay in an acute BALB/c model of infection (Treerat et al., 2015), whereas a *B. pseudomallei* 1026b *bapC* mutant showed no significant attenuation in a Syrian hamster model of melioidosis (Warawa and Woods, 2005).

## BapA (BPSS1528)

BapA (BPSS1528) has no known homology to any other bacterial or host cell proteins except the BapA orthologues of *B. pseudomallei* and the closely related species *B. thailandensis* and *B. mallei*. BapA is secreted by T3SS-3 in both a BsaS and BsaZ dependant manner (Treerat et al., 2015; Vander Broek et al., 2015). A 1026b *B. pseudomallei bapA* mutant showed no attenuation in a Syrian hamster model of infection (Warawa and Woods, 2005), whereas a *B. pseudomallei* K96243 *bapA* mutant was attenuated in a competitive growth assay in an acute BALB/c model of infection (Treerat et al., 2015).

# FUTURE PERSPECTIVES

While there has been a wealth of new information concerning *B. pseudomallei* T3S, there are still many significant gaps in knowledge, particularly with regard to the importance of T3SS-1 and T3SS-2 in melioidosis. It is possible that the plant pathogen-like T3SS-1 and T3SS-2 add fitness to *B. pseudomallei* in the environment, allowing infection/colonization of adjacent plant life. However, it is also possible that these systems are relevant in mammalian hosts, given their conservation amongst the *B. pseudomallei* strains sequenced to date, and the finding that T3SS-1 is required for full virulence in a murine model of melioidosis (D'Cruze et al., 2011).

It is still unclear whether T3SS-3 plays a significant role in invasion of host cells, particularly non-phagocytic cells. There have been many reports of T3SS-3 or its effector proteins playing a role in invasion (Stevens et al., 2003; Suparak et al., 2005; Muangsombut et al., 2008; Muangman et al., 2011; Kang et al., 2015). Yet in another study, T3SS-3 ATPase (*bsaS*) mutants did not show a decrease in invasion efficiency in HEK293 or HeLa cells (French et al., 2011). This observation is important because

it questions the involvement of T3SS-3 in invasion as well as highlighting a general lack of understanding of the pathways and mechanisms involved in *B. pseudomallei* entry into host cells.

To date CHBP is the only effector protein secreted by the *B. pseudomallei* T3SS-3 that is encoded outside of the T3SS-3 locus, and which is not present in the genome of all strains (Pumirat et al., 2014). This raises the question of whether other effector proteins secreted by T3SS-3, but encoded outside of the T3SS-3 locus, may be present in other strains. Full genome comparisons of almost 100 strains of *B. pseudomallei* identified 86% of genes as being conserved and present in all strains (Sim et al., 2008). The other 14% of genes, considered accessory genes, were disproportionally present in genomic islands and were associated with clinical isolates (Sim et al., 2008). The GIs in *B. pseudomallei* are highly variable between strains. A study of five clinical *B. pseudomallei* strains identified a total of 71 GIs distributed between the strains, with at least half being unique to the strain in which they were identified (Tuanyok et al., 2008). The variability in these regions is largely due to horizontal gene transfer and *B. pseudomallei* has a relatively high rate of lateral gene transfer compared to the mutation rates of other bacterial species (Pearson et al., 2009). As *B. pseudomallei* has a large amount of genomic diversity in its accessory genome and a high rate of lateral gene transfer, there is a strong possibility that other novel effector proteins are encoded in other strains of *B. pseudomallei* that have yet to be identified. Study of these effector proteins could provide important insights into strain differences as well as the potential for novel effector biology, but it is a difficult task as the secretome of *B. pseudomallei* is very complex (Vander Broek et al., 2015). Also, due to the temporal and hierarchical control of the T3SS, there is always the possibility that an effector protein will not be secreted under the conditions used in a given experiment (reviewed in Büttner, 2012). Previous methods of identifying T3SS-3 effector proteins have relied on initial bioinformatics prediction (Stevens et al., 2003; Muangman et al., 2011) or high throughput screens (Vander Broek et al., 2015), both of which may prove to be useful tools for further studies of *B. pseudomallei* T3S. Indeed it is timely to apply these approaches to the identification and characterization of effector proteins secreted by the lesser studied T3SS-1 and T3SS-2.

Another important outstanding area of research is characterizing the functions of those effector proteins that have already been identified. One common characteristic of many T3SS effector proteins that complicates this task is their functional redundancy (reviewed in Galán, 2009). Commonly, deletion of one effector protein yields little or no phenotype in infection models because other effector proteins target either the same host cell protein or pathway (reviewed in Galán, 2009). In a biological system this would increase the chance of effectors successfully carrying out their intended function and decrease the likelihood of host cell interference. This functional redundancy also highlights the evolutionary importance of dysregulating specific cellular pathways from the standpoint of the bacterium. Even where redundancy does not exist, the function of effector proteins are often subtle when compared to bacterial toxins and may not be easily measurable in *in vitro* or *in vivo* models of infection (reviewed in Dean, 2011). This lack of a phenotype to inform focused studies presents a challenge for investigators, creating the need for high throughput "fishing" assays, such as protein immunoprecipitation/pull-downs and yeast two-hybrid assays. These assays have been used successfully to identify host cell binding partners and the subsequent functions of effector proteins from other bacteria (Zhou et al., 2013; Pallett et al., 2014). Understanding the functions of T3SS-3 effector proteins may provide new insights into host-pathogen interactions in *B. pseudomallei* infection.

Finally, the T3SS-3 has been shown to be one of the most important virulence factors in *B. pseudomallei* models of infection, raising the question of whether T3SS-3 could be a useful target for protective vaccines or therapeutic intervention in melioidosis patients. Although several attempts have been made to use live-attenuated vaccines based on mutation of key T3SS-3 genes in murine models of melioidosis, none have proven to provide sterilizing immunity. Despite being a potent B- and T-cell antigen, attempts to utilize BipD as a subunit vaccine in murine models of melioidosis have shown little promise (Stevens et al., 2004; Druar et al., 2008). There have also been attempts to use the translocator proteins of T3SS-3 as subunit vaccines. The N-terminal region of BipB was tested as a protective antigen in mice, but showed no protection against subsequent challenge (Druar et al., 2008). The C-terminal and N-terminal regions of BipC have also been separately tested as a subunit vaccine in mice, but neither antigen showed any protection (Druar et al., 2008). Some studies have focused on the use of effector proteins as subunit vaccines. Out of these studies the BopA protein shows most promise, since mice immunized with recombinant BopA were protected against subsequent intranasal challenge with both *B. mallei* and *B. pseudomallei* (Whitlock et al., 2010). More recently interest in the use of small molecule inhibitors of the T3SS-3 has arisen (Gong et al., 2015). Treatment of *B. pseudomallei* infected RAW264.7 cells with a small molecule inhibitor targeting BsaS of the T3SS-3, resulted in a decrease in bacterial intracellular survival (Gong et al., 2015). However, the use of such inhibitors is still very much in its infancy, with important *in vivo* studies being required to determine whether such small molecules would be effective in murine models of melioidosis.

## AUTHOR CONTRIBUTIONS

CV and JS contributed equally to the writing of this review article.

## ACKNOWLEDGMENTS

The authors are supported by an Institute Strategic Programme Grant from the BBSRC.

## REFERENCES


Abe, A., De Grado, M., Pfuetzner, R. A., Sánchez-SanMartin, C., DeVinney, R., Puente, J. L. et al. (1999). Enteropathogenic *Escherichia coli* translocated intimin receptor. Tir, requires a specific chaperone for stable secretion. *Mol. Microbiol.* 33, 1162–1175. doi: 10.1046/j.1365-2958.1999.01558.x

Akeda, Y., and Galán, J. E. (2005). Chaperone release and unfolding of substrates in type III secretion. *Nature* 437, 911–915. doi: 10.1038/nature03992

Anderson, D. M., and Schneewind, O. (1997). A mRNA signal for the type III secretion of Yop proteins by *Yersinia enterocolitica*. *Science* 278, 1140–1143. doi: 10.1126/science.278.5340.1140

Angus, A. A., Agapakis, C. M., Fong, S., Yerrapragada, S., Estrada-De Los Santos, P., Yang, P., et al. (2014). Plant-associated symbiotic *Burkholderia* species lack hallmark strategies required in mammalian pathogenesis. *PLoS ONE* 9:e83779. doi: 10.1371/journal.pone.0083779

Attree, O., and Attree, I. (2001). A second type III secretion system in *Burkholderia pseudomallei*: who is the real culprit?. *Microbiology* 147, 3197–3199. doi: 10.1099/00221287-147-12-3197

Barrett, B. S., Picking, W. L., Picking, W. D., and Middaugh, C. R. (2008). The response of type three secretion system needle proteins MxiH$\Delta$5, BsaL$\Delta$5, and PrgI$\Delta$5 to temperature and pH. *Proteins* 73, 632–643. doi: 10.1002/prot.22085

Bast, A., Krause, K., Schmidt, I. H., Pudla, M., Brakopp, S., Hopf, V., et al. (2014). Caspase-1-dependent and -independent cell death pathways in *Burkholderia pseudomallei* infection of macrophages. *PLoS Pathog.* 10:e1003986. doi: 10.1371/journal.ppat.1003986

Birtalan, S., and Ghosh, P. (2001). Structure of the Yersinia type III secretory system chaperone SycE. *Nat. Struct. Mol. Biol.* 8, 974–978. doi: 10.1038/nsb1101-974

Blocker, A., Gounon, P., Larquet, E., Niebuhr, K., Cabiaux, V., Parsot, C., et al. (1999). The tripartite type III secreton of Shigella flexneri inserts IpaB and IpaC into host membranes. *J. Cell Biol.* 147, 683–693. doi: 10.1083/jcb.147.3.683

Blocker, A., Jouihri, N., Larquet, E., Gounon, P., Ebel, F., Parsot, C., et al. (2001). Structure and composition of the Shigella flexneri 'needle complex', a part of its type III secreton. *Mol. Microbiol.* 39, 652–663. doi: 10.1046/j.1365-2958.2001.02200.x

Botteaux, A., Sory, M. P., Biskri, L., Parsot, C., and Allaoui, A. (2009). MxiC is secreted by and controls the substrate specificity of the Shigella flexneri type III secretion apparatus. *Mol. Microbiol.* 71, 449–460. doi: 10.1111/j.1365-2958.2008.06537.x

Brett, P. J., DeShazer, D., and Woods, D. E. (1998). Note *Burkholderia thailandensis* sp. nov., a *Burkholderia pseudomallei*-like species. *Int. J. Syst. Bacteriol.* 48, 317–320. doi: 10.1099/00207713-48-1-317

Burtnick, M. N., Brett, P. J., Nair, V., Warawa, J. M., Woods, D. E., and Gherardini, F. C. (2008). *Burkholderia pseudomallei* type III secretion system mutants exhibit delayed vacuolar escape phenotypes in RAW 264.7 murine macrophages. *Infect. Immun.* 76, 2991–3000. doi: 10.1128/IAI.00263-08

Büttner, D. (2012). Protein export according to schedule: architecture, assembly, and regulation of type III secretion systems from plant-and animal-pathogenic bacteria. *Microbiol. Mol. Biol. Rev.* 76, 262–310. doi: 10.1128/MMBR.05017-11

Büttner, D., and He, S. Y. (2009). Type III protein secretion in plant pathogenic bacteria. *Plant Physiol.* 150, 1656–1664. doi: 10.1104/pp.109.139089

Cambronne, E. D., Cheng, L. W., and Schneewind, O. (2000). LcrQ/YscM1, regulators of the Yersinia yop virulon, are injected into host cells by a chaperone-dependent mechanism. *Mol. Microbiol.* 37, 263–273. doi: 10.1046/j.1365-2958.2000.01974.x

Campbell-Valois, F.-X., Sachse, M., Sansonetti, P. J., and Parsot, C. (2015). Escape of actively secreting *Shigella flexneri* from ATG8/LC3-positive vacuoles formed during Cell-To-Cell spread is facilitated by IcsB and VirA. *MBio* 6:e02567–14. doi: 10.1128/mBio.02567-14

Chang, J., Chen, J., and Zhou, D. (2005). Delineation and characterization of the actin nucleation and effector translocation activities of Salmonella SipC. *Mol. Microbiol.* 55, 1379–1389. doi: 10.1111/j.1365-2958.2004.04480.x

Chen, Y., Schröder, I., French, C. T., Jaroszewicz, A., Yee, X. J., The, B. E., et al. (2014). Characterization and analysis of the *Burkholderia pseudomallei* BsaN virulence regulon. *BMC Microbiol.* 14:206. doi: 10.1186/s12866-014-0206-6

Cheng, A. C., and Currie, B. J. (2005). Melioidosis: epidemiology, pathophysiology, and management. *Clin. Microbiol. Rev.* 18, 383–416. doi: 10.1128/CMR.18.2.383-416.2005

Chirakul, S., Bartpho, T., Wongsurawat, T., Taweechaisupapong, S., Karoonutaisiri, N., Talaat, A. M., et al. (2014). Characterization of BPSS1521 (bprD), a regulator of *Burkholderia pseudomallei* virulence gene expression in the mouse model. *PLoS ONE* 9:e104313. doi: 10.1371/journal.pone.0104313

Costa, T. R. D., Felisberto-Rodrigues, C., Meir, A., Prevost, M. S., Redzej, A., Trokter, M., et al. (2015). Secretion systems in Gram-negative bacteria: structural and mechanistic insights. *Nat. Rev. Microbiol.* 13, 343–359. doi: 10.1038/nrmicro3456

Cui, J., Yao, Q., Li, S., Ding, X., Lu, Q., Mao, H., et al. (2010). Glutamine deamidation and dysfunction of ubiquitin/NEDD8 induced by a bacterial effector family. *Science* 329, 1215–1218. doi: 10.1126/science.1193844

Cullinane, M., Gong, L., Li, X., Adler, N.-L., Tra, T., Adler, B., et al. (2008). Stimulation of autophagy suppresses the intracellular survival of *Burkholderia pseudomallei* in mammalian cell lines. *Autophagy* 4, 744–753. doi: 10.4161/auto.6246

Currie, B. J., Ward, L., and Cheng, A. C. (2010). The epidemiology and clinical spectrum of melioidosis: 540 cases from the 20 year Darwin prospective study. *PLoS Negl. Trop. Dis.* 4:e900. doi: 10.1371/journal.pntd.0000900

D'Cruze, T., Gong, L., Treerat, P., Ramm, G., Boyce, J. D., Prescott, M., et al. (2011). Role for the *Burkholderia pseudomallei* type three secretion system cluster 1 bpscN gene in virulence. *Infect. Immun.* 79, 3659–3664. doi: 10.1128/IAI.01351-10

Darwin, K. H., and Miller, V. L. (2001). Type III secretion chaperone-dependent regulation: activation of virulence genes by SicA and InvF in *Salmonella typhimurium*. *EMBO J.* 20, 1850–1862. doi: 10.1093/emboj/20.8.1850

Dean, P. (2011). Functional domains and motifs of bacterial type III effector proteins and their roles in infection. *FEMS Microbiol. Rev.* 35, 1100–1125. doi: 10.1111/j.1574-6976.2011.00271.x

Deng, W., Li, Y., Hardwidge, P. R., Frey, E. A., Pfuetzner, R. A., Lee, S., et al. (2005). Regulation of type III secretion hierarchy of translocators and effectors in attaching and effacing bacterial pathogens. *Infect. Immun.* 73, 2135–2146. doi: 10.1128/IAI.73.4.2135-2146.2005

Deng, W., Puente, J. L., Gruenheid, S., Li, Y., Vallance, B. A., Vázquez, A., et al. (2004). Dissecting virulence: systematic and functional analyses of a pathogenicity island. *Proc. Natl. Acad. Sci. U.S.A.* 101, 3597–3602. doi: 10.1073/pnas.0400326101

Diepold, A., Amstutz, M., Abel, S., Sorg, I., Jenal, U., and Cornelis, G. R. (2010). Deciphering the assembly of the Yersinia type III secretion injectisome. *EMBO J.* 29, 1928–1940. doi: 10.1038/emboj.2010.84

Diepold, A., and Wagner, S. (2014). Assembly of the bacterial type III secretion machinery. *FEMS Microbiol. Rev.* 38, 802–822. doi: 10.1111/1574-6976.12061

Diepold, A., Wiesand, U., and Cornelis, G. R. (2011). The assembly of the export apparatus (YscR. S, T, U, V) of the Yersinia type III secretion apparatus occurs independently of other structural components and involves the formation of an YscV oligomer*Mol. Microbiol.* 82, 502–514. doi: 10.1111/j.1365-2958.2011.07830.x

Druar, C., Yu, F., Barnes, J. L., Okinaka, R. T., Chantratita, N., Beg, S., et al. (2008). Evaluating *Burkholderia pseudomallei* Bip proteins as vaccines and Bip antibodies as detection agents. *FEMS Immunol. Med. Microbiol.* 52, 78–87. doi: 10.1111/j.1574-695X.2007.00345.x

Du, J., Reeves, A. Z., Klein, J. A., Twedt, D. J., Knodler, L. A., and Lesser, C. F. (2016). The type III secretion system apparatus determines the intracellular niche of bacterial pathogens.. *Proc. Natl. Acad. Sci. U.S.A.* 113, 4794–4799. doi: 10.1073/pnas.1520699113

Egan, F., Barret, M., and O'Gara, F. (2014). The SPI-1-like Type III secretion system: more roles than you think.. *Front. Plant Sci.* 5:34. doi: 10.3389/fpls.2014.00034

Ehrbar, K., Friebel, A., Miller, S. I., and Hardt, W.-D. (2003). Role of the Salmonella pathogenicity island 1 (SPI-1) protein InvB in type III secretion of SopE and SopE2, two Salmonella effector proteins encoded outside of SPI-1. *J. Bacteriol.* 185, 6950–6967. doi: 10.1128/JB.185.23.6950-6967.2003

Ehrbar, K., Hapfelmeier, S., Stecher, B., andHardt, W.-D. (2004). InvB is required for type III-dependent secretion of SopA in *Salmonella enterica* serovar Typhimurium. *J. Bacteriol.* 186, 1215–1219. doi: 10.1128/JB.186.4.1215-1219.2004

Ehrbar, K., Winnen, B., and Hardt, W.-D. (2006). The chaperone binding domain of SopE inhibits transport via flagellar and SPI-1 TTSS in the absence of InvB. *Mol. Microbiol.* 59, 248–264. doi: 10.1111/j.1365-2958.2005.04931.x

Epler, C. R., Dickenson, N. E., Olive, A. J., Picking, W. L., and Picking, W. D. (2009). Liposomes recruit IpaC to the *Shigella flexneri* type III secretion apparatus needle as a final step in secretion induction. *Infect. Immun.* 77, 2754–2761. doi: 10.1128/IAI.00190-09

Erhardt, M., Mertens, M. E., Fabiani, F. D., and Hughes, K. T. (2014). ATPase-independent type-III protein secretion in *Salmonella enterica*. *PLoS Genet.* 10:e1004800. doi: 10.1371/journal.pgen.1004800

Erskine, P. T., Knight, M. J., Ruaux, A., Mikolajek, H., Sang, N. W. F., Withers, J., et al. (2006). High resolution structure of BipD: an invasion protein associated with the type III secretion system of *Burkholderia pseudomallei*. *J. Mol. Biol.* 363, 125–136. doi: 10.1016/j.jmb.2006.07.069

Espina, M., Ausar, S. F., Middaugh, C. R., Baxter, M. A., Picking, W. D., and Picking, W. L. (2007). Conformational stability and differential structural analysis of LcrV, PcrV, BipD, and SipD from type III secretion systems. *Protein Sci.* 16, 704–714. doi: 10.1110/ps.062645007

Espina, M., Olive, A. J., Kenjale, R., Moore, D. S., Ausar, S. F., Kaminski, R. W., et al. (2006). IpaD localizes to the tip of the type III secretion system needle of *Shigella flexneri*. *Infect. Immun.* 74, 4391–4400. doi: 10.1128/IAI.00440-06

Forsberg, Å., Viitanen, A.-M., Skurnik, M., and Wolf-Watz, H. (1991). The surface-located YopN protein is involved in calcium signal transduction in *Yersinia pseudotuberculosis*. *Mol. Microbiol.* 5, 977–986. doi: 10.1111/j.1365-2958.1991.tb00773.x

French, C. T., Toesca, I. J., Wu, T.-H., Teslaa, T., Beaty, S. M., Wong, W., et al. (2011). Dissection of the Burkholderia intracellular life cycle using a photothermal nanoblade. *Proc. Natl. Acad. Sci. U.S.A.* 108, 12095–12100. doi: 10.1073/pnas.1107183108

Frithz-Lindsten, E., Rosqvist, R., Johansson, L., and Forsberg, Å. (1995). The chaperone-like protein YerA of *Yersinia pseudotuberculosis* stabilizes YopE in the cytoplasm but is dispensable for targeting to the secretion loci. *Mol. Microbiol.* 16, 635–647. doi: 10.1111/j.1365-2958.1995.tb02426.x

Fu, Y., and Galán, J. E. (1998). Identification of a specific chaperone for SptP, a substrate of the centisome 63 type III secretion system of *Salmonella typhimurium*. *J. Bacteriol.* 180, 3393–3399.

Galán, J. E. (2009). Common themes in the design and function of bacterial effectors. *Cell Host Microbe* 5, 571–579. doi: 10.1016/j.chom.2009.04.008

Galán, J. E., and Curtiss, R. (1989). Cloning and molecular characterization of genes whose products allow *Salmonella Typhimurium* to penetrate tissue culture cells. *Proc. Natl. Acad. Sci. U.S.A.* 86, 6383–6387. doi: 10.1073/pnas.86.16.6383

Galán,. J. E., Lara-Tejero, M., Marlovits, T. C., and Wagner, S. (2014). Bacterial type III secretion systems: specialized nanomachines for protein delivery into target cells. *Annu. Rev. Microbiol.* 68:415. doi: 10.1146/annurev-micro-092412-155725

Gemski, P., Lazere, J. R., Casey, T., and Wohlhieter, J. A. (1980). Presence of a virulence-associated plasmid in *Yersinia pseudotuberculosis*. *Infect. Immun.* 28, 1044–1047.

Gong, L., Cullinane, M., Treerat, P., Ramm, G., Prescott, M., Adler, B., et al. (2011). The *Burkholderia pseudomallei* type III secretion system and BopA are required for evasion of LC3-associated phagocytosis. *PLoS ONE* 6:e17852. doi: 10.1371/journal.pone.0017852

Gong, L., Lai, S.-C., Treerat, P., Prescott, M., Adler, B., Boyce, J. D., et al. (2015). *Burkholderia pseudomallei* Type III secretion system cluster 3 ATPase BsaS, a chemotherapeutic Target for Small-Molecule ATPase Inhibitors. *Infect. Immun.* 83, 1276–1285. doi: 10.1128/IAI.03070-14

Gophna, U., Ron, E. Z., and Graur, D. (2003). Bacterial type III secretion systems are ancient and evolved by multiple horizontal-transfer events. *Gene* 312, 151–163. doi: 10.1016/S0378-1119(03)00612-7

Gutierrez, M. G., Pfeffer, T. L., and Warawa, J. M. (2015a). Type 3 secretion system cluster 3 is a critical virulence determinant for lung-specific melioidosis. *PLoS Negl. Trop. Dis.* 9:e3441. doi: 10.1371/journal.pntd.0003441

Gutierrez, M. G., Yoder-Himes, D. R., and Warawa, J. M. (2015b). Comprehensive identification of virulence factors required for respiratory melioidosis using Tn-seq mutagenesis. *Front. Cell. Infect. Microbiol.* 5:78. doi: 10.3389/fcimb.2015.00078

Haque, A., Chu, K., Easton, A., Stevens, M. P., Galyov, E. E., Atkins, T., et al. (2006). A live experimental vaccine against *Burkholderia pseudomallei* Elicits CD4+ T Cell–Mediated Immunity. Priming T Cells Specific for 2 Type III Secretion System Proteins. *J. Infect. Dis.* 194, 1241-1248. doi: 10.1086/508217

Haraga, A., West, T. E., Brittnacher, M. J., Skerrett, S. J., and Miller, S. I. (2008). *Burkholderia thailandensis* as a model system for the study of the virulence-associated type III secretion system of *Burkholderia pseudomallei*. *Infect. Immun.* 76, 5402–5411. doi: 10.1128/IAI.00626-08

Hardt, W.-D., Chen, L.-M., Schuebel, K. E., Bustelo, X. R., and Galán, J. E. (1998). *S. Typhimurium* encodes an activator of Rho GTPases that induces membrane ruffling and nuclear responses in host cells. *Cell* 93, 815–826. doi: 10.1016/S0092-8674(00)81442-7

Hayward, R. D., Cain, R. J., McGhie, E. J., Phillips, N., Garner, M. J., and Koronakis, V. (2005). Cholesterol binding by the bacterial type III translocon is essential for virulence effector delivery into mammalian cells. *Mol. Microbiol.* 56, 590–603. doi: 10.1111/j.1365-2958.2005.04568.x

Hayward, R. D., and Koronakis, V. (1999). Direct nucleation and bundling of actin by the SipC protein of invasive Salmonella. *EMBO J.* 18, 4926–4934. doi: 10.1093/emboj/18.18.4926

Heine, S. J., Diaz-McNair, J., Martinez-Becerra, F. J., Choudhari, S. P., Clements, J. D., Picking, W. L., et al. (2013). Evaluation of immunogenicity and protective efficacy of orally delivered Shigella type III secretion system proteins IpaB and IpaD. *Vaccine* 31, 2919–2929. doi: 10.1016/j.vaccine.2013.04.045

Hemrajani, C., Berger, C. N., Robinson, K. S., Marchès, O., Mousnier, A., and Frankel, G. (2010). NleH effectors interact with Bax inhibitor-1 to block apoptosis during enteropathogenic *Escherichia coli* infection. *Proc. Natl. Acad. Sci. U.S.A.* 107, 3129–3134. doi: 10.1073/pnas.0911609106

Holden, M. T. G., Titball, R. W., Peacock, S. J., Cerdeño-Tárraga, A. M., Atkins, T., Crossman, L. C., et al. (2004). Genomic plasticity of the causative agent of melioidosis. *Burkholderia pseudomallei. Proc. Natil. Acad. Sci. U.S.A.* 101, 14240–14245. doi: 10.1073/pnas.0403302101

Hovis, K. M., Mojica, S., McDermott, J. E., Pedersen, L., Simhi, C., Rank, R. G., et al. (2013). Genus-optimized strategy for the identification of Chlamydial type III secretion substrates. *Pathog. Dis.* 69, 213–222. doi: 10.1111/2049-632X.12070

Hu, B., Lara-Tejero, M., Kong, Q., Galán, J. E., and Liu, J. (2017). *In situ* molecular architecture of the salmonella Type III secretion machine. *Cell* 168, 1065–1074. doi: 10.1016/j.cell.2017.02.022

Iriarte, M., Sory, M.-P., Boland, A., Boyd, A. P., Mills, S. D., Cornelis, G. R. et al. (1998). TyeA, a protein involved in control of Yop release and in translocation of Yersinia Yop effectors. *EMBO J.* 17, 1907–1918. doi: 10.1093/emboj/17.7.1907

Jarvis, K. G., Giron, J. A., Jerse, A. E., McDaniel, T. K., Donnenberg, M. S., and Kaper, J. B. (1995). Enteropathogenic *Escherichia coli* contains a putative type III secretion system necessary for the export of proteins involved in attaching and effacing lesion formation. *Proc. Natl. Acad. Sci. U.S.A.* 92, 7996–8000. doi: 10.1073/pnas.92.17.7996

Jitprasutwit, S., Thaewpia, W., Muangsombut, V., Lulitanond, A., Leelayuwat, C., Lertmemongkolchai, G., et al. (2010). Effect of acidic pH on the invasion efficiency and the type III secretion system of *Burkholderia thailandensis*. *J. Microbiol.* 48, 526–532. doi: 10.1007/s12275-010-0078-x

Johnson, S., Roversi, P., Espina, M., Olive, A., Deane, J. E., Birket, S., et al. (2007). Self-chaperoning of the type III secretion system needle tip proteins IpaD and BipD. *J. Biol. Chem.* 282, 4035–4044. doi: 10.1074/jbc.M607945200

Jones, A. L., Beveridge, T. J., and Woods, D. E. (1996). Intracellular survival of *Burkholderia pseudomallei*. *Infect. Immun.* 64, 782–790.

Kang, W. T., Vellasamy, K. M., Chua, E.-G., and Vadivelu, J. (2015). Functional characterizations of effector protein BipC, a type III secretion system protein, in *Burkholderia pseudomallei* pathogenesis. *J. Infect. Dis.* 211, 827–834. doi: 10.1093/infdis/jiu492

Kang, W. T., Vellasamy, K. M., Rajamani, L., Beuerman, R. W., and Vadivelu, J. (2016a). *Burkholderia pseudomallei* type III secreted protein BipC: role in actin modulation and translocation activities required for the bacterial intracellular lifecycle. *Peer J.* 4:e2532. doi: 10.7717/peerj.2532

Kang, W. T., Vellasamy, K. M., and Vadivelu, J. (2016b). Eukaryotic pathways targeted by the type III secretion system effector protein. BipC, involved in the intracellular lifecycle of Burkholderia pseudomallei. *Sci. Rep.* 6:33528. doi: 10.1038/srep33528

Kayath, C. A., Hussey, S., Nagra, K., Philpott, D., and Allaoui, A. (2010). Escape of intracellular Shigella from autophagy requires binding to

cholesterol through the type III effector, IcsB. *Microbes Infect.* 12, 956–966. doi: 10.1016/j.micinf.2010.06.006

Kim, J. S., Eom, J. S., Im Jang, J., Kim, H. G., Seo, D. W. Bang, I. S., et al (2011). Role of Salmonella pathogenicity island 1 protein IacP in *Salmonella enterica* serovar Typhimurium pathogenesis. *Infect. Immun.* 79, 1440–1450. doi: 10.1128/IAI.01231-10

Klein, J. A., Dave, B. M., Raphenya, A. R., McArthur, A. G., and Knodler, L. A. (2017). Functional relatedness in the Inv/Mxi-Spa type III secretion system family. *Mol. Microbiol.* 103, 973–991. doi: 10.1111/mmi.13602

Knight, M. J., Ruaux, A., Mikolajek, H., Erskine, P. T., Gill, R., Wood, S. P., et al. (2006). Crystallization and preliminary X-ray diffraction analysis of BipD, a virulence factor from *Burkholderia pseudomallei*. *Acta Crystallogr. Sect. F Struct. Biol. Cryst. Commun.* 62, 761–764. doi: 10.1107/S1744309106024857

Kresse, A. U., Beltrametti, F., Müller, A., Ebel, F., and Guzmán, C. A. (2000). Characterization of SepL of enterohemorrhagic *Escherichia coli*. *J. Bacteriol.* 182, 6490–6498. doi: 10.1128/JB.182.22.6490-6498.2000

Kubori, T., and Galán, J. E. (2002). Salmonella type III secretion-associated protein InvE controls translocation of effector proteins into host cells. *J. Bacteriol.* 184, 4699–4708. doi: 10.1128/JB.184.17.4699-4708.2002

Kubori, T., Matsushima, Y., Nakamura, D., Uralil, J., Lara-Tejero, M., Sukhan, A., et al. (1998). Supramolecular structure of the *Salmonella Typhimurium* type III protein secretion system. *Science* 280, 602–605. doi: 10.1126/science.280.5363.602

Kubori, T., Sukhan, A., Aizawa, S.-I., and Galán, J. E. (2000). Molecular characterization and assembly of the needle complex of the Salmonella Typhimurium type III protein secretion system. *Proc. Natl. Acad. Sci. U.S.A.* 97, 10225–10230. doi: 10.1073/pnas.170128997

Lafont, F., Tran Van Nhieu, G., Hanada, K., Sansonetti, P., and van der Goot, G. F. (2002). Initial steps of Shigella infection depend on the cholesterol/sphingolipid raft-mediated CD44–IpaB interaction. *EMBO J.* 21, 4449–4457. doi: 10.1093/emboj/cdf457

Lee, S. H., and Galán, J. E. (2003). InvB is a type III secretion-associated chaperone for the *Salmonella enterica* effector protein SopE. *J. Bacteriol.* 185, 7279–7284. doi: 10.1128/JB.185.24.7279-7284.2003

Lee, S. H., and Galán, J. E. (2004). Salmonella type III secretion-associated chaperones confer secretion-pathway specificity. *Mol. Microbiol.* 51, 483–495. doi: 10.1046/j.1365-2958.2003.03840.x

Lee, Y. H., Chen, Y., Ouyang, X., and Gan, Y.-H. (2010). Identification of tomato plant as a novel host model for *Burkholderia pseudomallei*. *BMC Microbiol.* 10:28. doi: 10.1186/1471-2180-10-28

Limmathurotsakul, D., Golding, N., Dance, D. A., Messina, J. P., Pigott, D. M., Moyes, C. L., et al. (2016). Predicted global distribution of *Burkholderia pseudomallei* and burden of melioidosis. *Nat. Microbiol.* 1:15008. doi: 10.1038/nmicrobiol.2015.8

Lipscomb, L., and Schell, M. A. (2011). Elucidation of the regulon and cis-acting regulatory element of HrpB, the AraC-type regulator of a plant pathogen-like type III secretion system in *Burkholderia pseudomallei*. *J. Bacteriol.* 193, 1991–2001. doi: 10.1128/jb.01379-10

Madan, R., Rastogi, R., Parashuraman, S., and Mukhopadhyay, A. (2012). *Salmonella acquires* lysosome-associated membrane protein 1 (LAMP1) on phagosomes from Golgi via SipC protein-mediated recruitment of host Syntaxin6. *J. Biol. Chem.* 287, 5574–5587. doi: 10.1074/jbc.M111.286120

Markham, A. P., Birket, S. E., Picking, W. D., Picking, W. L., and Middaugh, C. R. (2008). pH sensitivity of type III secretion system tip proteins. *Proteins* 71, 1830–1842. doi: 10.1002/prot.21864

Marlovits, T. C., Kubori, T., Sukhan, A., Thomas, D. R., Galán, J. E., and Unger, V. M. (2004). Structural insights into the assembly of the type III secretion needle complex. *Science* 306, 1040–1042. doi: 10.1126/science.1102610

Martinez-Becerra, F. J., Chen, X., Dickenson, N. E., Choudhari, S. P., Harrison, K., Clements, J. D., et al. (2013). Characterization of a novel fusion protein from IpaB and IpaD of Shigella sand its potential as a pan-Shigella vaccine. *Infect. Immun.* 81, 4470–4477. doi: 10.1128/IAI.00859-13

Martinez-Becerra, F. J., Kissmann, J. M., Diaz-McNair, J., Choudhari, S. P., Quick, A. M., Mellado-Sanchez, G., et al. (2012). Broadly protective Shigella vaccine based on type III secretion apparatus proteins. *Infect. Immun.* 80, 1222–1231. doi: 10.1128/IAI.06174-11

Maurelli, A. T., Baudry, B. H., d'Hauteville, H., Hale, T. L., and Sansonetti, P. J. (1985). Cloning of plasmid DNA sequences involved in invasion of HeLa cells by *Shigella flexneri*. *Infect. Immun.* 49, 164–171.

McGhie, E. J., Hayward, R. D., and Koronakis, V. (2001). Cooperation between actin-binding proteins of invasive Salmonella: SipA potentiates SipC nucleation and bundling of actin. *EMBO J.* 20, 2131–2139. doi: 10.1093/emboj/20.9.2131

Miao, E. A., Mao, D. P., Yudkovsky, N., Bonneau, R., Lorang, C. G., Warren, S. E., et al. (2010). Innate immune detection of the type III secretion apparatus through the NLRC4 inflammasome. *Proc. Natl. Acad. Sci. U.S.A.* 107, 3076–3080. doi: 10.1073/pnas.0913087107

Michiels, T., and Cornelis, G. R. (1991). Secretion of hybrid proteins by the Yersinia Yop export system. *J. Bacteriol.* 173, 1677–1685. doi: 10.1128/jb.173.5.1677-1685.1991

Moore, R. A., Reckseidler-Zenteno, S., Kim, H., Nierman, W., Yu, Y., Tuanyok, A., et al. (2004). Contribution of gene loss to the pathogenic evolution of *Burkholderia pseudomallei* and *Burkholderia mallei*. *Infect. Immun.* 72, 4172–4187. doi: 10.1128/IAI.72.7.4172-4187.2004

Muangman, S., Korbsrisate, S., Muangsombut, V., Srinon, V., Adler, N. L., Schroeder, G. N., et al. (2011). BopC is a type III secreted effector protein of *Burkholderia pseudomallei*. *FEMS Microbiol. Lett.* 323, 75–82. doi: 10.1111/j.1574-6968.2011.02359.x

Muangsombut, V., Suparak, S., Pumirat, P., Damnin, S., Vattanaviboon, P., Thongboonkerd, V., et al. (2008). Inactivation of *Burkholderia pseudomallei* bsaQ results in decreased invasion efficiency and delayed escape of bacteria from endocytic vesicles. *Arch. Microbiol.* 190, 623–631. doi: 10.1007/s00203-008-0413-3

Myeni, S. K., Wang, L., and Zhou, D. (2013). SipB-SipC complex is essential for translocon formation. *PLoS ONE* 8:e60499. doi: 10.1371/journal.pone.0060499

Myeni, S. K., and Zhou, D. (2010). The C terminus of SipC binds and bundles F-actin to promote Salmonella invasion. *J. Biol. Chem.* 285, 13357–13363. doi: 10.1074/jbc.M109.094045

Ng, M. Y., Wang, M., Casey, P. J., Gan, Y.-H., and Hagen, T. (2017). Activation of MAPK/ERK signaling by *Burkholderia pseudomallei* cycle inhibiting factor (Cif). *PLoS ONE* 12:e0171464. doi: 10.1371/journal.pone.0171464

Ngauy, V., Lemeshev, Y., Sadkowski, L., and Crawford, G. (2005). Cutaneous melioidosis in a man who was taken as a prisoner of war by the Japanese during World War II. *J. Clin. Microbiol.* 43, 970–972. doi: 10.1128/JCM.43.2.970-972.2005

Nougayrède, J.-P., Boury, M., Tasca, C., Marchès, O., Milon, A., Oswald, E., et al. (2001). Type III secretion-dependent cell cycle block caused in HeLa cells by enteropathogenic *Escherichia coli* O103. *Infect. Immun.* 69, 6785–6795. doi: 10.1128/IAI.69.11.6785-6795.2001

Olive, A. J., Kenjale, R., Espina, M., Moore, D. S., Picking, W. L., and Picking, W. D. (2007). Bile salts stimulate recruitment of IpaB to the *Shigella flexneri* surface, where it colocalizes with IpaD at the tip of the type III secretion needle. *Infect. Immun.* 75, 2626–2629. doi: 10.1128/IAI.01599-06

Osiecki, J. C., Barker, J., Picking, W. L., Serfis, A. B., Berring, E., Shah, S., et al. (2001). IpaC from Shigella and SipC from Salmonella possess similar biochemical properties but are functionally distinct. *Mol. Microbiol.* 42, 469–481. doi: 10.1046/j.1365-2958.2001.02654.x

Pal, M., Erskine, P. T., Gill, R. S., Wood, S. P., and Cooper, J. B. (2010). Near-atomic resolution analysis of BipD, a component of the type III secretion system of *Burkholderia pseudomallei*. *Acta Crystallogr. Sect. F Struct. Biol. Cryst. Commun.* 66, 990–993. doi: 10.1107/S1744309110026333

Pallett, M. A., Berger, C. N., Pearson, J. S., Hartland, E. L., and Frankel, G. (2014). The type III secretion effector NleF of enteropathogenic *Escherichia coli* activates NF-$\kappa$B early during infection. *Infect. Immun.* 82, 4878–4888. doi: 10.1128/IAI.02131-14

Panina, E. M., Mattoo, S., Griffith, N., Kozak, N. A., Yuk, M. H., and Miller, J. F. (2005). A genome-wide screen identifies a Bordetella type III secretion effector and candidate effectors in other species. *Mol. Microbiol.* 58, 267–279. doi: 10.1111/j.1365-2958.2005.04823.x

Parsot, C., Ménard, R., Gounon, P., and Sansonetti, P. J. (1995). Enhanced secretion through the *Shigella flexneri* Mxi-Spa translocon leads to assembly of extracellular proteins into macromolecular structures. *Mol. Microbiol.* 16, 291–300. doi: 10.1111/j.1365-2958.1995.tb02301.x

Paul, K., Erhardt, M., Hirano, T., Blair, D. F., and Hughes, K. T. (2008). Energy source of flagellar type III secretion. *Nature* 451, 489–492. doi: 10.1038/nature06497

Pearson, T., Giffard, P., Beckstrom-Sternberg, S., Auerbach, R., Hornstra, H., Tuanyok, A., et al. (2009). Phylogeographic reconstruction of a bacterial species with high levels of lateral gene transfer. *BMC Biol.* 7:78. doi: 10.1186/1741-7007-7-78

Pei, J., and Grishin, N. V. (2009). The Rho GTPase inactivation domain in *Vibrio cholerae* MARTX toxin has a circularly permuted papain-like thiol protease fold. *Proteins* 77, 413–419. doi: 10.1002/prot.22447

Persson, C., Carballeira, N., Wolf-Watz, H., and Fällman, M. (1997). The PTPase YopH inhibits uptake of Yersinia, tyrosine phosphorylation of p130Cas and FAK, and the associated accumulation of these proteins in peripheral focal adhesions. *EMBO J.* 16, 2307–2318. doi: 10.1093/emboj/16.9.2307

Picking, W. L., Nishioka, H., Hearn, P. D., Baxter, M. A., Harrington, A. T., Blocker, A., et al. (2005). IpaD of *Shigella flexneri* is independently required for regulation of Ipa protein secretion and efficient insertion of IpaB and IpaC into host membranes. *Infect. Immun.* 73, 1432–1440. doi: 10.1128/IAI.73.3.1432-1440.2005

Pilatz, S., Breitbach, K., Hein, N., Fehlhaber, B., Schulze, J., Brenneke, B., et al. (2006). Identification of *Burkholderia pseudomallei* genes required for the intracellular life cycle and *in vivo* virulence. *Infect. Immun.* 74, 3576–3586. doi: 10.1128/IAI.01262-05

Pruksachartvuthi, S., Aswapokee, N., and Thankerngpol, K. (1990). Survival of *Pseudomonas pseudomallei* in human phagocytes. *J. Med. Microbiol.* 31, 109–114. doi: 10.1099/00222615-31-2-109

Pumirat, P., Vander Broek, C., Juntawieng, N., Muangsombut, V., Kiratisin, P., Pattanapanyasat, K., et al. (2014). Analysis of the prevalence, secretion and function of a cell cycle-inhibiting factor in the melioidosis pathogen *Burkholderia pseudomallei*. *PLoS ONE* 9:e96298. doi: 10.1371/journal.pone.0096298

Radics, J., Königsmaier, L., and Marlovits, T. C. (2014). Structure of a pathogenic type 3 secretion system in action. *Nat. Struct. Mol. Biol.* 21, 82–87. doi: 10.1038/nsmb.2722

Rainbow, L., Hart, C. A., and Winstanley, C. (2002). Distribution of type III secretion gene clusters in *Burkholderia pseudomallei*. *B. thailandensis* and *B. mallei*. *J. Med. Microbiol.* 51, 374–384. doi: 10.1099/0022-1317-51-5-374

Roehrich, A. D., Bordignon, E., Mode, S., Shen, D.-K., Liu, X., Blocker, A. J. et al. (2016). Steps for Shigella Gatekeeper MxiC Function in Hierarchical Type III Secretion Regulation. *J. Biol. Chem.* 292, 1705–1723. doi: 10.1074/jbc.M116.746826

Roehrich, A. D., Guillossou, E., Blocker, A. J., and Martinez-Argudo, I. (2013). Shigella IpaD has a dual role: signal transduction from the type III secretion system needle tip and intracellular secretion regulation. *Mol. Microbiol.* 87, 690–706. doi: 10.1111/mmi.12124

Rossier, O., Wengelnik, K., Hahn, K., and Bonas, U. (1999). The Xanthomonas Hrp type III system secretes proteins from plant and mammalian bacterial pathogens. *Proc. Natl. Acad. Sci. U.S.A.* 96, 9368–9373. doi: 10.1073/pnas.96.16.9368

Rotz, L. D., Khan, A. S., Lillibridge, S. R., Ostroff, S. M., and Hughes, J. M. (2002). Public health assessment of potential biological terrorism agents. *Emerg. Infect. Dis.* 8, 225–230. doi: 10.3201/eid0802.010164

Roversi, P., Johnson, S., Field, T., Deane, J. E., Galyov, E. E., and Lea, S. M. (2006). Expression, purification, crystallization and preliminary crystallographic analysis of BipD, a component of the *Burkholderia pseudomallei* type III secretion system. *Acta Crystallogr. Sect. F Struct. Biol. Cryst. Commun.* 62, 861–864. doi: 10.1107/S1744309106027035

Sato, H., Frank, D. W., Hillard, C. J., Feix, J. B., Pankhaniya, R. R., Moriyama, K., et al. (2003). The mechanism of action of the *Pseudomonas aeruginosa*-encoded type III cytotoxin, ExoU. *EMBO J.* 22, 2959–2969. doi: 10.1093/emboj/cdg290

Schesser, K., Frithz-Lindsten, E., and Wolf-Watz, H. (1996). Delineation and mutational analysis of the *Yersinia pseudotuberculosis* YopE domains which mediate translocation across bacterial and eukaryotic cellular membranes. *J. Bacteriol.* 178, 7227–7233. doi: 10.1128/jb.178.24.7227-7233.1996

Schraidt, O., and Marlovits, T. C. (2011). Three-dimensional model of Salmonella's needle complex at subnanometer resolution. *Science* 331, 1192–1195. doi: 10.1126/science.1199358

Sim, S. H., Yu, Y., Lin, C. H., Karuturi, R. K., Wuthiekanun, V., Tuanyok, A., et al. (2008). The core and accessory genomes of *Burkholderia pseudomallei*: implications for human melioidosis. *PLoS Pathog.* 4:e1000178. doi: 10.1371/journal.ppat.1000178

Smith, M. D., Angus, B. J., Wuthiekanun, V., and White, N. J. (1997). Arabinose assimilation defines a nonvirulent biotype of *Burkholderia pseudomallei*. *Infect. Immun.* 65, 4319–4321.

Sory, M.-P., Boland, A., Lambermont, I., and Cornelis, G. R. (1995). Identification of the YopE and YopH domains required for secretion and internalization into the cytosol of macrophages, using the cyaA gene fusion approach. *Proc. Natl. Acad. Sci. U.S.A.* 92, 11998–12002.

Srinivasan, A., Kraus, C. N., DeShazer, D., Becker, P. M., Dick, J. D., Spacek, L., et al. (2001). Glanders in a military research microbiologist. *N. Engl. J. Med.* 345, 256–258. doi: 10.1056/NEJM200107263450404

Srinon, V., Muangman, S., Imyaem, N., Muangsombut, V. L. A., Adler, N. R., Galyov, E. E., et al. (2013). Comparative assessment of the intracellular survival of the *Burkholderia pseudomallei* bopC mutant. *J. Microbiol.* 51, 522–526. doi: 10.1007/s12275-013-2557-3

Stebbins, C. E., and Galán, J. E. (2001). Maintenance of an unfolded polypeptide by a cognate chaperone in bacterial type III secretion. *Nature* 414, 77–81. doi: 10.1038/35102073

Stensrud, K. F., Adam, P. R., La Mar, C. D., Olive, A. J., Lushington, G. H., Sudharsan, R., et al. (2008). Deoxycholate interacts with IpaD of Shigella flexneri in inducing the recruitment of IpaB to the type III secretion apparatus needle tip. *J. Biol. Chem.* 283, 18646–18654. doi: 10.1074/jbc.M802799200

Stevens, M. P., Friebel, A., Taylor, L. A., Wood, M. W., Brown, P. J., Galyov, E. E. et al. (2003). A Burkholderia pseudomallei type III secreted protein. BopE, facilitates bacterial invasion of epithelial cells and exhibits guanine nucleotide exchange factor activity. *J. Bacteriol.* 185, 4992–4996. doi: 10.1128/JB.185.16.4992-4996.2003

Stevens, M. P., Haque, A., Atkins, T., Hill, J., Wood, M. W., Easton, A., et al. (2004). Attenuated virulence and protective efficacy of a *Burkholderia pseudomallei* bsa type III secretion mutant in murine models of melioidosis. *Microbiology* 150, 2669–2676. doi: 10.1099/mic.0.27146-0

Stevens, M. P., Wood, M. W., Taylor, L. A., Monaghan, P., Hawes, P., Jones, P. W., et al. (2002). An Inv/Mxi-Spa-like type III protein secretion system in *Burkholderia pseudomallei* modulates intracellular behaviour of the pathogen. *Mol. Microbiol.* 46, 649–659. doi: 10.1046/j.1365-2958.2002.03190.x

Sun, G. W., Chen, Y., Liu, Y., Tan, G.-Y., Ong, C., Gan, H., et al. (2010). Identification of a regulatory cascade controlling Type III Secretion System 3 gene expression in *Burkholderia pseudomallei*. *Mol. Microbiol.* 76, 677–689. doi: 10.1111/j.1365-2958.2010.07124.x

Sun, G. W., Lu, J., Pervaiz, S., Cao, W. P., and Gan, Y.-H. (2005). Caspase-1 dependent macrophage death induced by *Burkholderia pseudomallei*. *Cell. Microbiol.* 7, 1447–1458. doi: 10.1111/j.1462-5822.2005.00569.x

Suparak, S., Kespichayawattana, W., Haque, A., Easton, A., Damnin, S., Lertmemongkolchai, G., et al. (2005). Multinucleated giant cell formation and apoptosis in infected host cells is mediated by *Burkholderia pseudomallei* type III secretion protein BipB. *J. Bacteriol.* 187, 6556–6560. doi: 10.1128/JB.187.18.6556-6560.2005

Teh, B. E., French, C. T., Chen, Y., Chen, I. G. J., Wu, T.-H., Gan, H., et al. (2014). Type three secretion system-mediated escape of *Burkholderia pseudomallei* into the host cytosol is critical for the activation of NF$\kappa$B. *BMC Microbiol.* 14:115. doi: 10.1186/1471-2180-14-115

Tippayawat, P., Pinsiri, M., Rinchai, D., Riyapa, D., Romphruk, A., Gan, Y. H., et al. (2011). *Burkholderia pseudomallei* proteins presented by monocyte-derived dendritic cells stimulate human memory T cells *in vitro*. *Infect. Immun.* 79, 305–313. doi: 10.1128/IAI.00803-10

Tippayawat, P., Saenwongsa, W., Mahawantung, J., Suwannasaen, D., Chetchotisakd, P., Limmathurotsakul, D., et al. (2009). Phenotypic and functional characterization of human memory T cell responses to *Burkholderia pseudomallei*. *PLoS Negl. Trop. Dis.* 3:e407. doi: 10.1371/journal.pntd.0000407

Treerat, P., Alwis, P., D'Cruze, T., Cullinane, M., Vadivelu, J., Devenish, R. J., et al. (2015). The *Burkholderia pseudomallei* Proteins BapA and BapC Are Secreted TTSS3 Effectors and BapB levels modulate expression of Bop. *PLoS ONE* 10:e0143916. doi: 10.1371/journal.pone.0143916

Tuanyok, A., Leadem, B. R., Auerbach, R. K., Beckstrom-Sternberg, S. M., Beckstrom-Sternberg, J. S., Mayo, M., et al. (2008). Genomic islands

from five strains of *Burkholderia pseudomallei*. *BMC Genomics* 9:566. doi: 10.1186/1471-2164-9-566

Tucker, S. C., and Galán, J. E. (2000). omplex function for SicA, a *Salmonella enterica* serovar typhimurium type III secretion-associated chaperone. *J. Bacteriol.* 182, 2262–2268. doi: 10.1128/JB.182.8.2262-2268.2000

Upadhyay, A., Wu, H., Williams, C., Field, T., Galyov, E. J., et al. (2008). The guanine-nucleotide-exchange factor BopE from *Burkholderia pseudomallei* adopts a compact version of the Salmonella SopE/SopE2 fold and undergoes a closed-to-open conformational change upon interaction with Cdc42. *Biochem. J.* 411, 485–493. doi: 10.1042/BJ20071546

Vander Broek, C. W., Chalmers, K. J., Stevens, M. P., and Stevens, J. M. (2015). Quantitative Proteomic analysis of *Burkholderia pseudomallei* Bsa Type III secretion system effectors using hypersecreting mutants. *Mol. Cell. Proteomics* 14, 905–916. doi: 10.1074/mcp.M114.044875

Van Zandt, K. E., Greer, M. T., and Gelhaus, H. C. (2013). Glanders: an overview of infection in humans. *Orphanet J. Rare Dis.* 8, 131. doi: 10.1186/1750-1172-8-131

Wagner, S., Königsmaier, L., Lara-Tejero, M., Lefebre, M., Marlovits, T. C., and Galán, J. E. (2010). Organization and coordinated assembly of the type III secretion export apparatus. *Proc. Natl. Acad. Sci. U.S.A.* 107, 17745–17750. doi: 10.1073/pnas.1008053107

Wang, Y., Ouellette, A. N., Egan, C. W., Rathinavelan, T., Im, W., and Da Guzman, R. N. (2007). Differences in the electrostatic surfaces of the type III secretion needle proteins PrgI, BsaL, and MxiH. *J. Mol. Biol.* 371, 1304–1314. doi: 10.1016/j.jmb.2007.06.034

Warawa, J., and Woods, D. E. (2005). Type III secretion system cluster 3 is required for maximal virulence of *Burkholderia pseudomallei* in a hamster infection model. *FEMS Microbiol. Lett.* 242, 101–108. doi: 10.1016/j.femsle.2004.10.045

Warren, S. M., and Young, G. M. (2005). An amino-terminal secretion signal is required for YplA export by the Ysa, Ysc, and flagellar type III secretion systems of *Yersinia enterocolitica* biovar 1B. *J. Bacteriol.* 187, 6075–6083. doi: 10.1128/JB.187.17.6075-6083.2005

West, T. E., Myers, N. D., Chantratita, N., Chierakul, W., Limmathurotsakul, D., Wuthiekanun, V., et al. (2014). NLRC4 and TLR5 each contribute to host defense in respiratory melioidosis. *PLoS Negl. Trop. Dis.* 8:e3178. doi: 10.1371/journal.pntd.0003178

Whitlock, G. C., Deeraksa, A., Qazi, O., Judy, B. M., Taylor, K., Propst, K. L., et al. (2010). Protective response to subunit vaccination against intranasal *Burkholderia mallei* and *B. pseudomallei* challenge. *Procedia Vaccinol.* 2, 73–77. doi: 10.1016/j.provac.2010.03.013

Whitlock,. G. C., Estes, D. M., Young, G. M., Young, B., and Torres, A. G. (2008). Construction of a reporter system to study *Burkholderia mallei* type III secretion and identification of the BopA effector protein function in intracellular survival. *Trans. R. Soc. Trop. Med. Hyg.* 102, S127–S133. doi: 10.1016/S0035-9203(08)70029-4

Whitlock, G. C., Valbuena, G. A., Popov, V. L., Judy, B. M., Estes, D. M., and Torres, A. G. (2009). *Burkholderia mallei* cellular interactions in a respiratory cell model. *J. Med. Microbiol.* 58, 554–562. doi: 10.1099/jmm.0.007724-0

Whitmore, A. (1913). An account of a glanders-like disease occurring in Rangoon. *J. Hyg.* 13, 1–34. doi: 10.1017/S0022172400005234

Wilharm, G., Lehmann, V., Krauss, K., Lehnert, B., Richter, S., Ruckdeschel, K., et al. (2004). *Yersinia enterocolitica* type III secretion depends on the proton motive force but not on the flagellar motor components MotA and MotB. *Infect. Immun.* 72, 4004–4009. doi: 10.1128/IAI.72.7.4004-4009.2004

Williamson, E. D. (2009). Plague. *Vaccine* 27, D56–D60. doi: 10.1016/j.vaccine.2009.07.068

Winstanley, C., Hales, B. A., and Hart, C. A. (1999). Evidence for the presence in *Burkholderia pseudomallei* of a type III secretion system-associated gene cluster. *J. Med. Microbiol.* 48, 649–656. doi: 10.1099/00222615-48-7-649

Yabuuchi, E., Kosako, Y., Oyaizu, H., Yano, I., Hotta, H., Hashimoto, Y., et al. (1992). Proposal of *Burkholderia gen*. nov. and transfer of seven species of the genus *Pseudomonas homology* group II to the new genus, with the type species *Burkholderia cepacia* (Palleroni and Holmes 1981) comb. nov. *Microbiol. Immunol.* 36, 1251–1275. doi: 10.1111/j.1348-0421.1992.tb02129.x

Yang, J., Zhao, Y., Shi, J., and Shao, F. (2013). Human NAIP and mouse NAIP1 recognize bacterial type III secretion needle protein for inflammasome activation. *Proc. Natl. Acad. Sci. U.S.A.* 110, 14408–14413. doi: 10.1073/pnas.1306376110

Young, B. M., and Young, G. M. (2002). YplA is exported by the Ysc, Ysa, and flagellar type III secretion systems of *Yersinia enterocolitica*. *J. Bacteriol.* 184, 1324–1334. doi: 10.1128/JB.184.5.1324-1334.2002

Young, G. M., Schmiel, D. H., and Miller, V. L. (1999). A new pathway for the secretion of virulence factors by bacteria: the flagellar export apparatus functions as a protein-secretion system. *Proc. Natl. Acad. Sci. U.S.A.* 96, 6456–6461. doi: 10.1073/pnas.96.11.6456

Yu, Y., Kim, H. S., Chua, H. H., Lin, C. H., Sim, S. H., Lin, D., et al. (2006). Genomic patterns of pathogen evolution revealed by comparison of *Burkholderia pseudomallei*, the causative agent of melioidosis, to avirulent *Burkholderia thailandensis*. *BMC Microbiol.* 6:46. doi: 10.1186/1471-2180-6-46

Zahrl, D., Wagner, M., Bischof, K., Bayer, M., Zavecz, B., Beranek, A., et al. (2005). Peptidoglycan degradation by specialized lytic transglycosylases associated with type III and type IV secretion systems. *Microbiology* 151, 3455–3467. doi: 10.1099/mic.0.28141-0

Zarivach, R., Deng, W., Vuckovic, M., Felise, H. B., Nguyen, H. V., Miller, S. I., et al. (2008). Structural analysis of the essential self-cleaving type III secretion proteins EscU and SpaS. *Nature* 453, 124–127. doi: 10.1038/nature06832

Zhang, L., Wang, Y., Picking, W. L., Picking, W. D., and Da Guzman, R. N. (2006). Solution structure of monomeric BsaL, the type III secretion needle protein of *Burkholderia pseudomallei*. *J. Mol. Biol.* 359, 322–330. doi: 10.1016/j.jmb.2006.03.028

Zhao, Y., Yang, J., Shi, J., Gong, Y.-N., Lu, Q., Xu, H., et al. (2011). The NLRC4 inflammasome receptors for bacterial flagellin and type III secretion apparatus. *Nature* 477, 596–600. doi: 10.1038/nature10510

Zhou, Y., Dong, N., Hu, L., and Shao, F. (2013). The Shigella type three secretion system effector OspG directly and specifically binds to host ubiquitin for activation. *PLoS ONE* 8:e57558. doi: 10.1371/journal.pone.0057558

**Conflict of Interest Statement:** The authors declare that the research was conducted in the absence of any commercial or financial relationships that could be construed as a potential conflict of interest.

frontiers in Cellular and Infection Microbiology

REVIEW
published: 15 June 2017
doi: 10.3389/fcimb.2017.00254

# Type VI Secretion Effectors: Methodologies and Biology

*Yun-Wei Lien*[1,2] *and Erh-Min Lai*[1,2]*

[1] Institute of Plant and Microbial Biology, Academia Sinica, Taipei, Taiwan, [2] Department of Plant Pathology and Microbiology, National Taiwan University, Taipei, Taiwan

The type VI secretion system (T6SS) is a nanomachine deployed by many Gram-negative bacteria as a weapon against eukaryotic hosts or prokaryotic competitors. It assembles into a bacteriophage tail-like structure that can transport effector proteins into the environment or target cells for competitive survival or pathogenesis. T6SS effectors have been identified by a variety of approaches, including knowledge/hypothesis-dependent and discovery-driven approaches. Here, we review and discuss the methods that have been used to identify T6SS effectors and the biological and biochemical functions of known effectors. On the basis of the nature and transport mechanisms of T6SS effectors, we further propose potential strategies that may be applicable to identify new T6SS effectors.

**Keywords: type VI secretion system, methodology, effector, toxin-immunity, proteomics, bioinformatics, library, protein-protein interaction**

OPEN ACCESS

***Edited by:***
*Sophie Bleves,*
*Aix-Marseille University, France*

***Reviewed by:***
*Dor Salomon,*
*Tel Aviv University, Israel*
*Tao Dong,*
*University of Calgary, Canada*
*Abdelrahim Zoued,*
*Harvard Medical School, United States*

***Correspondence:**
*Erh-Min Lai*
*emlai@gate.sinica.edu.tw*

***Received:*** *30 March 2017*
***Accepted:*** *31 May 2017*
***Published:*** *15 June 2017*

***Citation:***
*Lien Y-W and Lai E-M (2017) Type VI Secretion Effectors: Methodologies and Biology. Front. Cell. Infect. Microbiol. 7:254. doi: 10.3389/fcimb.2017.00254*

## INTRODUCTION

Cell-to-cell communication and interaction is a central theme for all life forms including single-cell organisms such as bacteria. Gram-negative bacteria have evolved a variety of protein secretion systems to export or import macromolecules across membranes for survival and fitness. The type VI secretion system (T6SS) is a versatile injection machine that can deliver effector molecules into the environment, eukaryotic hosts and prokaryotic competitors. The T6SS mainly functions in a contact-dependent manner to target bacterial competitors for interbacterial competition and eukaryotic hosts for pathogenesis (Durand et al., 2014; Russell et al., 2014a; Cianfanelli et al., 2016b). However, recent reports also suggested that some T6SS effectors may exert their functions extracellularly rather than inside target cells (Wang et al., 2015; Lin et al., 2017; Si et al., 2017).

Typically, the T6SS gene cluster encodes 13–14 conserved core components for machinery assembly and some less conserved accessory proteins and effectors related to T6SS regulation and biological functions (Records, 2011; Basler, 2015; Cianfanelli et al., 2016b). The system consists of a TssJLM (or TssLM) trans-membrane complex (Aschtgen et al., 2008; Ma et al., 2009, 2012; Felisberto-Rodrigues et al., 2011), which serves as a docking site for the TssEFGK baseplate complex (Brunet et al., 2015). TssA, a starfish-like dodecametic complex, connects the TssEFGK baseplate to the Hcp tube and TssBC sheath components for polymerization of this tail structure (Planamente et al., 2016; Zoued et al., 2016). TssB-TssC functions as a contractile sheath, which presumably wraps around the Hcp tube and dynamically propels the Hcp-VgrG puncturing device and associated T6SS effectors across bacterial membranes (Basler et al., 2012). After the firing action, ClpV AAA+ ATPase binds to the contracted TssBC outer sheath for disassembly into subunits, which can be recycled for the next T6SS assembly (Bonemann et al., 2009; Basler and Mekalanos, 2012). Furthermore, Hcp, VgrG, and associated effectors could be translocated into bacterial target cells and reused to assemble new T6SS machineries in target cells (Vettiger and Basler, 2016).

The T6SS has evolved multiple strategies for effector delivery. On the basis of the known effector transport mechanisms, effectors can be classified as "specialized" or "cargo" effectors (Cianfanelli et al., 2016b). Specialized effectors are fused to the C-terminus of T6SS structure proteins, such as Hcp, VgrG, or PAAR (Pro-Ala-Ala-Arg)-domain-containing protein known to sharpen the VgrG spike (Shneider et al., 2013). However, cargo effectors interact directly or require a specific chaperone or adaptor protein for loading onto the lumen of the Hcp tube or VgrG spike. T6SS adaptors/chaperones including DUF4123-, DUF1795-, and potentially DUF2169-containing proteins are required for loading a specific effector onto the cognate VgrG for delivery (Alcoforado Diniz and Coulthurst, 2015; Liang et al., 2015; Unterweger et al., 2015, 2016; Whitney et al., 2015; Bondage et al., 2016; Cianfanelli et al., 2016a). The DUF4123-containing protein functioning as a chaperone/adaptor was identified in the two studies in *Vibrio cholerae* with biochemical evidence showing its interaction with cognate VgrG (VgrG-1) and T6SS effector (TseL) by co-immunoprecipitation and bacterial two-hybrid analysis as well as genetic evidence for its requirement in mediating TseL secretion and TseL-mediated antibacterial activity (Liang et al., 2015; Unterweger et al., 2015). Together with its similar characteristics (i.e., low molecular weight protein with low isoelectric point, pI ∼5) with chaperones in phages and the type III secretion system (T3SS), the DUF4123-containing protein was named the T6SS effector chaperone (TEC) (Liang et al., 2015). Its chaperone feature is consistent with previous observation of a DUF4123-containing protein, Atu4349 in stabilizing the Tde1 effector in *Agrobacterium tumefaciens* and forming a complex with Tde1 co-purified from *Escherichia coli* (Ma et al., 2014). However, because of its requirement for TseL binding to the VgrG-1 spike with no detectable effect on TseL stability, the DUF4123-containing protein was also named T6SS adaptor protein 1 (Tap-1) by considering its function as an adaptor for loading TseL to the VgrG-1 spike (Unterweger et al., 2015). Although Tap-1 can interact with VgrG-1 in the absence of TseL in *V. cholerae* (Unterweger et al., 2015), the *A. tumefaciens* Tap-1/TEC ortholog and Tde1 each cannot interact with its cognate VgrG (VgrG1) in the absence of each other, so the formation of this adaptor/chaperone-effector complex occurs before loading onto the VgrG spike (Bondage et al., 2016). The DUF1795-containing protein, named effector-associated gene (Eag), can specifically interact with the PAAR domain of the cognate effectors, which are stabilized by specific Eag proteins in *Serratia marcescens* and *Pseudomonas aeruginosa* (Alcoforado Diniz and Coulthurst, 2015; Whitney et al., 2015; Cianfanelli et al., 2016a). Furthermore, EagR1 and EagR2 each interact with the cognate Rhs effector with specificity (i.e., EagR1 binds to Rhs1 but not Rhs2 and vice versa) (Cianfanelli et al., 2016a). In the absence of Rhs2, EagR2 can no longer load onto its cognate VgrG spike (VirG2) (Cianfanelli et al., 2016a). These data strongly suggest that Eag functions as a chaperone perhaps with specificity for PAAR-containing effectors. Another putative chaperone family protein is the DUF2169-containing protein, which was first identified in *A. tumefaciens* Atu3641 for its role in stabilizing the PAAR-like DUF4150-containing Tde2 effector for Tde2-dependent antibacterial activity (Bondage et al., 2016). The widespread genetic linkage between DUF2169- and DUF4150/PAAR-containing genes in several T6SS$^+$ proteobacterial genomes also implies a specific interaction between the two domains DUF2169 and DUF4150/PAAR. Taken together, Tap-1/TEC, Eag, and perhaps DUF2169-containing protein mainly function for loading specific effectors onto the cognate VgrG spike for secretion, but different adaptors/chaperones may have subtle differences in their modes of action, which awaits further structural and biochemical studies to clarify.

T6SS effectors with diverse biochemical activities have been identified. The major functions include the membrane-, cell wall-, or nucleic acid-targeting antibacterial effectors and several eukaryote-targeting effectors with a variety of enzymatic activities (Russell et al., 2014a; Alcoforado Diniz et al., 2015). In addition to the effectors functioning inside target cells, a few recent examples also suggested that T6SS effectors may function extracellularly rather than inside target cells. These identified extracellular effectors mainly function to bind or facilitate metal ions for their uptake (Wang et al., 2015; Lin et al., 2017; Si et al., 2017).

T6SS is widespread in Gram-negative bacteria, which include free-living bacteria and pathogens/symbionts of plants or animals. However, the number of identified effectors remains limited, in part because the annotation based on the primary genomic sequence information is often insufficient to properly annotate the function of effector genes. Nevertheless, almost all identified effectors are encoded with genetic linkage to the *vgrG* or *hcp* locus in the T6SS main gene cluster(s) or orphan *vgrG/hcp* island (De Maayer et al., 2011; Ma et al., 2014; Shyntum et al., 2014; Liang et al., 2015; Salomon et al., 2015; Abby et al., 2016). Various approaches have been successfully used to identify T6SS effectors. In this review, we summarize past and current methods as well as proposed potential strategies for identifying T6SS effectors. We hope such information can facilitate the discovery of novel T6SS effectors and elucidate their biochemical activities and biological functions.

## PAST AND CURRENT METHODS FOR IDENTIFYING T6SS EFFECTORS

With the current knowledge of biochemical characteristics and transport mechanisms of T6SS effectors, T6SS effectors can be identified via both discovery-driven and knowledge/hypothesis-based methodologies. The methods used for identifying T6SS effectors are described as follows and summarized in **Table 1**, which also lists the pros and cons of these methods.

### Bioinformatics Analysis

Some VgrG and Hcp proteins belong to specialized effectors by bearing a C-terminal effector domain (Pukatzki et al., 2009; Jamet and Nassif, 2015; Cianfanelli et al., 2016b; Ma et al., 2017a). Thus, VgrG or Hcp proteins with an additional C-terminal extension region are promising effector candidates with dual structural and biological roles. VgrG proteins can be classified into two categories: the canonical VgrG with gp27-gp5 domains as a sole structure function and the

**TABLE 1 |** Summary of current and potential methods for discovery of T6SS effectors.

| Method | Advantages | Limitation / Disadvantages |
|---|---|---|
| **CURRENT METHOD** | | |
| Bioinformatics analysis | Fast and robust in predicting putative effector candidates without experimental work | Prior knowledge or hypothesis is required |
| Genetic analysis of T6SS-associated genes | Easier to conduct without large-scale omics analysis or library construction and screening | Can only reveal effectors in the T6SS gene cluster or *hcp/vgrG* island |
| Proteomics-based method | Revealing effectors without known features | Limited to identifying proteins with significant secretion *in vitro* or a known chaperone for stability |
| Mutant library screening | Revealing effectors without known features; linking the gene to certain phenotypes directly | May identify genes other than T6SS effectors but with the same phenotypes; requires a testable phenotype |
| **POTENTIAL METHOD** | | |
| Expression library | Revealing effectors without known features | Limited to identifying genes with cytosolic toxicity or screenable phenotype; may identify genes other than T6SS effectors |
| Protein–protein interactions | Revealing effectors interacting with known T6SS components | Limited to effectors with direct or tight interactions with bait protein; toxic protein may be harmful for the bacterial/yeast two-hybrid host |

evolved VgrG with a C-terminal extended region conferring an additional domain(s) (Pukatzki et al., 2007). Therefore, several evolved VgrG proteins are identified, such as *V. cholerae* VgrG-1 containing an actin-crosslinking domain for a role in pathogenesis (Pukatzki et al., 2007) and the C-terminus of *V. cholerae* VgrG-3 with peptidoglycan degradation capability functioning as an antibacterial effector (Brooks et al., 2013; Dong et al., 2013). Besides bearing effector functions in the C-terminal extension of these evolved VgrG proteins, in entero-aggregative *E. coli* (EAEC), the VgrG1 harbors a C-terminal extension carrying DUF2345 and transthyretin (TTR) domains that are responsible for Tle1 effector binding (Flaugnatti et al., 2016). Co-immunoprecipitation (co-IP) and bacterial two-hybrid experiments suggested that the C-terminal extension is necessary and sufficient for interacting with the Tle1 effector, with the TTR domain involved in direct interaction with Tle1, whereas DUF2345 is required to stabilize the VgrG1–Tle1 interaction. In contrast to the widespread presence of evolved VgrG proteins harboring putative effector domains or an effector-binding domain in β-Proteobacteria and γ-Proteobacteria (Pukatzki et al., 2007; Boyer et al., 2009), Hcp proteins with a C-terminal extension have been found only in Enterobacteriaceae (Ma et al., 2017a). Although the C-terminal extension of some Hcp proteins was predicted to be a toxic domain, found in *Salmonella* in 2009 (Blondel et al., 2009), several Hcp proteins with a diverse C-terminal toxic domain (Hcp-ET) including Hcp-ET1 with DNase activity were recently characterized to exhibit antibacterial activity in Shiga toxin-producing *E. coli* (Ma et al., 2017a).

Besides searching for evolved VgrG or Hcp-ET, the conserved domains residing in known effectors can also be used as a query to search for potential effectors with available genome sequences. Russell et al. identified an amidase superfamily of T6SS effectors by searching for amidase catalytic cysteine and histidine residues combined with other features of T6SS effectors in their genome (Russell et al., 2012). With similar approaches, T6SS phospholipase effectors have been identified by the existence of a conserved motif, GXSXG, HXKXXXXD (Russell et al., 2013), or GXSXG (Flaugnatti et al., 2016). T6SS peptidoglycan glycoside hydrolase effectors were also identified by searching for the lysozyme-like fold (Whitney et al., 2013). Although they were not entirely identified by bioinformatics search, several nuclease effectors with predicted or verified conserved domains, such as the HXXD catalytic site motif of *A. tumefaciens* Tde (Zhang et al., 2012; Ma et al., 2014), HNH endonuclease domain of *S. marcescens* Rhs2 (Alcoforado Diniz and Coulthurst, 2015) and *Dickeya dadantii* RhsB (Koskiniemi et al., 2013), can be used to identify new T6SS effectors in any $T6SS^+$ bacterial genome via bioinformatics tools.

T6SS effectors also possess motifs or domains related to functions involved in translocation or other structural functions rather than biochemical or biological activity. In 2012, Zhang et al. proposed that a bacterial toxin could be divided into three parts: an N-terminal trafficking associated region, a central region, and a C-terminal toxic region. Rearrangement hotspot (Rhs)/YD repeats are common features of a central region in a toxin protein transported by diverse mechanisms. However, the PAAR domain is mostly located at the N-terminus of a T6SS effector, although some of these domains are followed by an N-terminal extension region (Zhang et al., 2012; Shneider et al., 2013). Of note, some classes of PAAR-containing proteins also harbor an Rhs region and a TTR domain located at the C-terminal extension region (Zhang et al., 2012; Shneider et al., 2013). Because the TTR domain of VgrG1 protein in EAEC is necessary and sufficient for Tle1 effector binding (Flaugnatti et al., 2016), the TTR domain of some PAAR-containing proteins may function as a carrier for effectors as suggested (Shneider et al., 2013). Indeed, several T6SS effectors were identified to have these characteristics. *P. aeruginosa* Tse5/RhsP1 and RhsP2 are typical Rhs effectors (Hachani et al., 2014; Whitney et al., 2014), whereas *S. marcescens* Rhs1 and Rhs2 (Alcoforado Diniz and Coulthurst, 2015), *D. dadantii* RhsA and RhsB (Koskiniemi et al., 2013), and Rhs-CT in Shiga toxin-producing *E. coli* (Ma et al., 2017b) harbor both N-terminal PAAR and central Rhs domains. Many T6SS effectors are featured with an N-terminal

PAAR domain followed by a C-terminal effector domain. The examples are *P. aeruginosa* Tse6/PA0093 carrying the typical PAAR (Hachani et al., 2014; Whitney et al., 2014); *A. tumefaciens* Tde2 (Ma et al., 2014) and *P. aeruginosa* PA0099 (Hachani et al., 2014) with the N-terminal PAAR-like domain DUF4150; and *Francisella novicida* IglG, an effector of non-canonical T6SS, containing another PAAR-like domain DUF4280 (Rigard et al., 2016). In addition to the Rhs/YD repeat and PAAR, some T6SS effectors possess the motif named marker for type six effectors (MIX), which was first found in *Vibrio parahaemolyticus* by a proteomics approach (Salomon et al., 2014). Further bioinformatics analysis revealed that this MIX motif is present in some proteins encoded within T6SS gene clusters or the *hcp*/*vgrG* island in T6SS$^+$ Proteobacteria. Moreover, these MIX effectors may be horizontally transferred among marine bacteria (Salomon et al., 2015; Salomon, 2016). However, whether the MIX motif is important for the effector function or translocation remains to be tested. With these findings, PAAR- and Rhs-containing effectors were predicted to be widespread in Proteobacterial genomes, indicating that the use of bioinformatics tools to identify the presence of the Rhs/YD repeat, PAAR, TTR, and MIX motifs as a preliminary screen for identifying T6SS effectors or their interacting proteins is a promising strategy, although these motifs are not exclusively related to T6SS.

Because of an essential role required in mediating the transport of specific cargo effectors, the conserved domains of the known T6SS adaptors/chaperones including DUF4123 of Tap-1/TEC (Liang et al., 2015; Unterweger et al., 2015; Bondage et al., 2016), DUF1795 of Eag (Whitney et al., 2015; Cianfanelli et al., 2016a), and DUF2169 (Bondage et al., 2016) can be used to identify the cognate effector gene due to their close genetic linkage. Indeed, the conservation of these chaperones/adaptors with genetic linkage to the cognate effector genes has led to identification of a new T6SS effector, such as the TseC effector mediated by TEC in *A. hydrophila*, by searching for DUF4123 in the genome (Liang et al., 2015) and several putative effectors that are genetically linked to DUF4123 and DUF2169 found in many Proteobacterial genomes (Liang et al., 2015; Bondage et al., 2016). Thus, by identifying the conserved domains of these chaperone/adaptor genes, one can identify the putative effector genes and perform functional assays to confirm their effector functions and relationship with the cognate chaperone/adaptor and VgrG spike.

In addition to the above-mentioned methods specifically for T6SS effector prediction, some online bioinformatics tools or databases provide a suggestion for potential effectors, such as an effector protein predictor, secretEPDB (An et al., 2016, 2017); a T6SS database; SecReT6 (Li et al., 2015); and T346hunter, which can annotate homologs of type III, IV and VI secretion systems automatically (Martínez-García et al., 2015). For researchers working on *Burkholderia* spp., DBSecSys is an online database for the *Burkholderia mallei* and *Burkholderia pseudomallei* secretion system (Memišević et al., 2014, 2016). The Pfam database also provides a resource to identify potential effectors with conserved effector domains (Finn et al., 2014). In conclusion, the bioinformatics-based approach to identify new T6SS effectors is a convenient and powerful tool for study of organisms with a sequenced genome. However, bioinformatics is limited to our current knowledge of biochemical features and transport mechanisms of T6SS effectors.

## Genetic Analysis of T6SS-Associated Genes

Some open reading frames in the T6SS main cluster encoding a hypothetical protein with unknown function could be candidate genes for T6SS effector or immunity proteins; combining deletion of these genes and phenotypic analysis such as interbacterial competition assay or virulence assay may lead to effector discovery. Hcp secretion is considered a hallmark of a functional T6SS and therefore can be used to determine the effects of the deletion mutant in T6SS assembly. In *S. marcescens*, two genes with unknown function in the T6SS gene cluster were found to be T6SS effectors, *ssp1* and *ssp2*, via bacterial competition assay and protein–protein interaction studies (English et al., 2012). The other case is the Tae and Tde1 effectors in *A. tumefaciens* C58, in which both Tae and Tde1 are secreted proteins, and their absence does not affect Hcp secretion (Lin et al., 2013; Ma et al., 2014). Follow-up experiments further demonstrated their functions as bacterial toxins and that their cognate immunity proteins are encoded from their adjacent genes (Ma et al., 2014). Some effectors are not encoded in the T6SS main cluster but are found in the *hcp*/*vgrG* island located outside the T6SS main cluster (Abby et al., 2016). Such effector genes include *tse5*/*rhsP1* and *rhsP2* in *P. aeruginosa*, found near *vgrG4* and *vgrG14*, respectively (Hachani et al., 2014; Whitney et al., 2014); *tde2* in *A. tumefaciens* C58, located in the *vgrG2* operon (Ma et al., 2014); and some effectors found located in the *vgrG*/*hcp* island in *Pantoea* and *Erwinia* species (De Maayer et al., 2011). Therefore, hypothetical proteins encoded in the T6SS gene cluster or orphan *vgrG*/*hcp* island can be analyzed genetically by virulence assay, antibacterial competition assay and/or protein secretion. Together with sequence- and structure-based search engines, such as NCBI blast searches (Ncbi Resource Coordinators, 2017) and Phyre2 (Kelley et al., 2015), one can identify T6SS effectors without large-scale omics approaches or library construction and screening.

## Proteomics-Based Method

Unlike the bioinformatics-based method depending on empirical known characteristics of T6SS effectors, proteomics is a discovery-driven approach that can identify T6SS effectors without prior knowledge. A simple experimental design is to identify T6SS effector candidates via a comparative proteomics analysis between a wild-type strain and a T6SS secretion-deficient mutant. The *P. aeruginosa* H1-T6SS effectors Tse1, Tse2, and Tse3 were found by comparing the secretome between the hyper-secreted *pppA* deletion mutant and *clpV1* secretion-deficient mutant (Hood et al., 2010). Similarly, a gel-free secretome analysis comparing the wild-type strain and *clpV* mutant of *V. cholerae* revealed a TseH effector possessing an amidase domain and two YD repeats (Altindis et al., 2015). The mutant of *vasH,* encoding a transcriptional regulator of T6SS (Kitaoka et al., 2011), was used to identify the new effectors VasX and VgrG1 in *V. cholerae* and *A. hydrophila*, respectively (Suarez et al., 2010;

Miyata et al., 2011). Both of these effectors were confirmed by a virulence assay with amoeba or HeLa cells as models. The use of the *tssC* mutant as a T6SS secretion-deficient mutant to analyze the comparative secretome also led to the discovery of Tae2 in *B. thailendensis*, Bte1 and Bte2 in *Burkholderia fragilis* and Fte2 in *Flavobacterium johnsoniae* (Russell et al., 2012, 2014b; Wexler et al., 2016). Comparison of the secretomes of the *S. marcescens clpV* mutant and the wild type revealed four new effectors: Ssp3, Ssp4, Ssp5, and Ssp6 (Fritsch et al., 2013). The effector function of Ssp4 was confirmed by interbacterial competition assay; the toxic effects of others were determined by examining the survival of effector-expressing *E. coli* cells. Comparison of the secretomes of the T6SS cluster-deletion mutant and the wild type of enterohemorragic *E. coli* (EHEC) revealed a magnesium (Mn)-containing catalase, KatN, as a T6SS effector (Wan et al., 2017). This study demonstrated that KatN is secreted in a T6SS-dependent secretion to the extracellular milieu *in vitro* and into the host cell cytosol after EHEC is phagocytized by macrophages. Interestingly, *katN* is not located in the T6SS cluster or the *hcp/vgrG* island. Thus, determining the molecular mechanisms underlying how KatN is transported via T6SS through VgrG or Hcp as a carrier or via another yet-to-be discovered mechanism would be of interest. In addition, secretome analysis of each specific *vgrG* mutant in *S. marcescens* was used to identify a VgrG-dependent effector, which led to the discovery of an Slp effector in *S. marcescens* with VgrG2-dependent secretion (Cianfanelli et al., 2016a).

The characteristics of a chaperone that stabilizes the cognate effector can also be used to identify new T6SS effectors. This idea led to the identification of Tse4 in *P. aeruginosa* (Whitney et al., 2014). Because Hcp1 in *P. aeruginosa* has the chaperone activity that stabilizes effectors (Silverman et al., 2013), comparing the intracellular proteome between the wild type and Δ*hcp1* was used as a unique method to identify candidate effectors with lower accumulation in Δ*hcp1* (Whitney et al., 2014). This gave us a hint that the same principle can be used to identify the effector requiring a cognate chaperone for stability by performing comparative cellular proteome analysis between the wild type and the mutant deficient in a specific chaperone, such as a DUF4123-, DUF2169-, or DUF1795-containing protein.

The proteomics-based method is a powerful tool to identify potential effectors in a hypothesis-driven or knowledge-independent manner. Thus, this approach may identify novel effectors with conserved motifs such as MIX motif-containing effectors found in *V. parahaemolyticus* (Salomon et al., 2014). However, since not all effectors can be secreted *in vitro* in significant amounts or require a chaperone for stability, current proteomics-based methods are limited to identify effectors with these criteria.

## Mutant Library Screening

In addition to proteomics approaches, mutant library screening is another powerful tool to identify T6SS effectors without known features yet is often a phenotype-dependent method. Of note, the very first T6SS reported in *V. cholerae* was identified by this approach, although discovery of a secretion system was not intentional. The key to identifying the T6SS involved in *V. chalerae* virulence is the use of a novel bacterial virulence assay with the eukaryotic amoebae organism *Dictyostelium discoiseum* as a host model system, which uptakes bacterial cells by phagocytosis, mimicking the behavior of macrophages (Steinert and Heuner, 2005; Pukatzki et al., 2006). The transposon insertion mutants, *vasH*, *vasA* (*tssF*), and *vasK* (*tssM*), were found to lose the anti-amoebae activity and later found deficient in secretion of a previously known secreted protein, Hcp (Williams et al., 1996; Pukatzki et al., 2006). Thus, a robust phenotype screening system is required for identifying T6SS effectors by mutant library screening. In *Burkholderia cenocepacia*, the T6SS effector TecA was found by selecting the transposon insertion mutants that cannot disrupt the actin of macrophages, and TecA was further demonstrated to function as a Rho-GTPase deaminase (Aubert et al., 2016). Because the immunity protein is essential for resistance against wild-type siblings with antibacterial activity but not T6SS-deficient siblings, Dong et al. used transposon insertion-site sequencing (Tn-seq) to identify the immunity gene and associated effector gene in a transposon mutant library screening (Dong et al., 2013). By this approach, they identified a new T6SS effector with lipase domain, TseL, and two known effectors: VgrG3, with peptidoglycan degradation activity, and VasX, which may interact with phospholipids. Because this study focused on identifying mutants that are absent in T6SS$^+$ but present in T6SS$^-$ *V. cholerae* strains, the mutants that are lethal in both T6SS$^+$ and T6SS$^-$ strains could not be selected. As a result, all three effectors identified are cell wall– or membrane-targeting effectors because the effectors only exhibit the function when delivered to the cell wall or membrane of target cells; thus, the respective immunity mutants remain viable for selection. For the effectors with cytosolic targets, one may identify the cognate immunity gene by directly sequencing the saturating mutant library because of the lethality of the mutants. Tn-seq technology was also used to identify a *V. cholerae* transposon insertion *tsiV3* mutant that cannot survive in the infant rabbit gut, which suggests a role for T6SS in antagonistic interbacterial interactions during infection (Fu et al., 2013). The *tsiV3* mutant of this *V. cholera* strain C6706 is viable when grown in regular growth medium because T6SS is not expressed during *in vitro* growth but is induced *in vivo* for bacterial colonization in the animal host.

Mutant library screening has been successfully used to identify T6SS effectors or cognate immunity, but mutant strains with impaired competitive growth or virulence phenotypes could be caused by mutation in genes involved in T6SS machine assembly or even other virulence-associated factors. In *B. pseudomallei*, transposon insertion mutant library screening revealed the T3SS as the main system related to host virulence, whereas T6SS-1 is important for the virulence in the Madagascar hissing cockroach model, and T6SS-5 may be associated with fitness in mice (Fisher et al., 2012; Gutierrez et al., 2015). Library screening approaches also identified T6SS associated with other phenotypes. For example, a transposon insertion in *clpV* highly attenuated the secretion of iron chelator pyoverdine from *Pseudomonas taiwanensis* with reduced antagonism ability (Chen et al., 2016). Transposon insertion mutations in *vgrG* or *hcp* operons in *Proteus mirabilis* altered swarming behavior (Alteri

et al., 2013). However, whether the impact on pyoverdine secretion or swarming ability are the direct phenotype or are secondary effects due to the absence of T6SS await further validation.

## POTENTIAL METHODS FOR IDENTIFYING T6SS EFFECTORS

In addition to the above-mentioned methods that have been successfully used to identify T6SS effectors directly or indirectly, we discuss two potential approaches that may help to identify T6SS effectors.

### Expression Library

Most of the T6SS effectors identified to date are usually toxic to eukaryotic hosts or competitor bacteria. Thus, we can take advantage of such characteristics to identify effector genes by screening a genome-wide expression library in yeast (for eukaryotic toxin) or *E. coli* cells (for bacterial toxins). Indeed, since the 2000s, yeast has been used as a model to find bacterial effectors of other secretion systems (Siggers and Lesser, 2008). The key is to use the tightly regulated inducible promoter to express the genes of interests and screen the construct with growth inhibition or arrest under inducible condition. This kind of approach has been used to identify T3SS effectors in *Shigella* sp., *P. aeruginosa* and *Xanthomonas campestris* pv. *vesicatoria*. In *Shigella* sp., a T3SS effector, IpaJ, encoded from *Shigella* virulence plasmids, was found to be toxic and inhibit growth when expressed in yeast cells and later confirmed to have T3SS-dependent secretion (Slagowski et al., 2008). A genome-wide expression library constructed from *P. aeruginosa* was transformed into yeast cells, and the expressed proteins leading to yeast cell death or growth inhibition after induction were selected for further virulence assay by infecting *Caenorhabditis elegans* and macrophages with wild-type *P. aeruginosa* or the respective deletion mutants. Such screening indeed identified several virulence factors of *P. aeruginosa*, but the delivery mechanism of these proteins has yet to be determined (Zrieq et al., 2015). In *X. campestris* pv. *vesicatoria*, this approach was used to determine the biological function of already identified T3SS effectors (Salomon et al., 2010). In addition to performing the screening experiments under normal growth conditions, various stress conditions can be used with transformants to identify the effectors targeting the conserved pathway activated only under stress (Slagowski et al., 2008; Salomon et al., 2010).

Toxin effector screening has been also performed in prokaryotic cells. By transforming a DNA library from 388 microbial genomes into *E. coli* and sequencing all surviving transformants, the gene (toxin) that could survive only when its adjacent gene is present on the same clone (antitoxin) was identified (Sberro et al., 2013). Hence, Sorek's group identified both known (238 pairs) and newly identified (123 pairs) toxin/antitoxin pairs. Thus, in view of the toxicity of T6SS effectors and co-existence relationship of the toxin-immunity pair, one can use the inducible expression library and toxin-immunity pair for survival screening to identify T6SS effectors. However, if the effector only exerts its function on the cell membrane/surface or extracellularly, its effector function cannot be uncovered because it may require the T6SS machine for delivery to the right compartments. Therefore, expression library screening may only identify effectors with a cytoplasmic target unless a signal peptide is fused to the expressed proteins for translocation across the inner membrane. Also, the expression library is not specifically designed for T6SS effector identification. Another may also identify genes unrelated to T6SS. Therefore, after identification of putative effector candidates, further elucidation of the delivery mechanism is required to conclude the genes encoding T6SS effectors. One limitation in the expression library is that effectors with subtle effects or other physiological functions not related to cell growth may be overlooked.

### Protein–Protein Interaction

As described previously, several T6SS cargo effectors are loaded to the VgrG spike via non-covalent binding with chaperone or adaptor proteins such as Eag or Tap-1/TEC (Pukatzki et al., 2009; Liang et al., 2015; Unterweger et al., 2015, 2016; Whitney et al., 2015; Bondage et al., 2016; Cianfanelli et al., 2016b). Others such as Tse2 in *P. aeruginosa* and Tae4 in *Salmonella typhimurium* are secreted by binding to the lumen of the Hcp hexamer (Silverman et al., 2013; Sana et al., 2016). Therefore, the T6SS effectors were found to be directly or indirectly associated with Hcp, VgrG, PAAR, Tap-1/TEC, or Eag in various bacteria (Shneider et al., 2013; Silverman et al., 2013; Hachani et al., 2014; Liang et al., 2015; Unterweger et al., 2015; Whitney et al., 2015; Bondage et al., 2016; Cianfanelli et al., 2016a; Rigard et al., 2016). Because the genes encoding these conserved T6SS components functioning as carriers or chaperones/adaptors for T6SS effectors are easier to be predicted than most effector genes in a sequenced genome, these proteins can be first identified and used as a bait in well-established protein–protein interaction platforms such as bacterial two-hybrid (Battesti and Bouveret, 2012), yeast two-hybrid (Mehla et al., 2015), or co-IP/pull-down assay (Brymora et al., 2004; Kaboord and Perr, 2008) to identify potential effectors. This idea was indeed proposed by Silverman et al., that interaction with the Hcp chaperone may be a novel method to identify new T6SS effectors (Silverman et al., 2013). One disadvantage of this method is that it can identify only effectors that directly or tightly bind with adaptors/chaperones or the T6SS machine. Because expression of the effector toxin may be harmful for the host used in bacterial or yeast two-hybrid assays, some key effector toxins may be missed by such screening.

## BIOCHEMICAL AND BIOLOGICAL FUNCTIONS OF KNOWN T6SS EFFECTORS

Numerous T6SS effectors have been identified with experimentally proven or predicted biochemical activities. In general, the effectors can be classified by their target cells as eukaryotic hosts or bacterial competitors, although the mode of action or biochemical function of effectors can be distinct or

**TABLE 2 |** Known T6SS effectors with defined biochemical activities.

| Effector | Organism | Biochemical activity | References |
|---|---|---|---|
| **EUKARYOTIC TARGET** | | | |
| VgrG1 | *A. hydrophila* | ADP-ribosyltransferase | Suarez et al., 2010 |
| TecA | *B. cenocepacia* | Deaminating Rho GTPase | Aubert et al., 2016 |
| VgrG-5 | *B. thailendensis* | Membrane fusion activity | Schwarz et al., 2014 |
| EvpP | *E. tarda* | Inhibition of NLRP3 inflammasome | Yang et al., 2015; Chen et al., 2017 |
| VgrG-1 | *V. cholerae* | Actin-crosslinking | Pukatzki et al., 2007; Ma and Mekalanos, 2010 |
| VgrG2b | *P. aeruginosa* | Interacting with microtubule | Sana et al., 2015 |
| KatN | Enterohemorragic *E. coli* | Mn-containing catalase | Wan et al., 2017 |
| **DUAL TARGET** | | | |
| PldA/Tle5, PldB | *P. aeruginosa* | Phospholipase, activation of Akt signaling pathway | Russell et al., 2013; Jiang et al., 2014 |
| VasX | *V. cholerae* | Membrane-targeting activity | Dong et al., 2013; Miyata et al., 2013 |
| TseL/Tle2 | *V. cholerae* | Phospholipase | Dong et al., 2013; Russell et al., 2013 |
| **BACTERIAL TARGET—LIPASE ACTIVITY** | | | |
| Tle1 | *Burkholderia thailandensis* | Phospholipase | Russell et al., 2013 |
| Tle1 | Entero-aggregative *E. coli* | Phospholipase | Flaugnatti et al., 2016 |
| **BACTERIAL TARGET—CELL WALL DEGRADATION ENZYME** | | | |
| Tse1 | *P. aeruginosa* | Amidase | Hood et al., 2010; Russell et al., 2011 |
| Tse3 | *P. aeruginosa* | Muramidase | Hood et al., 2010; Russell et al., 2011 |
| TseH | *V. cholerae* | Cell-wall degradation hydrolase | Altindis et al., 2015 |
| VgrG-3 | *V. cholerae* | Peptidoglycan degradation | Pukatzki et al., 2006; Brooks et al., 2013 |
| Tge2 | *P. aeruginosa* | Glycoside hydrolase | Whitney et al., 2013 |
| **BACTERIAL TARGET—DNASE** | | | |
| Tde1, Tde2 | *A. tumefaciens* | DNase | Ma et al., 2014 |
| RhsA, RhsB | *D. dadantii* | DNase | Koskiniemi et al., 2013 |
| Hcp-ET1 | Shiga toxin-producing *E. coli* | DNase | Ma et al., 2017a |
| Rhs2 | *S. marcescens* | DNase | Alcoforado Diniz and Coulthurst, 2015 |
| **BACTERIAL TARGET—OTHER BIOCHEMICAL ACTIVITY** | | | |
| Tse2 | *P. aeruginosa* | NAD-dependent toxicity | Hood et al., 2010; Robb et al., 2016 |
| Tse6 | *P. aeruginosa* | NAD(P)+ glycohydrolase | Whitney et al., 2014, 2015 |
| **EXTRACELLULAR** | | | |
| TseM | *B. thailendensis* | $Mn^{2+}$-binding protein | Si et al., 2017 |
| YezP | *Y. pseudotuberculosis* | Zinc-binding protein | Wang et al., 2015 |
| TseF | *P. aeruginosa* | Bind OMV for iron acquisition | Lin et al., 2017 |

shared between eukaryotic or prokaryotic effectors (**Table 2**). So far, the major biological functions of these effectors are to increase the competitive growth advantages of environmental or host-associated bacteria or virulence of the bacterial pathogen (Kapitein and Mogk, 2013; Durand et al., 2014; Russell et al., 2014a; Alcoforado Diniz et al., 2015; Hachani et al., 2016). In addition to functioning as a contact-dependent weapon against the host or bacterial competitor, some T6SSs may secrete effectors for scavenging cofactors to survive in oxidative stress and/or facilitate metal ion acquisition (Chen et al., 2016; Lin et al., 2017; Si et al., 2017; Wan et al., 2017). These findings suggest diversified T6SS functions for bacterial survival and fitness in its ecological niches.

The biological and biochemical functions of antihost T6SS effectors are quite diverse. Some of the virulence-associated T6SS effectors can interact with the cytoskeleton of the host cells directly. *V. cholerae* VgrG-1 can cause actin crosslinking, which is associated with the intestinal inflammation (Pukatzki et al., 2007; Ma and Mekalanos, 2010). *P. aeruginosa* VgrG2b interacts with microtubules causing the successful invasion of epithelial cells (Sana et al., 2015). VgrG1 in *A. hydrophila* has ADP-ribosyltransferase activity and can disrupt the cytoskeleton of HeLa cells (Suarez et al., 2010). Others can interact with the plasma membrane of host cells. *B. thailandensis* VgrG-5 has membrane fusion activity and is required for the multinucleated giant cell formation to spread between cells (Schwarz et al., 2014). Besides targeting the host cytoskeleton or membrane, an Mn-containing catalase, KatN, was shown to be translocated from the enterohemorrhagic *E. coli* (EHEC) into host cells in a T6SS-dependent manner and reduce the reactive oxygen species concentration in host macrophages in a T6SS-dependent manner (Wan et al., 2017). Although T6SS appears to be important for EHEC virulence, as demonstrated in mouse model, no virulence phenotype could be observed in the *katN* mutant. In *B. cenocepacia*, TecA deaminates Rho GTPase in host cells and triggers the inflammation reaction and actin disruption (Aubert et al., 2016). Although infection of the *tecA* mutant will not trigger inflammation, it can kill mice, as compared with the survival of all mice infected with wild-type *B. cenocepacia*. The authors proposed that TecA may limit the bacterial cell number in the host and cause the bacteria to evolve toward a mutual relationship with the host. In contrast, the fish pathogen *Edwardsiella tarda* produces a unique T6SS effector EvpP, which does not harbor any known functional domain, to suppress inflammasome activation and promote colonization in the host (Chen et al., 2017). Thus, bacterial pathogens seem to evolve

different T6SS effectors in modulating the host immunity for survival and fitness, but much more remains to be learned about their host targets and mode of actions (Yu and Lai, 2017).

The antibacterial T6SS effectors identified so far can be divided into membrane-, cell wall-, and nucleic acid-targeting effectors as well as other biological functions (Durand et al., 2014; Russell et al., 2014a; Alcoforado Diniz et al., 2015). Membrane-targeting effectors include Tle phospholipase superfamily such as *P. aeruginosa* PldA/Tle5, *V. cholerae* Tle2/TseL, and *Burkholderia thailandensis* Tle1 (Russell et al., 2013) and entero-aggregative *E. coli* Tle1 (Flaugnatti et al., 2016). VgrG3 and TseH in *V. cholerae* (Brooks et al., 2013; Altindis et al., 2015) and Tse1 amidase and Tse3 muramidase (Russell et al., 2011) in *P. aeruginosa* belong to cell wall-targeting effectors. *S. marcescens* Rhs2 (Alcoforado Diniz and Coulthurst, 2015), *D. dadantii* RhsA and RhsB (Koskiniemi et al., 2013), *A. tumefaciens* Tde1 and Tde2 (Ma et al., 2014), and Shiga toxin-producing *E. coli* Hcp-ET1 (Ma et al., 2017a) can hydrolyze DNA. Some effectors have other toxic effects in bacterial cytoplasm; for example, *P. aeruginosa* Tse6 is an NAD(P)+ glycohydrolase toxin inducing bacteriostasis by depleting cellular NAD(P)+ levels (Whitney et al., 2015) and Tse2 is likely an NAD-dependent enzyme from the structure information (Robb et al., 2016).

Many T6SS effectors can be secreted into the extracellular milieu during *in vitro* culture, but these antihost or antibacterial toxin effectors exhibit their effector functions inside the target cells. A few reports recently provided compelling biochemical evidence for some T6SS effectors functioning extracellularly rather than in target cells. These effectors so far identified mainly function to bind or facilitate metal ions for their uptake. *Yersinia pseudotuberculosis* T6SS-4 encodes a unique zinc-binding effector protein, YezP, that is involved in environmental stress resistance in the host body (Wang et al., 2015). The double mutant lacking this effector and classical zinc transporter exhibits almost no virulence toward mice. Similar to *Y. pseudotuberculosis*, TseM secreted by T6SS-4 of *Burkholderia thailandensis* functions as an $Mn^{2+}$-binding protein in interacting with the $Mn^{2+}$-specific TonB-dependent outer-membrane protein MnoT to activate transport for resistance to oxidative stress (Si et al., 2017). Deletion of *tseM* caused reduced virulence toward *Galleria mellonella* wax moth larvae. Although not functioning as a metal-binding protein, TseF secreted by H3-T6SS of *P. aeruginosa* can bind to and recruit outer-membrane vesicles for iron (Fe) acquisition (Lin et al., 2017). By engaging the Fe(III)-pyochelin receptor FptA and the porin OprF, TseF can facilitate the delivery of outer-membrane vesicle-associated Fe for bacterial cells.

Although many effectors target only eukaryotic cells (i.e., *V. cholerae* VgrG-1 with an actin cross-linking domain) or prokaryotic cells (i.e., *P. aeruginosa* Tse1 amidase and Tse3 muramidase for targeting peptidoglycan), some effectors may have dual targets. PldA/Tle5 and PldB, phospholipase D effectors secreted from *P. aeruginosa,* can target both bacterial and eukaryotic cells (Jiang et al., 2014). Both PLD effectors can inhibit bacterial growth by increasing membrane permeability when translocated into the periplasm of bacterial recipient cells while activating phosphorylation of the protein kinase B (Akt) signaling pathway to lead to the internalization of the bacteria into the host cell. TseL/Tle2 in *V. cholerae* is phospholipase, which exhibits both T6SS-dependent antibacterial activity and a virulence role toward *D. discoideum* (Dong et al., 2013; Russell et al., 2013). In addition, *V. cholerae* VasX is a membrane targeting toxin that can interact with phosphoinositides important for virulence toward the eukaryotic amoebae *D. discoideum* and compromise the integrity of the inner membrane in bacterial target cells for antibacterial activity (Miyata et al., 2011, 2013; Dong et al., 2013). The *P. aeruginosa* Tse2 toxin naturally attacks bacterial cells for interbacterial competition but can also cause toxicity when ectopically expressed in eukaryotic cells (Robb et al., 2016). Thus, although current data show that the DNase effectors such as Tde and NAD(P)+ glycohydrolase effectors such as Tse6 are involved in antibacterial activity, whether they can also be translocated into eukaryotic host cells remains to be tested. In considering the role of T6SS in bacterial colonization inside hosts such as *A. tumefaciens* T6SS for competitive growth advantage *in planta* (Ma et al., 2014), *V. cholera* T6SS for survival in the infant rabbit gut (Fu et al., 2013), and T6SS for survival of the bacterial symbionts Bacteroidetes in human guts (Wexler et al., 2016), such possibility could be explored.

## PERSPECTIVES

The T6SS is known to have important roles in bacterium–host interaction, bacterium–bacterium interaction and even other functions associated with bacterial physiology. Considering the expanded and diversifying functions of the T6SS discovered since its identification more than a decade ago, the system may have more functions, especially biological significance at polymicrobial ecological niches yet to be uncovered. The methodologies and biology of T6SS effectors we discuss in this review can be a foundation for future identification and studies of the T6SS and effectors.

## AUTHOR CONTRIBUTIONS

YL and EL discussed the review content and wrote the paper together.

## FUNDING

Funding is provided by the Ministry of Science and Technology (MOST 104-2311-B-001-025-MY3), Taiwan to EL.

## ACKNOWLEDGMENTS

We thank the members of Lai laboratory for critical readings of this manuscript.

## REFERENCES


Abby, S. S., Cury, J., Guglielmini, J., Néron, B., Touchon, M., and Rocha, E. P. (2016). Identification of protein secretion systems in bacterial genomes. *Sci. Rep.* 6:23080. doi: 10.1038/srep23080

Alcoforado Diniz, J., and Coulthurst, S. J. (2015). Intraspecies competition in *Serratia marcescens* is mediated by type VI-secreted rhs effectors and a conserved effector-associated accessory protein. *J. Bacteriol.* 197, 2350–2360. doi: 10.1128/JB.00199-15

Alcoforado Diniz, J., Liu, Y. C., and Coulthurst, S. J. (2015). Molecular weaponry: diverse effectors delivered by the Type VI secretion system. *Cell. Microbiol.* 17, 1742–1751. doi: 10.1111/cmi.12532

Alteri, C. J., Himpsl, S. D., Pickens, S. R., Lindner, J. R., Zora, J. S., Miller, J. E., et al. (2013). Multicellular bacteria deploy the type VI secretion system to preemptively strike neighboring cells. *PLoS Pathog.* 9:e1003608. doi: 10.1371/journal.ppat.1003608

Altindis, E., Dong, T., Catalano, C., and Mekalanos, J. (2015). Secretome analysis of *Vibrio cholerae* type VI secretion system reveals a new effector-immunity pair. *MBio* 6, e00075-15. doi: 10.1128/mBio.00075-15

An, Y., Wang, J., Li, C., Leier, A., Marquez-Lago, T., Wilksch, J., et al. (2016). Comprehensive assessment and performance improvement of effector protein predictors for bacterial secretion systems III, IV and VI. *Brief Bioinform.* doi: 10.1093/bib/bbw100. [Epub ahead of print].

An, Y., Wang, J., Li, C., Revote, J., Zhang, Y., Naderer, T., et al. (2017). SecretEPDB: a comprehensive web-based resource for secreted effector proteins of the bacterial types III, IV and VI secretion systems. *Sci. Rep.* 7:41031. doi: 10.1038/srep41031

Aschtgen, M. S., Bernard, C. S., De Bentzmann, S., Lloubès, R., and Cascales, E. (2008). SciN is an outer membrane lipoprotein required for type VI secretion in enteroaggregative *Escherichia coli*. *J. Bacteriol.* 190, 7523–7531. doi: 10.1128/jb.00945-08

Aubert, D. F., Xu, H., Yang, J., Shi, X., Gao, W., Li, L., et al. (2016). A burkholderia type VI effector deamidates rho GTPases to activate the pyrin inflammasome and trigger inflammation. *Cell Host Microbe* 19, 664–674. doi: 10.1016/j.chom.2016.04.004

Basler, M. (2015). Type VI secretion system: secretion by a contractile nanomachine. *Philoso. Trans. R. Soc. B Biol. Sci.* 370:20150021. doi: 10.1098/rstb.2015.0021

Basler, M., and Mekalanos, J. J. (2012). Type 6 secretion dynamics within and between bacterial cells. *Science* 337, 815–815. doi: 10.1126/science.1222901

Basler, M., Pilhofer, M., Henderson, G. P., Jensen, G. J., and Mekalanos, J. J. (2012). Type VI secretion requires a dynamic contractile phage tail-like structure. *Nature* 483, 182–186. doi: 10.1038/nature10846

Battesti, A., and Bouveret, E. (2012). The bacterial two-hybrid system based on adenylate cyclase reconstitution in *Escherichia coli*. *Methods* 58, 325–334. doi: 10.1016/j.ymeth.2012.07.018

Blondel, C. J., Jiménez, J. C., Contreras, I., and Santiviago, C. A. (2009). Comparative genomic analysis uncovers 3 novel loci encoding type six secretion systems differentially distributed in Salmonella serotypes. *BMC Genomics* 10:354. doi: 10.1186/1471-2164-10-354

Bondage, D. D., Lin, J. S., Ma, L. S., Kuo, C. H., and Lai, E. M. (2016). VgrG C terminus confers the type VI effector transport specificity and is required for binding with PAAR and adaptor–effector complex. *Proc. Natl. Acad. Sci. U.S.A.* 113, E3931–E3940. doi: 10.1073/pnas.1600428113

Bonemann, G., Pietrosiuk, A., Diemand, A., Zentgraf, H., and Mogk, A. (2009). Remodelling of VipA/VipB tubules by ClpV-mediated threading is crucial for type VI protein secretion. *EMBO J.* 28, 315–325. doi: 10.1038/emboj.2008.269

Boyer, F., Fichant, G., Berthod, J., Vandenbrouck, Y., and Attree, I. (2009). Dissecting the bacterial type VI secretion system by a genome wide *in silico* analysis: what can be learnt from available microbial genomic resources? *BMC Genomics* 10:104. doi: 10.1186/1471-2164-10-104

Brooks, T. M., Unterweger, D., Bachmann, V., Kostiuk, B., and Pukatzki, S. (2013). Lytic activity of the *Vibrio cholerae* type VI secretion toxin VgrG-3 is inhibited by the antitoxin TsaB. *J. Biol. Chem.* 288, 7618–7625. doi: 10.1074/jbc.M112.436725

Brunet, Y. R., Zoued, A., Boyer, F., Douzi, B., and Cascales, E. (2015). The type VI secretion TssEFGK-VgrG phage-like baseplate is recruited to the TssJLM membrane complex via multiple contacts and serves as assembly platform for tail tube/sheath polymerization. *PLoS Genet.* 11:e1005545. doi: 10.1371/journal.pgen.1005545

Brymora, A., Valova, V. A., and Robinson, P. J. (2004). Protein-protein interactions identified by pull-down experiments and mass spectrometry. *Curr. Protoc. Cell Biol.* Chapter 17, Unit 17.15. doi: 10.1002/0471143030.cb1705s22

Chen, H., Yang, D., Han, F., Tan, J., Zhang, L., Xiao, J., et al. (2017). The bacterial T6SS effector EvpP prevents NLRP3 inflammasome activation by inhibiting the $Ca^{2+}$-dependent MAPK-Jnk pathway. *Cell Host Microbe* 21, 47–58. doi: 10.1016/j.chom.2016.12.004

Chen, W. J., Kuo, T. Y., Hsieh, F. C., Chen, P. Y., Wang, C. S., Shih, Y. L., et al. (2016). Involvement of type VI secretion system in secretion of iron chelator pyoverdine in *Pseudomonas taiwanensis*. *Sci. Rep.* 6:32950. doi: 10.1038/srep32950

Cianfanelli, F. R., Alcoforado Diniz, J., Guo, M., De Cesare, V., Trost, M., and Coulthurst, S. J. (2016a). VgrG and PAAR proteins define distinct versions of a functional type VI secretion system. *PLoS Pathog.* 12:e1005735. doi: 10.1371/journal.ppat.1005735

Cianfanelli, F. R., Monlezun, L., and Coulthurst, S. J. (2016b). Aim, load, fire: the type VI secretion system, a bacterial nanoweapon. *Trends Microbiol.* 24, 51–62. doi: 10.1016/j.tim.2015.10.005

De Maayer, P., Venter, S. N., Kamber, T., Duffy, B., Coutinho, T. A., and Smits, T. H. (2011). Comparative genomics of the type VI secretion systems of Pantoea and Erwinia species reveals the presence of putative effector islands that may be translocated by the VgrG and Hcp proteins. *BMC Genomics* 12:576. doi: 10.1186/1471-2164-12-576

Dong, T. G., Ho, B. T., Yoder-Himes, D. R., and Mekalanos, J. J. (2013). Identification of T6SS-dependent effector and immunity proteins by Tn-seq in *Vibrio cholerae*. *Proc. Natl. Acad. Sci. U.S.A.* 110, 2623–2628. doi: 10.1073/pnas.1222783110

Durand, E., Cambillau, C., Cascales, E., and Journet, L. (2014). VgrG, Tae, Tle, and beyond: the versatile arsenal of Type VI secretion effectors. *Trends Microbiol.* 22, 498–507. doi: 10.1016/j.tim.2014.06.004

English, G., Trunk, K., Rao, V. A., Srikannathasan, V., Hunter, W. N., and Coulthurst, S. J. (2012). New secreted toxins and immunity proteins encoded within the Type VI secretion system gene cluster of *Serratia marcescens*. *Mol. Microbiol.* 86, 921–936. doi: 10.1111/mmi.12028

Felisberto-Rodrigues, C., Durand, E., Aschtgen, M. S., Blangy, S., Ortiz-Lombardia, M., Douzi, B., et al. (2011). Towards a structural comprehension of bacterial type VI secretion systems: characterization of the TssJ-TssM complex of an *Escherichia coli* pathovar. *PLoS Pathog.* 7:e1002386. doi: 10.1371/journal.ppat.1002386

Finn, R. D., Bateman, A., Clements, J., Coggill, P., Eberhardt, R. Y., Eddy, S. R., et al. (2014). Pfam: the protein families database. *Nucleic Acids Res.* 42, D222–D230. doi: 10.1093/nar/gkt1223

Fisher, N. A., Ribot, W. J., and DeShazer, D. (2012). The Madagascar hissing cockroach as a novel surrogate host for *Burkholderia pseudomallei*, *B. mallei* and *B. thailandensis*. *BMC Microbiol.* 12:117. doi: 10.1186/1471-2180-12-117

Flaugnatti, N., Le, T. T., Canaan, S., Aschtgen, M. S., Nguyen, V. S., Blangy, S., et al. (2016). A phospholipase A1 antibacterial Type VI secretion effector interacts directly with the C-terminal domain of the VgrG spike protein for delivery. *Mol. Microbiol.* 99, 1099–1118. doi: 10.1111/mmi.13292

Fritsch, M. J., Trunk, K., Diniz, J. A., Guo, M., Trost, M., and Coulthurst, S. J. (2013). Proteomic identification of novel secreted antibacterial toxins of the *Serratia marcescens* type VI secretion system. *Mol. Cell. Proteomics* 12, 2735–2749. doi: 10.1074/mcp.M113.030502

Fu, Y., Waldor, M. K., and Mekalanos, J. J. (2013). Tn-Seq analysis of *Vibrio cholerae* intestinal colonization reveals a role for T6SS-mediated antibacterial activity in the host. *Cell Host Microbe* 14, 652–663. doi: 10.1016/j.chom.2013.11.001

Gutierrez, M. G., Yoder-Himes, D. R., and Warawa, J. M. (2015). Comprehensive identification of virulence factors required for respiratory melioidosis using Tn-seq mutagenesis. *Front. Cell. Infect. Microbiol.* 5:78. doi: 10.3389/fcimb.2015.00078

Hachani, A., Allsopp, L. P., Oduko, Y., and Filloux, A. (2014). The VgrG proteins are "à la Carte" delivery systems for bacterial type VI effectors. *J. Biol. Chem.* 289, 17872–17884. doi: 10.1074/jbc.M114.563429

Hachani, A., Wood, T. E., and Filloux, A. (2016). Type VI secretion and anti-host effectors. *Curr. Opin. Microbiol.* 29, 81–93. doi: 10.1016/j.mib.2015.11.006

Hood, R. D., Singh, P., Hsu, F., Güvener, T., Carl, M. A., Trinidad, R. R., et al. (2010). A Type VI SECRETION SYSTEM of *Pseudomonas aeruginosa* targets a toxin to bacteria. *Cell Host Microbe* 7, 25–37. doi: 10.1016/j.chom.2009.12.007

Jamet, A., and Nassif, X. (2015). New players in the toxin field: polymorphic toxin systems in bacteria. *MBio* 6, e00285-15. doi: 10.1128/mBio.00285-15

Jiang, F., Waterfield, N. R., Yang, J., Yang, G., and Jin, Q. (2014). A *Pseudomonas aeruginosa* type VI secretion phospholipase D effector targets both prokaryotic and eukaryotic cells. *Cell Host Microbe* 15, 600–610. doi: 10.1016/j.chom.2014.04.010

Kaboord, B., and Perr, M. (2008). Isolation of proteins and protein complexes by immunoprecipitation. *Methods Mol. Biol.* 424, 349–364. doi: 10.1007/978-1-60327-064-9_27

Kapitein, N., and Mogk, A. (2013). Deadly syringes: type VI secretion system activities in pathogenicity and interbacterial competition. *Curr. Opin. Microbiol.* 16, 52–58. doi: 10.1016/j.mib.2012.11.009

Kelley, L. A., Mezulis, S., Yates, C. M., Wass, M. N., and Sternberg, M. J. E. (2015). The Phyre2 web portal for protein modelling, prediction and analysis. *Nat. Protoc.* 10, 845–858. doi: 10.1038/nprot.2015.053

Kitaoka, M., Miyata, S. T., Brooks, T. M., Unterweger, D., and Pukatzki, S. (2011). VasH is a transcriptional regulator of the type VI secretion system functional in endemic and pandemic *Vibrio cholerae*. *J. Bacteriol.* 193, 6471–6482. doi: 10.1128/JB.05414-11

Koskiniemi, S., Lamoureux, J. G., Nikolakakis, K. C., t'Kint de Roodenbeke, C., Kaplan, M. D., Low, D. A., et al. (2013). Rhs proteins from diverse bacteria mediate intercellular competition. *Proc. Natl. Acad. Sci. U.S.A.* 110, 7032–7037. doi: 10.1073/pnas.1300627110

Li, J., Yao, Y., Xu, H. H., Hao, L., Deng, Z., Rajakumar, K., et al. (2015). SecReT6: a web-based resource for type VI secretion systems found in bacteria. *Environ. Microbiol.* 17, 2196–2202. doi: 10.1111/1462-2920.12794

Liang, X., Moore, R., Wilton, M., Wong, M. J., Lam, L., and Dong, T. G. (2015). Identification of divergent type VI secretion effectors using a conserved chaperone domain. *Proc. Natl. Acad. Sci. U.S.A.* 112, 9106–9111. doi: 10.1073/pnas.1505317112

Lin, J. S., Ma, L. S., and Lai, E. M. (2013). Systematic dissection of the agrobacterium type VI secretion system reveals machinery and secreted components for subcomplex formation. *PLoS ONE* 8:e67647. doi: 10.1371/journal.pone.0067647

Lin, J., Zhang, W., Cheng, J., Yang, X., Zhu, K., Wang, Y., et al. (2017). A Pseudomonas T6SS effector recruits PQS-containing outer membrane vesicles for iron acquisition. *Nat. Commun.* 8:14888. doi: 10.1038/ncomms14888

Ma, A. T., and Mekalanos, J. J. (2010). *In vivo* actin cross-linking induced by *Vibrio cholerae* type VI secretion system is associated with intestinal inflammation. *Proc. Natl. Acad. Sci. U.S.A.* 107, 4365–4370. doi: 10.1073/pnas.09151 56107

Ma, J., Pan, Z., Huang, J., Sun, M., Lu, C., and Yao, H. (2017a). The Hcp proteins fused with diverse extended-toxin domains represent a novel pattern of antibacterial effectors in type VI secretion systems. *Virulence*. doi: 10.1080/21505594.2017.1279374. [Epub ahead of print].

Ma, J., Sun, M., Dong, W., Pan, Z., Lu, C., and Yao, H. (2017b). PAAR-Rhs proteins harbor various C-terminal toxins to diversify the antibacterial pathways of type VI secretion systems. *Environ Microbiol.* 19, 345–360. doi: 10.1111/1462-2920. 13621

Ma, L. S., Hachani, A., Lin, J. S., Filloux, A., and Lai, E. M. (2014). *Agrobacterium tumefaciens* deploys a superfamily of type VI secretion dnase effectors as weapons for interbacterial competition in planta. *Cell Host Microbe* 16, 94–104. doi: 10.1016/j.chom.2014.06.002

Ma, L. S., Lin, J. S., and Lai, E. M. (2009). An IcmF family protein, ImpLM, is an integral inner membrane protein interacting with ImpKL, and its walker a motif is required for type VI secretion system-mediated Hcp secretion in *Agrobacterium tumefaciens*. *J. Bacteriol.* 191, 4316–4329. doi: 10.1128/JB.00029-09

Ma, L. S., Narberhaus, F., and Lai, E. M. (2012). IcmF family protein TssM exhibits ATPase activity and energizes type VI secretion. *J. Biol. Chem.* 287, 15610–15621. doi: 10.1074/jbc.M111.301630

Martínez-García, P. M., Ramos, C., and Rodríguez-Palenzuela, P. (2015). T346Hunter: a novel web-based tool for the prediction of type III, type IV and type VI secretion systems in bacterial genomes. *PLoS ONE* 10:e0119317. doi: 10.1371/journal.pone.0119317

Mehla, J., Caufield, J. H., and Uetz, P. (2015). The yeast two-hybrid system: a tool for mapping protein-protein interactions. *Cold Spring Harb. Protoc.* 2015, 425–430. doi: 10.1101/pdb.top083345

Memišević, V., Kumar, K., Cheng, L., Zavaljevski, N., DeShazer, D., Wallqvist, A., et al. (2014). DBSecSys: a database of *Burkholderia mallei* secretion systems. *BMC Bioinformatics* 15:244. doi: 10.1186/1471-2105-15-244

Memišević, V., Kumar, K., Zavaljevski, N., DeShazer, D., Wallqvist, A., and Reifman, J. (2016). DBSecSys 2.0: a database of *Burkholderia mallei* and *Burkholderia pseudomallei* secretion systems. *BMC Bioinformatics* 17:387. doi: 10.1186/s12859-016-1242-z

Miyata, S. T., Kitaoka, M., Brooks, T. M., McAuley, S. B., and Pukatzki, S. (2011). *Vibrio cholerae* requires the type VI secretion system virulence factor VasX To kill dictyostelium discoideum. *Infect. Immun.* 79, 2941–2949. doi: 10.1128/IAI.01266-10

Miyata, S. T., Unterweger, D., Rudko, S. P., and Pukatzki, S. (2013). Dual expression profile of Type VI secretion system immunity genes protects pandemic *Vibrio cholerae*. *PLoS Pathog.* 9:e1003752. doi: 10.1371/journal.ppat.1003752

Ncbi Resource Coordinators (2017). Database resources of the national center for biotechnology information. *Nucleic Acids Res.* 45, D12–D17. doi: 10.1093/nar/gkw1071

Planamente, S., Salih, O., Manoli, E., Albesa-Jové, D., Freemont, P. S., and Filloux, A. (2016). TssA forms a gp6-like ring attached to the type VI secretion sheath. *EMBO J.* 35, 1613–1627. doi: 10.15252/embj.201694024

Pukatzki, S., Ma, A. T., Revel, A. T., Sturtevant, D., and Mekalanos, J. J. (2007). Type VI secretion system translocates a phage tail spike-like protein into target cells where it cross-links actin. *Proc. Natl. Acad. Sci. U.S.A.* 104, 15508–15513. doi: 10.1073/pnas.0706532104

Pukatzki, S., Ma, A. T., Sturtevant, D., Krastins, B., Sarracino, D., Nelson, W. C., et al. (2006). Identification of a conserved bacterial protein secretion system in *Vibrio cholerae* using the Dictyostelium host model system. *Proc. Natl. Acad. Sci. U.S.A.* 103, 1528–1533. doi: 10.1073/pnas.0510322103

Pukatzki, S., McAuley, S. B., and Miyata, S. T. (2009). The type VI secretion system: translocation of effectors and effector-domains. *Curr. Opin. Microbiol.* 12, 11–17. doi: 10.1016/j.mib.2008.11.010

Records, A. R. (2011). The type VI secretion system: a multipurpose delivery system with a phage-like machinery. *Mol. Plant Microbe Interact.* 24, 751–757. doi: 10.1094/MPMI-11-10-0262

Rigard, M., Bröms, J. E., Mosnier, A., Hologne, M., Martin, A., Lindgren, L., et al. (2016). Francisella tularensis IglG belongs to a novel family of PAAR-Like T6SS proteins and harbors a unique N-terminal extension required for virulence. *PLoS Pathog.* 12:e1005821. doi: 10.1371/journal.ppat.1005821

Robb, C. S., Robb, M., Nano, F. E., and Boraston, A. B. (2016). The structure of the toxin and type six secretion system substrate Tse2 in complex with its immunity protein. *Structure* 24, 277–284. doi: 10.1016/j.str.2015.11.012

Russell, A. B., Hood, R. D., Bui, N. K., LeRoux, M., Vollmer, W., and Mougous, J. D. (2011). Type VI secretion delivers bacteriolytic effectors to target cells. *Nature* 475, 343–347. doi: 10.1038/nature10244

Russell, A. B., LeRoux, M., Hathazi, K., Agnello, D. M., Ishikawa, T., Wiggins, P. A., et al. (2013). Diverse type VI secretion phospholipases are functionally plastic antibacterial effectors. *Nature* 496, 508–512. doi: 10.1038/nature12074

Russell, A. B., Peterson, S. B., and Mougous, J. D. (2014a). Type VI secretion effectors: poisons with a purpose. *Nat. Rev. Microbiol.* 12, 137–148. doi: 10.1038/nrmicro3185

Russell, A. B., Singh, P., Brittnacher, M., Bui, N. K., Hood, R. D., Carl, M. A., et al. (2012). A widespread bacterial type VI secretion effector superfamily identified using a heuristic approach. *Cell Host Microbe* 11, 538–549. doi: 10.1016/j.chom.2012.04.007

Russell, A. B., Wexler, A. G., Harding, B. N., Whitney, J. C., Bohn, A. J., Goo, Y. A., et al. (2014b). A type VI secretion-related pathway in Bacteroidetes mediates interbacterial antagonism. *Cell Host Microbe* 16, 227–236. doi: 10.1016/j.chom.2014.07.007

Salomon, D. (2016). MIX and match: mobile T6SS MIX-effectors enhance bacterial fitness. *Mob. Genet. Elements* 6:e1123796. doi: 10.1080/2159256x.2015.1123796

Salomon, D., Dar, D., Sreeramulu, S., and Sessa, G. (2010). Expression of *Xanthomonas campestris* pv. vesicatoria Type III effectors in yeast affects cell growth and viability. *Mol. Plant Microbe Interact.* 24, 305–314. doi: 10.1094/MPMI-09-10-0196

Salomon, D., Kinch, L. N., Trudgian, D. C., Guo, X., Klimko, J. A., Grishin, N. V., et al. (2014). Marker for type VI secretion system effectors. *Proc. Natl. Acad. Sci. U.S.A.* 111, 9271–9276. doi: 10.1073/pnas.1406110111

Salomon, D., Klimko, J. A., Trudgian, D. C., Kinch, L. N., Grishin, N. V., Mirzaei, H., et al. (2015). Type VI secretion system toxins horizontally shared between marine bacteria. *PLoS Pathog.* 11:e1005128. doi: 10.1371/journal.ppat.1005128

Sana, T. G., Baumann, C., Merdes, A., Soscia, C., Rattei, T., Hachani, A., et al. (2015). Internalization of *Pseudomonas aeruginosa* strain PAO1 into epithelial cells is promoted by interaction of a T6SS effector with the microtubule network. *MBio* 6, e00712–15. doi: 10.1128/mBio.00712-15

Sana, T. G., Flaugnatti, N., Lugo, K. A., Lam, L. H., Jacobson, A., Baylot, V., et al. (2016). *Salmonella Typhimurium* utilizes a T6SS-mediated antibacterial weapon to establish in the host gut. *Proc. Natl. Acad. Sci. U.S.A.* 113, E5044–E5051. doi: 10.1073/pnas.1608858113

Sberro, H., Leavitt, A., Kiro, R., Koh, E., Peleg, Y., Qimron, U., et al. (2013). Discovery of functional toxin/antitoxin systems in bacteria by shotgun cloning. *Mol. Cell* 50, 136–148. doi: 10.1016/j.molcel.2013.02.002

Schwarz, S., Singh, P., Robertson, J. D., LeRoux, M., Skerrett, S. J., Goodlett, D. R., et al. (2014). VgrG-5 is a burkholderia type VI secretion system-exported protein required for multinucleated giant cell formation and virulence. *Infect. Immun.* 82, 1445–1452. doi: 10.1128/IAI.01368-13

Shneider, M. M., Buth, S. A., Ho, B. T., Basler, M., Mekalanos, J. J., and Leiman, P. G. (2013). PAAR-repeat proteins sharpen and diversify the Type VI secretion system spike. *Nature* 500, 350–353. doi: 10.1038/nature12453

Shyntum, D. Y., Venter, S. N., Moleleki, L. N., Toth, I., and Coutinho, T. A. (2014). Comparative genomics of type VI secretion systems in strains of Pantoea ananatis from different environments. *BMC Genomics* 15:163. doi: 10.1186/1471-2164-15-163

Si, M., Zhao, C., Burkinshaw, B., Zhang, B., Wei, D., Wang, Y., et al. (2017). Manganese scavenging and oxidative stress response mediated by type VI secretion system in *Burkholderia thailandensis*. *Proc. Natl. Acad. Sci. U.S.A.* 114, E2233–E2242. doi: 10.1073/pnas.1614902114

Siggers, K. A., and Lesser, C. F. (2008). The yeast Saccharomyces cerevisiae: a versatile model system for the identification and characterization of bacterial virulence proteins. *Cell Host Microbe* 4, 8–15. doi: 10.1016/j.chom.2008.06.004

Silverman, J. M., Agnello, D. M., Zheng, H., Andrews, B. T., Li, M., Catalano, C. E., et al. (2013). Haemolysin co-regulated protein is an exported receptor and chaperone of type VI secretion substrates. *Mol. Cell* 51, 584–593. doi: 10.1016/j.molcel.2013.07.025

Slagowski, N. L., Kramer, R. W., Morrison, M. F., LaBaer, J., and Lesser, C. F. (2008). A functional genomic yeast screen to identify pathogenic bacterial proteins. *PLoS Pathog.* 4:e9. doi: 10.1371/journal.ppat.0040009

Steinert, M., and Heuner, K. (2005). Dictyostelium as host model for pathogenesis. *Cell. Microbiol.* 7, 307–314. doi: 10.1111/j.1462-5822.2005.00493.x

Suarez, G., Sierra, J. C., Erova, T. E., Sha, J., Horneman, A. J., and Chopra, A. K. (2010). A type VI secretion system effector protein, VgrG1, from aeromonas hydrophila that induces host cell toxicity by ADP RIBOSYLATION OF ACTIN. *J. Bacteriol.* 192, 155–168. doi: 10.1128/JB.01260-09

Unterweger, D., Kostiuk, B., and Pukatzki, S. (2016). Adaptor proteins of type VI secretion system effectors. *Trends Microbiol.* 25, 8–10. doi: 10.1016/j.tim.2016.10.003

Unterweger, D., Kostiuk, B., Ötjengerdes, R., Wilton, A., Diaz-Satizabal, L., and Pukatzki, S. (2015). Chimeric adaptor proteins translocate diverse type VI secretion system effectors in *Vibrio cholerae*. *EMBO J.* 34, 2198–2210. doi: 10.15252/embj.201591163

Vettiger, A., and Basler, M. (2016). Type VI secretion system substrates are transferred and reused among sister cells. *Cell* 167, 99–110.e112. doi: 10.1016/j.cell.2016.08.023

Wan, B., Zhang, Q., Ni, J., Li, S., Wen, D., Li, J., et al. (2017). Type VI secretion system contributes to Enterohemorrhagic *Escherichia coli* virulence by secreting catalase against host reactive oxygen species (ROS). *PLoS Pathog.* 13:e1006246. doi: 10.1371/journal.ppat.1006246

Wang, T., Si, M., Song, Y., Zhu, W., Gao, F., Wang, Y., et al. (2015). Type VI secretion system transports $Zn^{(2+)}$ to combat multiple stresses and host immunity. *PLoS Pathog.* 11:e1005020. doi: 10.1371/journal.ppat.1005020

Wexler, A. G., Bao, Y., Whitney, J. C., Bobay, L. M., Xavier, J. B., Schofield, W. B., et al. (2016). Human symbionts inject and neutralize antibacterial toxins to persist in the gut. *Proc. Natl. Acad. Sci. U.S.A.* 113, 3639–3644. doi: 10.1073/pnas.1525637113

Whitney, J. C., Beck, C. M., Goo, Y. A., Russell, A. B., Harding, B., De Leon, J. A., et al. (2014). Genetically distinct pathways guide effector export through the type VI secretion system. *Mol. Microbiol.* 92, 529–542. doi: 10.1111/mmi.12571

Whitney, J. C., Chou, S., Russell, A. B., Biboy, J., Gardiner, T. E., Ferrin, M. A., et al. (2013). Identification, structure, and function of a novel type VI secretion peptidoglycan glycoside hydrolase effector-immunity pair. *J. Biol. Chem.* 288, 26616–26624. doi: 10.1074/jbc.M113.488320

Whitney, J. C., Quentin, D., Sawai, S., LeRoux, M., Harding, B. N., Ledvina, H. E., et al. (2015). An interbacterial NAD(P)(+) glycohydrolase toxin requires elongation factor tu for delivery to target cells. *Cell* 163, 607–619. doi: 10.1016/j.cell.2015.09.027

Williams, S. G., Varcoe, L. T., Attridge, S. R., and Manning, P. A. (1996). *Vibrio cholerae* Hcp, a secreted protein coregulated with HlyA. *Infect. Immun.* 64, 283–289.

Yang, W., Wang, L., Zhang, L., Qu, J., Wang, Q., and Zhang, Y. (2015). An invasive and low virulent Edwardsiella tarda esrB mutant promising as live attenuated vaccine in aquaculture. *Appl. Microbiol. Biotechnol.* 99, 1765–1777. doi: 10.1007/s00253-014-6214-5

Yu, M., and Lai, E. M. (2017). Warfare between host immunity and bacterial weapons. *Cell Host Microbe* 21, 3–4. doi: 10.1016/j.chom.2016.12.012

Zhang, D., de Souza, R. F., Anantharaman, V., Iyer, L. M., and Aravind, L. (2012). Polymorphic toxin systems: comprehensive characterization of trafficking modes, processing, mechanisms of action, immunity and ecology using comparative genomics. *Biol. Direct* 7, 18–18. doi: 10.1186/1745-6150-7-18

Zoued, A., Durand, E., Brunet, Y. R., Spinelli, S., Douzi, B., Guzzo, M., et al. (2016). Priming and polymerization of a bacterial contractile tail structure. *Nature* 531, 59–63. doi: 10.1038/nature17182

Zrieq, R., Sana, T. G., Vergin, S., Garvis, S., Volfson, I., Bleves, S., et al. (2015). Genome-wide screen of *Pseudomonas aeruginosa* in saccharomyces cerevisiae identifies new virulence factors. *Front. Cell. Infect. Microbiol.* 5:81. doi: 10.3389/fcimb.2015.00081

**Conflict of Interest Statement:** The authors declare that the research was conducted in the absence of any commercial or financial relationships that could be construed as a potential conflict of interest.

frontiers in Cellular and Infection Microbiology

REVIEW
published: 16 June 2017
doi: 10.3389/fcimb.2017.00256

# Biological Functions of the Secretome of *Neisseria meningitidis*

*Jan Tommassen * and Jesús Arenas*

*Department of Molecular Microbiology and Institute of Biomembranes, Utrecht University, Utrecht, Netherlands*

*Neisseria meningitidis* is a Gram-negative bacterial pathogen that normally resides as a commensal in the human nasopharynx but occasionally causes disease with high mortality and morbidity. To interact with its environment, it transports many proteins across the outer membrane to the bacterial cell surface and into the extracellular medium for which it deploys the common and well-characterized autotransporter, two-partner and type I secretion mechanisms, as well as a recently discovered pathway for the surface exposure of lipoproteins. The surface-exposed and secreted proteins serve roles in host-pathogen interactions, including adhesion to host cells and extracellular matrix proteins, evasion of nutritional immunity imposed by iron-binding proteins of the host, prevention of complement activation, neutralization of antimicrobial peptides, degradation of immunoglobulins, and permeabilization of epithelial layers. Furthermore, they have roles in interbacterial interactions, including the formation and dispersal of biofilms and the suppression of the growth of bacteria competing for the same niche. Here, we will review the protein secretion systems of *N. meningitidis* and focus on the functions of the secreted proteins.

**Keywords: *Neisseria meningitidis*, secretome, autotransporters, two-partner secretion system, host-pathogen interactions, immune evasion, biofilms**

OPEN ACCESS

***Edited by:***
*Sophie Bleves,*
*Aix-Marseille University, France*

***Reviewed by:***
*Susu M. Zughaier,*
*Emory University, United States*
*Charlene Kahler,*
*University of Western Australia, Australia*

****Correspondence:***
*Jan Tommassen*
*j.p.m.tommassen@uu.nl*

***Received:*** *17 March 2017*
***Accepted:*** *29 May 2017*
***Published:*** *16 June 2017*

***Citation:***
*Tommassen J and Arenas J (2017) Biological Functions of the Secretome of Neisseria meningitidis. Front. Cell. Infect. Microbiol. 7:256. doi: 10.3389/fcimb.2017.00256*

## INTRODUCTION

The gram-negative diplococcus *Neisseria meningitidis* is a commensal bacterium residing in the upper respiratory tract of humans. It is transmitted through aerosols and can asymptomatically be present in up to 30% of the population for long periods exceeding 2 years. It is a close relative of another commensal of the nasopharynx, *Neisseria lactamica*, and of the pathogen *Neisseria gonorrhoeae*, which causes infections of the urogenital system. Incidentally, also *N. meningitidis* is pathogenic when it crosses the epithelial barriers of the nasopharynx to reach the bloodstream causing septicemia. From there, it can cross the blood-brain barrier causing meningitis (Pace and Pollard, 2012; Takada et al., 2016). Meningococcal disease has an incidence rate that ranges from <1 to 1,000 cases per 100,000 per year with large geographical and temporal differences (Rouphael and Stephens, 2012). It is lethal in 10% of the cases and causes severe sequelae in 30–50% of the survivors, including neurologic disabilities, seizures, hearing or visual loss, or cognitive impairment (Pace and Pollard, 2012). The high morbidity and mortality of the disease has urged in the past decades the development of suitable vaccines.

Based on the structure of the capsular polysaccharide, *N. meningitidis* is divided into 13 serogroups, five of which (A, B, C, W, and Y) are responsible for the majority of meningococcal disease. Vaccines have been developed based on the capsular polysaccharides of serogroups A, C, W, and Y (Crum-Cianflone and Sullivan, 2016). However, the capsule of serogroup B is not

immunogenic and, therefore, a capsule-based vaccine for this serogroup could not be developed. Vaccines based on outer-membrane vesicles (OMVs) have been designed against serogroup B strains, but their efficacy was restricted to determined geographic areas affected by certain clones (Bjune et al., 1991; Oster et al., 2005). In the quest for alternative vaccine candidates, new cell-surface-exposed and secreted proteins have been identified and extensively studied in recent years. These studies have resulted in two vaccine formulations, Bexsero® (4CMenB) and Trumenba® (MenB-FHbp), with an expected broader spectrum than OMV-based vaccines (Crum-Cianflone and Sullivan, 2016). In addition, they have provided extensive insights into the functions of the surface-exposed and secreted proteins and their role in the biology of *N. meningitidis*.

Although certain lineages of *N. meningitidis* are highly invasive and frequently associated with the disease, the bacteria have evolved to live in the host asymptomatically. After entering a host, the bacteria adhere to epithelial surfaces in the nasopharynx, where they form microcolonies (Sim et al., 2000). These structures resemble biofilms and help the bacteria to persist under adverse conditions. As a commensal, *N. meningitidis* has evolved different mechanisms to evade the host immune system and to compete with other members of the oral microbiome. It has to scavenge the environment for nutrients, which are restricted in this niche. In all these processes, various components of the secretome, i.e., the total of proteins that are secreted across the cell envelope to the cell surface or beyond, are implicated. It has been a decade since the last review of the secretome of *N. meningitidis* (van Ulsen and Tommassen, 2006). Since then, significant progress has been made in solving the functions of the secreted proteins. In this review, we first briefly describe the protein translocation systems that are relevant for the secretion of proteins in *N. meningitidis*. Then, we describe the current insights into the functions of the secreted proteins.

## PROTEIN TRANSLOCATION SYSTEMS IN *N. MENINGITIDIS*

In Gram-negative bacteria, several conserved pathways have evolved for the translocation of proteins across the cell envelope into the extracellular milieu (Costa et al., 2015). Of these pathways, the autotransporter, two-partner secretion (TPS), and the type I secretion (T1S) systems are active in *N. meningitidis*. In addition, these bacteria use a recently discovered mechanism, which is dependent on a member of a protein family called Slam, for the cell-surface exposure of lipoproteins (Hooda et al., 2016). The T1S system (T1SS) mediates the secretion of substrates in one step from the bacterial cytoplasm across the two membranes into the milieu. In the other pathways, the substrates are first translocated across the inner membrane, after which the periplasmic intermediate is translocated across the outer membrane. To varying extent, these two-step pathways deploy general machinery for the localization of envelope proteins, i.e., the Sec and Tat systems for protein translocation across the inner membrane, the Lol system for shuttling lipoproteins across the periplasm, and the BAM system for the assembly of integral outer membrane proteins (OMPs). In this section, we briefly describe the protein transport systems that are relevant in *N. meningitidis* and emphasize what is known about these systems in this organism. It is noteworthy that fundamental research in *Neisseria* spp. has played a leading role in uncovering some of these systems, particularly the autotransporter mechanism, the BAM system, and the Slam-dependent pathway. Except for Sec and Tat, the other translocation systems have been studied at least to some extent in *N. meningitidis*. For more extensive descriptions of the pathways, we refer in each subsection to specialized recent reviews.

### Transport and Assembly of Integral OMPs

Integral OMPs are not part of the secretome as they are not translocated across the entire cell envelope. Therefore, their functions are not discussed in this review. However, since their translocation and assembly machinery is deployed by protein secretion systems, this machinery will be described here.

The vast majority of integral OMPs consists of antiparallel amphipathic β-strands that form closed cylindrical structures, called β-barrels. They are synthesized in the cytoplasm as precursors with an N-terminal signal sequence, which marks them for transport across the inner membrane via the Sec system (von Heijne, 1990). The Sec system (for recent reviews, see Lycklama a Nijeholt and Driessen, 2012; Tsirigotaki et al., 2017) has, so far, not been studied in *N. meningitidis*, but homologs of all components have been identified in the available genome sequences (van Ulsen and Tommassen, 2006), and, therefore, it presumably functions similarly as in model organisms like *Escherichia coli*. In *E. coli*, the Sec system includes a chaperone, SecB, which prevents aggregation of client proteins in the cytoplasm and guides them to the inner membrane components of the system (**Figure 1A**). In the inner membrane, the heterotrimeric SecYEG complex forms the protein-translocating channel. Energy for transport is provided by the motor protein SecA, which hydrolyzes ATP, and by the proton-motive force, which is coupled to the translocation process presumably by the SecDF-YajC complex (Tsukazaki et al., 2011). After passage of the precursor through the Sec translocon, its signal sequence is removed by the signal peptidase LepB (Auclair et al., 2012).

All integral OMPs studied so far use the Sec system for translocation across the inner membrane. The channel in the SecYEG translocon is narrow and only allows for the translocation of completely unfolded proteins in a linear fashion. Some proteins have to be exported in a folded form, e.g., because they bind a co-factor in the cytoplasm. Such proteins share a consensus "twin-arginine" motif ([S/T]-R-R-x-F-L-K) in the N-terminal region of their signal sequences, and they use an alternative apparatus, the twin-arginine translocation (Tat) system, to cross the inner membrane (for recent reviews, see Palmer and Berks, 2012; Patel et al., 2014). The Tat system of *E. coli* consists of three proteins, TatA, TatB, and TatC, all of which are also present in *N. meningitidis* (van Ulsen and Tommassen, 2006).

Once OMPs are released from the Sec machinery, chaperones, such as SurA and Skp, bind the mature proteins to prevent their aggregation in the periplasm (**Figure 1A**). In *E. coli*, SurA appears

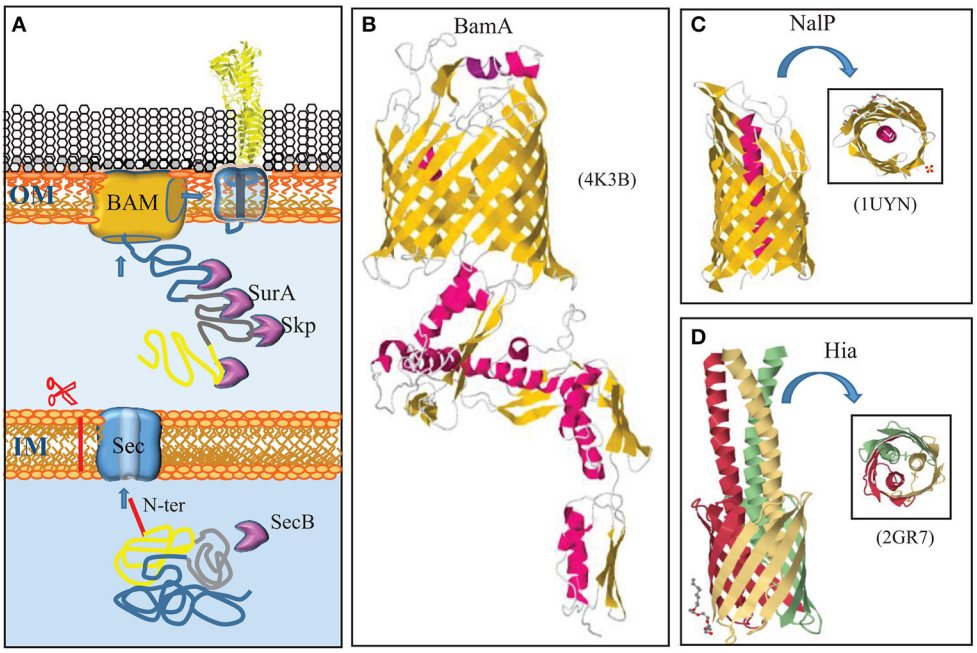


**FIGURE 1 |** Autotransporter secretion system. **(A)** Autotransporters use the same machinery to reach the outer membrane (OM) as integral OMPs. They are synthesized with a cleavable N-terminal signal sequence (red) for translocation across the inner membrane (IM) via the Sec translocon. After periplasmic transit, escorted by chaperones like Skp and SurA, the C-terminal β-domain (blue) is integrated as a β-barrel into the OM by the BAM complex. Presumably during this integration, the passenger domain (yellow) is transported to the cell surface. A segment that connects the passenger with the β-domain (gray) forms an α-helix that plugs the channel within the barrel. **(B)** Structure of the central component of the BAM system, BamA, from *N. gonorrhoeae* (Noinaj et al., 2013). BamA is constituted of a β-barrel in the outer membrane and five periplasmic POTRA domains. α-Helices and β-strands are shown in red and yellow, respectively. **(C)** Structure of the β-domain of the autotransporter NalP with the α-helix that plugs the β-barrel and exposes the passenger, if connected, at the cell surface, indicated in red (Oomen et al., 2004). **(D)** Structure of the β-domains of the trimeric autotransporter Hia of *H. influenzae* (Meng et al., 2006). Each subunit is indicated with a different color. In panels **(C,D)**, a top view is shown in the insets. The structural data were retrieved from the Protein Data Bank (PDB) and access codes are provided in brackets. References are provided in the text.

to be the main periplasmic chaperone for OMPs as its depletion drastically reduces the OMP content, whereas depletion of Skp had only minor effects (Sklar et al., 2007). In sharp contrast, mutational analysis indicated that SurA has no appreciable role in OMP biogenesis in *N. meningitidis*, whereas deletion of *skp* affected the major OMPs, i.e., the porins (Volokhina et al., 2011). Also the protease DegP has been suggested to have a role as a periplasmic chaperone in OMP biogenesis (Sklar et al., 2007; Krojer et al., 2008). However, its primary role in this process presumably is the degradation of toxic and membrane-damaging misfolded OMPs in the periplasm (Ge et al., 2014). Inactivation of DegQ, the DegP homolog of *N. meningitidis*, did not have any appreciable effect on OMP biogenesis (Volokhina et al., 2011).

After transit of the periplasm, OMPs are assembled into the outer membrane by the β-barrel assembly machinery (BAM) (**Figure 1A**) (for a recent review, see Noinaj et al., 2017). The central component of the BAM was originally discovered by Voulhoux et al. (2003) in *N. meningitidis*. This protein, previously known as Omp85 and now called BamA, is essential for bacterial viability and homologs are found in all Gram-negative bacteria and even in mitochondria, where it performs a similar function (Walther et al., 2009). The first complete BamA crystal structure solved was that of *N. gonorrhoeae* (Noinaj et al., 2013). The protein consists of a C-terminal 16-stranded β-barrel, which is inserted into the outer membrane, and five repeated polypeptide transport-associated (POTRA) domains extending into the periplasm (**Figure 1B**). In *E. coli*, BamA forms a complex with four lipoproteins, BamB, C, D, and E. These lipoproteins are less conserved, and only BamD is essential (Ricci and Silhavy, 2012; Noinaj et al., 2017). The BAM of *N. meningitidis* lacks the BamB component, but it contains the peptidoglycan-associated OMP RmpM, which stabilizes the complex (Volokhina et al., 2009). Also in *N. meningitidis*, BamD is essential (Volokhina et al., 2009), but a *bamD* mutant (originally described as *comL* mutant) of *N. gonorrhoeae* appeared to be viable (Fussenegger et al., 1996).

## Autotransporter Secretion

The first autotransporter ever described is the IgA protease of *N. gonorrhoeae* (Pohlner et al., 1987). It is a classical autotransporter that consists of an N-terminal signal sequence for transport across the inner membrane via the Sec system, a secreted passenger domain, and a C-terminal β-domain. The β-domain was suggested to insert as a β-barrel into the outer membrane to form a pore through which the passenger domain is secreted without assistance of any other proteins, hence the

name autotransporter. The first crystal structure of such a β-domain that was solved, i.e., that of the autotransporter NalP of *N. meningitidis*, seemed to confirm this idea (Oomen et al., 2004). This structure revealed a 12-stranded β-barrel with an internal hydrophilic pore filled by an N-terminal α-helix that would expose the passenger, if connected, at the cell surface (**Figure 1C**). However, it was also noticed that the internal pore was very narrow, probably too narrow to allow for the passage of a linear polypeptide that contains even small structural elements such as oligopeptide loops formed by disulfide bonds.

It is clear now that the name autotransporter is an oversimplification of the secretion pathway that is used. Autotransporters largely utilize for their secretion the machinery that is used by OMPs (**Figure 1A**) (for a recent review, see Grijpstra et al., 2013). First, they are translocated across the inner membrane by the Sec machinery. In the periplasm, they are escorted by chaperones, such as SurA, Skp, and DegP (Purdy et al., 2007; Ieva and Bernstein, 2009; Ruiz-Perez et al., 2009), although inactivation of the corresponding genes had no noticeable effect on autotransporter biogenesis in *N. meningitidis* (Volokhina et al., 2011). Also the BAM complex in the outer membrane is required for autotransporter biogenesis (Voulhoux et al., 2003), presumably for the insertion of the β-domain but possibly also for the translocation of the passenger domain, as a passenger stalled in the translocation process could be cross-linked to BamA (Ieva and Bernstein, 2009). It was proposed that the β-domain of the autotransporter and the β-barrel of BamA form a hybrid barrel with an internal diameter that is wide enough to allow for the translocation of the passenger, even if it contains small folded domains (Ieva et al., 2011). Protein folding at the cell surface probably provides the energy source to drive translocation (Drobnak et al., 2015). After outer membrane translocation, the passenger domain can remain attached to the β-domain, or it can be released into the extracellular milieu by one of several proteolytic mechanisms (Grijpstra et al., 2013). For the mechanisms relevant in *N. meningitidis*, we refer to the description of the individual autotransporters below. Besides the BAM complex, also the TAM complex may play a role in the secretion of a subset of autotransporters (Selkrig et al., 2012). The TAM complex consists of an OMP, TamA, which is a homolog of BamA, and an inner membrane protein TamB, which spans the periplasm and interacts with TamA. The precise role of the TAM complex is unclear. Reconstitution experiments showed that the BAM complex and chaperone SurA were necessary and sufficient to mediate the translocation of an autotransporter into proteoliposomes (Roman-Hernandez et al., 2014). Perhaps, TAM can substitute for BAM for some autotransporters. The role of TAM in autotransporter secretion has not been investigated in *N. meningitidis*.

Among autotransporters, four subcategories can be distinguished (Grijpstra et al., 2013). Two of them are present in *N. meningitidis*, the classical autotransporters, which include IgA protease and NalP, and the trimeric autotransporters. In trimeric autotransporters, the β-domains of each subunit contribute four β-strands to form a similar 12-stranded β-barrel as does the β-domain of the classical autotransporters (**Figure 1D**) (Meng et al., 2006). The structure of the passenger domain, however, is entirely different, as will be discussed further below.

## Two-Partner Secretion (TPS) System

The TPS system facilitates the secretion of very large β-helical proteins with often virulence-related functions (for a recent review, see Jacob-Dubuisson et al., 2013). The two partners are the secreted protein, which is generically called TpsA, and a dedicated transporter in the outer membrane called TpsB (**Figure 2A**). TpsB is a homolog of BamA. From the C to the N terminus, it consists of a 16-stranded β-barrel, two POTRA domains at the periplasmic side, and an α-helix that plugs the channel in the barrel (**Figure 2B**) (Clantin et al., 2007). TpsA is transported across the inner membrane by the Sec system and escorted in the periplasm by chaperones (Jacob-Dubuisson et al., 2013). The mature TpsA contains a conserved TPS domain near the N terminus that is recognized by the POTRA domains of TpsB (**Figure 2B**). This interaction leads to removal of the plug helix and further conformational changes in TpsB (Maier et al., 2015), allowing for the transport of TpsA to the cell surface via the barrel of TpsB. *N. meningitidis* strains generally contain at least one conserved locus with *tps* genes, but genome sequence analysis indicated that various strains can contain up to five different *tpsA* genes and two *tpsB* genes (van Ulsen and Tommassen, 2006; van Ulsen et al., 2008). One of the TpsB proteins was shown to have broad substrate specificity, whereas the other one was specific for the TpsA encoded by the same operon (ur Rahman and van Ulsen, 2013). Substrate specificity was shown to be determined by the POTRA domains (ur Rahman et al., 2014).

## Transport of Lipoproteins to the Outer Membrane

Besides integral OMPs, the outer membrane contains lipoproteins, which are peripherally attached to the membrane via an N-terminal lipid moiety. Lipoproteins are synthesized as precursors with an N-terminal signal sequence for export via the Sec or Tat machinery. Their signal sequences contain at the C terminus a conserved motif, [LVI][ASTVI][GAS]C, called lipobox, where the conserved cysteine represents the first residue of the mature protein (Hayashi and Wu, 1990). After translocation across the inner membrane, this cysteine is modified (for a recent review, see Buddelmeijer, 2015). First, a diacylglycerol moiety derived from phosphatidylglycerol is covalently attached to the sulfhydryl group of the cysteine by the enzyme lipoprotein diacylglyceryl transferase (Lgt) (**Figure 3**). Then, the signal sequence is cleaved by the dedicated lipoprotein signal peptidase LspA, after which the α-amino group of the cysteine is acylated by the enzyme apolipoprotein N-acyltransferase (Lnt) (**Figure 3**). In *E. coli*, these three enzymes are essential. However, the *lnt* gene could be inactivated in *N. meningitidis* and *N. gonorrhoeae* (LoVullo et al., 2015; da Silva et al., 2016). As the outer membrane contains essential lipoproteins, such as BamD (see above), this implies that these *Neisseria* spp., in contrast to *E. coli*, can transport diacylated lipoproteins to the outer membrane, which was indeed demonstrated in *N. meningitidis* (da Silva et al., 2016).

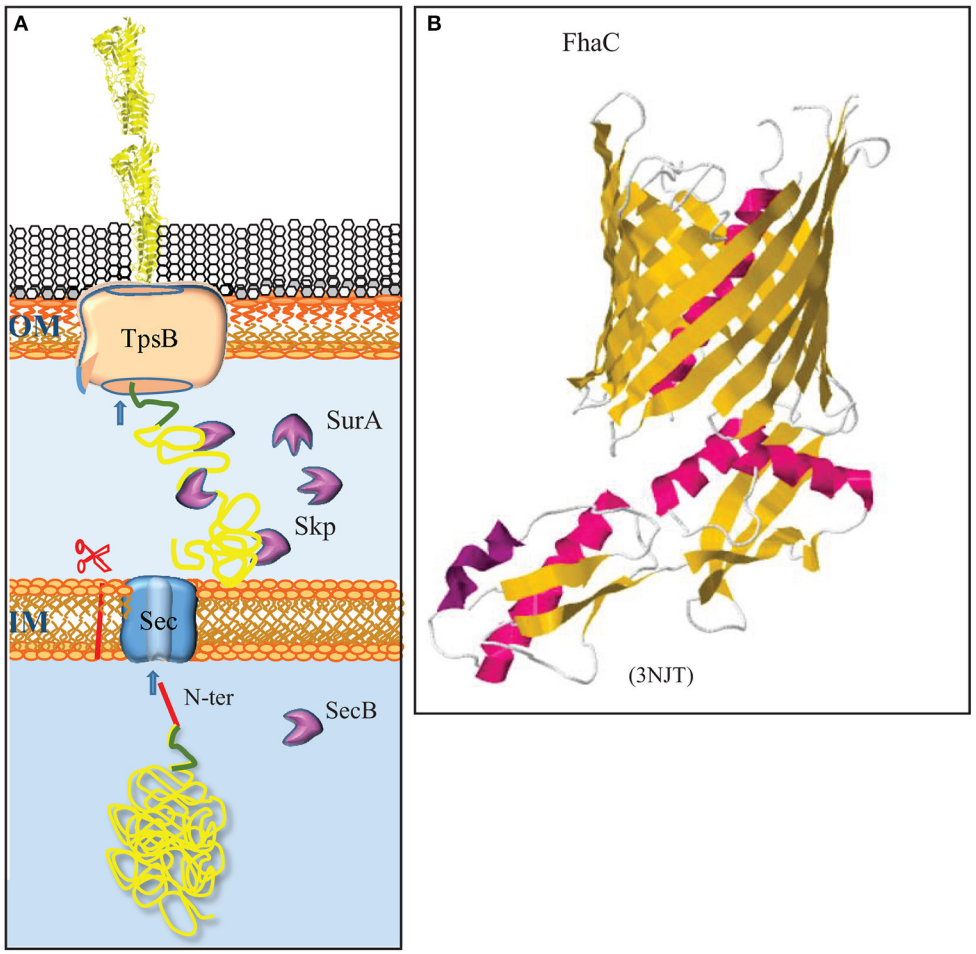


**FIGURE 2 |** The two-partner secretion system. **(A)** The TpsA substrates contain a cleavable signal sequence (red) for Sec-mediated translocation across the inner membrane (IM). After chaperone-escorted transit of the periplasm, the N-terminal TPS domain (green) interacts with the integral OMP TpsB, which mediates transport across the outer membrane (OM). **(B)** Structure of the TpsB FhaC of *B. pertussis* (Clantin et al., 2007). TpsB consists of a β-barrel domain embedded in the OM and two periplasmic POTRA domains that interact with the TPS domain of substrates. The first POTRA domain is connected via a linker with an N-terminal α-helix that plugs the β-barrel in the resting state. The structure of the R450A mutant of FhaC is depicted to show the plugging of the channel. β-Strands and α-helices are colored yellow and red, respectively. The PDB access code is provided in brackets.

After their maturation, lipoproteins can remain attached to the inner membrane or be transported to the outer membrane. In *E. coli*, the destination of the lipoprotein is determined by the identity of the amino-acid residue directly adjacent to the lipidated N-terminal cysteine (Yamaguchi et al., 1988). Basically, an aspartate residue at the +2 position functions as an inner-membrane-retention signal, whilst lipoproteins destined to outer membrane have a different residue at this position. However, this signal appears to be species specific as other sorting rules were reported for lipoproteins in other bacteria (Schulze and Zückert, 2006; Narita and Tokuda, 2007). The sorting rules for lipoproteins in *N. meningitidis* have not been determined, but the simple +2 rule of *E. coli* does not seem to apply as a DsbA lipoprotein with a serine at the +2 position was experimentally demonstrated to localize to the inner membrane (Tinsley et al., 2004).

Lipoproteins are targeted to the periplasmic side of the OM by the Lol system. This system consists of an ATP-binding cassette (ABC) transporter LolCDE in the inner membrane, a periplasmic chaperone LolA, and LolB, which functions as a receptor in the outer membrane (**Figure 3**) (for a recent review, see Narita and Tokuda, 2016). The LolCDE complex consists of a heterodimer of two homologous integral membrane proteins, LolC and LolE, which is associated with a dimer of the cytoplasmic ABC protein LolD. This complex selects the substrate lipoproteins that don't carry an inner-membrane retention signal and provides the energy to release them from the inner membrane by ATP hydrolysis (Yakushi et al., 2000). Interestingly, *N. meningitidis* and *N. gonorrhoeae*, as well as many other Gram-negative bacteria, each contain only a single protein that is homologous to LolC and LolE and that has specific characteristics of both of them (**Figure 3**) (LoVullo et al., 2015). This protein, which

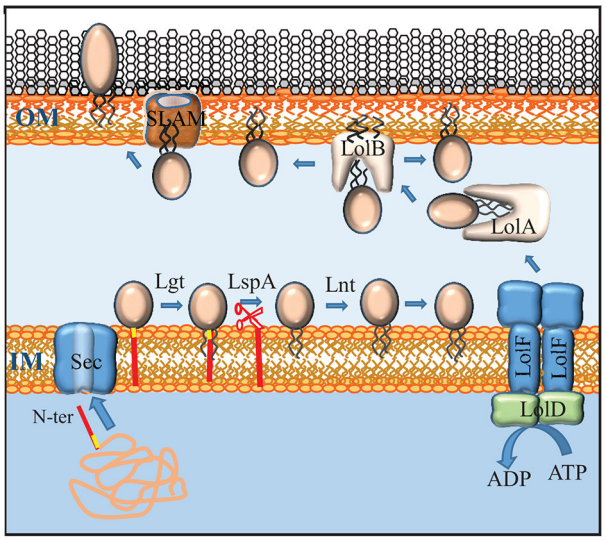


**FIGURE 3 |** Maturation, transport and secretion of lipoproteins. Lipoproteins contain a lipobox (yellow) at the C terminus of their signal sequence (red). After transport across the inner membrane (IM) by the Sec system, the lipoprotein precursor is modified by the addition of a diacylglyceryl moiety to the sulfhydryl group of the cysteine in the lipobox by Lgt, followed by cleavage of the signal sequence by LspA, and the addition of a third, amide-linked fatty acyl chain by Lnt. Lipoproteins that don't contain an IM-retention signal (also called Lol-avoidence motif) are expelled from the IM by an ABC transporter that, in *Neisseria*, consists of a dimer of LolF (instead of the LolCE heterodimer found in *E. coli*) and a dimer of LolD. The chaperone LolA shields the lipid moiety of the lipoprotein during periplasmic transit and shuttles it to the receptor LolB that inserts it into the inner leaflet of the OM. Some lipoproteins are translocated to the outer face of the OM via a mechanism that requires a SLAM protein. Whether SLAM forms the actual translocation channel itself is not known.

is called LolF, presumably forms a homodimer in the inner membrane, and it was suggested that the presence of a LolF instead of LolCE is related to the capacity of these bacteria to transport diacylated lipoproteins, i.e., lipoproteins not modified by Lnt, to the outer membrane (LoVullo et al., 2015). After release from the inner membrane, the lipoprotein is captured by the chaperone LolA, which shields its hydrophobic lipid moiety from the aqueous environment of the periplasm, thus forming a water-soluble complex (Matsuyama et al., 1995). From LolA, the lipoprotein is transferred to LolB, which is a structural homolog of LolA. LolB is a lipoprotein itself and it is attached with its lipid moiety in the OM (**Figure 3**). LolB then mediates the insertion of the lipoprotein into the inner leaflet of the OM (Matsuyama et al., 1997).

## Transport of Lipoproteins to the Cell Surface

How lipoproteins are translocated across the outer membrane to reach the cell surface has only been studied in few exceptional cases but is an emerging field of research (for a recent review, see Wilson and Bernstein, 2017). In the best studied cases, the lipoproteins utilize conserved protein secretion systems to reach the cell surface, such as the type 2 secretion system (T2SS) (for a review, see Nivaskumar and Francetic, 2014), a system that is related to the machinery required for the biogenesis of type IV pili but is not operational as a protein secretion system in *N. meningitidis*. In this case, the lipoproteins contain an inner membrane retention signal to avoid the Lol system after their transport across the inner membrane via Sec or Tat (Pugsley and Kornacker, 1991; Putker et al., 2013). These lipoproteins are directly secreted from the periplasmic side of the inner membrane to the cell surface using the T2S machinery. Other lipoproteins, such as NalP of *N. meningitidis* (van Ulsen et al., 2003), are autotransporters. Before translocation across the outer membrane, these autotransporter lipoproteins presumably use the Lol system to reach the inner face of the outer membrane, although this has experimentally not yet been proven. Recently, a new general pathway dedicated to the transport of lipoproteins to the cell surface was uncovered in *N. meningitidis* (Hooda et al., 2016). This pathway is an extension of the Lol pathway as the substrates appear to use the Lol system to reach the outer membrane. A family of proteins named surface lipoprotein assembly modulator (Slam) was found to be involved in the subsequent translocation across the outer membrane (**Figure 3**). Slam proteins consist of an N-terminal periplasmic domain containing two tetratricopeptide repeats and a C-terminal 14-stranded β-barrel embedded in the outer membrane. There is no homolog of Slam proteins in *E. coli*, and the synthesis of cell-surface-exposed lipoproteins from *N. meningitidis* in *E. coli* does not lead to their cell-surface exposition. However, when Slam was co-expressed, these lipoproteins were transported to the *E. coli* cell surface (Hooda et al., 2016). Whether Slam forms the actual translocation channel for the lipoproteins or guides them to an alternative translocation apparatus, such as BAM, remains to be investigated. *N. meningitidis* has two Slam proteins with different substrate specificity. Slam1 has broad specificity and is involved in the translocation of at least the transferrin-binding protein B (TbpB), the lactoferrin-binding protein B (LbpB), and the factor H-binding protein (fHbp). Slam2 appears to be specific for hemoglobin-haptoglobin utilization protein A (HpuA). Interestingly, these lipoproteins, as well as another cell-surface-exposed lipoprotein, i.e., neisserial heparin-binding antigen (NHBA), show considerable structural similarity (see below), which may reflect a prerequisite for Slam-dependent transport and/or a common evolutionary origin. Slam homologs are widely distributed among proteobacteria (Hooda et al., 2016), suggesting that they represent a new general pathway dedicated to the secretion of lipoproteins. It is noteworthy, however, that TbpB expressed in *N. gonorrhoeae* without its lipid moiety was secreted into the culture supernatant (Ostberg et al., 2013), suggesting that the Slam-dependent pathway may have broader specificity than just lipoproteins.

## Type 1 Secretion System (T1SS)

The T1SS is composed of three proteins: an ABC protein in the inner membrane, a TolC-type channel protein in the outer membrane, and a membrane-fusion protein that connects the integral inner and outer membrane components (**Figure 4A**) (for a recent review, see Lenders et al., 2013). The outer membrane component is trimeric protein that forms a 12-stranded β-barrel

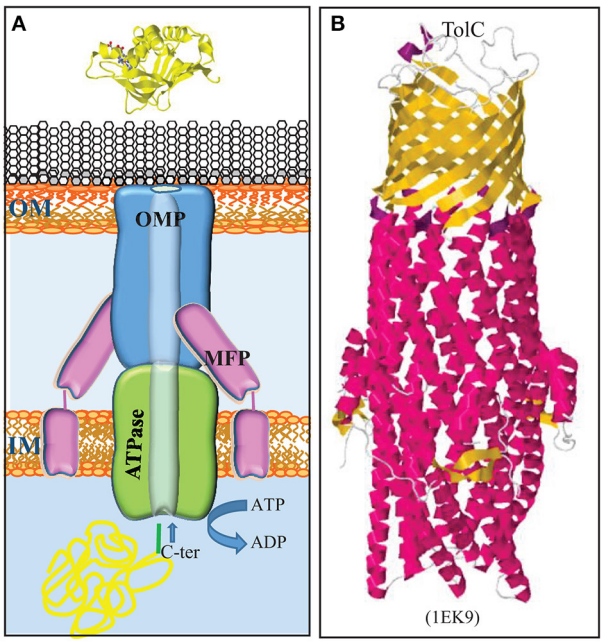


**FIGURE 4 |** Type 1 secretion system. **(A)** The T1SS consists of three proteins, a trimeric OMP (blue), an ABC transporter in the inner membrane (IM) (green), and an IM-anchored membrane-fusion protein (MFP) (pink), which together form a translocation channel for substrates directly from the bacterial cytoplasm to the external milieu. Substrates contain a secretion signal at their C terminus (green) for recognition by the machinery. **(B)** Structure of the homotrimeric OM T1SS component of *E. coli*, TolC (Koronakis et al., 2000). The trimer consists of a β-barrel in the OM and long α-helices, which form a tunnel that deeply penetrates into the periplasm. β-Strands and α-helices are colored yellow and red, respectively. The PDB access code is given in brackets.

in the outer membrane to which each protomer contributes four β-strands (**Figure 4B**). At the periplasmic side, the β-strands are connected by long α-helices that form together a long hollow conduit that spans the periplasm and reaches the ABC transporter in the inner membrane (Koronakis et al., 2000). This machinery mediates the secretion of substrates directly from the cytoplasm into the extracellular milieu without a periplasmic intermediate (**Figure 4A**). Thus, these substrates do not contain an N-terminal signal sequence for recognition by the Sec or Tat systems. Instead, they contain a recognition signal at the C terminus to interact with the ABC component of the T1SS. Many T1SS substrates belong to the RTX protein family, where RTX stands for repeats in toxin (Linhartová et al., 2010). These proteins contain glycine-rich repeats with the consensus sequence GGxGxDxxx (where x is any amino acid) near the secretion signal. These repeats bind calcium ions, which promotes folding in the extracellular medium where, in contrast to the cytoplasm, the concentration of calcium is high. Thus, besides ATP hydrolysis and the proton-motive force, extracellular folding might provide a driving force for translocation (Lenders et al., 2013). The components constituting the T1SS of *N. meningitidis* have been identified (Wooldridge et al., 2005).

## STRUCTURE AND FUNCTION OF SECRETED PROTEINS

**Table 1** summarizes the functions of the secreted proteins that are discussed in detail below.

### Cell-Surface-Exposed Lipoproteins

In this section, we discuss the structure and function of five well-characterized cell-surface-exposed lipoproteins. Two other such lipoproteins, i.e., the autotransporter NalP and FrpD, which has a role in the T1SS, are discussed in subsequent sections. Several other lipoproteins have been suggested in the literature to be exposed at the cell surface in *N. meningitidis*. However, even if their function is known, it is not clear why they are transported to the cell surface to exert such function, and in some cases, their function is even incompatible with surface localization. We don't discuss these lipoproteins here and feel that their localization should be further investigated. For a discussion about caveats and pitfalls in assessing lipoprotein localization, see Wilson and Bernstein (2017).

#### Lipoproteins Involved in Iron Acquisition: TbpB, LbpB, and HpuA

One of the primary defense mechanisms of a host against invading bacterial pathogens is to deprive them from essential nutrients, such as iron, a defense mechanism that is known as nutritional immunity. In the human host, iron is bound by proteins, such as transferrin in serum, lactoferrin in secretions and mucosal surfaces, and hemoglobin and ferritin within cells. These proteins have very high affinities for iron, and, consequently, the concentration of free iron in the human fluids is too low to support microbial growth (Weinberg, 2009). Many bacteria produce siderophores, which are low-molecular-weight iron chelators that sequester otherwise inaccessible ferric iron from the environment. However, *Neisseria* spp. do not secrete siderophores; instead, they synthesize receptors that directly hijack iron sequestered in the iron-binding proteins of the host (Schryvers and Stojiljkovic, 1999). Several of these receptors consist of two proteins, a surface-exposed lipoprotein and an integral OMP. The integral OMP belongs to the TonB-dependent family (Tdf) of receptors, which includes also siderophore receptors. These receptors form 22-stranded β-barrels that are closed by an N-terminal plug. They interact with the TonB complex in the inner membrane, which deploys the proton-motive force to energize transport across the outer membrane (for a review, see Noinaj et al., 2010).

The transferrin receptor in *Neisseria* spp. consists of the Tdf member TbpA and the surface-exposed lipoprotein TbpB. The synthesis of these proteins is induced under iron limitation. In *N. meningitidis*, both proteins are essential for the acquisition of iron from human transferrin (Irwin et al., 1993), whilst TbpB is dispensable in *N. gonorrhoeae*, although its presence considerably enhances the efficiency of the process (Anderson et al., 1994). Both proteins can bind transferrin, but, in contrast to TbpA, TbpB preferably binds the iron-loaded form (Cornelissen and Sparling, 1996; Boulton et al., 1998). Thus, TbpB may enhance iron acquisition by selecting holo-transferrin to bind to the

**TABLE 1 |** Secretion mechanism and functions of secreted proteins.

| Protein | Secretion system[a,b] | Biological functions[c] |
|---|---|---|
| TbpB | Slam | Iron acquisition from transferrin |
| LbpB | Slam | Iron acquisition from lactoferrin |
| | | Protection against lactoferricin |
| HpuA | Slam | Heme iron acquisition from hemoglobin(-haptoglobin) |
| fHbp | Slam | Prevention of complement activation by binding factor H |
| | | Protection against host defense peptide LL-37 |
| NHBA | Slam? | Serum resistance by binding heparin |
| | | Adhesion by binding heparan sulfate proteoglycans |
| | | Initiation of biofilm formation |
| | | Increase of endothelial permeability |
| IgA protease | Classical AT | Cleavage of IgA and other host proteins |
| | | Immune modulation by cleavage transcription factor NF-κB |
| | | Initiation of biofilm formation |
| | | Binding heparin |
| NalP | Classical AT | Proteolytic release of bacterial cell-surface-exposed proteins Cleavage of complement factor C3 |
| App, AusI | Classical AT | Binding of histones and cleavage of histone H3 |
| | | Induction of apoptosis |
| | | Adhesion |
| AutA | Classical AT | Autoaggregation |
| | | Stimulation of $CD4^+$ T-cells and B-cells |
| AutB | Classical AT | Biofilm formation |
| NadA | Trimeric AT | Adhesion and invasion |
| | | Binding Hsp90 |
| NhhA | Trimeric AT | Adhesion |
| | | Binding laminin and heparan sulfate |
| | | Serum resistance by binding vitronectin |
| | | Apoptosis of macrophages |
| | | Immune modulation by affecting differentiation monocytes |
| TpsA | TPS | Interbacterial competition |
| | | Intracellular survival |
| | | Adhesion |
| | | Biofilm formation |
| FrpC | T1SS | Adhesion |
| FrpD | Slam? | Adhesion |
| MafB | Unknown | Interbacterial competition |
| TspB | Unknown | Binding immunoglobulins |
| | | Biofilm formation |

[a] *Question marks indicate that suggested secretion mechanism is not demonstrated.*
[b] *AT, autotransporter.*
[c] *For references, see text.*

receptor. In addition, TbpB's affinity for the holo form may help in the release of the apo form from the receptor once iron is delivered. TbpB is a bilobed protein probably resulting from gene duplication. Each lobe consists of a β-barrel domain and an adjacent handle domain, which is also rich in β-sheet structure (**Figure 5**) (Calmettes et al., 2012; Noinaj et al., 2012). Human transferrin is also a bilobed protein with a $Fe^{3+}$-binding site within each lobe (Hall et al., 2002). Structural analysis revealed that TbpA and TbpB both bind the C-lobe of transferrin using non-overlapping binding sites (Noinaj et al., 2012). The C-lobe of transferrin consists of two subdomains, C1 and C2, which are connected by a hinge at the base of a deep cleft that contains the $Fe^{3+}$-binding site. TbpB binds both the C1 and C2 subdomains of holo-transferrin via the handle and β-barrel domains in its N-lobe, respectively (Calmettes et al., 2012). This explains the selectivity of TbpB for holo-transferrin as the apo-form shows a 51° rotation of the C2 domain which would drastically reduce the TbpB-transferrin interface (Calmettes et al., 2012). In the available structures, the C-lobe of TbpB is not involved in transferrin binding, and its function is unclear. An α-helix from extracellular loop 3 of TbpA intrudes into the cleft between the C1 and C2 subdomains of transferrin, which induces a partial opening of the cleft and destabilizes the coordination site of the ferric ion (Noinaj et al., 2012), which facilitates its release. Released iron would enter a closed chamber formed by TbpA, TbpB, and transferrin, which prevents its diffusion into the medium and positions it for further transport through the barrel of TbpA (Noinaj et al., 2012).

The lactoferrin receptor is constituted by the Tdf member LbpA and the surface-exposed lipoprotein LbpB (Pettersson et al., 1994b, 1998; Prinz et al., 1999). Whilst the corresponding genes are ubiquitous in *N. meningitidis*, they are disrupted in about half of the *N. gonorrhoeae* isolates (Anderson et al., 2003). Nevertheless, expression of a functional lactoferrin receptor in *N. gonorrhoeae* provided a competitive advantage in a human infection model, and it was essential for infection by a strain lacking the transferrin receptor (Anderson et al., 2003). LbpA and LbpB both bind lactoferrin, but LbpB is not essential for its utilization as an iron source in both species (Pettersson et al., 1998; Biswas et al., 1999). Whilst lactoferrin and transferrin are homologous proteins, also LbpA and LbpB share extensive sequence similarity with TbpA and TbpB, respectively (Pettersson et al., 1994a, 1998). Crystallization of the N lobe of LbpB revealed a structure very similar to that of the corresponding part of TbpB. It also consists of two domains, a handle domain and a β-barrel domain with long loops projecting from both domains and forming an extended cap region (**Figure 5**) (Brooks et al., 2014). *In silico* docking experiments indicated that the cap region constitutes the binding site to which lactoferrin binds with its N-lobe (Brooks et al., 2014). However, recent biochemical analysis revealed that it preferentially binds the C-lobe of iron-loaded lactoferrin (Ostan et al., 2017), just like TbpB binds the C-lobe of iron-loaded transferrin (see above), suggesting a similar role for LbpB as for TbpB in selecting iron-loaded ligands. LbpB appears to have an additional role in protecting the bacteria against the bactericidal activity of lactoferricin (Morgenthau et al., 2012).

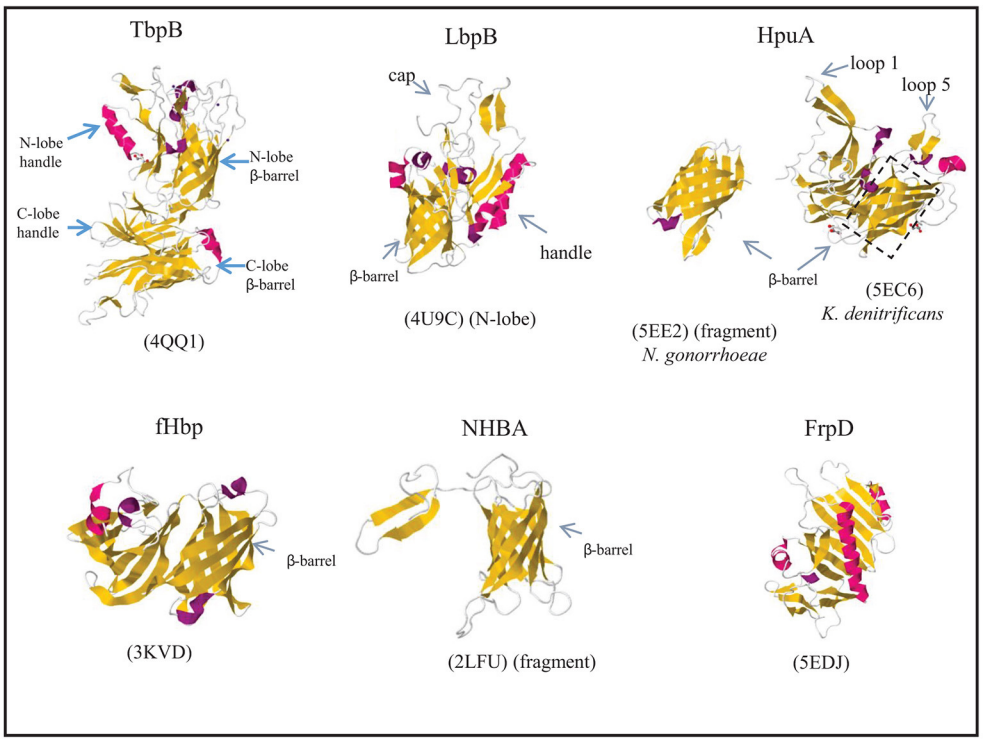


**FIGURE 5 |** Structures of surface-exposed lipoproteins in *N. meningitidis*. Where indicated, the structure of only a fragment of the complete protein is available. The structure of *N. meningitidis* HpuA has not been solved; instead, those of *K. denitrificans* HpuA and a C-terminal fragment of *N. gonorrhoeae* HpuA are shown. β-Strands and α-helices are colored yellow and red, respectively, and relevant domains of each protein are indicated. The PDB access codes are given in brackets and references are provided in the text.

Lactoferricin is a small cationic peptide, which is released from the N terminus of lactoferrin by proteolysis (Bellamy et al., 1992; Gifford et al., 2005). LbpB contains two highly variable stretches rich in negatively charged amino-acid residues in its C-lobe (Pettersson et al., 1999) that have been shown to mediate protection against this cationic peptide (Morgenthau et al., 2014). Thus, binding of the N-lobe of lactoferrin to the C-lobe of LbpB may prevent proteolysis events that generate lactoferricin. In addition or alternatively, the C-lobe may also be able to bind the free peptide, thus neutralizing its toxic effects (Ostan et al., 2017).

*N. meningitidis* can express two receptors for hemoglobin, HmbR and HpuAB, which enable it to extract heme from hemoglobin and use it as an iron source (Stojiljkovic et al., 1995; Lewis et al., 1997). Of these, the HpuAB system is also capable of extracting heme from hemoglobin-haptoglobin complexes (Lewis et al., 1997). Expression of the corresponding genes is controlled by iron availability and is prone to phase variation by slipped-strand mispairing (Lewis et al., 1999). HpuAB is a bipartite receptor, in which HpuB is a Tdf member and HpuA is a surface-exposed lipoprotein. In the absence of HpuA, HpuB still binds its ligands but with low affinity, and they cannot be used as an iron source (Rohde et al., 2002; Rohde and Dyer, 2004). Ligands did not bind to cells expressing only HpuA (Rohde and Dyer, 2004), but a direct interaction could be demonstrated in pull-down assays with purified HpuA (Wong et al., 2015). The crystal structure was solved of *Kingella denitrificans* HpuA alone and in complex with hemoglobin, and of a C-terminal fragment of *N. gonorrhoeae* HpuA (Wong et al., 2015). HpuA is about half the size of TbpB, and its structure shows a similar fold as a single lobe of TbpB (**Figure 5**). It consists of a compact C-terminal β-barrel and an N-terminal open β-sandwich domain. Two large loops, loops 1 and 5, extend from the core of the protein. These exposed loops show high sequence variability, suggesting they are under immune selection. In spite of their solvent exposure, these loops have a high content of hydrophobic amino-acid residues, and although they display high sequence variability, they are the major interaction sites of hemoglobin, with loops 1 and 5 contacting the β- and α-chains, respectively, of a hemoglobin dimer. Additional interactions involve residues on two other loops.

## Factor H Binding Protein (fHbp)

The complement system plays a key role in the host's defense against microbial invaders. Host cells are protected from complement activation, amongst others by binding the soluble factor H, a major negative regulator of the alternative complement pathway. By producing fHbp (a.k.a. GNA1870 or LP2086), *N. meningitidis* hijacks factor H and thereby limits complement activation at its surface (Madico et al., 2006; Schneider et al., 2006). Indeed, fHbp expression was found to improve bacterial survival in human blood and serum (Seib et al., 2009). Additionally, fHbp synthesis was found to protect

the bacteria against the cationic antimicrobial peptide LL-37, a host defense peptide that destabilizes negatively charged bacterial membranes (Seib et al., 2009). Presumably, LL-37 interacts with fHbp also by electrostatic interaction.

fHbp is highly immunogenic and induces bactericidal antibodies that activate the classical complement pathway. In addition, antibodies may prevent binding of factor H to fHbp and thereby prevent inhibition of the alternative pathway. Based on sequence variation, two different subfamilies (Fletcher et al., 2004) or three variant groups (Masignani et al., 2003) were distinguished, with very limited immunological cross-reactivity between the groups (Masignani et al., 2003). One and two variants are included as components in the recently developed vaccines Bexsero® and Trumenba®, respectively.

The level of expression of fHbp varies considerably between different strains (Biagini et al., 2016), which may affect vaccine efficacy. Synthesis of the protein is induced under oxygen limitation (Oriente et al., 2010). Furthermore, fHbp synthesis is post-transcriptionally controlled by temperature due to the presence of a secondary structure at the 5′ end of its mRNA, which could function as a thermosensor; expression is considerably lower at 30°C than at 37°C (Loh et al., 2016). Thus, the synthesis of fHbp is presumably low on the mucosal surfaces of the nasopharynx, where the temperature is relatively low and the oxygen concentration is high. Consequently, vaccines solely based on fHbp will possibly not prevent carriage and spreading of the bacteria amongst the population and offer limited herd immunity (Loh et al., 2016). The synthesis of fHbp will increase as the bacteria reach the submucosal epithelial surfaces and the bloodstream, i.e., when protection against the host's defense mechanisms becomes essential. The synthesis of fHbp is also influenced by iron availability. However, whilst expression is reduced under iron limitation in most strains, it is increased in some lineages (Sanders et al., 2012), which makes it difficult to speculate about the biological significance of this phenomenon. Whether there is a relation with the reported capacity of fHbp to bind siderophores produced by other bacteria (Veggi et al., 2012) is questionable as fHbp synthesis is reduced in most strains under iron limitation when siderophore production is induced. A physiological role for the siderophore-binding capacity of fHbp has not been demonstrated.

The structure of fHbp has been determined by NMR and crystallography (Cantini et al., 2009; Schneider et al., 2009). The overall fold resembles those of HpuA and of the individual lobes of TbpB and LbpB and consists of a C-terminal β-barrel and an N-terminal taco-shaped barrel-like structure (**Figure 5**). Factor H consists of 20 complement control protein repeats, and of these, repeats 6 and 7 were found to bind fHbp with extensive interactions in co-crystals (Schneider et al., 2009). Interestingly, this binding site overlaps with the binding site for glycosaminoglycans to which factor H binds on mammalian cells to prevent complement activation.

## Neisseria Heparin-Binding Antigen (NHBA)

Like fHbp, NHBA (a.k.a. GNA2132) is a component of the Bexsero® vaccine. In spite of considerable sequence variability, particularly near the N terminus (Bambini et al., 2009), NHBA elicits broadly cross-reactive bactericidal antibodies that conferred passive protection in a rat model (Welsch et al., 2003; Giuliani et al., 2010; Serruto et al., 2010).

NHBA was shown to bind heparin and heparan sulfate (Serruto et al., 2010). It consists of two domains. The structure of the conserved C-terminal domain has been determined by NMR and shows a similar 8-stranded β-barrel as those in the lipoproteins described above (**Figure 5**) (Esposito et al., 2011). The structure of the N-terminal domain has not been solved; it was predicted to be an intrinsically unfolded polypeptide (Esposito et al., 2011). In between these domains, NHBA contains an arginine-rich segment that binds heparin and heparan sulfate by electrostatic interaction (Serruto et al., 2010). The binding of heparin and heparin-like molecules has several functions. First, heparin binding was shown to correlate with increased survival of an unencapsulated *N. meningitidis* strain in human serum. In an encapsulated strain, such effect of NHBA synthesis was not observed, presumably because of the dominant role of the capsule in mediating serum resistance. As heparin is known to interact with complement proteins, including factor H, C4b-binding protein and C1 inhibitor (Yu et al., 2005), it was suggested that heparin bound at the cell surface might impart serum resistance by its capacity to bind such complement-regulatory molecules (Serruto et al., 2010). Alternatively, it might form a negatively charged capsule-like structure resembling the classical polysaccharide capsule (Serruto et al., 2010). NHBA has also been shown to function as an adhesin by binding to heparan sulfate proteoglycans that are present on surface of epithelial cells (Vacca et al., 2016).

Besides heparin and heparin-like molecules, NHBA also binds other polyanionic structures, including DNA (Arenas et al., 2013a). *N. meningitidis* forms microcolonies on the epithelial surfaces in the nasopharynx (Sim et al., 2000). Extracellular DNA (eDNA) is an important component of the extracellular matrix of these biofilm-like structures, and it is essential in the initiation of biofilm formation in most clonal lineages (Lappann et al., 2010). NHBA binds eDNA and inactivation of the *nhbA* gene in these lineages impairs biofilm formation (Arenas et al., 2013a).

NHBA can be cleaved immediately upstream of the arginine-rich segment by the autotransporter protease NalP (see below). Consequently, a C-terminal fragment including the arginine-rich segment is released into the milieu (Serruto et al., 2010). This fragment is taken up by endothelial cells and accumulates in mitochondria, where it induces the production of reactive oxygen species. The resulting phosphorylation of the adherens junction protein VE-cadherin and its subsequent internalization leads to increased endothelial permeability (Casellato et al., 2014). Thus, the released fragment of NHBA may contribute to the extensive vascular leakage that is typical for meningococcal sepsis. The arginine-rich segment was essential for this role of the NHBA C-terminal fragment presumably by functioning as a mitochondrial targeting signal. A slightly smaller fragment that is released from NHBA by lactoferrin-mediated cleavage and that lacks the arginine-rich segment did not induce endothelial leakage (Casellato et al., 2014).

## Autotransporters

### IgA Protease

IgA protease is produced by both *N. meningitidis* and *N. gonorrhoeae*. The passenger domain consists of two subdomains, an N-terminal domain containing the protease activity and a polypeptide called the α-peptide; these domains are connected via a small γ-peptide (Pohlner et al., 1987). The passenger is connected to the β-domain via a linker peptide. The protease domain can be released into the extracellular milieu by autocatalytic cleavage at sites (PAPSP, PPSP, or PPAP) located in between the protease domain and the γ-peptide, between the γ-peptide and the α-peptide, and between the α-peptide and the linker peptide. The presence of the latter processing site is strain dependent (Roussel-Jazédé et al., 2014). Alternatively, the entire passenger including the linker peptide can be released after cleavage by the autotransporter protease NalP (see below) (van Ulsen et al., 2003). IgA protease cleaves human IgA1 at a site (TPPTPSPS), which resembles the autocatalytic processing sites and is located in the hinge region between the Fab and the Fc domains (Plaut et al., 1975). IgA protease does not cleave IgA2, which lacks such a cleavage site (Plaut et al., 1975). Cleavage of IgA1 may inhibit IgA-mediated agglutination and subsequent mechanical clearance of the bacteria in the nasopharynx. IgA protease has also been shown to cleave the lysosome-associated membrane protein LAMP1 (Hauck and Meyer, 1997), which was reported to promote bacterial survival within epithelial cells (Lin et al., 1997) and transcytosis across polarized epithelia (Hopper et al., 2000). In addition, IgA protease cleaves the vesicular membrane protein synaptobrevin II in chromaffin cells (Binscheck et al., 1995) and the human chorionic gonadotropin hormone (Senior et al., 2001), but the physiological implications are not clear. All these alternative substrates have a target site resembling the autocatalytic cleavage sites.

The α-peptide contains a variable number of nuclear localization signals (NLS), which are arginine-rich peptide segments (Pohlner et al., 1995; Roussel-Jazédé et al., 2014), and it was indeed demonstrated to target an attached reporter protein to the nucleus of eukaryotic cells (Pohlner et al., 1995). When NalP releases IgA protease with attached α-peptide from the bacterial cell surface, the IgA protease is targeted to the nucleus where it cleaves the p65/RelA component of transcription factor NF-κB, thus silencing the expression of several NF-κB-responsive genes, including those encoding interleukin 8 and the anti-apoptotic protein cFLIP (Besbes et al., 2015). This altered gene expression results in sustained activation of c-Jun N-terminal kinase and apoptosis. Interestingly, purified IgA protease without attached α-peptide has been shown to inhibit TNFα-induced apoptosis of monocytes, presumably by the observed cleavage of the TNF receptor II (Beck and Meyer, 2000).

When NalP is not expressed and the autocleavage site between the α-peptide and the linker peptide is absent, the α-peptide is exposed at the bacterial cell surface covalently connected to the β-domain. Since NLS are positively charged protein segments, they bind polyanions like eDNA, thus stimulating biofilm formation (Arenas et al., 2013a). The α-peptide also binds heparin (Roussel-Jazédé et al., 2014) and may have similar functions in conferring serum resistance and mediating adhesion as discussed above for NHBA. Whether the α-peptide also directly affects gene expression by binding DNA after it has been targeted to the nucleus of eukaryotic cells has not been investigated yet.

### NalP

The *nalP* gene is found in the vast majority of *N. meningitidis* isolates, with the notable exception of invasive isolates of clonal complexes ST-269 and ST-461 (Oldfield et al., 2013). Its expression is prone to phase variation by slipped-strand mispairing at a poly-C tract in the coding region (Turner et al., 2002; van Ulsen et al., 2003). An analysis of its phase variation status revealed that approximately half of the strains were phased on, and no significant differences were found in this respect between carriage and invasive strains (Oldfield et al., 2013).

NalP is a subtilisin-like serine protease. Its passenger is released from the cell surface by autoproteolytic cleavage. However, after cleavage between the passenger and the β-domain, the passenger remains temporarily attached at the cell surface by an N-terminal lipid anchor (Roussel-Jazédé et al., 2013). In this position, it releases several autotransporters and lipoproteins from the bacterial cell surface. The release of these proteins has relevant consequences. As already discussed above, the NalP-mediated release of IgA protease with attached α-peptide and of the C-terminal part of NHBA from the cell surface stimulates apoptosis and increases the permeability of endothelial and epithelial cell layers. In contrast, when *nalP* is phased off, the α-peptide and complete NHBA are retained at the cell surface, which stimulates biofilm formation and adhesion and protects against host defenses. Thus, the absence of *nalP* expression appears to favor colonization and biofilm formation, whilst *nalP* expression may lead to dispersal of biofilms and invasion or spreading to a new host.

Another target of NalP is the LbpB component of the lactoferrin receptor (Roussel-Jazédé et al., 2010). LbpB is a very immunogenic protein, and its NalP-mediated release from the cell surface imparted protection against the complement-mediated killing by LbpB-specific bactericidal antibodies (Roussel-Jazédé et al., 2010). As discussed above, LbpB is not essential for the acquisition of iron from lactoferrin, although it may enhance the process by selecting holo-lactoferrin for binding to the receptor. The latter function may be lost when LbpB is cleaved from the cell surface by NalP, but this is compensated by protection against LbpB-specific bactericidal antibodies. Another function of LbpB discussed above, i.e., offering protection against the membrane-damaging effects of lactoferricin, is probably retained, even if the protein is released into the extracellular milieu. Thus, due to the phase-variable expression of *nalP*, a subpopulation of the bacterial cells will lose LbpB from the cell surface, and this subpopulation may be less efficient in iron acquisition but will have a competitive advantage when LbpB-specific antibodies are elicited in the host. It is noteworthy that in *N. gonorrhoeae*, which does not produce NalP because the gene is disrupted, the expression of *lbpB* itself is prone to phase variation (Anderson et al., 2003).

Besides bacterial proteins, NalP also cleaves at least one host protein, i.e., the complement factor C3. Thereby, it avoids complement activation and confers serum resistance (Del

Tordello et al., 2014). Consistently, *nalP* expression was earlier reported to be upregulated during growth in an *ex vivo* human whole-blood model and to be essential for survival under these conditions (Echenique-Rivera et al., 2011b).

### Two Additional Proteases: App and AusI

App and AusI (a.k.a. MspA) are both chemotrypsin-like serine proteases with homology to IgA protease (Abdel Hadi et al., 2001; van Ulsen et al., 2001, 2006; Turner et al., 2006). Whereas, an intact *app* gene is ubiquitous among *N. meningitidis* strains, the *ausI* gene is disrupted by premature stop codons in several strains, and its expression is prone to phase variation by the presence of a poly-C tract in the coding region (Martin et al., 2003; van Ulsen et al., 2006). Interestingly, an extensive study in mostly serogroup B and Y isolates revealed that the *ausI* gene was phased on in 90% of both invasive and carriage strains of serogroup B. As 33% phased on would be expected in the case of random on and off switching, this suggests an important role for AusI in the biology of serogroup B (Oldfield et al., 2013). Such a preference for the on phase of *ausI* was not found in the serogroup Y isolates.

App and AusI are both released from the bacterial cell surface by autoproteolytic cleavage. However, like for IgA protease, a larger form of these proteins with a C-terminal extension, called α-peptide, can be released by NalP-mediated cleavage (van Ulsen et al., 2003, 2006; Turner et al., 2006). The α-peptide of App contains two NLS similar to those in the α-peptide of IgA protease, but such sequences are not present in the α-peptide of AusI. Nevertheless, both proteins with attached α-peptides were shown to be targeted to the nucleus after being taken up by dendritic cells and to induce apoptosis, presumably by their capacity to bind histones and to cleave histone H3 (Khairalla et al., 2015). Uptake into the dendritic cells was shown to be mediated by the mannose receptor and the transferrin receptor 1 to which the proteases could be crosslinked.

Earlier, both App and AusI were reported to function as adhesins (Serruto et al., 2003; Turner et al., 2006), a function which is difficult to reconcile with their cleavage from the cell surface. Perhaps, the proteins remain temporarily associated with the cell surface before they are released. Heterologous expression of App and AusI in *E. coli* mediated adhesion of the bacteria to Chang epithelial cells, whereas variable adhesion to other cell lines was observed (Serruto et al., 2003; Turner et al., 2006). App-mediated adhesion to Chang cells could also be demonstrated in *N. meningitidis* (Serruto et al., 2003). The presence of a capsule did not seem to interfere with the adhesin function, suggesting that this large protein (∼160 kDa) extends beyond the capsule to interact with its receptor on the Chang cells. However, deletion analysis suggested that the α-peptide, which is located close to the bacterial cell surface in uncleaved App and is unlikely to extend beyond the capsule, is the main determinant for adhesion (Serruto et al., 2003). Protease treatment indicated the involvement of a proteinaceous receptor on Chang cells, but it is not known whether the transferrin receptor 1 or the mannose receptor, which mediate uptake of App and AusI in dendritic cells (see above), are involved. App was also shown to mediate interbacterial aggregation on cell layers (Serruto et al., 2003); possibly, this is mediated by the binding of the NLS in the α-peptide to eDNA, analogous to the role of the α-peptide of IgA protease in biofilm formation (see above).

### Surface-Exposed Classical Autotransporters: AutA and AutB

AutA and AutB are two related, relatively small autotransporters of ∼75 kDa including the β-domain. The *autA* gene is broadly distributed among *Neisseria* spp., whereas the presence of the *autB* gene is restricted to the pathogenic *Neisseria* spp., *N. meningitidis* and *N. gonorrhoeae* (Arenas et al., 2015a, 2016). Also some, but not all, strains of *Haemophilus influenzae* and closely related *Haemophilus* spp. contain an *autB* gene. Analysis of the *autB*-flanking sequences in both genera suggested that a common ancestor of the two pathogenic *Neisseria* spp. has acquired the gene from a *H. influenzae* strain by horizontal gene transfer (Davis et al., 2001; Arenas et al., 2016).

The expression of *autA* and *autB* is prone to phase variation by slipped-strand mispairing at AAGC nucleotide repeats located immediately downstream of the start codon (Peak et al., 1999). In addition, the *autA* gene was disrupted in 76% of the meningococcal genomes analyzed by premature stop codons, insertions and/or deletions (Arenas et al., 2015a) suggesting selection pressure against expression of the gene. However, the gene was phased on in ∼33% of the strains with an intact *autA*, consistent with random on and off switching. In contrast to *autA*, *autB* was disrupted in only 8% of the *N. meningitidis* genomes analyzed (Arenas et al., 2016). Curiously, the gene is phased off in the vast majority of the genomes with an intact *autB*, and in only ∼2% of the strains the gene could be expressed. This strongly suggests that, even if an intact *autB* is retained, its expression is under negative selection pressure probably already in the nasopharynx as no significant difference between invasive and carriage isolates was observed in this respect (Arenas et al., 2016).

The passenger domains of AutA and AutB are not proteolytically released, and they are exposed at the bacterial cell surface covalently attached to the β-domain (Arenas et al., 2015a, 2016). AutA expression was shown to cause bacterial autoaggregation (Arenas et al., 2015a), a trait associated with resistance to host immune defenses such as phagocytosis (Ochiai et al., 1993). Autoaggregation is mediated by mutual interaction of AutA proteins on neighboring cells. In addition, AutA was found to bind DNA, which acts as an adhesive between cells (Arenas et al., 2015a; Arenas and Tommassen, 2017). Autoaggregation also has consequences for the architecture of biofilms formed. Besides, AutA was reported to be a potent $CD4^+$ T-cell and B-cell stimulating antigen (Ait-Tahar et al., 2000). Expression of *autB* was shown to enhance biofilm formation, and it retarded the passage of the bacteria through epithelial cell layers (Arenas et al., 2016). This suggests that AutB could have a role during host colonization.

### Trimeric Autotransporters: NadA and NhhA

NadA shows high sequence similarity to the well-known virulence factors YadA from *Yersinia enterocolitica* and UspA2 from *Moraxella catarrhalis* (van Ulsen et al., 2001). It is a

component of the Bexsero® vaccine. However, the gene is present in only ∼30% of *N. meningitidis* isolates with a lower prevalence in carriage strains (∼15%) (Comanducci et al., 2002, 2004). Furthermore, based on sequence variability, two main groups of NadA variants can be discriminated (Bambini et al., 2014) with limited immunological cross-reactivity between the groups (Comanducci et al., 2004), and the expression levels are highly variable (Martin et al., 2003), which also may impact on vaccine efficacy (Comanducci et al., 2002). Expression levels are determined by phase variation at a TAAA tetranucleotide repeat region upstream of the *nadA* promoter (Martin et al., 2003), whilst also on/off switching can occur by phase variation at a poly-C stretch within the coding region of some *nadA* variants (Bambini et al., 2014). Expression of *nadA* is transcriptionally controlled by the repressor NadR (Schielke et al., 2009), which binds operator sequences upstream and downstream of the TAAA repeat region, the latter overlapping with the -10 region of the promoter (Metruccio et al., 2009). The metabolite 4-hydroxyphenylacetic acid was found to act as an inducer of *nadA* expression (Metruccio et al., 2009). This metabolite is secreted in human saliva, suggesting that *nadA* expression will be induced on the mucosal surfaces of the nasopharynx. Interestingly, upon derepression, the expression levels were similar independent of the number of TAAA repeats, indicating that the number of repeats determines the level of repression by NadR rather than the expression levels in the induced state.

NadA functions as an adhesin and invasin. Its heterologous expression in *E. coli* promoted adherence of the bacteria to and invasion of Chang epithelial cells, and this function was confirmed in *N. meningitidis* (Capecchi et al., 2005). NadA function could also be reconstituted in a *yadA* mutant of *Y. enterocolitica*, and it was shown that β1 integrins function as its receptor on host cells (Nägele et al., 2011). Curiously, NadA was also shown to bind the heat shock protein Hsp90, a normally cytoplasmic chaperone, and purified Hsp90 was shown to inhibit NadA-mediated adhesion and invasion *in vitro* (Montanari et al., 2012). The physiological significance of these observations is not clear.

Whilst the passenger domains of classical autotransporters usually form a long β-helical structure that displays globular functional domains, trimeric autotransporters have a completely different architecture consisting of a stalk domain that displays one or several head domains (Grijpstra et al., 2013). The stalk is a coiled-coil structure that extends from the α-helices that occupy the membrane-embedded β-barrel (**Figure 1D**). NadA has a similar overall architecture but is somewhat atypical in that a separate globular head domain is lacking (Malito et al., 2014). Instead, the coiled coils extend up to the N terminus and the head is formed by insertions of 36 residues that protrude from the stalk and form wing-like structures (**Figure 6**). The adhesin activity was mapped to the head region (Capecchi et al., 2005; Tavano et al., 2011), which is apparently sufficiently exposed from the bacterial cell surface to be functional also in encapsulated strains (Capecchi et al., 2005).

NhhA (a.k.a. Msf) was identified as a homolog of the adhesin Hia of non-typeable *H. influenzae* (Peak et al., 2000; van Ulsen et al., 2001), and the *nhhA* gene was found to be ubiquitously present in all *N. meningitidis* strains examined, although disrupted in some of them (Peak et al., 2000). Expression levels varied widely and were affected in one particular lineage, i.e., ST41/44, by an amino-acid substitution in the β-domain, which prevents trimerization and surface exposition of the passenger domain (Echenique-Rivera et al., 2011a). The function of NhhA as an adhesin was demonstrated after its heterologous production in *E. coli*, which mediated adherence of the bacteria to epithelial cell lines, and was confirmed after constructing an *nhhA* mutant in an encapsulated *N. meningitidis* strain (Scarselli et al., 2006). It was demonstrated that purified NhhA and NhhA-producing cells bind the extracellular matrix components laminin and heparan sulfate (Scarselli et al., 2006). In addition, NhhA was shown to bind activated vitronectin, a complement regulatory protein, and, thus, to impart serum resistance to the bacteria by inhibiting the formation of the membrane-attack complex (Griffiths et al., 2011). Consistently, an *nhhA* mutant was less virulent and showed reduced survival in blood after intraperitoneal challenge of mice (Sjölinder et al., 2008). Expression of the protein appeared to be essential also for the colonization of the nasopharyngeal mucosa and for disease development after intranasal challenge in a murine model of meningococcal disease. The reduced colonization levels are probably related to the *in vitro* observations that wild-type bacteria are more resistant than the *nhhA* mutant to phagocytosis (Sjölinder et al., 2008) and that NhhA induces apoptosis of macrophages (Sjölinder et al., 2012). In addition, immune modulatory activities of NhhA were reported (Wang et al., 2016). NhhA blocked differentiation of monocytes into dendritic cells and induced their differentiation into macrophages that failed to produce proinflammatory mediators but produced

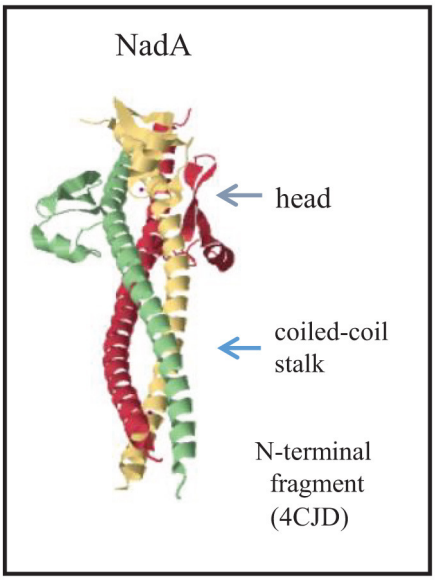


**FIGURE 6 |** Structure of the passenger of the trimeric autotransporter NadA. The structure of the N-terminal part of the passenger is provided (Malito et al., 2014). Each subunit is colored differently, and the major structural domains of the complex are indicated. The PDB access code is provided in brackets.

anti-inflammatory responses. These differentiated macrophages were highly efficient in eliminating the bacteria. Hence, this response prevents dissemination and sustains asymptomatic colonization (Wang et al., 2016).

## The Two-Partner Secretion (TPS) System

The substrates of the TPS systems, TpsA, are very large proteins (>2,000 amino-acid residues), which, like most classical autotransporters, display a β-helical conformation (Jacob-Dubuisson et al., 2013). *N. meningitidis* strains can produce up to five different TpsA proteins (van Ulsen and Tommassen, 2006). The genes for one TPS system are widely distributed among *N. meningitidis* isolates, whereas the genes for other TPS systems are associated with invasive clonal complexes (van Ulsen et al., 2008). Only the function of the conserved TpsA, a.k.a. HrpA, has been investigated, particularly in strains that produce this protein as the only TpsA. Substrates of TPS systems can have various, often virulence-related functions. Several functions have been attributed to the meningococcal TpsA, including a role in intracellular survival and escape from infected cells (Talà et al., 2008), adhesion to epithelial cell lines (Schmitt et al., 2007), and biofilm formation (Neil and Apicella, 2009). More recently, it was demonstrated that TpsA is involved in interbacterial competition in a process called contact-dependent growth inhibition (CDI) (Arenas et al., 2013b). CDI was originally described in *E. coli* and has evolved to inhibit the growth of closely related bacteria, usually of the same species, in niche competition (Aoki et al., 2005). In the proposed model, the surface-exposed TpsA interacts with a receptor in the outer membrane of a target cell, after which a small C-terminal part of TpsA of ∼300 amino-acid residues is proteolytically released and transported into the target cell, where it exerts one of different toxic activities, e.g., by functioning as a DNase or an RNase (Aoki et al., 2010). The producing cells themselves are protected against this toxic activity by the production of a small immunity protein, here called TpsI. TpsA proteins with CDI activity are polymorphic toxins, i.e., comparison of their sequences in different strains revealed that they can display a wide variety of toxic domains at their C terminus, each of which is associated with its own cognate TpsI (Aoki et al., 2010).

The genes for the conserved TPS system of *N. meningitidis* are organized in an operon (**Figure 7**). Downstream of the *tpsI* gene, a variable number of 5′ truncated *tpsA*-related genes are located, called *tpsC* cassettes. In their 5′ end, the *tpsC* cassettes show homology with a segment immediately upstream of the 3′ end encoding the toxic domain of *tpsA*. At their 3′ end, however, the *tpsC* cassettes encode different toxic domains (**Figure 7**). Thus, the *tpsC* cassettes provide a broad repertoire of toxic domains and each of them is associated with a cognate *tpsI* gene to impart immunity to the producer. However, the products of these *tpsC* cassettes, if expressed, cannot be secreted because they lack an N-terminal signal sequence and a TPS domain, required for recognition by the Sec system and the TpsB protein, respectively. It was proposed that the 3′ end of *tpsA* along with the downstream *tpsI* can be replaced by *tpsC* cassettes and the cognate *tpsI* through genetic recombination, thus resulting in the production of a TpsA with a different toxic domain (Arenas et al., 2013b). Examination of the 3′ end of the *tpsA* genes in available genome sequences indeed suggested a high rate of recombination between *tpsA* and *tpsC* cassettes (van Ulsen and Tommassen, 2006). However, a detailed analysis of the 3′ end of the *tpsA* gene in large panels of meningococcal isolates from the same lineage collected over several decades from different parts of the world revealed a very low rate of exchange (Arenas et al., 2013b). It was suggested that the availability of a large collection of *tpsI* genes might be more important for the bacteria than the ability to replace the toxic domain of TpsA by a variety of others encoded by the *tpsC* cassettes.

## The T1SS

FrpC and related proteins (some called FrpA) are the substrates of the meningococcal T1SS; they are produced under iron limitation (Thompson and Sparling, 1993; Thompson et al., 1993a,b). FrpC-like proteins are large proteins of 120–200 kDa. They are members of the RTX family of proteins and differ largely with respect to the number of glycine-rich calcium-binding repeats (see above); in addition they show considerable sequence variability in a small N-terminal domain of ∼350 amino-acid residues (van Ulsen and Tommassen, 2006), possibly due to immune pressure. The RTX family includes important cytotoxins in several pathogens (Linhartová et al., 2010). However, *N. meningitidis* mutants lacking functional *frpC* genes or the T1SS machinery were not attenuated in animal infection models (Klee et al., 2000; Forman et al., 2003).

After secretion, the FrpC protein is autocatalytically cleaved at an Asp-Pro bond at physiological concentrations of calcium ions (Osička et al., 2004). The N-terminal part of ∼45 kDa is retained at the bacterial cell surface by binding FrpD with high affinity (Prochazkova et al., 2005). FrpD is a cell-surface-exposed lipoprotein that is encoded by the same operon as FrpC. Its structure is different from those of the surface-exposed lipoproteins discussed above, although it also has a high β-sheet content, which may be relevant for its transport to the cell surface (**Figure 5**) (Sviridova et al., 2017). During autocatalytic processing, the released carboxyl group of the C-terminal aspartate of the N-terminal FrpC fragment forms a covalent linkage with an adjacent ε-amino group of a lysine generating a new Asp-Lys isopeptide bond (Prochazkova et al., 2005). In this way, the N-terminal FrpC fragment may be covalently linked to membrane proteins on the host epithelial cells (Sviridova et al., 2017). Thus, together with FrpD, the N-terminal fragment of FrpC may function as an adhesin, mediating the adhesion of the bacteria to epithelial cells.

## Other Secretion Systems and Secreted Proteins

Besides the secretion systems discussed above, some *N. meningitidis* strains contain a type 4 secretion system (T4SS). The genes for a T4SS were first identified in gonococcal strains on a genomic island called gonococcal genomic island (Dillard and and Seifert, 2001), and the system was shown to mediate the secretion of single-stranded DNA (Hamilton et al., 2005). Subsequently, it was found that also some meningococcal strains contain genes for the T4SS (Snyder et al., 2005; Woodhams

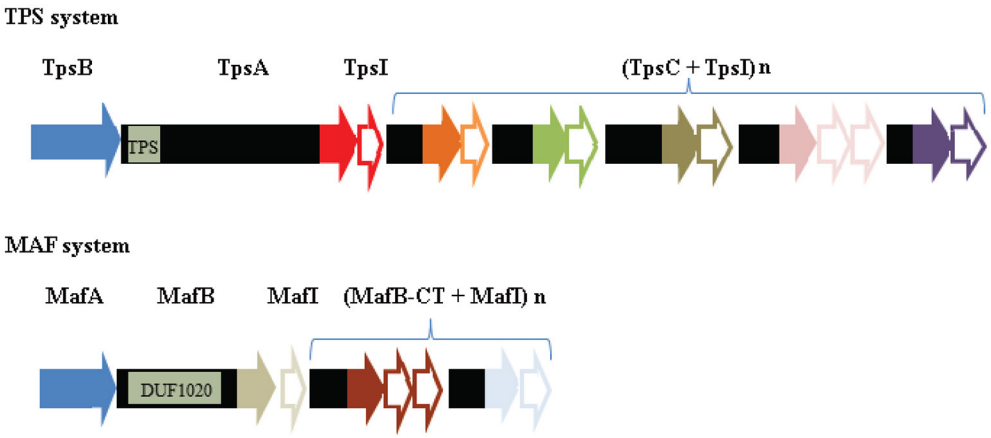


**FIGURE 7 |** Comparison of the genetic organization of the genes encoding a TPS system and a MAF system. In the top panel, the genetic island encoding the TPS system of strain B16B6 is depicted (Arenas et al., 2013b). TPS islands consist of genes encoding the transporter TpsB (blue), the secreted toxin TpsA, an immunity protein TpsI, and a variable repertoire of *tpsC* cassettes interspersed with genes encoding immunity proteins. The position of the gene segment of *tpsA* that encodes the TPS domain, which is recognized by TpsB, is indicated. The segments of *tpsA* and *tpsC* cassettes that encode toxic domains are colored, with different colors indicating different toxic domains. The *tpsI* genes encoding the cognate immunity proteins are indicated as open arrows with the same colors. In the bottom panel, the genetic island MGI-1 of B16B6 is depicted (Arenas et al., 2015b). The MGI islands consist of genes encoding MafA, the secreted toxin MafB, an immunity protein MafI, and a variable repertoire of *mafB-CT* cassettes interspersed with genes encoding immunity proteins. The position of the gene segment that encodes the conserved DUF1020 domain in MafB is indicated. Sequences encoding toxic domains and cognate immunity proteins are indicated as in the TPS island. Note that no evidence for MafA representing the transporter of MafB has been reported so far.

et al., 2012). However, in most of these strains, these genes are disrupted, and those strains with a complete T4SS do not appear to exhibit increased DNA release. As no function has been assigned to the T4SS in *N. meningitidis*, it won't be discussed here in detail. *N. meningitidis* also produce type IV pili, which are retractile pili involved in adhesion to host cells, interbacterial interaction, DNA uptake, and surface motility. These surface organelles are topic of several focused reviews to which we refer (e.g., see Berry and Pelicic, 2015; Mayer and Wong, 2015). In this section, we focus on a number of secreted proteins for which the secretion mechanism has not yet been solved.

## MafB

Like the TpsA proteins, the MafB proteins are polymorphic toxins that display a small variable toxic domain at their C terminus (Arenas et al., 2015b; Jamet et al., 2015). The *mafB* genes are localized on the chromosome on genomic islands designated Maf Genomic Islands (MGI) (Jamet et al., 2015). Up to three MGI can be present in a single meningococcal strain. The gene organization on the MGI is reminiscent of the loci encoding the TPS systems (**Figure 7**). The *mafB* genes are usually flanked by a *mafA* and a *mafI* gene. The *mafI* gene encodes a small immunity protein, which has been shown to interact with the toxic domain of MafB and to neutralize its toxic activity (Arenas et al., 2015b; Jamet et al., 2015). Indeed, MafB producers were shown to inhibit the growth of congeners that do not produce the cognate immunity protein. Downstream of the *mafI* gene, a variable number of 5′ truncated *mafB*-related genes are located, called *mafB-CT* cassettes (**Figure 7**). Like the *tpsC* cassettes, these *mafB-CT* cassettes offer a reservoir of alternative toxic domains, which could potentially be displayed at the C terminus of MafB after a genetic recombination event.

Apart from the presence of a toxic domain, MafB proteins do not show any similarity with TpsA proteins. They are synthesized with a signal sequence for transport across the inner membrane via the Sec machinery. Immediately after the signal sequence, all MafB proteins contain a conserved domain of unknown function, DUF1020, followed by the C-terminal toxic domain (**Figure 7**). In some MafB proteins, a Hint domain, which is expected to mediate protein splicing (Amitai et al., 2003), separates the DUF1020 from the toxic domain. How MafB is translocated across the outer membrane is unclear. Considering the parallelism with the TPS loci (**Figure 7**), MafA would be an obvious candidate for a protein involved in the secretion process. Earlier studies in *N. gonorrhoeae* indicated that MafA is an adhesin that binds host glycolipids (Paruchuri et al., 1990). Accordingly, these proteins were designated members of a multiple adhesin family (maf). MafA doesn't show any similarity with TpsB. It is produced with a signal sequence containing a lipobox motif, suggesting it's a lipoprotein, and secondary structure predictions didn't suggest a β-barrel structure, which is difficult to reconcile with its possible role as a transporter (Arenas et al., 2015b). Indeed, MafB was found in the extracellular medium when expressed in a *Neisseria cinerea* mutant lacking MafA (Jamet et al., 2015), suggesting that MafB secretion is independent of MafA. Furthermore, MafB was not secreted when produced in *E. coli* suggesting that it is not a novel type of autotransporter and that the transport mechanism involved is not present in *E. coli* (Jamet et al., 2015). It was suggested that MafB may be released with OMVs, which are

abundantly shed from the surface in *N. meningitidis* (Jamet et al., 2015).

### T and B Cell-Stimulating Protein B (TspB)

The name TspB, for T- and B-cell-stimulating protein B, may be a misnomer as evidence for such a function has, to the best of our knowledge, never been published. TspB was identified as a protein that binds immunoglobulins (Ig) (Müller et al., 2013). The protein is encoded by a prophage that is associated with invasive-disease isolates (Bille et al., 2005; Müller et al., 2013), and its synthesis is induced in the presence of human serum (Müller et al., 2013). Up to four copies of the *tspB* gene can be found in a genome.

The TspB proteins contain variable sequences at the N- and C-terminal ends and a conserved core region followed by a variable proline-rich segment (Müller et al., 2013). The core region of TspB binds the Fcγ region of IgG2. Ig-binding proteins are produced by several human pathogens, and they prevent the activation of complement. Indeed, TspB was shown to contribute to the survival of *N. meningitidis* in normal human serum by inhibiting IgM-mediated activation of the classical complement pathway (Müller et al., 2015). Since TspB binds IgM only poorly (Müller et al., 2013), this effect is probably indirect. TspB was found to bind DNA and to the form a biofilm-like matrix consisting of TspB, IgG, and DNA surrounding bacterial aggregates (Müller et al., 2013, 2015). Possibly, the presence of IgG in the matrix stimulates the non-productive activation of complement far away from the bacterial cell surface.

The secretion mechanism of TspB remains unclear. It could be released as a minor coat protein of filamentous phage particles, which was demonstrated to be mediated by the secretin PilQ, a protein also responsible for extrusion of type IV pili from the bacteria (Bille et al., 2005). However, in the studies of Müller et al. (2013), TspB appeared not to be associated with phage particles. The protein is produced with an N-terminal signal sequence for Sec-mediated transport across the inner membrane and a hydrophobic region near the C terminus that should act as a stop-transfer signal and anchor the protein in the membrane. Thus, possibly, the protein is only released after cell lysis.

## CONCLUDING REMARKS

The quest for novel vaccine antigens has enormously stimulated research into cell-surface-exposed and secreted proteins in *N. meningitidis*. These investigations have not only resulted in the development of two new registered vaccines, but they have also uncovered the functions of many of these proteins, which have roles in host-pathogen interactions, including adhesion, invasion, and immune evasion, in nutrient acquisition, and in interbacterial interactions, including biofilm formation and competition. Thus, these studies have provided important novel insights into biology of the meningococcus. In addition, they have led to the discovery of new transport mechanisms and machineries of general (micro)biological significance, such as the BAM and SLAM discussed above and the LPT machinery for the transport of lipopolysaccharides (Bos et al., 2004). Because they are essential in most Gram-negative bacteria and cell-surface exposed, particularly the integral OMPs of the BAM and LPT systems are attractive targets for the development of new antimicrobials (Srinivas et al., 2010; Urfer et al., 2016).

With respect to the transport mechanisms, there is still much to be learned. For lipoproteins, for example, it will be important to establish the sorting rules in *N. meningitidis*, which will help to predict on the basis of the sequence whether a lipoprotein is transported to the cell surface or is retained at the periplasmic side of either the inner or the outer membrane. In the MAF system, it is still unknown how MafB is transported to the cell surface, and how its toxic domain is cleaved off and imported into the target cell. Molecular insights in these mechanisms could lead to novel antimicrobial therapies.

Competition between different meningococci is a new field of study. A relatively large part of the rather small genome is occupied by genes encoding toxins and their cognate immunity proteins and transporters. It should be noted that CDI activity has, so far, only been demonstrated in competition assays between wild-type strains and their mutant derivatives lacking specific immunity proteins. What happens in a competition between two wild-type strains that express different toxins and immunity proteins is unknown. Although colonization by different strains has been demonstrated in carriage studies, it was very rare and detected in only ∼1% of the carriers (Caugant et al., 2007), suggesting that competition in the nasopharynx may be very effective. In contrast, such competition was recently not observed *in vitro* in dual-strain biofilm-formation experiments (Pérez-Ortega et al., 2017).

It is evident that many components of the secretome exert similar functions. It is particularly remarkable how many of them function as adhesins. Some redundancy in function is to be expected considering the high capacity of the meningococcus to change its cell surface, e.g., by phase variation, presumably as a mechanism to escape from the immune response of the host. Thus, one protein may take over the function of another one that is switched off. However, adhesins may also work in combination or sequentially or target other receptors and, thereby, other host cells. It is also evident that many secreted proteins have multiple functions, which is conceivable considering their large size. In addition, the secreted proteases may have multiple targets and, thus, interfere with the host's metabolism and immune response in multiple ways. It is likely that new functions of the secretome will be uncovered in the coming years. In this respect, it is important to note that most functions were discovered so far in *in vitro* systems. The development of transgenic mouse models for nasopharyngeal colonization of *N. meningitidis* (Joshwich et al., 2013) certainly opens new avenues for understanding the role of secretome components in host-pathogen interactions, although limitations will persist considering the large number of host-specific components involved.

## AUTHOR CONTRIBUTIONS

All authors listed, have made substantial, direct and intellectual contribution to the work, and approved it for publication.

## REFERENCES


Abdel Hadi, H., Wooldridge, K. G., Robinson, K., and Ala'Aldeen, D. A. (2001). Identification and characterization of App: an immunogenic autotransporter protein of *Neisseria meningitidis*. *Mol. Microbiol.* 41, 611–623. doi: 10.1046/j.1365-2958.2001.02516.x

Ait-Tahar, K., Wooldridge, K. G., Turner, D. P., Atta, M., Todd, I., and Ala'Aldeen, D. A. (2000). Auto-transporter A protein of *Neisseria meningitidis*: a potent $CD4^+$ T-cell and B-cell stimulating antigen detected by expression cloning. *Mol. Microbiol.* 37, 1094–1105. doi: 10.1046/j.1365-2958.2000.02061.x

Amitai, G., Belenkiy, O., Dassa, B., Shainskaya, A., and Pietrokovski, S. (2003). Distribution and function of new bacterial intein-like protein domains. *Mol. Microbiol.* 47, 61–73. doi: 10.1046/j.1365-2958.2003.03283.x

Anderson, J. E., Hobbs, M. M., Biswas, G. D., and Sparling, P. F. (2003). Opposing selective forces for the expression of the gonococcal lactoferrin receptor. *Mol. Microbiol.* 48, 1325–1337. doi: 10.1046/j.1365-2958.2003.03496.x

Anderson, J. E., Sparling, P. F., and Cornelissen, C. N. (1994). Gonococcal transferrin-binding protein 2 facilitates but is not essential for transferrin utilization. *J. Bacteriol.* 176, 3162–3170.

Aoki, S. K., Diner, E. J., t'Kint de Roodenbeke, C., Burgess, B. R., Poole, S. J., Braaten, B. A., et al. (2010). A widespread family of polymorphic contact-dependent toxin delivery systems in bacteria. *Nature* 468, 439–442. doi: 10.1038/nature09490

Aoki, S. K., Pamma, R., Hernday, A. D., Bickham, J. E., Braaten, B. A., and Low, D. A. (2005). Contact-dependent inhibition of growth in *Escherichia coli*. *Science* 309, 1245–1248. doi: 10.1126/science.1115109

Arenas, J., and Tommassen, J. (2017). Meningococcal biofilm formation: let's stick together. *Trends Microbiol.* 25, 113–124. doi: 10.1016/j.tim.2016.09.005

Arenas, J., Cano, S., Nijland, R., van Dongen, V., Rutten, L., van der Ende, A., et al. (2015a). The meningococcal autotransporter AutA is implicated in autoaggregation and biofilm formation. *Environ. Microbiol.* 17, 1321–1337. doi: 10.1111/1462-2920.12581

Arenas, J., de Maat, V., Catón, L., Krekorian, M., Herrero, J. C., Ferrara, F., et al. (2015b). Fratricide activity of MafB protein of *N. meningitidis* strain B16B6. *BMC Microbiol.* 15:156. doi: 10.1186/s12866-015-0493-6

Arenas, J., Nijland, R., Rodriguez, F. J., Bosma, T. N. P., and Tommassen, J. (2013a). Involvement of three meningococcal surface-exposed proteins, the heparin-binding protein NHBA, the α-peptide of IgA protease and the autotransporter protease NalP, in initiation of biofilm formation. *Mol. Microbiol.* 87, 254–268. doi: 10.1111/mmi.12097.

Arenas, J., Paganelli, F. L., Rodríguez-Castaño, P., Cano-Crespo, S., van der Ende, A., van Putten, J. P., et al. (2016). Expression of the gene for autotransporter AutB of *Neisseria meningitidis* affects biofilm formation and epithelial transmigration. *Front. Cell. Infect. Microbiol.* 6:162. doi: 10.3389/fcimb.2016.00162

Arenas, J., Schipper, K., van Ulsen, P., van der Ende, A., and Tommassen, J. (2013b). Domain exchange at the 3′ end of the gene encoding the fratricide meningococcal two-partner secretion protein A. *BMC Genomics* 14:622. doi: 10.1186/1471-2164-14-622

Auclair, S. M., Bhanu, M. K., and Kendall, D. A. (2012). Signal peptidase I: cleaving the way to mature proteins. *Protein Sci.* 21, 13–25. doi: 10.1002/pro.757

Bambini, S., De Chiara, M., Muzzi, A., Mora, M., Lucidarme, J., Brehony, C., et al. (2014). *Neisseria* adhesin A variation and revised nomenclature scheme. *Clin. Vaccine Immunol.* 21, 966–971. doi: 10.1128/CVI.00825-13

Bambini, S., Muzzi, A., Olcen, P., Rappuoli, R., Pizza, M., and Comanducci, M. (2009). Distribution and genetic variability of three vaccine components in a panel of strains representative of the diversity of serogroup B meningococcus. *Vaccine* 27, 2794–2803. doi: 10.1016/j.vaccine.2009.02.098

Beck, S. C., and Meyer, T. F. (2000). IgA1 protease from *Neisseria gonorrhoeae* inhibits TNFα-mediated apoptosis of human monocytic cells. *FEBS Lett.* 472, 287–292. doi: 10.1016/S0014-5793(00)01478-2

Bellamy, W., Takase, M., Wakabayashi, H., Kawase, K., and Tomita, M. (1992). Antibacterial spectrum of lactoferricin B, a potent bactericidal peptide derived from the N-terminal region of bovine lactoferrin. *J. Appl. Bacteriol.* 73, 472–479.

Berry, J. L., and Pelicic, V. (2015). Exceptionally widespread nanomachines composed of type IV pilins: the prokaryotic Swiss Army knives. *FEMS Microbiol. Rev.* 39, 134–154. doi: 10.1093/femsre/fuu001

Besbes, A., Le Goff, S., Antunes, A., Terrade, A., Hong, E., Giorgini, D., et al. (2015). Hyperinvasive meningococci induce intra-nuclear cleavage of the NF-κB protein p65/RelA by meningococcal IgA protease. *PLoS Pathog.* 11:e1005078. doi: 10.1371/journal.ppat.1005078.

Biagini, M., Spinsanti, M., De Angelis, G., Tomei, S., Ferlenghi, I., Scarselli, M., et al. (2016). Expression of factor H binding protein in meningococcal strains can vary at least 15-fold and is genetically determined. *Proc. Natl. Acad. Sci. U.S.A.* 113, 2714–2719. doi: 10.1073/pnas.1521142113

Bille, E., Zahar, J. R., Perrin, A., Morelle, S., Kriz, P., Jolley, K. A., et al. (2005). A chromosomally integrated bacteriophage in invasive meningococci. *J. Exp. Med.* 201, 1905–1913. doi: 10.1084/jem.20050112

Binscheck, T., Bartels, F., Bergel, H., Bigalke, H., Yamasaki, S., Hayashi, T., et al. (1995). IgA protease from *Neisseria gonorrhoeae* inhibits exocytosis in bovine chromaffin cells like tetanus toxin. *J. Biol. Chem.* 270, 1770–1774.

Biswas, G. D., Anderson, J. E., Chen, J. E., Cornelissen, C. N., and Sparling, P. F. (1999). Identification and functional characterization of the *Neisseria gonorrhoeae lbpB* gene product. *Infect. Immun.* 67, 455–459.

Bjune, G., Høiby, E. A., Grønnesby, J. K., Fredriksen, J. H., Halstensen, A., Holten, E., et al. (1991). Effect of outer membrane vesicle vaccine against group B meningococcal disease in Norway. *Lancet* 338, 1093–1096.

Bos, M. P., Tefsen, B., Geurtsen, J., and Tommassen, J. (2004). Identification of an outer membrane protein required for the transport of lipopolysaccharide to the bacterial cell surface. *Proc. Natl. Acad. Sci. U.S.A.* 101, 9417–9422. doi: 10.1073/pnas.0402340101

Boulton, I. C., Gorringe, A. R., Allison, N., Robinson, A., Gorinsky, B., Joannou, C. L., et al. (1998). Transferrin-binding protein B isolated from *Neisseria meningitidis* discriminates between apo and diferric human transferrin. *Biochem. J.* 15, 269–273.

Brooks, C. L., Arutyunova, E., and Lemieux, M. J. (2014). The structure of lactoferrin-binding protein B from *Neisseria meningitidis* suggests roles in iron acquisition and neutralization of host defences. *Acta Crystallogr. F Struct. Biol. Commun.* 70, 1312–1317. doi: 10.1107/S2053230X14019372.

Buddelmeijer, N. (2015). The molecular mechanism of bacterial lipoprotein modification-How, when and why? *FEMS Microbiol. Rev.* 39, 246–261. doi: 10.1093/femsre/fuu006

Calmettes, C., Alcantara, J., Yu, R. H., Schryvers, A. B., and Moraes, T. F. (2012). The structural basis of transferrin sequestration by transferrin-binding protein B. *Nat. Struct. Mol. Biol.* 19, 358–360. doi: 10.1038/nsmb.2251

Cantini, F., Veggi, D., Dragonetti, S., Savino, S., Scarselli, M., Romagnoli, G., et al. (2009). Solution structure of the factor H-binding protein, a survival factor and protective antigen of *Neisseria meningitidis*. *J. Biol. Chem.* 284, 9022–9026. doi: 10.1074/jbc.C800214200

Capecchi, B., Adu-Bobie, J., Di Marcello, F., Ciucchi, L., Masignani, V., Taddei, A., et al. (2005). *Neisseria meningitidis* NadA is a new invasin which promotes bacterial adhesion to and penetration into human epithelial cells. *Mol. Microbiol.* 55, 687–698. doi: 10.1111/j.1365-2958.2004.04423.x

Casellato, A., Rossi Paccani, S., Barrile, R., Bossi, F., Ciucchi, L., Codolo, G., et al. (2014). The C2 fragment from *Neisseria meningitidis* antigen NHBA increases endothelial permeability by destabilizing adherens junctions. *Cell. Microbiol.* 16, 925–937. doi: 10.1111/cmi.12250

Caugant, D. A., Tzanakaki, G., and Kriz, P. (2007). Lessons from meningococcal carriage studies. *FEMS Microbiol. Rev.* 31, 52–63. doi: 10.1111/j.1574-6976.2006.00052.x

Clantin, B., Delattre, A. S., Rucktooa, P., Saint, N., Méli, A. C., Locht, C., et al. (2007). Structure of the membrane protein FhaC: a member of the Omp85-TpsB transporter superfamily. *Science* 317, 957–961. doi: 10.1126/science.1143860

Comanducci, M., Bambini, S., Brunelli, B., Adu-Bobie, J., Aricò, B., Capecchi, B., et al. (2002). NadA, a novel vaccine candidate of *Neisseria meningitidis*. *J. Exp. Med.* 195, 1445–1454. doi: 10.1084/jem.20020407

Comanducci, M., Bambini, S., Caugant, D. A., Mora, M., Brunelli, B., Capecchi, B., et al. (2004). NadA diversity and carriage in *Neisseria meningitidis*. *Infect. Immun.* 72, 4217–4223. doi: 10.1128/IAI.72.7.4217-4223.2004

Cornelissen, C. N., and Sparling, P. F. (1996). Binding and surface exposure characteristics of the gonococcal transferrin receptor are dependent on both transferrin-binding proteins. *J. Bacteriol.* 178, 1437–1444.

Costa, T. R., Felisberto-Rodrigues, C., Meir, A., Prevost, M. S., Redzej, A., Trokter, M., et al. (2015). Secretion systems in Gram-negative bacteria:

structural and mechanistic insights. *Nat. Rev. Microbiol.* 13, 343–359. doi: 10.1038/nrmicro3456

Crum-Cianflone, N., and Sullivan, E. (2016). Meningococcal vaccinations. *Infect. Dis. Ther.* 5, 89–112. doi: 10.1007/s40121-016-0107-0.

da Silva, R. A., Churchward, C. P., Karlyshev, A. V., Eleftheriadou, O., Snabaitis, A. K., Longman, M. R., et al. (2016). The role of apolipoprotein N-acyl transferase, Lnt, in the lipidation of factor H binding protein of *Neisseria meningitidis* strain MC58 and its potential as a drug target. *Br. J. Pharmacol.* doi: 10.1111/bph.13660. [Epub ahead of print].

Davis, J., Smith, A. L., Hughes, W. R., and Golomb, M. (2001). Evolution of an autotransporter: domain shuffling and lateral transfer from pathogenic *Haemophilus* to *Neisseria*. *J. Bacteriol.* 183, 4626–4635. doi: 10.1128/JB.183.15.000-000.2001

Del Tordello, E., Vacca, I., Ram, S., Rappuoli, R., and Serruto, D. (2014). *Neisseria meningitidis* NalP cleaves human complement C3, facilitating degradation of C3b and survival in human serum. *Proc. Natl. Acad. Sci. U.S.A.* 111, 427–432. doi: 10.1073/pnas.1321556111

Dillard, J. P., and Seifert, H. S. (2001). A variable genetic island specific for *Neisseria gonorrhoeae* is involved in providing DNA for natural transformation and is found more often in disseminated infection isolates. *Mol. Microbiol.* 41, 263–277. doi: 10.1046/j.1365-2958.2001.02520.x

Drobnak, I., Braselmann, E., and Clark, P. L. (2015). Multiple driving forces required for efficient secretion of autotransporter virulence proteins. *J. Biol. Chem.* 2090, 10104–10116. doi: 10.1074/jbc.M114.629170

Echenique-Rivera, H., Brunelli, B., Scarcelli, M., Taddei, A. R., Pizza, M., Aricò, B., et al. (2011a). A naturally occurring single-residue mutation in the translocator domain of *Neisseria meningitidis* NhhA affects trimerization, surface localization, and adhesive capacities. *Infect. Immun.* 79, 4308–4321. doi: 10.1128/IAI.00198-11

Echenique-Rivera, H., Muzzi, A., Del Tordello, E., Seib, K. L., Francois, P., Rappuoli, R., et al. (2011b). Transcriptome analysis of *Neisseria meningitidis* in human whole blood and mutagenesis studies identify virulence factors involved in blood survival. *PLoS Pathog.* 7:e1002027. doi: 10.1371/journal.ppat.1002027

Esposito, V., Musi, V., de Chiara, C., Veggi, D., Serruto, D., Scarselli, M., et al. (2011). Structure of the C-terminal domain of *Neisseria* heparin binding antigen (NHBA), one of the main antigens of a novel vaccine against *Neisseria meningitidis*. *J. Biol. Chem.* 286, 41767–41775. doi: 10.1074/jbc.M111.289314

Fletcher, L. D., Bernfield, L., Barniak, V., Farley, J. E., Howell, A., Knauf, M., et al. (2004). Vaccine potential of the *Neisseria meningitidis* 2086 lipoprotein. *Infect. Immun.* 72, 2088–2100. doi: 10.1128/IAI.72.4.2088-2100.2004

Forman, S., Linhartova, I., Osicka, R., Nassif, X., Sebo, P., and Pelicic, V. (2003). *Neisseria meningitidis* RTX proteins are not required for virulence in infant rats. *Infect. Immun.* 71, 2253–2257. doi: 10.1128/IAI.71.4.2253-2257.2003

Fussenegger, M., Facius, D., Meier, J., and Meyer, T. F. (1996). A novel peptidoglycan-linked lipoprotein (ComL) that functions in natural transformation competence of *Neisseria gonorrhoeae*. *Mol. Microbiol.* 19, 1095–1105. doi: 10.1046/j.1365-2958.1996.457984.x

Ge, X., Wang, R., Ma, J., Liu, Y., Ezemaduka, A. N., Chen, P. R., et al. (2014). DegP primarily functions as a protease for the biogenesis of β-barrel outer membrane proteins in the gram-negative bacterium *Escherichia coli*. *FEBS J.* 281, 1226–1240. doi: 10.1111/febs.12701

Gifford, J. L., Hunter, H. N., and Vogel, H. J. (2005). Lactoferricin: a lactoferrin-derived peptide with antimicrobial, antiviral, antitumor and immunological properties. *Cell. Mol. Life Sci.* 62, 2588–2598. doi: 10.1007/s00018-005-5373-z

Giuliani, M. M., Biolchi, A., Serruto, D., Ferlicca, F., Vienken, K., Oster, P., et al. (2010). Measuring bactericidal antigen-specific responses to a multicomponent vaccine against serogroup B meningococcus. *Vaccine* 28, 5023–5030. doi: 10.1016/j.vaccine.2010.05.014

Griffiths, N. J., Hill, D. J., Borodina, E., Sessions, R. B., Devos, N. I., Feron, C. M., et al. (2011). Meningococcal surface fibril (Msf) binds to activated vitronectin and inhibits the terminal complement pathway to increase serum resistance. *Mol. Microbiol.* 82, 1129–1149. doi: 10.1111/j.1365-2958.2011.07876.x

Grijpstra, J., Arenas, J., Rutten, L., and Tommassen, J. (2013). Autotransporter secretion: varying on a theme. *Res. Microbiol.* 146, 562–582. doi: 10.1016/j.resmic.2013.03.010

Hall, D. R., Hadden, J. M., Leonard, G. A., Bailey, S., Neu, M., Winn, M., et al. (2002). The crystal and molecular structures of diferric porcine and rabbit serum transferrins at resolutions of 2.15 and 2.60 Å, respectively. *Acta Crystallogr. D Biol. Crystallogr.* 58, 70–80. doi: 10.1107/S0907444901017309

Hamilton, H. L., Domínguez, N. M., Schwartz, K. J., Hackett, K. T., and Dillard, J. P. (2005). *Neisseria gonorrhoeae* secretes chromosomal DNA via a novel type IV secretion system. *Mol. Microbiol.* 55, 1704–1721. doi: 10.1111/j.1365-2958.2005.04521.x

Hauck, C. R., and Meyer, T. F. (1997). The lysosomal/phagosomal membrane protein h-lamp-1 is a target of the IgA1 protease of *Neisseria gonorrhoeae*. *FEBS Lett.* 405, 86–90.

Hayashi, S., and Wu, H. C. (1990). Lipoproteins in bacteria. *J. Bioenerg. Biomembr.* 22, 451–471.

Hooda, Y., Lai, C. C., Judd, A., Buckwalter, C. M., Shin, H. E., Gray-Owen, S. D., et al. (2016). Slam is an outer membrane protein that is required for the surface display of lipidated virulence factors in *Neisseria*. *Nat. Microbiol.* 1:16009. doi: 10.1038/nmicrobiol.2016.9

Hopper, S., Vasquez, B., Merz, A., Clary, S., Wilbur, J. S., and So, M. (2000). Effects of immunoglobulin A1 protease on *Neisseria gonorrhoeae* trafficking across polarized T84 epithelial monolayers. *Infect. Immun.* 68, 906–911. doi: 10.1128/IAI.68.2.906-911.2000

Ieva, R., and Bernstein, H. D. (2009). Interaction of an autotransporter passenger domain with BamA during its translocation across the bacterial outer membrane. *Proc. Natl. Acad. Sci. U.S.A.* 106, 19120–19125. doi: 10.1073/pnas.0907912106

Ieva, R., Tian, P., Peterson, J. H., and Bernstein, H. D. (2011). Sequential and spatially restricted interactions of assembly factors with an autotransporter β domain. *Proc. Natl. Acad. Sci. U.S.A.* 108, E383–E391. doi: 10.1073/pnas.1103827108

Irwin, S. W., Averil, N., Cheng, C. Y., and Schryvers, A. B. (1993). Preparation and analysis of isogenic mutants in the transferrin receptor protein genes, *tbpA* and *tbpB*, from *Neisseria meningitidis*. *Mol. Microbiol.* 8, 1125–1133.

Jacob-Dubuisson, F., Guérin, J., Baelen, S., and Clantin, B. (2013). Two-partner secretion: as simple as it sounds? *Res. Microbiol.* 164, 583–595. doi: 10.1016/j.resmic.2013.03.009

Jamet, A., Jousset, A. B., Euphrasie, D., Mukorako, P., Boucharlat, A., Ducousso, A., et al. (2015). A new family of secreted toxins in pathogenic *Neisseria* species. *PLoS Pathog.* 11:e1004592. doi: 10.1371/journal.ppat.1004592

Joshwich, K. O., McCaw, S. E., Islam, E., Sintsova, A., Gu, A., Shively, J. E., et al. (2013). *In vivo* adaptation and persistence of *Neisseria meningitidis* within the nasopharyngeal mucosa. *PLoS Pathog.* 9:e1003509. doi: 10.1371/journal.ppat.1003509

Khairalla, A. S., Omer, S. A., Mahdavi, J., Aslam, A., Dufailu, O. A., Self, T., et al. (2015). Nuclear trafficking, histone cleavage and induction of apoptosis by the meningococcal App and MspA autotransporters. *Cell. Microbiol.* 17, 1008–1020. doi: 10.1111/cmi.12417.

Klee, S. R., Nassif, X., Kusecek, B., Merker, P., Beretti, J. L., Achtman, M., et al. (2000). Molecular and biological analysis of eight genetic islands that distinguish *Neisseria meningitidis* from the closely related pathogen *Neisseria gonorrhoeae*. *Infect. Immun.* 68, 2082–2095. doi: 10.1128/IAI.68.4.2082-2095.2000

Koronakis, V., Sharff, A., Koronakis, E., Luisi, B., and Hughes, C. (2000). Crystal structure of the bacterial membrane protein TolC central to multidrug efflux and protein exports. *Nature* 405, 914–919. doi: 10.1038/35016007

Krojer, T., Sawa, J., Schäfer, E., Saibil, H. R., Ehrmann, M., and Clausen, T. (2008). Structural basis for the regulated protease and chaperone function of DegP. *Nature* 453, 885–890. doi: 10.1038/nature07004

Lappann, M., Claus, H., van Alen, T., Harmsen, M., Elias, J., Molin, S., et al. (2010). A dual role of extracellular DNA during biofilm formation in *Neisseria meningitidis*. *Mol. Microbiol.* 75, 1355–1371. doi: 10.1111/j.1365-2958.2010.07054.x

Lenders, M. H. H., Reimann, S., Smits, S. H., and Schmitt, L. (2013). Molecular insights into type I secretion systems. *Biol. Chem.* 394, 1371–1384. doi: 10.1515/hsz-2013-0171.

Lewis, L. A., Gipson, M., Hartman, K., Ownbey, T., Vaughn, J., and Dyer, D. W. (1999). Phase variation of HpuAB and HmbR, two distinct haemoglobin receptors of *Neisseria meningitidis* DNM2. *Mol. Microbiol.* 32, 977–989.

Lewis, L. A., Gray, E., Wang, Y. P., Roe, B. A., and Dyer, D. W. (1997). Molecular characterization of *hpuAB*, the haemoglobin-haptoglobin-utilization operon of *Neisseria meningitidis*. *Mol. Microbiol.* 23, 737–749.

Lin, L., Ayala, P., Larson, J., Mulks, M., Fukuda, M., Carlsson, S. R., et al. (1997). The *Neisseria* type 2 IgA1 protease cleaves LAMP1 and promotes survival of bacteria within epithelial cells. *Mol. Microbiol.* 24, 1083–1094.

Linhartová, I., Bumba, L., Mašín, J., Basler, M., Osička, R., Kamanová, J., et al. (2010). RTX proteins: a highly diverse family secreted by a common mechanism. *FEMS Microbiol. Rev.* 34, 1076–1112. doi: 10.1111/j.1574-6976.2010.00231.x

Loh, E., Lavender, H., Tan, F., Tracy, A., and Tang, C. M. (2016). Thermoregulation of meningococcal fHbp, an important virulence factor and vaccine antigen, is mediated by anti-ribosomal binding site sequences in the open reading frame. *PLoS Pathog.* 12:e1005794. doi: 10.1371/journal.ppat.1005794

LoVullo, E. D., Wright, L. F., Isabella, V., Huntley, J. F., and Pavelka, M. S. Jr. (2015). Revisiting the Gram-negative lipoprotein paradigm. *J. Bacteriol.* 197, 1705–1715. doi: 10.1128/JB.02414-14

Lycklama a Nijeholt, J. A., and Driessen, A. J. (2012). The bacterial Sec-translocase: structure and mechanism. *Philos. Trans. R. Soc. Lond. B* 367, 1016–1028. doi: 10.1098/rstb.2011.0201

Madico, G., Welsch, J. A., Lewis, L. A., McNaughton, A., Perlman, D. H., Costello, C. E., et al. (2006). The meningococcal vaccine candidate GNA1870 binds the complement regulatory protein factor H and enhances serum resistance. *J. Immunol.* 177, 501–510. doi: 10.4049/jimmunol.177.1.501

Maier, T., Clantin, B., Gruss, F., Dewitte, F., Delattre, A. S., Jacob-Dubuisson, F., et al. (2015). Conserved Omp85 lid-lock structure and substrate recognition in FhaC. *Nat. Commun.* 6:7452. doi: 10.1038/ncomms8452

Malito, E., Biancucci, M., Faleri, A., Ferlenghi, I., Scarselli, M., Maruggi, G., et al. (2014). Structure of the meningococcal vaccine antigen NadA and epitope mapping of a bactericidal antibody. *Proc. Natl. Acad. Sci. U.S.A.* 111, 17128–17133. doi: 10.1073/pnas.1419686111

Martin, P., van de Ven, T., Mouchel, N., Jeffries, A. C., Hood, D. W., and Moxon, E. R. (2003). Experimentally revised repertoire of putative contingency loci in *Neisseria meningitidis* strain MC58: evidence for a novel mechanism of phase variation. *Mol. Microbiol.* 50, 245–257. doi: 10.1046/j.1365-2958.2003.03678.x

Masignani, V., Comanducci, M., Giuliani, M. M., Bambini, S., Adu-Bobie, J., Arico, B., et al. (2003). Vaccination against *Neisseria meningitidis* using three variants of the lipoprotein GNA1870. *J. Exp. Med.* 197, 789–799. doi: 10.1084/jem.20021911

Matsuyama, S., Tajima, T., and Tokuda, H. (1995). A novel periplasmic carrier protein involved in the sorting and transport of *Escherichia coli* lipoproteins destined for the outer membrane *EMBO J.* 14, 3365–3372.

Matsuyama, S., Yokota, N., and Tokuda, H. (1997). A novel outer membrane lipoprotein, LolB (HemM), involved in the LolA (p20)-dependent localization of lipoproteins to the outer membrane of *Escherichia coli*. *EMBO J.* 16, 6947–6955.

Mayer, B., and Wong, G. C. (2015). How bacteria use type IV pili machinery on surfaces. *Trends Microbiol.* 23, 775–788. doi: 10.1016/j.tim.2015.09.002

Meng, G., Surana, N. K., St Geme, J. W. III., and Waksman, G. (2006). Structure of the outer membrane translocator domain of the *Haemophilus influenzae* Hia trimeric autotransporter. *EMBO J.* 25, 2297–2304. doi: 10.1038/sj.emboj.7601132

Metruccio, M. M., Pigozzi, E., Roncarati, D., Berlanda Scorza, F., Norais, N., Hill, S. A., et al. (2009). A novel phase variation mechanism in the meningococcus driven by a ligand-responsive repressor and differential spacing of distal promoter elements. *PLoS Pathog.* 5:e1000710. doi: 10.1371/journal.ppat.1000710

Montanari, P., Bozza, G., Capecchi, B., Caproni, E., Barrile, R., Norais, N., et al. (2012). Human heat shock protein (Hsp) 90 interferes with *Neisseria meningitidis* adhesin A (NadA)-mediated adhesion and invasion. *Cell. Microbiol.* 14, 368–385. doi: 10.1111/j.1462-5822.2011.01722.x

Morgenthau, A., Beddek, A., and Schryvers, A. B. (2014). The negatively charged regions of lactoferrin binding protein B, an adaptation against anti-microbial peptides. *PLoS ONE* 9:e86243. doi: 10.1371/journal.pone.0086243

Morgenthau, A., Livingstone, M., Adamiak, P., and Schryvers, A. B. (2012). The role of lactoferrin binding protein B in mediating protection against human lactoferricin. *Biochem. Cell. Biol.* 90, 417–423. doi: 10.1139/o11-074.

Müller, M. G., Ing, J. Y., Cheng, M. K., Flitter, B. A., and Moe, G. R. (2013). Identification of a phage-encoded Ig-binding protein from invasive *Neisseria meningitidis*. *J. Immunol.* 191, 3287–3296. doi: 10.4049/jimmunol.1301153

Müller, M. G., Moe, N. E., Richards, P. Q., and Moe, G. R. (2015). Resistance of *Neisseria meningitidis* to human serum depends on T and B cell stimulating protein B. *Infect. Immun.* 83, 1257–1264. doi: 10.1128/IAI.03134-14

Nägele, V., Heesemann, J., Schielke, S., Jiménez-Soto, L. F., Kurzai, O., and Ackermann, N. (2011). *Neisseria meningitidis* adhesin NadA targets β1 integrins: functional similarity to *Yersinia* invasin. *J. Biol. Chem.* 286, 20536–20546. doi: 10.1074/jbc.M110.188326

Narita, S. I., and Tokuda, H. (2007). Amino acids at positions 3 and 4 determine the membrane specificity of *Pseudomonas aeruginosa* lipoproteins. *J. Biol. Chem.* 4, 13372–13378. doi: 10.1074/jbc.M611839200

Narita, S., and Tokuda, H. (2016). Bacterial lipoproteins: biogenesis, sorting and quality control. *Biochim. Biophys. Acta.* doi: 10.1016/j.bbalip.2016.11.009. [Epub ahead of print].

Neil, R. B., and Apicella, M. A. (2009). Role of HrpA in biofilm formation of *Neisseria meningitidis* and regulation of the *hrpBAS* transcripts. *Infect. Immun.* 77, 2285–2293. doi: 10.1128/IAI.01502-08

Nivaskumar, M., and Francetic, O. (2014). Type II secretion system: a magic beanstalk or a protein escalator. *Biochim. Biophys. Acta* 1843, 1568–1577. doi: 10.1016/j.bbamcr.2013.12.020

Noinaj, N., Easley, N. C., Oke, M., Mizuno, N., Gumbart, J., Boura, E., et al. (2012). Structural basis for iron piracy by pathogenic *Neisseria*. *Nature* 483, 53–58. doi: 10.1038/nature10823

Noinaj, N., Guillier, M., Barnard, T. J., and Buchanan, S. K. (2010). TonB-dependent transporters: regulation, structure, and function. *Annu. Rev. Microbiol.* 64, 43–60. doi: 10.1146/annurev.micro.112408.134247

Noinaj, N., Gumbart, J. C., and Buchanan, S. K. (2017). The β-barrel assembly machinery in motion. *Nat. Rev. Microbiol.* 15, 197–204. doi: 10.1038/nrmicro.2016.191

Noinaj, N., Kuszak, A. J., Gumbart, J. C., Lukacik, P., Chang, H., Easley, N. C., et al. (2013). Structural insight into the biogenesis of β-barrel membrane proteins. *Nature* 501, 385–390. doi: 10.1038/nature12521

Ochiai, K., Kurita-Ochiai, T., Kamino, Y., and Ikeda, T. (1993). Effect of co-aggregation on the pathogenicity of oral bacteria. *J. Med. Microbiol.* 39, 183–190. doi: 10.1099/00222615-39-3-183

Oldfield, N. J., Matar, S., Bidmos, F. A., Alamro, M., Neal, K. R., Turner, D. P., et al. (2013). Prevalence and phase variable expression status of two autotransporters, NalP and MspA, in carriage and disease isolates of *Neisseria meningitidis*. *PLoS ONE* 25:e69746. doi: 10.1371/journal.pone.0069746

Oomen, C. J., van Ulsen, P., van Gelder, P., Feijen, M., Tommassen, J., and Gros, P. (2004). Structure of the translocator domain of a bacterial autotransporter. *EMBO J.* 23, 1257–1266. doi: 10.1038/sj.emboj.7600148

Oriente, F., Scarlato, V., and Delany, I. (2010). Expression of factor H binding protein of meningococcus responds to oxygen limitation through a dedicated FNR-regulated promoter. *J. Bacteriol.* 192, 691–701. doi: 10.1128/JB.01308-09

Osička, R., Procházková, K., Šulc, M., Linhartová, I., Havlíček, V., and Šebo, P. (2004). A novel "clip-and-link" activity of repeat in toxin (RTX) proteins from Gram-negative pathogens. Covalent protein cross-linking by and Asp-Lys isopeptide bond upon calcium-dependent processing at an Asp-Pro bond. *J. Biol. Chem.* 279, 24944–24956. doi: 10.1074/jbc.M314013200

Ostan, N. K. H., Yu, R.-H., Ng, D., Lai, C. C.-L., Pogoutse, A. K., Sarpe, V., et al. (2017). Lactoferrin binding protein B – a bifunctional bacterial receptor protein. *PLoS Pathog.* 13:e1006244. doi: 10.1371/journal.ppat.1006244

Ostberg, K. L., DeRocco, A. J., Mistry, S. D., Dickinson, M. K., and Cornelissen, C. N. (2013). Conserved regions of gonococcal TbpB are critical for surface exposure and transferrin utilization. *Infect. Immun.* 81, 3442–3450. doi: 10.1128/IAI.00280-13

Oster, P., Lennon, D., O'Hallahan, J., Mulholland, K., Reid, S., and Martin, D. (2005). MeNZB$^{TM}$: a safe and highly immunogenic taylor-made vaccine against the New Zealand *Neisseria meningitidis* serogroup B disease epidemic strain. *Vaccine* 23, 2191–2196. doi: 10.1016/j.vaccine.2005.01.063

Pace, D., and Pollard, A. J. (2012). Meningococcal disease: clinical presentation and sequelae. *Vaccine* 30, B3–B9. doi: 10.1016/j.vaccine.2011.12.062

Palmer, T., and Berks, B. C. (2012). The twin-arginine translocation (Tat) protein export pathway. *Nat. Rev. Microbiol.* 10, 483–496. doi: 10.1038/nrmicro2814

Paruchuri, D. K., Seifert, H. S., Ajioka, R. S., Karlsson, K. A., and So, M. (1990). Identification and characterization of a *Neisseria gonorrhoeae* gene encoding a glycolipid-binding adhesin. *Proc. Natl. Acad. Sci. U.S.A.* 87, 333–337.

Patel, R., Smith, S. M., and Robinson, C. (2014). Protein transport by the bacterial Tat pathway. *Biochim. Biophys. Acta* 1843, 1620–1628. doi: 10.1016/j.bbamcr.2014.02.013

Peak, I. R., Jennings, M. P., Hood, D. W., and Moxon, E. R. (1999). Tetranucleotide repeats identify novel virulence determinant homologues in *Neisseria meningitidis*. *Microb. Pathog.* 26, 13–23.

Peak, I. R., Srikhanta, Y., Dieckelmann, M., Moxon, E. R., and Jennings, M. P. (2000). Identification and characterisation of a novel conserved outer membrane protein from *Neisseria meningitidis*. *FEMS Immunol. Med. Microbiol.* 28, 329–334. doi: 10.1111/j.1574-695X.2000.tb01494.x

Pérez-Ortega, J., Rodríguez, A., Ribes, E., Tommassen, J., and Arenas, J. (2017). Interstrain cooperation in meningococcal biofilms: role of the autotransporters NalP and AutA. *Front. Microbiol.* 8:434. doi: 10.3389/fmicb.2017.00434

Pettersson, A., Klarenbeek, V., van Deurzen, J., Poolman, J. T., and Tommassen, J. (1994a). Molecular characterization of the structural gene for the lactoferrin receptor of the meningococcal strain H44/76. *Microb. Pathog.* 17, 395–408. doi: 10.1006/mpat.1994.1085

Pettersson, A., Maas, A., and Tommassen, J. (1994b). Identification of the *iroA* gene product of *Neisseria meningitidis* as a lactoferrin receptor. *J. Bacteriol.* 176, 1764–1766.

Pettersson, A., Prinz, T., Umar, A., van der Biezen, J., and Tommassen, J. (1998). Molecular characterization of LbpB, the second lactoferrin-binding protein of *Neisseria meningitidis*. *Mol. Microbiol.* 27, 599–610.

Pettersson, A., van der Biezen, J., Joosten, V., Hendriksen, J., and Tommassen, J. (1999). Sequence variability of the meningococcal lactoferrin-binding protein LbpB. *Gene* 231, 105–110.

Plaut, A. G., Gilbert, J. V., Artenstein, M. S., and Capra, J. D. (1975). *Neisseria gonorrhoeae* and *Neisseria meningitidis*: extracellular enzyme cleaves human immunoglobulin A. *Science* 190, 1103–1105.

Pohlner, J., Halter, R., Beyreuther, K., and Meyer, T. F. (1987). Gene structure and extracellular secretion of *Neisseria gonorrhoeae* IgA protease. *Nature* 325, 458–462. doi: 10.1038/325458a0

Pohlner, J., Langenberg, U., Wölk, U., Beck, S. C., and Meyer, T. F. (1995). Uptake and nuclear transport of *Neisseria* IgA1 protease-associated α-proteins in human cells. *Mol. Microbiol.* 17, 1073–1083. doi: 10.1111/j.1365-2958.1995.mmi_17061073.x

Prinz, T., Meyer, M., Pettersson, A., and Tommassen, J. (1999). Structural characterization of the lactoferrin receptor from *Neisseria meningitidis*. *J. Bacteriol.* 181, 4417–4419.

Prochazkova, K., Osicka, R., Linhartova, I., Halada, P., Sulc, M., and Sebo, P. (2005). The *Neisseria meningitidis* outer membrane lipoprotein FrpD binds the RTX protein FrpC. *J. Biol. Chem.* 280, 3251–3258. doi: 10.1074/jbc.M411232200

Pugsley, A. P., and Kornacker, M. G. (1991). Secretion of the cell surface lipoprotein pullulanase in *Escherichia coli*. Cooperation or competition between the specific secretion pathway and the lipoprotein sorting pathway? *J. Biol. Chem.* 266, 13640–13645.

Purdy, G. E., Fisher, C. R., and Payne, S. M. (2007). IcsA surface presentation in *Shigella flexneri* requires the periplasmic chaperones DegP, Skp, and SurA. *J. Bacteriol.* 189, 5566–5573. doi: 10.1128/JB.00483-07

Putker, F., Tommassen-van Boxtel, R., Stork, M., Rodríguez-Herva, J. J., Koster, M., and Tommassen, J. (2013). The type II secretion system (Xcp) of *Pseudomonas putida* is active and involved in the secretion of phosphatases. *Environ. Microbiol.* 15, 2658–2671. doi: 10.1111/1462-2920.12115

Ricci, D. P., and Silhavy, T. J. (2012). The Bam machine: a molecular cooper. *Biochim. Biophys. Acta* 1818, 1067–1084. doi: 10.1016/j.bbamem.2011.08.020

Rohde, K. H., and Dyer, D. W. (2004). Analysis of haptoglobin and hemoglobin-haptoglobin interactions with the *Neisseria meningitidis* TonB-dependent receptor HpuAB by flow cytometry. *Infect. Immun.* 72, 2494–2506. doi: 10.1128/IAI.72.5.2494-2506.2004

Rohde, K. H., Gillaspy, A. F., Hatfield, M. D., Lewis, L. A., and Dyer, D. W. (2002). Interactions of haemoglobin with the *Neisseria meningitidis* receptor HpuAB: the role of TonB and an intact proton motive force. *Mol. Microbiol.* 43, 335–354. doi: 10.1046/j.1365-2958.2002.02745.x

Roman-Hernandez, G., Peterson, J. H., and Bernstein, H. (2014). Reconstitution of bacterial autotransporter assembly using purified components. *Elife* 3:e04234. doi: 10.7554/eLife.04234

Rouphael, N. G., and Stephens, D. S. (2012). *Neisseria meningitidis*: biology, microbiology, and epidemiology. *Methods Mol. Biol.* 799, 1–20. doi: 10.1007/978-1-61779-346-2_1

Roussel-Jazédé, V., Arenas, J., Langereis, J. D., Tommassen, J., and van Ulsen, P. (2014). Variable processing of the IgA protease autotransporter at the cell surface of *Neisseria meningitidis*. *Microbiology* 160, 2421–2431. doi: 10.1099/mic.0.082511

Roussel-Jazédé, V., Grijpstra, J., van Dam, V., Tommassen, J., and van Ulsen, P. (2013). Lipidation of the autotransporter NalP of *Neisseria meningitidis* is required for its function in the release of cell-surface-exposed proteins. *Microbiology* 159, 286–295. doi: 10.1099/mic.0.063982-0

Roussel-Jazédé, V., Jongerius, I., Bos, M. P., Tommassen, J., and van Ulsen, P. (2010). NalP-mediated proteolytic release of lactoferrin-binding protein B from the meningococcal cell surface. *Infect. Immun.* 78, 3083–3089. doi: 10.1128/IAI.01193-09

Ruiz-Perez, F., Henderson, I. R., Leyton, D. L., Rossiter, A. E., Zhang, Y., and Nataro, J. P. (2009). Role of the periplasmic chaperone proteins in the biogenesis of serine protease autotransporters of *Enterobacteriaceae*. *J. Bacteriol.* 191, 6571–6583. doi: 10.1128/JB.00754-09

Sanders, H., Brehony, C., Maiden, M. C., Vipond, C., and Feavers, I. M. (2012). The effect of iron availability on transcription of the *Neisseria meningitidis* fHbp gene varies among clonal complexes. *Microbiology* 158, 869–876. doi: 10.1099/mic.0.054957-0.

Scarselli, M., Serruto, D., Montanari, P., Capecchi, B., Adu-Bobie, J., Veggi, D., et al. (2006). *Neisseria meningitidis* NhhA is a multifunctional trimeric autotransporter adhesin. *Mol. Microbiol.* 61, 631–644. doi: 10.1111/j.1365-2958.2006.05261.x

Schielke, S., Huebner, C., Spatz, C., Nägele, V., Ackermann, N., Frosch, M., et al. (2009). Expression of the meningococcal adhesin NadA is controlled by a transcriptional regulator of the MarR family. *Mol. Microbiol.* 72, 1054–1067. doi: 10.1111/j.1365-2958.2009.06710.x

Schmitt, C., Turner, D., Boesl, M., Abele, M., Frosch, M., and Kurzai, O. (2007). A functional two-partner secretion system contributes to adhesion of *Neisseria meningitidis* to epithelial cells. *J. Bacteriol.* 189, 7968–7976. doi: 10.1128/JB.00851-07

Schneider, M. C., Exley, R. M., Chan, H., Feavers, I., Kang, Y. H., Sim, R. B., et al. (2006). Functional significance of factor H binding to *Neisseria meningitidis*. *J. Immunol.* 176, 7566–7575. doi: 10.4049/jimmunol.176.12.7566

Schneider, M. C., Prosser, B. E., Caesar, J. J., Kugelberg, E., Li, S., Zhang, Q., et al. (2009). *Neisseria meningitidis* recruits factor H using protein mimicry of host carbohydrates. *Nature* 458, 890–893. doi: 10.1038/nature07769

Schryvers, A. B., and Stojiljkovic, I. (1999). Iron acquisition systems in the pathogenic *Neisseria*. *Mol. Microbiol.* 32, 1117–1123. doi: 10.1099/mic.0.068874-0

Schulze, R. J., and Zückert, W. R. (2006). *Borrelia burgdorferi* lipoproteins are secreted to the outer surface by default. *Mol. Microbiol.* 59, 1473–1484. doi: 10.1111/j.1365-2958.2006.05039.x

Seib, K. L., Serruto, D., Oriente, F., Delany, I., Adu-Bobie, J., Veggi, D., et al. (2009). Factor H-binding protein is important for meningococcal survival in human whole blood and serum and in the presence of the antimicrobial peptide LL-37. *Infect. Immun.* 77, 292–299. doi: 10.1128/IAI.01071-08

Selkrig, J., Mosbahi, K., Webb, C. T., Beloussoff, M. J., Perry, A. J., Wells, T. J., et al. (2012). Discovery of an archetypical protein transport system in bacterial outer membranes. *Nat. Struct. Mol. Biol.* 19, 506–510. doi: 10.1038/nsmb.2261

Senior, B. W., Stewart, W. W., Galloway, C., and Kerr, M. A. (2001). Cleavage of the hormone human chorionic gonadotropin, by the Type 1 IgA1 protease of *Neisseria gonorrhoeae*, and its implications. *J. Infect. Dis.* 184, 922–925. doi: 10.1086/323397

Serruto, D., Adu-Bobie, J., Scarselli, M., Veggi, D., Pizza, M., Rappuoli, R., et al. (2003). *Neisseria meningitidis* App, a new adhesin with autocatalytic serine protease activity. *Mol. Microbiol.* 48, 323–334. doi: 10.1046/j.1365-2958.2003.03420.x

Serruto, D., Spadafina, T., Ciucchi, L., Lewis, L. A., Ram, S., Tontini, M., et al. (2010). *Neisseria meningitidis* GNA2132, a heparin-binding protein that induces protective immunity in humans. *Proc. Natl. Acad. Sci. U.S.A.* 107, 3770–3775. doi: 10.1073/pnas.0915162107

Sim, R. J., Harrison, M. M., Moxon, E. R., and Tang, C. M. (2000). Underestimation of meningococci in tonsillar tissue by nasopharyngeal swabbing. *Lancet* 356, 1653–1654. doi: 10.1016/S0140-6736(00)03162-7

Sjölinder, H., Eriksson, J., Maudsdotter, L., Aro, H., and Jonsson, A. B. (2008). Meningococcal outer membrane protein NhhA is essential for colonization and disease by preventing phagocytosis and complement attack. *Infect. Immun.* 76, 5412–5420. doi: 10.1128/IAI.00478-08

Sjölinder, M., Altenbacher, G., Hagner, M., Sun, W., Schedin-Weiss, S., and Sjölinder, H. (2012). Meningococcal outer membrane protein NhhA triggers apoptosis in macrophages. *PLoS ONE* 7:e29586. doi: 10.1371/journal.pone.0029586

Sklar, J. G., Wu, T., Kahne, D., and Silhavy, T. J. (2007). Defining the roles of the periplasmic chaperones SurA, Skp, and DegP in *Escherichia coli*. *Genes Dev.* 21, 2473–2484. doi: 10.1101/gad.1581007

Snyder, L. A., Jarvis, S. A., and Saunders, N. J. (2005). Complete and variant forms of the 'gonococcal genetic island' in *Neisseria meningitidis*. *Microbiology* 151, 4005–4013. doi: 10.1099/mic.0.27925-0

Srinivas, N., Jetter, P., Ueberbacher, B. J., Werneburg, M., Zerbe, K., Steinmann, J., et al. (2010). Peptidomimetic antibiotics target outer-membrane biogenesis in *Pseudomonas aeruginosa*. *Nature* 327, 1010–1013. doi: 10.1126/science.1182749

Stojiljkovic, I., Hwa, V., de Saint Martin, L., O'Gaora, P., Nassif, X., Heffron, F., et al. (1995). The *Neisseria meningitidis* haemoglobin receptor: its role in iron utilization and virulence. *Mol. Microbiol.* 15, 531–541.

Sviridova, E., Rezacova, P., Bondar, A., Veverka, V., Novak, P., Schenk, G., et al. (2017). Structuraal basis of the interaction between the putative adhesion-involved and iron-regulated FrpD and FrpC proteins of *Neisseria meningitidis*. *Sci. Rep.* 7:40408. doi: 10.1038/srep40408

Takada, S., Fujiwara, S., Inoue, T., Kataoka, Y., Hadano, Y., Matsumoto, K., et al. (2016). Meningococcemia in adults: a review of the literature. *Intern. Med.* 55, 567–572. doi: 10.2169/internalmedicine.55.3272

Talà, A., Progida, C., De Stefano, M., Cogli, L., Spinosa, M. R., Bucci, C., et al. (2008). The HrpB-HrpA two-partner secretion system is essential for intracellular survival of *Neisseria meningitidis*. *Cell. Microbiol.* 10, 2461–2482. doi: 10.1111/j.1462-5822.2008.01222.x

Tavano, R., Capecchi, B., Montanari, P., Franzoso, S., Marin, O., Sztukowska, M., et al. (2011). Mapping of the *Neisseria meningitidis* NadA cell-binding site: relevance of predicted α-helices in the $NH_2$-terminal and dimeric coiled-coil regions. *J. Bacteriol.* 193, 107–115. doi: 10.1128/JB.00430-10

Thompson, S. A., and Sparling, P. F. (1993). The RTX cytotoxin-related FrpA protein of *Neisseria meningitidis* is secreted extracellularly by meningococci and by $HlyBD^+$ *Escherichia coli*. *Infect. Immun.* 61, 2906–2911.

Thompson, S. A., Wang, L. L., and Sparling, P. F. (1993a). Cloning and nucleotide sequence of *frpC*, a second gene from *Neisseria meningitidis* encoding a protein similar to RTX cytotoxins. *Mol. Microbiol.* 9, 85–96. doi: 10.1111/j.1365-2958.1993.tb01671.x

Thompson, S. A., Wang, L. L., West, A., and Sparling, P. F. (1993b). *Neisseria meningitidis* produces iron-regulated proteins related to the RTX family of exoproteins. *J. Bacteriol.* 175, 811–818. doi: 10.1128/jb.175.3.811-818.1993

Tinsley, C. R., Voulhoux, R., Beretti, J. L., Tommassen, J., and Nassif, X. (2004). Three homologues, including two membrane-bound proteins, of the disulfide oxidoreductase DsbA in *Neisseria meningitidis*: Effects on bacterial growth and biogenesis of functional type IV pili. *J. Biol. Chem.* 279, 27078–27087. doi: 10.1074/jbc.M313404200

Tsirigotaki, A., de Geyter, J., Šoštarik, N., Economou, A., and Karamanou, S. (2017). Protein export through the bacterial Sec pathway. *Nat. Microbiol. Rev.* 15, 21–36. doi: 10.1038/nrmicro.2016.161

Tsukazaki, T., Mori, H., Echizen, Y., Ishitan, R., Fukai, S., Tanaka, T., et al. (2011). Structure and function of a membrane component SecDF that enhances protein export. *Nature* 474, 235–238. doi: 10.1038/nature09980

Turner, D. P., Marietou, A. G., Johnston, L., Ho, K. K., Rogers, A. J., Wooldridge, K. G., et al. (2006). Characterization of MspA, an immunogenic autotransporter protein that mediates adhesion to epithelial and endothelial cells in *Neisseria meningitidis*. *Infect. Immun.* 74, 2957–2964. doi: 10.1128/IAI.74.5.2957-2964.2006

Turner, D. P., Wooldridge, K. G., and Ala'Aldeen, D. A. (2002). Autotransported serine protease A of *Neisseria meningitidis*: an immunogenic, surface-exposed outer membrane, and secreted protein. *Infect. Immun.* 70, 4447–4461. doi: 10.1128/IAI.70.8.4447-4461.2002

ur Rahman, S., and van Ulsen, P. (2013). System specificity of the TpsB transporters of coexpressed two-partner secretion systems of *Neisseria meningitidis*. *J. Bacteriol.* 195, 788–797. doi: 10.1128/JB.01355-12

ur Rahman, S., Arenas, J., Öztürk, H., Dekker, N., and van Ulsen, P. (2014). The polypeptide transport-associated (POTRA) domains of TpsB transporters determine the system specificity of two-partner secretion systems. *J. Biol. Chem.* 289, 19799–19809. doi: 10.1074/jbc.M113.544627

Urfer, M., Bogdanovic, J., Lo Monte, F., Moehle, K., Zerbe, K., Omasits, U., et al. (2016). A peptidomimetic antibiotic targets outer membrane proteins and disrupts selectively the outer membrane in *Escherichia coli*. *J. Biol. Chem.* 291, 1921–1932. doi: 10.1074/jbc.M115.691725

Vacca, I., Del Tordello, E., Gasperini, G., Pezzicoli, A., Di Fede, M., Rossi Paccani, S., et al. (2016). Neisserial heparin binding antigen (NHBA) contributes to the adhesion of *Neisseria meningitidis* to human epithelial cells. *PLoS ONE* 11:e0162878. doi: 10.1371/journal.pone.0162878

van Ulsen, P., Adler, B., Fassler, P., Gilbert, M., van Schilfgaarde, M., van der Ley, P., et al. (2006). A novel phase-variable autotransporter serine protease, AusI, of *Neisseria meningitidis*. *Microbes Infect.* 8, 2088–2097. doi: 10.1016/j.micinf.2006.03.007

van Ulsen, P., and Tommassen, J. (2006). Protein secretion and secreted proteins in pathogenic *Neisseriaceae*. *FEMS Microbiol. Rev.* 30, 292–319. doi: 10.1111/j.1574-6976.2006.00013.x

van Ulsen, P., Rutten, L., Feller, M., Tommassen, J., and van der Ende, A. (2008). Two-partner secretion systems of *Neisseria meningitidis* associated with invasive clonal complexes. *Infect. Immun.* 76, 4649–4658. doi: 10.1128/IAI.00393-08.

van Ulsen, P., van Alphen, L., Hopman, C. T., van der Ende, A., and Tommassen, J. (2001). *In vivo* expression of *Neisseria meningitidis* proteins homologous to the *Haemophilus influenzae* Hap and Hia autotransporters. *FEMS Immunol. Med. Microbiol.* 32, 53–64. doi: 10.1111/j.1574-695X.2001.tb00534.x

van Ulsen, P., van Alphen, L., ten Hove, J., Fransen, F., van der Ley, P., and Tommassen, J. (2003). A Neisserial autotransporter NalP modulating the processing of other autotransporters. *Mol. Microbiol.* 50, 1017–1030. doi: 10.1046/j.1365-2958.2003.03773.x

Veggi, D., Gentile, M. A., Cantini, F., Lo Surdo, P., Nardi-Dei, V., Seib, K. L., et al. (2012). The factor H binding protein of *Neisseria meningitidis* interacts with xenosiderophores *in vitro*. *Biochemistry* 51, 9384–9393. doi: 10.1021/bi301161w

Volokhina, E. B., Beckers, F., Tommassen, J., and Bos, M. P. (2009). The β-barrel outer membrane protein assembly complex of *Neisseria meningitidis*. *J. Bacteriol.* 191, 7074–7085. doi: 10.1128/JB.00737-09

Volokhina, E. B., Grijpstra, J., Stork, M., Schilders, I., Tommassen, J., and Bos, M. P. (2011). Role of the periplasmic chaperones Skp, SurA and DegQ in outer membrane protein biogenesis in *Neisseria meningitidis*. *J. Bacteriol.* 193, 1612–1621. doi: 10.1128/JB.00532-10

von Heijne, G. (1990). The signal peptide. *J. Membr. Biol.* 115, 195–201.

Voulhoux, R., Bos, M. P., Geurtsen, J., Mols, M., and Tommassen, J. (2003). Role of a highly conserved bacterial protein in outer membrane protein assembly. *Science* 299, 262–265. doi: 10.1126/science.1078973

Walther, D. M., Rapaport, D., and Tommassen, J. (2009). Biogenesis of β-barrel membrane proteins in bacteria and eukaryotes: evolutionary conservation and divergence. *Cell. Mol. Life Sci.* 66, 2789–2804. doi: 10.1007/s00018-009-0029-z

Wang, X., Sjölinder, M., Gao, Y., Wan, Y., and Sjölinder, H. (2016). Immune homeostatic macrophages programmed by the bacterial surface protein NhhA potentiate nasopharyngeal carriage of *Neisseria meningitidis*. *mBio* 7, e01670–e01615. doi: 10.1128/mBio.01670-15

Weinberg, E. D. (2009). Iron availability and infection. *Biochim. Biophys. Acta* 1790, 600–605. doi: 10.1016/j.bbagen.2008.07.002

Welsch, J. A., Moe, G. R., Rossi, R., Adu-Bobie, J., Rappuoli, R., and Granoff, D. M. (2003). Antibody to genome-derived neisserial antigen 2132, a *Neisseria meningitidis* candidate vaccine, confers protection against bacteremia in the absence of complement-mediated bactericidal activity. *J. Infect. Dis.* 188, 1730–1740. doi: 10.1086/379375

Wilson, M. M., and Bernstein, H. D. (2017). Surface-exposed lipoproteins: an emerging secretion phenomenon in Gram-negative bacteria. *Trends Microbiol.* 24, 198–208. doi: 10.1016/j.tim.2015.11.006

Wong, C. T., Xu, Y., Gupta, A., Garnett, J. A., Matthews, S. J., and Hare, S. A. (2015). Structural analysis of haemoglobin binding by HpuA from

the *Neisseriaceae* family. *Nat. Commun.* 6:10172. doi: 10.1038/ncomms10172

Woodhams, K. L., Benet, Z. L., Blonsky, S. E., Hackett, K. T., and Dillard, J. P. (2012). Prevalence and detailed mapping of the gonococcal genetic island in *Neisseria meningitidis*. *J. Bacteriol.* 194, 2275–2285. doi: 10.1128/JB.00094-12.

Wooldridge, K. G., Kizil, M., Wells, D. B., and Ala'Aldeen, D. A. (2005). Unusual genetic organization of a functional type I protein secretion system in *Neisseria meningitidis*. *Infect. Immun.* 73, 5554–5567. doi: 10.1128/IAI.73.9.5554-5567.2005

Yakushi, T., Masuda, K., Narita, S., Matsuyama, S., and Tokuda, H. (2000). A new ABC transporter mediating the detachment of lipid-modified proteins from membranes. *Nat. Cell Biol.* 2, 212–218. doi: 10.1038/35008635

Yamaguchi, K., Yu, F., and Inouye, M. (1988). A single amino acid determinant of the membrane localization of lipoproteins in *E. coli*. *Cell* 53, 423–432.

Yu, H., Muñoz, E. M., Edens, R. E., and Linhardt, R. J. (2005). Kinetic studies on the interactions of heparin and complement proteins using surface plasmon resonance. *Biochim. Biophys. Acta* 1726, 168–176. doi: 10.1016/j.bbagen.2005.08.003

**Conflict of Interest Statement:** The laboratory of JT has received research funding from GlaxoSmithKline Biologicals. The other author declares that the research was conducted in the absence of any commercial or financial relationships that could be construed as a potential conflict of interest.

frontiers in Cellular and Infection Microbiology

ORIGINAL RESEARCH
published: 28 August 2017
doi: 10.3389/fcimb.2017.00380

# Targeting the Type II Secretion System: Development, Optimization, and Validation of a High-Throughput Screen for the Identification of Small Molecule Inhibitors

*Ursula Waack[1], Tanya L. Johnson[1,2], Khalil Chedid[1], Chuanwu Xi[3], Lyle A. Simmons[4], Harry L. T. Mobley[1] and Maria Sandkvist[1]**

[1] Department of Microbiology and Immunology, University of Michigan Medical School, Ann Arbor, MI, United States, [2] Department of Chemistry, Eastern Michigan University, Ypsilanti, MI, United States, [3] Department of Environmental Health Sciences, University of Michigan School of Public Health, Ann Arbor, MI, United States, [4] Department of Molecular, Cellular, and Developmental Biology, University of Michigan, Ann Arbor, MI, United States

Nosocomial pathogens that develop multidrug resistance present an increasing problem for healthcare facilities. Due to its rapid rise in antibiotic resistance, *Acinetobacter baumannii* is one of the most concerning gram-negative species. *A. baumannii* typically infects immune compromised individuals resulting in a variety of outcomes, including pneumonia and bacteremia. Using a murine model for bacteremia, we have previously shown that the type II secretion system (T2SS) contributes to *in vivo* fitness of *A. baumannii.* Here, we provide support for a role of the T2SS in protecting *A. baumannii* from human complement as deletion of the T2SS gene *gspD* resulted in a 100-fold reduction in surviving cells when incubated with human serum. This effect was abrogated in the absence of Factor B, a component of the alternative pathway of complement activation, indicating that the T2SS protects *A. baumannii* against the alternative complement pathway. Because inactivation of the T2SS results in loss of secretion of multiple enzymes, reduced *in vivo* fitness, and increased sensitivity to human complement, the T2SS may be a suitable target for therapeutic intervention. Accordingly, we developed and optimized a whole-cell high-throughput screening (HTS) assay based on secreted lipase activity to identify small molecule inhibitors of the T2SS. We tested the reproducibility of our assay using a 6,400-compound library. With small variation within controls and a dynamic range between positive and negative controls, the assay had a z-factor of 0.65, establishing its suitability for HTS. Our screen identified the lipase inhibitors Orlistat and Ebelactone B demonstrating the specificity of the assay. To eliminate inhibitors of lipase activity and lipase expression, two counter assays were developed and optimized. By implementing these assays, all seven tricyclic antidepressants present in the library were found to be inhibitors of the lipase, highlighting the potential of identifying alternative targets for approved pharmaceuticals. Although no T2SS inhibitor was identified among

OPEN ACCESS

**Edited by:**
*Sophie Bleves, Aix-Marseille University, France*

**Reviewed by:**
*Olivera Francetic, Institut Pasteur, France*
*Katrina T. Forest, University of Wisconsin-Madison, United States*

***Correspondence:**
*Maria Sandkvist*
*mariasan@umich.edu*

**Received:** *31 May 2017*
**Accepted:** *09 August 2017*
**Published:** *28 August 2017*

**Citation:**
*Waack U, Johnson TL, Chedid K, Xi C, Simmons LA, Mobley HLT and Sandkvist M (2017) Targeting the Type II Secretion System: Development, Optimization, and Validation of a High-Throughput Screen for the Identification of Small Molecule Inhibitors. Front. Cell. Infect. Microbiol. 7:380. doi: 10.3389/fcimb.2017.00380*

the compounds that reduced lipase activity by ≥30%, our small proof-of-concept pilot study indicates that the HTS regimen is simple, reproducible, and specific and that it can be used to screen larger libraries for the identification of T2SS inhibitors that may be developed into novel *A. baumannii* therapeutics.

**Keywords: *Acinetobacter baumannii*, type II secretion, high-throughput screening, small molecule inhibitors, LipA, lipase activity, antibiotic resistance, antidepressants**

## INTRODUCTION

A growing concern in hospitals, nursing homes, and other healthcare facilities is the increasing frequency of antibiotic resistant infections that result in longer hospital stays, higher costs, and increased mortality. The ESKAPE pathogens *Enterococcus faecium, Staphylococcus aureus, Klebsiella pneumoniae, Acinetobacter baumannii, Pseudomonas aeruginosa,* and *Enterobacter* species have attracted considerable attention as they cause the majority of nosocomial infections (Rice, 2008). Infections caused by *A. baumannii* are prevalent with ∼45,000 cases per year in the United States alone. Globally, there are about 1 million cases annually (Spellberg and Rex, 2013) and reports suggest that *A. baumannii* may be the leading cause of nosocomial infections in some countries (Wong et al., 2016). It is estimated that 50% of these infections are caused by antibiotic-resistant strains (Spellberg and Rex, 2013). Exposure to *A. baumannii* can result in a variety of infections including pneumonia, urinary tract infection, bacteremia, meningitis, skin, and wound infections that may lead to sepsis (Bergogne-Berezin and Towner, 1996; Maragakis and Perl, 2008). Considered an opportunist, *A. baumannii* typically infects immune-compromised individuals but more recently isolated strains may not be restricted to this patient population, possibly as a consequence of increased virulence (Jones et al., 2015; Paterson and Harris, 2015). The remarkable ability of *A. baumannii* to form biofilm and resist dry environments (Jawad et al., 1998; Espinal et al., 2012) may explain its prevalence in healthcare environments (Weernink et al., 1995; Catalano et al., 1999). Additional contributing factors include multi- or pan-antibiotic resistance (Maragakis and Perl, 2008; Leite et al., 2016), which is due, in part, to intrinsic properties of the outer membrane of *A. baumannii* and its notable ability to acquire foreign DNA through horizontal gene transfer (de Vries and Wackernagel, 2002).

The rise in antibiotic resistance rapidly reduces the options of effective treatment and calls for the identification of new therapeutic approaches. A recommended strategy combines antibiotics with drugs that target resistance mechanisms such as Augmentin, which consists of Amoxicillin and the β-lactamase inhibitor Clavulanate. Other feasible options include the combination of antibiotics with inhibitors of drug efflux pumps or outer membrane permeabilizers (Gill et al., 2015). Identification of new therapeutic targets is also necessary. These may include essential processes such as lipopolysaccharide synthesis and transport as well as factors that contribute to *in vivo* fitness and virulence.

One of the first studies to target virulence factors using HTS of small molecule libraries identified a compound that inhibits dimerization of ToxT, a virulence regulator in *Vibrio cholerae* (Hung et al., 2005; Shakhnovich et al., 2007). This inhibitor abolishes the production of cholera toxin and decreases TCP-mediated colonization in an infant mouse model (Hung et al., 2005). Other studies have screened for biologicals or chemical compounds that target colonization factors, such as curli and type 1 pili, toxins, protein secretion pathways or quorum sensing systems (Steadman et al., 2014; Gill et al., 2015; Ruer et al., 2015; Hauser et al., 2016). With a few exceptions, it is too soon to evaluate the outcome of these studies and their success; however, some of these potential anti-virulence drugs are in various stages of development and are being analyzed in animal models or clinical trials (Pan et al., 2009; Rasko and Sperandio, 2010; Hauser et al., 2016). An IgG antibody that targets the binding of anthrax toxin to its receptor is currently used as an antitoxin in combination therapy for the treatment of *Bacillus anthracis* infections (Hendricks et al., 2014) and demonstrates the feasibility of targeting disease-causing components of pathogens.

Secretion systems are particularly attractive targets for alternative therapeutics as their inactivation interferes with the delivery of entire batteries of secreted virulence factors. Therefore, several HTSs have been designed to identify small molecule inhibitors of the type III secretion system, which is present in many gram-negative human pathogens and secretes a wide variety of virulence effectors (Nordfelth et al., 2005; Aiello et al., 2010). Another secretion system, the type II secretion system (T2SS), is responsible for the secretion of numerous degradative enzymes and toxins that contribute to survival in the environment and the mammalian host and may also be a suitable target for alternative therapeutics (Sandkvist, 2001; Cianciotto, 2005; Cianciotto and White, 2017). As with many gram-negative pathogens, *A. baumannii* possesses a functional T2SS (Elhosseiny et al., 2016; Johnson et al., 2016). The T2SS forms an apparatus that spans both the inner and outer membrane and is encoded by 12 essential genes, *gspC-M* and *pilD* (Korotkov et al., 2012; Thomassin et al., 2017). T2S substrates are synthesized with an N-terminal signal peptide that allows for translocation from the cytoplasm to the periplasm via the general export (Sec) or twin arginine translocation (Tat) pathways. Once in the periplasm, the signal sequence is cleaved, the protein folds, and interacts with the T2SS to finally exit the cell via a gated outer membrane pore formed by GspD (Reichow et al., 2010; Douzi et al., 2011; Yan et al., 2017). GspD connects to GspC, one of the components of the inner membrane platform that also consists of the transmembrane proteins GpsF, L, and M (Sandkvist et al.,

1999; Py et al., 2001; Michel et al., 2007; Abendroth et al., 2009; Douzi et al., 2011; Korotkov et al., 2011). The pseudopilins GspG, H, I, J, and K make a pseudopilus, a structure homologous to the Type IV pilus, while PilD cleaves and methylates the pseudopilin subunits prior to their assembly (Nunn and Lory, 1993; Durand et al., 2005; Cisneros et al., 2012). The entire system is powered by a cytoplasmic ATPase, GspE (Camberg and Sandkvist, 2005; Camberg et al., 2007). All of these proteins, including their expression and interactions, are potential targets for a therapeutic compound (**Figure 1**).

Recent work by our laboratory and others has demonstrated the benefit of having a functional T2SS for colonization by *A. baumannii* and *A. nosocomialis* (Elhosseiny et al., 2016; Harding et al., 2016; Johnson et al., 2016). Inactivation of the T2SS or one of its substrates results in diminished survival in murine models for bacteremia and pneumonia, indicating that screening for compounds that target the T2SS may lead to the identification of *A. baumannii* virulence inhibitors. In this study, we describe the development and optimization of a HTS to identify small molecule inhibitors of the T2SS in *A. baumannii*. In addition, we highlight the need for inclusion of high-throughput counter-screens to remove compounds with alternative targets.

# METHODS

## Bacterial Strains and Plasmids

All bacterial strains and plasmids are described in **Table 1**. All strains were cultured overnight in Luria-Bertani (LB) broth. When necessary, LB broth was supplemented with carbenicillin (100 μg/ml) for plasmid maintenance. The studies were conducted under biosafety level 2 conditions.

## Compound Library

All compounds tested in this study are from commercially available libraries acquired and maintained in 384-well plates in DMSO at −20°C at a concentration of 2 mM by the Center for Chemical Genomics at the University of Michigan. The five libraries include MS2400, NCC, Pathways, Prestwick, and LOPAC. MS2400 is a collection of FDA approved drugs plus compounds with known biological activity obtained from Microscource Discovery (Spectrum Collection). NCC is a library with compounds that have been used in human clinical trials. The Pathways collection is comprised of known active compounds with a variety of targets. The Prestwick library is composed of approved drugs which are safe for use in humans. Finally, the LOPAC collection is the Library of Pharmacologically Active Compounds from Sigma.

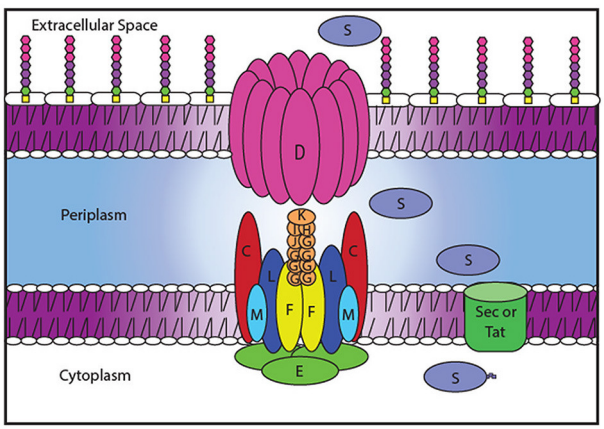


**FIGURE 1 |** Potential Targets of a T2SS inhibitor. T2SS inhibitors may block transcription of the T2SS genes or translation, post-translational modification, protein-protein interactions or function of the T2SS proteins. Blocking the recognition by GspC/GspD of the T2SS substrates (S) to be secreted by the T2SS system could also halt secretion.

## Serum Bactericidal Assay

After cultures were grown overnight in LB, the cells were separated from supernatant by centrifugation for 10 min at 3,500 rpm. The cells were washed in PBS and diluted 1:100. Equal volumes of cells and either 100% normal human serum, heat-inactivated human serum or factor depleted sera were incubated together for 30 min at 37°C. Samples were diluted and plated on LB agar to obtain CFUs.

**TABLE 1 |** List of bacterial strains and plasmids used in study.

| Strain or plasmid | Characteristics | Source or study |
|---|---|---|
| **STRAIN** | | |
| 17978 | WT for this study | ATCC |
| 17978Δ*gspD* | T2SS mutant | Johnson et al., 2016 |
| 17978Δ*gspN* | | Johnson et al., 2016 |
| 17978Δ*lipA* | | Johnson et al., 2016 |
| AB031 | Clinical strain | Tilley et al., 2014 |
| AB031 Δ*gspD* | T2SS mutant | Waack et al., in preparation. |
| AB 0057 | Clinical strain, $tet^R$, $chl^R$, $trim^R$, $carb^R$ | Adams et al., 2008 |
| AB 5075 | Clinical strain, $tet^R$, $rif^R$, $carb^R$, $trim^R$ | Jacobs et al., 2014 |
| P020 | Clinical strain, $cef^R$ | Greene et al., 2016 |
| C038 | Clinical strain, $cef^R$ | Greene et al., 2016 |
| C058 | Clinical strain, $mer^R$, $azt^R$, $cef^R$, $cip^R$, $lev^R$, $imi^R$ | Greene et al., 2016 |
| C076 | Clinical strain, $azt^R$, $cef^R$, $cip^R$, $lev^R$, $trim^R$ | Greene et al., 2016 |
| P084 | Clinical strain, $mer^R$, $azt^R$, $cef^R$, $cip^R$, $lev^R$, $imi^R$ | Greene et al., 2016 |
| C097 | Clinical strain | Greene et al., 2016 |
| P102 | Clinical strain, $mer^R$, $azt^R$, $cef^R$, $cip^R$, $lev^R$, $imi^R$ | Greene et al., 2016 |
| P143 | Clinical strain, $azt^R$, $cef^R$ | Greene et al., 2016 |
| **PLASMID** | | |
| pMMB67EH | Low copy vector ($Ap^r$) | Fürste et al., 1986 |
| p*lipBA* | pMMB67EH-*lipBA* ($Ap^r$) | Johnson et al., 2016 |
| p*gfp* | pMMB67EH-*gfp* ($Ap^r$) | Scott et al., 2001 |

*azt, aztreonam; carb, carbapenems; cef, cefazolin; chl, chloramphenicol; cip, ciprofloxacin; gent, gentamycin; imi, imipenem; lev, levofloxacin; mer, meropenem; rif, rifampin; tet, tetracycline; trim, trimethoprim-sulfate; tob, tobramycin.*

## High-Throughput Lipase Assay

Overnight cultures of wild-type (WT) *A. baumannii* 17978/p*lipBA* and 17978Δ*gspD*/p*lipBA* were grown in LB broth. After growth, the cultures were centrifuged for 10 min at 3500 rpm to separate cells and supernatant. The supernatant was removed and the pellet was washed in Mueller-Hinton 2 (MH) and resuspended in the original volume. 10 μL of MH was added to each well of a 384-well Greiner 784080 plate. Compounds in DMSO or the DMSO control were added to the wells (0.05 μL) using Perkin Elmer Sciclone liquid handler with a 50 nl pintool attachment (in primary assay). For concentration-response assays, the TTP LabTech Mosquito X1 was used to place variable volumes (0.02–1.2 μL) of compounds to the wells. 17978/p*lipBA* was diluted and added to all the negative control wells as well as to the sample wells while 17978Δ*gspD*/p*lipBA* was diluted and added to the positive control wells. All cultures had a starting $OD_{600}$ of 0.005 and were supplemented with 50 μM IPTG (isopropyl-β-D-thiogalactopyranoside) to induce expression of the *lipBA* genes. Plates were centrifuged 1 min at 1,000 rpm to ensure all liquid was at the bottom of the well. Plates were incubated overnight at 24°C in a humidified incubator. After 16 h incubation, the $OD_{600}$ value of each culture was recorded. An optimized lipase assay was used to measure lipase activity. Briefly, the cultures were incubated with 0.45 mM 4-nitrophenyl myristate, 80 mM Tris-HCl (pH 8.0), and 0.15% Triton X-100 and the absorbance at 415 nm was measured over time using the PE EnVision Multimode Plate Reader. All data were uploaded to MScreen for analysis. MScreen is a data analysis and storage system created by the Center for Chemical Genomics intended for the processing of high-throughput data generated by users of the center (Jacob et al., 2012).

## Lipase Inhibitor Assay

Cultures of *A. baumannii* 17978/p*lipBA* and 17978Δ*gspD*/p*lipBA* were grown overnight in LB broth with 50 μM IPTG and the supernatant and cells were separated by centrifugation. For concentration-response assays, the TTP LabTech Mosquito X1 was used to add variable volumes (0.02–1.2 μl) of compounds. Supernatant was added to the wells, buffer with lipase substrate was added and the change in $OD_{415}$ was recorded as above. All data were uploaded to MScreen for analysis.

## GFP Expression Assay

*A. baumannii* 17978/p and 17978/p*gfp* cultures were grown O/N as above. Cells were washed as described above for the lipase assay. Compounds in DMSO or the DMSO control were added to the wells of a black low-volume Greiner 784073 plate using Perkin Elmer Sciclone liquid handler with a 50 nl pintool attachment calibrated to deliver 200 nM. For concentration-response assays, the TTP LabTech Mosquito X1 was used to place variable volumes (0.02–1.2 μl). Cultures were diluted to $OD_{600}$ = 0.005 in LB supplemented with 75 μM IPTG. Plates were centrifuged for 1 min at 1,000 rpm to ensure all liquid was at the bottom of the well and incubated overnight at room temperature in a humidified incubator. Fluorescence was measured after growth using a BMGLabtech PHERAstar (485 nm excitation, 520 nm emission). All data were uploaded to MScreen.

## Lipase Assay

A modified version of the lipase assay reported by Johnson et al. (2016) was used. Briefly, overnight cultures of *A. baumannii* strains were cultured in LB broth. The lipase activity of each culture was measured by a spectrophotometer after addition of 0.9 mM of the substrate, 4-nitrophenyl myristate in 80 mM Tris/0.15% Triton X-100 buffer. The absorbance at 415 nm was measured over time at 37°C. All assays were performed in triplicate with means and standard deviations presented.

# RESULTS

Recent studies have demonstrated the significance of the T2SS in colonization by *A. baumannii* and *A. nosocomialis* in murine models of bacteremia and pneumonia (Elhosseiny et al., 2016; Harding et al., 2016; Johnson et al., 2016). In our study, we also revealed that one of the secreted proteins, LipA, contributes to colonization (Johnson et al., 2016), possibly by aiding in nutrient acquisition through lipid hydrolysis. It is quite likely that other T2S substrates including the lipase LipH, the phospholipase LipAN, and/or proteases and other putative enzymes identified by proteomics similarly contribute to *in vivo* survival of *A. baumannii* (Elhosseiny et al., 2016; Harding et al., 2016).

In addition, a "serum resistance factor" may be secreted by the T2SS, as a previous study aimed at identifying factors that contribute to *A. baumannii* proliferation in human serum identified a *gspN* transposon insertion mutant with diminished serum survival (Jacobs et al., 2010). Here, we followed up on this finding and tested the possibility that an intact T2SS is required for *A. baumannii* ATCC 17978 to resist serum complement. Many isolates of *A. baumannii* survive in the presence of 100% serum; however, ATCC 17978 is sensitive to this concentration and, therefore, we conducted our experiments using 50% serum. The WT and Δ*gspD* mutant strains were incubated in 50% pooled human sera, and the CFUs were determined after 30 min incubation at 37°C. As a control, we used the Δ*lipA* mutant that has an intact T2SS but lacks one of the T2S substrates, LipA. We also treated the WT and mutant strains with heat-inactivated (HI; 56°C, 30 min) serum, in which the complement system is inactivated. While no loss of viability was observed for the WT and Δ*lipA* strains, only 1% of the Δ*gspD* mutant cells survived 30 min in normal serum (**Figure 2A**). Next, we subjected the Δ*gspD* mutant cells to factor C1q-depleted and factor B-depleted human sera. The majority of Δ*gspD* mutant cells survived in the absence of factor B, which is required for activation of the alternative complement pathway; while in the C1q-depleted serum, which is deficient in the classical pathway yet contains factor B, <0.05% of the Δ*gspD* mutant cells were viable (**Figure 2B**). This result suggests that the T2SS directs the outer membrane translocation of a factor that provides protection from the alternative pathway. In contrast, the Δ*gspN* mutant was not affected by human serum (**Figure 2A**), a result that differs from the study published by Jacobs et al. (2010). The lack of a serum sensitive phenotype for the Δ*gspN* mutant is consistent with our earlier finding that GspN is not required for T2S in *A. baumannii* and with the discovery by Wang et al. that showed GspN is not needed for

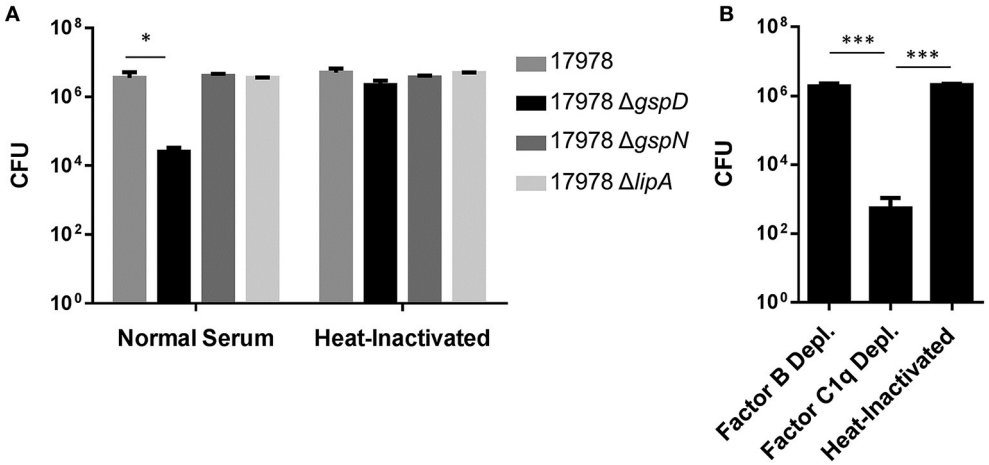


**FIGURE 2 |** Survival in serum depends on the T2SS. **(A)** Cells from overnight cultures were washed and incubated for 30 min at 37°C with either 50% normal human serum or heat-inactivated serum. Cells were plated for CFUs following incubation. $^{*}p < 0.05$ by Student *t*-test; $n = 3$. **(B)** Cells from overnight cultures were washed and incubated as above with Factor B deficient, C1q deficient, or heat-inactivated serum. $n = 3$, $^{***}p < 0.001$ by Student *t*-test.

survival of *A. baumannii* in a mouse model of pneumonia (Wang et al., 2014). We suggest, therefore, that the diminished growth observed for the *gspN* transposon mutant in human serum is due to a polar effect of the transposon on the downstream gene, *gspD*, which we show here is required for full protection from serum complement. Taken together with earlier findings, these results support the model that extracellular proteins secreted by the T2SS play important roles in the pathogenesis of *A. baumannii* and suggest that the T2SS may be an attractive target for therapeutic intervention.

Inhibiting the function of the T2SS would simultaneously prevent the secretion of many substrates causing a greater impact on *A. baumannii* survival than targeting individual T2S substrates. The T2SS components and their interactions (**Figure 1**) provide ideal targets for therapeutics because they are unique to the T2SS and are absent from most members of the human microbiota. Compounds could block the function of the outer membrane pore, inhibit interactions between the different components of the secretion apparatus, prevent recognition of the substrates by the apparatus, or interfere with the expression of the T2S proteins (**Figure 1**). To identify inhibitors of the T2SS, we developed a novel HTS approach.

## Development of HTS Assay

In our previous study, we used a colorimetric lipase assay to measure the activity of the T2S lipase, LipA, in culture supernatant of strains overexpressing plasmid encoded *lipBA* genes. We used an overexpression strain because endogenous lipase production is very low during growth of *A. baumannii* ATCC 17978 in LB presenting a challenge for detection (Johnson et al., 2016). Further, because lipase activity is undetectable in the culture supernatant of T2SS mutants, this provides a robust assay that can be used as a readout for T2SS activity (Johnson et al., 2016) for the purpose of identifying T2SS inhibitors. However, testing the effect of a large number of compounds on LipA activity in cell-free culture supernatants would be cumbersome as it would involve an extra processing step. Thus, we compared cell-free culture supernatants and unfractionated cultures for T2SS activity (**Figure 3**). The culture supernatant and unfractionated culture of the 17978/p*lipBA* strain both showed significant lipase activity toward 4-nitrophenyl myristate, while there was little to no activity either in the supernatant or culture of the T2SS mutant, 17978Δ*gspD*/p*lipBA*. More importantly, the vast majority of the lipase activity in the unfractionated culture was generated by extracellular LipA thus allowing us to omit the step in which the culture supernatant is separated from cells. Consequently, we were able to develop an assay for HTS of small molecule inhibitors of T2SS that involved the addition of the lipase substrate directly to the bacterial cultures following growth in the presence and absence of compounds.

In our first attempt to miniaturize the assay we grew cultures of the WT 17978 strain and Δ*gspD* mutant in the wells of clear 96-well microtiter plates to which we then added 4-nitrophenyl myristate and determined the lipase activity by measuring the increase in absorbance at 415 nm over time. Prior to adding the lipase substrate, we measured the density of the cultures at 600 nm. This is an important step because many compounds, including known antibiotics, will affect the growth of the bacteria resulting in false positives. While the move to the microtiter format required titration of IPTG to induce *lipBA* expression, a reproducible difference in lipase activity could be measured in the WT and mutant cultures. We further developed the lipase secretion assay in flat-bottom 384-well plates using a MicromultiDrop liquid dispenser. As the conditions developed for the 96-well plates did not generate reproducible data in the 384-well format, we set up a systematic analysis in which we evaluated a variety of conditions to obtain the most consistent data. We varied growth media, culture volume, IPTG concentration, starting $OD_{600}$ of the culture, growth temperature, length of growth, aeration, and

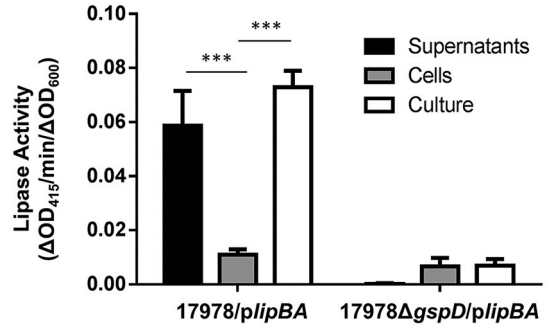


**FIGURE 3 |** Detection of T2S lipase activity in either culture supernatants, cells, or unfractionated bacterial cultures. Enzymatic activity of either the supernatants, cells, or unfractionated cultures of 17978/p*lipBA* or 17978Δ*gspD*/p*lipBA* strains cultured overnight in LB broth. The substrate 4-nitrophenyl-myristate was added to the samples and the change in $OD_{415}$ was recorded over time. Activities were normalized to the $OD_{600}$ of the original cultures. $n = 3$, $^{***}p < 0.001$ by One-Way Anova.

**TABLE 2 |** Optimization of assay conditions for development of a HTS.

| Variables | Conditions tested | Final assay condition |
|---|---|---|
| Plate format | 96 well vs. 384 well | 384 well |
| Start OD | 0.005, 0.0025, 0.001, 0.0005 | 0.005 |
| Media | LB vs. Mueller-Hinton (MH) | MH |
| Volume | 10, 15, 20, or 30 μL | 10 μL |
| Temperature | 20°, 24° (RT), 30°, 37°C | RT |
| Aeration | Shaking vs. non-shaking | Non-shaking |
| Substrate Concentration | 0.225, 0.45, 0.9, 1.8 mM | 0.45 mM |

finally, 4-nitrophenyl myristate concentration (**Table 2**). The experimental setup that yielded the most consistent growth and reproducible lipase activity from well-to-well and plate-to-plate were obtained when cultures were grown in 10 μL MH broth (from a starting $OD_{600}$ of 0.005) with 50 μM IPTG, in a humidified chamber at 24°C without shaking for 16 h (**Table 2**).

## Pilot Screen

Following optimization, we screened 6,400 pharmacologically active compounds as well as FDA-approved drugs from the following libraries available at the University of Michigan Center for Chemical Genomics: MS2400, Prestwick, LOPAC, BioFocus NCC, and Focused Collections. This pilot screen was performed to evaluate the strength of the assay before moving on to larger compound libraries. Each 384-well plate contained 320 sample wells, 32 positive control wells, and 32 negative control wells. As the ultimate goal of the HTS is to identify T2SS inhibitors, the T2SS mutant, 17978Δ*gspD*/p*lipBA* served as our positive control while 17978/p*lipBA* served as the negative control. Both negative and positive controls were cultured in the presence of 0.5% DMSO while the sample wells containing 17978/p*lipBA* received the compounds resuspended in DMSO yielding a 0.5% final DMSO concentration. Following growth, the absorbance at 600 nm was measured for the cultures in each well. The average $OD_{600}$ for the negative and positive controls were 0.21 ± 0.02 and 0.19 ± 0.02, respectively. The lipase substrate was then added, and the absorbance at 415 nm was measured over a period of 20 min at ambient temperature. The pilot screen yielded a z-factor of 0.65 [$z' = 1-(3*(\sigma_p + \sigma_n)/(|\mu_p - \mu_n|))$](Zhang et al., 1999; **Figure 4A**) and coefficient of variation (CV, $CV = \sigma/\mu$) of 0.03 and 0.07 for the negative and positive controls, respectively. Initial active compounds were identified using statistical comparisons to positive and negative controls present on every plate. In the triage process, we selected compounds that resulted in all of the following: a reduction in lipase activity that was equal or >3 *SD* of the negative control, a minimum cut-off at 30% inhibition of lipase activity and an $OD_{600}$ value >0.17 (**Figure 4**). Implementing these criteria yielded 191 compounds (3% hit rate). From these, we removed 22 compounds that are known antibiotics, such as gatifloxacin, clarithromycin, and levofloxacin and retested the remaining 169 compounds.

Each compound was re-tested twice in a concentration-dependent manner using the original DMSO stock and covering two orders of magnitude. $IC_{50}$ values were calculated. Forty-eight compounds gave $IC_{50}$ values of <30 μM. Following removal of compounds that affected growth, 34 active compounds remained (0.5% hit rate). Fresh powder of these compounds were ordered and retested. Of these compounds, 21 were confirmed as active. The compounds with the lowest $IC_{50}$ values are known lipase inhibitors, Orlistat and Ebelactone B, and therefore likely had a direct effect on the lipase activity itself. Orlistat, a pancreatic lipase inhibitor, was the most potent of the compounds tested with an $IC_{50}$ of 40.6 nM (**Figure 5A**). The other compounds exhibited $IC_{50}$s between 4.3 and 27 μM (**Table 3**). The titration curves of Orlistat (**Figure 5A**) and Oxyclozanide (**Figure 5B**) are shown as examples. Of note, compounds with low $IC_{50}$ values included tricyclic antidepressants that are known to act as serotonin-norepinephrine re-uptake inhibitors. While these latter compounds may act on the secretion system, it is possible they also bind directly to the lipase via their hydrophobic rings. Our proof-of-concept pilot screen with z' = 0.65 and CV of 0.03 and 0.07 for the negative and positive controls, respectively, showed that our assay was reproducible and was capable of identifying compounds that result in a statistically significant reduction in lipase activity. However, the identification of compounds that are known lipase inhibitors emphasized the importance of developing counter screens and other follow-up assays to remove false positives and to assure specificity in order to identify T2S inhibitors.

## Counter Screening

As the most potent compounds identified in our pilot screen described above represented lipase inhibitors, we developed a screen to eliminate these types of compounds. In this counter screen the bacterial cultures were not grown in the presence of compounds. Instead, a large batch of 17978p/*lipBA* culture was grown without compounds and following removal of cells, the

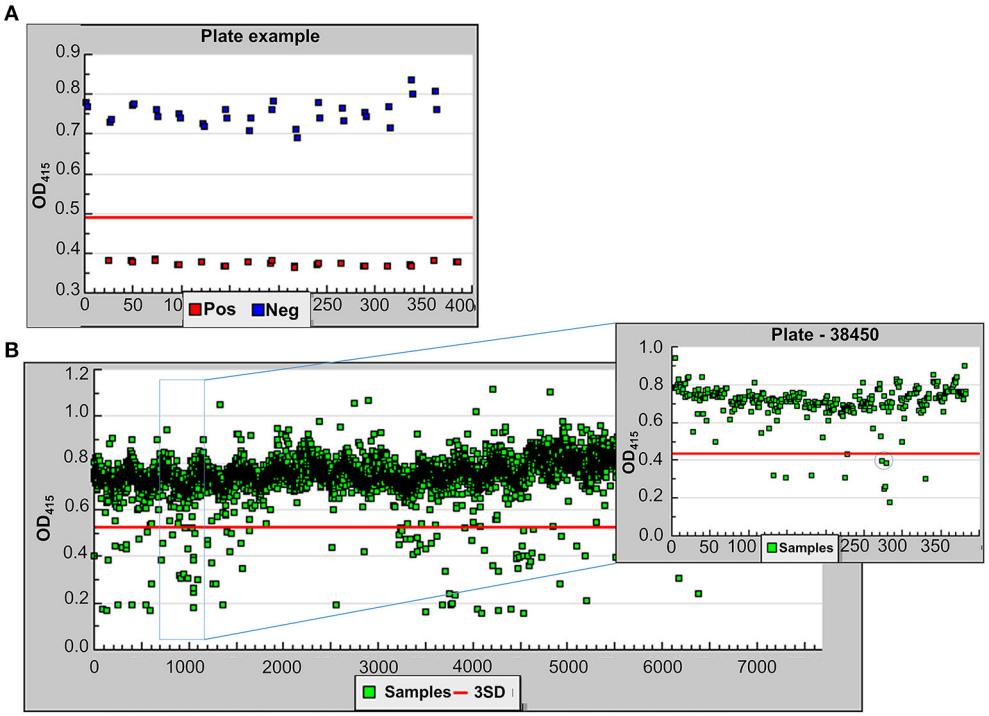


**FIGURE 4 |** Demonstrating the feasibility of the lipase assay for HTS. **(A)** One sample plate from the pilot screen showing the $OD_{415}$ values for the positive (red) and negative (blue) controls. The z-factor for the entire pilot screen was calculated using $1-(3^*(\sigma_p + \sigma_n)/(|\mu_p-\mu_n|))$ where σ is the standard deviation and μ is the mean. **(B)** The results for 6,400 compounds tested in the pilot screen. All samples below the red line (3 *SD* from negative controls) were taken into consideration. A single sample plate is highlighted in the inset. The compound, Orlistat, indicated by the circle represents a hit in the primary screen and was tested further.

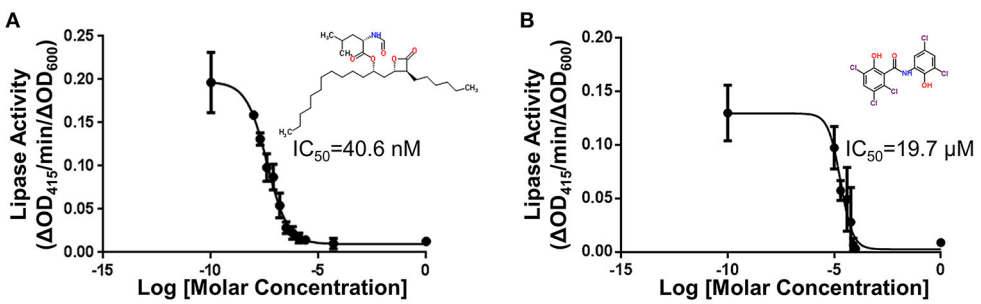


**FIGURE 5 |** Titrations of compounds and the corresponding $IC_{50}$. **(A)** Titration of Orlistat, a pancreatic lipase inhibitor that was identified in the primary screen. Increasing amounts of Orlistat was included during growth of 17978/p*lipBA*. After overnight incubation in 96-well plates, the substrate 4-nitrophenyl myristate was added and the lipase activity was measured. Activities have been normalized to $OD_{600}$ of the cultures. $n = 3$, bars represent standard deviation from the mean. In follow-up counter screening, Orlistat was classified as an inhibitor of LipA activity **(B)** Titration of Oxyclozanide, an anthelmintic that was identified in the primary screen. Lipase activity in the presence of Oxyclozanide was measured as above. Activities have been normalized to $OD_{600}$ of culture. $n = 3$, bars represent standard deviation from the mean. Following counter screening, Oxyclozanide was classified as an inhibitor of *lipA* expression from the plasmid.

cell-free culture supernatant containing the lipase was distributed in 384-well plates and incubated with the compounds, thus allowing us to identify compounds that inhibit the lipase itself. Following optimization, we identified the following conditions for the counter screen: (1) grow 17978p/*lipBA* with 50 μM IPTG for 16 h and remove cells by centrifugation; (2) dilute the supernatant 1:10 and add 10 μL to 384-well plates containing compounds; (3) add 10 μL 4-nitrophenyl myristate at 0.45 mM, incubate 10 min, and measure the change in absorbance at 415 nm.

An additional counter screen was developed for the elimination of compounds that interfere with plasmid-encoded *lipBA* expression. For this, we used the same plasmid backbone as p*lipBA* but substituted the *lipBA* gene with the *gfp* gene, which codes for Green Fluorescent Protein (p*gfp*). This plasmid was introduced into the WT 17978 strain (17978/p*gfp*), and without

**TABLE 3 |** $IC_{50}$ values of compounds identified in primary screen and tested for concentration dependent inhibition.

| Compound | $IC_{50}$ (μM) |
|---|---|
| **LIPASE INHIBITORS** | |
| Ebelactone B ($n = 2$) | 4.3 |
| **ANTI-DEPRESSANTS** | |
| Vivactil | 10 |
| Fluoxetine | 10.5 |
| Aventyl | 14.5 |
| Duloxetine | 16 |
| Norcyclobenzaprine | 16 |
| Maprotiline | 16 |
| Desiprimine | 16.5 |
| Lofepramine | 21 |
| Sertraline | 23.5 |
| **OTHER** | |
| Perhexiline Maleate | 4.7 |
| Febuxostat | 8 |
| Alfuzosin | 11 |
| Stattic | 12.5 |
| Fendiline | 13 |
| Tomoxetine | 14.5 |
| Indatraline | 27 |

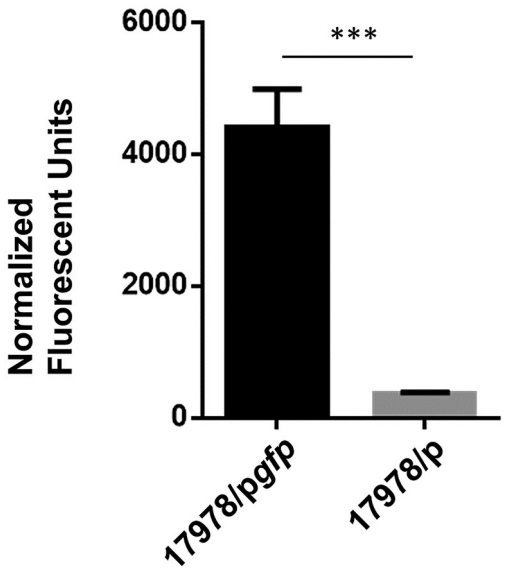


**FIGURE 6 |** Detection of GFP fluorescence. Strains of 17978/p and 17978/p*gfp* were grown overnight in the presence of IPTG to induce the expression of GFP. After growth, fluorescence of intact cells of each strain was measured at 485 nm excitation, 520 nm emission and normalized to the $OD_{600}$ of the cultures. $n = 3$, $^{***}p < 0.001$ by Student *t*-test.

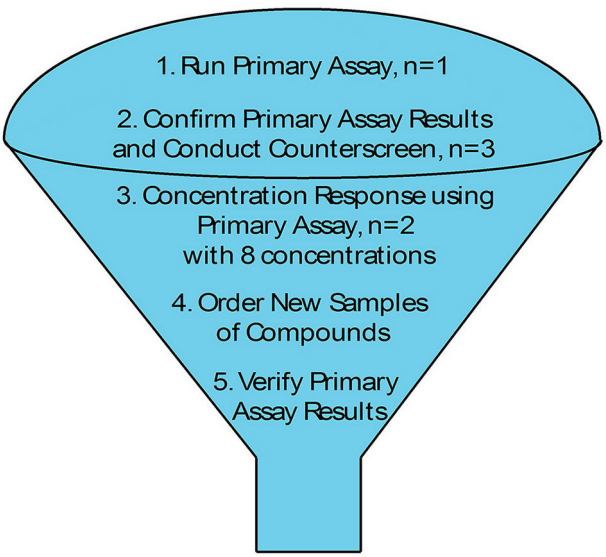


**FIGURE 7 |** HTS Schematic.

lysing the cells, reproducible GFP fluorescence was significantly higher than the fluorescence detected for 17978 with the vector alone negative control (17978/p; **Figure 6**). We optimized the conditions and applied them in the following counter screen: cultures were grown in 10 μL MH from a starting $OD_{600}$ of 0.005, with 75 μM IPTG in a humid chamber at 24°C without shaking for 16 h using 17978/p*gfp* and 17978/p as negative and positive controls, respectively. For this counter screen, the compounds would be added to the cultures at the start of growth, with the fluorescence measured after growth. Any compound that is positive in both the primary screen and this counter screen is likely targeting expression of the plasmid-encoded lipase and should be removed from the pool of potential hits.

Twenty-one compounds that had responded in a concentration-dependent manner in the primary HTS and then confirmed when using fresh powders, were subjected to the lipase inhibitor and GFP counter screens. All of these compounds were identified as either lipase inhibitors ($n = 18$; **Table 3** and **Figure 5A**) or inhibitors of *lipBA* expression from the plasmid ($n = 3$; representative compound shown in **Figure 5B**) highlighting the necessity of utilizing counter screens before pursuing detailed characterization of false positives.

As we move forward to screen larger libraries to identify T2SS inhibitors, our protocol will involve the following order of analysis (**Figure 7**): the active compounds from the primary HTS (step 1) will be delivered in triplicates to three different sets of 384-well plates using the original DMSO stock solutions (step 2). The first set of plates will represent a repetition of the primary screen. The second and third sets of plates will be used to counter screen for compounds that inhibit lipase activity or plasmid-borne gene expression, respectively (**Figure 7**). Compounds that are positive in the counter screens will be eliminated from further consideration, and the remaining compounds will be tested for their ability to prevent secretion over a range of concentrations (step 3). Fresh compounds will be reordered and tested (steps 4 and 5). Active compounds will then be analyzed for inhibition of secretion in additional *A. baumannii* strains, as T2SS inhibitors should ideally be functional against

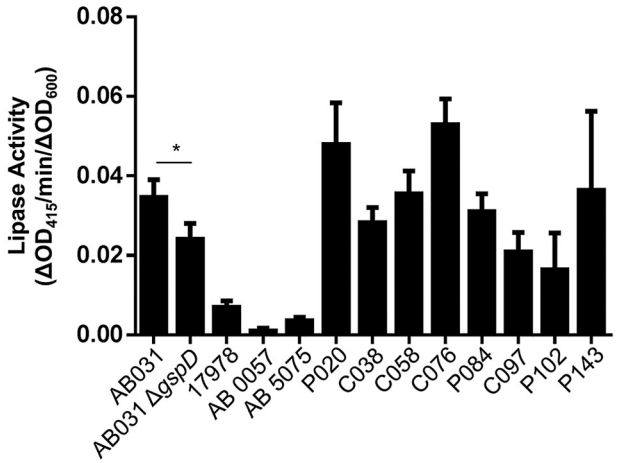


**FIGURE 8 |** T2S lipase activity of *A. baumannii* strains. The lipase substrate, 4-nitrophenyl myristate was added to overnight cultures of the indicated *A. baumannii* strains and the lipase activity was measured. Activities were normalized to the $OD_{600}$ readings of each culture. Bars show standard deviations from the means, $n = 3$. $^*p < 0.05$ by Student *t*-test.

the T2SS of all the *A. baumannii* isolates regardless of antibiotic resistance phenotype. To this effect, we have begun to test lipase activity of other strains of *A. baumannii* that were isolated from different body sites, are resistant to different antibiotics and produce different amounts of biofilm (**Figure 8**). While we have previously shown that detection of lipase activity in the culture supernatant of ATCC 17978 grown in LB in the absence of lipids requires overexpression of LipA from a plasmid, other strains display lipase activity without the need for LipA overexpression (**Figure 8**). The difference in lipase activity among the strains may be due to differences in expression of *lipA* as well as the presence of other lipases, such as LipH, which may or may not be dependent on the T2SS for extracellular secretion. We constructed a T2SS mutant of one of the strains, AB031 (to be described elsewhere). This Δ*gspD* mutant had a statistically significant reduction in lipase activity compared to the WT AB031 strain indicating that a detectable portion of the lipase activity stems from a T2SS dependent lipase(s) (**Figure 8**). This strain, as well as any others we may find as we continue to screen *A. baumannii* isolates for extracellular lipase activity, may be used to further analyze active hits to help determine which compounds to pursue. Analysis of additional strains such as AB0057 and AB5075 that show low lipase activity, however, will likely involve plasmid-expression of LipA.

## DISCUSSION

Here, we provide additional information on the T2SS in *A. baumannii*. In addition to supporting colonization, in part through the secretion of LipA, we show that the T2SS also contributes to serum resistance as there is a ≥100-fold reduction in recoverable CFUs of ATCC 17978 Δ*gspD* mutant following exposure to human complement. The mechanism by which the T2SS protects *A. baumannii* from human complement is not known, but published reports have shown that *A. baumannii* expresses secreted and surface-associated proteins that contribute to serum resistance and it is possible that they use the T2SS for outer membrane translocation. The serine protease PKF is produced with an N-terminal signal peptide, a prerequisite for T2S, and CipA, another serum resistance factor is a predicted lipoprotein (King et al., 2013; Koenigs et al., 2016). Lipoproteins, such as pullulanase and SslE, are examples of surface-associated T2S substrates, and CipA may similarly localize to the cell surface via the T2SS (Pugsley et al., 1986; Baldi et al., 2012). While PKF is a member of the HtrA family of chaperone-proteases that refold or degrade misfolded proteins in the periplasmic compartment (Hansen and Hilgenfeld, 2013), it is detected in *A. baumannii* culture supernatants possibly due to its secretion via the T2SS.

The reduced *in vivo* fitness in mouse models of bacteremia (Johnson et al., 2016) and pneumonia (Elhosseiny et al., 2016) and the increased sensitivity to complement killing of T2SS deficient *A. baumannii* (**Figure 2**) suggest that the T2SS plays an important part during infection through the action of specific T2S substrates and, thus, shows great potential for therapeutic targeting. GspD may be an especially promising target, as it forms a gated channel in the outer membrane through which transport occurs. Potential drugs, therefore, would not need to penetrate membranes to reach their target and would not be subject to the effect of drug efflux pumps. This latter point may be of particular importance in the treatment of bacteremic *A. baumannii*, as the expression of several efflux pumps are upregulated when *A. baumannii* is cultured in human serum (Jacobs et al., 2012). Here, we describe the development and optimization of a HTS to identify small molecule inhibitors of the T2SS in *A. baumannii*. Using a previously published assay, we developed, optimized, and tested a high-throughput assay on a small library of pharmacologically active compounds. Our proof-of-concept study demonstrated little fluctuations within controls and showed an acceptable dynamic range between positive and negative controls yielding a z-factor of 0.65 (Zhang et al., 1999). It also indicated that the assay is simple, straightforward, reproducible, robust, and specific as it identified the lipase inhibitors Orlistat and Ebelactone B twice and all seven tricyclic antidepressants present among the 6,400 compounds tested. In addition, the pilot study underscored the importance of including counter screens to reduce the number of false-positives. Though we are confident that our primary lipase screen and counter screens have been sufficiently optimized to be used to screen larger libraries of compounds, we may add an additional assay to reduce the number of potential hits early in the course of triage. If active compounds identified in the HTS are true inhibitors of the T2SS they should also block the secretion of other T2S substrates. Therefore, we may consider employing a double screen that simultaneously detects a reduction of the extracellular amount of LipA and another T2S enzyme. This assay has yet to be developed; however, mass spectrometry analysis of culture supernatants of *A. baumannii* and the related *A. nosocomialis* indicate that several Acinetobacter enzymes besides LipA are secreted by the T2SS (Elhosseiny et al., 2016; Harding et al., 2016), suggesting that a double screen is feasible.

Once larger libraries are subjected to this HTS and the primary assay results have been verified with fresh powders (**Figure 7**), the high-purity compounds will be further tested for specificity. While inhibitors that target the essential Sec system and signal peptidase (Tsirigotaki et al., 2017) would be detected and removed in the primary screen due to their negative impact on growth, a partial growth defect may not be observed in our end point measurement of cell density. This will be addressed in two ways. First, cultures will be grown in microtiter plates in the absence or presence of verified compounds and the $OD_{600}$ will be measured over time. Second, the activity of a periplasmic enzyme, such as alkaline phosphatase, will be determined. This activity will be reduced when the activity of the Sec system is diminished. Other compounds may target periplasmic chaperones or disulfide isomerases such as DsbA (Goemans et al., 2014). The alkaline phosphatase assay will also be instrumental in the detection and subsequent removal of these compounds.

Other studies have implemented similar HTS approaches for the identification of secretion inhibitors with notable differences. The first screen developed and validated, used a gain-of-signal screen to identify inhibitors of SecA, an essential component of the Sec export pathway in *P. aeruginosa* (Moir et al., 2011). No inhibitors were identified to directly interfere with the Sec pathway as the transport of the periplasmic enzyme β-lactamase was not affected. However, following application of secondary assays, a set of compounds was found to reduce the extracellular activity of T2SS substrates although they had no effect on the secreted substrates themselves, suggesting that the compounds inhibit their secretion (Moir et al., 2011). Our screen differs from the Sec screen in that we use a T2SS mutant as our positive control, thus increasing the specificity of our assay. In addition, our screen is designed to include high-throughput counter screens for the removal of false positives early in the triage process. The screen developed and validated by Tran et al., utilized the plant pathogen *Dickeya dadantii* (Tran et al., 2013). Similar to our screen, the authors measured $OD_{600}$ after growth to detect antibiotics and used the activity of a T2S substrate to measure the functionality of the T2SS. As with the Moir et al., screen, the Tran et al., screen did not have counter screens developed to be utilized in the HTS process (Moir et al., 2011; Tran et al., 2013). What is apparent in all three studies is that identified compounds have to be subjected to many additional tests, including those mentioned above, before they can be classified as true T2SS inhibitors. In addition, subcellular fractionation of cells grown in the presence of active T2S inhibitors should confirm an accumulation of T2S substrates in the periplasmic compartment, although some T2S substrates may be degraded by periplasmic proteases when their outer membrane translocation is perturbed. Once we implement our screen for the identification of T2SS inhibitors in *A. baumannii*, it will be advantageous to compare any active compounds to the compounds discovered in these two screens and search for similarities amongst the compounds.

While the primary goal of this pilot screen was to develop a HTS regimen for the identification of compounds to target the T2SS, our data indicate that our dual screen combined with counter screens also have the potential to identify compounds with antibiotic properties and reveal new targets for known pharmacological compounds already in use. An example of this is our discovery that the tricyclic antidepressants are efficient inhibitors of *A. baumannii* LipA (**Table 3**). Less surprising was the finding that the pancreatic lipase inhibitors Orlistat and Ebelactone B efficiently inhibit LipA activity. However, as our previous study has shown that LipA enhances *A. baumannii* colonization (Johnson et al., 2016) and that *A. baumannii* secretes several lipolytic enzymes including LipH and LipAN that may also support *in vivo* survival of *A. baumannii* (Elhosseiny et al., 2016; Harding et al., 2016), a lipase inhibitor could have potential for therapeutic use. Along with T2SS inhibitors, our HTS may also isolate inhibitors of LipB, the chaperone for both LipA and another T2S substrate, LipH (Harding et al., 2016), and they may also be developed for therapeutic intervention.

Identification of T2SS inhibitors for therapeutic purposes is the ultimate goal; however, we are also interested in pursuing small molecules, which can be used as tools to study T2S in multidrug resistant strains as they are often genetically intractable and very difficult to systematically study. Therefore, development of chemical probes to advance virulence studies of these antibiotic resistant isolates is also critically important.

## AUTHOR CONTRIBUTIONS

MS, UW, HM, and LS conceived the experiments. CX provided clinical strains. UW, TJ, and KC performed the experiments. UW and MS analyzed the data and wrote the manuscript. All authors have read and approved the manuscript.

## FUNDING

We would like to thank MCubed and the Center for Discovery of New Medicine at University of Michigan for funding. This work was supported in part by AI49294 (to MS) from the National Institute of Allergy and Infectious Diseases. HM and LS were supported by AI107184 and GM107312, respectively.

## ACKNOWLEDGMENTS

The authors would like to thank the staff of the Center for Chemical Genomics, especially Thomas McQuade and Martha Larsen, for assistance with experiments and data analysis.

## REFERENCES

Abendroth, J., Mitchell, D. D., Korotkov, K. V., Johnson, T. L., Kreger, A., Sandkvist, M., et al. (2009). The three-dimensional structure of the cytoplasmic domains of EpsF from the type 2 secretion system of *Vibrio cholerae*. *J. Struct. Biol.* 166, 303–315. doi: 10.1016/j.jsb.2009.03.009

Adams, M. D., Goglin, K., Molyneaux, N., Hujer, K. M., Lavender, H., Jamison, J. J., et al. (2008). Comparative genome sequence analysis of multidrug-resistant

*Acinetobacter baumannii*. *J. Bacteriol.* 190:8053. doi: 10.1128/JB.00834-08

Aiello, D., Williams, J. D., Majgier-Baranowska, H., Patel, I., Peet, N. P., Huang, J., et al. (2010). Discovery and characterization of inhibitors of *Pseudomonas aeruginosa* type III secretion. *Antimicrob. Agents Chemother.* 54, 1988–1999. doi: 10.1128/AAC.01598-09

Baldi, D. L., Higginson, E. E., Hocking, D. M., Praszkier, J., Cavaliere, R., James, C. E., et al. (2012). The Type II secretion system and its ubiquitous lipoprotein substrate SslE, are required for biofilm formation and virulence of enteropathogenic *Escherichia coli*. *Infect. Immun.* 80, 2042–2052. doi: 10.1128/IAI.06160-11

Bergogne-Berezin, E., and Towner, K. J. (1996). Acinetobacter spp as nosocomial pathogens: microbiological, clinical and epidemiological features. *Clin. Microbiol. Rev.* 9, 148–165.

Camberg, J. L., and Sandkvist, M. (2005). Molecular analysis of the *Vibrio cholerae* type II secretion ATPase EpsE. *J. Bacteriol.* 18, 249–256. doi: 10.1128/JB.187.1.249-256.2005

Camberg, J. L., Johnson, T., L., Patrick, M., Abendroth, J., Hol, W. G., and Sandkvist, M. (2007). Synergistic stimulation of EpsE ATP hydrolysis by EpsL and acidic phospholipids. *EMBO J.* 26, 19–27. doi: 10.1038/sj.emboj.7601481

Catalano, M., Quelle, L. S., Jeric, P. E., Di Martino, A., and Maimonet, S. M. (1999). Survival of *Acinetobacter baumannii* on bed rails during an outbreak and during sporadic cases. *J. Hosp. Infect.* 42, 27–35. doi: 10.1053/jhin.1998.0535

Cianciotto, N. P. (2005). Type II secretion: a protein secretion system for all seasons. *Trends Microbiol.* 13, 581–588. doi: 10.1016/j.tim.2005.09.005

Cianciotto, N. P., and White, R. C. (2017). Expanding role of type II secretion in bacterial pathogenesis and beyond. *Infect. Immun.* 85, e00014–00017. doi: 10.1128/IAI.00014-17

Cisneros, D. A., Bond, P. J., Pugsley, A. P., Campos, M., and Francetic, O. (2012). Minor pseudopilin self-assembly primes type II secretion pseudopilus elongation. *EMBO J.* 31, 1041–1053. doi: 10.1038/emboj.2011.454

de Vries, J., and Wackernagel, W. (2002). Integration of foreign DNA during natural transformation of *Acinetobacter* sp. by homology-facilitated illegitimate recombination. *Proc. Natl. Acad. Sci. U.S.A.* 99, 2094–2099. doi: 10.1073/pnas.042263399

Douzi, B., Ball, G., Cambillau, C., Tegoni, M., and Voulhoux, R. (2011). Deciphering the Xcp *Pseudomonas aeruginosa* Type II secretion machinery through multiple interactions with substrates. *J. Biol. Chem.* 286, 40792–40801. doi: 10.1074/jbc.M111.294843

Durand, E., Michel, G., Voulhoux, R., Kurner, J., Bernadac, A., and Filloux, A. (2005). XcpX controls biogenesis of the *Pseudomonas aeruginosa* XcpT-containing Pseudopilus. *J. Biol. Chem.* 280, 31378–31389. doi: 10.1074/jbc.M505812200

Elhosseiny, N. M., El-Tayeb, O. M., Yassin, A. S., Lory, S., and Attia, A. S. (2016). The secretome of *Acinetobacter baumannii* ATCC 17978 type II secretion system reveals a novel plasmid encoded phospholipase that could be implicated in lung colonization. *Int. J. Med. Microbiol.* 306, 633–641. doi: 10.1016/j.ijmm.2016.09.006

Espinal, P., Marti, S., and Vila, J. (2012). Effect of biofilm formation on the survival of *Acinetobacter baumannii* on dry surfaces. *J. Hosp. Infect.* 80, 56–60. doi: 10.1016/j.jhin.2011.08.013

Fürste, J. P., Pansegrau, W., Frank, R., Blöcker, H., Scholz, P., Bagdasarian, M., et al. (1986). Molecular cloning of the plasmid RP4 primase region in a multi-host-range tacP expression vector. *Gene* 48, 119–131. doi: 10.1016/0378-1119(86)90358-6

Gill, E. E., Franco, O. L., and Hancock, R. E. W. (2015). Antibiotic adjuvants: diverse strategies for controlling drug-resistant pathogens. *Chem. Biol. Drug Des.* 85, 56–78. doi: 10.1111/cbdd.12478

Goemans, C., Denoncin, K., and Collet, J.-F. (2014). Folding mechanisms of periplasmis proteins. *Biochim. Biophys. Acta* 1843, 1517–1528. doi: 10.1016/j.bbamcr.2013.10.014

Greene, C., Vadlamudi, G., Newton, D., Foxman, B., and Xi, C. (2016). The influence of biofilm formation and multidrug resistance on environmental survival of clinical and environmental isolates of *Acinetobacter baumannii*. *Am. J. Infect. Control* 44, e65–e71. doi: 10.1016/j.ajic.2015.12.012

Hansen, G., and Hilgenfeld, R. (2013). Architecture and regulation of HtrA-family proteins involved in protein quality control and stress response. *Cell. Mol. Life Sci.* 70, 761–775. doi: 10.1007/s00018-012-1076-4

Harding, C. M., Kinsella, R. L., Palmer, L. D., Skaar, E. P., and Feldman, M. F. (2016). Medically relevant Acinetobacter species require a type II secretion system and specific membrane-associated chaperones for the export of multiple substrates and full virulence. *PLoS Pathog.* 12:e1005391. doi: 10.1371/journal.ppat.1005391

Hauser, A. R., Mecsas, J., and Moir, D. T. (2016). Beyond antibiotics: new therapeutic approaches for bacterial infections. *Clin. Infect. Dis.* 63, 89–95. doi: 10.1093/cid/ciw200

Hendricks, K. A., Wright, M. E., Shadomy, S. V., Bradley, J. S., Morrow, M. G., Pavia, A. T., et al. (2014). Centers for disease control and prevention expert panel meetings on prevention and treatment of anthrax in adults. *Emerging Infect. Dis.* 20:e130687. doi: 10.3201/eid2002.130687

Hung, D. T., Shakhnovich, E. A., Pierson, E., and Mekalanos, J. J. (2005). Small-molecule inhibitor of *Vibrio cholerae* virulence and intestinal colonization. *Science* 310, 670–674. doi: 10.1126/science.1116739

Jacob, R. T., Larsen, M. J., Larsen, S. D., Kirchhoff, P. D., Sherman, D. H., and Neubig, R. R. (2012). MScreen. *J. Biomol. Screen.* 17, 1080–1087. doi: 10.1177/1087057112450186

Jacobs, A. C., Hood, I., Boyd, K. L., Olson, P. D., Morrison, J. M., Carson, S., et al. (2010). Inactivation of phospholipase D diminishes *Acinetobacter baumannii* pathogenesis. *Infect. Immun.* 78, 1952–1962. doi: 10.1128/IAI.00889-09

Jacobs, A. C., Sayood, K., Olmsted, S. B., Blanchard, C. E., Hinrichs, S., Russell, D., et al. (2012). Characterization of the *Acinetobacter baumannii* growth phase-dependent and serum responsive transcriptomes. *FEMS Immunol. Med. Microbiol.* 64, 403–412. doi: 10.1111/j.1574-695X.2011.00926.x

Jacobs, A. C., Thompson, M. G., Black, C. C., Kessler, J. L., Clark, L. P., McQueary, C. N., et al. (2014). AB5075, a highly virulent isolate of *Acinetobacter baumannii*, as a model strain for the evaluation of pathogenesis and antimicrobial treatments. *MBio* 5:e01076-14. doi: 10.1128/mBio.01076-14

Jawad, A., Seifert, H., Snelling, A. M., Heritage, J., and Hawkey, P. M. (1998). Survival of *Acinetobacter baumannii* on dry surfaces: comparison of outbreak and sporadic isolates. *J. Clin. Microbiol.* 36, 1938–1941.

Johnson, T. L., Waack, U., Smith, S., Mobley, H., and Sandkvist, M. (2016). *Acinetobacter baumannii* is dependent on the type II secretion system and its substrate LipA for lipid utilization and *in vivo* fitness. *J. Bacteriol.* 198, 711–719. doi: 10.1128/JB.00622-15

Jones, C. L., Clancy, M., Honnold, C., Singh, S., Snesrud, E., Onmus-Leone, F., et al. (2015). Fatal outbreak of an emerging clone of extensively drug-resistant *Acinetobacter baumannii* with enhanced virulence. *Clin. Infect. Dis.* 61, 145–154. doi: 10.1093/cid/civ225

King, L. B., Pangburn, M. K., and McDaniel, L. S. (2013). Serine protease PKF of *Acinetobacter baumannii* results in serum resistance and suprression of biofilm formation. *J. Infect. Dis.* 207, 1128–1134. doi: 10.1093/infdis/jis939

Koenigs, A., Stahl, J., Averhoff, B., Göttig, S., Wichelhaus, T. A., Wallich, R., et al. (2016). CipA of *Acinetobacter baumannii* is a novel plasminogen binding and complement inhibitory protein. *J. Infect. Dis.* 213, 1388–1399. doi: 10.1093/infdis/jiv601

Korotkov, K. V., Johnson, T. L., Jobling, M. G., Pruneda, J., Pardon, E., Héroux, A., et al. (2011). Structural and functional studies on the interaction of GspC and GspD in the type II secretion system. *PLoS Pathog.* 7:e1002228. doi: 10.1371/journal.ppat.1002228

Korotkov, K. V., Sandkvist, M., and Hol, W. G. J. (2012). The type II secretion system: biogenesis, molecular architecture and mechanism. *Nat. Rev. Microbiol.* 10, 336–351. doi: 10.1038/nrmicro2762

Leite, G. C., Oliveira, M. S., Perdigão-Neto, L. V., Rocha, C. K. D., Guimarães, T., Rizek, C., et al. (2016). Antimicrobial combinations against pan-resistant *Acinetobacter baumannii* isolates with different resistance mechanisms. *PLoS ONE* 11:e0151270. doi: 10.1371/journal.pone.0151270

Maragakis, L. L., and Perl, T. M. (2008). *Acinetobacter baumannii*: epidemiology, antimicrobial resistance, and treatment options. *Clin. Infect. Dis.* 46, 1254–1263. doi: 10.1086/529198

Michel, G. P. F., Durand, E., and Filloux, A. (2007). XphA/XqhA, a novel GspCD subunit for type II secretion in *Pseudomonas aeruginosa*. *J. Bacteriol.* 189, 3776–3783. doi: 10.1128/JB.00205-07

Moir, D. T., Di, M., Wong, E., Moore, R., A., Schweizer, H., P., Woods, D. E., et al. (2011). Development and application of a cellular, gain-of-signal, bioluminescent reporter screen for inhibitors of Type II secretion in

*Pseudomonas aeruginosa* and *Burkholderia pseudomallei*. *J. Biomol. Screen.* 16, 694–705. doi: 10.1177/1087057111408605

Nordfelth, R., Kauppi, A. M., Norberg, H. A., Wolf-Watz, H., and Elofsson, M. (2005). Small-molecule inhibitors specifically targeting type III secretion. *Infect. Immun.* 73, 3104–3114. doi: 10.1128/IAI.73.5.3104-3114.2005

Nunn, D. N., and Lory, S. (1993). Cleavage, methylation, and localization of the *Pseudomonas aeruginosa* export proteins XcpT, -U, -V, and -W. *J. Bacteriol.* 175, 4375–4382. doi: 10.1128/jb.175.14.4375-4382.1993

Pan, N. J., Brady, M. J., Leong, J. M., and Goguen, J. D. (2009). Targeting type III secretion in *Yersinia pestis*. *Antimicrob. Agents Chemother.* 53, 385–392. doi: 10.1128/AAC.00670-08

Paterson, D. L., and Harris, P. N. A. (2015). Editorial commentary: the new acinetobacter equation: hypervirulence plus antibiotic resistance equals big trouble. *Clin. Infect. Dis.* 61, 155–156. doi: 10.1093/cid/civ227

Pugsley, A. P., Chapon, C., and Schwartz, M. (1986). Extracellular pullulanase of *Klebsiella pneumonia* is a lipoprotein. *J. Bacteriol.* 166, 1083–1088. doi: 10.1128/jb.166.3.1083-1088.1986

Py, B., Loiseau, L., and Barras, F. (2001). An inner membrane platform in the type II secretion machinery of Gram-negative bacteria. *EMBO Rep.* 2, 244–248. doi: 10.1093/embo-reports/kve042

Rasko, D. A., and Sperandio, V. (2010). Anti-virulence strategies to combat bacteria-mediated disease. *Nat. Rev. Drug Discov.* 9, 117–128. doi: 10.1038/nrd3013

Reichow, S. L., Korotkov, K. V., Hol, W. G. J., and Gonen, T. (2010). Structure of the cholera toxin secretion channel in its closed state. *Nat. Struct. Mol. Biol.* 17, 1226–1232. doi: 10.1038/nsmb.1910

Rice, L. B. (2008). Federal funding for the study of antimicrobial resistance in nosocomial pathogens: no ESKAPE. *J. Infect. Dis.* 197, 1079–1081. doi: 10.1086/533452

Ruer, S., Pinotsis, N., Steadman, D., Waksman, G., and Remaut, H. (2015). Virulence-targeted antibacterials: concept, promise, and susceptibility to resistance mechanisms. *Chem. Biol. Drug Des.* 86, 379–399. doi: 10.1111/cbdd.12517

Sandkvist, M. (2001). Type II secretion and pathogenesis. *Infect. Immun.* 69, 3523–3535. doi: 10.1128/IAI.69.6.3523-3535.2001

Sandkvist, M., Hough, L. P., Bagdasarian, M. M., and Bagdasarian, M. (1999). Direct interaction of the EpsL and EpsM proteins of the general secretion apparatus in *Vibrio cholerae*. *J. Bacteriol.* 181, 3129–3135.

Scott, M. E., Dossani, Z. Y., and Sandkvist, M. (2001). Directed polar secretion of protease from single cells of *Vibrio cholerae* via the type II secretion pathway. *Proc. Natl. Acad. Sci. U.S.A.* 98, 13978–13983. doi: 10.1073/pnas.241411198

Shakhnovich, E. A., Hung, D. T., Pierson, E., Lee, K., and Mekalanos, J. J. (2007). Virstatin inhibits dimerization of the transcriptional activator ToxT. *Proc. Natl. Acad. Sci. U.S.A.* 104, 2372–2377. doi: 10.1073/pnas.0611643104

Spellberg, B., and Rex, J. H. (2013). The value of single-pathogen antibacterial agents. *Nat. Rev. Drug Discov.* 12:963. doi: 10.1038/nrd3957-c1

Steadman, D., Lo, A., Waksman, G., and Remaut, H. (2014). Bacterial surface appendages as targets for novel antibacterial therapeutics. *Future Microbiol.* 9, 887–900. doi: 10.2217/fmb.14.46

Thomassin, J.-L., Moreno, J. S., Guilvout, I., Van Nheiu, G. T., and Francetic, O. (2017). The trans-envelope architecture and function of the type 2 secretion system: new insights raising new questions. *Mol. Microbiol.* 105, 211–226. doi: 10.1111/mmi.13704

Tilley, D., Law, R., Warren, S., Samis, J. A., and Kumar, A. (2014). CpaA a novel protease from *Acinetobacter baumannii* clinical isolates deregulates blood coagulation. *FEMS Microbiol. Lett.* 356, 53–61. doi: 10.1111/1574-6968.12496

Tran, N., Zielke, R. A., Vining, O. B., Azevedo, M. D., Armstrong, D. J., Banowetz, G. M., et al. (2013). Development of a quantitative assay amenable for high-throughput screening to target the type ii secretion system for new treatments against plant-pathogenic bacteria. *J. Biomol. Screen.* 18, 921–929. doi: 10.1177/1087057113485426

Tsirigotaki, A., De Geyter, J., Sostaric, N., Economou, A., and Karamanou, S. (2017). Protein export through the bacterial Sec pathway. *Nat. Rev. Microbiol.* 15, 21–36. doi: 10.1038/nrmicro.2016.161

Wang, N., Ozer, E. A., Mandel, M. J., and Hauser, A. R. (2014). Genome-wide identification of *Acinetobacter baumannii* genes necessary for persistence in the lung. *MBio* 5:e01163-14. doi: 10.1128/mBio.01163-14

Weernink, A., Severin, W. P. J., Tjernberg, I., and Dijkshoorn, L. (1995). Pillows, an unexpected source of acinetobacter. *J. Hosp. Infect.* 29, 189–199. doi: 10.1016/0195-6701(95)90328-3

Wong, D., Nielsen, T. B., Bonomo, R. A., Pantapalangkoor, P., Luna, B., and Spellberg, B. (2016). Clinical and pathophysiological overview of acinetobacter infections: a century of challenges. *Clin. Microbiol. Rev.* 30, 409–447. doi: 10.1128/CMR.00058-16

Yan, Z., Yin, M., Xu, D., Zhu, Y., and Li, X. (2017). Structural insights into the secretin translocation channel in the type II secretion system. *Nat. Struct. Mol. Biol.* 24, 177–183. doi: 10.1038/nsmb.3350

Zhang, J.-H., Chung, T. D. Y., and Oldenburg, K. R. (1999). A simple statistical parameter for use in evaluation and validation of high throughput screening assays. *J. Biomol. Screen.* 4, 67–73. doi: 10.1177/108705719900400206

**Conflict of Interest Statement:** The authors declare that the research was conducted in the absence of any commercial or financial relationships that could be construed as a potential conflict of interest.

frontiers in Cellular and Infection Microbiology

ORIGINAL RESEARCH
published: 07 November 2017
doi: 10.3389/fcimb.2017.00464

# A New Strain Collection for Improved Expression of Outer Membrane Proteins

*Ina Meuskens*[1,2], *Marcin Michalik*[1], *Nandini Chauhan*[1], *Dirk Linke*[1]* and *Jack C. Leo*[1]*

[1] Section for Evolution and Genetics, Department of Biosciences, University of Oslo, Oslo, Norway, [2] Interfaculty Institute for Biochemistry, Eberhard Karls University, Tübingen, Germany

Almost all integral membrane proteins found in the outer membranes of Gram-negative bacteria belong to the transmembrane β-barrel family. These proteins are not only important for nutrient uptake and homeostasis, but are also involved in such processes as adhesion, protein secretion, biofilm formation, and virulence. As surface exposed molecules, outer membrane β-barrel proteins are also potential drug and vaccine targets. High production levels of heterologously expressed proteins are desirable for biochemical and especially structural studies, but over-expression and subsequent purification of membrane proteins, including outer membrane proteins, can be challenging. Here, we present a set of deletion mutants derived from *E. coli* BL21(DE3) designed for the over-expression of recombinant outer membrane proteins. These strains harbor deletions of four genes encoding abundant β-barrel proteins in the outer membrane (OmpA, OmpC, OmpF, and LamB), both single and in all combinations of double, triple, and quadruple knock-outs. The sequences encoding these outer membrane proteins were deleted completely, leaving only a minimal scar sequence, thus preventing the possibility of genetic reversion. Expression tests in the quadruple mutant strain with four test proteins, including a small outer membrane β-barrel protein and variants thereof as well as two virulence-related autotransporters, showed significantly improved expression and better quality of the produced proteins over the parent strain. Differences in growth behavior and aggregation in the presence of high salt were observed, but these phenomena did not negatively influence the expression in the quadruple mutant strain when handled as we recommend. The strains produced in this study can be used for outer membrane protein production and purification, but are also uniquely useful for labeling experiments for biophysical measurements in the native membrane environment.

**Keywords: outer membrane, β-barrel protein, recombinant protein expression, P1 transduction, production strain**

OPEN ACCESS

***Edited by:***
*Bérengère Ize, Centre National de la Recherche Scientifique (CNRS), France*

***Reviewed by:***
*Ralf Koebnik, Institut de Recherche pour le Développement, France*
*Guillaume Duret, Rice University, United States*
*Jeremy Guerin, National Institute of Diabetes and Digestive and Kidney Diseases, United States*

***Correspondence:**
*Dirk Linke*
*dirk.linke@ibv.uio.no*
*Jack C. Leo*
*j.c.leo@ibv.uio.no*

***Received:*** *19 July 2017*
***Accepted:*** *20 October 2017*
***Published:*** *07 November 2017*

***Citation:***
*Meuskens I, Michalik M, Chauhan N, Linke D and Leo JC (2017) A New Strain Collection for Improved Expression of Outer Membrane Proteins. Front. Cell. Infect. Microbiol. 7:464. doi: 10.3389/fcimb.2017.00464*

## INTRODUCTION

The envelope of Gram-negative bacteria such as, *Escherichia coli* consists of two membranes, the inner and the outer membrane. This double membrane system protects the bacteria from environmental insult and makes them resistant to many antibiotics and host immune defenses, but allows the efficient uptake of nutrients. The outer membrane is permeable to small hydrophilic molecules due to the presence of porins. Porins, and almost all other transmembrane outer

membrane proteins (OMPs), are composed of a transmembrane β-barrel domain (Fairman et al., 2011). β-barrels consist of an antiparallel β-sheet that closes in on itself; the proteins thus adopt a cylindrical shape, with hydrophobic residues facing the membrane environment and mostly hydrophilic residues lining the inside of the β-barrel, which in the case of porins acts as an aqueous channel permitting the diffusion of water and other nutrients through the outer membrane (Delcour, 2009). Other OMPs act as secretion pores, transporting a variety of macromolecules across the outer membrane, such as, lipopolysaccharide (Dong et al., 2014), biofilm matrix components (Hufnagel et al., 2015), other proteins (Chagnot et al., 2013), or, in the case of autotransporters, parts of the same polypeptide chain (Leo et al., 2012). OMPs are further involved in such functions as self-recognition (Aoki et al., 2005, 2008), protein hydrolysis (Haiko et al., 2009), and virulence (Monteiro et al., 2016).

All β-barrel OMPs in Gram-negative bacteria are homologous (Remmert et al., 2010), and follow a conserved route of membrane insertion. OMPs are transported across the inner membrane via the Sec machinery in an unfolded conformation (Walther et al., 2009b). In the periplasm, chaperones such as, SurA, Skp, and DegP help to keep the OMPs in an unfolded state (Goemans et al., 2014). Insertion of OMPs into the outer membrane is accomplished by the β-barrel assembly machinery or BAM complex (Bakelar et al., 2016; Gu et al., 2016; Han et al., 2016). A recent study has shown that OMPs are inserted into the outer membrane at discreet sites near the cell center and move laterally toward the cell poles (Rassam et al., 2015). As the periplasm is devoid of adenosine triphosphate and ionic gradients cannot be maintained across the outer membrane, the energy for insertion into the outer membrane must be provided by the folding of the β-barrel itself (Moon et al., 2013).

Insertion of OMPs is thus dependent on the two constitutive membrane insertase/translocase systems, the Sec, and the BAM. For efficient recombinant production of properly folded OMPs, sufficient capacity is required for both systems to process the additional burden of heterologously expressed protein. When the BAM copy number is reduced, OMPs are inefficiently integrated into the outer membrane, though cell viability is not significantly affected (Aoki et al., 2008). Thus, under OMP over-expression conditions, the BAM may become congested, resulting in a bottleneck for efficient OMP integration. In addition to misfolding, this may also lead to induction of the envelope stress response, and thus indirectly to induction of protease expression (Alba and Gross, 2004) including the periplasmic protease DegP (Grosskinsky et al., 2007).

The Sec system is also prone to saturation, based e.g., on observations that, in some over-expression conditions, cytosolic inclusion bodies are formed where the signal peptide was not properly processed, or periplasmic inclusion bodies are observed due to follow-up problems of improper processing (Georgiou and Segatori, 2005). Over-expression of inner membrane proteins leads to accumulation of cytoplasmic inclusion bodies and aggregates, but also reduces the amount of proteins secreted into the periplasm and outer membrane (Wagner et al., 2007). Congestion of the Sec machinery further affects cell viability and the maximum rate at which heterologous OMPs can be transported into the periplasm (Schlegel et al., 2013). The Sec machinery also transports soluble periplasmic proteins, lipoproteins, integral inner membrane proteins, and several types of secreted proteins in addition to OMPs (Kudva et al., 2013). Therefore, for over-expression of heterologous OMPs in *E. coli*, it would be advisable to knock out abundant but non-essential OMPs to relieve some of the burden on the BAM and Sec machineries. In addition, removing these abundant proteins from the membrane leaves more space for recombinant proteins, potentially influencing the maximum yield per cell; limited membrane area can be a bottleneck for the over-production of membrane proteins (Arechaga et al., 2000; Wagner et al., 2006).

Koebnik and coworkers have previously developed such a set of strains derived from the common expression strain BL21(DE3) (Prilipov et al., 1998b). These strains lack one or more of the most abundant OMPs: OmpA, OmpC, OmpF, or LamB (maltoporin). We have successfully used some of these strains for expression and purification of OMPs, especially BL21 Omp2 and BL21 Omp8 (Wollmann et al., 2006; Arnold et al., 2007; Leo et al., 2011; Mikula et al., 2012; Oberhettinger et al., 2012; Shahid et al., 2012), but also for NMR experiments using native membranes (Shahid et al., 2015). However, in our hands these strains have proven to be genetically unstable and prone to sudden lysis, possibly due to mobilization of the Tn*5* transposon under stress conditions, used in generating these knock-out strains (Prilipov et al., 1998b; Supplementary Figure 1).

In this work, we present a series of knock-out strains lacking one, two, three, or all four of the genes encoding the proteins OmpA, OmpC, OmpF, and LamB. These strains are designed for use in over-expression of recombinant OMPs, and are equivalent to some of the strains produced earlier (Prilipov et al., 1998b). However, our series is more complete than that produced by Prilipov et al. and we used a different strategy to produce our knock-outs resulting in genetically more stable strains. Particularly, we have not observed spontaneous lysis of our quadruple knock-out strain lacking all four abundant OMPs (similar to the Omp8 strain produced earlier) when handled as we recommend. We also demonstrate that the quadruple mutant strain shows improved levels of four test proteins in the outer membrane compared to the BL21(DE3) parent strain.

# MATERIALS AND METHODS

## Bacteria, Media, and Growth Conditions

The *E. coli* strains produced in this work are derivatives of the commonly used expression strain BL21(DE3) (Studier and Moffatt, 1986). In addition to being widely utilized for expression, this strain also lacks the outer membrane protease OmpT, which we reasoned would be beneficial for over-expression of OMPs in particular. For transductions, we used the generally transducing bacteriophage P1 *vir*. The donor strains harboring the kanamycin cassettes for gene deletion were from the Keio collection (Baba et al., 2006). The K-12 reference strain was BW25113 (Datsenko and Wanner, 2000).

Bacteria were grown in lysogeny broth (LB) unless stated otherwise. For most experiments, we used the "Lennox"

formulation: 10 g tryptone, 5 g yeast extract, and 5 g NaCl per liter. In the text below, we mean this formulation when referring to LB. For growth curves, we also used the "Miller" formulation (10 g tryptone, 5 g yeast extract, and 10 g NaCl per liter)—we refer to this as LB-Miller. Where necessary, media were supplemented with kanamycin (kan) or ampicillin (amp) at 25 μg/ml and 100 μg/ml, respectively. SOC medium was used after transformations as described elsewhere (Hanahan, 1983). As a defined medium, we used the minimal medium M9 (Miller, 1972) supplemented with glucose 0.2% (w/v) and 18 amino acids (all except cysteine and tyrosine) at 0.1 mg/ml each. Bacteria were usually grown at 37°C, unless harboring the plasmid pCP20, in which case they were grown either at 30°C for plasmid maintenance or 42°C to cure the plasmid. Some of the *omp* deletion strains, such as, the quadruple mutant BL21ΔABCF, grew significantly better at 30°C than at 37°C, and these were thus propagated at 30°C.

## Plasmids

Plasmid pCP20 encoding the FLP recombinase (Flippase) was used for excising the kanamycin cassette after transduction into the knock-out strains (Cherepanov and Wackernagel, 1995). For λ red recombination, we employed the plasmid pKD46 (Datsenko and Wanner, 2000). The expression constructs used for testing our strains have been described previously: pET3b containing the genes encoding *ompX* and variants thereof (Arnold et al., 2007), pASK-IBA2 with *Yersinia enterocolitica* YadA membrane anchor domain (YadAM) (Wollmann et al., 2006) or Intimin (Oberhettinger et al., 2012). pET3b-OmpX was also modified for the purpose of this study by inserting a double haemagglutinin (HA)-tag with GSG linkers (GSGYPYDVPDYAGSGYPYDVPDYAGSG) in the position between S53 and S54 of OmpX for easier detection (pET3b-OmpX-HA). The insertion was created by site-directed mutagenesis (Byrappa et al., 1995) using the primers given in **Table 1**.

## P1 Phage Transduction

P1 phage transduction was performed essentially as described (Thomason et al., 2007). Briefly, the *E. coli* strains from the Keio collection were grown in LB medium to an optical density at 600 nm ($OD_{600}$) of 1.0 and infected with P1 *vir* phages at various dilutions (e.g., $10^{-5}$, $10^{-6}$, $10^{-7}$), mixed with 3 ml liquid top agar and poured onto pre-warmed LB plates. The following day, a semi-confluent plate was chosen and the top agar scraped off. This was mixed with 2 ml LB medium supplemented with a drop of chloroform, vortexed for 2 min and centrifuged for 10 min at 5,000 × g. Another drop of chloroform added to the supernatant, which was then stored at 4°C. The parent strain *E. coli* BL21(DE3) was infected with dilution series of each P1 phage lysate and the titer of the lysates was calculated from the number of plaques formed on the plates.

For the transduction experiments, *E. coli* BL21(DE3) and derivatives were grown in LB medium overnight, diluted 1:100 in the morning and grown until an $OD_{600}$ of ∼1.0, and then supplemented with 10 mM $CaCl_2$ and mixed the P1 phage lysate harboring the kan cassette specific for the desired knock-out at a multiplicity of infection (MOI) of 0.5, assuming $10^9$ bacteria/ml culture. After incubating for 20 min at 37°C, the infection was stopped by addition of 100 mM sodium citrate pH 5.5. The mix was centrifuged for 2 min at 5,000 × *g*. The pellet was washed in LB medium supplemented with 100 mM sodium citrate and centrifuged as before. This washing step was repeated twice and then the bacteria were incubated for ∼1 h at 37°C in LB containing 100 mM sodium citrate. Finally, the bacteria were centrifuged for 2 min at 4,000 × *g* diluted in 100 μl LB medium and streaked out on LB agar plates supplemented with kanamycin and 10 mM sodium citrate.

## Introduction of the Kan Cassette by λ Red Recombination

To delete the *ompF* locus, we amplified the FLP recognition target (FRT)-kanamycin cassette flanked by sequence directly outside the sequence coding for OmpF, using the Keio collection Δ*ompF* strain and the same primer sequences described in that study (Baba et al., 2006). Insertion of the kan cassette was achieved by λ red recombination, essentially as described (Datsenko and Wanner, 2000): the plasmid pKD46 was transformed into recipient strains by electroporation, and transformants were selected for by plating on ampicillin and growing at 30°C. To introduce the kan cassette into the *ompF* locus, the pKD46-containing bacteria were grown to mid-log phase at 30°C, at which time the λ red genes were induced by the addition of 1 mM L-arabinose. After 1 h of induction, the cells were harvested and made electrocompetent. One hundred nanograms of PCR product was transformed into the cells by electroporation, after which cells were allowed to recover for 1 h at 30°C in SOC medium supplemented with 1 mM L-arabinose. Transformants were then selected for by growing on LB with kanamycin at 30°C. To remove pKD46, bacteria were grown on LB + kan at 37°C, and then tested for ampicillin sensitivity. Insertion of the kan cassette into the *ompF* locus was verified by colony PCR.

## Excision of the Kan Cassette

For excision of the kan cassette, kan-resistant transductants were transformed with the conditionally replicating plasmid pCP20 encoding the FLP recombinase by electroporation, following the procedure suggested by Baba et al. (2006). After electroporation the cells were quickly mixed with 1 ml SOC medium and incubated for 1 h at 30°C. The bacteria were then plated on LB agar plates with ampicillin and incubated overnight at 30°C. To cure pCP20, one amp-resistant colony was streaked out onto an LB agar plate and incubated at 42°C overnight. To screen for mutants strains, colonies were streaked out on LB plates containing kan, amp, and no antibiotic, respectively, using a grid, and then incubated at 37°C overnight. Clones sensitive to both kan and amp were chosen, and correct deletions were verified using colony PCR.

## Colony PCR

For verification of the right gene deletions in our mutants PCR with primers specific for the upstream and downstream region of the gene to be deleted was used. The primers sequences are given in **Table 1**. Colony PCR was performed using Taq polymerase

**TABLE 1 |** Primers used in this study.

| **COLONY PCR** | | |
|---|---|---|
| **Gene** | **Direction** | **Sequence (5′ → 3′)** |
| *ompA* | Forward | ATTTTGGATGATAACGAGGCGCAAAAAATG |
| *ompA* | Reverse | GAACTTAAGCCTGCGGCTGAGTTAC |
| *lamB* | Forward | AAAAGAAAAGCAATGACTCAGGAGATAGAATG |
| *lamB* | Reverse | GGTTTTGCTATTACCACCAGATTTCCATCTG |
| *ompF* | Forward | AGGTGTCATAAAAAAAACCATGAGGGTAATAAATAAT |
| *ompF* | Reverse | GAGGTGTGCTATTAGAACTGGTAAACGATACC |
| *ompC* (common) | Forward | CAATCGGTGCAAATGCCAGATAAGACAC |
| *ompC* (*E. coli* K-12) | Forward | GCAAATAAAGGCATATAACAGAGGGTTAATAACATG |
| *ompC* | Reverse | ATATCAATCGAGATTAGAACTGGTAAACCAGACC |
| **MUTAGENESIS** | | |
| **Product** | **Direction** | **Sequence (5′ → 3′)** |
| HA-OmpX | Forward | GTTATCCATACGACGTACCTGATTACGCAGGTTCTGGGTCTGGTGACTACAACAAAAACCAG |
| HA-OmpX | Reverse | CTGAGCCCGCATAATCCGGAACATCATACGGGTAACCAGAACCGCTTGCAGTACGGCTTTTCTC |

(New England Biolabs) and 20 pmol of primer per reaction. A typical colony PCR program was as follows: initial denaturation for 3 min at 94°C, followed by 25 cycles of denaturation (30 s at 94°C), annealing (20 s 50°C), and extension [1.5 min (or 5 min with *ompC* common primers) at 70°C]. After a final extension of 5 min at 70°C, samples were mixed with loading buffer and applied to a 1% agarose gel (0.8% for *ompC* common primers). The primer pair used amplified the coding sequences of each locus are indicated in **Table 1**.

## Outer Membrane Preparations

Outer membrane isolations were performed essentially as described in Leo et al. (2015). Briefly, 20 ml of an overnight culture at $OD_{600}$ 1.0 were pelleted and washed with 10 mM HEPES buffer at pH 7.4. To promote lysis, 0.1 mg/ml lysozyme was added, along with $MgCl_2$ and $MnCl_2$ to 10 mM and a pinch of DNase I (Sigma). The cells were then disrupted using a bead beater (SpeedMill Plus from Analytik Jena, Germany). The lysates were centrifuged at 15,600 × *g* for 30 s in a tabletop centrifuge and the supernatant was then moved to a fresh 2 ml microcentrifuge tube and centrifuged at 15,600 × *g* for another 30 min. The supernatant was decanted and the brownish membrane pellet resuspended in 400 µl 10 mM HEPES pH 7.4 with 1% (w/v) *N*-lauroyl sarcosine. The inner membranes were solubilized at room temperature (RT) for 30 min. Following this, the tubes were centrifuged at 15,600 × *g* for 30 min to pellet the outer membrane. The pellet was washed with 10 mM HEPES pH 7.4 and then resuspended in 30 µl HEPES buffer. For SDS-PAGE, 10 µl of 4 × non-reducing SDS sample buffer was added. Fifteen percentage SDS-PAGE gels were used for experimental verification of the knockout mutants at the protein level. For Coomassie G-250 (colloidal) staining of polyacrylamide gels, 12 µl of the outer membrane samples were used. For silver staining (Nesterenko et al., 1994), 8 µl of the outer membrane prep samples were run in a polyacrylamide gel and for Western blots 6 µl of the outer membrane prep samples were used.

## Growth Curves

To draw growth curves, starter cultures were grown in 5 ml LB or supplemented M9 medium and the $OD_{600}$ values were measured. The bacteria were then diluted to an $OD_{600}$ value of 0.01 and 5 µl of this suspension was added to 200 µl of medium (LB, LB-Miller, or supplemented M9) in a sterile microtiter plate. For blanks, no bacteria were added. The plates were sealed with a BreathEasy® membrane (from Sigma-Aldrich). The plates were incubated in a Biotek Synergy plate reader with controlled temperature and orbital rotation at the "slow" setting; absorbance at 600 nm was recorded at 20-min intervals. For plotting, values from four biological replicates were averaged.

## Aggregation Assays

For sedimentation assays, an overnight culture was diluted 1:100 in fresh LB (total volume 10 ml). The cultures were grown with shaking at 30°C in a flask till late log phase ($OD_{600}$ ~1.0), at which point $MgCl_2$ or $CaCl_2$ were added to 10 mM to some of the cultures. After a further hour of incubation at 30°C with shaking, the bacteria were transferred carefully to 18 mm tubes so as not to disrupt any floccules. The tubes were then incubated statically at RT. One hundred and fifty microliter samples were taken from the very top of the cultures at 5-min intervals for 20 min and the absorbance at 600 nm was measured using a microcuvette (light path 1 cm). To estimate autoaggregation, the absorbance at each time point was compared to the absorbance at time point zero and expressed as a percentage:

$$(A_t * 100)/A_0,$$

where $A_t$ is the absorbance at the relevant time point and $A_0$ is the absorbance at time point zero. For plotting, three biological replicates were used.

For photography, 5 ml cultures were grown to late log phase ($OD_{600} \approx 0.8$) and $MgCl_2$ or $CaCl_2$ were added as above. After a further hour of shaking, the tubes were incubated statically at RT and photographed after 20 min and 2 h.

## Recombinant Protein Expression and Detection

For inducing recombinant protein production, plasmids encoding the test proteins were transform into the quadruple mutant strain (BL21ΔABCF). For production, a 5 ml overnight culture of a transformed clone was diluted 1:100 in fresh LB and grown at 30°C till mid-log phase ($OD_{600}$ ∼0.5). The culture was then induced with either isopropyl thiogalactoside (at 1 mM) or anhydrotetracycline (at 50 ng/ml). The cultures were incubated at 30°C for a further 2 h, after which the cells were harvested and outer membranes were isolated. The OMPs were separated by SDS-PAGE. Over-expressed YadAM, OmpX, and its duplicated variant OmpX88 were detected by colloidal Coomassie G-250 staining. Overexpression of a HA-tagged variant of OmpX and Intimin was detected by immunoblotting. The proteins were transferred to a 0.45 μm polyvinylidine difluoride membrane (Thermo Scientific) using a semi-dry transfer unit (Hoefer TE70X). The membranes were blocked with 2% skimmed milk powder dissolved in phosphate-buffered saline (PBS; 20 mM sodium phosphate pH 7.4, 150 mMNaCl) for 1 h at RT or overnight at 4°C. This was followed by incubation for an hour with primary antibodies; 1:2,000 dilution of rabbit anti-HA tag antibody (for OmpX-HA) and 1:5000 dilution of rabbit anti-Intimin antibody (Oberhettinger et al., 2012). The membrane was washed three times with PBS+0.05% Tween20 followed by incubation with a 1:10,000 dilution of goat anti-rabbit IgG horseradish peroxidase-conjugate (Santa Cruz Biotech) in PBS+2% skimmed milk powder for an hour. The membrane was washed three times with PBS+0.05% Tween20. The bands were detected using enhanced chemiluminescence (Pierce ECL western blotting substrate) and a Kodak 4000R Image station.

## Whole-Cell ELISAs

For quantitative examination of Intimin and OmpX-HA expression, we performed whole-cell enzyme-linked immunosorbent assays (ELISAs). Bacteria transformed with the corresponding plasmids were grown overnight at 30°C in 5 ml LB medium with ampicillin. The following day, the bacteria were diluted 1:10 in fresh medium (5 ml, with amp) and grown till mid-log ($OD_{600}$ ∼0.5; about 2 h), at which time they were induced with anhydrotetracycline or isopropyl thiogalactoside as in the section on Recombinant Protein Expression and Detection. The bacteria were grown at 30°C for another 2 h. The $OD_{600}$ of the cultures was measured and the bacteria were diluted in PBS to an $OD_{600}$ value of 0.2. One hundred microliters of this suspension were applied to the wells of a polystyrene microtiter plate and bacteria were allowed to adhere to the surface of the well for 1 h at RT. The wells were washed three times with 200 μl washing buffer [PBS + 0.1% bovine serum albumin (BSA, from VWR)] and then blocked for 1 h with PBS + 2% BSA. The wells were washed once with 200 μl washing buffer, and 100 μl of the primary antibody diluted into blocking buffer was applied. The antibodies were the same as in the section on Recombinant Protein Expression and Detection, anti-HA (1:2,000), and anti-Intimin (1:1,000). After an hour's incubation, the wells were washed three times as above, and the secondary antibody (anti-rabbit-HRP, from Agrisera) was added, diluted 1:2,000 in blocking buffer. The plate was incubated for 1 h at RT, after which the wells were washed three times as above. Detection was performed using the colorimetric HRP substrate ABTS (ThermoScientific) according to the manufacturer's instructions. After color development (40 min) the reactions were stopped with 1% SDS and absorbances were recorded at 405 nm.

# RESULTS

## Production of Knock-Out Strains

To avoid the problems we had encountered with the strains from Prilipov et al. we pursued a different strategy in making our knock-out strains. We decided to delete the entire coding sequences for the four genes encoding the OMPs lacking in the Omp8 strain of Prilipov et al. namely *ompA*, *ompC*, *ompF,* and *lamB* (Prilipov et al., 1998b). We reasoned that this strategy would prevent the possibility of a genetic reversion, thus improving the genetic stability of the newly generated knock-out strains. BL21 strains probably do not express *ompC* naturally, due to an insertion element-mediated deletion of the upstream region of the *ompC* locus, including the signal peptide of OmpC (Pugsley and Rosenbusch, 1983; Studier et al., 2009; Han et al., 2012). Nevertheless, we decided to delete the entire *ompC* coding sequence to fully prevent the possibility of reversion, e.g., by a recombination event restoring a functional signal peptide. To make the deletions, we employed the Keio collection, a set of 3,985 single-gene deletions in *E. coli*, where virtually the entire coding sequence of the deleted genes is replaced by a kanamycin resistance cassette (Baba et al., 2006). This cassette is flanked by sequences targeted by the FLP recombinase; thus, when FLP is supplied in trans, the kan cassette can be excised from the genome leaving only a ∼100 bp-long scar sequence.

We produced the single knock-outs in *E. coli* BL21(DE3) by phage P1 transduction: a phage lysate was produced from the Keio strains harboring the desired OMP gene deletions. This lysate was used to infect the recipient strain, and kan-resistant transductants were then selected for by plating on kanamycin plates. To remove the kan cassette, we introduced the FLP-containing plasmid pCP20 into the kan-resistant bacteria and selected for amp-resistant colonies without the addition of kanamycin. To cure pCP20, clones were plated onto LB (no selection) and grown at 42°C. Clones that were sensitive to both amp and kan were chosen for PCR screening to verify the loss of the kan cassette and the loss of the wild-type allele. Using this strategy, we produced the four individual knock-outs, and then by re-iterating the process, we obtained five double knock-outs, three triple knock-outs, and the quadruple knock-out strain (**Table 2**).

We experienced particular problems producing the *ompA-ompF* double knock-out and the *ompA-ompF-ompC* triple knock-out. The *ompA* and *ompF* loci are situated relatively close to each other in the *E. coli* genome (distance ∼32 kb; P1 can transduce fragments ∼ three times this size); therefore, we often obtained revertants for one mutant while trying to produce the other. To circumvent this problem, we employed a different strategy: we amplified the FRT-kan cassette from the Keio Δ*ompF* strain by PCR, with 50 bp overhangs identical to

**TABLE 2 |** Knock-out strains produced in this study.

| Knock-outs | Strain | Genes deleted | Addgene ID |
|---|---|---|---|
| **SINGLE KNOCK-OUTS** | | | |
| | BL21ΔA | *ompA* | 102256 |
| | BL21ΔB | *lamB* | 102257 |
| | BL21ΔC | *ompC* | 102258 |
| | BL21ΔF | *ompF* | 102259 |
| **DOUBLE KNOCK-OUTS** | | | |
| | BL21ΔAB | *ompA*, *lamB* | 102260 |
| | BL21ΔAC | *ompA*, *ompC* | 102261 |
| | BL21ΔAF | *ompA*, *ompF* | 102262 |
| | BL21ΔBC | *lamB*, *ompC* | 102263 |
| | BL21ΔBF | *lamB*, *ompF* | 102264 |
| | BL21ΔCF | *ompC*, *ompF* | 102265 |
| **TRIPLE KNOCK-OUTS** | | | |
| | BL21ΔABC | *ompA*, *lamB*, *ompC* | 102266 |
| | BL21ΔABF | *ompA*, *lamB*,*ompF* | 102267 |
| | BL21ΔACF | *ompA*, *ompC*, *ompF* | 102268 |
| | BL21ΔBCF | *lamB*, *ompC*, *ompF* | 102269 |
| **QUADRUPLE KNOCK-OUT** | | | |
| | BL21ΔABCF | *ompA*, *lamB*, *ompC*, *ompF* | 102270 |

*All strains are derived from BL21(DE3).*

the sequence flanking the *ompF* coding region, as was used to make the *ompF* mutant in the original Keio collection (Baba et al., 2006). We then produced the BL21ΔAF and BL21ΔACF strains by λ red recombination in the BL21ΔA and BL21ΔAC strains (Datsenko and Wanner, 2000). We then selected for kan-resistant colonies and subsequently removed the kan cassette as described for the transduction experiments. Indeed, this strategy proved successful.

## Verification of the Knock-Out Mutant Strains

To verify that the correct gene had been deleted, we amplified the target coding sequence by colony PCR. Using primers specific for each of the four loci, we could show that the mutant strains had lost the wild-type allele (**Figure 1A**). The sequences remaining in the deletion mutants correspond to ∼150 bp, the size of the scar sequence and flanking regions, indicating that the gene was actually replaced by the kan cassette, which in turn was excised by FLP. The size of the wild-type coding sequence is 1041 bp for *ompA*, 1089 bp for *ompF*, 1104 bp for *ompC,* and 1341 bp for *lamB*. These sizes are consistent with the PCR products obtained from the parent strain BL21(DE3). For verification of the *ompC* deletion, another forward primer binding downstream the *rcsC* locus was used due to the fact that in *E. coli* BL21 the upstream region of *ompC* is deleted (Studier et al., 2009). Thus, the forward primer amplifying the *ompC* locus in *E. coli* K-12 strains does not produce a product in B strains. The common forward primer, which binds downstream of the *rscC* gene, produces a product in both strains when combined with the same reverse primer used for amplifying the K-12 locus (**Table 1**). In BL21(DE3), this results in a product of ∼1.9 kb. In K-12, the product also contains the region deleted in BL21(DE3), so the total length of the product is ∼5.3 kb. For the mutants, where the *ompC* coding sequence is deleted within the K-12 context, the product is ∼4.2 kb (**Figure 1B**). These results confirm that the kan cassette had correctly replaced the *ompC* sequence of BL21(DE3).

In order to show that the PCR-positive knock-out strains lack the corresponding proteins, we prepared outer membrane samples from all the strains and analyzed these by SDS-PAGE and silver staining (**Figure 1C**). *E. coli* BL21(DE3) was included as a positive sample showing outer membrane protein bands of interest. Maltoporin (LamB) has a size of ∼49 kDa. OmpC and OmpF are approximately the same size and run as a single band at ∼39 kDa, and OmpA has the smallest size of ∼35 kDa. All of these protein bands are visible in the parent strain. The single knock-out strain BL21ΔA shows all bands of interest except the 35 kDa OmpA band indicating that this protein is lacking in this strain. The ΔB strain shows the bands of interest at 35 kDa for OmpA and at 37 kDa for OmpC and OmpF but no band at 49 kDa. As a note, maltoporin is not well expressed in *E. coli* B strains, including BL21, which makes the confirmation of the *lamB* knock-out difficult on the protein level (Ronen and Raanan-Ashkenazi, 1971; Han et al., 2012); thus, the *lamB* knock-outs could only be fully confirmed by PCR. Single *ompC* and *ompF* knock-outs show a reduction in band intensity at 39 kDa, and only the double knock-outs lack the band at 39 kDa completely, suggesting that our strategy of knocking out *ompC* was a reasonable approach to make sure the gene is entirely inactivated. A possible explanation for a residual band at 39 kDa (e.g. for BL21ΔF) is expression of the cryptic porin OmpN (Prilipov et al., 1998a). Taken together, the PCR results and OMP profiles of the strains show that we have successfully deleted the genes encoding the major OMPs, either singly or in all combinations.

## Growth Properties of the Quadruple Knock-Out Strain BL21ΔABCF

While working with the new strains, it became obvious that by altering the outer membrane protein composition the growth behavior changed. BL21ΔABCF grew significantly more slowly than the parent strain BL21(DE3). The strain grew initially faster at 37°C than at 30°C, but the culture at 37°C saturated at a lower $OD_{600}$ (**Figure 2A**). However, even at 30°C, BL21ΔABCF did not reach the same $OD_{600}$ value as BL21(DE3).

We also observed that when using the Miller formulation of LB (with 10 g sodium chloride per liter), BL21ΔABCF grew significantly slower than in our standard LB (5 g NaCl/l), also at 30°C, whereas BL21(DE3) showed no significant differences in growth in the two media (**Figure 2B**). We do not currently have an explanation for this phenomenon; perhaps BL21ΔABCF is unable to compensate efficiently for the increased osmolarity of LB-Miller.

We also tested the growth of BL21ΔABCF in defined medium (**Figure 2C**). For this, we used minimal medium M9 supplemented with 18 amino acids. Though growth was slower than in LB, BL21ΔABCF reached higher optical densities than in the rich, undefined medium. It apparently also reached a higher density than BL21(DE3); however, part of the higher

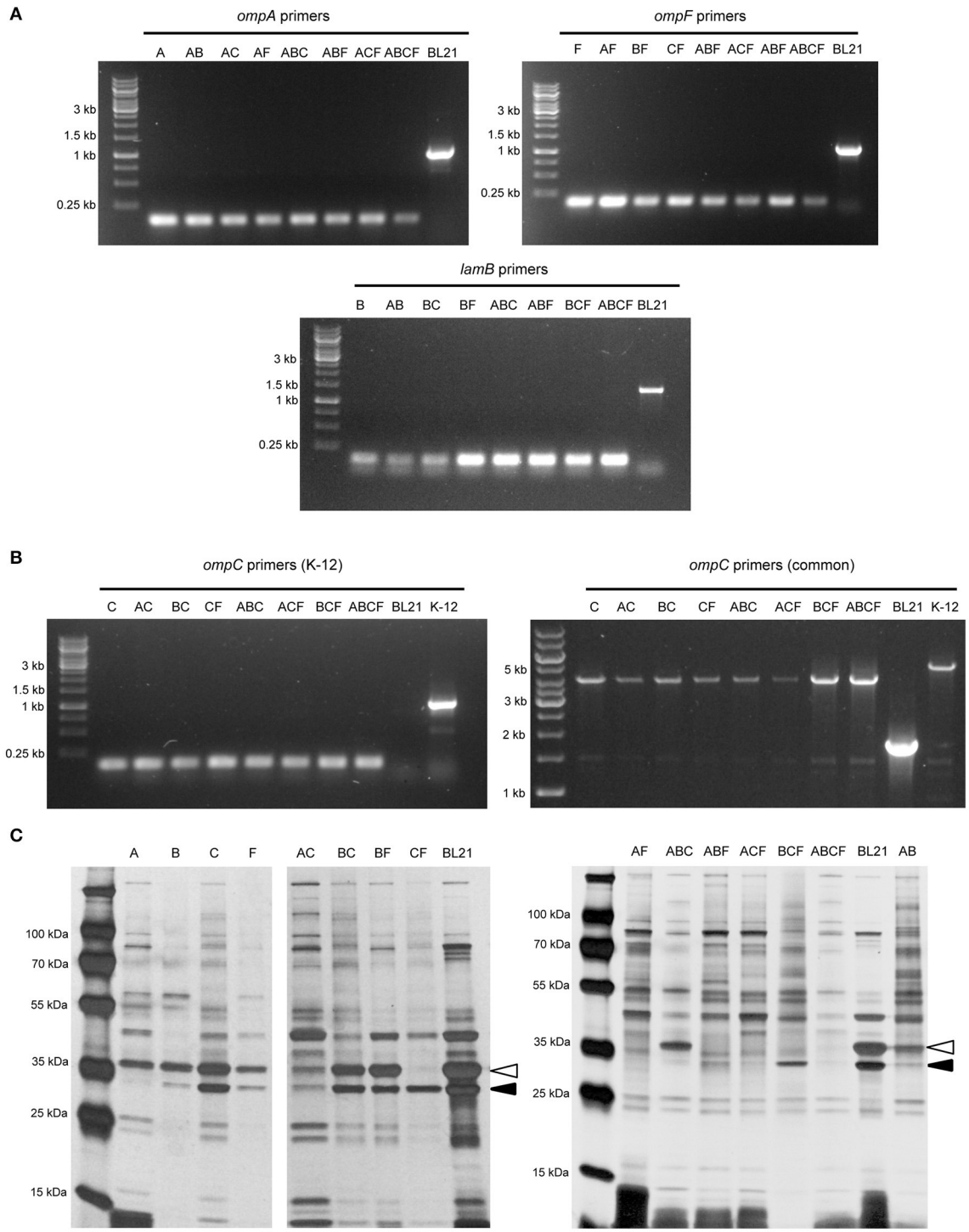


**FIGURE 1 |** Verification of the BL21 OMP knock-out strains. **(A)** Colony PCR results with primers for *ompA*, *ompF,* and *lamB* showing that in the mutant strains only a scar sequence (130–150 bp) remains at the locus. BL21 = parent strain BL21(DE3) control (expected sizes: *ompA* 1072, *ompF* 1135, *lamB* 1380 bp). **(B)** Colony PCR results of *ompC*. On the left, results using primers specific for the K-12 *ompC* locus are shown, where BL21(DE3) does not give a product and the deletion strains show just a short scar sequence (∼150 bp). The expected size for K-12 *ompC is* 1101 bp. On the right, results using common primers amplifying a larger region around the *ompC* locus in both BL21 and K-12. Here, the expected product for BL21(DE3) is 1.9 kb, the size expected for *E. coli* K-12 product is 5.3 kb and for the deletion strains 4.2 kb. **(C)** Silver-stained 15% polyacrylamide gel of BL21 OMP knock-out strains. The positions of OmpA (black arrowhead) and OmpC/F (open arrowhead) bands are indicated for the parent strain control (BL21). LamB is poorly expressed in *E. coli* B strains when grown at temperatures above 30°C and in the presence of other carbon sources (Ronen and Raanan-Ashkenazi, 1971), so this protein is not evident in most of the samples. Note that the Δ symbol has been omitted in the figure texts due to space constraints.

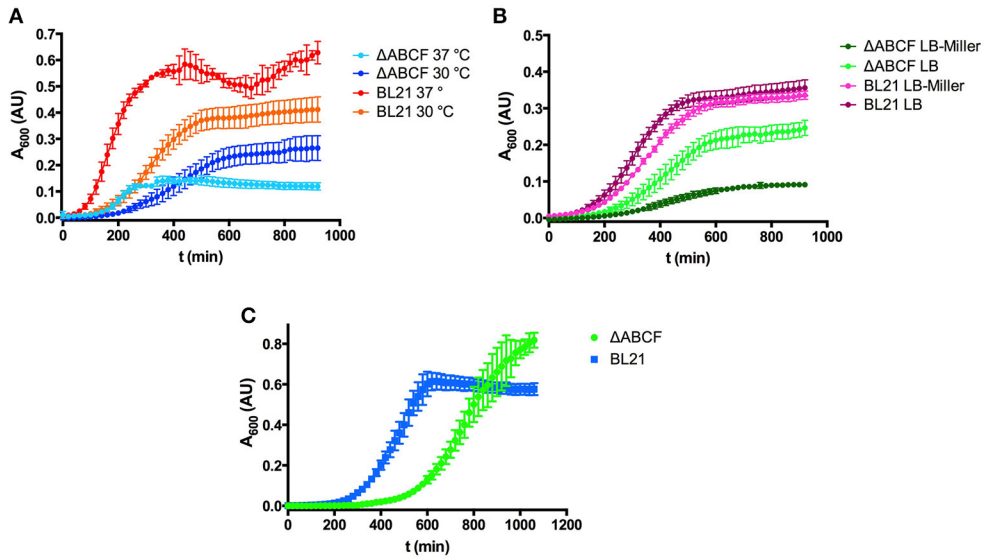


**FIGURE 2 |** Growth properties of the quadruple mutant BL21ΔABCF. **(A)** Growth of BL21ΔABCF in LB medium at 30 and 37°C. The parent strain BL21(DE3) is shown for comparison. Data points are the mean of four biological replicates; error bars denote the standard deviation. **(B)** Growth of BL21ΔABCF in LB (0.5% NaCl) and LB-Miller (1% NaCl) medium at 30°C. The parent strain BL21(DE3) is shown for comparison. Data points are the mean of four biological replicates; error bars denote the standard deviation. **(C)** Growth of BL21ΔABCF in supplemented M9 medium at 30°C. The parent strain BL21(DE3) is shown for comparison. Data points are the mean of four biological replicates; error bars denote the standard deviation. Note that the absorbance values shown here are not directly comparable to those measured with a 1 cm cuvette, due to the difference in light path length.

absorbance readings of the quadruple mutant cultures could be attributed to the tendency of BL21ΔABCF to clump in the defined medium, presumably due to the relatively high concentration of magnesium (2 mM; see section Aggregation of BL21ΔABCF in the Presence of Divalent Cations).

## Aggregation of BL21ΔABCF in the Presence of Divalent Cations

As noted above, BL21ΔABCF tends to aggregate in the presence of divalent cations. When $Mg^{2+}$ or $Ca^{2+}$ is added to the medium, BL21ΔABCF flocculates and settles rapidly at the bottom of the tube under static condition (**Figures 3A,B**). In contrast, the parent strain does not aggregate in the presence of either ion during the short time frame of the experiment (**Figures 3A,C**). However, upon prolonged incubation (>1 h), also BL21(DE3) began to flocculate in the presence of $Ca^{2+}$ (**Figure 3D**). The reason for the rapid aggregation of BL21ΔABCF is not clear. A possibility might be the increased binding of divalent cations by the more exposed lipid A phosphates in the BL21ΔABCF strain, leading to electrostatic attraction through bridging divalent cations. In principle, the aggregation caused by $CaCl_2$ might cause problems when preparing chemically competent cells; however, in our hands BL21ΔABCF can be made competent and transformed efficiently using the standard $CaCl_2$ protocol (data not shown).

## BL21ΔABCF Is Superior in Producing Recombinant OMPs

To qualitatively test the performance of our new quadruple mutant strain, we over-expressed four test proteins from our laboratory. For comparison, we used the parent strain *E. coli* BL21 (DE3). The test proteins were OmpX, a native OMP of *E. coli*, a duplicated variant of this protein with 16 β-strands rather than the usual eight (Arnold et al., 2007), and another OmpX variant containing a HA tag in one of the extracellular loops. Additionally, we tested the expression of two autotransporter proteins: the membrane anchor domain of the *Yersinia* adhesin YadA (Wollmann et al., 2006) and the inverse autotransporter Intimin from enteropathogenic *E. coli* (Oberhettinger et al., 2012).

The expression of wild-type OmpX can be seen as a band at 15 kDa when stained with Coomassie G-250 (**Figure 4A**). The band is more intense for BL21ΔABCF than for the parent strain. Other bands of native proteins, for example the band at 18 kDa that presumably represents OmpW, show that the same amount of sample was loaded. Note that there is no clear difference between the strains for the duplicated variant OmpX88 (∼37 kDa). The OmpX-HA construct was also expressed in BL21(DE3) and BL21ΔABCF. A Western blot of outer membrane preparations (**Figure 4B**) shows that for the quadruple knock-out strain, the total amount of expressed OmpX-HA is higher compared to the parent strain BL21(DE3). An additional band was detected at an increased molecular weight (∼25 kDa) that we originally attributed to non-denatured OmpX-HA (**Figure 4B**, right panel), similar to previous findings on OmpX gel shifts (Arnold et al., 2007), Based on the OMP gel shift phenomenon (Rosenbusch, 1974; Schweizer et al., 1978), we know that native and denatured forms of OMPs can migrate differently in SDS-PAGE. However, when comparing heated and unheated samples, the band did not change, suggesting that it is an artifact yet to be explained (data

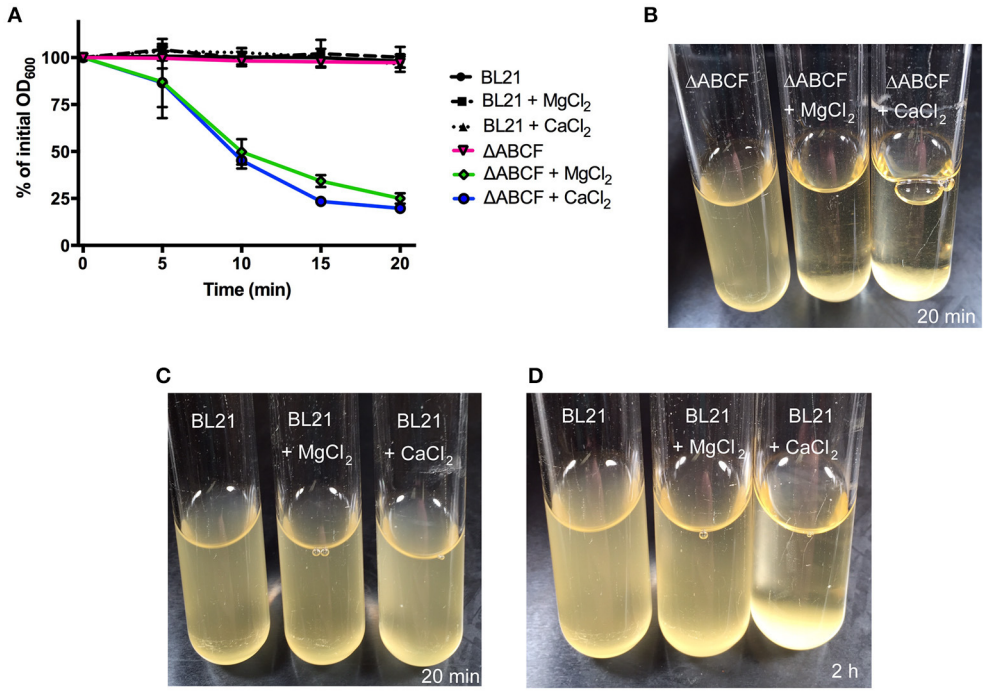


**FIGURE 3 |** Divalent cation-mediated aggregation of BL21ΔABCF. **(A)** Quantitative sedimentation assay. Cultures of BL21ΔABCF or the parent strain were cultured in LB medium (with or without the addition of $MgCl_2$ or $CaCl_2$ at 10 mM) at 30°C with shaking (200 rpm). For the sedimentation assay, the cultures were incubated statically and the $OD_{600}$ value was measured from the very top of the culture at 5-min intervals. The data points represent the percentage of the initial $OD_{600}$ value as the mean of three biological replicates; error bars denote standard deviations. **(B)** Photograph of BL21ΔABCF cultures after 20 min of static incubation. In the presence of 10 mM $MgCl_2$ or $CaCl_2$, BL21ΔABCF flocculates and rapidly settles at the bottom of the tube, leaving the medium clear. **(C)** Photograph of BL21(DE3) cultures after 20 min of static incubation. Turbidity is not reduced by the addition of 10 mM $MgCl_2$ or $CaCl_2$ to cultures of BL21(DE3). **(D)** Photograph of BL21(DE3) cultures after 2 h of static incubation. In the presence of $CaCl_2$, also BL21(DE3) flocculates.

not shown). The third specific band at ∼50 kDa is presumably a folded dimer of OmpX at very low concentration (Chaturvedi and Mahalakshmi, 2013).

YadA is an obligate homotrimer and an adhesin of enteropathogenic *Yersiniae* (Mühlenkamp et al., 2015). It is an extremely stable protein which remains trimeric in the presence of denaturants such as, SDS and urea (Wollmann et al., 2006). In SDS-PAGE, YadAM (membrane anchor domain of YadA) migrates at an apparent molecular weight of 45 kDa (Wollmann et al., 2006). The expression of YadAM in BL21(DE3) and BL21ΔABCF is shown in **Figure 4C**. The colloidal Coomassie G250-stained gel shows better expression of YadAM in BL21ΔABCF than BL21(DE3). As mentioned above, many native outer membrane protein bands (e.g., ∼30 kDa and ∼60 kDa) are absent in the ΔABCF strain.

The expression of Intimin is shown in **Figure 4D**. Here, a construct including a StrepII tag was used and its expression visualized specifically in a Western blot using an anti-Intimin antibody (Oberhettinger et al., 2012). The blot shows two bands for the parent strain: one at ∼95 kDa corresponding to the molecular weight of Intimin and a second band at ∼120 kDa. This latter band is sometimes observed in Intimin blots, though its provenance is not clear (Heinz et al., 2016; Leo et al., 2016). For the ΔABCF strain, the 95 kDa band is more intense, and the ∼120 kDa band fainter, suggesting better membrane insertion. In addition, some apparent degradation product can be seen for the quadruple mutant (band at ∼70 kDa). The superiority of the BL21ΔABCF strain is demonstrated by a higher yield of the "correct" Intimin band and less of the (presumably mis-incorporated) 120 kDa band.

To gain a more quantitative view of OMP production in BL21ΔABCF and to assess reproducibility between culture batches, we performed whole-cell ELISA on bacteria expressing OmpX-HA and Intimin. We compared expression of these two proteins in BL21(DE3), BL21ΔABCF, and the Prilipov strain BL21 Omp8. We also tested the expression of YadAM in these strains, but due to technical problems with detecting the StrepII tag on the bacterial surface combined with the tendency of YadAM-expressing cells to clump, we did not obtain reliable results (data not shown). In this construct, only a short stretch of YadAM is exposed to the surface, so the StrepII tag is presumably not fully accessible to antibodies (Shahid et al., 2012).

BL21ΔABCF produced both Intimin and OmpX-HA at higher amounts than the parent strain BL21(DE3) (**Figure 5**). Somewhat unexpectedly, BL21ΔABCF also outperformed the Omp8 strain, though the difference is not large. The ELISA also demonstrate that the variability between biological replicates is low, though for Intimin there is more variability between replicates. Incidentally, in the whole-cell assays the detected proteins must be surface-exposed, showing that the detected species must be correctly processed and inserted into the membrane.

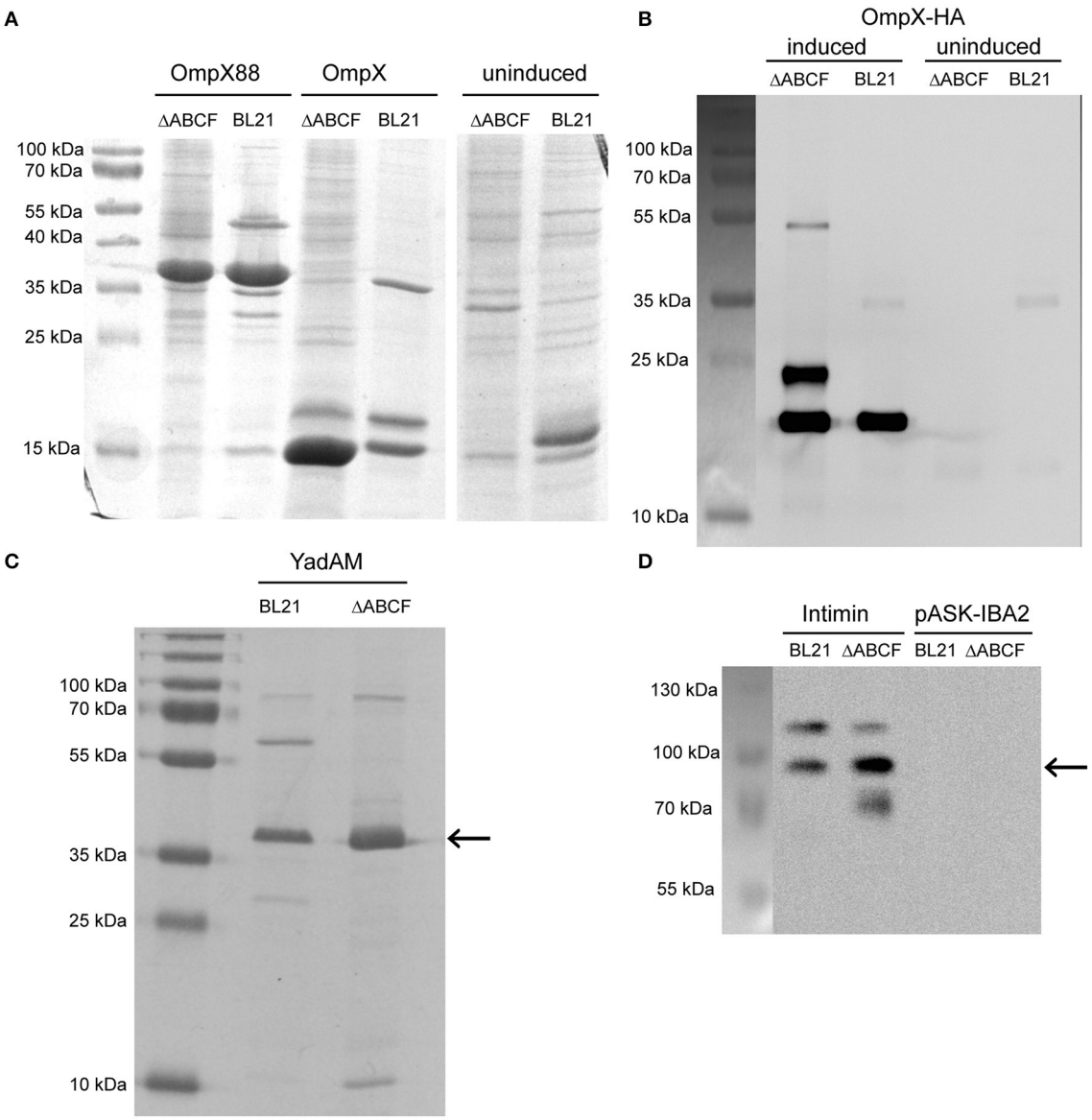


**FIGURE 4 |** Improved over-production of recombinant OMPs in BL21ΔABCF. **(A)** Coomassie-stained 15% polyacrylamide gel showing production levels of recombinant OmpX and duplicated OmpX (OmpX88) in BL21(DE3) and BL21ΔABCF. Uninduced cultures of the OmpX construct are shown as a control. Note that the artificial construct OmpX88 does not show significantly improved expression, while the expression of OmpX is massively improved in the BL21ΔABCF strain. **(B)** Western blot of OmpX-HA produced in both BL21(DE3) and BL21ΔABCF probed with an anti-HA antibody. An equal amount of cells (based on $OD_{600}$ measurement) was lysed by heating in sample buffer and loaded onto the gel. Uninduced samples are shown as controls. A picture showing the positions of the pre-stained molecular weight marker bands on the blotting membrane is shown on the left. **(C)** Colloidal Coomassie G250-stained 15% polyacrylamide gel showing production levels of the YadA membrane anchor (YadAM; position denoted by the arrow) produced in both BL21 and BL21ΔABCF. **(D)** Western blot of Intimin produced in both BL21 and BL21ΔABCF probed with an anti-Intimin antibody. An equal amount of cells (based on OD600 measurement) was lysed by heating in sample buffer and loaded onto the gel. Strains with the empty vector (pASK-IBA2) serve as controls. The arrow shows the position of the main Intimin band (~95 kDa). A picture showing the positions of the pre-stained molecular weight marker bands on the blotting membrane is shown on the left.

## DISCUSSION

We have produced a series of *E. coli* knock-out strains for use in over-expressing OMPs with deletions of at least one of four abundant OMP protein genes. Our series contains the four single deletions, all combinations of double and triple deletions, and the quadruple deletion strain BL21ΔABCF. The strains all contain the DE3 lysogen and can therefore be used with vectors requiring the T7 polymerase for expression.

We noted some unusual properties when culturing the quadruple mutant strain BL21ΔABCF: the strain grows poorly at 37°C and does not tolerate high salt concentrations. In addition, BL21ΔABCF aggregates in the presence of divalent cations. We therefore recommend that BL21ΔABCF be grown at 30°C in

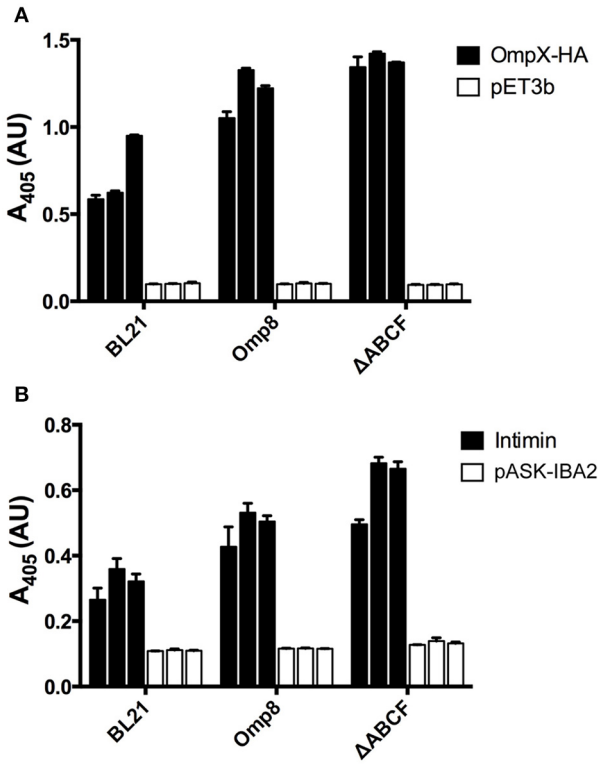


**FIGURE 5 |** Quantitative assessment of recombinant OMP production by BL21ΔABCF **(A)** Whole-cell ELISA of bacteria producing OmpX-HA. Bacteria were coated onto wells of a microtiter plate and probed with an anti-HA tag antibody. The primary antibody was detected with a HRP-conjugated secondary antibody and colorimetric staining using the substrate ABTS. Black bars denote the biological replicates (three for each strain) expressing OmpX-HA; white bars show values for empty vector controls. Each bar represent the mean of three technical replicates; error bars denote the standard deviation of three technical replicates. **(B)** Whole-cell ELISA of bacteria producing Intimin. The experimental set up was similar to **(A)**; the primary antibody was an anti-Intimin antibody. Black bars denote biological replicates expressing Intimin, white bars represent vector controls. Each bar represent the mean of three technical replicates; error bars denote the standard deviation of three technical replicates.

medium with low sodium chloride (≤5 g/l) and without excess divalent cations.

We demonstrated the superiority of the quadruple mutant strain in producing four different test proteins (OmpX, artificial OmpX variants, YadA, and Intimin) compared with BL21(DE3). This strain has mutations in the same genes as the Omp8 strain previously produced (Prilipov et al., 1998b), and we assumed that there would be no major differences between these two strains regarding OMP production capability. However, our whole-cell ELISAs showed that BL21ΔABCF is slightly better at over-expressing OMPs than Omp8, and significantly better than the parent strain BL21(DE3). In addition, as our strain lacks the transposon found in Omp8, and the full deletion of the OMP coding sequences prevents any reversion to wild-type, it is more stable than the Omp8 strain has proven to be, at least in our hands. A second advantage of the ΔABCF strain is the lack of any intrinsic antibiotic resistance markers, allowing it to host a broader choice of vector plasmids.

An additional advantage of these OMP deletion strains, similarly to the strains of Prilipov et al., is the low level of endogenous OMPs. Especially the ΔABCF strain can be used for *in situ* studies of OMP functions, without interference from endogenous proteins, where efficient labeling of the protein of interest against a low background is required. The power of such approaches can be seen in work where YadA was expressed in the original Omp8 strain in isotope-labeled medium for nuclear magnetic resonance (NMR) studies, where it was then possible to directly measure NMR spectra of the protein in native membranes (Shahid et al., 2015). This would not have been possible using wild-type *E. coli* due to the high background from other abundant OMPs.

Furthermore, the lack of all major naturally occurring OMPs in this strain may aid in purifying heterologous OMPs for functional or structural studies. As the amount of competing OMPs is low, heterologous OMPs can be purified efficiently and simply with e.g., ion exchange chromatography, without the need to introduce affinity tags, which might compromise protein function. This applies even to transmembrane β-barrel proteins of eukaryotic origin, some of which have been produced in bacteria (Walther et al., 2009a).

## STRAIN AVAILABILITY

All strains produced in this study are available through Addgene (http://www.addgene.org). See **Table 2** for strain identifiers.

## AUTHOR CONTRIBUTIONS

DL conceived the project; JL and DL designed the project; IM and JL performed the recombinant DNA work; IM, JL, MM, and NC performed the strain characterization; and all authors were involved in analyzing the data and writing the manuscript.

## FUNDING

This work was funded by an Erasmus student exchange fellowship (to IM), FriMedBio funding by the Research Council of Norway (to DL), and a grant from VISTA, a basic research program funded by Statoil in collaboration with the NorwegianAcademy of Science and Letters (to JL).

## ACKNOWLEDGMENTS

We thank Sophie Krauss, Pao Jané, and Hawzeen Salah Khalil for technical assistance. The strains from the Keio collection were obtained from the National BioResource Project (NIG, Japan): *E. coli*.

## SUPPLEMENTARY MATERIAL

The Supplementary Material for this article can be found online at: https://www.frontiersin.org/articles/10.3389/fcimb.2017.00464/full#supplementary-material

## REFERENCES


Alba, B. M., and Gross, C. A. (2004). Regulation of the *Escherichia coli* sigma(E)-dependent envelope stress response. *Mol. Microbiol.* 52, 613–619. doi: 10.1111/j.1365-2958.2003.03982.x

Aoki, S. K., Malinverni, J. C., Jacoby, K., Thomas, B., Pamma, R., Trinh, B. N., et al. (2008). Contact-dependent growth inhibition requires the essential outer membrane protein BamA (YaeT) as the receptor and the inner membrane transport protein AcrB. *Mol. Microbiol.* 70, 323–340. doi: 10.1111/j.1365-2958.2008.06404.x

Aoki, S. K., Pamma, R., Hernday, A. D., Bickham, J. E., Braaten, B. A., and Low, D. A. (2005). Contact-dependent inhibition of growth in *Escherichia coli*. *Science* 309, 1245–1248. doi: 10.1126/science.1115109

Arechaga, I., Miroux, B., Karrasch, S., Huijbregts, R., de Kruijff, B., Runswick, M. J., et al. (2000). Characterisation of new intracellular membranes in *Escherichia coli* accompanying large scale over-production of the b subunit of F(1)F(o) ATP synthase. *FEBS Lett.* 482, 215–219. doi: 10.1016/S0014-5793(00)02054-8

Arnold, T., Poynor, M., Nussberger, S., Lupas, A. N., and Linke, D. (2007). Gene duplication of the eight-stranded beta-barrel OmpX produces a functional pore: a scenario for the evolution of transmembrane β-barrels. *J. Mol. Biol.* 366, 1174–1184. doi: 10.1016/j.jmb.2006.12.029

Baba, T., Ara, T., Hasegawa, M., Takai, Y., Okumura, Y., Baba, M., et al. (2006). Construction of *Escherichia coli* K-12 in-frame, single-gene knockout mutants: the Keio collection. *Mol. Syst. Biol.* 2:2006.0008. doi: 10.1038/msb4100050

Bakelar, J., Buchanan, S. K., and Noinaj, N. (2016). The structure of the β-barrel assembly machinery complex. *Science* 351, 180–186. doi: 10.1126/science.aad3460

Byrappa, S., Gavin, D. K., and Gupta, K. C. (1995). A highly efficient procedure for site-specific mutagenesis of full-length plasmids using Vent DNA polymerase. *Genome Res.* 5, 1–5. doi: 10.1101/gr.5.4.404

Chagnot, C., Zorgani, M. A., Astruc, T., and Desvaux, M. (2013). Proteinaceous determinants of surface colonization in bacteria: bacterial adhesion and biofilm formation from a protein secretion perspective. *Front. Microbiol.* 4:303. doi: 10.3389/fmicb.2013.00303

Chaturvedi, D., and Mahalakshmi, R. (2013). Methionine mutations of outer membrane protein X influence structural stability and beta-barrel unfolding. *PLoS ONE* 8:e79351. doi: 10.1371/journal.pone.0079351

Cherepanov, P. P., and Wackernagel, W. (1995). Gene disruption in *Escherichia coli*: TcR and KmR cassettes with the option of Flp-catalyzed excision of the antibiotic-resistance determinant. *Gene* 158, 9–14. doi: 10.1016/0378-1119(95)00193-A

Datsenko, K. A., and Wanner, B. L. (2000). One-step inactivation of chromosomal genes in *Escherichia coli* K-12 using PCR products. *Proc. Natl. Acad. Sci. U.S.A.* 97, 6640–6645. doi: 10.1073/pnas.120163297

Delcour, A. H. (2009). Outer membrane permeability and antibiotic resistance. *Biochim. Biophys. Acta.* 1794, 808–816. doi: 10.1016/j.bbapap.2008.11.005

Dong, H., Xiang, Q., Gu, Y., Wang, Z., Paterson, N. G., Stansfeld, P. J., et al. (2014). Structural basis for outer membrane lipopolysaccharide insertion. *Nature* 511, 52–56. doi: 10.1038/nature13464

Fairman, J. W., Noinaj, N., and Buchanan, S. K. (2011). The structural biology of β-barrel membrane proteins: a summary of recent reports. *Curr. Opin. Struct. Biol.* 21, 523–531. doi: 10.1016/j.sbi.2011.05.005

Georgiou, G., and Segatori, L. (2005). Preparative expression of secreted proteins in bacteria: status report and future prospects. *Curr. Opin. Biotechnol.* 16, 538–545. doi: 10.1016/j.copbio.2005.07.008

Goemans, C., Denoncin, K., and Collet, J. F. (2014). Folding mechanisms of periplasmic proteins. *Biochim. Biophys. Acta* 1843, 1517–1528. doi: 10.1016/j.bbamcr.2013.10.014

Grosskinsky, U., Schütz, M., Fritz, M., Schmid, Y., Lamparter, M. C., Szczesny, P., et al. (2007). A conserved glycine residue of trimeric autotransporter domains plays a key role in *Yersinia* adhesin A autotransport. *J. Bacteriol.* 189, 9011–9019. doi: 10.1128/JB.00985-07

Gu, Y., Li, H., Dong, H., Zeng, Y., Zhang, Z., Paterson, N. G., et al. (2016). Structural basis of outer membrane protein insertion by the BAM complex. *Nature* 531, 64–69. doi: 10.1038/nature17199

Haiko, J., Suomalainen, M., Ojala, T., Lähteenmäki, K., and Korhonen, T. K. (2009). Breaking barriers–attack on innate immune defences by omptin surface proteases of enterobacterial pathogens. *Innate Immun.* 15, 67–80. doi: 10.1177/1753425909102559

Han, L., Zheng, J., Wang, Y., Yang, X., Liu, Y., Sun, C., et al. (2016). Structure of the BAM complex and its implications for biogenesis of outer-membrane proteins. *Nat. Struct. Mol. Biol.* 23, 192–196. doi: 10.1038/nsmb.3181

Han, M. J., Lee, S. Y., and Hong, S. H. (2012). Comparative analysis of envelope proteomes in *Escherichia coli* B and K-12 strains. *J. Microbiol. Biotechnol.* 22, 470–478. doi: 10.4014/jmb.1110.10080

Hanahan, D. (1983). Studies on transformation of *Escherichia coli* with plasmids. *J. Mol. Biol.* 166, 557–580. doi: 10.1016/S0022-2836(83)80284-8

Heinz, E., Stubenrauch, C. J., Grinter, R., Croft, N. P., Purcell, A. W., Strugnell, R. A., et al. (2016). Conserved features in the structure, mechanism, and biogenesis of the inverse autotransporter protein family. *Genome Biol. Evol.* 8, 1690–1705. doi: 10.1093/gbe/evw112

Hufnagel, D. A., Depas, W. H., and Chapman, M. R. (2015). The biology of the *Escherichia coli* extracellular matrix. *Microbiol. Spectr.* 3:249. doi: 10.1128/microbiolspec.MB-0014-2014

Kudva, R., Denks, K., Kuhn, P., Vogt, A., Müller, M., and Koch, H. G. (2013). Protein translocation across the inner membrane of gram-negative bacteria: the Sec and Tat dependent protein transport pathways. *Res. Microbiol.* 164, 505–534. doi: 10.1016/j.resmic.2013.03.016

Leo, J. C., Grin, I., and Linke, D. (2012). Type V secretion: mechanism(s) of autotransport through the bacterial outer membrane. *Philos. Trans. R. Soc. Lond. B Biol. Sci.* 367, 1088–1101. doi: 10.1098/rstb.2011.0208

Leo, J. C., Lyskowski, A., Hattula, K., Hartmann, M. D., Schwarz, H., Butcher, S. J., et al. (2011). The structure of *E. coli* IgG-binding protein D suggests a general model for bending and binding in trimeric autotransporter adhesins. *Structure* 19, 1021–1030. doi: 10.1016/j.str.2011.03.021

Leo, J. C., Oberhettinger, P., and Linke, D. (2015). Assessing the outer membrane insertion and folding of multimeric transmembrane β-barrel proteins. *Methods Mol. Biol.* 1329, 157–167. doi: 10.1007/978-1-4939-2871-2_12

Leo, J. C., Oberhettinger, P., Yoshimoto, S., Udatha, D. B., Morth, P. J., Schütz, M., et al. (2016). Secretion of the intimin passenger domain is driven by protein folding. *J. Biol. Chem.* 291, 20096–20112. doi: 10.1074/jbc.M116.731497

Mikula, K. M., Leo, J. C., Łyskowski, A., Kedracka-Krok, S., Pirog, A., and Goldman, A. (2012). The translocation domain in trimeric autotransporter adhesins is necessary and sufficient for trimerization and autotransportation. *J. Bacteriol.* 194, 827–838. doi: 10.1128/JB.05322-11

Miller, J. H. (1972). *Experiments in Bacterial Genetics*. Cold Spring Harbor, NY: Cold Spring Harbor Laboratory.

Monteiro, R., Ageorges, V., Rojas-Lopez, M., Schmidt, H., Weiss, A., Bertin, Y., et al. (2016). A secretome view of colonisation factors in Shiga toxin-encoding *Escherichia coli* (STEC): from enterohaemorrhagic *E. coli* (EHEC) to related enteropathotypes. *FEMS Microbiol. Lett.* 363:fnw179. doi: 10.1093/femsle/fnw179

Moon, C. P., Zaccai, N. R., Fleming, P. J., Gessmann, D., and Fleming, K. G. (2013). Membrane protein thermodynamic stability may serve as the energy sink for sorting in the periplasm. *Proc. Natl. Acad. Sci. U.S.A.* 110, 4285–4290. doi: 10.1073/pnas.1212527110

Mühlenkamp, M., Oberhettinger, P., Leo, J. C., and Linke, D. (2015). Yersinia adhesin A (YadA)-beauty & beast. *Int. J. Med. Microbiol.* 305, 252–258. doi: 10.1016/j.ijmm.2014.12.008

Nesterenko, M. V., Tilley, M., and Upton, S. J. (1994). A simple modification of Blum's silver stain method allows for 30 minute detection of proteins in polyacrylamide gels. *J. Biochem. Biophys. Methods* 28, 239–242. doi: 10.1016/0165-022X(94)90020-5

Oberhettinger, P., Schütz, M., Leo, J. C., Heinz, N., Berger, J., Autenrieth, I. B., et al. (2012). Intimin and invasin export their C-terminus to the bacterial cell surface using an inverse mechanism compared to classical autotransport. *PLoS ONE* 7:e47069. doi: 10.1371/annotation/cb7e47be-dd4b-46cd-b4e5-18b7077f64df

Prilipov, A., Phale, P. S., Koebnik, R., Widmer, C., and Rosenbusch, J. P. (1998a). Identification and characterization of two quiescent porin genes, *nmpC* and *ompN*, in *Escherichia coli* BE. *J Bacteriol* 180, 3388–3392.

Prilipov, A., Phale, P. S., Van Gelder, P., Rosenbusch, J. P., and Koebnik, R. (1998b). Coupling site-directed mutagenesis with high-level expression: large scale production of mutant porins from *E. coli*. *FEMS Microbiol. Lett.* 163, 65–72. doi: 10.1111/j.1574-6968.1998.tb13027.x

Pugsley, A. P., and Rosenbusch, J. P. (1983). OmpF porin synthesis in *Escherichia coli* strains B and K-12 carrying heterologous ompB and/or ompF loci. *FEMS Microbiol. Lett.* 16, 143–148. doi: 10.1111/j.1574-6968.1983.tb00275.x

Rassam, P., Copeland, N. A., Birkholz, O., Tóth, C., Chavent, M., Duncan, A. L., et al. (2015). Supramolecular assemblies underpin turnover of outer membrane proteins in bacteria. *Nature* 523, 333–336. doi: 10.1038/nature14461

Remmert, M., Biegert, A., Linke, D., Lupas, A. N., and Söding, J. (2010). Evolution of outer membrane β-barrels from an ancestral ββ hairpin. *Mol. Biol. Evol.* 27, 1348–1358. doi: 10.1093/molbev/msq017

Ronen, A., and Raanan-Ashkenazi, O. (1971). Temperature sensitivity of maltose utilization and lambda resistance in *Escherichia coli* B. *J. Bacteriol.* 106, 791–796.

Rosenbusch, J. P. (1974). Characterization of the major envelope protein from *Escherichia coli*. regular arrangement on the peptidoglycan and unusual dodecyl sulfate binding. *J. Biol. Chem.* 249, 8019–8029.

Schlegel, S., Rujas, E., Ytterberg, A. J., Zubarev, R. A., Luirink, J., and de Gier, J. W. (2013). Optimizing heterologous protein production in the periplasm of *E. coli* by regulating gene expression levels. *Microb. Cell Fact.* 12:24. doi: 10.1186/1475-2859-12-24

Schweizer, M., Hindennach, I., Garten, W., and Henning, U. (1978). Major proteins of the *Escherichia coli* outer cell envelope membrane. Interaction of protein ii with lipopolysaccharide. *Eur. J. Biochem.* 82, 211–217. doi: 10.1111/j.1432-1033.1978.tb12013.x

Shahid, S. A., Bardiaux, B., Franks, W. T., Krabben, L., Habeck, M., van Rossum, B.-J., et al. (2012). Membrane-protein structure determination by solid-state NMR spectroscopy of microcrystals. *Nat. Methods* 9, 1212–1217. doi: 10.1038/nmeth.2248

Shahid, S. A., Nagaraj, M., Chauhan, N., Franks, T. W., Bardiaux, B., Habeck, M., et al. (2015). Solid-state NMR study of the YadA membrane-anchor domain in the bacterial outer membrane. *Angew. Chem. Int. Ed. Engl.* 54, 12602–12606. doi: 10.1002/anie.201505506

Studier, F. W., and Moffatt, B. A. (1986). Use of bacteriophage T7 RNA polymerase to direct selective high-level expression of cloned genes. *J. Mol. Biol.* 189, 113–130. doi: 10.1016/0022-2836(86)90385-2

Studier, F. W., Daegelen, P., Lenski, R. E., Maslov, S., and Kim, J. F. (2009). Understanding the differences between genome sequences of *Escherichia coli* B strains REL606 and BL21(DE3) and comparison of the *E. coli* B and K-12 genomes. *J. Mol. Biol.* 394, 653–680. doi: 10.1016/j.jmb.2009.09.021

Thomason, L. C., Costantino, N., and Court, D. L. (2007). *E. coli* genome manipulation by P1 transduction. *Curr. Protoc. Mol. Biol.* 79, 1.17.1–1.17.8. doi: 10.1002/0471142727.mb0117s79

Wagner, S., Baars, L., Ytterberg, A. J., Klussmeier, A., Wagner, C. S., Nord, O., et al. (2007). Consequences of membrane protein overexpression in *Escherichia coli*. *Mol. Cell. Proteomics* 6, 1527–1550. doi: 10.1074/mcp.M600431-MCP200

Wagner, S., Bader, M. L., Drew, D., and de Gier, J. W. (2006). Rationalizing membrane protein overexpression. *Trends Biotechnol.* 24, 364–371. doi: 10.1016/j.tibtech.2006.06.008

Walther, D. M., Bos, M. P., Rapaport, D., and Tommassen, J. (2009a). The mitochondrial porin, VDAC, has retained the ability to be assembled in the bacterial outer membrane. *Mol. Biol. Evol.* 27, 887–895. doi: 10.1093/molbev/msp294

Walther, D. M., Rapaport, D., and Tommassen, J. (2009b). Biogenesis of β-barrel membrane proteins in bacteria and eukaryotes: evolutionary conservation and divergence. *Cell. Mol. Life Sci.* 66, 2789–2804. doi: 10.1007/s00018-009-0029-z

Wollmann, P., Zeth, K., Lupas, A. N., and Linke, D. (2006). Purification of the YadA membrane anchor for secondary structure analysis and crystallization. *Int. J. Biol. Macromol.* 39, 3–9. doi: 10.1016/j.ijbiomac.2005.11.009

**Conflict of Interest Statement:** The authors declare that the research was conducted in the absence of any commercial or financial relationships that could be construed as a potential conflict of interest.

This work has been included in a patent application (U.S. Patent Office application number 62438094).

# Advantages of publishing in Frontiers

**OPEN ACCESS**
Articles are free to read for greatest visibility and readership

**FAST PUBLICATION**
Around 90 days from submission to decision

**HIGH QUALITY PEER-REVIEW**
Rigorous, collaborative, and constructive peer-review

**TRANSPARENT PEER-REVIEW**
Editors and reviewers acknowledged by name on published articles

**Frontiers**
Avenue du Tribunal-Fédéral 34
1005 Lausanne | Switzerland

**Visit us:** www.frontiersin.org
**Contact us:** info@frontiersin.org | +41 21 510 17 00

**REPRODUCIBILITY OF RESEARCH**
Support open data and methods to enhance research reproducibility

**DIGITAL PUBLISHING**
Articles designed for optimal readership across devices

**FOLLOW US**
@frontiersin

**IMPACT METRICS**
Advanced article metrics track visibility across digital media

**EXTENSIVE PROMOTION**
Marketing and promotion of impactful research

**LOOP RESEARCH NETWORK**
Our network increases your article's readership